4th International Probabilistic Symposium

12th-13th October 2006, Berlin, Germany

Federal Institute for Material Research and Testing (BAM), Berlin

University of Natural Resources and Applied Life Sciences, Department of Civil Engineering and Natural Hazards, Vienna

Academia Morksa Szczecin

Dirk Proske, Milad Mehdianpour & Lucjan Gucma (Eds.): 4th International Probabilistic Symposium, 12th-13th October 2006, Berlin, BAM (Federal Institute for Materials Research and Testing),
Universität für Bodenkultur, Bundesanstalt für Materialforschung und -prüfung, Maritime University of Szczecin
Wien • Berlin • Szczecin 2006
ISBN-10: 3-00-019232-8
ISBN-13: 978-3-00-019232-6

Dirk Proske
Milad Mehdianpour
Lucjan Gucma (Eds.)

4th International Probabilistic Symposium

12th-13th October 2006
Berlin, BAM

Preface

The world today is shaped by high dynamics. Multitude of processes evolves parallel and partly connected invisible. For example, the globalisation is such a process. Here one can observe the exponential growing of connections form the level of single humans to the level of cultures. Such connections guide as to the term complexity. Complexity is often understood as product of the number of elements and the amount of connections in the system. In other words, the world is going more complex, if the connections increase. Complexity itself is a term for a system, which is not fully understood, which is partly uncontrollable and indeterminated: exactly as humans. Growing from a single cell, the humans will show latter a behaviour, which we can not predict in detail. After all, the human brain consists of 10^{11} elements (cells). If the social dynamical processes yield to more complexity, we have to accept more indetermination. Well, one has to hope, that such an indetermination does not affect the basic of human existence. If we look at the field of technology, we can detect, that here indetermination or uncertainty is often be dealt with explicitly. This is valid for natural risk management, for nuclear engineering, civil engineering or for the design of ships. And so different the fields are which contribute to this symposium for all is valid: People working in this field have realised, that a responsible usage of technology requires consideration of indetermination and uncertainty. This level is not yet reached in the social sciences. It is the wish of the organisers of this symposium, that not only civil engineers, mechanical engineers, mathematicians, ship builders take part in this symposium, but also sociologists, managers and even politicians. Therefore there is still a great opportunity to grow for this symposium. Indetermination does not have to be negative: it can also be seen as chance.

Dr.-Ing. Milad Mehdianpour
Federal Institute for Materials Research and Testing

Prof. DDr. Konrad Bergmeister
University of Natural Resources and Applied Life Sciences, Vienna, Institute of Structural Engineering

Prof. Lucjan Gucma
Maritime University of Szczecin

Dr.-Ing. Dirk Proske
University of Natural Resources and Applied Life Sciences, Vienna, Institute of Mountain Risk Engineering

Vorwort

Die heutige Welt der Menschen wird durch große Dynamik geprägt. Eine Vielzahl verschiedener Prozesse entfaltet sich parallel und teilweise auf unsichtbare Weise miteinander verbunden. Nimmt man z.B. den Prozess der Globalisierung: Hier erleben wir ein exponentielles Wachstum der internationalen Verknüpfungen von der Ebene einzelner Menschen und bis zur Ebene der Kulturen. Solche Verknüpfungen führen uns zum Begriff der Komplexität. Diese wird oft als Produkt der Anzahl der Elemente eines Systems mal Umfang der Verknüpfungen im System verstanden. In anderen Worten, die Welt wird zunehmend komplexer, denn die Verknüpfungen nehmen zu. Komplexität wiederum ist ein Begriff für etwas unverstandenes, unkontrollierbares, etwas unbestimmtes. Genau wie bei einem Menschen: Aus einer Zelle wächst ein Mensch, dessen Verhalten wir im Detail nur schwer vorhersagen können. Immerhin besitzt sein Gehirn 10^{11} Elemente (Zellen). Wenn also diese dynamischen sozialen Prozesse zu höherer Komplexität führen, müssen wir auch mehr Unbestimmtheit erwarten. Es bleibt zu Hoffen, dass die Unbestimmtheit nicht existenzielle Grundlagen betrifft. Was die Komplexität der Technik angeht, so versucht man hier im Gegensatz zu den gesellschaftlichen Unsicherheiten die Unsicherheiten zu erfassen und gezielt mit ihnen umzugehen. Das gilt für alle Bereiche, ob nun Naturgefahrenmanagement, beim Bau und Betrieb von Kernkraftwerken, im Bauwesen oder in der Schifffahrt. Und so verschieden diese Fachgebiete auch scheinen mögen, die an diesem Symposium teilnehmen: Sie haben erkannt, das verantwortungsvoller Umgang mit Technik einer Berücksichtigung der Unbestimmtheit bedarf. Soweit sind wir in gesellschaftlichen Prozessen noch nicht. Wünschenswert wäre, dass in einigen Jahren nicht nur Bauingenieure, Maschinenbauer, Mathematiker oder Schiffsbauer an einem solchen Probabilistik-Symposium teilnehmen, sondern auch Soziologen, Politiker oder Manager. Es bleibt also noch viel Entwicklungspotential für dieses Symposium. Bleiben wir gespannt, Unbestimmtheit kann auch positiv sein.

Dr.-Ing. Milad Mehdianpour
Bundesanstalt für Materialforschung und -prüfung

Prof. DDr. Konrad Bergmeister
Universität für Bodenkultur Wien,
Institut für Konstruktiven Ingenieurbau

Prof. Lucjan Gucma
Maritime University of Szczecin

Dr.-Ing. Dirk Proske
Universität für Bodenkultur Wien,
Institut für Alpine Naturgefahren

Organising Committee

Dr.-Ing. Milad Mehdianpour
Federal Institute for Materials Research and Testing

Prof. DDr. Konrad Bergmeister
University of Natural Resources and Applied Life Sciences, Vienna, Institute of Structural Engineering

Prof. Lucjan Gucma
Maritime University of Szczecin

Dr.-Ing. Dirk Proske
University of Natural Resources and Applied Life Sciences, Vienna, Institute of Mountain Risk Engineering

Monika Stanzer
University of Natural Resources and Applied Life Sciences, Vienna, Institute of Mountain Risk Engineering

Evelin Kamper
University of Natural Resources and Applied Life Sciences, Vienna, Institute of Structural Engineering

Scientific Committee

Content

Modelling human behaviour in the assessment of navigational safety in restricted areas

Zbigniew Pietrzykowski
Institute of Marine Navigation, Maritime University of Szczecin

Abstract: This article presents a problem of modeling processes of navigators' decision making during simulation research on ships' movement in a restricted area. The acquisition and representation of navigators' knowledge makes it possible to build a model of behaviour which takes into consideration decision making criteria used by the human being. The use of behaviour models in simulation research on ship movement in a restricted area allows to analyze and evaluate the navigational safety in these areas with the human factor taken into account.

1 Introduction

Increasing awareness of societies and economical factors make people draw more attention to problems of navigational safety. The safety of personnel, ships, cargo and environment has to be ensured both at sea and in inland navigation as the vessel traffic increases and so does vessel size, maximum speeds. The concern particularly refers to ships carrying hazardous goods: tankers, gas carriers, chemical tankers. At the same time the human factor becomes of more importance due to the fact that human errors are most often causes of navigational accidents.

The assessment of navigational safety is essential in both analyses and project works (off line) and in ship control and management (on line). These problems, or in more general terms, qualitative and quantitative description of vessel traffic in restricted areas are dealt with by the discipline called marine traffic engineering.

Modelling human decision making processes – those referring to a navigator steering a ship in a restricted area is a detailed research problem of marine traffic engineering. Navigators' behaviour models are used for designing systems of autonomous ship movement control and for simulation tests of ship movement. Such models can also be used for a cur-

rent assessment of a navigational situation and safety analysis in project research as well as navigator training.

One essential component of the models is navigators' knowledge acquired and properly represented. This knowledge refers to. e.g. criteria for navigational situation assessment. Besides, the knowledge can be used in the classical risk analysis, based on probabilistic methods in designing work, ship control and vessel traffic control.

2 Decision making models

The decision process can be divided into stages. Their correct execution is a prerequisite for the decision to be correct, which, consequently, affects the effectiveness of decision maker's actions (Fig. 1).

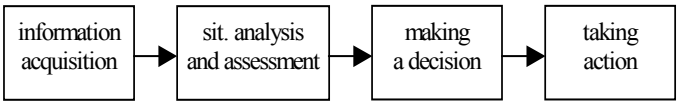

Fig. 1. The stages of the decision making process

The correctness of decisions made by a navigator depends, among others, on the scope and quality of available information, navigator's knowledge, experience and skills and his knowledge of the problem being solved. It also refers to the assessment of a navigational situation and decisions made during sea-going ship movement control. In this case it is important which model of a situation is used, adopted methods of analysis and assessment and the type and scope of decisions considered by the navigator as admissible.

Information describing a navigational situation may be of various character in the decision making process:

- deterministic (the parameters and state vector values of own and target ships are known),
- probabilistic (information describing the problem is expressed by appropriate probability distributions),
- uncertainty (probability distributions are not known),
- fuzziness (uncertainty relates to both an occurrence of an event and its significance).

In the classical approach the deterministic form of the mentioned elements is adopted.

A number of classification criteria can be distinguished for decision making models, such as the character (form) of a model, type of controlled system, number of decision stages,

number of criteria and number of decision makers. In work [5] two main approaches are proposed for decision making modelling:

- descriptive approach; it is not based on the knowledge of a model defining the output (effect) as a function of input (cause), but on knowing what input values are to be selected in order to obtain desired output values;
- prescriptive (normative) approach; this approach is based on the knowledge of a model defining the output (effect) as a function of input (cause), and it uses a relevant conventional optimizing algorithm for gaining an optimal process control.

Both descriptive and prescriptive approaches can be used for decision making modelling in various system optimization and control problems:

- deterministic (transition from one state to another at a preset control input, described by a deterministic relation),
- statistical (transition from one state at a preset control input to next states at a defined probability),
- fuzzy (transition from one crisp or fuzzy state – at a preset control input, defined by a crisp or fuzzy relation).

Deterministic, statistical and fuzzy models are created depending on the type of the system being controlled, decision variables and goals.

There exists a class of problems in which the searched for decision has to account for more than one criterion. This necessitates finding a compromise as goals are often much different. Another difficulty in the modeling decision processes executed by human beings is that the human often fails to maximize, preferring to reach a defined value of the goal function, called the aspiration level.

The decision process can comprise one (e.g. one-stage optimization) or many stages (control). In the case of multi-stage control we can identify problems with various times of their completion: preset in advance, or set in a covert manner, fuzzy or indefinite.

The number of decision makers is also significant. Problems of decision making where there are more than one decision makers are a subject of group decision, human teams and N-person game theories. This diversification results from taking into account decision makers' preferences (identical or different) and access to information (identical or different).

The variety of decision making models is a consequence of diversity of systems, existing constraints, goals and criteria used. It also refers to models of navigators' behaviour in the process sea-going ship movement control.

3 Navigators' behaviour models

The navigator, making a decision, to a greater or lesser degree relies on approximate values, uses approximate models of objects and approximate constraints and goals. Therefore, one should consider all possible combinations of „certainties" and „uncertainties" affecting ship control. In order to simplify thus formulated problem, the following assumptions were made [10]:

- The navigator uses a simplified model of own ship. It is assumed that it is a deterministic model, and refers to other objects as well.
- The navigator, planning manoeuvre execution, assesses a given navigational situation and determines ship movement trajectory: ship's positions and necessary courses at subsequent instants. This refers in particular to difficult and complicated situations. S/he optimizes ship's trajectory looking for a series of control inputs such as courses that will assure performing a manoeuvre as s/he has planned.
- In situations where neither difficult nor complex decisions have to be made the navigator applies simpler solutions. S/he replaces a prescriptive decision making model by a descriptive one, based on solutions found by a deterministic method or on fuzzy inference.
- Depending on a situation, the navigator uses deterministic or fuzzy goals and constraints.
- Deviations from the worked out trajectory at defined discrete instants are corrected by him/her on the basis of a descriptive model.

In this way navigator's behaviour models – decision process models – can be presented as these superimposed models:

- prescriptive (decision making) and descriptive (ship movement control) (Fig. 2),
- descriptive (decision making) and descriptive (ship movement control) (Fig. 3)

Modelling navigators' behaviour calls for the identification of goals and constraints used by them. These include the assurance of navigational safety, incorporation of good sea practice principles, economical aspect (loss of way, loss of time, fuel consumption). The navigator implements the goals by using corresponding criteria while making decisions.

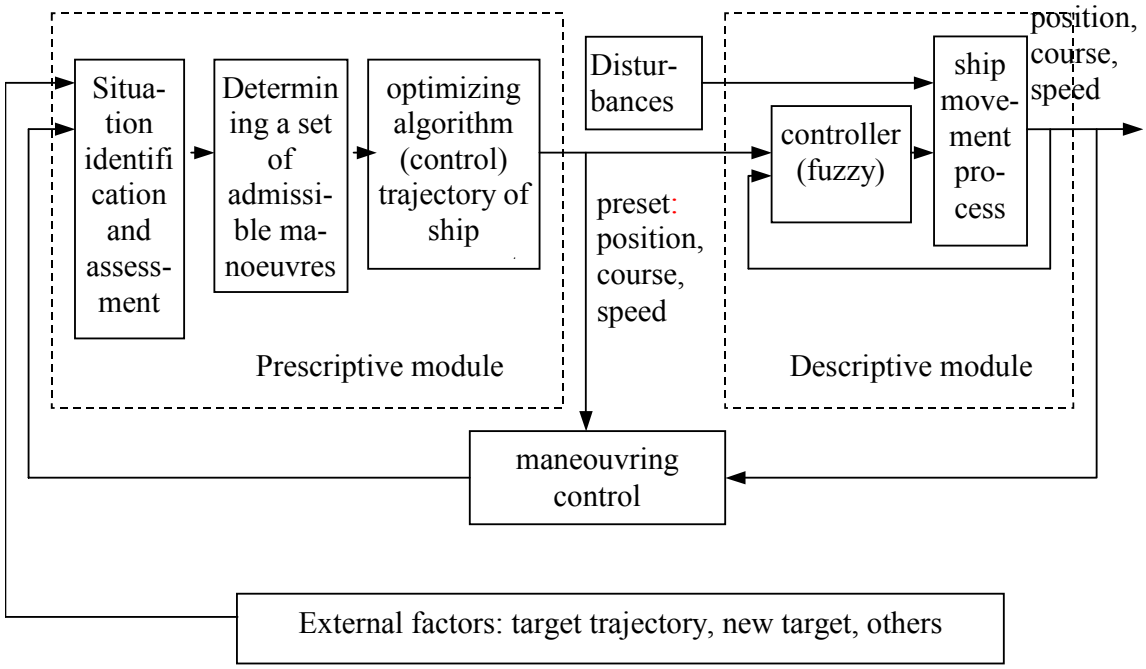

Fig. 2. A prescriptive model of navigator's behaviour

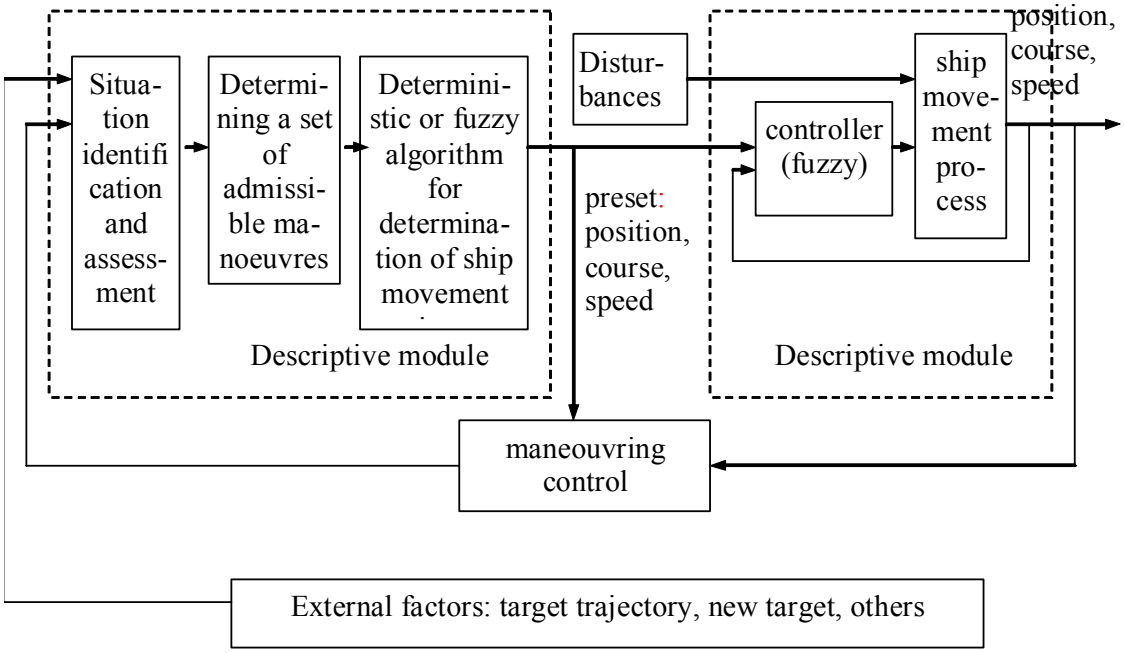

Fig. 3 A descriptive model of navigator's behaviour.

4 Classical criteria of navigational situation assessment

The assurance of navigational safety is strictly connected with continuous analysis and assessment of a navigational situation based on adequate assessment criteria:

- those resulting directly from regulations (general ones (Colreg [1], local and specific), and
- those resulting from navigators' knowledge and experience.

It should be emphasized that even in the regulations that are references to navigators' knowledge and experience.

The use of criteria of navigational situation assessment requires that quantitative or qualitative measures and indicators are introduced (distance, time, impact energy, safety level indicators). These are, among others, distance to other objects, closest point of approach (CPA) and time to the closest point of approach (TCPA), indicators of safety/danger level, ship's domain. If the relevant regulation do not state otherwise, it is the navigator who specifies the criteria.

The criterion known as the closest point of approach (CPA) is commonly employed in the assessment of a navigational situation, and used in automatic radar plotting aids (ARPA). This criterion assumes that the navigator specifies a minimum (safe) distance for the passing of another object – minimum closest point of approach (CPA_L). An additional criterion is the time to the closest point of approach ($TCPA$) – its minimum value $TCPA_L$ is defined by the navigator as well. There are also criteria taking into account the magnitudes CPA_L and $TCPA_L$ at the same time. Examples of such criteria are the risk level indicators or the collision risk coefficients. In this case the navigator also defines its minimum admissible value.

In the process of ship conduct the navigator tries to keep a certain area around the ship free from other navigational objects. The area is referred to as ship's domain [3]. The presence of another vessel in the domain area is interpreted as a hazard to navigational safety. Analytical and statistical methods are mainly used for the determination of ship's domain.

Generally the determination of navigation safety level is connected with the determination of navigation safety indicator. The indicator can be written as the functional P [4]:

$$\mathrm{P} = F(B, R, S, M) \tag{1}$$

Where B – area parameters,
R – vessel parameters,
S – position determination system parameters,
M – hydro-meteorological parameters.

The principal problem is that it is difficult to describe the functional in analytical terms.

5 Criteria of navigational situation assessment based of knowledge representation

Each decision in ship movement control is based on the situation analysis and assessment. That is why more and more attention is drawn to the problems of acquisition, extraction and representation of navigators' knowledge on the subject, so that it can be utilized in decision support systems. These problems are dealt with by knowledge engineering. This discipline uses methods and tools for the acquisition of and structuring of experts' knowledge as well as the matching and selection of proper methods of inference and clarification of problems being solved. This refers to both procedural knowledge – procedure formulated by the experts – and declarative i.e. descriptive knowledge, defined by sets of facts, statements, rules. Declarative knowledge is particularly difficult to acquire and represent, as is typical of elements of uncertainty and fuzziness. These elements result from, among others, inaccurate and imprecise parameters characterizing the analyzed phenomenon and from the fact the expert uses linguistic concepts in the description of parameters (e.g. dangerous / (very) safe distance, etc.).

The work [6] proposes a method of navigational safety level determination based on the representation of expert navigators' knowledge, using artificial neural networks with the fuzzy logic.

These networks, after the learning process, make it possible to assess navigational situations according to the criteria used by navigators. The learning data comprise facts collected within expert research (simulation and questionnaire research): parameters characterizing a navigational situation (such as ship's state vector parameters) and the assessment of navigational safety level of the situations recorded. The network was supposed to implement the development (Fig. 1)

$$\gamma = f(\Delta y, \Delta\varphi, \omega) \tag{2}$$

where Δy – deviation from the fairway center line [m],
$\Delta\phi$ – deviation from the preset course [°],
ω – the turn rate.

Both the *CPA* criterion as well as ship's domain (see Chapter 4) divide navigational situations into safe and dangerous ones. The concept of ship's domain has been generalised and extended to the concept of ship's fuzzy domain [7]: area around the ship which the navigator should maintain free from other vessels and objects; the shape and size of that area depends on the assumed navigational safety level.

The determination of ship's fuzzy domain is based on the representation of navigators' knowledge, making it possible to determine navigational safety level for any navigational situation that may occur. Using the method discussed in [8] and employing an artificial neural network with fuzzy logic we can determine areas of a preset navigational safety level. Fig. 4. presents fuzzy domains of ships of various sizes in an area 200 m wide.

Similarly to the notion of ship's fuzzy domain we can introduce and define the concept of fuzzy closest point of approach. The criterion of fuzzy closest point of approach is inter-

preted as follows: the navigator, setting the value of the closest point of approach CPAL, determines a safe passing distance between ships. The passing at a 'slightly' larger distance will assure a higher level of safety. Besides, a 'slightly lower' value of CPA ($CPA < CPA_L$) is allowed. When two ships pass each other at such a distance, there will be no collision and the situation is acceptable. Thus the tolerance interval $\langle CPA_{Lmin}, \mathrm{CPA}_{Lmax}\rangle$ is assumed, described by the values of the navigational safety level, as is the case for the ship's fuzzy domain.

6 Restrictions in choosing the right track

While steering a ship in a restricted area the navigator has to maintain a safe distance to other objects and at the same time s/he has to account for the regulations in force, specific character of the area and the current traffic situation. There is no choice of track, which results from the shape of the navigable restricted area, from increased vessel traffic and the necessity to execute such manoeuvres as passing, overtaking, crossing, following another ship, passing a berthing or anchoring ship and others.

All this requires maximum caution, and to maintain it several criteria are used:

- navigational safety of own ship,
- safe distance of passing, overtaking, crossing courses of other ships or objects,
- clear (noticeable) admissible course alteration,
- steering (if applicable) along the defined fairway centre line, or recommended trajectory,
- economical: loss of way, loss of time, fuel consumption, etc.

For instance, in the passing manoeuvre (ships on opposite courses) in the fairway safe distance to the other ship has to be maintained (goal) and to the fairway limit (constraint). The same applies to overtaking. When passing a berthed or anchored ship, the main goal is to maintain safe distance such that no damage will be done to the other ship, e.g. breaking of mooring lines or anchor chain, while a safe distance to the area limit has to be kept as well. Another constraint is a noticeable admissible alteration of ship's course.

These criteria can be determined on the basis of expert research. Tools of the fuzzy set theory were used for their identification and representation. Some of them are as follows:

- ship's fuzzy domain D_{SF} – criterion of own and other ship's navigational safety,
- fuzzy sets of trajectory shift relative to the recommended trajectory (fairway centre line) C_{RF}, noticeable admissible course alteration C_{CF} and, if they occur, safe distance from a berthed or anchored ship, respectively C_{MF} and C_{AF} , described by corresponding functions of membership μ_{CRF}, μ_{CMF} and μ_{CAF}.

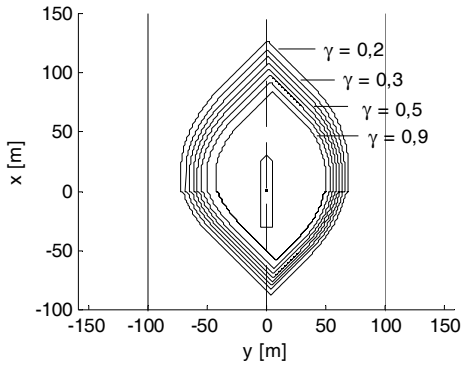

(a)ship 60 m in length, 10,5 m breadth and 3,5 m draft

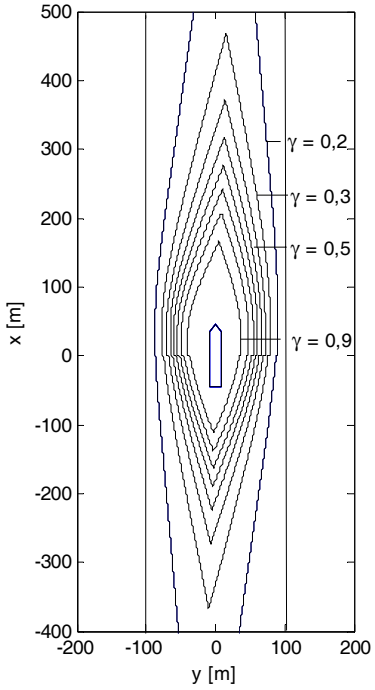

b) ship 95 m in length, 18 m breadth and 5,5 m draft

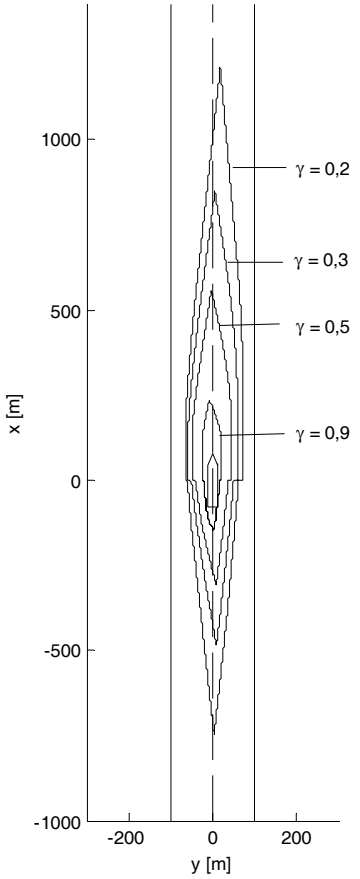

c) ship 156 m in length, 24 m breadth and 9,3 m draft

Fig. 4. Ship's fuzzy domain on the waterway of 200 m wide. Navigational safety level γ: 0 – safe; 1 – dangerous (collision) [12]

These and not other methods and tools of fuzzy set theory have been used because they offer, among others, the following possibilities:

- description of criteria for the choice of way (including the navigational safety criterion) intuitively follows the human pattern, accounting for imprecision (fuzziness) of the criteria – gradual transition from elements belonging to the sets to those not belonging to the sets of such elements,
- aggregation of criteria defined in various spaces (e.g. distance, course),
- description of human decision making process as an optimization one-stage or multi-stage problem with fuzzy goals and constraints.

- Use of classical optimization methods for solving thus formulated optimization problem.

7 Assessment of navigational safety in the fairway

The criterion of ship's fuzzy domain can be used for the current assessment of a navigational situation (on line), as well as for an analysis of traffic processes (off line) in restricted areas, which may comprise various parts of fairways, i.e. straight sections and bends. For instance, the above criterion was used for assessing navigational safety of a ship proceeding in a fairway bend 200 metres wide. Figures 5 and 6 present, respectively, an "ideal" and "dangerous" passages of a ship 95 m in length, 18 m breadth, moving within a fairway bend, with recorded values of the safety level.

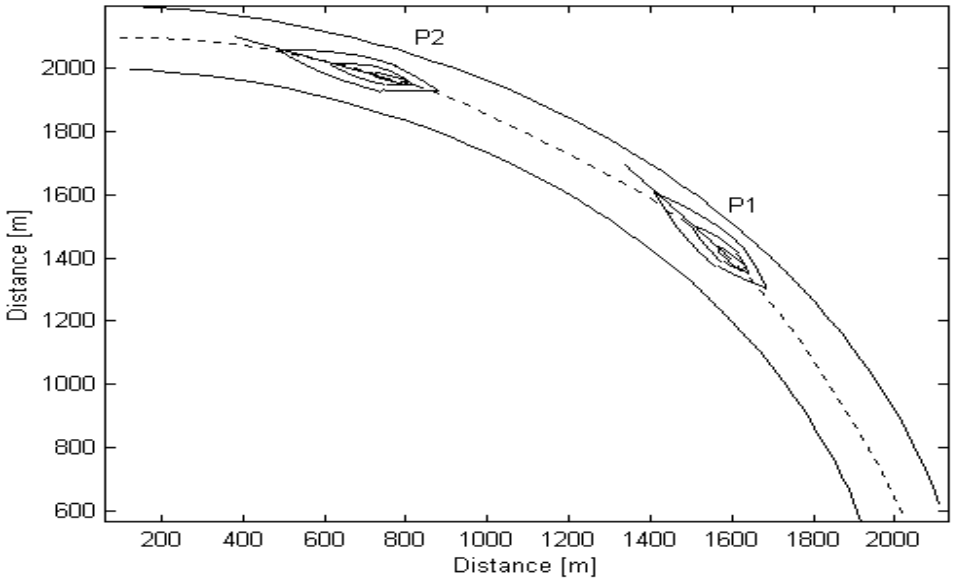

(a) ship's trajectory

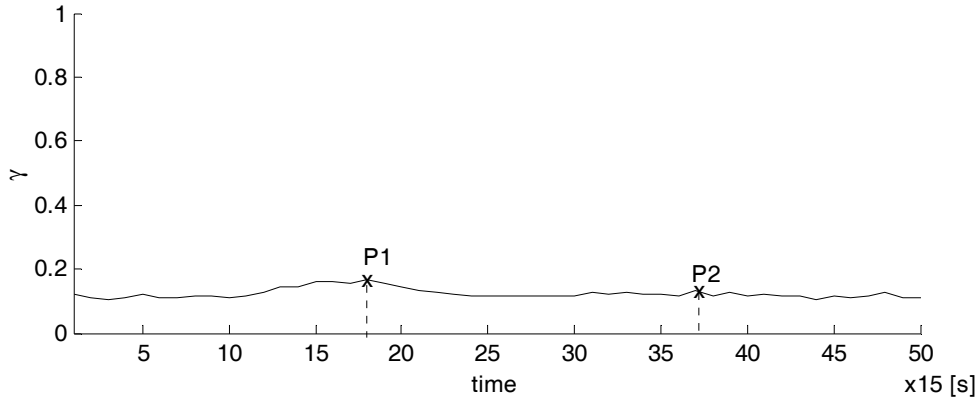

(b) values of the navigational safety level γ

Fig. 5."Ideal"ship's passage on a fairway bend [2]

8 Assessment of navigational safety of the manoeuvre of passing a mooring ship

Ships moving in a restricted area are forced to manoeuvre by passing or overtaking other moving or stationary objects. While assessing navigational safety, the navigator has to take into account the safety of his/her own ship and that of other objects. Figure 7 shows an example of passing a moored ship and the recorded values of navigational safety level: of own ship, (passing ship), mooring ship and overall assessment of navigational situation. This allows to make a more detailed analysis of manoeuvres executed.

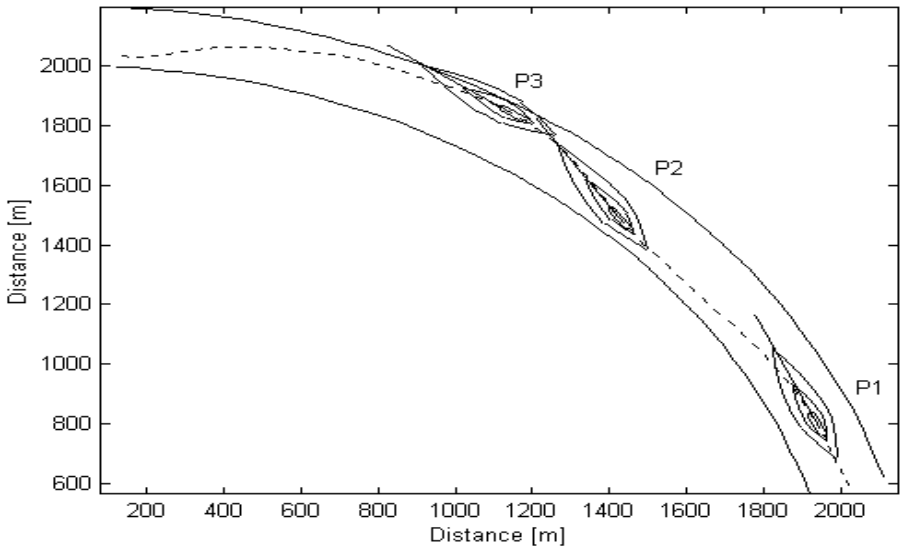

(a) ship's trajectory

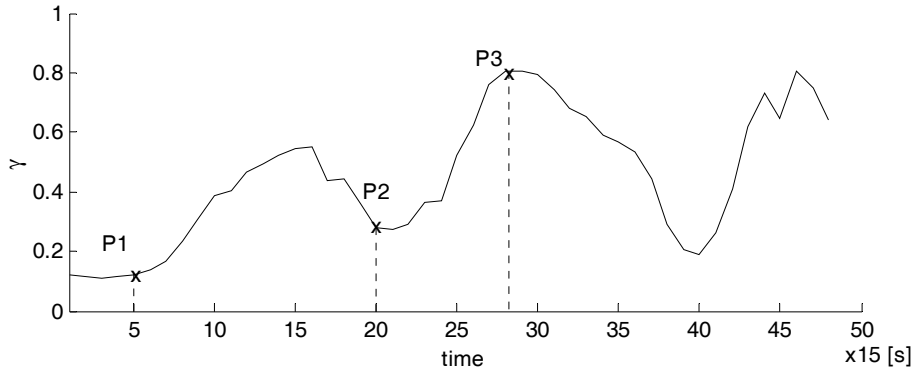

(b) values of the navigational situation assessment γ

Fig. 6. "Dangerous" passage on a fairway bend [2]

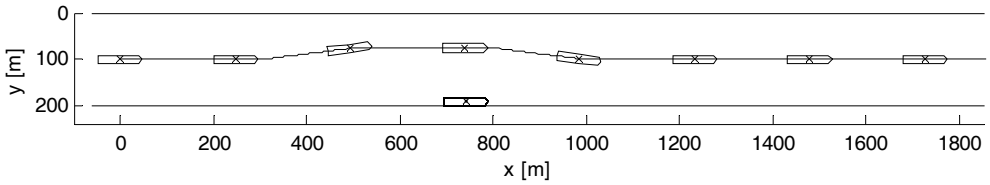

(a) own ship movement trajectory

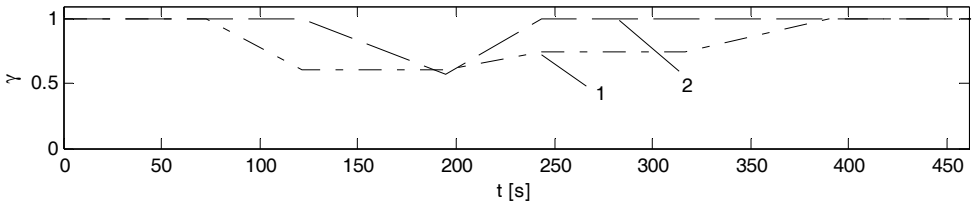

(b) navigational situation assessment: 1- navigational safety level γ of the own ship; 2 - safety level of the mooring ship

Fig. 7 Manoeuvre of passing a mooring ship

9 The probabilistic-fuzzy method for manoeuvring risk assessment

Modelling human behaviour, particularly the acquisition and representation of human knowledge and experience, enables us to extend methods of manoeuvring risk assessment used so far. This will be useful in a current analysis of navigational safety and in designing work. The probabilistic-fuzzy method of manoeuvring assessment is one example of this approach [9]. The method was used in assessing the safety of a ship manoeuvring within a fairway bend being in the stage of designing. The presented approach makes it possible to assess navigational safety taking into account dangerous situations, i.e. situations when a ship comes too close to the fairway border, which may result in safety failure situation. The probability of such a situation can be determined on the basis of the density function in which the random variables are locations of extreme points of the ship in the fairway (separately for the straboard and port sides of fairway limits), as well as on the basis of the defined fuzzy set: dangerous situation – dangerous distance to the port (left) and starboard (right-hand) fairway limit.

The relevant research was carried out in a fairway bend, 150m broad at the bottom, with the radius of 600m [9]. The fairway was divided into sections with limits running perpendicular to its centre line. The ship used for research was a loaded tanker with 40000 DWT capacity, length overall L=196m, beam B=28m and draft T=11m. Figures 8 and 9 illustrate the determined values of a probability of a collision and of dangerous situation occurrence.

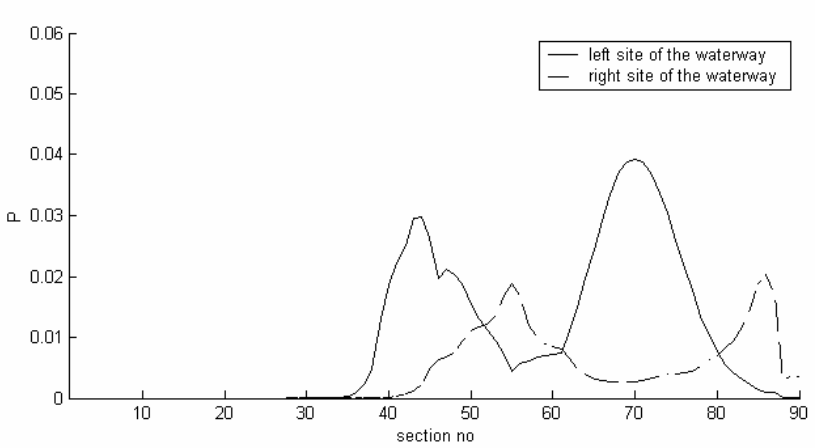

Fig. 8. Probability of an accident on the starboard (right) and port (left) side of the waterway [9].

10 Models of navigators' behaviour in the process of ship control

The models of navigators' behaviour introduced in Chapter 3 were implemented in the problem of the ship's safe trajectory determination. Examples of the trajectories obtained by using an optimization algorithm – multi-stage control in a fuzzy environment – are shown in Figure 10.

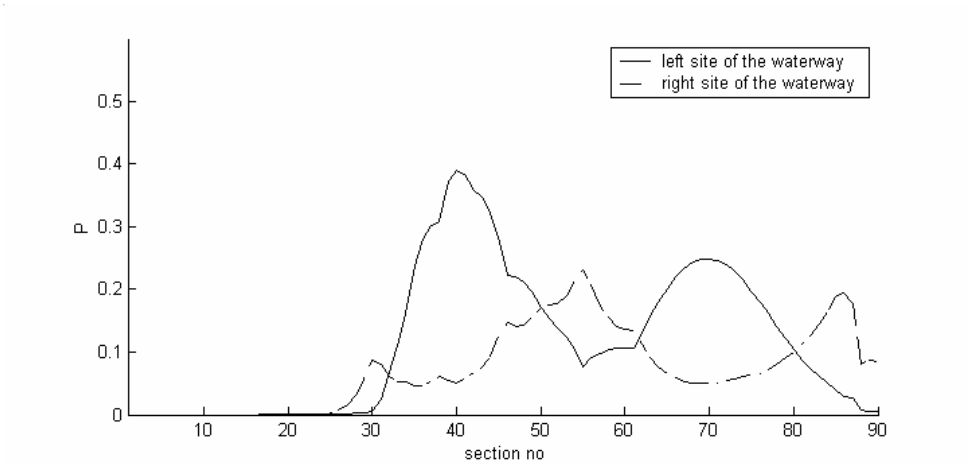

Fig. 9. Probability of dangerous situation occurrence for the waterway starboard and port sides (Zadeh's approach) [9].

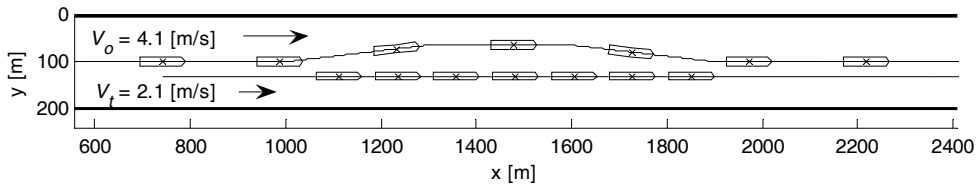

(a) overtaking manoeuvre

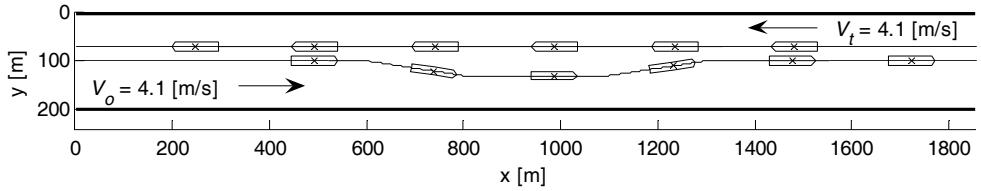

(b) passing manoeuvre

Fig.10. Trajectories of ship movement in a restricted area; positions (x) on 60 [s] time intervals [11]

It is possible to implement the mentioned models in simulation research into ship movement processes in restricted areas. The diversification of criteria of situation assessment and the choice of way will enable modelling movement of ships as autonomous objects, with consideration given to individual behaviour of navigators. In this way the possibility arises for a comprehensive analysis and assessment of navigational safety in restricted areas.

11 Summary

The analysis and assessment of navigational safety in restricted areas is essential in the process of ship movement control in order to prevent accidents as well as in designing new or modernizing existing waterways. Such tasks have to account for the human factor – namely navigator's behaviour. This article presents models of human behaviour which take into account criteria used by the navigator in the process of ship movement control in a restricted area. Examples are shown of the use of these models in navigational situation analysis and assessment.

References

[1] COLREG: Convention on the International Regulations for Preventing Collisions at Sea, International Maritime Organization, 1972

[2] Dziedzic T, Pietrzykowski Z., Uriasz J. Knowledge-based System for Evaluation of Ship's Navigational Safety. In: V. Bertram (Ed.): *Proc. of 1st Conf. COMPIT 2000*. Potsdam, 2000, pp.132-140

[3] Goodwin E.M. 1975, A statistical study of ship domains, *Journal of Navigation* 28 (1975), pp. 328-344

[4] Gucma S., *Marine Traffic Engineering*, Gdansk: Okretownictwo i Zegluga Gdansk, 2001 (in Polish)

[5] Kacprzyk J., *Multi-stage fuzzy control*, Warszawa: WNT, 2001 (in Polish).

[6] Pietrzykowski, Z. Applications of neuro-fuzzy networks for identifications of distress situations in vessel traffic in restricted areas. In: *Proc. of 7th International Scientific and Technical Conference on Sea Traffic Engineering*, Szczecin, 1997, pp. 131-142 (in Polish).

[7] Pietrzykowski Z., Ship fuzzy domain in assessment of navigational safety in restricted areas. In: *Proc. of IIIrd Navigational Symposium*, Gdynia, **I**, 1999, pp. 253-264 (in Polish).

[8] Pietrzykowski Z., The analysis of a ship fuzzy domain in a restricted area. In: R. Katebi (Ed.): *IFAC Conference Computer Applications in Marine Systems CAMS'2001*, Kidlington, Oxford: Elsevier Science Ltd, 2002, pp. 45-50.

[9] Pietrzykowski Z., Gucma L., Application of the probabilistic-fuzzy method for assessment of dangerous situation of a ship manoeuvring in a restricted area, *Annual of Navigation* 4 (2002), Gdynia, pp. 59-70

[10] Pietrzykowski Z., *Modelling of Decision Processes in Sea-Going Ship Movement Control*, Studies No 49, Szczecin: Maritime University of Szczecin, 2004 (in Polish).

[11] Pietrzykowski Z., Modelling of navigators' behaviour in restricted area navigation, *Journal of KONBIN* No 2 (2006), Warszawa, 2006, pp. 27-34

[12] Z. Pietrzykowski, Navigational safety in restricted area – ship fuzzy domain for ships of different size, In: *EXPLO-SHIP 2006*, Scientific Papers of Maritime University of Szczecin No 11(83), Szczecin, 2006, pp. 223-232 (in Polish)

Stochastic structural modelling

Konrad Bergmeister& Simon Hoffmann
BOKU, Department of Civil Engineering + Natural Hazards, Vienna, Austria

Abstract: The Department of Civil Engineering & Natural Hazards has a more than 5 year long experience in stochastic modelling of complex structures. This contribution gives a brief introduction to the models generated during this period. Several applications are demonstrated to show the capabilities of this software system for structural analysis. Their specific characteristics regarding geometry, load cases and modelling is outlined. The sampling used for the single applications is described. Basic results taken from each single analysis are discussed. The contributions extend allow no detailed presentation of all results obtained during the last 5 years, but a substantial list of references shall help for further investigations.

1 Introduction

During the last few decades practical methods for the reliability assessment of structural infrastructure have been developed to assist engineers in probabilistic analysis. These methods help to quantify reliability within the inspection and assessment, as well as immanent uncertainties by sensitivity analysis. Eventually decision making about the structural resistance is eased. The considered structures can still be in the design phase, under construction or already in use. Therefore it is essential to apply the basic principles and methods as a problem related reliability analysis including the posing of possible risks. The objective is to confirm the updating and decision making methods.

1.1 Structural analysis SARA

The procedures used for the applications is implemented in the integrated software system SARA (Safety Analysis and Reliability Analysis), which was developed in the course of a project called “Structure Analysis and Reliability Assessment”. Based on a deterministic nonlinear FEM model finally a Reliability index β is obtained by the calculation of multiple models simulating the distribution of the input parameters. The concept of the reliability assessment with its main steps is demonstrated in figure 1, taken from a more detailed description of the system in [8] and [9].

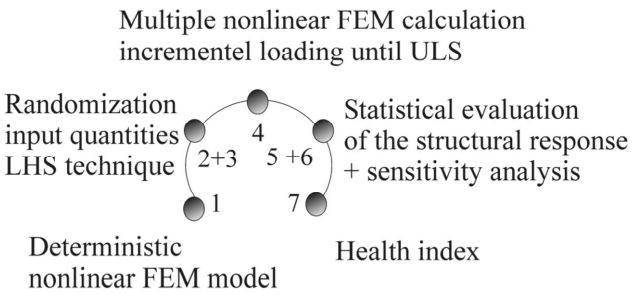

Figure 1: Concept of reliability assessment

2 Application Examples

2.1 Segmental bridge in Vienna

The single span bridge in Vienna over Highway A23 is 25 years old. Due to an ongoing construction project the bridge was demolished in 2002. During the demolition a range of non-destructive tests as well as finally a full-scale destructive load test were performed. The presented reliability assessment was a part of the predictive numerical study [6] for planning and optimizing the test setup.

2.1.1 Geometry

The length of the bridge is 44.60 m, the width 6.40 m and the height 2.10 m (Figure 2).

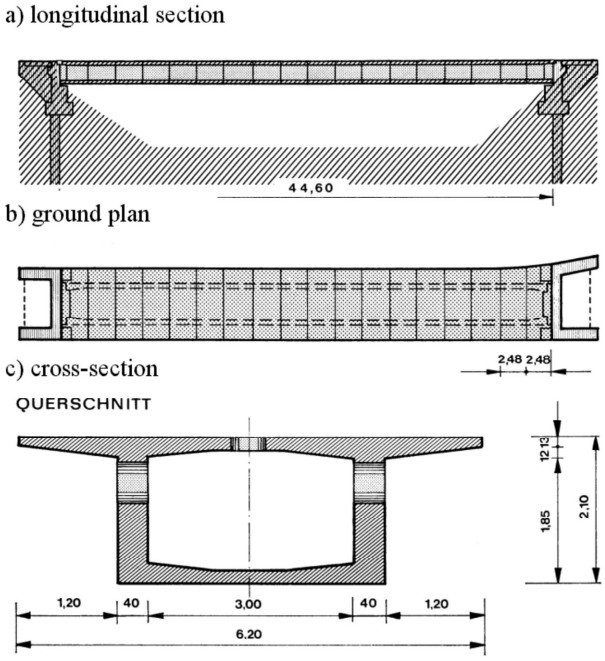

Figure 2: Side elevation of the bridge from the west.

The fully post-tensioned box-girder bridge was made of 18 segments with lengths of 2.485 m each. The segmental joints were filled with epoxy resin. The segments were cast from concrete B500 and are rein-forced with mild steel St 50. The post-tensioning tendons consist of 20 strands St 160/180.

2.1.2 Load cases

The bridge was pre-stressed and then loaded with prescribed displacement in the middle of the span. The ultimate failure load and the descending branch were obtained. The bridge girder failed typically in the middle of the span. First the prestressing tendons yielded, tensile cracks developed, and consequently the concrete in the compression flange of the box girder crushed and split.

2.1.3 Modelling

Mean values of the material properties for concrete B500 were generated using ATENA defaults (based on recommendations by CEB, fib, RILEM etc.). Tensile cracking model in ATENA is based on the smeared crack approach, which replaces the discrete cracks, occurring in real concrete structures, by strain localization in a continuous displacement field. Concrete fracture is covered by nonlinear fracture mechanics based on fracture energy with an exponential softening law derived experimentally by Hordijk [2] demonstrated in Figure 3 and equation 1. The objectivity of the finite element solution is assured by crack band approach - the descending branch of the stress-strain relationship is adjusted according to the finite element size and mesh orientation.

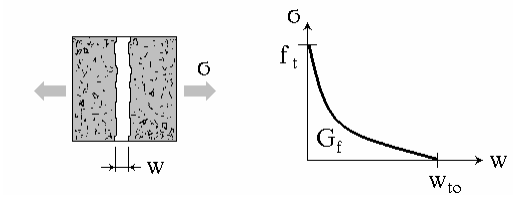

Figure 3: Stress - crack-opening law according to Hordijk [2].

$$\frac{\sigma}{f_t} = \left(1 + c_1 \frac{w}{w_{t0}}\right)^3 \exp\left(-c_2 \frac{w}{w_{t0}}\right) - \frac{w}{w_{t0}}\left(1 + c_1^3\right)\exp\left(-c_2\right) \tag{1}$$

with $c_1 = 3$, $c_2 = 6.93$ and $w_{t0} = 5.14\frac{G_f}{f_t}$

A more detailed contribution to the material modelling within the software ATENA can be found in the contribution “Uncertainties of material properties in nonlinear computer simulation” by R. Pukl, included in these proceedings. The used mean values, coefficients of variation and suitable pdfs of the concrete and steel properties are presented in Table 1. Statistical correlation among random variables was considered according to the prescribed correlation matrix as shown in the upper triangle of Table 2.

Tab. 1: Basic variables used for the simulation.

Variable	Material	Properties	Units	Distribution	Mean	CoV
E_c	Concrete	Modulus of elasticity	Gpa	Lognormal	36.95	0.15
ν		Poisson' ratio	-	Lognormal	0.2	0.05
f_t		Tensile strength	MPa	Weibull	3.275	0.18
f_c		Compressive strength	MPa	Lognormal	42.5	0.10
G_f		Fracture energy	N/m	Weibull	81.43	0.20
ε_c		uniaxial compressive strain at compressive strength	-	Lognormal	0.0023	0.15
c_{Red}		reduction of compressive strength due to damage	-	Rectangular	0.8	0.06
w_d		critical compressive displacement	m	Lognormal	0.0005	0.10
ρ		specific material weight	MN/m³	Normal	0.023	0.1
E_s	Pre-stressed steel	Modulus of elasticity	GPa	Lognormal	200	0.03
f_{yp}		Yield strength	MPa	Lognormal	630	0.03
F_p		Prestressing force	MN	Normal	21.85	0.04
A_s		Area of strands	m²	Normal	0.0237	0.001

Tab. 2: Correlation matrix for concrete properties.

Parameter	E_c	f_t	f_c	G_f	ε_c
E_c	1	0.7	0.9	0.5	0.9
f_t	0.7	1	0.8	0.9	0.6
f_c	0.9	0.8	1	0.6	0.6
G_f	0.5	0.9	0.6	1	0.5
ε_c	0.9	0.6	0.6	0.5	1

2.1.4 Analysis

For the estimation of the basic statistical parameters of the ultimate load different numbers of samples have been used by total numbers of 8 and 32 samples [6]. In both cases comparable results were obtained. Furthermore the results have been used to estimate a reliability index for the structure considering different levels of the load (mean values) and two alternatives of variability (coefficient of variation 0.1 and 0.2). The analysis verified the feasibility of the used complex stochastic nonlinear program system integrating nonlinear fracture finite element analysis wit probabilistic tools.

2.2 Colle Isarco Viaduct

The goal of the stochastic fracture analysis for the Colle Isarco Viaduct was to estimate the reliability of the structure and to show the efficiency of the procedures used by SARA ([8] and [9]). A detailed statistical failure simulation and reliability assessment of the existing bridge structure was performed. The Colle Isarco Viaduct is a cantilever beam bridge in Italy with a total length of 1,000 m. Built in 1969, it is a fully post-tensioned box-girder

bridge and is part of the Brenner Highway in Italy. Several objects of this type are found in the two separated lanes which form this bottleneck crossing the Alps.

2.2.1 Geometry

The northern cast-in-place balanced cantilever beams are the most sensitive elements of bridge systems. Therefore, these elements, with varying box girder depths, have been chosen for the analyses. The total length of the beams is 167.5 m. They are subdivided by the mid-span with a length of 91 m and the cantilever beams with a length of 59 m and 17.5 m, see Figure 4. The lane slab has a width of 10.60 m and the lower girder slab a width of 6.00 m. Both of them have a thickness of about 0.20 m. The height of the box girder varies from 10.80 m over the middle support to 2.85 m at the end of the cantilever beams. A summary of the geometric data used for the analysis is given in Table 3.

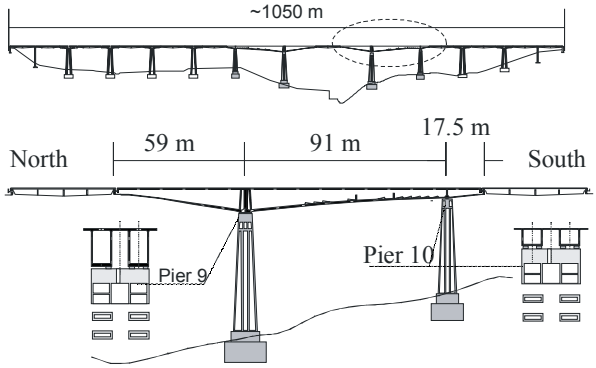

Figure 4: Side elevation of the bridge from the west.

Tab. 3: Deterministic geometric data used for the analysis.

Component	Location	Magnitude (m)
Cantilever north	North of pier 9	59.0
Middle-span	Pier 9 to pier 10	91.0
Cantilever south	South of pier 10	17.5
Width of lane slab	Entire slab	10.6
Box section width	Entire box	6.0
Box section height	Pier 10	4.5
Box section height	Pier 9	10.8
Box section height	Both ends	2.85
Total length	-	167.5

2.2.2 Load cases

A structure is exposed to numerous actions. The groups of load cases examined for this structure were dead loads, pre-stressing loads, traffic loads, and the boundary conditions. In addition to the dead load of the box girder, the dead loads of the neighbouring sus-

pended spans were taken into account (pro rata). The traffic loads acting on the neighbouring suspended span were treated in the same way as the dead loads. The traffic loads were modelled as regularly distributed loads with a magnitude of 70kN/m. These loads acting downwards on the pavement of the box girder were incrementally increased until failure. To find the smallest load capacity, this procedure was performed for differently located line loads along the longitudinal axis of the bridge. The uniform load along the entire girder was identified as relevant load case for the smallest load capacity. For the probabilistic assessment coefficients of variation of 15%, 30% and 45% for the traffic load were analyzed. The load case pre-stressing is given by 211 bar cable elements each with a diameter of 32 mm of type 850/970. The configuration of the bearing ensured a statically determined support of the girder.

2.2.3 Modelling

The finite element model was built in ATENA by using the previously mentioned geometric data. A detailed description of the non linear material models and discretisation of the structure can be found in [8]. The uncertainties of the materials caused by natural influences were included using for the specification their complete distribution function. The used mean values, coefficients of variation and suitable pdfs of the concrete and steel properties are presented in Table 4. The reinforcement was modelled multilinearly with a yield strength f_{ys} = 500 MPa to capture the break down by exceeding the yield strength. For the pre-stressed steel a similar model was used with a yield strength f_{yp} = 630 MPa which equals 75% of the nominal yield strength to allow for wedge slip, shrinkage and creep. The coefficients of correlation between the different concrete material properties, which have been considered during sampling by simulated annealing, can be found in Table 5.

Tab. 4: Basic variables used for the simulation.

Variable*	Material	Properties	Units	Distribution	Mean	CoV
E_c	Concrete	Modulus of elasticity	GPa	Lognormal	37	0.15
f_t		Tensile strength	MPa	Weibull	3.26	0.18
f_c		Compressive strength	MPa	Lognormal	42.5	0.10
G_f		Fracture energy	N/m	Weibull	120	0.20
f_{ys}	Reinforcement	Yield strength	MPa	Lognormal	500	0.05
f_{yp}	Pre-stressed Steel	Yield strength	MPa	Lognormal	630	0.03
r_V	Reinforcement	Ratio vertical A_s/A_c	-	Normal	0.003	0.10
r_M	Reinforcement	Ratio horizontal A_s/A_c	-	Normal	0.003	0.10

Tab. 5: Basic variables used for the simulation.

Parameter	E_c	f_t	f_c	G_f
E_c	1	0.7	0.9	0.5
f_t	0.7	1	0.8	0.9
f_c	0.9	0.8	1	0.6
G_f	0.5	0.9	0.6	1

2.2.4 Analysis

Based on probability simulations of the structure with a total number of 30 samples detailed analysis regarding the reliability index of the structure has been performed [8]. Monitoring data taken from a permanent measurement system [7] was considered for this analysis. Present and future reliability indices for the ultimate and service limit state have been estimated based on different load levels and scenarios for the structure's degradation. A sensitivity analysis for the single basic variables identified already major parameters for the structural response. Based on this analysis a specific strengthening concept for the bridge was developed. Recent works [8] have a closer look on the structure's behaviour on degradation and discussed different degradation functions characterisation of the time dependent reliability performance of the structure like the one introduced by Mori [3], (2).

$$g(t) = 1 - a \cdot t^b \tag{2}$$

Within these studies different damage scenarios as global or local degradation of the pre-stressed steel are discussed. Furthermore different failure scenarios are identified by a more detailed sensitivity analysis of the basic variables.

2.3 Footbridge

The pre-stressing system used for the Colle Isarco Viaduct with massive bars is generally not applied any more for modern pre-stressed bridges. For many years already tendons made of single wires typically app. 5 mm in diameter are applied. These wires are designed for much higher stresses and degree of utilization. Furthermore these tendons allow higher curvature and are much more likely to show single wire ruptures caused by degradation. All these differences to the analysed structure of the Colle Isarco Viaduct encouraged the additional analysis [8] of a structure more typical for the majority of pre-stressed bridge structures built since the 1970's. Based on [11] a theoretical sample of a pre-stressed bridge, not realized as an existing structure, was chosen.

2.3.1 Geometry

The 3 span continuous tee-beam with a total length of 65 m consists of a middle span of 26 m and 2 side spans of 19.5 m. The width for the bridge deck was chosen to be 2.8 m with a thickness of 0.18 m. The detailed dimensions of the tee-beams 0.86 m high cross section can be taken from Figure 5. The detailed characteristic of the tendons run described by (3) is shown in Figure 6. The geometric data used for the analysis is summarized in Table 6.

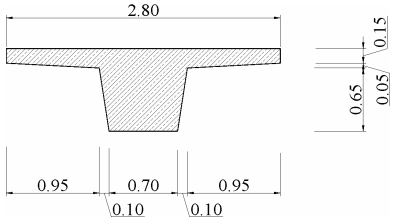

Figure 5: Cross section of tee-beam.

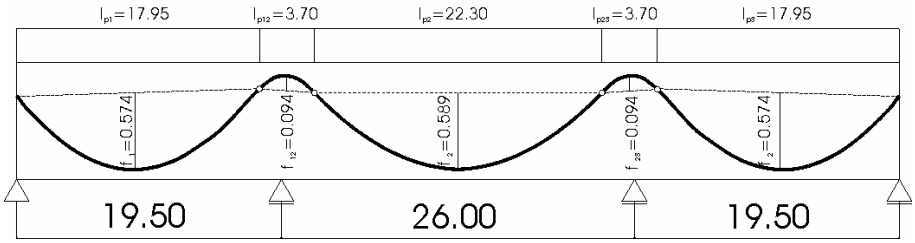

Figure 6: Characteristic of tendons run (10x enlarged in height).

$$z(x) = 4f\left(\xi - \xi^2\right) \text{ with } \xi = \frac{x}{l_p} \tag{3}$$

Tab. 6: Deterministic geometric data used for the analysis.

Component	Magnitude (m)
Middle-span	26.0
Side-spans	19.5
Width of deck	2.8
Thickness of deck	0.18
Cross section height	0.86
Web height	0.65
Total length	65.0

2.3.2 Load cases

The groups of load cases examined for this structure were dead loads, pre-stressing loads, traffic loads, and the boundary conditions. In addition to the dead load of the tee-beam itself the dead loads of the surfacing and rails were taken into account. The traffic loads were modelled as regularly distributed loads with a magnitude of 11.76 kN/m. These loads acting downwards on the pavement of the tee-beam were incrementally increased until failure. The uniform load along the entire 3 spans was identified as relevant load case for the smallest load capacity. The load case pre-stressing is given by 4 tendons consisting of 7 tension wires with a diameter of app. 5 mm each of type 1570/1770. The configuration of the bearing ensured an almost statically determined support of the entire structure.

2.3.3 Modelling

The finite element model was built in ATENA 2D using the previously mentioned geometric data. The cross section of the tee-beam acc. figure 7 was idealised using 3 rectangles with constant thickness. For the discretisation of the structure 2D-Quadrileterals CCIsoQQuad Elements have been selected. The element size of the finite element mesh was chosen to be 0.20 m and 0.10 m for the deck respectively, which led to a total number of 3,155 elements and 12,107 nodes. The elements could be grouped into 7 macro elements, considering material and geometrical qualities. Similar to the assessment for the Colle Isarco Viaduct the nonlinear concrete behaviour was specified using the SBETA material model [1]. Horizontal und vertical smeared reinforcement, modelled using a multilinear stress-

strain law with yield strength of f_{ys} = 500 MPa, was used in the web. The bending reinforcement in the web was realized as discrete reinforcement bars with yield strength of f_{ys} = 500 MPa. The tendons were modelled as polyline acc. to figure 8. For the pre-stressed steel a multilinear law with yield strength f_{yp} = 1170 MPa was used too, again allowing for wedge slip, shrinkage and creep. The materials uncertainties caused by natural influences were included using their complete distribution function for the specification. The used mean values, coefficients of variation and suitable pdfs of the concrete and steel properties are presented in Table 7. The coefficients of correlation of the concrete material properties, which have been considered during sampling by simulated annealing, are the same as the ones choosen for the Colle Isarco according Table 5.

Tab. 7: Basic variables used for the simulation.

Variable*	Material	Properties	Units	Distribution	Mean	CoV
E_c	Concrete	Modulus of elasticity	GPa	Lognormal	35.57	0.15
f_t		Tensile strength	MPa	Weibull	3.04	0.18
f_c		Compressive strength	MPa	Lognormal	38.3	0.10
G_f		Fracture energy	N/m	Weibull	120	0.20
f_{ys}	Reinforcement	Yield strength	MPa	Lognormal	500	0.05
f_{yp}	Pre-stressed Steel	Yield strength	MPa	Lognormal	1170	0.03

2.3.4 Analysis

A study based on 45 samples at a time demonstrated several differences to the results for the Colle Isarco [9]. The free cantilever construction of the Colle Isarco created a significant spare of performance for the final state of the bridge, which is missing for the analysed footway bridge. The different type of pre-stressing allowed to study in addition the rupture of single wires in the tendons including the local drop out of the pre-stress, rebuild by the bond to the concrete. The importance of changes of failure modes for different grades of degradation to the reliability index of the structure is demonstrated.

2.4 Gantry sign

Gantry signs are simple steel structures with wind as significant dominant load case. Their high level of standardisation makes them an ideal object for a detailed and sophisticated optimisation process based on probabilistic methods. In contradiction to bridge structures shown before, wind as the main load component orthogonal to the main axes of the structure makes the use of a 3dimensional model inescapable.

2.4.1 Geometry

For the analysis a most typical geometry was chosen. Shafts and bar are build of 8 mm plates bended to half shells and welded together to almost rectangular profiles. The main dimensions including the size of the sign exposed to the wind load can be found in Figure 7.

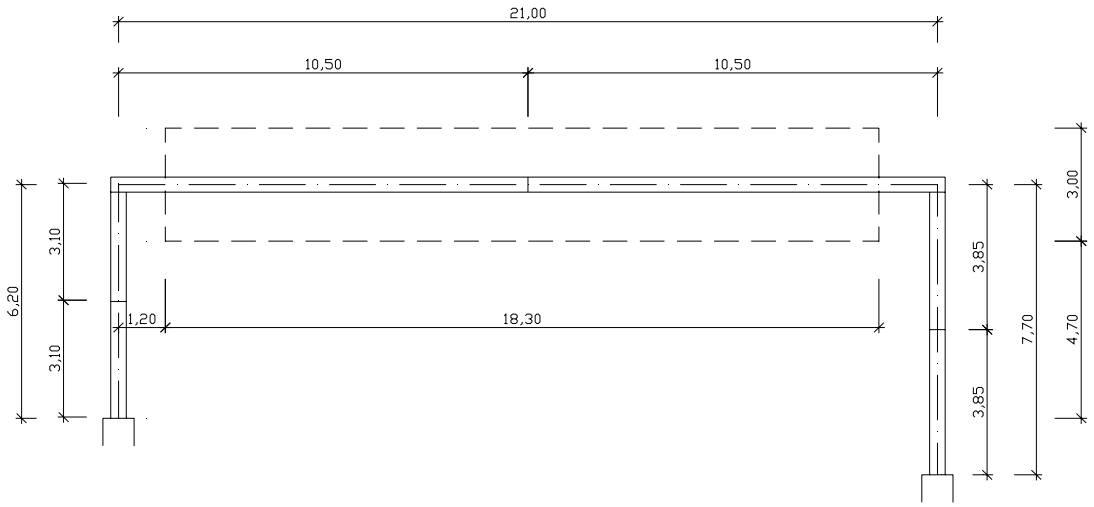

Figure 7: Side elevation of the analysed gantry sign.

2.4.2 Load cases

As only body force and wind load had to be considered for the analysis a specific non deterministic description could have been extended to the load side. Primal variances of the loading to the structure are caused by different wind speeds. Therefore its scattering have been directly included while generating the samples for the probabilistic analysis. In this case a mean value of 32.88 m/s and standard derivation of 5.31 m/s describing a Rayleight pdf (4) was chosen, corresponding to a mean wind load of 1.275 kN/m² on the sign.

$$f(v) = \frac{\pi}{2} \cdot \frac{v}{\bar{v}^2} e^{-\frac{\pi}{4}\left(\frac{v}{\bar{v}^2}\right)^2} \tag{4}$$

2.4.3 Modelling

The finite element model was built in ATENA 3D using the previously mentioned geometric data. All bended plates of the shafts and bar were modelled by quadratic Ahmad shell elements with a minimum of 9 integrational points and a number of 4 layers of similar height in its thickness were chosen. Only the head plates had to be modelled as linear brick elements and the connection of shafts and bar with linear tetra elements. A simple linear elastic material model could have been chosen because for the service limit state, as a maximum deflection, no non linearity had to be considered and the ultimate limit state was defined as the yielding of the steel plates of the shafts and the bar. This allowed estimating the reliability index for the service limit state only by a variation of the young's modulus of all elements and for the ultimate limit state by a comparison of the computed maximum stress to the yield stress of the used material. Detailed studies on steel probes of plates produced in Austria were used for the non deterministic description of the yield stress [10]. By the use of the multipurpose probability-based software for statistical sensitivity and reliability analysis of engineering problems FREET ([4] and [5]) the best description of the yield stress distribution of all 444 probes was identified as Gumble max. pdf with a mean value of 286.27 N/mm² and standard derivation of 17.88 N/mm² as shown in Figure 8.

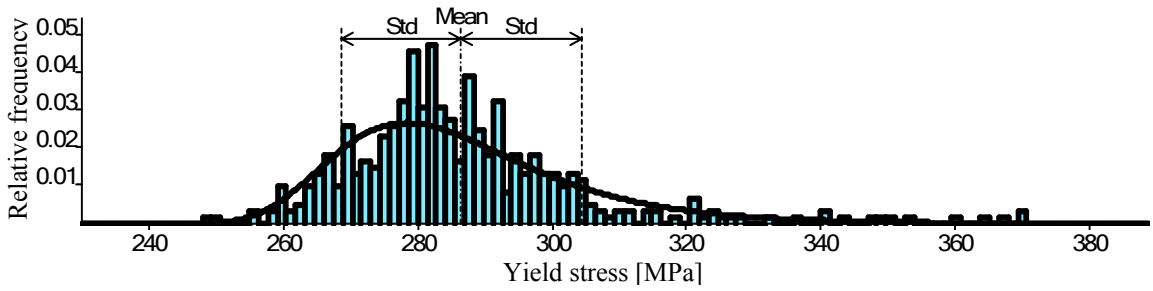

Figure 8: Yield stress distribution for a material S235JRG2 with a plate thickness of 8 mm.

2.4.4 Analysis

Based on 30 samples at a time an analysis for the service limit state and ultimate limit state was conducted within a diploma thesis. It could have been proved, that the actual design of the structure shows sufficient reliability for the service limit state and exceeds by far the demands for the ultimate limit state. Studies using differing plate thicknesses, dimensions and connections of the shafts and the bar showed possibilities for an optimized design of the structure and have to be discussed regarding their technical feasibility.

3 Conclusion and Outlook

The paper gives a wide overview of practical applications of the state of the art stochastic modelling tool SARA. The first three applications are reliability assessments of prestressed concrete bridge structures. The nonlinearities of their structural behaviour produce in most cases additional potential of the structure for its ultimate limit state and therefore lower failure probabilities than those calculated by neglecting these effects. Though for the service limit state these changes in stiffness might cause more deflection and consequently a lower reliability for its service limit state. Thus it appears that nonlinearities of the structures behaviour have to be considered for a reliability assessment of the entire structures in most cases. The non linear FEM software ATENA implemented in SARA allows to consider these effects. Especially the studies regarding the Colle Isarco and the Footbridge showed the necessity to include as well specific damage scenarios and types of degradation to gain a realistic description of the structures reliability. The implementation of monitoring data and sophisticate degradation functions into the reliability assessment is still a wide scope of research. Future progress in this field will help us to have not only current assessment of structures reliability, but a forecast of its probable development. Therefore SARA can build a powerful tool for maintenance planning of structures of different kinds, not only bridges. Supported by identification methods, which use for several approaches already some of the resources given by ATENA and FREET, the assistance in cost planning will not be limited to the maintenance. The last application showed the potential of stochastic modelling for the optimization of structural design. The extension of the system by supporting the modelling of 3D structures opens a wide range too of complete structures and details for a design based on more specific and sophisticated stochastic proof of its reliability as it is given by level II and III methods in Eurocode 0.

4 References

[1] Červenka, V., Libor Jendele, L. and Červenka, J., *ATENA Program Documentation, Part I, Theorie*, Distributed by Cervenka Consulting, 2005

[2] Hordijk, D.A., *Local Approach to Fatigue of Concrete*. Ph.D. Thesis, Delft University of Technology, The Nether-lands 1991

[3] Mori, Y. and Kato, T., *Practical method of reliability-based condition assessment of existing structures*. In *Applications of Statistics and Probability in Civil Engineering*, edited by Der Kiureghian, A., Madanat, S. and Pestana, JM., (Millpress: Rotterdam), pp. 613-620, 2003

[4] Novák, D., Teplý, B. and Keršner, Z., *The role of Latin Hypercube Sampling method in reliability engineering*, Proc. of ICOSSAR-97; Kyoto, Japan, 1998, pp. 403-409

[5] Novák, D., Rusina, R., and Vořechovský, M. (2003). *Small-sample statistical analysis - software FREET*. Proc., 9th International Conference on Applications of Statistics and Probability in Civil Engineering, (ICASP9), Rotterdam Millpress, San Francisco, USA, pp. 91-96, 2003

[6] Pukl, R., Novák, D. and Eichinger, E.M., Stochastic Nonlinear Fracture Analysis. In: *1st International Conference on Bridge Maintenance, Safety and Management (IABMAS'02)*, Barcelona, Spain, 2002

[7] Santa, U., *"Bauwerkinspektionen und -überwachung."* (in German) Ph.D Thesis at the Department of Structural Engineering + Natural Hazards, University of Natural Resources and Applied Life Sciences, Vienna, Austria, 2004

[8] Strauss, A., Bergmeister, K., Hoffmann, S., Pukl, R. and Novak, D., *Advanced life-cycle analysis of existing concrete bridges*, ASCE Journal of Materials in Civil Engineering (under Review), 2006

[9] Strauss, A., Hoffmann, S., Wendner, R. and Bergmeister, K., *Structural assessment and reliability analysis for existing engineering structures, applications on real structures*, Structure and Infrastructure Engineering (under Review), 2006

[10] Strauss, A., Kala, Z., Bergmeister, K., Novak, D., Hoffmann, S., Melcher, J., Fakus, M., Rozlivka, L., *„Materialcharakteristika von Stählen"* (in German), Stahlbau, 2006

[11] Thomsing Martin, *Spannbeton, Grundlagen – Berechnungsverfahren – Beispiele* (in German), Leipzig, 1998

[12] Wiedenegger, G., *„Probabilistische Betrachtung von Dreidimensionalen Strukturen aus Stahl"* (in German) Diploma Thesis at the Department of Structural Engineering + Natural Hazards, University of Natural Resources and Applied Life Sciences, Vienna, Austria, 2006

Analysis and modelling of autocorrelation in concrete strength series

Luc Taerwe
Ghent University, Department of Structural Engineering,
Magnel Laboratory for Concrete Research

Abstract : Consecutive concrete strength values are often considered to be independent. However, analysis of extensive concrete strength records reveals that generally a significant autocorrelation is present, which can be explained on the basis of the concrete production process. The following aspects will be addressed in the paper :

- analysis of the autocorrelation structure in concrete strength records (total number of observations varying between 500 and 1800)
- influence of autocorrelation on the common sample statistics (mean, standard deviation, ...)
- physical background of the autocorrelation structure
- modelling of the autocorrelation structure

1 Introduction

Concrete strength is a random variable which is usually modelled by means of a normal or lognormal distribution function. Generally it is assumed that consecutive strength values are independent. However, the detailed investigation of strength records that is presented below reveals that significant autocorrelation exists between consecutive values. Information concerning the correlation structure which is present in concrete strength records is only scarcely available in the literature. The time-dependent variation of consecutive strength values was mentioned by SOROKA [1] who investigated the evolution of the standard deviation as a function of the number of specimens that gradually became available as the length of the production period became longer. This variable increased with time and approached a constant value. The phenomenon was explained by RACKWITZ on the basis of an autoregressive model of order 1 [2]. Some empirical serial correlation functions were reported by DEGERMAN [3] who made use of strength values from the Swedish concrete industry. A thorough analysis of the problem based on the analysis of empirical concrete strength records can be found in [4, 5, 6].

2 General characteristics of the analyzed series

A general survey of the five concrete strength series that will be analyzed in the following is given in Tab. 1. The compressive strength of the specimens is determined at 28 days and expressed in MPa. The series are subdivided into subseries each covering a maximum of 200 results. This subdivision was found useful because this number of observations is sufficiently large to characterize the concrete production process during a certain period, while on the other hand, the corresponding period is not too long with respect to the inclusion of possible long-term changes in the basic variables influencing concrete strength.

The complete series are designated as A, B, C, D and E whereas the subseries notation contains an additional figure. The time period between the days that the first and the last specimens were tested, is mentioned in the fourth column of Tab. 1. For series A, B and C the number of specimens per casting day is variable and for series D and E, the daily sample rate equals 4 or 2. The first three series were obtained at building sites in Belgium whereas the two other series came from precasting plants all having their own concrete mixing equipment.

Tab. 1 : General survey of the concrete strength series

Series	n (*)	Division in subseries	Observation period (days)	Type of specimen	Mean daily sample rate
A	1786	A1...A9	1158	cubes (200 mm)	3.26
B	945	B1...B5	1044	cylinders	2.59
C	534	C1...C3	1233	cylinders	2.32
D	1468	D1...D8	303 (D1...D4)	cubes (158 mm)	4
			422 (D5...D8)		4
E	1158	E1...E6	267 (E1...E3)	cubes (158 mm)	4
			526 (E4...E6)		2

(*) Total number of test results

In Tab. 2 and 3, the mean $\bar{x}_n$, the standard deviation s_n and the coefficient of variation $\delta = s_n / \bar{x}_n$ are given for the complete series and the subseries respectively. The consecutive values of subseries A4 and B4 are shown in Figs. 1 and 2 in chronological order.

Tab. 2 : General characteristics of the concrete strength series

Series	N	$\bar{x}_n$ (MPa)	s_n (MPa)	δ (%)
A	1786	46.5	6.56	14.1
B	945	36.8	5.30	14.4
C	534	42.1	6.62	15.7
D	1468	59.9	3.68	6.1
E	1158	72.3	5.94	8.2

Tab. 3 : General characteristics of the subseries

Subseries	n	$\bar{x}_n$ (MPa)	s_n (MPa)	δ (%)
A1	200	45.8	5.47	11.9
A2	199	48.8	6.35	13.0
A3	200	50.2	6.78	13.5
A4	200	48.3	5.73	11.9
A5	200	44.5	5.74	12.9
A6	200	44.8	5.89	13.1
A7	200	46.3	6.33	13.7
A8	200	43.2	6.08	14.1
A9	187	46.8	7.13	15.2
B1	200	39.0	5.40	13.9
B2	200	34.9	4.83	13.8
B3	200	36.5	5.33	14.6
B4	200	37.0	4.69	12.7
B5	145	36.4	5.52	15.2
C1	200	46.1	6.67	14.5
C2	200	40.9	5.17	13.6
C3	134	37.9	5.01	13.2
D1	200	59.8	3.64	6.1
D2	196	59.6	3.17	5.3
D3	200	61.7	3.52	5.7
D4	200	59.0	4.25	7.2
D5	200	59.3	3.96	6.7
D6	200	59.8	3.44	5.8
D7	200	60.5	3.05	5.0
D8	72	58.1	2.95	5.1
E1	200	68.0	4.06	6.0
E2	199	69.0	4.05	5.9
E3	200	69.3	4.91	7.1
E4	200	76.7	4.61	6.0
E5	200	75.6	4.95	6.5
E6	158	75.7	5.53	7.3

3 Serial correlation

For series which are not random there will be dependencies of one kind or another between successive terms. One very useful measure of this effect is the correlation coefficient between pairs of strength values, where the components of each pair are k units apart in the sequential sampling process. Given n values x_1, ..., x_n the so-called serial correlation of lag k is defined [5] by

$$r_k = \frac{\frac{1}{(n-k)} \sum_{i=1}^{n-k} (x_i - \bar{x}_n)(x_{i+k} - \bar{x}_n)}{\frac{1}{n} \sum_{i=1}^{n} (x_i - \bar{x}_n)^2} \qquad (1)$$

where - n, the total number of observations
- $\bar{x}_n$, the mean of the series

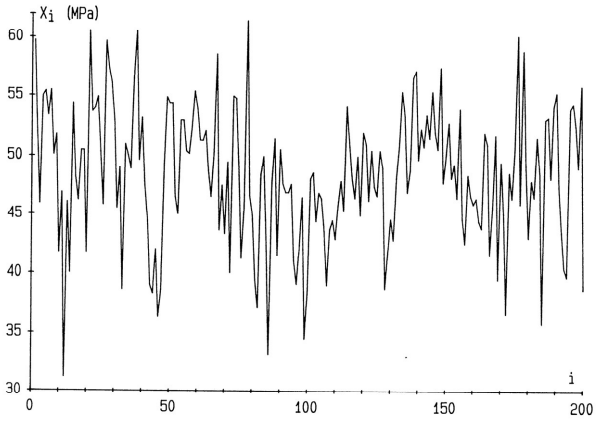

Fig. 1: Representation of subseries A4

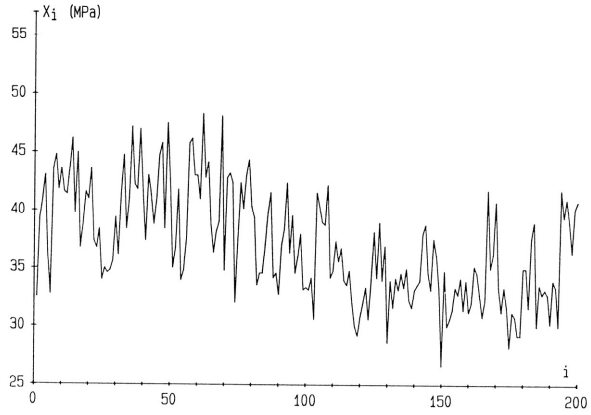

Fig. 2: Representation of subseries B4

If the series is regarded as a parent form which is infinitely long, we refer to the autocorrelations, instead of the serial correlations, and denote them by ρ_k where

$$\rho_k = \frac{\mathrm{Cov}\left[X_i, X_{i+k}\right]}{\left\{\mathrm{Var}\left[X_i\right]\mathrm{Var}\left[X_{i+k}\right]\right\}^{1/2}} \tag{2}$$

This accords with the usual convention in statistics of denoting parent values by Greek letters and sample values by roman type. The serial correlation of lag 0 equals 1. In the case of independent observations, $r_k = 0$ for $k \geq 1$. It is important to note that the strength results must be available in chronological order, otherwises the calculation of r_k does not make sense.

In the following, the structure of equation (1) is briefly discussed. The numerator is part of the sample covariance which is a sum of products, the factors of which are related to observations k units apart. In the case of a perfectly random series, the possibility that both x_i

and x_{i+k} are at the same side of the mean level $\bar{x}_n$ is as likely as the event that both are at a different side. This means that in the long run both positive and negative contributions to the numerator compensate each other and that r_k is zero. However, in the case of a correlated series, positive contributions will be dominating for a series with slow fluctuations whereas negative contributions will predominantly occur for a series with rapid fluctuations. The resulting values or r_k will be either positive or negative and significantly different from zero. As the dependency between observations, sufficiently far apart, tends to become negligible, r_k will approach zero for high k values. The denominator may be considered as a standardization factor and is equal to the sum appearing in the sample variance.

The consecutive values of r_k yield an instructive picture of the internal structure of a series consisting of correlated observations. The graphical representation of r_k as a function of k is called a correlogram. The correlograms of subseries A4 and B4 are represented in Figs. 3 and 4. The main difference between these two typical examples is that the first correlogram (subseries A4) decays rather rapidly, whereas in the second case (subseries B4) the values of r_k decrease very slowly. The reason for this is that the mean level of subseries A4 remains almost constant whereas in subseries B4 a significant downward trend is present (Figs. 1 and 2).

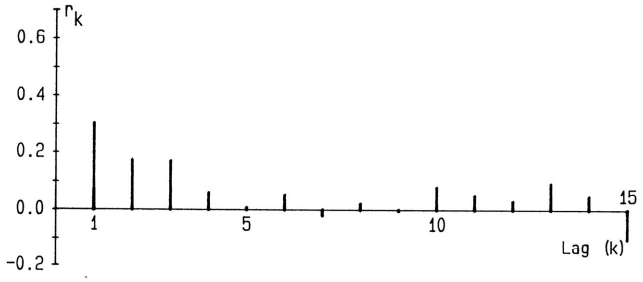

Fig. 3: Correlogram of subseries A4

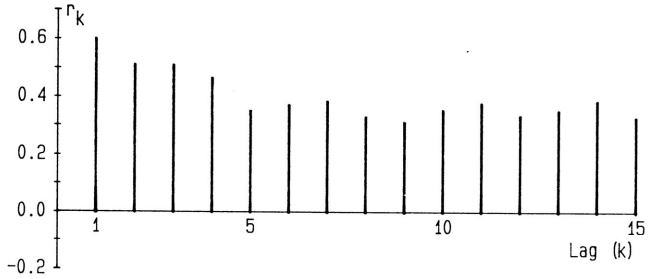

Fig. 4: Correlogram of subseries B4

In Tab. 4 the values of r_k, with $k = 1, ..., 5$ are given for the 31 series. It may be concluded that, on the mean, r_1 ranges between 0.2 and 0.6 whereas r_2 varies between 0.1 and 0.5. The same order of magnitude is mentioned in [4] for strength series of Swedish origin.

In order to test whether the serial correlation of lag k is significantly different from zero, use is made of the property that if $r_k = 0$ then [7, 8]

$$\mathrm{Var}[r_k] = \frac{1}{n}\left(1 + 2\sum_{i=1}^{k-1} r_i^2\right) \quad \text{for} \quad k > 1 \tag{3}$$

In case that

$$r_k < 2\sqrt{\mathrm{Var}[r_k]} \tag{4}$$

it is concluded that r_k is not significantly different from zero [6]. The highest lag for which r_k is significantly different from zero is also shown in Tab. 4. Obviously, these values vary rather widely depending of the correlation structure of the subseries concerned.

Tab. 4: Serial correlations r_1 to r_5 of the 31 subseries

Subseries	r_1	r_2	r_3	r_4	r_5	Highest lag of significant r_k
A1	0.425	0.386	0.276	0.263	0.286	8
A2	0.258	0.128	0.113	-0.011	0.028	1
A3	0.226	0.084	0.091	0.072	0.083	1
A4	0.302	0.173	0.169	0.060	0.006	3
A5	0.196	0.115	0.044	0.011	0.096	1
A6	0.286	0.090	0.177	0.033	-0.023	3
A7	0.277	0.213	0.185	0.174	0.121	4
A8	0.227	0.089	0.145	0.143	0.120	7
A9	0.462	0.375	0.337	0.300	0.343	5
B1	0.323	0.287	0.077	0.149	0.076	2
B2	0.493	0.412	0.409	0.202	0.134	6
B3	0.536	0.535	0.449	0.393	0.358	12
B4	0.600	0.511	0.509	0.464	0.351	14
B5	0.199	0.145	-0.039	0.015	-0.097	1
C1	0.451	0.401	0.372	0.362	0.325	7
C2	0.437	0.319	0.300	0.328	0.244	6
C3	0.384	0.194	0.210	0.183	0.223	5
D1	0.432	0.326	0.306	0.237	0.080	4
D2	0.488	0.385	0.242	0.132	0.185	11
D3	0.461	0.412	0.246	0.269	0.217	5
D4	0.586	0.513	0.431	0.402	0.416	10
D5	0.561	0.341	0.272	0.198	0.103	3
D6	0.366	0.201	0.053	0.037	0.064	2
D7	0.389	0.211	0.180	0.221	0.241	5
D8	0.341	0.211	0.133	0.023	0.009	1
E1	0.369	0.144	0.227	0.146	0.116	3
E2	0.255	0.030	-0.018	0.107	0.104	1
E3	0.575	0.412	0.388	0.396	0.330	9
E4	0.358	0.278	0.263	0.179	0.104	6
E5	0.252	0.148	0.089	0.125	-0.037	1
E6	0.360	0.168	0.095	0.028	-0.010	1

4 Physical background of the correlation structure

A possible explanation for the existence of the correlation structure may be found in the nature of the concrete production process. A given strength value is to a certain extent dependent on the previous values due to the fact that the basic factors which contribute to the variation of concrete strength, namely cement strength, and moisture content and grading of the sand, maintain a certain value during a more or less long time interval. On this basic process, random variations proper to each concrete mix are superimposed. The processes that describe the fluctuations of the basic variables, may also present a correlation structure. This complex input function is transformed, during the production process, into the output variable namely concrete strength. Further, a certain number of control activities are performed resulting in slight modifications of the cement or water content of the mix. The efficiency of this procedure strongly depends on the magnitude of the time lag between the observation of a significant change of a variable and the appropriate adjustment of a parameter. The general interaction scheme is represented in Fig. 5 [2].

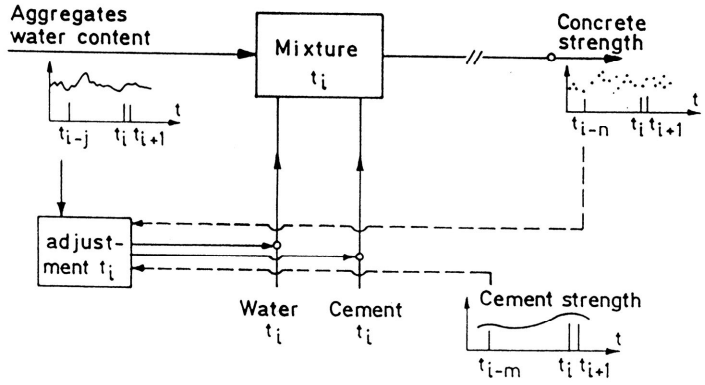

Fig. 5: Schematic representation of concrete production; adapted from [2]

In [5] and [6] the correlation structure of some input variables was also investigated. In 4 cement strength series, each consisting of 400 observations, also a significant serial correlation was found.

Values of the fineness modulus and moisture content of 378 consecutive deliveries of sand at a certain concrete plant were recorded. These data cover a period of about four and a half years. The main statistical characteristics of both series are shown in Tab. 5, whereas the five first serial correlations are given in Tab. 6.

Tab. 5: Properties of sand data (378 observations)

	Mean value	Standard deviation	Coefficient of variation
Fineness modulus	2.991	0.154	5.1%
Moisture content (%)	6.09	1.92	31.5%

Tab. 6: Serial correlations of sand data (378 observations)

	r_1	r_2	r_3	r_4	r_5
Fineness modulus	0.380	0.243	0.283	0.199	0.154
Moisture content (%)	-0.026	0.100	0.083	0.013	0.056

For the fineness modulus, the highest lag for which r_k is significantly different from zero is 7. On the other hand, the moisture content data present no significant serial correlation.

In the concrete production process, the moisture content of sand is generally compensated by adjusting the amount of mixing water, so the initial variations are only partly reflected in the concrete properties. However, it is difficult in practice to take into account variations in the grading of the sand by adjusting the mix proportions. Hence, variations of this variable are, to a great deal, transmitted to the concrete properties and probably this also holds for the correlation which appears to be present between consecutive values of the fineness modulus.

5 Practical consequences of the correlation structure

The presence of serial correlation has important consequences on the distribution of the usual sample statistics. The distribution of $\overline{X}_n$ remains normal but its variance increases compared to the case of independent observations. Both the expectation and the variance of S_n are influenced. Moreover, $(n-1)\, S_n^2 / \sigma^2$ has no longer a χ^2-distribution, and $\overline{X}_n$ and S_n are no longer independent [5].

These particularities have to be duly considered for the calculation of OC-lines of compliance criteria [9] because otherwises the calculated probabilities of acceptance will not accurately reflect reality.

It can be shown [8] that

$$\mathrm{Var}\left[\overline{X}_n\right] = \frac{\sigma_X^2}{n}\left[1 + \frac{2}{n}\sum_{j=1}^{n-1}(n-j)\,.\,\rho_j\right] \tag{5}$$

and

$$\mathrm{E}\left[S_n^2\right] = \sigma_X^2\left[1 - \frac{2}{n(n-1)}\sum_{j=1}^{n-1}(n-j)\,.\,\rho_j\right] \tag{6}$$

where σ_X^2 represents the variance of the strength variable X. In the case of independent observations $\rho_j = 0$ for $j \geq 1$ which yields the classical results $\mathrm{Var}\left[\overline{X}_n\right] = \sigma_X^2 / n$ and $\mathrm{E}\left[S_n^2\right] = \sigma^2$.

In the boundary case of equicorrelation ($\rho_k = \rho$ for $k = 1, ..., n$) the previous expressions reduce to

$$\mathrm{Var}\left[\overline{X}_n\right] = \frac{\sigma_X^2}{n}\left[1 + (n-1)\,\rho\right] \tag{7}$$

$$\mathrm{E}\left[S_n^2\right] = \sigma_X^2\,(1-\rho) \tag{8}$$

In case the correlation structure can be modelled by means of an autoregressive model of order 1 (see section 6.1) and for n = 3 ($\rho_k = \rho_1^k = \rho$) one finds respectively

$$\mathrm{Var}\left[\overline{X}_3\right] = \frac{\sigma_X^2}{9}\left[3 + 4\rho + 2\rho^2\right] \tag{9}$$

$$\mathrm{E}\left[S_3^2\right] = \sigma_X^2\left[1 - \frac{1}{3}(2\rho + \rho^2)\right] \tag{10}$$

In Tab. 7, some values of $\left(\mathrm{Var}\left[\overline{X}_n\right]\right)^{1/2}/\sigma_X$ are mentioned for the case of an AR(1) model and for the case of equicorrelation. It appears for example that for $n = 10$, the fact that $\rho = 0.7$ makes the reduction of the variance due to averaging half as efficient compared to the case of independent observations.

Tab. 7: Values of $\left(\mathrm{Var}\left[\overline{X}_n\right]\right)^{1/2}/\sigma_X$

ρ	AR(1) model					Equicorrelation	
	$n = 3$	$n = 5$	$n = 10$	$n = 15$	$n = 20$	$n = 3$	$n = 20$
0	0.5774	0.4472	0.3162	0.2582	0.2236	0.5774	0.2236
0.3	0.6976	0.5680	0.4165	0.3441	0.2997	0.7303	0.5788
0.5	0.7817	0.6671	0.5099	0.4269	0.3742	0.8165	0.7247
0.7	0.8680	0.8747	0.6446	0.5559	0.4944	0.8944	0.8456

Some values of $\left(\mathrm{E}\left[S_n^2\right]\right)^{1/2}/\sigma_X$ are mentioned in Tab. 8.

Tab. 8: Values of $\left(\mathrm{E}\left[S_n^2\right]\right)^{1/2}/\sigma_X$

ρ	AR(1) model					Equicorrelation
	$n = 3$	$n = 5$	$n = 10$	$n = 15$	$n = 20$	
0	1	1	1	1	1	1
0.3	0.8775	0.9202	0.9583	0.9719	0.9788	0.8366
0.5	0.7638	0.8329	0.9067	0.9361	0.9515	0.7071
0.7	0.6083	0.6931	0.8059	0.8605	0.8918	0.5477

From the foregoing results it is clear that autocorrelation has important consequences on the distribution of the usual sample statistics.

6 Development of stochastic models

6.1 Time-series models [4, 7]

Time-series are ordered observations of a random variable, which are typically obtained at different points in time. Time-series models are widely used in economics, also with the purpose of forecasting.

A first class of time-series models are the so-called autoregressive processes, abbreviated as AR(p) where p is the order of the model. The general equation of the AR(p)-model is

$$u_i = \phi_i\, u_{i-1} + \phi_2\, u_{i-2} + ... + \phi_p\, u_{i-p} + \varepsilon_i = \sum_{j=1}^{p} \phi_j\, u_{i-j} + \varepsilon_i \tag{11}$$

Where E[u] = 0 and ε_i is N(0,σ_ε). It appears that a particular value u_i is a weighed sum of p previous values, to which a random fluctuation is added. In case X is distributed according to N(μ,σ) and ε according to N(0,1) then (11) can be written as

$$x_i = \sum_{j=1}^{p} \phi_j\, x_{i-j} + \left(1 - \sum_{j=1}^{p} \phi_j\right) \mu + \sqrt{1 - \sum_{j=1}^{p} \rho_j\, \phi_j}\ .\sigma\,.\,\varepsilon_i \tag{12}$$

The most simple model is the AR(1) process or Markov series :

$$u_i = \rho\, u_{i-1} + \varepsilon_i \tag{13}$$

where $\phi_1 = \rho$ has been introduced. It can easily be shown that

$$\sigma_u^2 = \frac{\sigma_\varepsilon^2}{1-\rho^2} \tag{14}$$

The autocorrelation decays according to $\rho_k = \rho^k$.

The AR(2)-model, also called the Yule series, is given by

$$u_i = \phi_1\, u_{i-1} + \phi\, u_{i-2} + \varepsilon_i \tag{15}$$

It can be shown that

$$\rho_1 = \frac{\phi_1}{1-\phi_2} \qquad \rho_2 = \frac{\phi_1^2}{1-\phi_2} + \phi_2 \tag{16}$$

$$\sigma_u^2 = \frac{\left(1-\phi_2\right)\sigma_\varepsilon^2}{\left(1+\phi^2\right)\left(1-\phi_1-\phi_2\right)\left(1+\phi_1-\phi_2\right)} \tag{17}$$

The stationarity conditions are

$$-1 < \phi_2 < +1 \qquad \phi_1 + \phi_2 < 1 \qquad -\phi_1 + \phi_2 < 1$$

In order to find out which order is significant to maintain in the model, one can make use of the so-called Box-Jenkins approach in combination with the Ljung-Box test statistic which is based on the serial correlations of the residual series ε_i.

For subseries A4 and B4, depicted in Fig. 4, one finds the following AR-models.

A4 : AR(1) with $\phi_1 = 0.302$

B4 : AR(3) with $\phi_1 = 0.406$; $\phi_2 = 0.135$; $\phi_3 = 0.220$

However, for most of the subseries mentioned in Tab. 3, an AR-model of order 1 or 2 is sufficient. Typical values of the parameters are

AR(1)-model : - mean : $\phi_1 = 0.3$
- upper limit : $\phi_1 = 0.5$

AR(2)-model : - mean : $\phi_1 = 0.4$; $\phi_2 = 0.2$
- upper limit : $\phi_1 = 0.56$; $\phi_2 = 0.13$

Hence the following AR(2)-model was deemed to be rather representative for the concrete strength series considered :

$$u_i = 0.4\, u_{i-1} + 0.2\, u_{i-2} + \varepsilon_i \tag{18}$$

This model is used in [9] to analyse the influence of autocorrelation on OC-lines for conformity criteria for concrete strength.

The long-term effect which is present in several series can be related to the Hurst-effect (long-memory property) and the so-called stable distribution functions [11].

6.2 Renewal pulse process

6.2.1 General

We consider the following test statistic

$$q^2 = \frac{1}{2\,(n-1)} \sum_{i=1}^{n-1} (x_{i+1} - x_i)^2 \tag{19}$$

which is an unbiased estimate of σ^2 with efficiency equal to

$$\frac{\mathrm{Var}[s^2]}{\mathrm{Var}[q^2]} = \frac{2}{3}\left(1 + \frac{1}{3\,n-4}\right) \tag{20}$$

The latter ratio equals 1 for $n = 2$ and approaches 2/3 for $n \to \infty$. The statistic $2\,q^2$ is called the mean square successive difference.

The use of q^2 is particularly useful when the mean of the population, from which the observations are successively drawn, exhibits gradual or stepwise changes, the variance remaining constant. In that case the estimate s^2 of σ^2 will tend to be too large because s^2 also includes the variation of the population mean. If, during the observation period, a change in population mean takes place, the effect of this change on the estimate q^2 will be relatively small since q^2 includes only the differences between successive values, and generally only one difference will be rather high. Therefore, the estimate s^2 is much more sensitive to changes in the population mean than is the estimate q^2.

If we take as null hypothesis that the population mean μ remains constant during the observation period, and as an alternative that μ changes in one way or another, we can make use of the test statistic

$$r = \frac{q^2}{s^2} \tag{21}$$

small values of r being significant. Note that $E[r] = 1$.

When r is calculated for the subseries mentioned in Tab. 3, one always finds a significantly low value. This also holds for the cement strength series mentioned in [6].

The foregoing investigation suggests that the processes which produce the concrete strength results can hardly be considered as being "under control" in the classical statistical sense. However, this remark mainly holds for short-term variations and not for the long-term behavior. This statement is not meant as criticism on the current production methods, but shows that in practice it is very difficult to obtain a production process with perfectly homogeneous output properties. This comment is also applicable to other types of production processes and for many time-dependent phenomena that are influenced by random disturbances.

6.2.2 Model

Once it is found that the population mean doesn't remain stable at short term, it is attractive to find out what part of the total variation is due to these changes. In fact, we want to dispose of a rational procedure to divide the strength records into subgroups such that the conditions are essentially the same within each subgroup. However, in this case we have no prior knowledge of the occurrence of assignable causes of variation in the mean level. A possible way to proceed is to divide a record into subgroups of equal size n. However, the choice of n is quite arbitrary and the estimated values of the variances within and between subgroups depend on the chosen length of the subgroups. Hence it is necessary to develop an appropriate stochastic model and an associated practical estimation procedure.

To elaborate the model, we premise that the mean strength level does not vary in a continuous way but rather in a discontinuous one and that it presents jumps at certain points in

time. In between these jumps, the mean level remains constant. Whether these jumps are caused by the production process itself, or follow from a similar behaviour of the input variables, is not investigated here. Thus, a series of successive observations consists of consecutive subgroups, each group corresponding to a certain mean strength level that remains constant in between the mentioned jumps. Each subgroup, which may be considered as a sub-population, is called a "segment". The number of test results in segment j is denoted T_j, the mean value of the T_j results is denoted m_j, and the standard deviation of the T_j-values with respect to m_j is denoted s_j (Fig. 6). The distinction between consecutive segments is made on the basis of jumps in the mean strength level, although the standard deviation, too, may show a similar piecewise constant evolution (Fig. 6). In the theory of stochastic processes this type of behaviour is called a "renewal pulse process". The individual values of the random variable X (here cement strength) arise from random variations which are superimposed on a step-function. The complete model is fully determined by the distribution functions of the random variables m, s and T.

In [4,6] a statistical procedure was developed to devide the observed series according to the previous scheme, based on a likelihood ratio test.

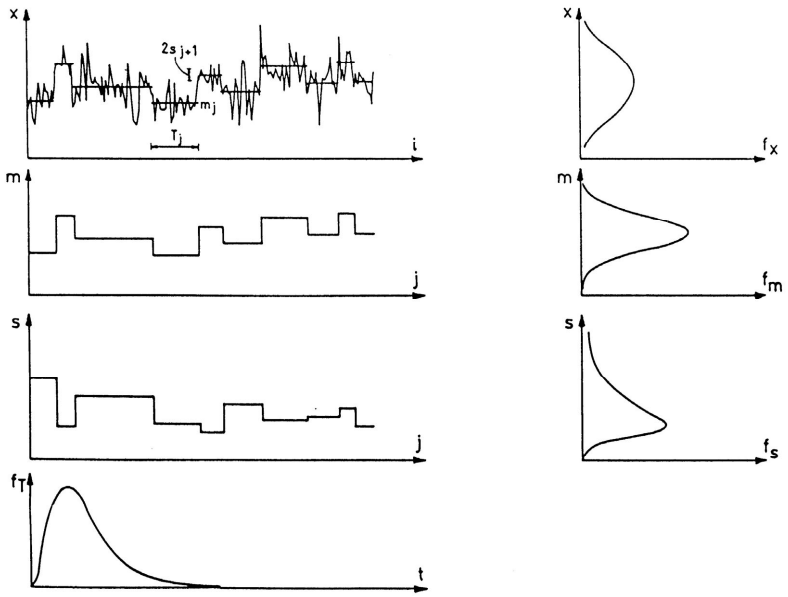

Fig. 6 : General representation of the stochastic model

7 Conclusions

- From the analysis presented in this paper it follows that successive concrete strength values are not indepedent as is usually assumed. Significant serial correlation is present in empirical concrete strength records.

- Five extensive series of concrete strength values, arranged in chronological order, are available. The total number of observations ranges between 534 and 1786.

- The analysis of 31 subseries, each consisting of almost 200 observations, reveals that r_1, the serial correlation of order 1, ranges between 0.2 and 0.6 whereas r_2 may vary between 0.1 and 0.5.

- The existence of serial correlation influences the distribution of the usual sample statistics used in quality control procedures. The variance of the sample mean $\bar{x}_n$ is higher compared to the case of independent observations whereas the mean value of s_n^2 is reduced by serial correlation.

- The origin of serial correlation in concrete strength records may be related to the nature of the production process and more particularly to the characteristics of the input variables. It was found that cement strength records from several cement plants also present significant serial correlation. The same conclusion holds for the fineness modulus of sand used at one concrete plant.

- The observed autocorrelation structure is modelled by means of an AR(2) time series model and a particular renewal pulse process.

- The conclusions raised in this paper are not only relevant to a better understanding of the random nature of concrete strength but also have practical consequences with respect to production control techniques and the calculation of OC-lines for compliance criteria.

8 References

[1] Soroka, I.; Length of concreting period and compressive strength variation in concrete, *Document 017-213*, Technion, Israel, Institute of Technology, December 1972, pp. 1-10.

[2] Rackwitz, R.; A simple stochastic model for in situ concrete strength, *Miscellaneous papers in civil engineering*, *Dialog*, *Danmarks Ingeniorakademi*, bygningsafdelingen, Lyngby, 1977, pp. 117-133.

[3] Degerman, T.; Design of concrete structures with probabilistic methods, *Report TVBK-1003*, Department of Building Technology, Lund Institute of Technology, 1981, pp. 116-125 (in Swedish).

[4] Taerwe, L.; Aspects of the stochastic nature of concrete strength including compliance control, *Doctoral thesis*, Ghent University, Ghent, Belgium, 1985, pp. 3.1-3.44 (in Dutch).

[5] Taerwe, L.; Serial correlation in concrete strength records, *Special Publication ACI SP-104-12*, Lewis H. Tuthill International Symposium on Concrete and Concrete Construction, G.T. Halvorsen Ed., Detroit, 1987, pp. 223-240.

[6] Taerwe, L.; Detection of inherent heterogeneities in cement strength records by means of segmentation, Uniformity of Cement strength, *ASTM STP 961*, E. Farkas and P. Klieger, Eds., ASTM, Philadelphia, 1987.

[7] Anderson, O.D.; Time series analysis and forecasting ; The Box-Jenkins approach, Butterworths, Boston, 1976, pp. 1-11.

[8] Kendall, M., Stuart, A. and Ord, J.; *The advanced theory of statistics*, Vol. 3, Griffin, London, 1983, pp. 422-656.

[9] Taerwe, L.; The influence of autocorrelation on OC-lines of compliance criteria for concrete strength, *Materials and Structures*, 1987, vol. 20, pp. 418-427.

[10] Hold, D.; Statistical theory with engineering applications, *Wiley*, New York, 1952, p. 357.

[11] Taerwe, L.; Long-memory property of concrete strength records, *Applications of Statistics and Probability (ICASP 7)*, Vol. 1, Eds. M. Lemaire, J.-L. Favre and A. Mébarki, Paris, July 1995, pp. 193-200.

Intervention Strategies for Concrete Structures including Material Uncertainties

Alfred Strauss[1], Dan Frangopol[2] & Konrad Bergmeister[1]
[1] Institute for Structural Engineering,
University of Natural Resources and Applied Life Sciences, Vienna, Austria
[2] Lehigh University, Bethlehem, Pennsylvania, USA

Abstract: Intervention strategies for cost optimized maintenance of concrete structures become in recent years important matters under bridge owners as well as persons immediately concerned with the preservation. Intervention strategies should support the preservation of national wealth and should allow in consequence a structured maintenance planning. The intervention strategies are closely connected to optimization algorithm. The optimization algorithm has to include several structural qualities, like the geometrical design, the material properties, the results of the visual inspection, the results of monitoring programs, the numerical reliability assessment (BERGMEISTER et al. [1]) etc. Most of these qualities are time dependent and are afflicted with uncertainties. The time-dependent structural qualities can usually clearly be torn up by means of condition profiles and reliability profiles. Costs can be assigned to the elements determining these profiles. Cost models for the elements of the reliability profiles have already been developed by KONG et al. [2] & FRANGOPOL et al. [3]. Since the visual inspection is the most frequent used methodology in bridge maintenance, it is necessary to develop also cost models for the associated condition profile and to combine both of them for a global optimization process. A global realistic optimization process must have the ability to capture the uncertainties of the material qualities and their temporal variability-degradation. The aim therefore is to transfer and to deduce the cost models for the elements of the reliability profiles to the elements of the condition profiles to combine the cost models and to include adequate the uncertainties of the material qualities.

1 Introduction

Management systems have to support decision-makers as to when and how to repair, rehabilitate, replace, and/or shut down deteriorating facilities. Therefore effective cost evaluation methods have to include; construction costs, inspection costs, maintenance costs, user costs, and failure costs, which are essential factors for life-cycle cost analysis of deteriorating structures (CHANG & SHINOZUKA [4]); (ANG & DE LEON [5]); (FRANGOPOL et al. [6], [7]). Inspection and maintenance measures, also called interventions, are the most easily influence able quantities during the structural preservation. The kind of interventions and their duration are based on various parameters, e.g. material properties, degradation ratio of material properties, the reliability level of a structure etc.. Intervention strategies are closely connected to cost optimization algorithms. They also have to include several structural qualities, like the geometrical design, the material properties, the results of the visual inspection, the results of monitoring programs, the results from numerical reliability assessment methods (BERGMEISTER et al. [1]) etc.. Most of these qualities are time dependent and are afflicted with uncertainties. The time-dependent structural qualities can usually clearly be torn up by means of condition profiles and reliability profiles. Costs can be assigned to the elements determining these profiles. Cost models for the elements of the reliability profiles already are developed by KONG et al. [2] & FRANGOPOL et al. [3]. Since the visual inspection is the most frequent used methodology in bridge maintenance, it is necessary to develop also cost models for the associated condition profile and to combine it with the cost models of the reliability profile to allow a global optimization process. In this contribution a method will be shown, which permits the combination of the two cost models to a global cost optimization model considering also the uncertainties in the time dependent material qualities. The combination can be carried out heuristically based on engineering experience, by means of multiobjective optimization (NEVES et al. 2006), or by means of a Cost Optimized Reliability – Condition Profile function *CRCP*. The *CRCP* is less computationally costly than the multiobjective generic algorithm optimization. The time-saving *CRCP* function can be extended for the inclusion of uncertainties in the material qualities but also the uncertainties of the profiles defining elements to a probabilistic basis (STRAUSS et al. [8]).

2 Condition – Reliability Profiles

The reliability profile, the condition profile and their cost models mainly characterize the cost optimization process for structures. Its course is essential influenced by the definition of the objective function or analytical formulation, respectively. The objective function has to meet the demands of the profiles, cost models and their boundary conditions. Since the descriptive elements of the profiles and the objective function itself are afflicted by uncertainties, it is necessary to perform the cost optimization considerations on a probabilistic level. A probabilistic concept concerning cost optimization strategies requires the inclusion of the following considerations:

- Conventional optimization processes are time expensive calculation processes

- Mostly, it is a target at the optimized cost considerations to carry them out as a function of a property of the reliability profile or the condition profile. The necessary calculation processes therefore increase according to the bounds and the step width of the variables property.
- Cost combined reliability profile as well as the condition profile consists of nearby 24 elements to be expressed as random variables.

These facts require the inclusion of an efficient statistical tool in the cost optimization model, which has to permit a simple definition of random variables and has to include an advanced Monte Carlo (MC) technique that allow a small number of realizations for random variables. FREeT is one of those statistical software packages that include an easy user-friendly definition of the stochastic models and an advanced MC technique the Latin Hypercube Sampling (LHS) technique [9]. FREeT was therefore in the following selected to support the probabilistic treatment of the objective function and the analytical model, respectively.

The condition profile can be defined as the variation of the condition index with time. This approach is deviated from a proposal for the reliability profile already suggested by THOFT CHRISTENSEN [10]; ESTES and FRANGOPOL [11]; NOWAK et al. [12]. The main elements describing the condition profile are (i) the initial condition index C_{0I}, (ii) the time of condition change initiation t_{CI}, (iii) the condition index deterioration rate α_C without lifetime extension, (iv) the time of first application of preventive lifetime-extending maintenance t_{PI}, (v) the time of reapplication of preventive lifetime-extending maintenance t_P, (vi) the duration of preventive lifetime-extending maintenance effect on condition t_{PDC}, (vii) the deterioration rate change of the condition index during preventive lifetime-extending maintenance effect δ_c, (viii) the improvement in the condition index (if any) immediately after the application of preventive lifetime-extending maintenance $\Delta\gamma$, see Fig. 1.

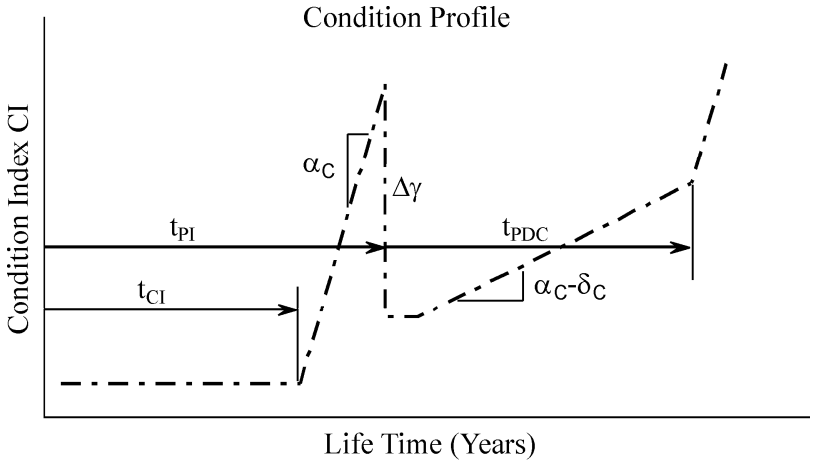

Fig. 1: Characteristic Elements of the Condition profile

In a first approach, the elements of the condition profile can be considered deterministic. Elements as shown in Table 1 are in general predefined and, as shown in Table 2, are variables. These two sets of elements are the descriptive ones for the condition index

profile optimization. The optimization can be performed with regard to several aspects: e.g. (1) to minimize the number of interventions for a specified life time t_H and a demanded index; (2) to minimize the overall costs of maintaining the condition or/and reliability over the demanded index during the specified lifetime.

Table 1: Predefined elements for the optimization strategy

Name	Unit	Condition Profile	Reliability Profile
		Symbol	Symbol
Time of condition change initiation / damage initiation*): lower bound	Year	$t_{CI,lower}$	$t_{RI,lower}$
Time of condition change initiation / damage initiation*): upper bound	Year	$t_{CI,upper}$	$t_{RI,upper}$
Time of first application of preventive lifetime-extending maintenance: upper bound	Year	$t_{PI,upper}$	$t_{PI,upper}$
Specified lifetime	Year	t_H	t_H
Initial condition index / initial reliability index*)	-	C_{0I}	β_{0I}
Condition index at t_H / reliability index at t_H*)	-	C_H	β_H
Condition index deterioration rate / reliability index deterioration rate*) without lifetime extension	-	α_C	α_R
Improvement in the condition index / reliability index*)	-	$\Delta\gamma$	$\Delta\beta$
Initial duration of preventive lifetime extending	Year	t_{CD}	t_{RD}
Deterioration rate change of the condition index / reliability index*) during preventive lifetime-extending maintenance effect	-	δ_c	$\Delta\alpha$

*) reliability profile

Table 2: Variable elements for the optimization strategy

Parameter	Vari-able	Condition Profile	Reliability Profile
		Symbol	Symbol
First application of preventive lifetime-extending maintenance	X(1)	t_{PI}	t_{PI}
Time of condition change initiation / damage initiation*)	X(2)	t_{CI}	t_{RI}
Duration of preventive lifetime-extending maintenance	X(3)	t_{PDC}	t_{PDR}
Unprotected period	X(4)	t_A	t_A
Number of interventions	X(5)	n	N

*) reliability profile

The optimization by minimization of the overall costs needs the definition of cost functions that can be assigned to the interventions. Suitable formulations of cost functions already proposed for interventions regarding the reliability profile can be found in Kong and Frangopol [2], see Table 3.

Since the measures of improvement in the condition index γ are not independent of the level of C_I, the level of the condition index at the measure of γ has to be included in the cost formulation. The polynomial formulation, also shown in Table 3, yields an increasing factor λ for the improvement in the condition index γ.

Table 3: Intervention-related cost functions

		Condition Profile		Reliability Profile	
Parameter	Unit	Intervention / Cost Eq.	Symbol	Intervention / Cost Eq.	Symbol
Fixed cost	$	$\Delta\gamma$ $C\gamma=C\gamma_0+p\times(\Delta\gamma)^q$	$C_{\gamma 0,}$	$\Delta\beta$ $C_\beta=C_{\beta 0}+p*(\Delta\beta)^q$	$C_{\beta 0,}$
Var. cost factor	-		p		P
Var. cost factor	-		q		Q
Fixed cost	$	δ_c $C_\delta=C_{\delta 0}+g\times(\delta_c)^h$	$C_{\delta 0,}$	$\Delta\alpha$ $C\alpha=C\alpha_0+p*(\Delta\alpha)^q$	$C_{\alpha 0,}$
Var. cost factor	-		g		G
Var. cost factor	-		h		H
Var. cost factor	-	$\lambda_{Ci}=p_1\times Ci^2+p_2\times Ci+p_3$	P_1	$\lambda_{\beta i}=p_1*\beta i^2+p_2*\beta i+p_3$	$C_{\gamma 0,}$
Var. cost factor	-		P_2		P
Var. cost factor	-		P_3		Q

3 Objective Function

3.1 Condition Profile

The analytical model of the above mentioned condition profile could be expressed as shown in Eq. (1). The equation consists of three main parts: (1) the initial time described by the C_{0I} index and the time without deterioration *x(2)*; (2) the period of deterioration without interventions, described by *x(1), x(2)* and α_C; (3) the time of interventions and reapplication of measures dominated by t_P and the value of *x(5)*.

$$CI = C_{0I} + [x(1) - x(2)]\cdot\alpha_c + [\Delta\gamma - \mathrm{x}(3)\cdot(\alpha_c - \delta_c) - \mathrm{x}(4)\cdot\alpha_c]\cdot x(5) \tag{1}$$

Based on this classification, Eq. (1) can further be divided into four parts, C_0, C_1, C_2, and C_3, see Eqs. (2) to (5). C_0 is the more or less constant part that is not influenced by the number of interventions. The remaining parts are directly related to the interventions.

$$C_0 = C_{0I} + [x(1) - x(2)]\cdot\alpha_c \tag{2}$$

$$C_1 = \Delta\gamma \tag{3}$$

$$C_2 = -[\mathrm{x}(3)\cdot(\alpha_c - \delta_c)] \tag{4}$$

$$C_3 = -[\mathrm{x}(4)\cdot\alpha_c] \tag{5}$$

Since C_1 to C_3 are in a linearly relation to *x(5)*, they can be combined in ΔC, which results in Eq. (6).

$$CI = C_0 + (C_1 + C_2 + C_3)\cdot x(5) = C_0 + \Delta C\cdot x(5) \tag{6}$$

This aggregation has the advantage that the cost-increasing factor λ can be handled as a global coefficient, as shown in Eq. (7).

$$\lambda_{CI,ges} = \sum_{i=1}^{n=x(5)} p_1 \cdot \left(C0 + \Delta C \cdot (i-1)\right)^2 + p_2 \cdot \left(C0 + \Delta C \cdot (i-1)\right) + p_3 \tag{7}$$

Applying the global coefficient $\lambda_{CI,ges}$ to the cost function as shown in Table 3 yields C_γ and C_δ respectively.

$$C_\gamma = \left(C_{\gamma 0} + p \cdot \Delta\gamma^q\right) \cdot \lambda_{CI,ges} \tag{8}$$

$$C_\delta = \left(C_{\delta 0} + g \cdot \delta_c^{\ h}\right) \cdot x(5) \tag{9}$$

The cost due to the δ_c interventions, see Eq. (9), is not correlated with the level of C_I. The cost terms thus associated result in the overall cost for maintaining a condition profile:

$$C_{CI} = C_\gamma + C_\delta \tag{10}$$

The aim is to minimize the overall cost for maintaining a condition profile by means of an optimization method. The optimization will rely mainly on the parameters as shown in Eq. (11).

$$C_{CI} = f(t_{PI}, t_{CI}, t_{PDC}, t_A, n) = f(\mathbf{x}) \tag{11}$$

Eq. (11) represents the objective function, a constrained nonlinear multivariable function, which has to be minimized. The optimization of the objective function is performed in this study by a line search medium-scale method. To ensure a reasonable course of the condition profile, the nonlinear multivariable function must be subjected to inequalities *c(x)*, equalities *ceq(x)*, and the lower (*lb*) and upper (*ub*) boundary conditions as shown in Eq. (13)

$$c(\mathbf{x}) \le 0; \quad c_{eq}(\mathbf{x}) = 0; \quad l_b \le \mathbf{x} \le u_b \tag{13}$$

where *x, lb*, and *ub* are vectors, *c(x)* and *ceq(x)* are functions that return vectors, and *f(x)* is the function that returns the minimum of the cost as a scalar. *f(x)* and *c(x)* are (or can be) nonlinear functions.

3.2 Reliability Profile

The reliability profile can also be created based on the variation of the reliability index, similar to the above performed remarks. The main elements describing the reliability profile are (i) the initial reliability index β_{0I}, (ii) the time of damage initiation t_{RI}, (iii) the reliability index deterioration rate α_R without lifetime extension, (iv) the time of first application of preventive lifetime-extending maintenance t_{PI}, (v) the time of reapplication of preventive lifetime-extending maintenance t_p, (vi) the duration of preventive lifetime-extending maintenance effect on reliability t_{RD}, (vii) the deterioration rate change of the reliability index during preventive lifetime-extending maintenance effect Δ_α, (viii) the improvement in the reliability index (if any) immediately after the application of preventive lifetime-extending maintenance Δ_β. Similar to the condition profile, there are

predefined and variable elements describing the reliability profile optimization process (see Table 1 and Table 2 respectively). The set up of the associated objective function can be performed analogously the previous explanations, which yields to.

$$C_{\beta} = \left(C_{\beta 0} + p \cdot \Delta\beta^{q}\right) \cdot \lambda_{\beta,ges} \tag{14}$$

$$C_{\alpha} = \left(C_{\alpha 0} + g \cdot \Delta\alpha^{h}\right) \cdot x(5) \tag{15}$$

and in consequence to:

$$C_{\beta H} = C_{\beta} + C_{\alpha} \tag{16}$$

There are therefore two objective functions, see Eq. (10) and Eq. (16):

a) which are used for the cost optimization,
b) which ones have to be combined with each other to get a global cost optimization,
c) for whom the specification factors have to be formulated by random variables to capture their uncertainties,
d) for whom one or more specification factors should be selectable as variables to allow a scope examination of cost influence quantities.

4 Objective Function – Probabilistic Treatment

The independent deterministic cost optimization of the objective functions regarding the condition profile and the reliability profile do not meet all the maintenance requirements. It is necessary to combine both objective functions and to include the uncertainties of the describing elements of the profiles. The uncertainties intrinsic in the profiles can be treated by random variables and an advanced Monte Carlo simulation technique. The high scores of simulations, necessary for a Monte Carlo Simulation, can be reduced by the Latin Hypercube Sampling (LHS) technique by a factor 1000 [9]. A special subdivision concept applied to each of the random variables within the LHS technique allows the reduction to a small number of necessary realizations and simulations, respectively. Consequently, each of the objective functions has to be evaluated *n* times according to the number of the necessary realizations for one specified initial set of random variables. The scattering input parameters, together with the simulated scattering output parameters, can be used for sensitivity analyses. These analyses give already essential insights into the mutual relation under the profiles parameter.

The main aim of the probabilistic consideration is to deliver the variables of Table 2 as scattering sizes under the claim of the minimal costs. The minimal costs are also due to the *n* simulations scattering quantities. These results permit the decision maker a more realistic assessment of the costs to be expected and the assessment of the sensitivity of the elements of the profiles regarding the costs. A more extensive assessment of cost developments enables the consideration of one or several variables of Table 1 and Table 2 as variable quantities within a defined range.

For the necessary requirements, mentioned above, Strauss et al. [8] developed a MATLAB routine for cost optimization strategies. It contains the LHS technique, FREeT as statistical software and allows the flexible choice of one or more quantities of the Table 1 and Table 2 as variables.

Fig. 2 shows the results of a probabilistic cost optimization for which β_H and C_H are selected as variables, for more details see [8]. This kind of investigation gives insight into the development of the costs and its spread as a function of the variables. Since a cost optimized profile is assigned to each of the presented points, – simulation results – the main elements describing the profiles are also available in a statistical/ spreading manner. These statistical results can be consulted to demonstrate the significance of each single main element in the cost optimization. Nevertheless there are two independent optimized courses – condition and reliability profile, respectively – which have to be entangled for a global cost optimization.

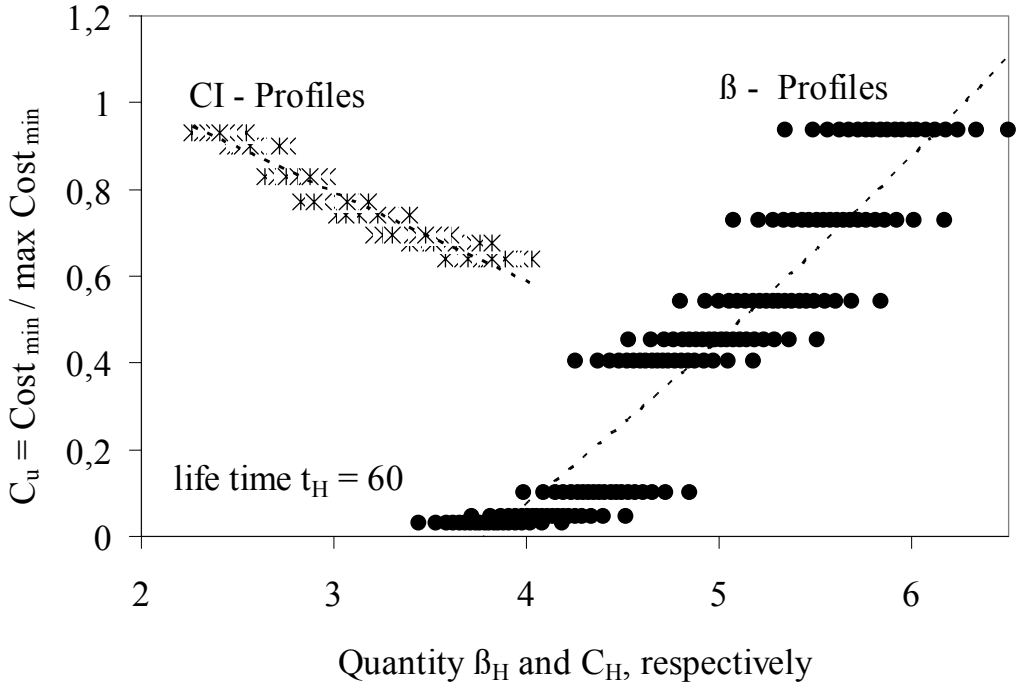

Fig. 2: Optimized cost $Cost_{RE}$ and $Cost_{CI}$ vs. β_H and C_H, respectively.

A strategy proposed by [8] to combine the two optimized courses is to assign the minimized costs, reliability and condition cost, respectively, to a normalized expression and sum them, see Eqs.(17).

$$\frac{Cost_{RE}}{Cost_{\max,RE} + Cost_{\min,CI}} + \frac{Cost_{CI}}{Cost_{\max,RE} + Cost_{\min,CI}} = \min \tag{17}$$

This kind of combining the Cost-Optimized Reliability Profile β with the Cost-Optimized Condition Profile *CI*, results in a structure's characteristic health profile *CRCP*, see Fig. 3.

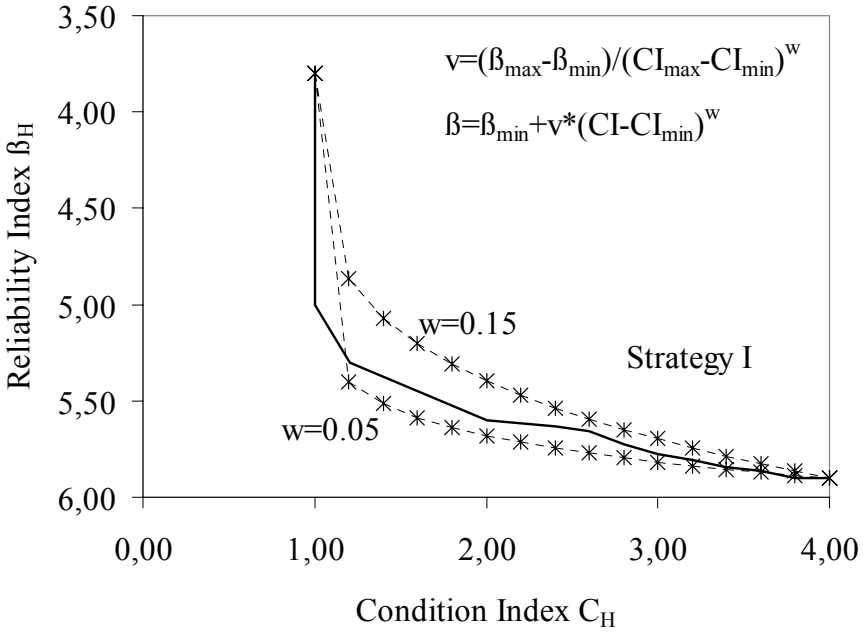

Fig. 3: Optimized cost profile regarding C_H and β_H [8]

As can be seen from Fig. 3, the β_H/C_H Cost Index Profile (CRCP) is more or less a derived numerical result that is different for every structure or structural component and that can be captured in a more general form as shown in Eq. (18):

$$\beta_H = \min \beta_H + v \cdot [C_H - \min C_H]^w \tag{18}$$

The parameters v and w can be obtained by the boundary conditions and a curve-fitting operation, respectively, see Fig. 3. This function can be understood as a characteristic size of the structure or the component looked at. The above considerations were carried out under the acceptance of a constant deterioration rate α. The deterioration rate is determined mainly by the changes in the material in the cross section or the structure itself. Therefore the demand is given to design the deterioration rate more flexible e.g.:

- in form of a linear function
- in form of a nonlinear function
- combined with a monitoring program.

The last approach captures the actual structural qualities best. It allows the realistic indication of material, cross section and structural properties. However, the approach requires the inclusion of an identification algorithm (STRAUSS et al. [13]) and of a prognosis model by TEPLY et al [15], MAORI [14] etc.

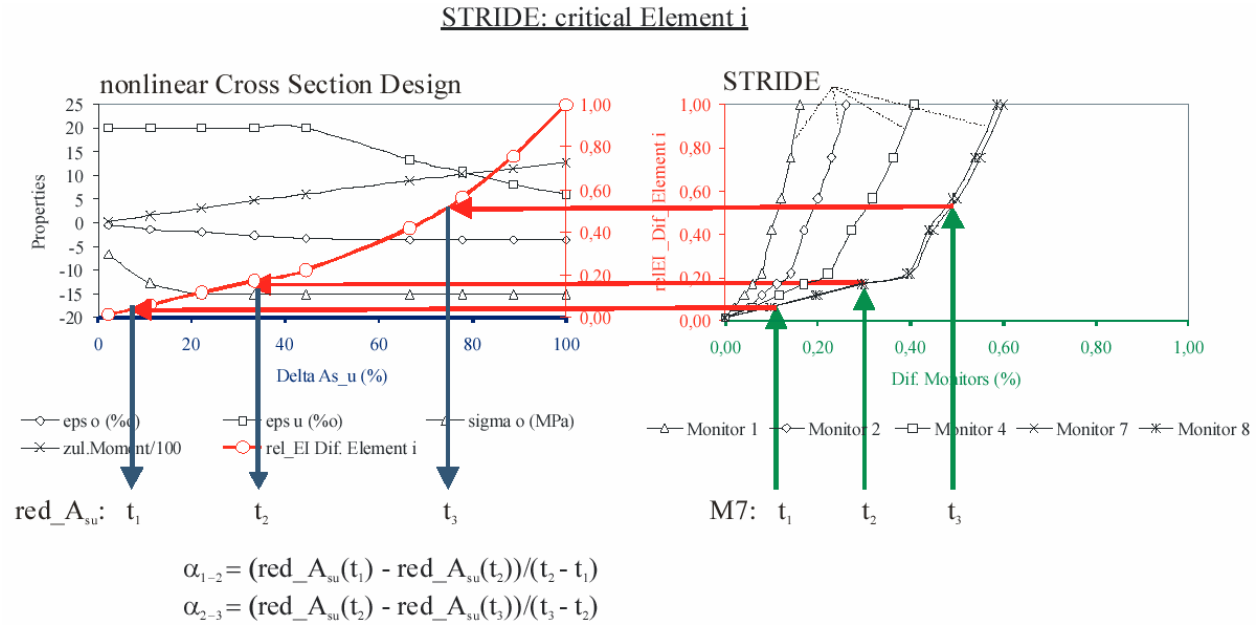

Fig. 4: Development of failure ratio factors α_i

How obviously from

Fig. 4 the identification algorithm has the following tasks at different times

- Identifying critical elements of the structure
- Due to the changes in the monitoring to identify the changes in the structure (reliability index ß) or the changes in the cross sections (e.g. resistances and in consequence the material properties based on cross section or sensitivity analyses, see Fig.3 on the right)

The changes of the reliability level or the changes of the material properties serve for the determination of the current degradation rate. Prognoses models like the Weibul functions, MAORI [14] approaches and TEPLY [15] degradations models can be used in consequence to derive the future development of the deterioration rate α. Since the monitoring systems and the identification methods are based on scattering date the prognoses models are too characterized by scattering. These prognoses models, expressible in most cases inform of functions, has to be included in Eqs. (18) which leads to:

$$\beta_H\left(f(\alpha(t))\right) = \min\beta_H + v\left(f(\alpha(t))\right)\cdot\left[C_H - \min C_H\right]^{w(f(\alpha(t)))} \qquad (19)$$

5 Conclusion

The aim of this contribution was to present a cost optimization concept for the maintenance planning of engineering structures. In the concept both the reliability considerations and

the condition consideration (visual inspections) are included. How it is obviously from the above explanations both considerations can be led to a structure characteristic property, the „structure's characteristic health profile CRCP". The active inclusion of time variable material qualities requires, however, an extension of this approach. The extension comprehends the description of the degradation rate α by the use of inverse identification algorithms and prognoses models. This concept allows a permanent updating of the CRCP profiles.

References

[1] Bergmeister, K., Novák, D., Pukl, R., and Cervenka, V. (2006). „Structural assessment and reliability analysis for existing engineering structures, theoretical background." *J. Infrastruct. Syst.,* under progress

[2] Kong, J. S. and Frangopol, D. M. (2005). "Cost-Reliability Interaction in Life-Cycle Cost Optimization of Deteriorating Structures." *Journal of Structural Engineering* ASCE, November 2004, 1704 – 1712

[3] Frangopol, D. M. and Neves, L. C. (2003). "Probabilistic Performance Prediction of Deteriorating Structures Under Different Maintenance Strategies: Condition, Safety and Cost." *ASCE - American Society of Civil Engineers (Ed.)* ASCE, Reston; ISBN 0-7844-0707-X., August 2003, 9 – 18.

[4] Chang, S. E., and Shinozuka, M. (1996). ''Life-cycle cost analysis with natural hazard risk.'' *J. Infrastruct. Syst.*, 2~3, 118–126.

[5] Ang, A. H-S., and De Leon, D. (1997). ''Target reliability for structural design based on minimum expected life-cycle cost.'' *Reliability and optimization of structural systems, D. M. Frangopol, R. B. Corotis, and R. Rackwitz, eds.*, Pergamon, New York, 71–83.

[6] Frangopol, D. M., Lin, K-Y., and Estes, A. C. (1997). ''Life-cycle cost design of deteriorating structures.'' *J. Struct. Eng., 123~10*, 1390–1401.

[7] Frangopol, D. M., Gharaibeh, E. S., Kong, J. S., and Miyake, M. (2000).''Optimal network-level bridge maintenance planning based on minimum expected cost.'' *Journal of the Transportation Research Board, Transportation Research Record*, 1696~2, National Academy Press, Washington, D.C., 26–33.

[8] Strauss, A., Frangopol, D. M., Bergmeister K. (2006). "Probabilistic Lifetime Optimization of Structures Combined Condition-Reliability Cost Profiles." *Journal of Structural Engineering* ASCE, under progress

[9] Novák, D., Rusina, R. and Vořechovský, M., Small-sample statistical analysis - software FREET. In *9th International conference on applications of statistics and probability in civil engineering (ICASP9)*, Berkeley, California, USA, 2003.

[10] Thoft-Christensen (1996). "Reliability profiles for concrete bridges." *In D.M. Frangopol and G. Hearn, editors, Structural Reliability in Bridge Engineering*, McGraw-Hill, New York, 239–244.

[11] Estes, A.C., and D.M. Frangopol (1996). "Life-cycle reliability-based optimal repair planning for highway bridges: A case study" *In D.M. Frangopol and G. Hearn, editors, Structural Reliability in Bridge Engineering*, McGraw-Hill, New York, 54–59.

[12] Nowak, A.S., Park, C.H., and Szersen, M.M. (1998). "Lifetime reliability profiles for steel girder bridges" *In D.M. Frangopol, editor, Optimal Performance of Civil Infrastructure Systems* , ASCE, Reston, Virginia, 139–154.

[13] Strauss, A., Frangopol, D. M., Bergmeister K. (2006). "Assessment of Existing Structures based on Inverse Statistical FEM Analysis." *Journal of Structural Engineering* ASCE, under progress

[14] Mori, Y. and Kato, T., Practical method of reliability-based condition assessment of existing structures. In *Applications of Statistics and Probability in Civil Engineering*, edited by Der Kiureghian, A., Madanat, S. and Pestana, JM., 2003 (Millpress: Rotterdam), pp. 613-620

[15] Teply, B., Chroma, M., Matesova, D. and Kersner, Z., *FReET-D, Program Documentation Part I + Part II*, Distributed by Cervenka Consulting, 2006.

Conformity control of concrete: some basic aspects

Luc Taerwe, Robby Caspeele
Ghent University, Department of Structural Engineering,
Magnel Laboratory for Concrete Research

Abstract : Conformity control is an important step in the quality control of manufactured items. This also holds for concrete where an additional problem arises by the fact that the main mechanical characteristics can only be determined at a certain age, typically 28 days. In the European Standard EN 206-1, specific rules for conformity control of concrete strength are given. In the paper the following aspects will be covered :

- current types of conformity criteria for concrete strength
- derivation of the probability of acceptance of current conformity criteria and discussion of OC-lines
- dependency in the case of compound conformity criteria
- influence of autocorrelation on OC-lines
- basic criteria for the parameter selection in conformity criteria
- discussion of the conformity criteria in EN 206-1.

1 Introduction

When concrete is produced, one or more properties are specified depending on the field of application and the environmental conditions. It has to be verified whether the produced concrete complies with the specified properties. This verification is called conformity control. In the case of concrete with product certification or production control certification, a more or less continuous production process takes place. Identity testing may be performed on a particular volume of concrete and shall be agreed between the supplier and the purchaser.

The most commonly specified property of concrete is compressive strength and most control plans have been derived for this property. However, also conformity criteria for other properties than strength are mentioned in EN 206-1 “Concrete – Part 1: Specification, performance, production and conformity” as e.g. consistence, density, W/C-ratio, cement content, air content and chloride content. The latter properties are related to durability requirements.

Conformity control is always based on a sample of limited size, from which inferences are made for the whole population. Hence, there is always a risk of taking the wrong decision. This means that in some cases "good" concrete will be rejected and "bad" concrete will be accepted. The associated risks are called respectively the producer's risk and the consumer's or client's risk. It is not straightforward to elaborate a control plan which satisfies all parties involved and to fix the mentioned risks for which no absolute criteria are available. Traditionally, a large variety of conformity criteria have been proposed in national design guidelines. This paper gives a review of several aspects which have to be considered when deriving conformity criteria. It also reviews the first author's earlier proposals for a general approach for conformity control [1].

2 Basic concepts

In the sequel we shall focus on the compressive strength as the quantity to be tested. For design and production purposes the specified characteristic strength f_{ck} corresponds to the 5%-fractile of the theoretical strength distribution of the concrete class considered (Fig. 1). In practice, the fraction below the specified f_{ck} will be smaller or higher than 5%. We shall call θ the fraction of test results below f_{ck} in the offered strength distribution (Fig. 1), hence

$$P\left[X \le f_{ck}\right] = \theta \tag{1}$$

with X the compressive strength, considered as a random variable.

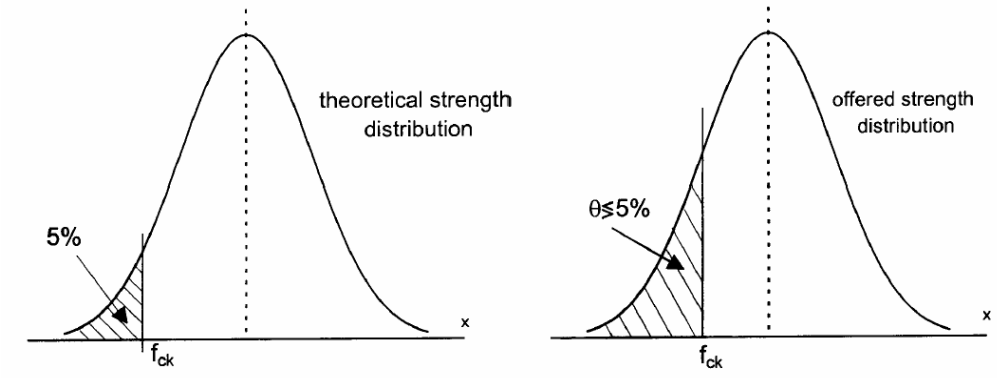

Fig. 1 : Theoretical and offered strength distributions

For an assumed strength distribution function and for a given conformity criterion, one can calculate the probability that a concrete lot, characterized by a value of θ, is accepted. This probability is called the probability of acceptance and denoted as P_a. The function $P_a(\theta)$ is called the operating characteristic of the criterion and is commonly abbreviated as OC-line. The OC-line has a typical shape as shown in Fig. 2. The ideal OC-line would be the line ABCD, which is described as $P_a = 1$ for $\theta < 0.05$ and $P_a = 0$ for $\theta > 0.05$. This OC-line, corresponding to a hypothetical sample of infinite size, has the greatest discriminating capacity i.e. the related conformity criterion allows to make a perfect distinction between good and bad productions. Practical OC-lines like AED show no specific variation at θ_2 =

0.05. A production with $\theta_2 > 0.05$ still has a significant probability of acceptance and a producer realizing $\theta_1 < 0.05$, will find out that his production is not always accepted.

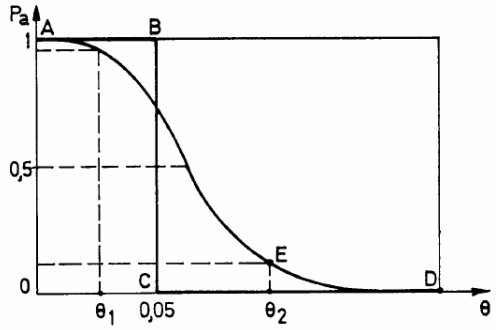

Fig. 2 : General shape of an OC-line

3 Types of conformity criteria

Common conformity criteria are of the following types

$$\bar{x}_n \geq f_{ck} + \lambda \cdot \sigma \tag{2}$$

$$\bar{x}_n \geq f_{ck} + \lambda \cdot s_n \tag{3}$$

$$\bar{x}_n \geq f_{ck} + k_1 \tag{4}$$

$$x_{min} \geq f_{ck} - k_2 \tag{5}$$

where $\bar{x}_n$ is the sample mean, σ the known standard deviation of the strength population, s_n the sample standard deviation, x_{min} the smallest strength value in the sample and λ, k_1 and k_2 parameters.

Consider criterion (2). Assuming a normal strength distribution, it can be shown that

$$P_a = \Phi\left[-\sqrt{n}\,(u_\theta + \lambda)\right] \tag{6}$$

where $\Phi(.)$ is the standardized cumulative normal distribution function and u_θ is the standardized normal variable corresponding to θ for which holds $\theta = \Phi(u_\theta)$. It is quite common to represent the corresponding OC-line in a diagram with transformed scales according to the inverse of the function $\Phi(.)$. In this case, the OC-line becomes a straight line as can be seen in Fig. 3. In this figure line A is the OC-line for $\lambda = 1.64$ and $n = 10$. The slope of the OC-line is proportional to $n^{0.5}$. This is in agreement with the fact that the larger the sample, the better the discriminating capacity of the conformity criterion. If λ increases (decreases) for constant n, then the OC-line shifts to the left (right). For $u_\theta = -\lambda$, $P_a = 50\%$. The corresponding value of θ is called the indifference quality level. As there are two parame-

ters in the criterion i.e. λ and n, it is possible to derive a conformity criterion for which the OC-line passes through two fixed points in the (θ, P_a) diagram.

For criterion (3) the exact probability of acceptance is given by the non-central t-distribution. However, generally good approximations are obtained by making use of the normal distribution. A possible approximation is given by

$$P_a = \Phi\left[-\sqrt{\frac{n}{1+\frac{\lambda^2}{2}}}\,(u_\theta + \lambda)\right] \tag{7}$$

which means that, by the fact that σ is not known but replaced by the sample estimate s_n, the slope of the OC-line is reduced by a factor $(1 + \lambda^2/2)$. In case $\lambda = 1.4$, then $1 + \lambda^2/2 = 1.98$ which means that the sample size needs to be doubled in order to obtain the same OC-line as for the case that σ is known.

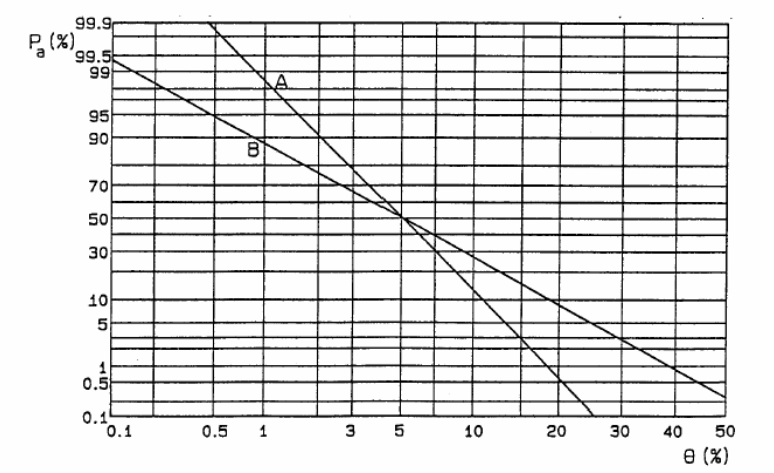

Fig. 3 : OC-lines for $\bar{x}_{10} \geq f_{ck} + 1.64 \cdot \sigma$ (A: independent observations ; B: correlated observations)

Criteria of the type (4) can be rewritten as

$$\bar{x}_n \geq f_{ck} + \left(\frac{k_1}{\sigma}\right) \cdot \sigma \quad \text{or} \quad \bar{x}_n \geq f_{ck} + \lambda' \cdot \sigma \tag{8}$$

which is the same structure as (2) with $\lambda' = k_1/\sigma$. A value of σ needs to be adopted for the evaluation of λ' and the calculation of the OC-line. Generally criteria of the type (4) are only applied to small samples (n = 3 to 10). OC-lines for criteria of the type (5) can be calculated by making use of the binomial distribution. Generally these criteria are used in combination with criteria of the type (3) and (4) which results in the following compound criteria

$$\begin{cases} \bar{x}_n \geq f_{ck} + \lambda \cdot s_n \\ x_{min} \geq f_{ck} - k_2 \end{cases} \quad (9)$$

$$\begin{cases} \bar{x}_n \geq f_{ck} + k_1 \\ x_{min} \geq f_{ck} - k_2 \end{cases} \quad (10)$$

The usual interpretation is that both criteria must be satisfied in order to accept the concrete production in case of product certification or the lot in case of identity testing. The calculation of the probability of acceptance of compound criteria is complicated by the fact that both criteria are not independent. This means that the global probability of acceptance P_a is not equal to the product of the probabilities of acceptance of the separate criteria i.e. $P_{a1} \times P_{a2}$. This is due to the fact that the events expressed by both inequalities are dependent. In case x_{min} is very small, it is likely that also $\bar{x}_n$ will tend to be small. This trend should not be accounted for twice as would be the case by the application of the product rule. Hence $P_a > P_{a1} \times P_{a2}$. The exact calculation of P_a is quite complicated [5]. Generally, one has to make use of Monte-Carlo simulation or numerical integration of integral expressions. It is interesting to point out that, especially for high n-values, the major contribution of the minimum value criterion to rejection takes place in the region with low θ values where it is not necessary to reduce P_{a1} of the mean value criterion.

OC-lines corresponding to criteria of the type $\bar{x}_n \geq f_{ck} + \lambda \cdot s_n$ are independent of the standard deviation σ of the strength distribution (Fig. 4, case A). OC lines for criteria: $\bar{x}_n \geq f_{ck} + k_1$ shift to the right with increasing σ (case B), whereas the opposite effect is found for criteria of the type $x_{min} \geq f_{ck} + k_2$ (case C). In the case of compound criteria, the first effect is generally predominant and a shift to the right results with increasing σ (case D). This different behaviour has some particular consequences with respect to the concrete producer's strategy.

In cases B and D (Fig. 4) it follows that, for a given θ, a production with low σ values has a lower probability of acceptance compared to a production with higher σ, which can give rise to the following situation. Consider the two basic types of behaviour that are depicted in the left hand side of Fig. 5, and premise that a target of P_a is available. In order that two producers (with different values σ_1 and σ_2), have the same probability of acceptance, it is necessary that they realize different fraction defectives ($\theta_2 > \theta_1$) in the first case of Fig. 5, whereas in the second case $\theta_1 = \theta_2$ (lower part of figure). For the rather extreme case depicted in the upper part of Fig. 5 it is possible that both producers can realize the same mean value. In other words, to obtain the same target P_a value, the influence of the mean value is predominant whereas the standard deviation is of less importance. However, the situation represented in the lower part of Fig. 5 is completely in accordance with the notion of characteristic strength and clearly reflects the fact that in the case of high σ values, it is necessary to strive for a higher μ value in order to reach the target probability of acceptance. The situation represented in the upper part of Fig. 5 is rather extreme because the equality of the means only occurs for a target P_a equal to 50%. Nevertheless, the effect is still important for realistic target values.

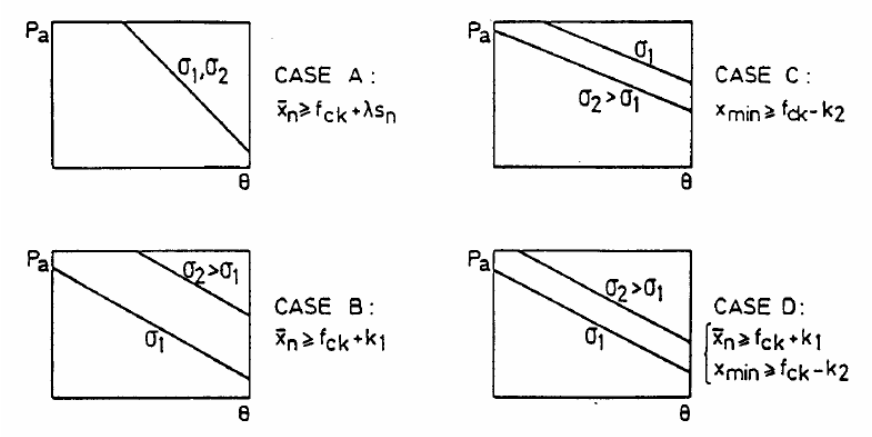

Fig. 4 : Influence of σ on the location of OC-lines for different criteria

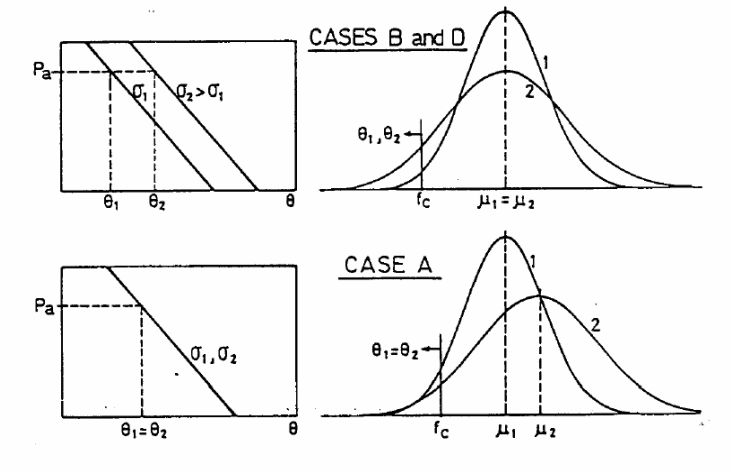

Fig. 5 : Comparison of offered distributions which yield the same probability of acceptance

In the case of correlated observations the variance of $\bar{x}_n$ is larger than in the case of independent observations, for which it equals σ^2/n. The result is that the slope of an OC-line also decreases as shown in Fig. 3 for the criterion $\bar{x}_{10} \geq f_{ck} + 1.64 \cdot \sigma$ (line B). Hence, there is a significant influence of the correlation structure on OC-lines. More details can be found in [6].

4 Derivation of conformity criteria

4.1 Traditional approach

Traditionally, the parameters appearing in conformity criteria are derived on the basis of an Acceptable Quality Level (AQL) or Limiting Quality (LQ) (Fig. 6). The AQL is a numerical definition of "good" quality. It is the maximum percent below the specified characteristic strength that can be considered satisfactory over a production period. The producer's risk α is the probability that a good lot will be rejected by the sampling plan (Fig. 6). A

sampling plan should have a low producer's risk for quality which is equal to or better than the AQL. In some plans α is fixed at 5%, in other plans it varies from about 1% to 10%.

The consumer's risk β is the probability that a "non-conforming" lot will be accepted by the sampling plan (Fig. 6). The risk is stated in conjunction with a numerical definition of "bad" quality such as the Limiting Quality (LQ). The LQ is the level of results below the specified characteristic strength that is unsatisfactory and therefore should be rejected by the sampling plan. A consumer's risk of 10% is common. The criteria presented in ISO 3951 "Sampling procedures and charts for inspection by variables for percent nonconforming" are of the type given in equation (3) and based on the AQL concept.

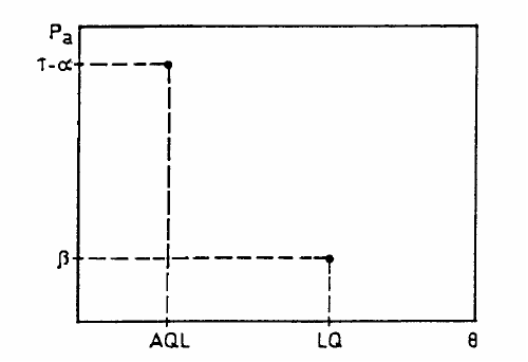

Fig. 6 : AQL (Acceptable Quality Limit), LQ (Limiting Quality) and associated risks

4.2 General remarks

Before the introduction of unified design guidelines at the European level, quite different conformity criteria for concrete strength were used in the various European countries, although the procedures for the design of structural elements were nearly the same. An attempt to arrive at a more unified approach can be found in the 1978 Edition of the CEB-FIP Model Code for Concrete Structures (MC 78) [8] where compound criteria of the type (9) and (10) were introduced. These types of criteria are also mentioned in ENV 206 (1989) and EN 206-1 (2000) [9].

Once the type of criterion is fixed, the next stage is to derive numerical values for the parameters. In principle, two points in the θ-P_a diagram could be fixed (see e.g. Fig. 6) and the corresponding parameter values calculated. This yields one value for λ and one value for n.

However, 2 problems occur. Primarily it is not easy to find representative values for AQL, LQ, α and β which satisfy the needs of both producers and purchasers. Choices of these parameters are to a large degree arbitrary. Secondly conformity control is often performed on the basis of samples with different sizes.

An obvious choice could be λ = 1.64. The corresponding OC-line for the criterion $\bar{x}_n \geq f_{ck} + 1.64 \cdot \sigma$ gives P_a = 50% for θ = 5%, which means that a producer who produces the target 5%-fractile, can expect a rejection of his production in one out of two cases. In

Fig. 3 the OC-line for n = 10 is shown. For lower values of θ, the probability of rejection remains fairly high, unless n would be increased. Hence, an approach is needed which yields sufficiently safe and economic solutions. A first attempt in this sense can be found in MC78 where so-called “unsafe” and “uneconomic” regions were indicated in the θ-P_a diagram. However, the origin of these regions is unclear.

4.3 The average outgoing quality limit

Another index which is used for sampling plans is the Average Outgoing Quality Limit (AOQL). The AOQL is the worst, or "limit", of average quality of outgoing product including accepted lots and rejected lots which have been screened. The AOQL concept stems from the relationship between the fraction defective before inspection (incoming quality) and the fraction defective after inspection (outgoing quality) when inspection is nondestructive and rejected lots are screened.

If θ is the incoming quality, $P_r = 1 - P_a$ the probability of lot rejection and if all rejected lots are screened and made free of defects (i.e. $\theta = 0$), then

$$\mathrm{AOQ} = \theta \cdot P_a + 0 \cdot P_r = \theta \cdot P_a \tag{11}$$

The calculation assumes that all defective units in the accepted lots are retained in the lots while all defective units in rejected lots are identified and either repaired or replaced by nondefective units. As θ increases with θ and P_a decreases with increasing θ, the function $\theta \cdot P_a$ goes through a maximum which is the AOQL (Fig. 7). The AOQL is most frequently used for inspection by attributes. However, there is no principle objection in using it for inspection by variables too [7]. The fact that all rejected lots have to be made free of defects is no major problem for concrete since rejected lots are subjected to more detailed inspection. In case of low strength, upgrading measures will be taken in order to assure adequate structural safety. From this point of view we can state that a rectification of rejected lots will take place such that $\theta \approx 0$ is a reasonable assumption.

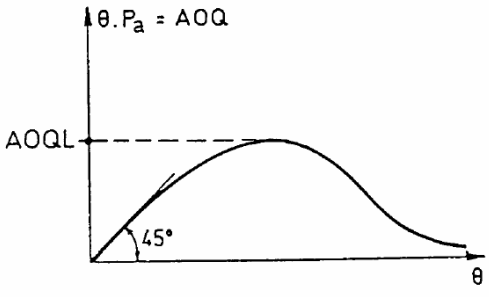

Fig. 7 : General evolution of AOQ as a function of θ

The OC-lines derived by Taerwe [1] are based on the AOQL concept, whereby AOQL = 5%, or from (11) AOQL = $(\theta.P_a)_{max} = 0.05$. As in the commonly applied semi-probabilistic safety format f_{ck} is defined as the 5 %-fractile, it results that the curve

$$\theta \cdot P_a = 0.05 \tag{12}$$

is a boundary for the unsafe region. This boundary line is plotted in Fig. 8, in the region θ > 5%. It is located in the same region as the former CEB-boundary, which proves the operational suitability. Values of λ for criteria corresponding to AOQL = 5% or $(\theta P_a)_{max} \leq$ 0.05 are given in Tab. 1 for the case of independent observations and for the case of correlated observations according to a particular AR(2)-model [2,3,6]. OC-lines tangent to the unsafe region for the case of independent observations are shown in Fig. 8.

Tab. 1 : Values of λ of the type $\bar{x}_n \geq f_{ck} + \lambda \cdot s_n$ with OC-line tangent to (12)

n	Independent observations	AR(2)-model
3	1.76	2.67
4	1.52	2.20
5	1.43	1.99
6	1.38	1.87
7	1.36	1.77
8	1.34	172
9	1.33	1.67
10	1.33	1.62
11	1.32	1.58
12	1.32	1.55
13	1.32	1.52
14	1.32	1.50
15	1.32	1.48

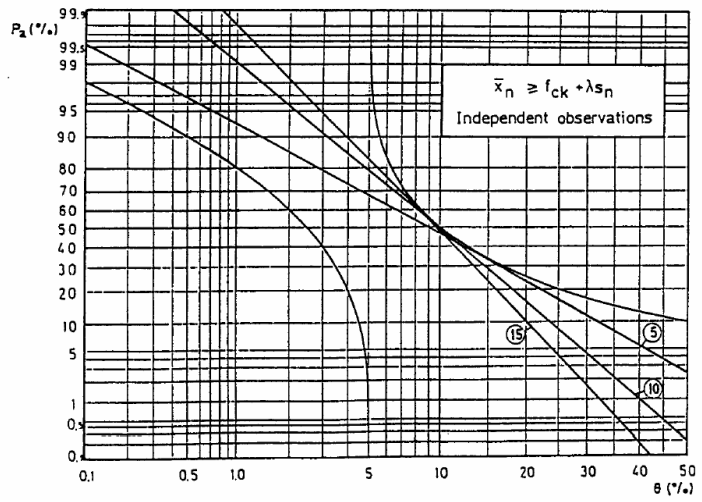

Fig. 8 : OC-lines for independent observations and n = 5, 10, 15

When the AOQL concept is used, its value is fixed at 5%, corresponding to the definition of f_{ck}. This choice is quite fundamental since for safety reasons we are interested in the average fraction defective of the outgoing lots. No arbitrary assumptions had to be introduced for determining the parameter λ, and no discussion about balancing risks between different parties is necessary. When n decreases, the slope of the OC-line decreases as well as its discriminating capacity. In that case, both the producer's and consumer's risk increase. Hence the consequences of changes in sample size are balanced between the two parties involved.

5 OC-curves for conformity criteria in EN 206-1

In the current standard EN 206-1 the following two conformity criteria are mentioned for concrete strength:

1. A compound criterion of the type (13) in the case of initial production with $n = 3$ and $k_1 = k_2 = 4$

$$\begin{cases} \bar{x}_n \geq f_{ck} + k_1 \\ x_{min} \geq f_{ck} - k_2 \end{cases} \tag{13}$$

2. A compound criterion of the type (14) in the case of continuous production with $n \geq 15$ and $\lambda = 1.48$

$$\begin{cases} \bar{x}_n \geq f_{ck} + \lambda \cdot \sigma \\ x_{min} \geq f_{ck} - k_2 \end{cases} \tag{14}$$

Although it was indicated in this paper that a criterion of the type $\bar{x}_n \geq f_{ck} + \lambda \cdot s_n$ is more appropriate according to the notion of characteristic strength (cf. Fig. 5), the European standard makes use of a criterion of the type (14). In this case σ has to be estimated on the basis of at least 35 consecutive strength values taken over a period exceeding three months and which is immediately prior to the production period during which conformity is to be checked. This σ value may be introduced in (14) on condition that the standard deviation of the latest 15 results (s_{15}) does not deviate significantly from σ. This is considered to be the case if

$$0.63 \cdot \sigma \leq s_{15} \leq 1.37 \cdot \sigma \tag{15}$$

which is the 95% acceptance interval. If condition (15) is not satisfied a new estimate of σ has to be calculated from the last available 35 test results.

Let us first investigate the case of independent observations. For different values of σ, Fig. 9 illustrates the probability of acceptance in the case of initial production. Except for the case $\sigma = 3$ MPa, the OC-curves cross the unsafe region given by (12).

Fig. 10 illustrates the probability of acceptance in the case of continuous production (without autocorrelation) and $n = 15$. For all σ values the curves remain in the acceptable region, but the OC-line is far from optimal, because it doesn't reach the unsafe region.

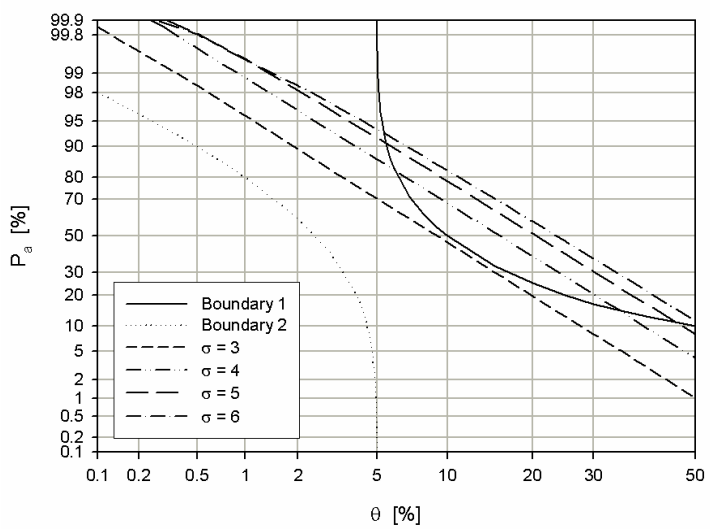

Fig. 9: Compound criterion for initial production (EN 206-1) and independent observations

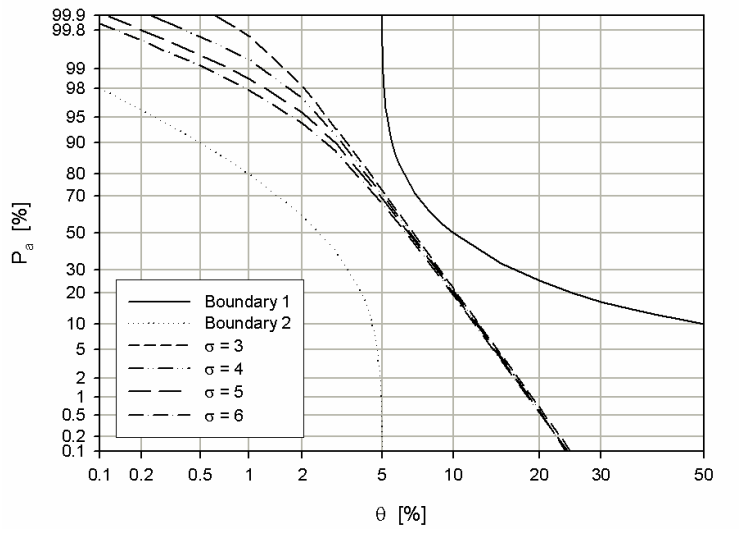

Fig. 10 : Compound criterion for continuous production (EN 206-1) and independent observations

Let us now consider the fact that realistic concrete strength records present an undeniable autocorrelation between consecutive values [2, 6]. This autocorrelation can easily be applied in the Monte Carlo simulations by using an AR(2)-model as selected in [3, 6]. Application of this model on the compound criteria in EN 206-1 yields Figs. 11 and 12, for the case of initial production and continuous production respectively. The same conclusions as the independent observations can be indicated. The slope of the OC-curves decreases significantly. Hence, autocorrelation needs to be incorporated in the derivation of the parameters in conformity criteria.

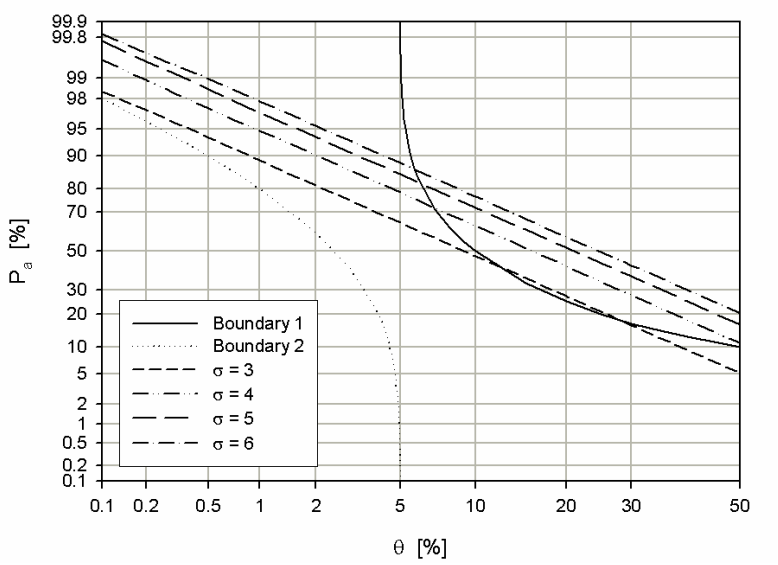

Fig. 11 : Compound criterion for initial production (EN 206-1) and correlated observations

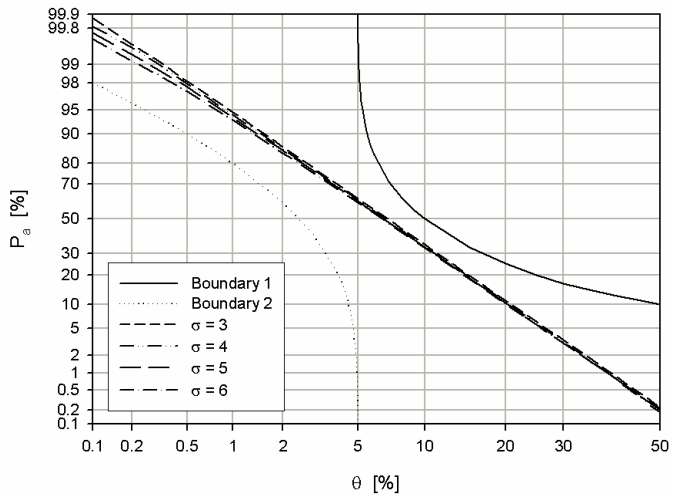

Fig. 12 : Compound criterion for continuous production (EN 206-1) and correlated observations

6 Conclusions

1. The calculation of OC-lines is briefly explained. The influencing factors and the particular aspects of the different types of criteria are indicated.

2. It is proposed to derive conformity criteria on the basis of the AOQL concept (Average Outgoing Quality Limit). In this way OC-curves that are tangent to the AOQL-boundary can be derived, which leads to balanced producer's and consumer's risks.

3. The OC-lines corresponding to the conformity criteria for concrete strength in EN 206-1 fall within the zone on the OC-plot that is both safe and economic. The OC-curves could however be optimized using the approaches mentioned in this paper.

4. Autocorrelation of subsequent strength records can be modelled by means of auto-regressive time-series. Incorporation of this aspect significantly decreases the descriminating capacity of the conformity criteria.

7 Acknowledgement

ROBBY CASPEELE is a Research Assistant of the FWO Research Foundation of Flanders. The authors wish to thank the FWO for the financial support on the research project "Probabilistic formulation of the influence of conformity control on the strength distribution of concrete and the safety level of concrete structures by means of Bayesian updating techniques".

8 References

[1] Taerwe, L.; A general basis for the selection of compliance criteria, *IABSE Proceedings P-102/86*, 1986, pp. 113-127.

[2] Taerwe, L.; Serial correlation in concrete strength records, *Special Publication ACI SP-104 "Lewis H. Tuthill International Symposium on Concrete and Concrete Construction"*, Detroit, 1987, pp. 223-240.

[3] Taerwe, L.; Aspects of the stochastic nature of concrete strength including compliance control (in Dutch), *Doctoral thesis*, Ghent University, Ghent, Belgium, 1985.

[4] Taerwe, L.; Detection of inherent heterogeneities in cement strength records by means of segmentation, Uniformity of Cement Strength, *ASTM STP 961*, E. Farkas and P. Klieger Eds., American Society for Testing and Materials, Philadelphia, 1987, pp. 42-65.

[5] Taerwe, L.; Evaluation of compound compliance criteria for concrete strength, *Materials and Structures*, 1988, pp. 13-20.

[6] Taerwe, L.; Influence of autocorrelation on OC-lines of compliance criteria for concrete strength, *Materials and Structures*, 1987, Vol. 20, pp. 418-427.

[7] Govindaraju, K.; Single sampling plans for variables indexed by AQL and AOQL, *Journal of Quality Technology*, Vol. 22, No. 4, pp. 310-313.

[8] CEB-FIP Model Code for Concrete Structures, *CEB-Bulletin d'Information no. 124/125*, Paris, 1978.

[9] CEN Concrete – Part 1 : Specification, performance, production and conformity, *EN-206-1*, 2000.

Tragfähigkeitsbewertung aus Versuchen- Probenanzahl versus Aussagesicherheit

Dr.-Ing. Milad Mehdianpour
Bundesanstalt für Materialforschung und -prüfung, Berlin

Zusammenfassung: Der Einfluss der Probenanzahl auf die erreichbare Aussagesicherheit bei der experimentellen Tragfähigkeitsbewertung wird anhand von zwei statistischen Methoden, der variablen und der attributiven Methode, vorgestellt. Der mathematische Hintergrund der attributiven Methode wird kurz beleuchtet. Bei der attributiven Methode zeigt sich insbesondere der Vorteil, in vielen Fällen ohne Zerstörung der Prüflinge, Aussagen hinsichtlich der Tragsicherheit im Gebrauchszustand machen zu können. Es wird eine Möglichkeit gezeigt, bei unveränderten Anforderungen an Aussagesicherheit die Prüflast und den Stichprobenumfang zu variieren und gegeneinander aufzurechnen. Der Einsatz der attributiven Methode wird an zwei Fallbeispielen vorgeführt.

1 Einleitung

Die Bewertung der Tragfähigkeit von Bauteilen erfolgt in der Regel rechnerisch, experimentell oder kombiniert aus beiden Methoden. Bei der rechnerischen Modellierung stellt die realitätsnahe Annahme der Materialeigenschaft bzw. -verhalten häufig ein größeres Problem dar als die Erfassung der realen Bauteilgeometrie. In vielen Fällen eröffnet die experimentelle Untersuchung die einzige Möglichkeit einer realistischen Bewertung der Tragfähigkeit, wenn präzise Eingangsinformationen für ein Rechenmodell oder gar ein geeignetes Rechenmodell fehlt. Die richtige Anwendung experimenteller Methoden setzt ein fundiertes Know How über die Versuchstechnik, über die mechanischen Zusammenhänge und oft die Beachtung der Probabilistik voraus. Bei falscher Anwendung kann die experimentelle Methode die Realität verfälscht widerspiegeln. Neben einer sorgfältigen Planung der Belastungskonfiguration, der Lagerungsbedingungen und der Versuchsdurchführung spielt die Auswertung bzw. die Bewertung der Versuchsergebnisse eine sehr wichtige Rolle. Jeder Bauteilwiderstand ist infolge vieler Einflussparameter in Wirklichkeit eine Zufallsgröße, weshalb zur Auswertung statistische Verfahren angewandt werden müssen, wenn Ergebnisse aus mehreren Prüfungen vorliegen. Die durchgeführten Prüfungen

stellen im Sinne der Statistik eine Stichprobe dar. Der Umfang der Stichprobe stellt einen wichtigen Parameter dar, von der die Sicherheit der Aussage über die Grundgesamtheit entscheidend abhängt. Es ist einleuchtend, dass diese Aussagesicherheit mit sinkender Probenanzahl schwindet.

Aus Kostengründen bzw. auch aus Gründen des Denkmalschutzes besteht häufig die Aufgabe darin, anhand von Untersuchungen an einer repräsentativen Stichprobe möglichst geringen Umfangs, zuverlässige Aussagen für die Grundgesamtheit abzuleiten.

2 Theoretische Grundlagen

2.1 Allgemein

Zur Auswertung von Versuchsergebnissen wird ausgehend von einer statistischen Verteilung der Tragfähigkeitswerte ein Grenzwert geschätzt, welcher von einem Mindestprozentsatz aller Bauteile erreicht wird. Häufig beeinflusst die Materialeigenschaft die Tragfähigkeit eines Bauteils dominierend bzw. in vielen Fällen ist es möglich, andere Unsicherheiten des Systems vor dem Versuch zu erfassen, zu eliminieren und gesondert zu berücksichtigen. Im Bauwesen wird hinsichtlich der Materialeigenschaft i. d. R. die 5%-Fraktile als Grenzwert festgelegt. Ein Sicherheitsfaktor $\gamma_M = \gamma_m \cdot \gamma_{m,sys}$ deckt noch weitere Unsicherheiten bei der Ermittlung der Beanspruchbarkeit eines Bauteils ab.

Die Aussage über den 5%-Fraktilwert, basierend auf der Untersuchung einer Stichprobe begrenzten Umfangs, ist nur als Schätzung möglich, d. h. sie trifft nur mit einer gewissen Wahrscheinlichkeit zu, welche als Aussagewahrscheinlichkeit bzw. Konfidenz bezeichnet wird. Sie wird in verschiedenen Bereichen des Bauwesens unterschiedlich festgelegt (Bsp. Stahlbau DIN 18800: 5%-Fraktile bei 75% Aussagewahrscheinlichkeit oder Betonstahl DIN 488: 5%-Fraktile bei 90% Aussagewahrscheinlichkeit). Das Fraktil bei einer geforderten Aussagesicherheit lässt sich in Abhängigkeit des Umfangs der getesteten Stichprobe ermitteln. Es gibt verschiedene Methoden, eine Stichprobe zu prüfen und den Fraktilwert zu schätzen. Man unterscheidet zwischen der „variablen“ und der „attributiven“ Prüfmethode, wobei die attributive Methode die strengere Prüfmethode ist und konservativere Ergebnisse liefert. Während bei der variablen Methode aus dem Mittelwert und Standardabweichung einer Versuchsreihe die konkrete Größe der Beanspruchbarkeit als 5%-Fraktil ermittelt wird, wird bei der attributiven Methode lediglich bewertet, wie viele Proben eine gewisse Eigenschaft z. B. die Mindestfestigkeit als 5%-Fraktil besitzen.

2.2 Variable Methode

Bei der variablen Methode wird bei jedem Versuch der Zahlenwert für eine Messgröße bestimmt und aus den vorliegenden Zahlenwerten unter Beachtung des begrenzten Stichprobenumfangs n eine statistisch abgesicherte „Größe“ entwickelt. Wie bereits oben erwähnt, handelt es sich bei der statistisch abgesicherten Größe hier um den 5%-Fraktilwert bei einer bestimmten Konfidenz. Unter Zugrundelegung einer Normalverteilung der Ver-

suchswerte liefert die mathematische Statistik aufbereitete Gleichungen, woraus der im Bauwesen geforderte statistisch abgesicherte Schätzwert der $\hat{x}_p$ ermittelt werden kann:

$$\hat{x}_p = \bar{x} - k_1 \cdot s_x \qquad (1)$$

mit $k_1 = k(n, p, 1-\alpha)$ — k_1-werte der nicht-zentralen t-Verteilung

n — Umfang der Stichprobe

p — p-Fraktil

$1\text{-}\alpha$ — Vertrauensniveau bzw. Aussagesicherheit

$$\bar{x} = \frac{1}{n}\sum_{i=1}^{n} x_i \qquad \text{Mittelwert der Stichprobe} \qquad (2)$$

$$s_x = \sqrt{\frac{1}{1-n}\sum_{i=1}^{n}(x_i - \bar{x})^2} \qquad \text{Standardabweichung} \qquad (3)$$

und x_i — i-te Realisation der Stichprobe (Nummer des Einzelversuchs).

Die k_1-Werte sind in den einschlägigen Statistikbüchern tabelliert. Abbildung 1 zeigt exemplarisch den Verlauf der k_1-Werte zur Ermittlung des 5%-Fraktilwertes einer Versuchsreihe in Abhängigkeit der Probenanzahl für 90% bzw. 75% Aussagesicherheit. Aus dem steil abfallenden Verlauf der Kurven ist zu erkennen, dass insbesondere bei geringen Pro-

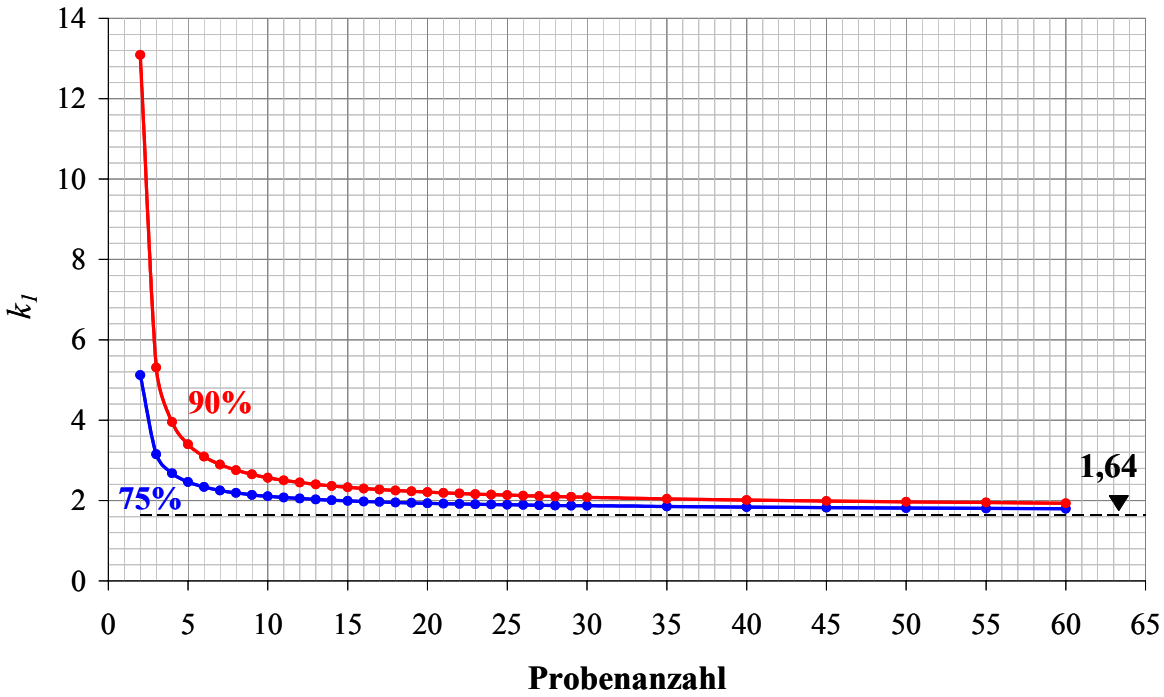

Abb. 1: Verlauf der k_1-Werte der nicht-zentralen t-Verteilung für die 5%-Fraktile in Abhängigkeit der Probenanzahl für 90% bzw. 75% Aussagesicherheit

benzahlen etwa unter 5 jeder zusätzlicher Versuch erheblich zu Steigerung der Aussagesicherheit beitragen kann. Da für $n \to \infty$ die t-Verteilung in die Normalverteilung übergeht, konvergieren die Kurven gegen den Wert 1,645. Der Betrag 1,645 entspricht dem z-Wert der Standardnormalverteilung für die 95%- bzw. 5%-Fläche unter der Verteilungskurve. Zur Ermittlung des p-Fraktils $\hat{x}_p$ wird nach (1) das Produkt aus dem k_1-Wert und der Standardabweichung S_x von dem Mittelwert $\bar{x}$ der Versuchsreihe subtrahiert. Die Subtraktion kann insbesondere bei großer Streuung der Versuchswerte - worauf man als Prüfer keinen Einfluss hat- sehr kleine bzw. gar negative Werte liefern, die physikalisch nicht sinnvoll sind. Dies liegt unter anderem an der zugrunde gelegten Normalverteilung der Versuchswerte. Ab einem Variationskoeffizienten von etwa 0,2 empfiehlt es sich daher eine andere Verteilung wie z. B. die Log-Normalverteilung anzunehmen [1]. Das p-Fraktil ergibt sich dann aus der Multiplikation des Mittelwertes $\bar{x}$ mit einem anderen Beiwert k_2, der ähnlich wie der k_1-Wert der einschlägigen Literatur entnommen werden kann.

2.3 Attributive Methode

Die attributive Methode wird häufig zum Zwecke der Qualitätsprüfung von Serienprodukten eingesetzt. Bei der attributiven Methode wird aus einem Los eine Stichprobe des Umfangs n entnommen und durchgeprüft. Das Los soll einen gewissen Maximalanteil an „schlechten“ Proben (Schlechtanteil p) besitzen. Diese Hypothese ist auf Wahrheit zu prüfen. Es sind entsprechend viele Proben im Los vorhanden, sodass die Stichprobenentnahme den Schlechtanteil kaum beeinflusst. Bei jedem Test der n Proben wird lediglich kontrolliert, ob die Probe die erwartete Eigenschaft hat und damit „gut“ ist oder nicht (sog. „ ja-nein-Prüfung“). Das Prüfergebnis entscheidet darüber, ob die Hypothese über den maximalen Schlechtanteil p im Los zutrifft und das gesamte Los anzunehmen oder abzulehnen ist. Ist dabei die Anzahl i der „schlechten“ Stücke größer als eine festgelegte Annahmezahl A_c, so wird das gesamte Los abgelehnt. Im Sinne von Bauteilprüfungen zeigen beispielsweise gute Bauteile eine Mindesttragfähigkeit, schlechte nicht. Nach bestandener Prüfung einer Stichprobe des Umfangs n, kann auf die Tragsicherheit aller ähnlichen Bauteile des Bauwerks geschlossen werden.

Zur mathematischen Erläuterung der attributiven Methode werden zunächst die wichtigsten Parameter nochmals zusammengefasst:

- n der Stichprobenumfang = Anzahl der Prüfungen
- p Schlechtanteil im Los in %
- A_c Annahmezahl (die maximal akzeptierbare Anzahl der schlechten Proben, wenn n Stück getestet werden)
- P_a Annahmewahrscheinlichkeit (Wahrscheinlichkeit, dass die Prüfung positiv ausfällt und das Los angenommen wird)

Die Wahrscheinlichkeit P_a, das Los nach der Prüfung anzunehmen, hängt ab von p, n und vor allem von A_c. Sie ergibt sich nach Überlegungen, welche auf dem Gesetz des

BERNOULLI-Experiments basieren. Die Wahrscheinlichkeit bei einem Schlechtanteil von p, nach n Tests genau i schlechte Stücke zu erhalten ergibt sich zu

$$P(\text{"genau i Treffer"}) = \binom{n}{i} \cdot p^i \cdot (1-p)^{n-i} \tag{4}$$

Die Wahrscheinlichkeit, höchstens A_c schlechte Stücke zu erhalten (also $i=0$ oder $i=1$ oder ... $i=A_c$) ergibt sich aus der Summe der Einzelwahrscheinlichkeiten (Unabhängigkeit der Proben vorausgesetzt) zu

$$P(i \le A_c) = \sum_{i=0}^{A_c} \binom{n}{i} \cdot p^i \cdot (1-p)^{n-i} \tag{5}$$

Mit einer Wahrscheinlichkeit von $P(i \le A_c)$ treten höchstens A_c schlechte Stücke auf, was gleichzeitig die Wahrscheinlichkeit dafür ist, dass die Stichprobe die Prüfung besteht und damit das gesamte Los angenommen wird. Die Annahmewahrscheinlichkeit $P(i \le A_c)$ ist bei „strengen" Testbedingungen oder durch Festlegung einer kleinen Annahmezahl A_c entsprechend gering. Je kleiner A_c ist, umso kleiner ist $P(i \le A_c)$ und umso geringer ist das „Risiko", ein evtl. schlechtes Los zu akzeptieren. Wird in einer Hypothese behauptet, dass es im Los maximal den p-Anteil an schlechten Proben gibt und es wird auf maximal A_c in n geprüft, so stellt $P(i \le A_c)$ die Unsicherheit α der Hypothese dar. Das Einserkomplement $W = 1 - P(i \le A_c)$ ist demnach dann Testsicherheit bzw. Aussagesicherheit [2].

$$W = 1 - \alpha \tag{6}$$

Anders als bei der Qualitätskontrolle einer laufenden Produktion ist bei Bauwerksprüfungen häufig die vorliegende Stichprobenzahl gering und man ist folglich bestrebt, auch die Annahmezahl möglichst gering zu halten und setzt von vornherein $A_c=0$. Solche Prüfungen werden in der Literatur als „Success-Run" bzw. „Erfolgslauf" bezeichnet [3]. Dadurch vereinfacht sich die Gleichung (5) zu:

$$P(i=0) = \binom{n}{0} \cdot p^0 \cdot (1-p)^n$$

$$P(i=0) = (1-p)^n \tag{7}$$

bzw.

$$\alpha(i=0) = (1-p)^n$$

Durch Umstellung von (7) kann dann festgestellt werden, wie viele Prüfungen erforderlich sind, um auf ein bestimmtes Sicherheitsniveau schließen zu können. Werden beispielsweise Stahlbauteile untersucht, deren Tragfähigkeit vorwiegend von der Materialeigenschaft bestimmt wird, ist es sinnvoll, die Kombination des 5%-Fraktils bei einer Aussagesicherheit von 75% zugrunde zulegen [4]. Geprüft wird dann gegen ein aus dem Fraktilwert der Beanspruchbarkeit abgeleitetes Mindestmaß an Tragfähigkeit ${}_{min}x$, das ggf. weitere Systemunsicherheiten in Form von höherer Prüfkraft berücksichtigen könnte. Löst man die Gleichung (7) nach n auf, erhält man die Gleichung (8), nach der dann 27 Success-Run-

Tests erforderlich wären. Da es sich hier um Success-Run-Tests handelt, wurde $\alpha(i=0)$ durch α abgekürzt.

$$\alpha = (1-p)^n \Rightarrow n = \frac{\ln \alpha}{\ln(1-p)}$$

$$0{,}25 = 0{,}95^n \Rightarrow n = \frac{\ln 0{,}25}{\ln 0{,}95} = 27 \qquad (8)$$

In der Regel ist die Entnahme bzw. die Prüfung von 27 Bauteilen nicht erwünscht und wäre, abgesehen von dem Aufwand, häufig aus der Sicht des Bestandschutzes nicht vertretbar. Um dennoch mit einer praxisgerechten Anzahl von Proben die gewünschten Zuverlässigkeitsaussagen zu erhalten, können die Prüflasten über den geforderten Mindestmaß an Tragfähigkeit ${}_{min}x$, angehoben werden. Dabei ist natürlich darauf zu achten, dass die technischen Grenzen nicht verletzt werden. Im Folgenden soll gezeigt werden, wie bei unveränderten Anforderungen an Zuverlässigkeit bzw. Konfidenz die Prüflast und der Stichprobenumfang variiert und gegeneinander aufgerechnet werden können.

Abbildung 2 zeigt beispielhaft die angenommene Dichte- und die Wahrscheinlichkeitsverteilung der Tragfähigkeit aller Bauteile eines Loses (Grundgesamtheit) unter Zugrundelegung einer Normalverteilung (σ und μ nicht genau bekannt). Die Annahme einer normalverteilten Grundgesamtheit wird hier als gut zutreffend postuliert. In der Praxis sollte dies immer mit Hilfe von statistischen Tests gesondert geprüft werden, da das Ergebnis durch die zugrunde gelegte Verteilung entscheidend beeinflusst werden kann.

Das Los soll auf einen Schlechtanteil von maximal 5% geprüft werden, entsprechend wur-

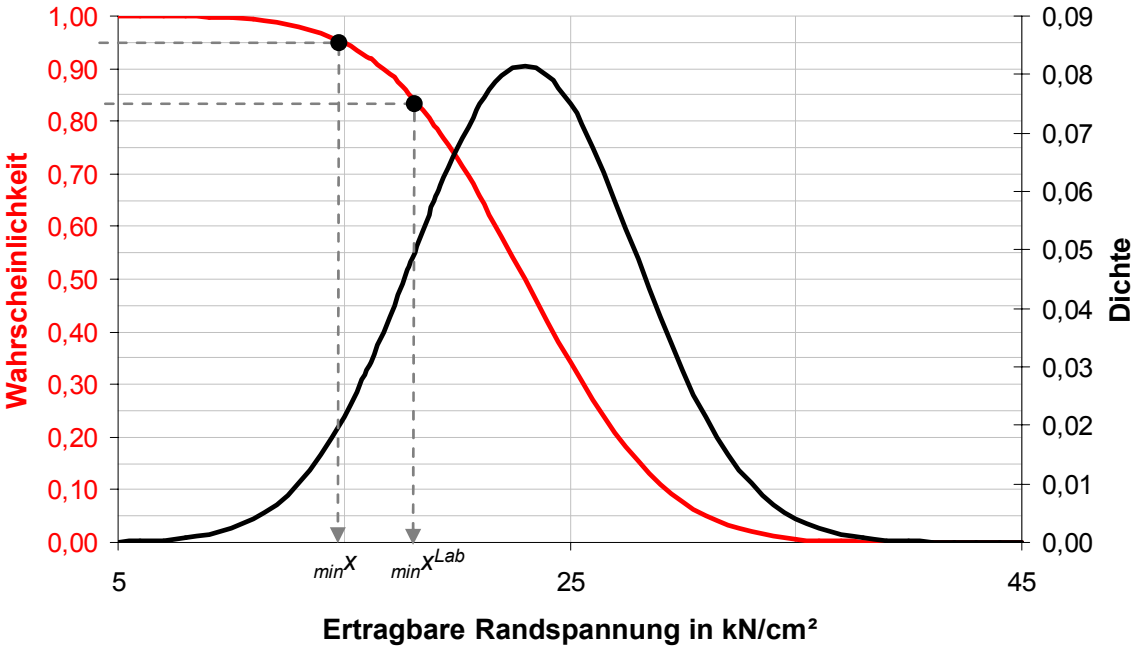

Abb. 2 geschätzte Dichte- und Wahrscheinlichkeitsverteilung von Tragfähigkeitswerten (Altstahlbauteile)

de ${}_{min}x$ (inklusive evtl. Sicherheitsbeiwert fürs System) festgelegt. Mit einer Wahrscheinlichkeit von 95% erreicht oder überschreitet jedes beliebig aus dem Los herausgegriffene Stück die Mindestbeanspruchbarkeit ${}_{min}x$. Würden 27 Bauteile geprüft werden, wobei alle ${}_{min}x$ erreichen, liegt die Annahmewahrscheinlichkeit bzw. die statistische Unsicherheit nach der Gleichung (7) bei

$$\alpha = (1 - 0{,}05)^{27} = 0{,}25 \tag{9}$$

und damit die Aussagesicherheit bei 0,75. Verschärfte man bei n = 27 die Prüfbedingungen, indem ${}_{min}x$ auf ${}_{min}x^{Lab}$ anhebt, sinkt naturgemäß die Annahmewahrscheinlichkeit. Sollten alle 27 Prüflinge den verschärften Test bestehen, hätte man hinsichtlich der Aussage „maximal 5% Schlechtanteil im Los“ eine viel größere Aussagesicherheit als zuvor gefordert. In dem Beispiel der Abbildung 2 bewirkt die erhöhte Prüflast, dass nur 84% aller Bauteile ${}_{min}x^{Lab}$ überschreiten könnten bzw. entsprechend evtl. 16% Schlechtanteil gibt. Die überhöhte Aussagesicherheit, wenn alle 27 Prüflinge ${}_{min}x^{Lab}$ überschreiten, liegt bei

$$\begin{aligned} \alpha &= (1 - 0{,}16)^{27} = 0{,}009 \\ W &= 1 - 0{,}009 = 0{,}991 \end{aligned} \tag{10}$$

Um bei der verschärften Prüfbedingung mit ${}_{min}x^{Lab}$ wie zuvor die gleiche Aussagesicherheit von 75% zu erhalten, müsste die Anzahl der Prüfungen reduziert werden.

$$0{,}25 = 0{,}84^{n} \Rightarrow n = \frac{\ln 0{,}25}{\ln 0{,}84} = 8 \tag{11}$$

Mit anderen Worten: Das Los wird nicht auf dem Niveau der 5%-Fraktile untersucht, sondern wie in dem Beispiel gezeigt auf dem Niveau der 16%-Fraktile, wodurch viele Proben eingespart werden können, falls der Success-Run-Test bestanden wird. Wegen des steilen Verlaufs der Wahrscheinlichkeitsverteilungskurve in dem Bereich, in dem üblich operiert wird und wegen der ln-Funktion bewirkt eine geringfügige Verschärfung der Prüfbedingung eine große Ersparnis an erforderlichen Proben.

Im Folgenden wird für das Beispiel eine Beziehung für die Festlegung der verschärften Prüfbedingung ${}_{min}x^{Lab}$ abgeleitet. Die Vorgehensweise lässt sich analog für andere Verteilungsformen und Fraktilwerte anwenden.

Um die Tabellen der standardisierten Normalverteilung verwenden zu können, werden die z-Transformierten nach Gleichung (12) betrachtet.

$$z = \frac{x - \mu}{\sigma} \tag{12}$$

Die z-Variablen der Standardnormalverteilung betragen jeweils

$$\begin{aligned} &\text{für } 95\% \qquad z_{5\,\%} = 1{,}64 \\ &\text{für } 84\% \qquad z_{16\%} = 1{,}00 \end{aligned} \tag{13}$$

Aus dem Verhältnis der z-Variablen

$$\frac{z_{5\,\%}}{z_{16\%}} = 1{,}64 \tag{14}$$

wird durch die Anwendung von (12) für ${}_{min}x$ und ${}_{min}x^{Lab}$ folgende Beziehung aufgestellt

$$1{,}64 = \frac{\frac{{}_{min}x - \mu}{\sigma}}{\frac{{}_{min}x^{Lab} - \mu}{\sigma}} = \frac{{}_{min}x - \mu}{{}_{min}x^{Lab} - \mu} \tag{15}$$

Nach der Umstellung erhält man für die verschärfte Prüfbedingung im Labor

$${}_{min}x^{Lab} = \frac{{}_{min}x + 0{,}64 \cdot \mu}{1{,}64} \tag{16}$$

Da es sich um die ein und dieselbe Grundgesamtheit handelt, ist ein Success-Run-Test mit 8 Proben auf dem Niveau von ${}_{min}x^{Lab}$ hinsichtlich der Zuverlässigkeitsaussage gleichwertig mit einem Success-Run-Test mit 27 Proben auf dem Niveau von ${}_{min}x$. Während sich ${}_{min}x$ aus dem charakteristischen Wert der Beanspruchbarkeit ableiten lässt, ist für Gleichung (16) μ als Mittelwert der Grundgesamtheit zu schätzen oder der einschlägigen Literatur zu entnehmen.

3 Fallbeispiele

3.1 Deutschlandhalle Berlin

Der mittlere Bereich der Deutschlandhalle (sog. Laterne) wird auf einer rechteckigen Fläche von 95 m x 58 m von einer stützenfreien Dachkonstruktion überspannt, bestehend aus 58 m langen Spannbetonbindern, verlegt im Abstand von 11 Metern. Zwischen den Spannbetonbindern liegen Stahlbetonpfetten im Abstand von 2 m. Den Raumabschluss bilden ca.

Abb. 3: Deutschlandhalle in Berlin
Bildquelle: http://www.berlin-china.net/zonglan/lueyou/berlin360/images/messe_deutschlandhalle.jpg

5200 Porenbetonplatten (Ytong) von 2,00 m x 0,50 m mit einer Dicke von 7,5 cm. Über den Porenbetonplatten befindet sich eine bituminöse Ausgleichsschicht von einigen Zentimetern und eine mehrlagige Dachpappenabdichtung. Die mit statisch anrechenbaren punktgeschweißten Bewehrungsmatten (glatte Stäbe) versehenen Porenbetonplatten tragen die Dachlasten und dienen gleichzeitig als Wärmeisolierung. Das Dach ist für Revisionsarbeiten begehbar. In den vergangenen Jahren wurde das Dach regelmäßig inspiziert und teilsaniert. Es wurden trotzdem immer wieder kleinere Stücke Porenbeton auf dem Hallenboden und im Tribünenbereich gefunden. Gegen herabfallende Bruchstücke wurden schließlich Abfangnetze unterhalb der Decke angebracht. Durch zahlreiche Untersuchungen und Gutachten wurden die Gefahrenpotentiale der Dachkonstruktion hinreichend dokumentiert. Ein großer Teil der Schadensaufnahmen (Sichtprüfung) konnte von einer Zwischentribüne aus, 8 m unterhalb der Deckenplatten erfolgen, vgl. Abbildung 4 links. Insbesondere in einer der letzten BAM-Gutachten wurde auf die Problematik von schadhaften Porenbetonplatten, deren Anzahl damals unbekannt war, eingegangen, vgl. Abbildung 4 rechts. Da die Bewehrung nicht gerippt ist, spielt die Betondeckung für die Tragfähigkeit der Porenbetonplatte eine große Rolle.

Im Rahmen einer umfangreichen Prüfmaßnahme wurde zunächst eine komplette Schadenskartierung durchgeführt. Alle 5200 Platten wurden zunächst einer Sichtprüfung aus nächster Nähe unterzogen. Ein direkter Zugang zu der Dachunterseite besteht nicht. Daher musste die Schadensaufnahme durch Industriekletterer durchgeführt werden. Da die Ursache für die in Abbildung 4 rechts dargestellten Schäden nicht feststand, war es umso wichtiger, möglichst alle betroffenen Platten ausfindig zu machen. Hierzu gehörte auch der Anteil derjenigen Platten, bei denen eine schalenartige Ablösung der Betondeckung bzw. eine horizontale Trennung im Material auf der Höhe der Bewehrung (bzw. Hohlstellen), welche jedoch durch die Rissverzahnung gerade noch am Bauteil hängt, vermutet wurde. Ein solcher Schaden bleibt bei einer Sichtprüfung unerkannt und kann nur durch mechanische Prüfung der Plattenunterseite z. B. durch Klopfen entdeckt werden. Eine Abklopfprüfung stellte aber einen viel höheren Prüfaufwand dar als die Sichtprüfung, da der Industriekletterer hierzu die Platte mit der Hand erreichen mussten. Da hierbei auch der Klang beim Klopfen zu beurteilen ist, ist die unmittelbare Nähe zwingend erforderlich.

Die Abklopfprüfung der Platten stellt eine ja-nein-Prüfung dar, d. h. entweder weist die

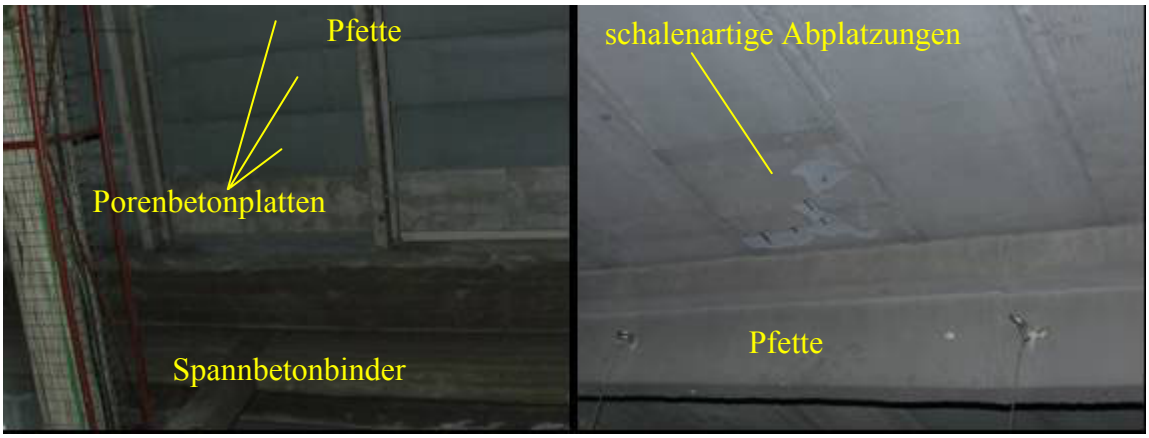

Abb. 4: links: Untersicht der Decke von der Zwischenbühne aus; rechts: schadhafte Porenbetonplatte mit schalenartiger Abplatzung der Betondeckung

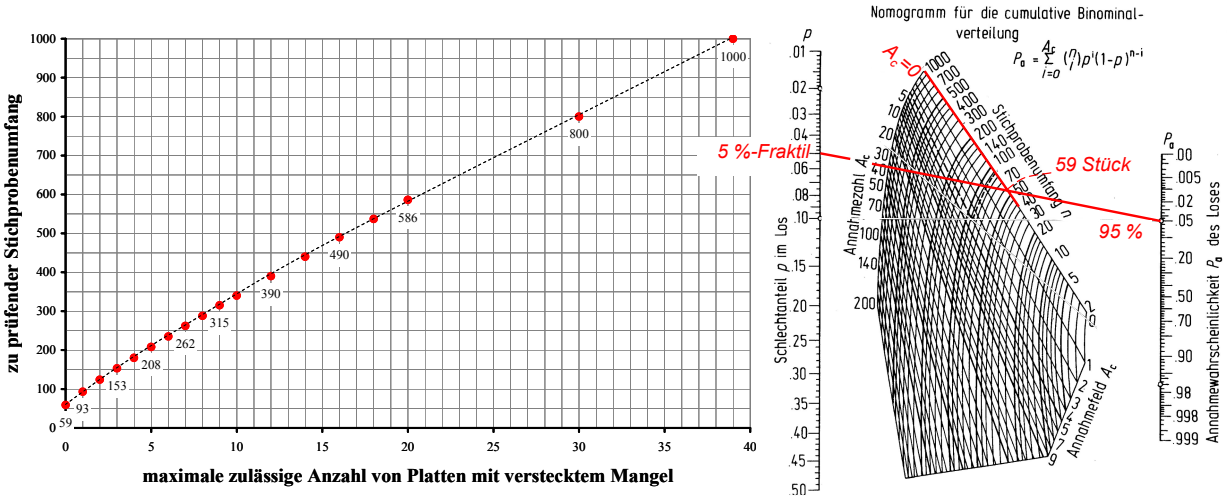

Abb. 5: Links: Prüfplan für die Abklopfprüfung; statistische Rahmenbedingungen bei maximal 5% schadhaften Platten aus einer Grundgesamtheit bei 95% Aussagesicherheit. Rechts: Nomogramm für die cumulative Binominalverteilung nach H. R. LARSON [5]

Platte einen (für die einfache Sichtprüfung versteckten) Mangel auf oder nicht. Wenn ja, ist sie im Sinne der Ausführungen unter Kapitel 2.3 als „schlecht“ zu bezeichnen. Mit Hilfe der attributiven Methode wurde ein Prüfplan aufgestellt, mit dem der Maximalanteil an schlechten Platten mit vertretbarem Aufwand abgeschätzt werden konnte. Der Prüfplan ist in Abbildung 5 im linken Diagramm dargestellt. Die einzelnen Wertepaare lassen sich mit Hilfe der Gleichung (5) berechnen oder aus dem rechts abgebildeten Nomogramm ablesen. Dort ist beispielhaft das Ablesen des ersten Wertepaares des Prüfplans rot eingezeichnet.

Ein Beispiel soll die Anwendung des Prüfplans verdeutlichen: wenn **59** (optisch unauffällige) Platten einer Abklopfprüfung unterzogen werden (vgl. Ordinate in Abbildung 5 links) und dabei **keine** fehlerhafte Platte (vgl. Abszisse in Abbildung 5 links) entdeckt wurde, dann liegt der Anteil der "schlechten" Platten bei maximal 5 %. Diese Aussage hat eine Sicherheit von 95%. Wurde aber bei der Prüfung **eine** "schlechte" Platte entdeckt, so muss der Prüfumfang auf **93** Platten erweitert werden, um eine gleichwertige Aussage machen zu können. Dabei darf keine weitere "schlechte" Platte entdeckt werden, sonst ist der Umfang wieder gemäß Prüfplan zu erhöhen.

Die Festlegung der Eingangsparameter für den Prüfplan, maximal 5% Schlechtanteil bei 95% Aussagesicherheit, erfolgte in diesem Sonderfall durch eingehende Abwägung der Gefahrensituation und die Abschätzung des Risikos eines versteckten Mangels und Berücksichtigung der Ergebnisse einer Ausfallrechnung für eine einzelne Platte. Zur Erhöhung der Sicherheit wurden die 5200 Platten bereichsweise nach Lage und früheren Beanspruchung (wie etwa Durchfeuchtung) in mehreren Grundgesamtheiten aufgeteilt und gesondert geprüft. Die Prüfung war lediglich für die optisch unauffälligen Platten vorgesehen. Platten mit offensichtlichem Schaden waren generell auszutauschen, oder abzufangen. Die zu prüfenden Platten wurden zuvor auf einem Plan festgelegt. Häufig konnte der Prüfer aus seiner Kletterposition heraus ebenso die benachbarten Platten abklopfen. Diese Maßnahme erhöhte naturgemäß den Stichprobenumfang und trug erheblich zur Aussagesicherheit bei bzw. es konnte bei gleich bleibender Aussagesicherheit von 95% auf einen

geringeren Schlechtanteil von ca. 2% geschlossen werden. Erfreulicherweise gelangen die Prüfungen als Success-Run-Tests.

3.2 Ritterschaftsbank Berlin Mitte

Das vor *1900* gebaute vierstöckige Gebäude der ehemaligen Ritterschaftsbank in der Mohrenstr. *66* in Berlin Mitte sollte saniert und teilweise umgebaut werden. Für die Sanierung des Gebäudes sollte der Bestand weitgehend erhalten bleiben. Es wurde insbesondere angestrebt, die vorhandenen Decken weiter zu nutzen. Das Deckensystem besteht, gemäß den damaligen Bauweisen, aus Stahlträgern mit zwischenliegenden preußischen Kappen. Ersten Materialuntersuchungen zur Folge weisen viele der Altstahlträger die Merkmale eines Puddelstahls auf, einige auch die eines Flußstahls. Von Altstahl sind einige ungünstige Eigenschaften bekannt, wie z. B. geringe Bruchdehnung, große Streuung der Materialeigenschaften, Inhomogenität innerhalb des Querschnitts sowie Anisotropie. Daher sollte vor der Sanierungsmaßnahme die Tragfähigkeit der Altstahlträger für den Bau- und den Endzustand untersucht und hinsichtlich der zu erwartenden Beanspruchungen beurteilt werden. Zum Einen waren für den Endzustand Deckenbelastungen bis zu 5,0 kN/m² geplant, zum Anderen wurden für den Bauzustand stoßartige Beanspruchungen durch herabfallende Trümmer erwartet. Insgesamt befinden sich an die 400 Altstahlträger im Bauwerk. Für Untersuchungen wurden 8 Träger (Walzprofile) aus dem Bestand entfernt und der BAM zur Verfügung gestellt. Die Trägerentnahme erfolgte aus verschiedenen Bereichen des Gebäudes. Es wurden statische sowie dynamische Tragfähigkeitstests an Bauteilen durchgeführt. Dem Planer sollte für den Gebrauchszustand ein Grenzwert der Beanspruchbarkeit als „zulässige Spannung“ basierend auf einem globalen Sicherheitsbeiwert im Sinne des alten Bemessungskonzepts geliefert werden. Außerdem sollte neben der Beurteilung der Beanspruchbarkeit gegenüber stoßartiger Belastung noch das Tragverhalten von Altstahlbauteilen unter kombinierter Beanspruchung durch Moment und Querkraft untersucht werden. In diesem Beitrag wird nur auf die Abschätzung des Grenzwertes der Beanspruchbarkeit als „zulässige Spannung“ eingegangen. Da die Anzahl der Proben gering war und eine Reihe von Untersuchungen unterschiedlicher Art anstand, war es wich-

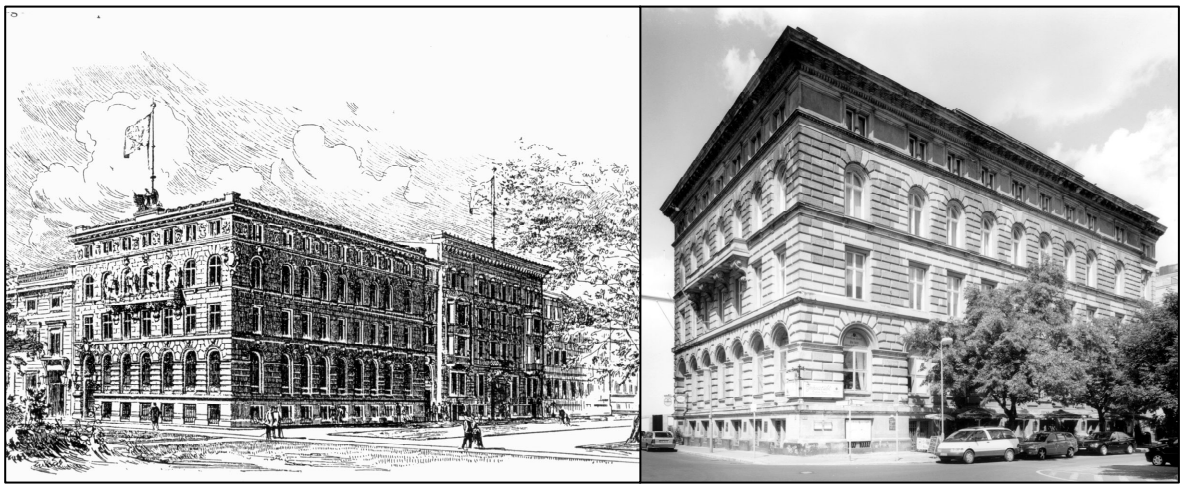

Abb. 6: Ritterschaftsbankgebäude. Links: Zeichnung von 1896: " Berlin und seine Bauten " hg. vom Architektenverein zu Berlin 1896, II. und III. Hochbau S. 372 Abb. 395. Rechts: Berlin Mohrenstr.66, Bild mit freundlicher Genehmigung von: Pitz&Hoh Werkstatt für Architektur und Denkmalpflege, September 2003

tig, den Grenzwert der Beanspruchbarkeit im Gebrauchszustand abzuschätzen, ohne die Träger zu beschädigen. Die Gewissheit, hierzu im Anschluss an alle anderen Untersuchungen abschließende Traglastversuche durchführen zu können, war vor allem wegen der anstehenden Stoßversuche nicht gegeben. Mit Hilfe der attributiven Methode war es möglich, Ergebnisse von Gebrauchslastversuchen, bei denen keine Beschädigung der Bauteile befürchtet wurde, auszuwerten und Aussagen zur Tragsicherheit im Gebrauchszustand zu treffen. Die geringe Probenanzahl wurde durch schärfere Prüfbedingungen ausgeglichen.

In Gebrauchslastversuchen wurden die Träger im Dreipunktbiegeversuch bis zu einer Grenzlast ${}_{min}x$ mehrmals be- und entlastet und die Tragfähigkeit anhand der Linearität der Kraft-Verformungskurve beurteilt. Dabei wurde kontrolliert, ob das Tragverhalten linear bleibt. Das vom Planer vorgegebene Gebrauchslastniveau entsprach einer Randfaserspannung von *10 kN/cm²*. Berücksichtigt man noch in Anlehnung an die alte Stahlbaunorm *DIN 18800 Teil 1 (3.81)* einen globalen Sicherheitsfaktor von *1,5* , so ergibt sich der geforderte Mindestwert der *5%*-Fraktile für die Tragfähigkeit der Träger im Versuch zu *15 kN/cm²*. Träger, deren Tragfähigkeit auch nur geringfügig unterhalb ${}_{min}x$ liegt, sollten im Sinne der attributiven Methode als „schlecht“ bezeichnet werden.

Unter Kapitel 2.3 wurde mit Hilfe der Gleichung (8) die Zahl *27* als die Mindestanzahl an Success-Run-Tests ermittelt, welche erforderlich wären, um bei *75%* Aussagewahrscheinlichkeit nicht mehr als *5%* Schlechtanteil in einer Grundgesamtheit anzunehmen. Hier standen aber nur *8* Träger, also höchstens nur *8* Success-Run-Tests zur Verfügung. Wie bei *8* Proben die gleiche Zuverlässigkeitsaussage erreicht werden kann, wenn die Tests mit einer höheren Laborbelastung ${}_{min}x^{Lab}$ durchgeführt werden, wurde als Beispiel in Gleichung (16) ermittelt. Für die Gleichung (16) ist die Abschätzung des Mittelwertes der Grundgesamtheit μ erforderlich. Der Mittelwert der Grundgesamtheit μ wurde unter Berücksichtigung der hauseigenen Datenbank auf der sicheren Seite liegend möglichst hoch abgeschätzt. Die statistische Berechnung der oberen Schranke für μ_{max} erfolgte mit Hilfe der *Student-t*-Verteilung unter Zulassung einer Irrtumswahrscheinlichkeit von maximal *5%*. Das Ergebnis beträgt $\mu_{max}=28,04\ kN/cm^2$.

Nach Einsetzen erhält man für die Gleichung (16)

$$ {}_{min}x^{Lab} = \frac{15 + 0,64 \cdot 28}{1,64} = 20,1 \frac{kN}{cm^2} , \qquad (17) $$

Alle 8 Bauteile konnten jeweils ihren Test auf dem mit (17) ermittelten erhöhten Beanspruchungsniveau von *20,1 kN/cm²* unbeschadet bzw. ohne Nichtlinearitäten in der Kraft-Verformungskurve bestehen. Daher wurde mit ausreichender Sicherheit auf einen Grenzwert der Beanspruchbarkeit von *10 kN/cm²* geschlossen.

4 Literatur

[1] Fischer, L.: Sicherheitskonzept für neue Normen – ENV und DIN-neu. Grundlagen und Hintergrundinformationen. Teil 3: Statistische Auswertung von Stichproben im eindimensionalen Fall (1. Forts.). Bautechnik 76 (1999), Heft 3, S. 236-253

[2] Wegener, P.: Vergleichende Untersuchungen zum Tragverhalten von Klemmkupplungen für Stahlrohrgerüste nach bestehenden deutschen Prüfvorschriften und geplanten europäischen bzw. internationalen Prüfnormen. Forschungsbericht 73, Bundesanstalt für Materialprüfung Berlin, 1980.

[3] Meyna, A.; Pauli, B.: Taschenbuch der Zuverlässigkeits- und Sicherheitstechnik. Quantitative Bewertungsverfahren. Carl Hanser Verlag München Wien, 2003.

[4] Lindner, J.; Scheer, J.; Schmidt, H.: Stahlbauten. Erläuterungen zu DIN 18 800 Teil 1 bis Teil,4. Beuth Verlag GmbH, Berlin, Wien, Zürich. 2. Auflage 1994.

[5] Larson, H.R. : A nomograph of the cumulative binominal distribution, Industrial Quality Control 23 1966/67, S. 270-278

Deflection of Concrete Members Considering Random Behaviour of Loading and Material Properties

Guido Hausmann
Institute of Concrete and Masonry Structures, University of Technology Darmstadt

Summary: Within the present paper deflection computations concerning random behaviour of loading and system parameters for a prestressed and a reinforced concrete member were accomplished. Since the load history is of particular importance for the actual stiffness distribution, computations on basis of simulated load histories were carried out. This method requires the computation of the deflection at a lot of points in time, which does not lead to acceptable time and effort of computation for complex systems. Therefore a simplified modelling of the live loads was developed, which considers the effects of load history and resulting stiffness distribution implicitly.

1 Introduction

In modern structural engineering wide span slabs and the minimization of dead load to optimize the dimensions of columns and foundation are required. These needs can be done by the use of pre-stressed concrete slabs. Due to serviceability requirements of the construction the allowable deflection becomes the main design criterion in many cases. Besides loading conditions, reinforcement ratio and compressive strength of concrete or time-dependent behaviour like creep and shrinkage, the deflection of concrete slabs is influenced by the effects of pre-stressing, i.e. the induction of bending moments and normal forces. To approach the complex system of a pre-stressed concrete slab, initially investigations of a pre-stressed and a conventional reinforced single span concrete member are carried out. For this reason a MATLAB procedure was developed, which is based on the determination of deflection at a given time using the moment-curvature relationship. Consideration of the random behaviour of the material properties is offered using Latin Hypercube Sampling. Additionally the calculation is based on a realistic differentiation between cracked and uncracked regions to obtain the realistic stiffness at a given time. Furthermore effects of unloading and repeated loading should be taken into account. For this purpose the consideration of the load history is essential. Usually the load history is unknown, therefore the calculation is based on load history simulations. Basis of these simulations

are the user category dependent live load parameters taken from JOINT COMMITTEE ON STRUCTURAL SAFETY [1]. The results of the investigations of the relatively simple single span member can be used to model more complex structural systems, e.g. pre-stressed concrete slabs. Especially simplifications of the live load history are necessary regarding the computing time.

2 Mechanical Model for Calculation of Deflection

2.1 Material Models

For the description of material behaviour of concrete under compression the stress-strain-relationship according to JOINT COMMITTEE ON STRUCTURAL SAFETY [1] is used. In comparison to the material laws according to DIN 1045-1 [2] used for deformation analysis, this material law differs especially for high strains. For a deflection analysis the occurring concrete stresses are normally below maximum concrete stress, so this difference can be neglected.

The concrete tensile strength can be calculated in relation of the compression strength according to DIN 1045-1 [2]. For the present examinations a linear stress strain relation for concrete in tension was assumed, limited by tensile strength. Modelling of complex tension softening behaviour was disregarded. To regard long term effects concerning the tensile strength, the centric tensile strength is reduced by a factor of 0.85 according to MERTSCH [3]. For the determination of cracking moment the flexural tensile strength was assumed.

The time dependent material properties of concrete include compression strength, tensile strength, young's modulus and of course creep and shrinkage. Within the scope of the present investigations time variant material properties were neglected except for creep and shrinkage effects. Creep and shrinkage coefficients were calculated according to DAFSTB-HEFT 525 [4], whereby only linear creeping behaviour was implied.

2.2 Moment-Curvature Relationship

The carrying behaviour of reinforced concrete or pre-stressed concrete sections can be modelled by the moment-curvature-relationship in good approximation. For the present examinations the calculation model of moment-curvature-relationship according to CEB FIB MODEL CODE 1990 [5] was used. Therein the tension stiffening effect is regarded relatively simple expressed by the parameter β_b.

Time dependent effects due to creep can be considered directly by modification of the stress strain relation of concrete in dependence of the current creep coefficient. Based on this modified moment-curvature-relationship and creep inducing loading this part of deflection can be calculated.

Deformations due to shrinkage are considered by applying a centric shortening of the system, which leads under consideration of the compatibility conditions with asymmetrical reinforced cross sections to a cross section curvature, which is considered in the moment-curvature-relationship as an imposed deformation. It is of particular importance whether the regarded cross section is in state I or state II. In the cracked condition (state II) the curvatures due to shrinkage increase clearly. Therefore the effects of load history have to be considered also for the deformations due to shrinkage, which are actually independent of loading conditions.

The effect of prestressing without bond for the determination of moment-curvature-relationship can be considered by an appropriate normal force. The bending moment due to prestressing is treated like an external loading.

Depending on the kind of loading different moment-curvature-relations are used for calculation. If a load arises for the first time, the relationship for instantaneous loading is used. For the deformation due to creeping the moment-curvature-relationship with modified stress strain relation of concrete and the parameters for long-term load is used.

Repeated unloading/reloading is considered according to KRELLER [6], which provides a constant stiffness for the un- and reload procedure after exceeding the cracking moment for the first time. Reloading beyond the maximum value again the relationship for monotonous load applies.

2.3 Calculation of Deflection

From the moment-curvature-relationship for each bending moment the corresponding curvatures with consideration of the non-linearity of reinforced concrete can be easily determined. The integration of these curvatures over the system leads in good approximation to the deflection. In addition the distribution of the internal forces of the examined system must be known. In statically determinate systems the distribution of the internal forces is independent of the stiffness distribution and does not have to be determined by iteration.

For the present examinations the deflection is determined separately for the three components: for instantaneous loading, creep-inducing loadings and deformation due to shrinkage. The reasons for this procedure is that depending on the deflection component both different moment-curvature-relationship and different kinds of loading (e.g. only sustained loads for deformations due to creep) have to be considered.

3 Stochastic Modelling

3.1 Stochastic Modelling of Material and System Properties

The stochastic parameters of material and system properties were derived from JOINT COMMITTEE ON STRUCTURAL SAFETY [1], STRAUSS [7] and FLEDERER [8] and are assorted in Tab. 1. Among the dimensions (h, d_1, b) the material strength (f_c, E_c, f_{ct}, f_y) are regarded as stochastic values as well. The model used to determine the moment-curvature-relationship according to CEB FIB MODEL CODE 1990 [5] considers the tension-stiffening-effect by model parameter β_b. Uncertainties of β_b are regarded by model uncertainty θ_{β_b}.

For determination of creep- and shrinkage coefficients according to DAFSTB-HEFT 525 [4] the stochastic input variables relative humidity (RH), geometry, compressive strength of concrete) are considered. Additionally model uncertainties θ_{shr} and θ_{cr} for the prediction of creep- and shrinkage coefficients are implied.

For the investigation of prestressed concrete members the uncertainties of the prestressing force and location of the tendon (eccentricity) are mentioned by model uncertainties θ_P and θ_{e1}.

The scatter of the dead loads is composed by both scatter of specific weight and spatial scatter. Concerning both components the coefficient of variation is assumed as 5 % according to GRAUBNER & GLOWIENKA [9]

Tab. 1: Stochastic parameters of material and system properties

Variable X	Type of distribution	Mean	COV
h	Normal	h_m	3 %
d_1	Normal	d_{1m}	17 %
b	Normal	b_m	10 %
f_c	Lognormal	38 N/mm²	13 %
E_c	Lognormal	35000 N/mm²	15 %
f_{ct}	Lognormal	2.6 N/mm²	30 %
f_y	Lognormal	560 N/mm²	6 %
θ_{β_b}	Lognormal	0.8	20 %
RH	Normal	70 %	10 %
θ_{shr}	Lognormal	1	15 %
θ_{cr}	Lognormal	1	15 %
θ_P	Normal	1	5 %
θ_{e1}	Normal	1	5 %
g	Normal	$b_m \cdot h_m \cdot 25\ kN/m^2$	5 %

3.2 Live Load Modelling

The live load on floors in buildings can be divided into sustained and intermittent load. Both components are characterised by intensity, duration and the time between two loading periods. The intensity of sustained loads can be approximated by a gamma distribution, intermittent loads by an exponential distribution. The required stochastic parameters are given in Tab. 2, which is taken from JOINT COMMITTEE ON STRUCTURAL SAFETY [1]. Therein σ_u regards scatter of spatial distribution and σ_v variation between storeys respectively different buildings. Note that these parameters are point in time loads.

Tab. 2: parameters for live loads depending on the user category [1]

User category	Reference Area	Sustained Load				Intermittent Load		
	A_0 [m²]	m_{st} [kN/m²]	σ_v [kN/m²]	σ_u [kN/m²]	$1/\lambda$ [a]	m_{in} [kN/m²]	σ_u [kN/m²]	$1/\lambda$ [a]
Office	20	0.5	0.3	0.6	5	0.2	0.4	0.3
Residence	20	0.3	0.15	0.3	7	0.3	0.4	1

By means of this information the standard deviation of both components are given as following:

$$\sigma_{st} = \sqrt{\sigma_v^2 + \sigma_u^2 \cdot \frac{A_0}{A} \cdot \kappa} \tag{1}$$

$$\sigma_{in} = \sqrt{\sigma_u^2 \cdot \frac{A_0}{A} \cdot \kappa} \tag{2}$$

$$\kappa_{red} = \frac{A_0}{A} \cdot \kappa \qquad \leq 1 \tag{3}$$

Therein κ regards the shape of the influence line used to determine the equivalent uniformly distributed load. The present examinations are based on $\kappa_{red} = 1$. With arising values of influence area A the scatter of spatial distribution (σ_u) becomes less important.

By means of the present input parameters a live load simulation is carried out. The principles of this live load simulation applied here were developed by SCHMIDT [10], whereas the present analysis is based on input parameters according to Tab. 2. Result of each simulation is a random live load history (Fig. 1 a), which provides the basis for the determination of deflection at each point in time of load change. Furthermore such a live load history simulation is used for determination of extreme value distributions (Fig. 1 b) supposing sufficient number of simulations.

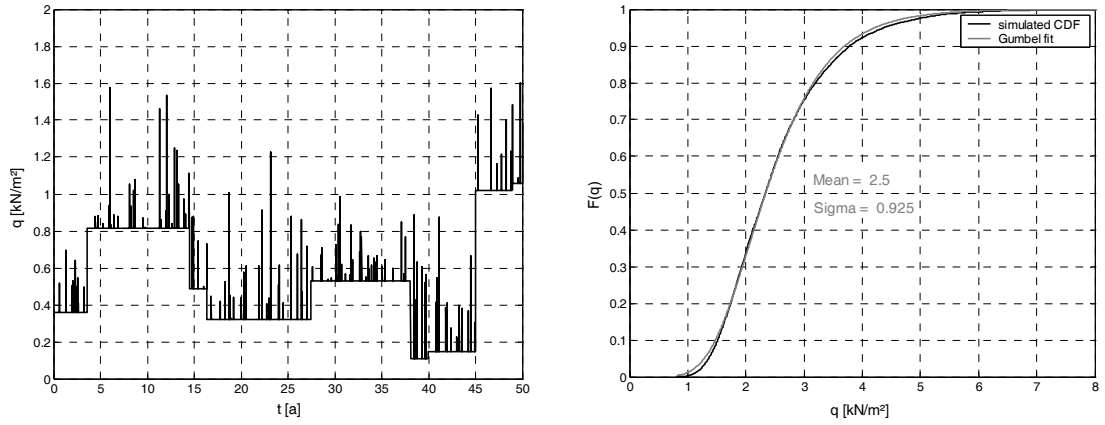

(a) Example of a simulated load history

(b) Extreme value distribution for a reference time period of 50 a including fitted Gumbel distribution

Fig. 1: Live loads for user category office

The discrete extreme value distribution based on simulation can now be fitted by an analytical extreme value distribution. GLOWIENKA & HAUSMANN [11] carried out such an analysis of extreme value distribution for extreme live loads based on simulations for different user categories, reference time periods and influence areas respectively influence line shape factors. For reference time periods longer than average occurrence rate of load changes the fitting to a Gumbel distribution is quite good. The parameters for total live loads approximated by a Gumbel distribution for reference time periods of 50 years respectively 10 years are given in Tab. 3. They are valid for the user categories office and residence which will be analysed in the following.

Tab. 3: parameters of fitted Gumbel distribution for live loads [3]

User category	T [a]	Mean	SD	COV
Office	50	2.50	0.925	37 %
	10	1.60	0.730	46 %
Residence	50	1.85	0.520	28 %
	10	1.26	0.515	41 %

4 Analysis of Selected Examples

4.1 General

Based on the input variables for material and system properties respectively load history simulations explained in chapter 3 both a prestressed concrete (example a) and a reinforced concrete member (example b) were investigated. Calculations were carried out using Latin

Hypercube sampling, an advancement of Monte Carlo method, in order to reduce the number of samples required. The main dimensions are displayed in Tab. 4.

Tab. 4: dimensions of calculated examples

Example	L [m]	h/b [cm]	A_{s1} [cm²]	A_{s2} [cm²]	A_p
a)	10	20 / 100	11.3	3.77	3 * 150 mm²
b)	6	30 / 100	9.24	---	---

4.2 Sequence of Computation

In the following section the principles of computation sequence of the deflection is represented briefly. The computations were carried out for a reference time period of 50 years. In the first step load history in dependence of the user category is simulated. At each time of a load change the deflection is computed separately due to instantaneous loading, due to creeping and due to shrinking. For the computation of the creep deformation only the sustained load portion is set as creep inducing load. The separate deformation components are summed up to get the total deformation. As result of a single computation one receives a time response of deflection. A simulated load history with associated time response of deflection is represented in Fig. 2 exemplarily for example b).

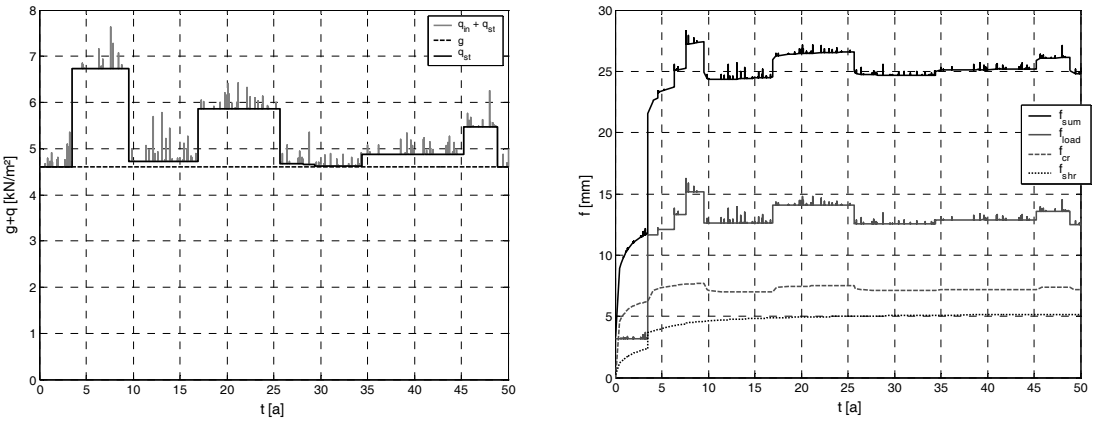

(a) simulated load history user category office (b) time response of deflection

Fig. 2: Results of a single calculation of deflection based on a simulated load history

This sequence of computation is repeated *n* times under random variation of the input parameters using Latin Hypercube Sampling. For the present investigations $n = 500$ simulations were performed. The results can be subjected to a statistic evaluation. In Fig. 3 is represented the time response of the average values, standard deviations (SD) and coefficient of variation (COV). Both examples were applied for user category office.

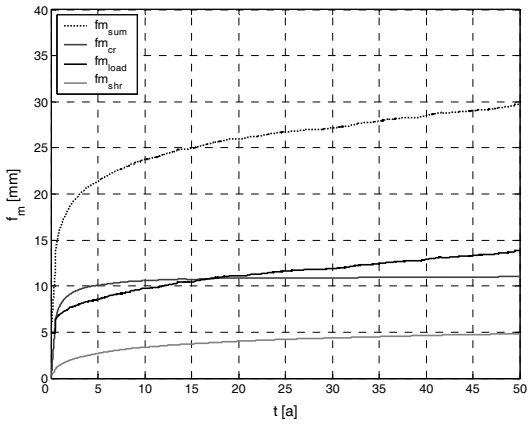

(a) time response of mean deflection example a)

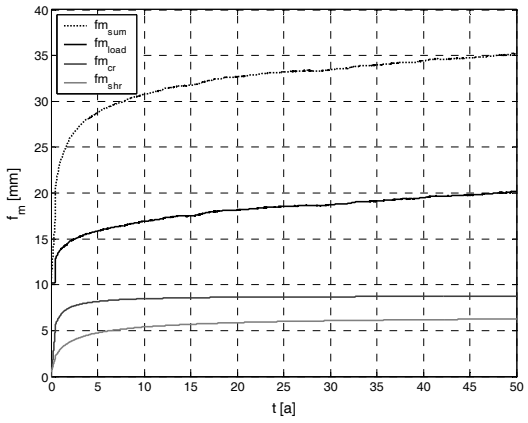

(b) time response of mean deflection example b)

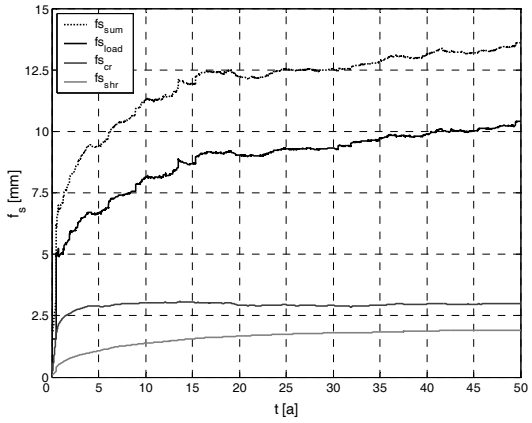

(c) time response of SD of deflection example a)

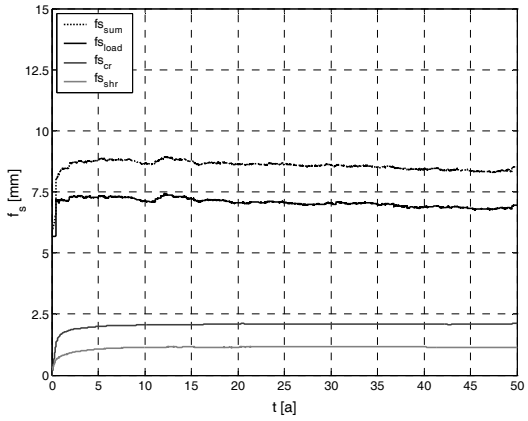

(d) time response of SD of deflection example b)

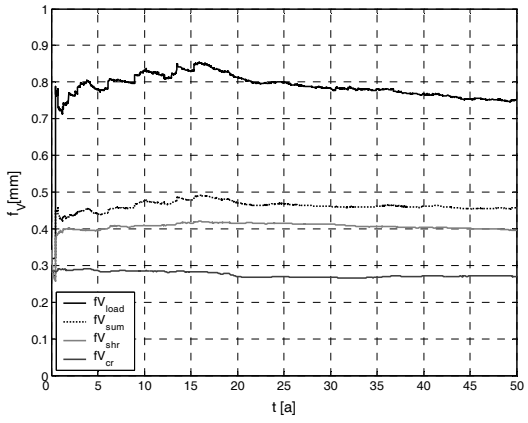

(e) time response of COV of deflection example a)

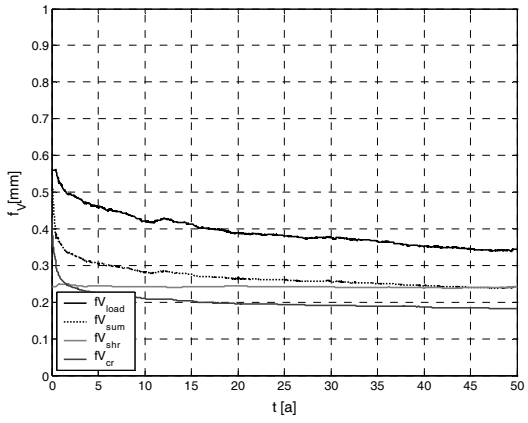

(f) time response of COV of deflection example b)

Fig. 3: statistical evaluation of deflection computation based on simulated load history

The results show that for the reinforced concrete beam a decreasing coefficient of variation of deflection with increasing service life. In contrast to this the coefficient of variation re-

mains almost constant for the prestressed concrete member. The proportional component of the creeping and shrinking deformation increases for prestressed concrete member in comparison to the reinforced concrete member, however the higher dispersion of the total deformation comes off mainly by the deformation component from instantaneous loading. Differences exist likewise in the kind of the distribution function. Fig. 4 and Fig. 5 present the extreme value distributions of the maximum deflection and the distribution functions at certain points in time (1 a, 5 a and 50 a). While for the reinforced concrete member all distribution functions can be approximated by a normal distribution, a Gumbel distribution fits well to the results of the prestressed concrete member. These differences are important for the computation of probabilities of exceeding of a defined limit value.

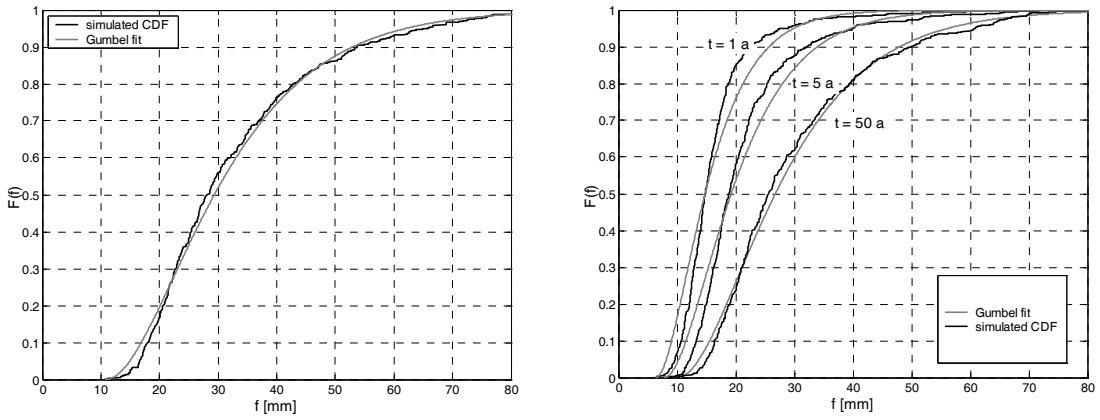

(a) Extreme value distribution of deflection

(b) distribution functions of deflection at certain points in time (1 a, 5 a, 50 a)

Fig. 4: distribution functions of deflection of prestressed concrete member (example a)

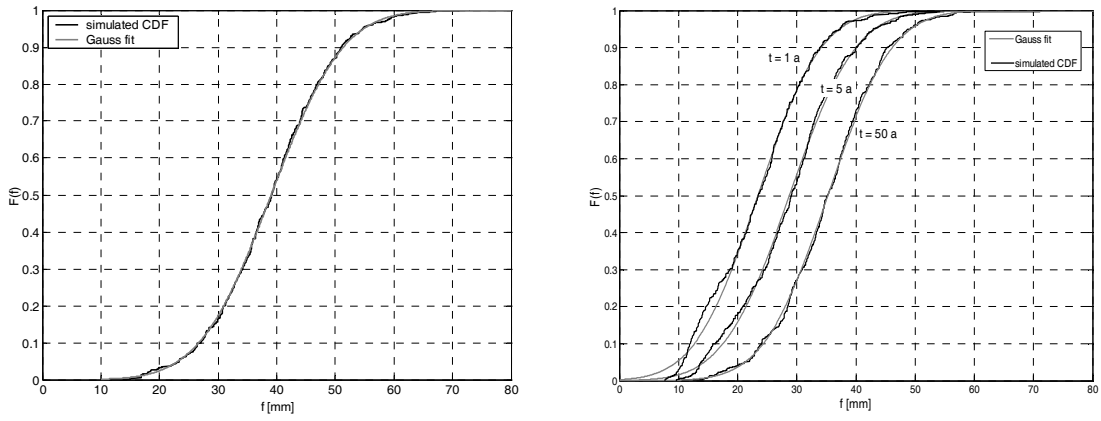

(a) Extreme value distribution of deflection

(b) distribution functions of deflection at certain points in time (1 a, 5 a, 50 a)

Fig. 5: distribution functions of deflection of a reinforced concrete member (example b)

4.3 Simplified Modelling of Live Loads

The investigations on basis of a simulated load history, as shown in section 4.2, are feasible for the relatively simple single span member still with an acceptable time and effort of computation. If more complex systems are examined e.g. prestressed concrete slabs the time and effort of computation increases substantially. Therefore a simplified modelling of live loads is suggested here, which considers the effects of load history implicitly and leads to the same results. On the one hand equivalent creep inducing loads are to be determined, on the other hand the effects of the extreme values arising in load history must be considered as well.

From comparative calculations has been obtained that the average value and the scatter of the creep deformations in good approximation a creep inducing load can be assumed which is constant in time. The value of the equivalent load corresponds to the sustained load indicated in tab. 2. Only during the first 5 years the deviations are larger in individual cases, since the value of the creep deformation depends strongly on the load amplitude at the early concrete age.

For the size of the deformations due to shrinking and direct load the extreme values occurring up to a given time is of importance. Subsequently two problems have to be solved. To obtain an extreme value distribution of the deflections for a certain reference time period (e.g. 50 a), it is sufficient to carry out the computation on basis of the appropriate extreme value distribution of the live loads. For other reference time periods T then the extreme value distribution of live loads has to be adapted accordingly. A comparison of the results of both procedures is represented in Fig. 6.

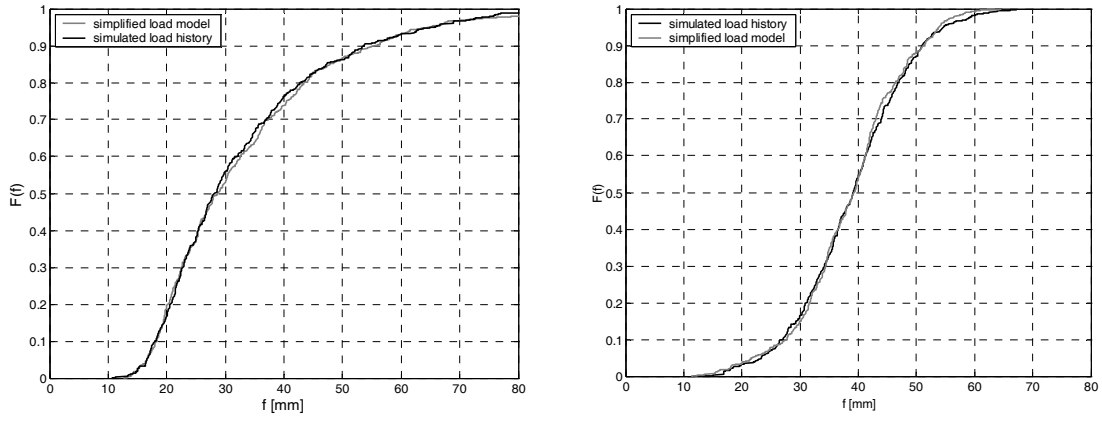

(a) pre-stressed concrete member (example a) (b) reinforced concrete member (example b)

Fig. 6: comparison of extreme value distribution based on simulated load history (user category office) and simplified load model

For the determination of the distribution function at a certain point in time t the simulated load history can be replaced by the computation of two different points in time. At the time $t\text{-}1$ the extreme value distribution of the live loads for the reference time period $T = t\text{-}1$ is used. Thus the maximum preloading of the system is included. At the point in time t the

point in time loads for the sustained load component according to Tab. 2 are applied. Thus all unloading procedures actually occurring during load history are replaced by only one unloading procedure. In Fig. 7 the distribution functions for the deflections for the points in time after 50 years for user category office are compared.

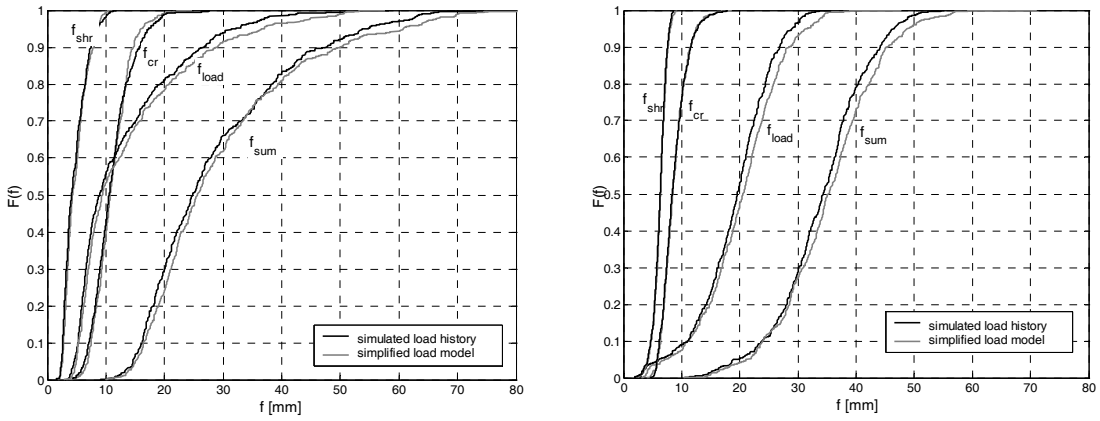

(a) pre-stressed concrete member (example a) (b) reinforced concrete member (example b)

Fig. 7: comparison of distribution functions of deflection and its components for 50 a

A good accordance of the results can be ascertained, so that the represented proceeding appears suitable to replace the extensive computation based on simulated load history. An examination of the validity for other user categories, which consist exclusively of sustained load (e.g. libraries) is still upcoming.

5 Conclusion and Outlook

In the present paper computations concerning random behaviour of loading and system parameters for a prestressed and a reinforced concrete member were conducted. Since the load history is of particular importance for the actual stiffness distribution, the computations on basis of simulated load histories were carried out. This method requires the computation of the deflection at a lot of certain points in time, which does not lead to acceptable time and effort of computation for complex systems. Therefore a simplified modelling of the live loads was developed, which considers the effects of load history and resulting stiffness distribution implicitly. Based on this load model reliability analyses can be accomplished for serviceability states of more complex structures without extensive consideration of load history and can consequently be used for the development of a design concept for limiting deflections based on a probabilistic approach.

6 References

[1] Joint Committee on Structural Safety: *Probabilistic Model Code.* (www.jcss.ethz.ch), 2001.

[2] DIN 1045-1: Tragwerke aus Beton, Stahlbeton und Spannbeton, Teil 1: Bemessung und Konstruktion. Beuth-Verlag, Berlin, 2001.

[3] Mertsch, O.: Zum Einfluss zeitvarianter Materialgesetze auf die Verformungsvorhersage von biegebeanspruchten Betonbauteilen. Universität Rostock: 2002 - Habilitation.

[4] Erläuterungen zu DIN 1045-1. *Deutscher Ausschuss für Stahlbeton (DAfStb)*, Heft 525, Beuth, 2003.

[5] CEB FIB Model Code 1990: Bulletin d'Information Nr. 203 und 204, Juli 1991.

[6] Kreller, H.: Zum nichtlinearen Trag- und Verformungserhalten von Stahlbetonstabtragwerken unter Last- und Zwangeinwirkung. Deutscher Ausschuss für Stahlbeton (DAfStb), Heft 409, Beuth, 1990.

[7] Strauss, A.: Stochastische Modellierung und Zuverlässigkeit von Betonkonstruktionen. Universität für Bodenkultur Wien, 2003 - Dissertation.

[8] Flederer, H.: Ein Beitrag zur Berechnung von Stahlverbundträgern im Gebrauchszustand unter Berücksichtigung stochastischer Größen. Dissertation Technische Universität Dresden: 2002 - Dissertation.

[9] Graubner C.-A., Glowienka S.: Zuverlässigkeitsanalysen von Stahlbetondruckgliedern unter besonderer Berücksichtigung des Teilsicherheitsbeiwertes γ_G auf der Einwirkungsseite. Abschlussbericht zum Forschungsvorhaben V 425 des DAfStb, Berlin 2005

[10] Schmidt, H.: Versagenswahrscheinlichkeit unbewehrter Wand-Decken-Verbindungen bei Gasexplosionen im Fertigteilbau. Technische Universität Darmstadt: 2003 - Dissertation.

[11] Glowienka, S.; Hausmann, G.: Hintergründe zur Festlegung der charakteristischen Werte von Nutzlasten. Manuscript Unpublished, 2006.

Structural Reliability of Sheet Pile Walls Using Finite Element Analysis

Timo Schweckendiek & Wim Courage
TNO Built Environment and Geosciences, Delft, The Netherlands

Abstract: In geotechnical design nowadays partial safety concepts like Load and Resistance Factor Design are applied in order to account for the uncertainties in the model and design parameters and to guarantee a minimum required level of reliability. It is, however, advantageous to determine the reliability level directly for many applications. It will be shown how reliability analysis for retaining structures can be carried out in a fully probabilistic manner within reasonable time effort. A case study of a deep excavation will be used to illustrate the presented concepts. Basically the approach follows the philosophy that all uncertain quantities in a design should be treated as stochastic variables instead of making conservative estimates. TNO Built Environment and Geosciences has developed the probabilistic toolbox ProBox that includes methods for reliability analysis and local sensitivity analysis. ProBox can be coupled with external models (e.g. FEM-codes) for the evaluation of the limit state function. Analytical models can be formulated in Probox directly as well. For the present example the Finite Element Code Plaxis was applied and coupled with ProBox. Level II as well as level III methods will be applied and the theory of Hohenbichler is applied to combine the failure probabilities of singular mechanisms to a system failure probability respectively reliability.

Keywords: Reliability, Retaining Structures, ProBox, Plaxis, Finite Element Method, Directional Sampling, Geotechnics, System Reliability

1 Introduction

There is a large variety of reliability methods available. However, these techniques are almost exclusively used by the scientific community and not in engineering practice. Our proposition is that this fact is not due to lack of suitable methods, but lack of user-friendliness and experience with applications.

Therefore we intend to demonstrate in this paper that reliability analysis can be carried out with reasonable time effort for specific structures whose system behavior is known. Level II as well as level III methods will be used in combination with finite element analysis. As specific example an excavation with a retaining structure consisting of a sheet pile wall and an anchor layer in layered soil is analyzed.

A significant advantage of determining the reliability of structures is that it supports the use of risk-based or probabilistic design concepts. The failure probabilities that are calculated by means of the reliability analysis are, of course, crucial elements in these approaches.

Furthermore, reliability analysis usually gives insight into the sensitivity with respect to the input variables. This information is especially useful as decision support for optimization or to know where the reduction of uncertainty or design changes have the largest effects.

The current example was chosen from the field of geotechnical engineering. The subsoil contains large uncertainties compared to other materials applied in civil engineering. The principal sources of uncertainties in soil properties are *imprecise measurements* and *inherent spatial variability*.

There are several possibilities for modeling these uncertainties. Spatial variability can for example be modeled be means of random fields. In this paper the random average approach is followed, where a soil deposit is modeled as a homogeneous material with random average properties. In fact, when following this approach, averaging effects can only be accounted for by adapting the input statistics. Since the calculation example is fictitious anyway, we do not pay attention to this detail here and assume the input parameters statistics to include the averaging effects already.

2 Proposed Methodology

For determining the *reliability* respectively the *failure probability* of a system the relevant *failure modes* and mechanisms are to be detected. In general we consider unacceptable states of the structural system as failure, like e.g. excessive deformations or plastic yielding of materials. Some of these mechanisms do not directly lead to a collapse of the system and the system exhibits some residual strength, even though it is already considered as failed. Considerations about residual strength are especially of interest for systems that might still fulfill their major essential function after reaching failure according to this definition, which is the case for water retaining structures like dikes (A dike might still retain

the water after partial failure of the inner slope.). In the present example, however, we consider residual strength to be irrelevant. The functional requirements of the structure are expressed by the limit states and omission of their fulfillments is considered failure.

For the presented approach the reliability analysis package *ProBox* (developed by TNO, The Netherlands) was coupled with the Finite Element code *Plaxis*, which is a program that is specifically suited for the analysis of geotechnical problems. The coupling of the programs consists essentially of two basic interfaces. On the one hand ProBox was enabled to amend the input data of each Plaxis calculation before its execution. Secondly the calculation output is to be accessed by ProBox in order to use it for the limit state function evaluation (see fig. 1).

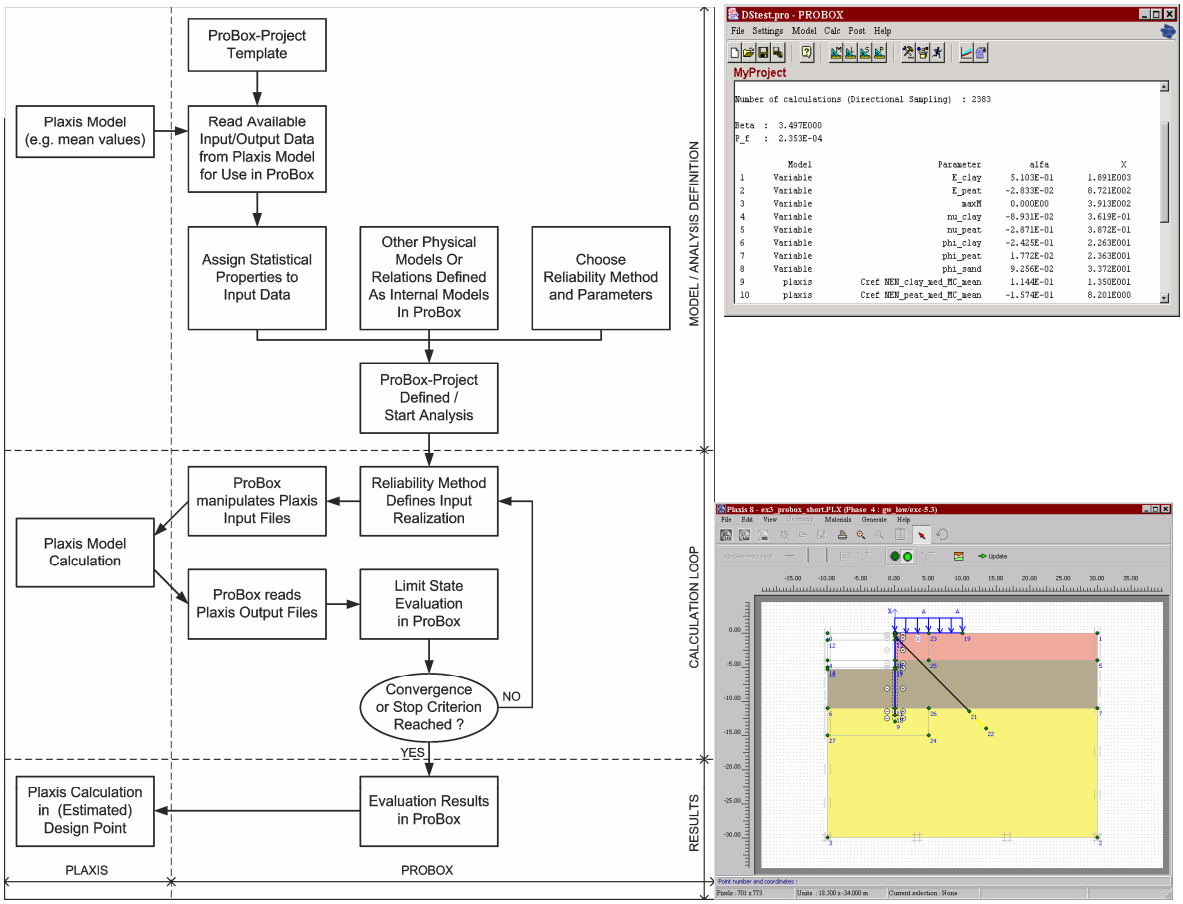

Figure 1: Coupled Reliability Analysis and Interfaces ProBox-Plaxis

In this approach the finite element analysis (FEA) is used as sort of a black box for elements of the limit state formulation. Due to the implicit nature of the limit state function, of course, all the available reliability methods in ProBox use numerical procedures, e.g. for the determination of partial derivatives. ProBox includes techniques like FORM/SORM, Crude Monte Carlo, Directional Sampling, Directional Adaptive Response Surface Sampling (DARS), Numerical Integration or combinations of these methods.

3 Example Description

The calculation example is presented before introducing the proposed method in order to give the reader a clear picture of the type of system that will be analyzed. The presented example is a simple retaining wall in sand. It consists of a sheet pile wall and one anchor layer with a whaling realized by means of two connected U-beams.

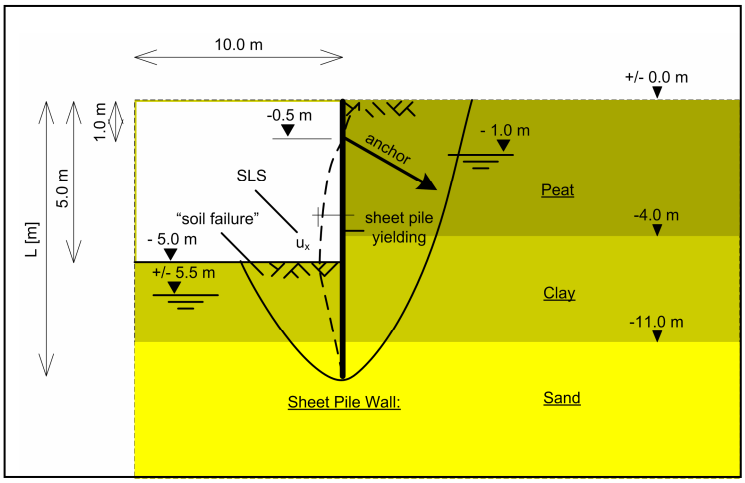

Figure 2: Retaining System Geometry

The sequence of execution is:

- 1. Installation sheet pile wall
- 2. Excavation phase 1 (-1.0 m)
- 3. Installation of anchors and whaling, prestressing of the anchors
- 4. Excavation phase 2 to final depth (-5.0 m)

The properties of the involved materials are given in table 1. For the characterization of the parameter statistics the first two central moments are used. These are based on back-calculation from typical 95%-characteristic values in the NEN6740 – table 1 (Dutch Standard for Geotechnical Design).

For stability of the calculations, avoiding ill-posed problems and physically impossible realizations of the parameters, the following distribution types are applied in the reliability analysis:

- Normal distribution: γ_{sat}
- Lognormal distribution (2-parametric): c, ϕ', ψ, E
- Beta distribution: ν ($0 \leq \nu \leq 0.5$), R_{inter} ($0 \leq R_{inter} \leq 1$)

A deterministic design was carried out on this example, which resulted in the following structural dimensions:

- Sheet pile: AZ17, length: 12.0 m
- Anchors: 440 kN capacity (S235) at mutual distance a = 2.0 m, inclination: 45°, embedment app. 1.0 m in the sand layer
- Whaling: 2xUPE220

The design was made according to the CUR 166 (Dutch Technical recommendation for Sheet Pile Structures). It was considered to belong to safety class two, which is based on a system reliability of $\beta = 3.4$.

Table 1: Soil Properties of the Calculation Example

PEAT, medium						
Name	Symbol	95%-Quantile	COV	Mean	STD	Unit
Saturated volumetric weight	γ_{sat}	12	5%	13.1	0.65	$[kN/m^3]$
Cohesion	c	5	20%	7.5	1.5	$[kPa]$
Friction angle	ϕ'	15	10%	23.9	2.39	[°]
Dilatation angle	ψ	0	0	0	0	[°]
Young's modulus	E	500	25%	850	212	$[kN/m^2]$
Poisson ratio	ν	n.a.	10%	0.35	0.035	[-]
Interface Strength	R_{inter}	n.a.	12%	0.6	0.1	[-]
CLAY, medium						
Name	Symbol	95%-Quantile	COV	Mean	STD	Unit
Saturated volumetric weight	γ_{sat}	17	5%	18.5	0.93	$[kN/m^3]$
Cohesion	c	10	20%	14.9	2.98	$[kPa]$
Friction angle	ϕ'	17.5	10%	20.9	2.09	[°]
Dilatation angle	ψ	0	0	0	0	[°]
Young's modulus	E	4000	25%	3400	850	$[kN/m^2]$
Poisson ratio	ν	n.a.	10%	0.35	0.035	[-]
Interface Strength	R_{inter}	n.a.	12%	0.6	0.1	[-]
SAND, dense						
Name	Symbol	95%-Quantile	COV	Mean	STD	Unit
Saturated volumetric weight	γ_{sat}	19	5%	-	-	$[kN/m^3]$
Cohesion	c	0	20%	-	-	$[kPa]$
Friction angle	ϕ'	35	10%	35	3.5	[°]
Dilatation angle	ψ	5	n.a.	-	-	[°]
Young's modulus	E	125,000	25%	-	-	$[kN/m^2]$
Poisson ratio	ν	0.35	n.a.	0.35	-	[-]
Interface Strength	R_{inter}	n.a.	n.a.	1.0	-	[-]

4 Failure Mechanisms

The following failure modes are the essential potential causes to set the system to the unwanted state – failure. Their definitions are applied for the formulation of the limit states of singular failure mechanisms.

4.1 Yielding of the Sheet Pile

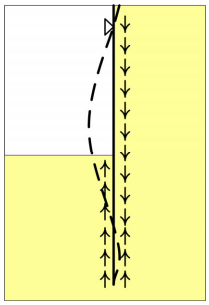

The sheet pile is subject to bending and the bending moments lead to compressive and tensile stresses. If these stresses exceed the *yield stress* σ_y of the applied steel, the structure can exhibit plastic behavior. As mentioned before, we consider plasticity in the sheet pile as failure, even though there is residual strength. There is a contribution of a normal force component, which can be accounted for via the limit state formulation.

Figure 3: Bending and Normal Loading of a Retaining Wall

If the normal force contribution is neglected, we can determine a maximum moment resistance of the sheet pile: $M_{adm} = W_{el} * \sigma_y$, where W_{el} is the elastic section modulus and σ_y is the steel yield strength. In this case the limit state can simply be formulated as:

$$Z = M_{adm} - M_{max}$$

where M_{max} is the maximum calculated bending moment.

This limit state formulation would be restricted to account for the uncertainties in the soil properties and the external loads. A more general formulation gives us the flexibility to include also the uncertainties on the resistance side and the earlier mentioned normal force contribution:

$$Z = \sigma_y - \left(\frac{M(z)}{W_{el}(z)} + \frac{N(z)}{A(z)} \right)$$

, where M(z) is the bending moment N(z) is the normal force and A(z) is the cross section area of the sheet pile.

As can be seen from the limit state formulation, some of the involved quantities are depth dependent. This distinction might is necessary, because

1. The maximum moment M_{max} and the maximum normal force N_{max} might not coincide in depth z.

2. The geometrical properties W_{el} and A might not be constant over depth, e.g. when they are effected by corrosion and this corrosion is estimated by a depth-dependent corrosion model.

Of course, all these quantities can be treated as stochastic variables, also the steel yield strength.

4.2 Failure of the Support

The principal function of an anchor in a retaining structure is its contribution to horizontal equilibrium. Basically this is composed of the *active and passive soil pressure* and the anchor force itself. Anchors consist of a grout body that serves as connection with the soil, a tensile element (e.g. a steel rod or steel cables) that connects the grout body with the retaining structure and connective elements that connect sheet pile and tensile element. We neglect the uncertainties in the connective elements, since the tensile element is considered to have a significantly higher failure probability. The grout body is treated in the next section. The tensile element itself has a certain cross section A_a and, in combination with a given anchor force F_a , the tensile stresses in the anchor can be determined by $\sigma_a = F_a / A_a$. As for

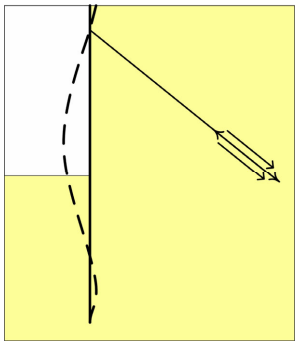

Figure 4: Anchor Loading

the sheet pile, reaching plasticity is considered as failure despite residual strength. Using design values in the above relation leads to a maximum anchor normal force capacity $F_{a,adm}$ and a simple version of the limit state would be:

$$Z = F_{a,adm} - F_a$$

, where F_a is the calculated normal force in the anchor.

The calculated normal force is constant over the anchor length, because no interaction between the anchor strands and the soil is accounted for. Another more flexible limit state function, formulated directly in terms of maximum stresses in the material, could be:

$$Z = \sigma_y - \frac{F_a}{A_a(x,z)}$$

As for the earlier described yielding of the sheet pile, this formulation has the advantage that the uncertainties can be accounted for on a more detailed level and that spatial influences (e.g. variations of the cross section area A_a due to corrosion etc.) can be examined as well.

The reliability of the waling can be determined based on the calculated anchor force F_a and the mutual anchor distance a:

$$Z = M_{adm} - \frac{F_a \cdot a^2}{8}$$

4.3 'Failure in the Soil'

In the following sections a few failure mechanisms are presented whose strength and load are determined either by the soil properties, by soil-structure interaction or both. For most of these mechanisms there are analytical approximations to determine a factor of safety or a margin of safety. However, the starting point of this research was the application of finite element analysis for the evaluation of the limit state function, because ideally it gives better approximations of the structural behavior taking interaction aspects automatically into account.

On the other hand this implies that we can usually not refer to these analytical methods in the limit state function. The limit state has to be formed based on information that is available in the results (or input) of the finite element analysis or in additional relations or material parameters.

Subsequently a number of those mechanisms are explained and possible approaches of limit state formulations are introduced, also highlighting potential problems. Finally a more crude, but robust approach is presented that would be sufficient to determine the system reliability as explained in section 5.

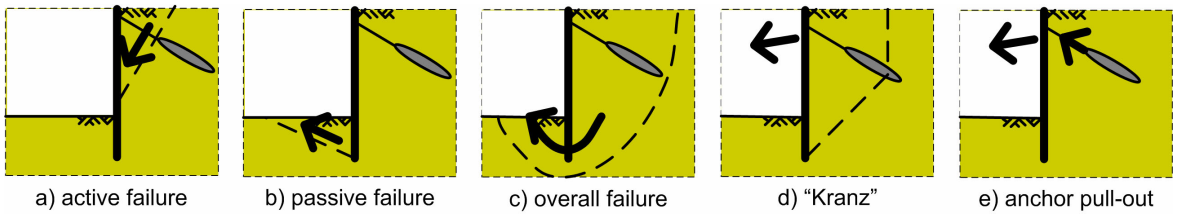

Figure 5: Failure Mechanisms in the Soil

4.3.1 Mobilized Shear Resistance in the Soil

In figure 5 we have summarized the most likely failure mechanisms for the contemplated system. The first three mechanisms are basically based on the idea that the soil shear resistance is insufficient for horizontal equilibrium (for active and passive failure a soil body is triggered to displace over a failure plane) or moment equilibrium (overall failure is comparable to a slope failure in e.g. a dike body) of the system. Therefore the available analytical methods for the handling of these mechanisms are usually based on the maximum shear resistance of the soil. The *Mohr-Coulomb* criterion can be used for this purpose.

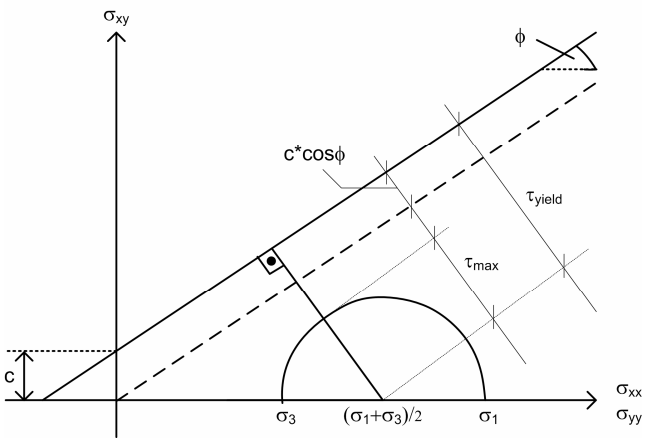

Figure 6: Mohr-Coulomb Yield Criterion (Plane-Strain)

On the one hand it is difficult to obtain the relevant quantities from the results of a finite element analysis that would be needed to directly use the earlier mentioned equilibrium approaches (active/passive soil resistance, Bishop slip circle analysis etc.). On the other hand the finite element method delivers us data that even refer more directly to the ideas where the analytical methods are based on, namely stresses and strains. As can be seen from figure 6, the stress state in a Gauss point in combination with the strength properties of the soil allow us to define a ratio between shear stress and shear resistance, which is commonly called the *mobilized shear resistance*:

$$\tau_{mob} = \frac{\tau_{\max}}{\tau_{yield}} = \frac{2\sqrt{\left(\frac{\sigma_{xx} - \sigma_{yy}}{2}\right)^2 + \tau_{xy}^{\ 2}}}{(\sigma_1 + \sigma_3)\cdot \sin\phi + c \cdot \cos\phi}$$

This ratio is a handy measure to define failure in an integration point. It is continuous in the 'safe' domain and therefore very useful for optimization or search algorithms, such as FORM or in parts also Directional Sampling. The question, however, arises where in the stress field we have to apply this measure. The fact that plasticity occurs in some integration points does certainly not imply structural failure directly. Ideally we would observe all the integration points along the expected failure surface(s). The problem is that it is not known beforehand where this surface will be situated.

One possible solution for this problem is the definition of areas around the expected failure planes. The average mobilized shear resistance $\overline{\tau_{mob}}$ can be calculated after each finite element analysis which can be used as a measure for the *margin* or *factor of safety* in the limit state function. The challenge with this approach is to define the failure criterion, i.e. how much mobilized shear resistance is equivalent to failure (unwanted state)?.

$$Z = \tau_{mob,\max} - \overline{\tau_{mob}}$$

Some tests with this criterion have shown that there are possibilities, e.g. using iterative procedures (stepwise increase of the failure criterion $\tau_{mox,\max}$) in combination with FORM, to calculate a reasonable estimate for an upper bound of the failure probability. It has to be stated that this method requires a considerable effort in adjustments and also a priori knowledge which makes it not generic and in a certain sense even subjective.

4.3.2 Displacement-Based Failure Criteria

From the previous section it becomes obvious that the definition of failure itself can be a difficult question for a whole structural system. The presented approach using information about the stress state was not robust enough to lead to answers in a generic manner. Therefore it was tried to use excessive displacements as definition of failure.

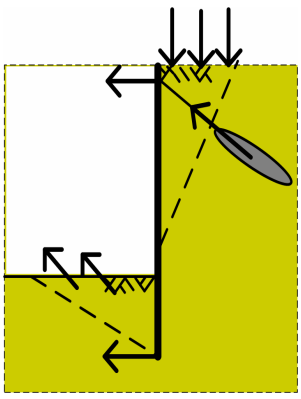

Figure 7: Possible Displacement Criteria

The arrows in figure 7 indicate locations where excessive displacements would be the result of the occurrence of one of the failure mechanisms. Therefore the limit state could theoretically be formulated as:

$$Z = \min(u_{\max,i} - u_i)$$

where $u_{\max,i}$ are admissible and u_i are calculated displacements.

There are, however, again several difficulties with the use of these criteria in combination with the reliability methods:

- Relatively large displacements are only reached in case of structural collapse. Often collapse means that the FEA does not find equilibrium and no results are available.

- If we apply algorithms like FORM, partial derivatives in a design point estimate are used for the subsequent estimate. For many of the deformation problems, these derivatives are larger with respect to stiffness parameters around the origin in parameter space, but the failure might be influenced more by strength parameters. This leads to convergence problems for algorithms including search or optimization routines.
- At some of the proposed points, like e.g. the sheet pile tip, significant displacements will not even be observed at all before failure is initiated. Again, methods like FORM have difficulties with convergence.
- If the displacements results are available and the other problems can be solved, the question arises what amount of displacements is considered as failure. As for the mobilized shear resistance a certain subjectivity is involved.
- FORM can only give a lower limit for the system failure probability which can be a bad estimate.

4.3.3 Equilibrium in the Finite Element Calculations

A more robust, generic and objective criterion for the failure of the structure respectively the soil surrounding it might be the information if the finite element analysis reached equilibrium in all calculation phases or not. In fact, this criterion is also used in the Dutch technical recommendations for retaining structures – the CUR 166. In its recommendations about the determination of the sheet pile length it is stated that, equilibrium is reached in all construction phases using design parameters, the length is sufficient. This implies at least the considerations about active and passive failure.

In this research this criterion was used in a broader sense including all the mentioned failure mechanisms in the soil. A disadvantage is that only the common failure probability of all the mechanisms is determined and not each one, which would give more insight into the system behavior:

$$P_{f,soil} = P\left(Z_1 \le 0 \cup ... \cup Z_n \le 0\right)$$

However, if the aim is to determine the system failure probability, this is sufficient, as explained in section 5. The limit state function simply becomes:

$Z = 1$ *, if equilibrium is reached in all construction phases*

$Z = -1$ *, if equilibrium is not reached in one or more construction phases*

In fact, most of the commonly used reliability methods do not perform well on this kind of discrete or even binary functions. In order to deal with this problem, the basic idea of *Directional Sampling* was adopted and a few modifications on the iterative procedures for the determination of the λ_i (vector length in parameter space for direction *i* for which *Z=0*) were necessary.

Due to its generic and robust properties this approach was considered to perform best and the presented results in the example calculation are also obtained with it.

5 System Failure

The singular failure mechanisms can either themselves lead to failure of the entire system, or in combination with others. The fault tree in figure 5 illustrates the singular failure mechanisms in their context of the system.

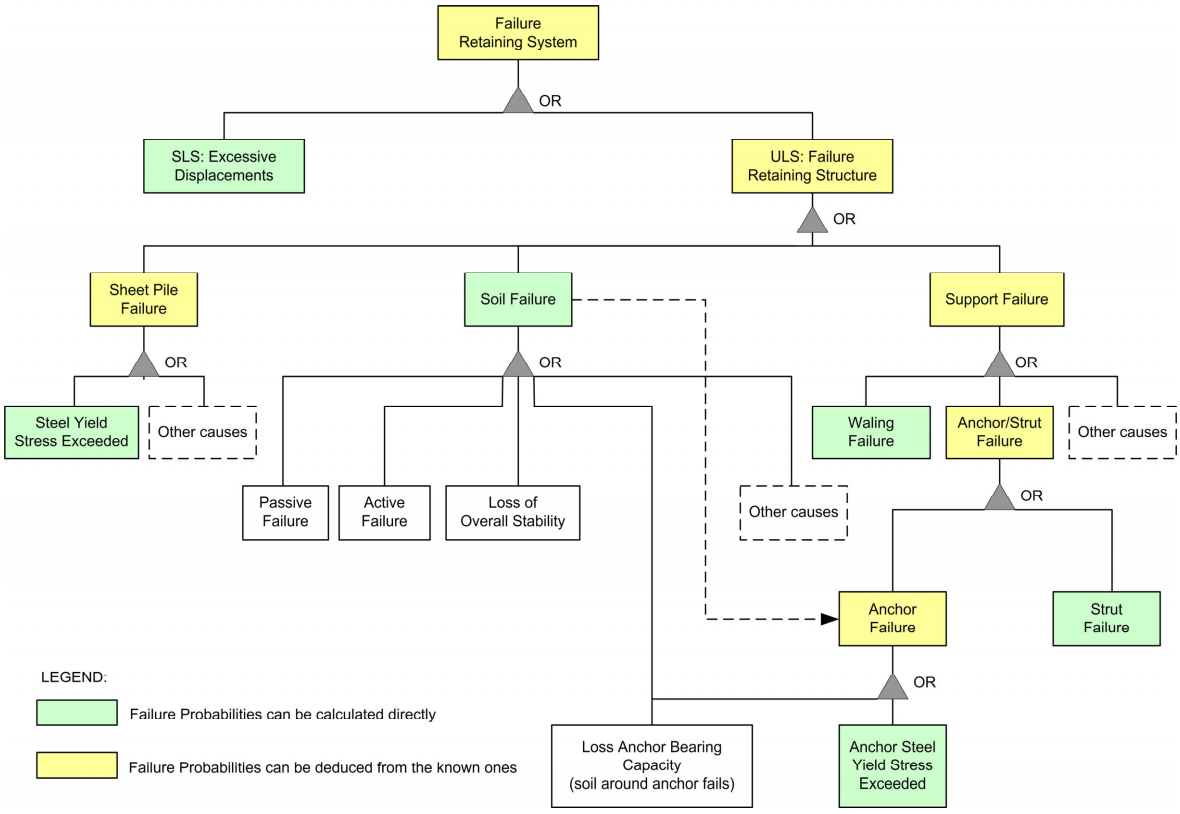

Figure 8: Fault Tree Retaining Structure With Support

The green limit states can be calculated directly from the results of the finite element analysis, whilst the yellow ones can be obtained by combining the green ones. In fact the top event is not a combination of the underlying failure probabilities, but both, the SLS (Serviceability Limit State) and the ULS (Ultimate Limit State) have to fulfill their requirements.

In the subsequent discussion of the calculation results it will be shown how the failure probabilities can be combined using the approach of Hohenbichler [5] to the system reliability.

Note: The probability of pull-out of the anchor is considered to be negligible in this configuration compared to the other failure mechanisms in the soil. Otherwise the probability of soil failure would have to be used as lower bound for the probability of anchor failure.

6 Calculation Results

The system that was defined in section 3 was modeled with the finite element package *Plaxis*. For the soil elements an elasto-plastic model with Mohr-Coulomb yield criterion was applied. The one- or two-dimensional structural elements (plates, anchors, grout body) were modeled as linear elastic. The *Plaxis* model was coupled with *ProBox* as explained in section 2. The results of the calculations using this coupled reliability-FEM analysis are presented in the following sections. 12 random variables were used whilst others with obviously negligible influence were taken deterministic with their mean value.

6.1 Reliability Analysis Results for Singular Failure Mechanisms

There are, of course, plenty of reliability techniques available in the literature. The applicability of a large number of them to reliability analysis of geotechnical structures has been investigated by one of the authors during his MSc-thesis [3]. The following sections summarize some results for the Ultimate Limit State terms of the failure probability and the most important influence coefficients α_i that are direct outcomes of a FORM analysis or approximations of these in case of other methods.

6.1.1 Yielding of the Sheet Pile

In this calculation example we consider only the uncertainties in the soil. Therefore it is sufficient to use the simplified limit state formulation from section 4.1 with $M_{adm} = 391.3$ *[kNm/m]* (corresponding to the deterministic design sheet pile). Thus:

$$Z = 391.3 - M_{max} \text{ [kNm/m]}$$

Table 2: Reliability Analysis Results for Yielding of Sheet Pile

Number of Calculations (FORM):	66
Reliability Index β:	3.73
Probability of Failure: P_f	3.72 E-04
Influence Coefficients:	
Parameter	alpha ; $\|\alpha\|>0.1$
E (clay)	0.94
E (peat)	0.14
ν (clay)	-0.23
R_{inter} (clay)	0.13
γ' (clay)	-0.12

The failure mechanism is clearly dominated by the stiffness of the two soft top layers.

6.1.2 Yielding of the Anchor

Again we use the simple formulation for the limit state function from section 4.2 with $F_{a,adm}$*=220 [kN/m]*, thus:

$$Z = 220 - F_a \text{ [kN/m]}$$

Table 3: Reliability Analysis Results Yielding of the Anchor

Number of Calculations (FORM):	66
Reliability Index β:	4.49
Probability of Failure: P_f	3.55 E-06
Influence Coefficients:	
Parameter	alpha ; |α|>0.1
E (clay)	0.97
ν (clay)	-0.16
γ' (peat)	-0.12

Again the shear modulus ($G = \frac{E}{2(1+\nu)}$) of the clay layer dominates the failure mechanism.

6.1.3 Yielding of the Waling

The limit state for the yielding of the waling can be formulated as (see also 4.2):

$$Z = 114.7 - \frac{F_a \cdot (2.0)^2}{8} [kNm]$$

Table 4: Reliability Analysis Results for Yielding of Waling

Number of Calculations (FORM):	66
Reliability Index β:	4.61
Probability of Failure: P_f	2.00 E-06

The influence coefficients are the same as for the previous limit state, since both limit state functions are linear combinations of F_a.

6.1.4 Failure in the Soil

The limit state used for the calculations is defined according to section 4.3.3.

Table 5: Reliability Analysis Results for Soil Failure

Number of Calculations (DS):	2929
Reliability Index β:	2.62
Probability of Failure: P_f	4.32 E-03
Influence Coefficients:	
Parameter	alpha ; |α|>0.1
E (clay)	0.48
ν (peat)	-0.26
ϕ' (peat)	-0.23
R_{inter} (clay)	0.12
γ' (clay)	0.69
γ' (peat)	0.16
c (clay)	0.11
c (peat)	-0.15

6.2 Combination To System Failure Probability

The method explained by Hohenbichler [5] enables us to obtain estimates for the system reliability, given the reliability indices of the singular mechanisms β_i, the influence coefficients α_{ij} and their mutual correlation coefficients ρ_{ijk} (which can be assumed as fully correlated, thus $\rho_{ijk} = 1$) in this case. Then the correlation between the mechanisms can be determined by:

$$\rho(Z_1, Z_2) = \alpha_{1j}\alpha_{2j}$$

If two mechanisms show a high degree of correlation, it is not worthwhile to carry out the calculations, because the common failure probability will be very close to the upper bound:

$$P_f = \max\{P(Z_1 \le 0); P(Z_2 \le 0)\}$$

Following this reasoning, we can conclude that the probability of the support failure can be approximated by the probability of yielding of the anchor: $\beta_{\text{support}} \approx 4.49$. The same approach for the combination of the yielding of the sheet pile and the support failure leads to $\beta_{\text{support} \cup \text{yielding sheet pile}} \approx 3.73$.

In the following we will consider for the correlation between this combination of mechanisms and the remaining 'failure in the soil' only the contribution of *E (clay)*, since the contribution of the rest is small and the assumption is conservative. Thus

$$\rho(Z_{combined}, Z_{soil\ failure}) = 0.94 \cdot 0.48 = 0.65$$

Using this information we obtain using Hohenbichler the following results for the system reliability:

Table 6: System Reliability Results

Number of Calculations (FORM / DS):	3127
Reliability Index β:	2.61
Probability of Failure: P_f	4.33 E-03

It can be observed that the approximated system failure probability does not significantly differ from the upper bound approach. This is due to the dominance of the large failure probability $P_{f,soil\ failure}$. It should be mentioned at this point that the equilibrium approach that was followed for determining this probability is still being refined and may have considered numerical problems in some cases as 'failure' and therefore increased the failure probability. This subject is being examined at the moment and the improved results will probably be presented on the symposium. We insist that this paper presents a methodology that in our opinion is suitable for reliability analysis of retaining structures in terms of its general framework, whereas the details are still undergoing developments. For the same reason the presented results should not yet be used to judge the reliability level of the deterministic design based on the CUR 166 or whatsoever.

The total calculation time for the 3127 FEM evaluations amounted about 52 hours.

7 Conclusions and Recommendations

The proposed methodology enables us to determine the system reliability of a retaining structure with reasonable effort. The total calculation time to obtain the results might amount about 3 days, but the calculations are carried out automatically, once the model and the reliability analysis parameters are defined. The following list includes some points of attention and recommendations for further improvements:

- The influence factors α are a result of the linearization of the limit state in methods like FORM. For other methods, as in this paper for Directional Sampling, these values are approximations and they are calculated in a way, as if linearization was implied. Therefore the quality and the significance of these α are questionable.
- The FEM analysis includes some conservatism at several points. The elasto-plastic model with Mohr-Coulomb yield criterion certainly overestimates the deflections of the retaining wall and the bending moments and anchor forces. Also the use of a plane-strain model (using e.g. friction angles determined by triaxial tests) implies un under-estimation of the strength. More realistic constitutive models and 3D analysis would lead to more realistic results.
- The pore pressures are supposed to represent a large contribution in the overall uncertainties. These should therefore also be modeled in a stochastic way.
- After the necessary calibrations (see section 6.2) of the reliability analysis for failure in soil the reliability analysis results might be compared with the requirements on which the deterministic design was based. We insist that the necessary refinements are not finished yet.
- Alternative to using level II influence coefficients for combining the failure mechanisms, one could think about a single *Directional Sampling* Calculation including all the limit state functions with an OR combination (serial system) and scaled in such a way that all the limit states are of similar importance respectively weight.

8 References

[1] Waarts, P.H.: *Structural Reliability using Finite Element Methods.* PhD-thesis. Delft: Delft University Press, 2000

[2] Brinkgreve, R.B.J. and Bakker, H.L.: *Non-linear finite element analysis of safety factors*. Computer Methods and Advances in Geotechnics, 1991.

[3] Schweckendiek, T.: *Structural Reliability in Geotechnics Using Finite Element Analysis*. MSc-Thesis, TU Delft, Section Hydraulic and Geotechnical Engineering. 2006

[4] *CUR 166 Damwandconstructies*, Dutch Technical Recommendation for Retaining Structures, Gouda, The Netherlands, 2006

[5] Hohenbichler, M. and Rackwitz R., *First-Order Concepts in System Reliability*, Journal of Structural Safety, (1): 178-188, 1983

Bewertung der Tragfähigkeit bestehender Stahlbetonbrücken mit Hilfe der Messungen von Betonstahldehnungen

Kerstin Bierbrauer & Manfred Keuser
Institut für Konstruktiven Ingenieurbau, Universität der Bundeswehr München

Zusammenfassung: Die Ermittlung der Tragfähigkeit bestehender Brücken aus Stahlbeton stellt eine Herausforderung dar, im Besonderen wenn über das Tragwerk keine Informationen in Form von statischen Berechnungen oder Zeichnungen zur Verfügung stehen. Die für die Tragfähigkeit relevanten Parameter müssen somit am Bauwerk selbst bestimmt werden. Da diese Parameter nur zum Teil gemessen werden können, müssen die fehlenden Werte zunächst abgeschätzt und die Schätzwerte anschließend verifiziert werden. Im Rahmen der Entwicklung einer Methode zur Ermittlung der Tragfähigkeit bestehender Brücken wurden Verfahren entwickelt, die es ermöglichen, die für die Tragfähigkeit relevanten Parameter - wie die Bewehrungsmenge - abzuschätzen und zu verifizieren. Mit Hilfe des Vergleichs von gemessenen und berechneten Betonstahldehnungen können die Eingangswerte für die Nachberechnung des Brückenüberbaus bewertet und der Berechnung der Tragfähigkeit zugrunde gelegt werden.

1 Motivation

An der Universität der Bundeswehr München wurde im Jahr 2000 ein Projekt initiiert mit der Aufgabenstellung die Tragfähigkeit bestehender Brücken zu ermitteln. Da bei Auslandseinsätzen der Bundeswehr für Brückenbauwerke oftmals keine Informationen in Form von Berechnungen oder Zeichnungen zur Verfügung stehen, muss deren Tragfähigkeit vor Ort untersucht werden.

Für die Ermittlung der Eigenschaften von Brückenüberbauwerken stehen zerstörende und zerstörungsfreie bzw. zerstörungsarme Messverfahren zur Verfügung. Diese ermöglichen – unter Berücksichtigung ihrer Anwendungsgrenzen – eine zuverlässige Ermittlung der Abmessungen des Brückenüberbaus und der Materialdaten. Bei Brücken in Massivbauweise ist jedoch besonders die Bestimmung der Bewehrung problematisch, auch unter Verwen-

dung moderner Messverfahren. Vor diesem Hintergrund wurden Verfahren entwickelt, die die Abschätzung der Bewehrungsmengen für bestehende Brückenüberbauten erlauben. Auf die Beschreibung dieser Verfahren wird in diesem Beitrag verzichtet. Detaillierte Informationen können entsprechender Literatur entnommen werden [1], [2], [3].

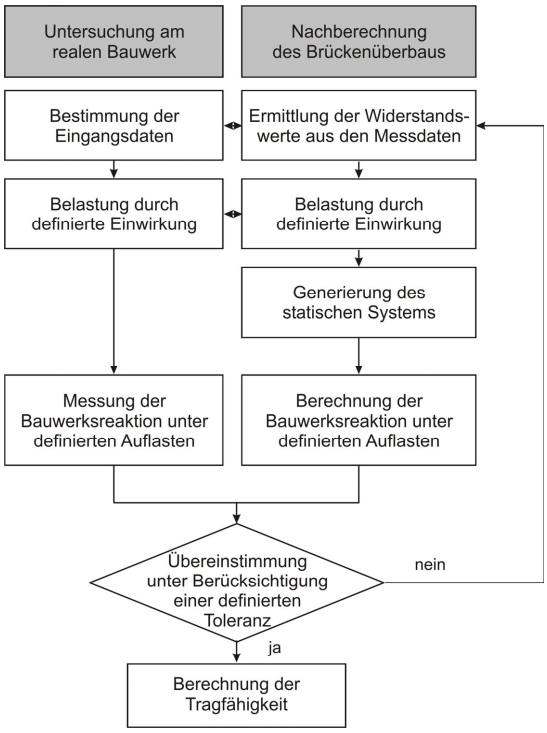

Abb. 1: Vorgehensweise bei der Ermittlung der Tragfähigkeit bestehender Brücken

Da die Bewehrungsmenge aus den Schätzverfahren von der im Tragwerk tatsächlich vorhandenen Bewehrung abweicht, unterscheiden sich die daraus resultierenden Bauwerksreaktionen von den tatsächlichen, am Brückenüberbau messbaren Reaktionen. Diese Abweichung muss mittels des Vergleichs der berechneten Bauwerksreaktionen mit den gemessenen verifiziert werden. Ergibt sich aus der Verifikation eine Diskrepanz, die einen vorgegebenen Toleranzwert überschreitet, muss die Bewehrungsmenge modifiziert werden. Auf der Basis der modifizierten Bewehrung kann ein neuer Wert für die Bauwerksreaktion berechnet werden. Wird der Toleranzwert eingehalten, wird die Bewehrungsmenge der Nachberechnung der Tragfähigkeit des Brückenüberbaus zugrunde gelegt. Die graphische Darstellung der Vorgehensweise zur Verifizierung der Bewehrungsmenge und der anschließenden Ermittlung der Tragfähigkeit zeigt Abbildung 1.

2 Lösungsansatz

Brückenüberbauten in Stahlbetonbauweise befinden sich in der Regel bereits unter Gebrauchslasten im gerissenen Zustand, d.h. in Zustand II. In der Zugzone treten infolge der Überschreitung der Zugfestigkeit des Betons Risse auf und führen an diesen Stellen zu deutlich erhöhten Spannungen und Dehnungen im Betonstahl. Im ungerissenen Bereich übernimmt der Beton weiterhin Zugspannungen (Tension - Stiffening - Effekt). Die Größe der in den Beton eingeleiteten Zugkraft hängt von der Verbundwirkung ab, die maßgeblich

durch die Lastgeschichte des Bauwerks beeinflusst wird [7]. Dabei spielen die durch veränderliche Lasten wie Verkehr erzeugten, dynamischen Beanspruchungen eine wesentliche Rolle.

Um die abgeschätzte Bewehrungsmenge am Bauwerk zu verifizieren, werden lokal messbare Größen benötigt, die die Verifizierung der Eigenschaften des Bauwerks auf der Grundlage einer **lokalen Aussage** erlauben. Hierfür werden in den Rissen gemessene **Betonstahldehnungen** unter definierten Einwirkungen im Gebrauchslastniveau verwendet.

Um den beschriebenen Lösungsansatz zu belegen, wurden im Labor für Konstruktiven Ingenieurbau der Universität der Bundeswehr München Versuche durchgeführt. Dabei ist der Versuchsablauf, dem die Versuchskörper ausgesetzt wurden, derart konzipiert, dass die Versuchskörper für die Versuchsdurchführung in gerissenem Zustand vorliegen. Als Beanspruchungen werden sowohl statische als auch zyklische Belastungen auf die Versuchskörper aufgebracht.

3 Ziel

Ziel dieser Untersuchungen ist es ein Verfahren zu entwickeln, das es ermöglicht, die abgeschätzte Bewehrungsmenge auf Gebrauchslastniveau zu verifizieren und zu validieren, um diesen Wert der Ermittlung der Tragfähigkeit des Brückenüberbaus zugrunde zu legen.

Als Parameter für die Verifizierung der Bewehrungsmengen auf Gebrauchslastniveau werden die Betonstahldehnungen in den Zugzonen des Bauwerks verwendet (vgl. Abschnitt 2). Die Verifizierung selbst geht einher mit der Gegenüberstellung der am Bauwerk gemessenen Betonstahldehnungen $\varepsilon_{s,meas.}$ und den Betonstahldehnungen, die in der Nachberechnung des Brückenüberbaus ermittelt werden, $\varepsilon_{s,calc.}$. Der Vergleich der Betonstahldehnungen erfolgt unter Berücksichtigung eines Toleranzwertes $\Delta\varepsilon_s$ entsprechend Gleichung (1).

$$\varepsilon_{s,meas.} = \varepsilon_{s,calc.} \cdot (1 \pm \Delta\varepsilon_s) \tag{1}$$

Sowohl die am Bauwerk bestimmten Eingangsdaten und die abgeschätzten Bewehrungsmengen als auch die berechneten Betonstahldehnungen enthalten Ungenauigkeiten. Diese sind z.B. auf Streuungen in den Materialeigenschaften und –mengen bzw. auf Idealisierungen in den mechanischen Modellen zurückzuführen. Dabei fließen zufällige und systematische Fehler in den Vergleich der Betonstahldehnungen ein. In dem Zahlenwert des Toleranzwerts, der die Abweichungen der gemessenen und berechneten Betonstahldehnungen abdeckt, müssen somit die Unsicherheiten von Messung und Berechnung berücksichtigt werden.

4 Berücksichtigung von Abweichungen der Eingangsdaten

Die Ergebnisse aus Versuchen bzw. die Ergebnisse der Berechnungen werden im Wesentlichen durch zwei Arten von Abweichungen beeinflusst:

- die systematischen Fehler und
- die zufälligen Fehler.

Unter einem systematischen Fehler versteht man z.B. einen instrumentellen Fehler wie die Messungenauigkeit eines Messgeräts. Der systematische Fehler ist unabhängig von der Anzahl der Stichproben und kann nur über alternative Vorgehensweisen minimiert bzw. ausgeschaltet werden [4], [5], [6]. In dem hier beschriebenen Fall erzeugen die Verfahren zur Messung der Betonstahldehnungen sowie die für die Berechnung verwendeten, idealisierten Werkstoffmodelle systematische Fehler.

Zufällige Fehler entstehen z.B. durch die Beschreibung von Parametern bei einer nicht ausreichenden Anzahl von Stichproben. Durch die Verwendung einer ausreichenden Anzahl von Stichproben können diese minimiert bzw. eliminiert werden. Im Fall der Versuchskörper erzeugen z.B. die Eigenschaften der Werkstoffe wie die Elastizitätmoduli, die Abmessungen der Versuchskörper sowie die Querschnittsfläche und die Betondeckung der Bewehrung zufällige Fehler.

Wurden aus einer Messreihe n Stichproben x_n ermittelt, so streuen die Messwerte um den Mittelwert $\bar{x}$ der Messreihe. Das Maß für die *Streuung eines Messwerts* um den Mittelwert ist die *Standardabweichung s*. Zur Beschreibung von Abweichungen der Messwerte vom Mittelwert ist die Standardabweichung nur bedingt geeignet, da sie nicht berücksichtigt, dass mit zunehmender Anzahl der Stichproben der berechnete arithmetische Mittelwert den wahren Mittelwert genauer beschreibt. Daher wird zur Beschreibung der Streuung einer Messreihe um den Mittelwert der mittlere quadratische Fehler Δx eingeführt. Für Zufallsgrößen, die der GAUSSschen Normalverteilung folgen, gilt Gleichung (2):

$$\Delta x = \pm \frac{s}{\sqrt{n}} = \pm \sqrt{\frac{1}{n(n-1)} \sum_{i=1}^{n} (x_i - \bar{x})^2} \tag{2}$$

In die Nachberechnung der Betonstahldehnungen fließen – wie bereits voran erläutert – Parameter ein, die zufällige und systematische Fehler enthalten. Daher enthalten die berechneten Betonstahldehnungen die Ungenauigkeiten der Eingangswerte der Berechnung.

Die Ermittlung der Abweichung der Betonstahldehnungen aufgrund der zufälligen Fehler der Eingangsgrößen $\Delta\varepsilon_{s,calc.,zuf.}$ kann mit Hilfe der **Fehlerfortpflanzung** ermittelt werden. Zur Ermittlung der Abweichung des Ergebnisses wird die Funktion $f(x_i)$ in eine Taylorreihe entwickelt. Sind die Abweichungen im Verhältnis zu den Werten der Bezugsgrößen klein, darf die Taylorreihe nach dem linearen Glied abgebrochen werden. Gemäß BRONSTEIN et al. [4] gilt für die Ermittlung der Abweichung des Ergebnisses die Formulierung entsprechend Gleichung (3). Die Abweichung $\Delta\varepsilon_{s,calc.,zuf.}$ entspricht dabei dem größten zu erwartenden Fehler [6].

$$\Delta\varepsilon_{s,calc.,zuf.} = \pm\sqrt{(\frac{\partial f}{\partial x_1}\Delta x_1)^2 + (\frac{\partial f}{\partial x_2}\Delta x_2)^2 + ... + (\frac{\partial f}{\partial x_n}\Delta x_n)^2} \quad (3)$$

Zur Ermittlung der Abweichung infolge systematischer Fehler $\Delta\varepsilon_{s,calc.,sys.}$ wird Gleichung (4) verwendet:

$$\Delta\varepsilon_{s,calc.,sys.} = \sum_{i=1}^{n} |\frac{\partial f}{\partial x_i}| \Delta x_i \quad (4)$$

Die Abweichungen $\Delta\varepsilon_{s,calc.,zuf.}$ und $\Delta\varepsilon_{s,calc.,sys.}$ erfassen nur die Ungenauigkeiten der **berechneten** Betonstahldehnungen. Im Zahlenwert des Toleranzwerts $\Delta\varepsilon_s$ sind darüber hinaus die Ungenauigkeiten der **Messung** zu berücksichtigen.

5 Versuche

5.1 Versuchskonzept

Für die Versuchsreihe wurden zehn Stahlbetonbalken mit einer Länge von 3,0m hergestellt. Die Querschnittsabmessungen betragen b/h = 0,20m/0,40m (siehe Abbildung 2). Alle Versuchsbalken wurden mit Beton der Festigkeitsklasse C30/37 hergestellt, die Aushärtedauer betrug 28 Tage. Die Probekörper unterscheiden sich hinsichtlich des Bewehrungsgrades ρ, des Stabdurchmessers d_s und der Betonüberdeckung c_{nom} entsprechend Tabelle 1.

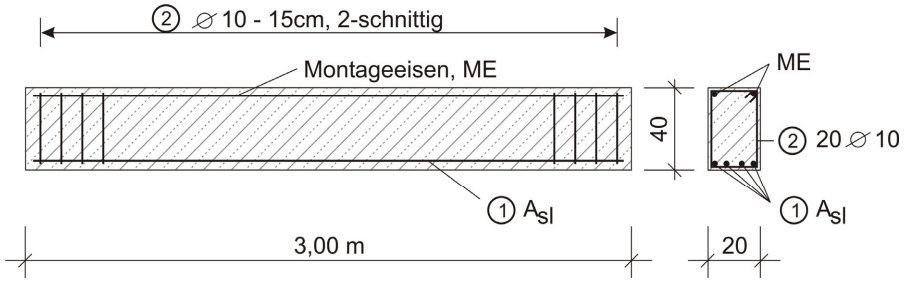

Abb. 2: Ansicht und Querschnitt sowie Bewehrungsmenge der Versuchskörper

Der **Versuchsaufbau** wurde als Vier-Punkt-Biegeversuch konzipiert. Für die Versuchsdurchführung wurden die Versuchsbalken auf Rollenlagern gelagert. Beidseitig kragten die Versuchsbalken jeweils 0,18m über die Rollenlager aus. Die Belastung der Balken erfolgte durch zwei Lasteinleitungsstellen in den Drittelspunkten zwischen den Rollenlagern (vgl. Abbildung 3).

Die Stahlbetonbalken wurden statischen und zyklischen Einwirkungen unterworfen. Zuvor wurden die Versuchskörper mit einer Initiallast vorbelastet. Diese erzeugt für jeden Versuchskörper ein Biegemoment, das oberhalb des Rissmoments M_{cr} liegt. Durch das Auf-

bringen der Initiallast wird sichergestellt, dass sich die Versuchskörper für die Versuchsdurchführung im Zustand II befinden.

Nach Aufbringen der Initiallast wurde die Bewehrung auf der Zugseite in Feldmitte und unter einem der Lasteinleitungspunkte auf einem etwa 5cm breiten Streifen vorsichtig freigelegt. An zwei Bewehrungsstäben jeder geöffneten Stelle wurden Dehnmessstreifen befestigt.

Tab. 1: Modifikation der Versuchskörper

Bezeichnung der Versuchskörper	Betongüte f_{ck}/ Betonstahlgüte f_{yk} [N/mm²]	Bewehrungsgrad ρ [%]	Betonüberdeckung c_{nom} [cm]	Anzahl der Stäbe / Anzahl der Bewehrungslagen	Stabstahldurchmesser d_s [mm]	Vorh. Bewehrungsquerschnitt A_{sl} [cm²]
R05	30 / 500	0,42	2	3 / 1	12	3,39
R08	30 / 500	0,70	2	5 / 1	12	5,65
R1	30 / 500	0,99	2	7 / 2	12	7,92
R16	30 / 500	1,40	2	10 / 2	12	11,30
St10	30 / 500	1,00	2	10 / 2	10	7,85
St14	30 / 500	1,00	2	5 / 1	14	7,69
St16	30 / 500	1,00	2	4 / 1	16	8,04
cnom3	30 / 500	0,57	3	4 / 1	12	4,52
cnom5	30 / 500	0,57	5	4 / 1	12	4,52
cnom7	30 / 500	0,57	7	4 / 1	12	4,52

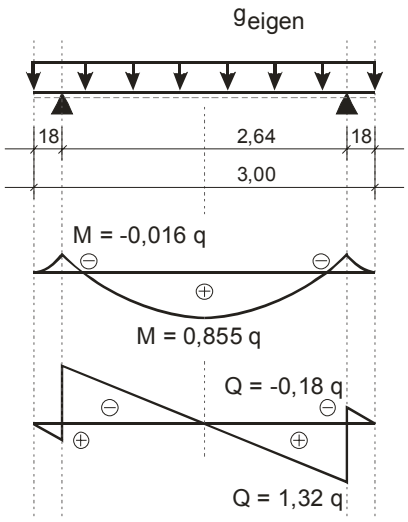

(a) Belastung des Versuchskörpers infolge Eigengewicht (oben), resultierender Biegemomentenverlauf (mittig) und Querkraftverlauf (unten)

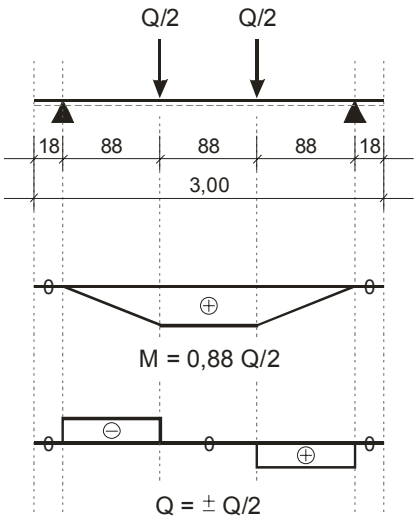

(b) Belastung des Versuchskörpers infolge Auflast (oben), resultierender Biegemomentenverlauf (mittig) und Querkraftverlauf (unten)

Abb. 3: Belastung und Reaktion der Versuchskörper unter Eigengewicht und Auflast

In den statischen Tests wurden stufenweise gesteigerte, statische Beanspruchungen gemäß Tabelle 2(a) auf die Versuchskörper aufgebracht. Zusätzlich zu den statischen Tests wurden die Versuchskörper zyklischen Belastungen ausgesetzt. Nach Durchführung der zyklischen Belastung, d.h. nach 20.000 und nach 40.000 Lastwechseln, wurden die Versuchskörper nochmals mit der höchsten Laststufe der statischen Versuche beansprucht.

Die Lasten für die statischen Tests sowie die Mittellasten und Amplituden für die zyklische Belastung wurden entsprechend des Gebrauchslastbereichs der Träger festgelegt (vgl. hierzu Tabelle 2(b)). Die zeitliche Abfolge ist in Abbildung 4 qualitativ dargestellt.

Tab. 2: Übersicht über die Auflasten für die statischen und zyklischen Versuchsabläufe

(a) Laststufen für die stufenweise gesteigerte, statische Belastung

Laststufe	Auflast [kN]
Q2	45,45
Q3	68,18
Q4	90,91
Q5	113,60
Q6	136,41
Q7	159,10
Q8	181,80
Q9	204,50

(b) Laststufen und Beanspruchungen der Versuchskörper für die statischen und zyklischen Versuchsabläufe

	Lastbild: Statische Belastung		Lastbild: Zyklische Belastung	
Versuchskörper	Minimale Laststufe	Maximale Laststufe	Mittellast [kN]	Amplitude [kN]
R05	Q2	Q3	50	± 20
R08	Q2	Q5	75	± 25
R1	Q2	Q6	90	± 40
R16	Q2	Q8	120	± 60
St10	Q2	Q6	90	± 40
St14	Q2	Q7	90	± 40
St16	Q2	Q7	95	± 45
cnom3	Q2	Q4	55	± 15
cnom5	Q2	Q4	50	± 10
cnom7	Q2	Q4	50	± 10

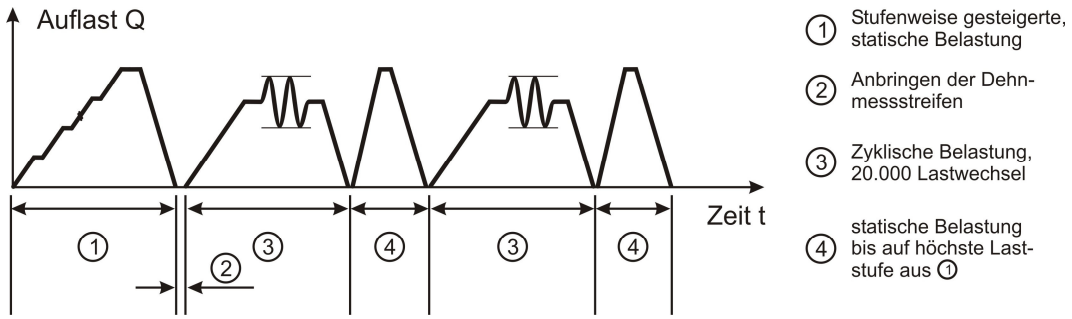

Abb. 4: Chronologischer Ablauf der Versuchsdurchführung

Mit Hilfe der Dehnmessstreifen wurden die Betonstahldehnungen während der stufenweise gesteigerten, statischen Belastung sowie in den statischen Belastungen nach der zyklischen Beanspruchung aufgezeichnet.

5.2 Versuchsergebnisse

Sowohl die Ergebnisse der Versuche mit stufenweise gesteigerter, statischer Last als auch die der Versuche mit zyklischer Beanspruchung zeigen - wie erwartet - deutlich den Einfluss des Bewehrungsgrades (Abbildung 5(a)). Der Einfluss der statischen Höhe, berücksichtigt über die veränderte Betonüberdeckung c_{nom}, zeichnet sich ebenfalls deutlich in den Betonstahldehnungen ab. Der Einfluss des Stabdurchmessers auf den Zusammenhang zwi-

schen Betonstahldehnung und Biegemoment ist vergleichsweise gering und somit vernachlässigbar. Dies bestätigen die Ergebnisse nach aufgebrachter zyklischer Belastung.

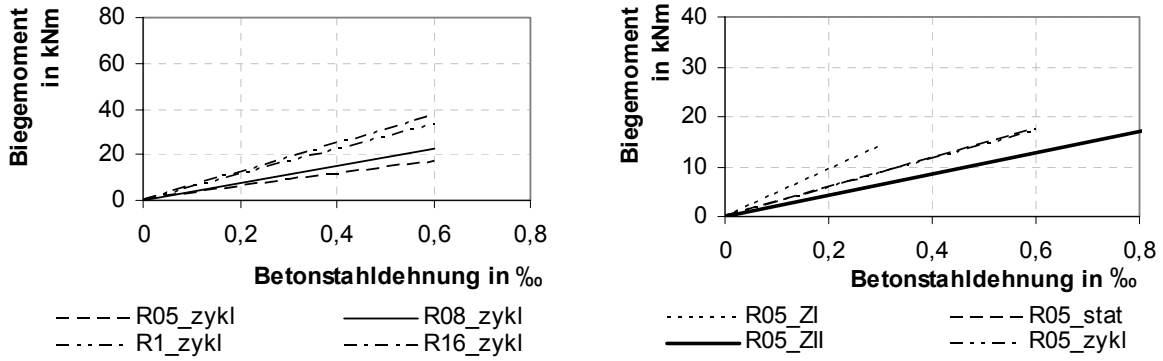

(a) Einfluss des Bewehrungsgrades

(b) Einfluss der Anzahl der Lastwechsel am Beispiel des Versuchskörpers R05

Abb. 5: Einfluss des Bewehrungsgrades und der Lastwechsel auf die Betonstahldehnungen

Die Gegenüberstellung der Betonstahldehnungen vor und nach aufgebrachter zyklischer Belastung ergab, dass es näherungsweise zu keiner Veränderung der Betonstahldehnungen kommt, wie die Abbildungen 5(b) und 6 zeigen. Dies ist in Hinblick auf die Messung der Betonstahldehnung **im Riss** zu erwarten. Im Riss wird die gesamte Zugkraft infolge der Auflast auf den Versuchskörper durch den Betonstahl übernommen. Da die Kraft im Betonstahl für gleiche Laststufen vor und nach zyklischer Beanspruchung **im Riss** unverändert bleibt, ergibt sich für die Betonstahldehnung ε_s keine Änderung zwischen statischer und zyklischer Belastung. Die Mitwirkung des Betons zwischen den Rissen hat keinen Einfluss auf die Messwerte.

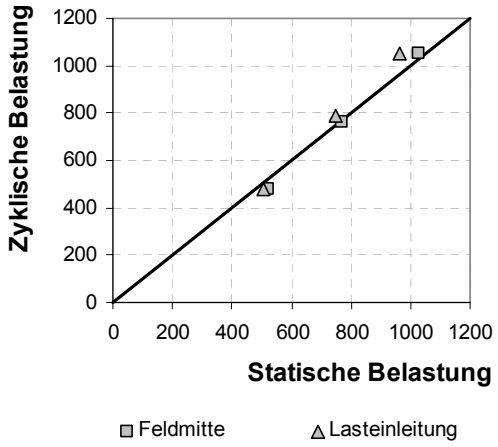

Abb. 6: Gegenüberstellung der Betonstahldehnungen vor und nach zyklischer Beanspruchung am Beispiel der Versuchskörper mit variierendem Bewehrungsgrad

Aus der Messung **über einen gerissenen Bereich** resultiert eine Betonstahldehnung, die den Anteil aus der Mitwirkung des Betons zwischen den Rissen enthält. Es ergibt sich ein mittlerer Wert für die Dehnungen im Betonstahl. Dieser wird durch zyklische Beanspruchung beeinflusst. In Versuchen wurde durch SEIBEL [7] der Einfluss der Anzahl der Lastwechsel auf die mittleren Betonstahldehnungen untersucht. Der Dehnungszuwachs im

Betonstahl beträgt nach 20.000 Lastwechseln etwa 5%. Die Veränderung des Verbundes resultiert aus der Schädigung des Betons der Kontaktzone in Rissnähe [8]. Für eine statische Belastung wird der Bereich, in dem der Verbund zwischen Beton und Betonstahl gestört ist, mit einer Länge des 2fachen bis 5fachen Stabdurchmessers angegeben (vgl. Abbildung 7). Durch die zyklische Belastung wird dieser gestörte Bereich vergrößert. Es verbleibt ein Resttraganteil des Betons auf Zug zwischen den Rissen.

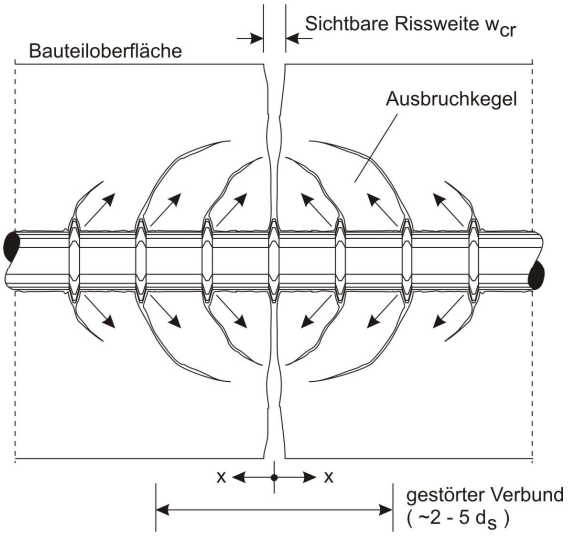

Abb. 7: Ausbruchkegel des Betons infolge statischer Belastung nach [8]

Für die Auswertung der Versuche wurde die Einwirkung infolge Eigengewichts nicht berücksichtigt, da durch die Kalibrierung der Dehnmessstreifen vor Versuchsdurchführung nur die Dehnungsänderungen in den Betonstählen infolge der Auflast gemessen werden.

5.3 Berechnung der Betonstahldehnungen

Für die Nachberechnung der Betonstahldehnungen wird ein vereinfachtes Berechnungsmodell verwendet (vgl. Abbildung 8). Das Berechnungsmodell setzt das Ebenbleiben der Querschnitte voraus. Des Weiteren findet die Mitwirkung des Betons zwischen den Rissen keine Berücksichtigung. Für die Berechnungen wurden die Versuchsträger als Stabmodell idealisiert, bei denen nichtlineares Materialverhalten berücksichtigt wurde.

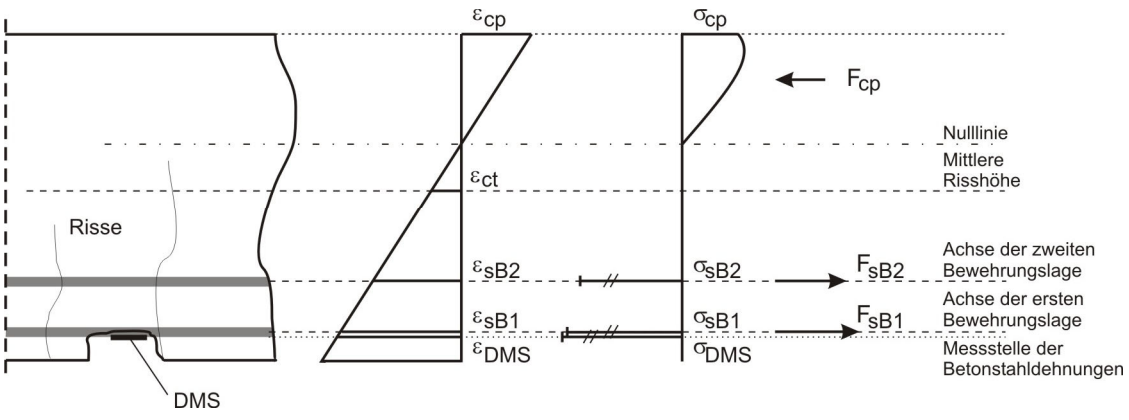

Abb. 8: Berechnungsmodell zur Ermittlung der Betonstahldehnungen

Das Werkstoffmodell für Beton wird gemäß DIN 1045-1 als Parabel angesetzt, der Betonstahl mittels des bilinearen Spannungs-Dehnungs-Verhalten abgebildet. Die geometrischen Daten und die Materialeigenschaften der Versuchskörper werden entsprechend der Versuchsplanung (vgl. Tabelle 1) angesetzt.

Wie bereits erläutert, werden die auf Gebrauchslastniveau verifizierten Bewehrungsmengen der Berechnung der Tragfähigkeit zugrunde gelegt. Zur Berechnung der Bewehrungsmenge können die gemessenen Betonstahldehnungen verwendet werden. Die gemessenen Betonstahldehnungen sind hierzu in die resultierende Lage der Bewehrung zu transformieren. Es ergibt sich eine resultierende Betonstahldehnung $\Delta\varepsilon_{s,res}$. Unter der Voraussetzung des Ebenbleibens der Querschnitte kann aus dem Biegemoment infolge der Änderung der Auflast ΔQ (vgl. hierzu Abschnitt 5.1) mittels der Abschätzung des Hebelarms des inneren Kräfte $z=0{,}85d$ (d: statische Höhe) die Kraft im Betonstahl berechnet werden. Unter der Annahme, dass für den Betonstahl linear elastisches Materialverhalten gilt, kann die Bewehrungsmenge gemäß Gleichung (5) ermittelt werden.

$$erf\ A_s = \frac{\Delta Q / 2 \cdot e}{z \cdot E_s \cdot \Delta\varepsilon_{s,res}} \tag{5}$$

5.4 Bewertung der Versuchsergebnisse

Um die in den Versuchen gemessenen Betonstahldehnungen zu bewerten, werden sie Betonstahldehnungen gegenübergestellt, die - wie in Abschnitt 5.3 beschrieben - rechnerisch ermittelt wurden (vgl. Abbildung 8).

Die berechneten Betonstahldehnungen zeigen eine recht gute Übereinstimmung mit den gemessenen Betonstahldehnungen nach stufenweise gesteigerter statischer Last entsprechend Abbildung 9(a) und nach zyklischer Beanspruchung gemäß Abbildung 9(b) (vgl. hierzu auch Abschnitt 5.2).

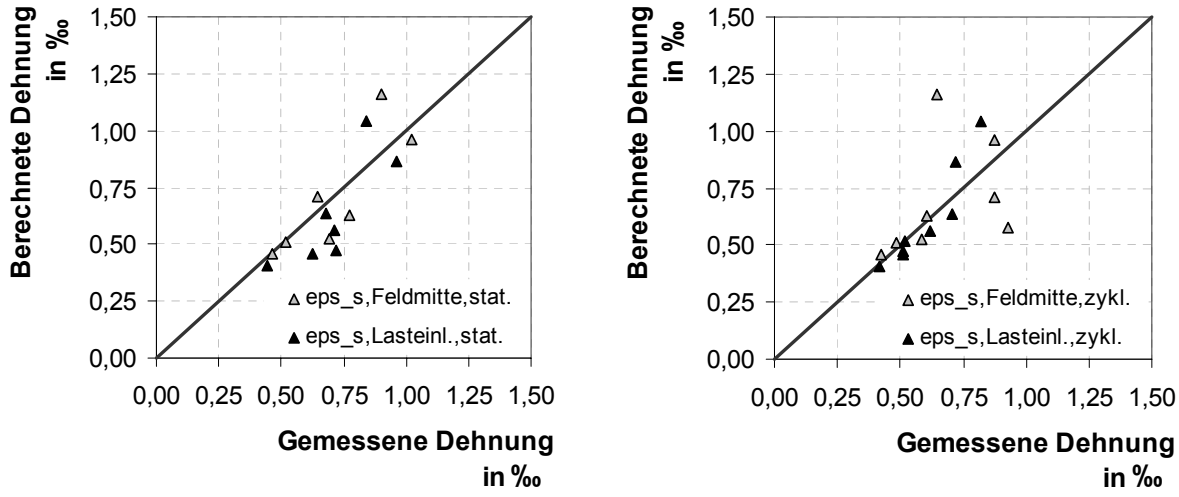

(a) Ergebnisse nach aufgebrachter stufenweise gesteigerter, statischer Last

(b) Ergebnisse nach aufgebrachter zyklischer Last

Abb. 9: Vergleich der gemessenen mit den berechneten Betonstahldehnungen in Feldmitte und im Bereich der Lasteinleitung

Um den Vergleich der berechneten Betonstahldehnungen mit den gemessenen zu bewerten, ist der Einfluss der Abweichungen infolge zufälliger und systematischer Fehler in den Einflussparametern der Berechnung und Messung zu berücksichtigen. Diese bilden die Grundlage für die Festlegung des Toleranzwerts $\Delta\varepsilon_s$ (vgl. hierzu auch Abschnitt 3).

Als Einflussparameter auf die Größe des Toleranzwerts $\Delta\varepsilon_s$ finden auf der **Seite der gemessenen Betonstahldehnungen** folgende Faktoren Berücksichtigung:

- die Messabweichung der Dehnmessstreifen,
- die Genauigkeit der Messapparatur,
- die Sorgfalt bei der Anbringung der Dehnmessstreifen auf den Betonstählen,
- die Einflüsse der Lasteinleitung und der Lagerung.

Auf der **Seite der Berechnung** wird das Ergebnis durch folgende Parameter beeinflusst:

- die Nennwerten zur Beschreibung der Eigenschaften der Versuchskörper und
- die vereinfachten, mechanischen Modelle zur Nachberechnung der Betonstahldehnungen.

Die Einflussgrößen auf der **Seite der Messung** sind mit systematischen Fehlern behaftet. Sie werden im Wesentlichen durch die Sorgfalt bei der Versuchsdurchführung beeinflusst. Das fehlerhafte Anbringen der Dehnmessstreifen an den Betonstählen wird im Weiteren nicht beachtet, da zur Festlegung der Betonstahldehnungen mehrere Messwerte entnommen und Ausreißer eliminiert werden.

Die Eingangsgrößen in die **Berechnung** der Betonstahldehnungen werden sowohl durch systematische (mechanische Formulierung) als auch durch zufällige Fehler (Geometrie und Material der Versuchskörper) beeinflusst. So beinhalten die mechanischen Modelle Idealisierungen, die nur durch die Verwendung anderer Modelle minimiert werden können. Zur Beschreibung der Abweichungen der Eigenschaften der Versuchskörper finden deren statistische Eigenschaften Berücksichtigung.

Bei der Anwendung dieses Verfahrens bei Brückenüberbauten ist es unbedingt erforderlich mehrere Messwerte für die Betonstahldehnungen am Bauwerk aufzunehmen. Somit kann zum einen der Auswertung der Betonstahldehnungen eine ausreichende Anzahl an Stichproben (vgl. hierzu auch Abschnitt 4) zugrunde gelegt werden, zum anderen können Systemreaktionen bestimmter Brückenquerschnitte, wie die Querverteilung bei Plattenbalken infolge exzentrisch angreifender Lasten, verifiziert werden.

6 Zusammenfassung und Ausblick

In diesem Beitrag wurde ein Verfahren vorgestellt, das es erlaubt Bewehrungsmengen von Stahlbetonbauteilen mit Hilfe gemessener Betonstahldehnungen auf Gebrauchslastniveau zu verifizieren. Die Verifizierung erfolgt mittels des Vergleichs von am Bauwerk gemessenen mit berechneten Betonstahldehnungen unter Berücksichtigung eines Toleranzwerts $\Delta\varepsilon_s$. Dieser Toleranzwert dient der Entscheidung, ob die abgeschätzte Bewehrungsmenge

akzeptiert und für die Berechnung der Tragfähigkeit verwendet wird oder modifiziert werden muss. Die Vorgehensweise zur Verifizierung abgeschätzter Bewehrungsmengen wurde mit Hilfe von Versuchen an Stahlbetonbalken verifiziert. Es konnte gezeigt werden, dass gemessene Betonstahldehnungen zur Verifizierung von Betonstahlmengen gut geeignet sind.

Die Grundlagen zur Festlegung des Toleranzwerts $\Delta\varepsilon_s$ wurden auf der Basis der Fehlergrößen in den berechneten und den gemessenen Betonstahldehnungen gelegt. Im nächsten Schritt ist ein Verfahren zur Festlegung des Toleranzwerts $\Delta\varepsilon_s$ zu entwickeln. Seine Quantifizierung geht einher mit der Bewertung der Eigenschaften der für die Ermittlung der Tragfähigkeit zu berücksichtigenden Größen.

Die Verifikation der am Bauwerk ermittelten Eingangsgrößen bildet die Basis für die Berechnung einer aktuellen Tragfähigkeit eines bestehenden Brückenüberbaus. Diese basiert auf der statistischen Auswertung der Messwerte zur Ableitung von Rechenwerten und die Modifikation der Teilsicherheitsbeiwerte der DIN 1055-100.

Ausdrücklicher Dank gilt dem Bundesamt für Wehrtechnik und Beschaffung in Koblenz als finanziellem Träger des Projekts „Ermittlung der Tragfähigkeit von Brücken“.

7 Literatur

[1] Bierbrauer, K.: *Ein Beitrag zur Ermittlung der Tragfähigkeit bestehender Brücken aus Stahlbeton – Abschätzung von Bewehrungsmengen.* Wien: Proceedings 45. Forschungskolloquium des DAfStb, Ernst&Sohn, 2005

[2] Bierbrauer K.; Keuser, M.: *A method for the quick estimation of the load bearing capacity of bridges.* München: Munich Bridge Assessment Conference 2005,

[3] Gebbeken, N.; Baumhauer, A. Ionita, M.; Keuser, M.; Bierbrauer, K.; Mangerig, I.; Retze, U.: *Zwischenbericht 2005, Klassifizierung von Brücken.* München: 2005 (unveröffentlicht)

[4] Bronstein, I.N.; Semandjajew, K.A.; Musiol, G.; Mühlig, H.: *Taschenbuch der Mathematik.* Frankfurt: Verlag Harri Deutsch, 1993

[5] Plate, E. J.: *Statistik und angewandte Wahrscheinlichkeitslehre für Bauingenieure.* Ernst&Sohn, 1993

[6] http://www-ekp.physik.uni-karlsruhe.de

[7] Seibel, P.: *Experimentelle und numerische Untersuchungen zur Mitwirkung des Betons zwischen den Rissen.* Kassel: 2001 - Dissertation

[8] Zilch, K.; Zehetmaier, G.: *Bemessung im konstruktiven Betonbau.* Springer Verlag, 2006

Ein systematischer Ansatz für eine Strategie zur Gewährleistung der Sicherheit von Gebäuden

Burkhard Switaiski
TÜV Rheinland Industrie Service GmbH

1 Einleitung

Infolge des gehäuften Auftretens von Hallendacheinstürzen im Januar und Februar 2006 gelangte die Frage nach einer generellen Prüfpflicht für Ingenieurbauten in den Mittelpunkt des öffentlichen Interesses. Die Befürworter sehen den Staat in der Pflicht, zum Schutz von Personen und Sachgütern entsprechende Vorschriften zu erlassen, die Gegner argumentieren mit der ohnehin bestehenden Verkehrssicherungspflicht des Besitzers oder Betreibers und lehnen jeden staatlichen Eingriff mit Hinweis auf Verstoß gegen die Grundsätze der Deregulierung und Liberalisierung ab.

Dieser Beitrag soll zur Versachlichung der Diskussion beitragen, indem er ausgehend von bereits bestehenden Regelungen und den Grundlagen der Risikobetrachtung das Modell einer Prüfsystematik entwickelt, das sowohl die Eigenverantwortung des Betreibers im Rahmen einer Eigenüberwachung als auch die Fremdüberwachung so kombiniert, dass eine Risikominderung mit vertretbarem Aufwand erreicht wird.

Die Diskussion wird hier auf die bauliche Substanz beschränkt. Betrachtungen der technischen Ausrüstung von Gebäuden sind somit ausgeschlossen.

2 Gesetzliche Regelungen

2.1 Die Verkehrssicherungspflicht nach BGB

Aus § 836 bis 838 BGB [1] ergibt sich die Verpflichtung zum sicheren Erhalt von Bauwerken und baulichen Anlagen (Verkehrssicherungspflicht genannt):

BGB § 836 Haftung des Grundstücksbesitzers.

(1) Wird durch den Einsturz eines Gebäudes oder eines anderen mit einem Grundstück verbundenen Werkes oder durch die Ablösung von Teilen des Gebäudes oder Werkes ein Mensch getötet, der Körper oder die Gesundheit eines Menschen verletzt oder eine Sache

beschädigt, so ist der Besitzer des Grundstücks, sofern der Einsturz oder die Ablösung die Folge fehlerhafter Errichtung oder mangelhafter Unterhaltung ist, verpflichtet, dem Verletzten den daraus entstehenden Schaden zu ersetzen. Die Ersatzpflicht tritt nicht ein, wenn der Besitzer zum Zwecke der Abwendung der Gefahr die im Verkehr erforderliche Sorgfalt beobachtet hat.

(2) Ein früherer Besitzer des Grundstücks ist für den Schaden verantwortlich, wenn der Einsturz oder die Ablösung innerhalb eines Jahres nach der Beendigung des Besitzes eintritt, es sei denn, dass er während seines Besitzes die im Verkehr erforderliche Sorgfalt beobachtet hat oder ein späterer Besitzer durch Beobachtung dieser Sorgfalt die Gefahr hätte abwenden können.

(3) Besitzer im Sinne dieser Vorschriften ist der Eigenbesitzer.

BGB § 837 Haftung des Gebäudebesitzers. *Besitzt jemand auf einem fremden Grundstück in Ausübung eines Rechts ein Gebäude oder ein anderes Werk, so trifft ihn an Stelle des Besitzers des Grundstücks die im § 836 bestimmte Verantwortlichkeit.*

BGB § 838 Haftung des Gebäudeunterhaltungspflichtigen. *Wer die Unterhaltung eines Gebäudes oder eines mit einem Grundstück verbundenen Werkes für den Besitzer übernimmt oder das Gebäude oder das Werk vermöge eines ihm zustehenden Nutzungsrechts zu unterhalten hat, ist für den durch den Einsturz oder die Ablösung von Teilen verursachten Schaden in gleicher Weise verantwortlich wie der Besitzer.*

Festzuhalten ist, dass eine Ersatzpflicht immer dann eintritt, wenn die erforderliche Sorgfalt zur Abwendung der Gefahr nicht beobachtet wurde. Dabei kann die Erfordernis nicht vom subjektiven Empfinden des Verantwortlichen abhängen; vielmehr ergibt sie sich aus demjenigen Verhalten, das zur Vermeidung des Schadens notwendig gewesen wäre. Nicht relevant sind hier übrigens Güterabwägungen im Sinne einer wirtschaftlichen Optimierung.

Wie aus einem höchstrichterlichen Urteil hervorgeht (BGH, Urteil vom 27. 4. 1999 - VI ZR 174/ 98), ist die Haftung auch dann gegeben, wenn Naturereignisse wie starke Sturmböen zum Schaden führen. Lediglich der Eintritt außergewöhnlicher Naturereignisse kann bei Nachweis der fehlerfreien Errichtung und der mit erforderlicher Sorgfalt vorgenommenen Unterhaltung des Bauwerks zu einem Haftungsausschluss führen (siehe auch BGHZ 58, 149, 153 f.; Senatsurteil vom 7. Oktober 1975 - VI ZR 103/ 74 - VersR 1976, 66; vom 23. März 1993 -).

2.2 Körperverletzung im Strafrecht

Der Straftatbestand der Körperverletzung ist im Strafgesetzbuch [2] geregelt:

StGB § 223 Körperverletzung.

(1) Wer eine andere Person körperlich misshandelt oder an der Gesundheit schädigt, wird mit Freiheitsstrafe bis zu fünf Jahren oder mit Geldstrafe bestraft.

(2) Der Versuch ist strafbar.

StGB § 226 Schwere Körperverletzung

(1) Hat die Körperverletzung zur Folge, dass die verletzte Person 1. das Sehvermögen auf einem Auge oder beiden Augen, das Gehör, das Sprechvermögen oder die Fortpflanzungsfähigkeit verliert, 2. ein wichtiges Glied des Körpers verliert oder dauernd nicht mehr gebrauchen kann oder 3. in erheblicher Weise dauernd entstellt wird oder in Siechtum, Lähmung oder geistige Krankheit oder Behinderung verfällt, so ist die Strafe Freiheitsstrafe von einem Jahr bis zu zehn Jahren.

(2) Verursacht der Täter eine der in Absatz 1 bezeichneten Folgen absichtlich oder wissentlich, so ist die Strafe Freiheitsstrafe nicht unter drei Jahren.

(3) In minder schweren Fällen des Absatzes 1 ist auf Freiheitsstrafe von sechs Monaten bis zu fünf Jahren, in minder schweren Fällen des Absatzes 2 auf Freiheitsstrafe von einem Jahr bis zu zehn Jahren zu erkennen.

StGB § 227 Körperverletzung mit Todesfolge

(1) Verursacht der Täter durch die Körperverletzung (§§ 223 bis 226) den Tod der verletzten Person, so ist die Strafe Freiheitsstrafe nicht unter drei Jahren.

(2) In minder schweren Fällen ist auf Freiheitsstrafe von einem Jahr bis zu zehn Jahren zu erkennen.

Da in der Regel bei Verstößen gegen die Verkehrssicherungspflicht nicht von Vorsatz auszugehen ist, liegt bei der aus Mängeln und Schäden an Bauwerken resultierenden körperlichen Schädigung von Personen Fahrlässigkeit vor: Hinsichtlich der Strafbarkeit fahrlässigen Handelns legt das StGB fest:

StGB § 15 Vorsätzliches und fahrlässiges Handeln

Strafbar ist nur vorsätzliches Handeln, wenn nicht das Gesetz fahrlässiges Handeln ausdrücklich mit Strafe bedroht.

Bei fahrlässiger Körperverletzung ist die Strafbarkeit gegeben durch

StGB § 229 Fahrlässige Körperverletzung.

Wer durch Fahrlässigkeit die Körperverletzung einer anderen Person verursacht, wird mit Freiheitsstrafe bis zu drei Jahren oder mit Geldstrafe bestraft.

Kennzeichnend für die Fahrlässigkeitstat ist die ungewollte Verwirklichung des gesetzlichen Tatbestandes durch eine pflichtwidrige Vernachlässigung der im Verkehr erforderlichen Sorgfalt.

3 Normen und Richtlinien

3.1 DIN 1076

DIN 1076 „Ingenieurbauwerke im Zuge von Straßen und Wegen, Überwachung und Prüfung“ (November 1999) [3] regelt Durchführung und Fristen für Untersuchungen sowie die Qualifikation der Prüfer u.a. an Straßenbrücken. Sie ist durch Allgemeine Rundschreiben des Bundesministeriums für Verkehr, Bau- und Wohnungswesen verbindlich eingeführt (Allg. Rundschreiben Straßenbau Nr. 25/199 v. 22.11.1999).

3.2 Richtlinie 804.8xxx

Die Richtlinie 804.8001 bis 804.8004 der Deutsche Bahn AG Netz „Ingenieurbauwerke planen, bauen u. Instand halten / Inspektion von Bauwerken“ [4] gilt für alle Ingenieurbauwerke, die Konzernunternehmen der DB AG nutzen bzw. für die eine Verkehrssicherungspflicht besteht.

RiL 804.8001 „Allgemeine Grundsätze“ legt die Inspektionsarten, den Umfang, die Qualifikation der Inspizierenden sowie die Inspektionsfristen fest. Neben Eisenbahnüberführungen (Brücken) (RiL 804.8002) und Überbauungen (RiL 804.8003) werden ausdrücklich sonstige Ingenieurbauwerke erfasst, zu denen auch Dächer und Hallen zählen (RiL 804.8004).

3.3 Vergleich

Die Begrifflichkeiten von DIN 1076 und RiL 804 können wie folgt zugeordnet werden:

DIN 1076	RiL 804
Laufende Beobachtung	Überwachung
Besichtigung	----------
Einfache Prüfung	Untersuchung
Hauptprüfung	Begutachtung
Prüfung aus besonderem Anlass	Sonderinspektion

Eine gewisse Unschärfe ist lediglich bei den Bauwerksüberwachungen nach DIN 1076 und der Inspektionsart „Überwachung“ nach RiL 804 festzustellen.

Die Prüffristen sind wie folgt festgelegt:

	DIN 1076	RiL 804
Lfde. Beobachtung/Überwachung	Laufend/halbjährl.	Halbjährlich
Besichtigung	Jährlich	----------
Einfache Prüfung/Untersuchung	Drei Jahre	Drei (Sechs) Jahre
Hauptprüfung/Begutachtung	Sechs Jahre	Sechs Jahre

Demnach ist die Besichtigung entsprechend DIN 1076 in der Ril 804 nicht vorgesehen. Weiter gibt RiL 804 die Möglichkeit, die Fristen für die Untersuchung bei einfachen Verhältnissen auf sechs Jahre auszudehnen. Für sehr risikoarme Bauwerke wird die Anwen-

dung der Richtlinie nicht gefordert. Die Einstufung erfolgt nach Anhang 1 zu RiL 804.8004.

Die geforderten Qualifikationen der Prüfer sind:

	DIN 1076	RiL 804
Lfde. Beobachtung/Überwachung	Sachkundige	Fachl. Qualifizierte Personen
Besichtigung	Sachkundige	
Einfache Prüfung/Untersuchung	Sachkundige Ingenieure	Ingenieure Bauwesen, Hochbau oder sonst. Befähigung
Hauptprüfung/Begutachtung	Sachkundige Ingenieure	Ingenieure Bauwesen, Hochbau, Architektur mit Berufserfahrung und speziellen Kenntnissen

Im Bereich der DB Netz wird insbesondere für die Durchführung der Begutachtungen explizit erheblich höhere Anforderungen angegeben als in DIN 1076, obwohl die dortige Formulierung, dass der sachkundige Ingenieur in der Lage sein muss, die statischen und konstruktiven Verhältnisse des Bauwerks zu beurteilen, bei entsprechend schwierigen Verhältnissen zu ähnlichen Qualifikationsmerkmalen führen muss.

Insgesamt ist also festzustellen, dass zwischen DIN 1076 und RiL 804 nur graduelle Unterschiede bestehen. Mit Bezug auf die Inspektion von sonstigen Ingenieurbauwerken wie Hallen und Dächern ist allerdings wesentlich, dass RiL 804 die Unterscheidung in Heft- und Buchbauwerke vornimmt, womit auch die Notwendigkeit von Begutachtungen entschieden wird. Zudem sieht RiL 804 die Verlängerung der Fristen für Untersuchungen auf sechs Jahre bei einfachen Verhältnissen bzw. in risikoarmen Fällen den Entfall der Verpflichtung zur Anwendung der Richtlinie vor.

4 Inspektionsmodell

4.1 Grundlegende Anforderungen

Die Inspektion eines Ingenieurbauwerks soll gewährleisten, dass innerhalb des gesamten Nutzungszyklus – beginnend mit der Abnahme und endend mit der Außerbetriebstellung – die Gefährdung von Personen und Sachen minimiert wird und die zur Erfüllung des definierten Zwecks des Bauwerks erforderlichen Eigenschaften erhalten bleiben. Sie ergänzt somit die Planung, Berechnung und Ausführung durch eine Komponente, die sich über die gesamte Nutzungsdauer bis hin zum Abriss erstreckt und Hinweise für die notwendigen Wartungs- und Reparaturmaßnahmen geben.

In einem Inspektionsmodell sind insbesondere folgende Parameter festzulegen:

- Umfang der Inspektion
- Zeitplan (Inspektionsintervalle)
- Qualifikation des Prüfpersonals

Diese sind so zu definieren, dass mit einem vertretbaren Aufwand Mängel und Schäden,

- die die Stand- und/oder Funktionssicherheit des Bauwerks beeinträchtigen, frühzeitig genug erkannt werden, um eine Gefährdung zu vermeiden;
- deren Nichtbeseitigung zu erhöhtem Sanierungsaufwand führt, erkannt und in Wartungs- und Reparaturanweisungen umgesetzt werden können.

Das Inspektionsmodell hat somit

- die Sicherheit des Bauwerks unter Beachtung der geltenden Gesetze und Richtlinien im Betrieb unter Beachtung des Sicherheitsbedürfnisses der Öffentlichkeit zu gewährleisten;
- zum wirtschaftlichen Betrieb und zum Werterhalt des Bauwerks durch rechtzeitige Initiierung geeigneter Wartungs-, und Reparaturarbeiten beizutragen.

Bei alledem ist festzuhalten, dass Sicherheit nicht in ein Bauwerk „hineingeprüft“ werden kann. Die mit dem Betrieb einer Anlage verbundenen Risiken sind in ihrer Größe durch die Planung, Ausführung und Nutzung vorgegeben, wobei Wartung und Instandhaltung eine bedeutsame Rolle spielen. Inspektionen dienen dazu, Abweichungen vom Sollzustand festzustellen und dadurch Hinweise auf notwendige Instandsetzungsarbeiten zu erhalten, die sowohl der Wiederherstellung des ursprünglichen Sicherheitsgrades als auch der vorbeugenden Instandhaltung dienen.

Insofern sind durch regelmäßige Prüfungen durchaus Kosten zu sparen und die Werthaltigkeit des Bauwerks über lange Zeiträume zu erreichen.

4.2 Begriffe

4.2.1 Sicherheit

4.2.1.1 Umgangssprachliche Bedeutung

Sicherheit ist umgangssprachlich definiert als Bedürfnis des Menschen, vor Gefahren für Leib und Leben sowie Hab und Gut geschützt zu sein. Die menschliche Psyche ist geneigt, Gefahren, die durch persönliches Verhalten – wenn auch nur vermeintlich – beeinflussbar sind, geringer einzuschätzen als solche, die von Naturereignissen oder nicht technischen Anlagen ausgehen, auch wenn dies objektiv nicht zutrifft. Beispielsweise werden die Gefahren bei der Teilnahme am öffentlichen Straßenverkehr in der Regel unterschätzt, diejenigen aus dem Betrieb technischer Großanlagen dagegen stark überschätzt. Zudem ist festzustellen, dass äußerst selten eintretende Schadensereignisse mit insbesondere hohen Opferzahlen sehr medienwirksam sind, häufig eintretende Fälle mit geringeren Schäden dagegen als normal angesehen werden, obwohl beispielsweise eine Risikobetrachtung letzteren ein um Größenordnung höheres Risiko zuordnen würde.

Das subjektive Sicherheitsempfinden muss dennoch beachtet werden, da die Akzeptanz einer Anlage oder der darin angebotenen Dienstleistung maßgeblichen Einfluss auf die Wirtschaftlichkeit hat. Bleiben etwa in einer Verkaufshalle die Käufer wegen tatsächlicher oder vermeintlicher sicherheitsrelevanter Mängel aus, so wird auf Dauer ein wirtschaftlich sinnvoller Betrieb nicht möglich sein. Meist ist es auch nur langfristig möglich, den einmal entstandenen negativen Eindruck durch Sanierungsmaßnahmen zu neutralisieren.

Das Sicherheitsbedürfnis ist somit ein „weicher" Faktor, der trotz seines schwer als Zahlenwert erfassbaren Charakters nicht vernachlässigt werden darf.

4.2.1.2 Der Sicherheitsbegriff in der Technik

In der Technik wird mit Sicherheit der Abstand einer vorhandenen oder der Planung zu Grunde gelegten Zustandes zu dem theoretischen Wert der Unbrauchbarkeit bezeichnet. Die Unbrauchbarkeit muss nicht zwangsläufig erst durch den Kollaps des Systems erreicht werden, vielmehr kann eine geometrische Lageänderung von Teilen oder das Überschreiten bestimmter Werkstoffkennwerte (z.B. der Fließgrenze) diese bereits bestimmen.

Für Bauwerke sind nach Eurocode [5] [6] folgende Nachweise zu führen:

- Nachweis der Tragsicherheit
- Nachweis der Lagesicherheit
- Nachweis der Gebrauchstauglichkeit.

Die Tragsicherheit ist gegeben, wenn die Beanspruchungen aus den Einwirkungen (Lasten) kleiner oder gleich den Beanspruchbarkeiten aus den Widerstandsgrößen (Steifigkeiten) sind.

Die Lagesicherheit ist gegeben, wenn unter Ansatz der zu erwartenden Beanspruchungen kein Gleiten, Abheben oder Umkippen des Bauwerks oder von Bauteilen eintritt.

Die Gebrauchstauglichkeit wird durch den Vergleich der Größe von Verformungen mit zulässigen Verformungen nachgewiesen.

Neben diesen Begriffen der genannten Normen treten auch die Begriffe

- Standsicherheit (in [3] und [4]
- Verkehrssicherheit (in [3] und [4])
- Dauerhaftigkeit (in [3])
- Betriebssicherheit (in [4])
- Funktionssicherheit (in [4])

auf.

Die Standsicherheit ist überraschenderweise in beiden Regelwerken nicht näher definiert. Aus dem Inhalt der Prüfungen kann aber darauf geschlossen werden, dass es sich hierbei um die Kombination der Begriffe der Tragsicherheit und der Lagesicherheit handelt.

Die Verkehrssicherheit erfasst nicht unmittelbar mit der baulichen Struktur zusammenhängende Aspekte der sicheren Nutzung des Bauwerks. Bei Brücken fallen hierunter beispielsweise Anfahrschutz (Leitplanken), Beleuchtungen, Geländer und Beschilderungen.

Auch der Begriff der Dauerhaftigkeit ist in den Vorschriften ohne weitere Erläuterung enthalten. Dem Sinn der Regelwerke entsprechend soll er hier definiert werden als die Fähigkeit einer Struktur, ihre Eigenschaften über einen längeren Zeitraum mit nur unwesentlichen negativen Veränderungen beizubehalten.

Die Betriebssicherheit betrachtet den Aspekt, dass ein Bauwerk einen Zweck zu erfüllen hat und diese Zweckerfüllung erhalten bleiben muss. So kann etwa eine Halle der Lagerung von Gütern dienen, die dort vor fremdem Zugriff und Witterungseinflüssen geschützt werden sollen. Übergeordneter Zweck ist hier das Betreiben und Aufrechterhalten eines logistischen Systems mit den Vorgängen der Ein- und Auslagerung.

Die Funktionssicherheit ist lediglich in der Ril 804.8004.01 „Dokumentationsblatt für sonstige Ingenieurbauwerke“ auf dem Titelblatt erwähnt. Da in der vorzunehmenden Einschätzung des Sicherheitsrisikos ausschließlich das Stand-, Betriebs- und Verkehrssicherheitsrisiko erwähnt werden und die Beurteilung der Standsicherheit auf dem Titelblatt gesondert ausgewiesen wird, ist zu vermuten, dass die Funktionssicherheit die Zusammenfassung von Betriebs- und Verkehrssicherheitsrisiko ist.

Insgesamt ist die Definition außerhalb der auf Eurocode basierenden Begrifflichkeiten Tragsicherheit, Lagesicherheit und Gebrauchstauglichkeit verwirrend und in sich nicht konsistent.

Es wird daher vorgeschlagen, folgende Gliederung vorzunehmen:

- • Standsicherheit
    - • Tragsicherheit
    - • Lagesicherheit
    - • Gebrauchstauglichkeit
- Funktionssicherheit
    - • Betriebssicherheit
    - • Verkehrssicherheit

vorzunehmen.

Der Aspekt der Dauerhaftigkeit ist auf alle Begriffe anzuwenden, da eine Beurteilung über den Zeitpunkt der Prüfung hinaus zumindest bis zur nächsten Prüfung gelten soll, wobei

besondere Ereignisse wie Unfälle, Gewalteinwirkung oder außer-gewöhnliche Unwetter die Gültigkeit der Prüfaussage beenden können.

Der Begriff der Verkehrssicherheit ist hier dahingehend zu erweitern, dass der Schutz von Menschen und Gütern nicht durch Schäden und Mängel beeinträchtigt werden darf, die die Standsicherheit nicht berühren (z.B. Herabfallen von Einbauteilen).

4.2.2 Risiko und Chance

4.2.2.1 Versicherungsmathematische Definition des Risikos

Das Risiko ist definiert als

Risiko = Eintrittswahrscheinlichkeit × Schadenseinheit

$$R = E_S \cdot S \qquad (1)$$

Die Schadenseinheit S wird dabei auf eine vorgegebene Schadensart beschränkt. Sie entsteht aus der statistischen Betrachtung von i Einzelereignissen mit dem zugeordneten Schadensumfang U_i. Aus der Gesamtheit der Einzelereignisse kann eine Verteilungsfunktion des Schadensumfangs $F(U)$ gewonnen werden [7] [8].

Diese Definition des Risikobegriffs wird allgemein im Versicherungswesen verwendet. Sie dient dazu, die Höhe von Versicherungsprämien festzulegen und den Umfang von Rückversicherungen sowie Rückstellungen zu bestimmen.

Als Schadenseinheit wird in der Regel die Leistung der Versicherung im Schadensfall angesetzt, die unter Einbeziehung etwaiger Selbstbeteiligungen des Versicherten nicht mit der Schadenshöhe identisch sein muss.

Die Eintrittswahrscheinlichkeit eines Schadensereignisses ergibt sich aus statistischen Daten für die jeweiligen Objekt- und Ereignisklassen. Die Angabe ist nur dann vergleichbar, wenn ein Bezug auf einen Zeitraum vorgenommen wird (z.B. Ereignisse pro Jahr).

Als Beispiel sei hier vereinfachend das Risiko dargestellt, das durch den Tod von Personen im Straßenverkehr entsteht. Wird von 7.000 Verkehrstoten pro Jahr ausgegangen, so ist die Eintrittswahrscheinlichkeit bei 70 Mio. Einwohnern 1×10^{-4}. Die Schadenseinheit soll mit 100.000 € festgelegt sein.

Damit wird das Risiko

$$R = 10^{-4}\ \text{Person/Jahr} \cdot 100000\ \text{Euro} = 10\ \text{Euro/(Person} \cdot \text{Jahr)}$$

Dieser Ansatz würde aber nur dann gelten, wenn alle Einwohner in eine Versicherung auf Tod durch Verkehrsunfall einzahlen würden. Bei einer Betrachtung bezüglich der Verursacher (z.B. Fahrzeuge) ist diese Berechnung anders aufzubauen:

Wird angenommen, dass die Objektklasse der Versicherten 35 Mio. Fahrzeuge umfasst, so kommen auf jedes Fahrzeug 2×10^{-4} Verkehrstote. Damit ist das Risiko

$$R = 2 \cdot 10^{-4} \text{ (Person/(Fahrzeuge} \cdot \text{Jahr)} \cdot 100000 \text{ (Euro/Person)} = 20 \text{ Euro/(Fahrzeug} \cdot \text{Jahr)}$$

Aus diesem einfachen Beispiel wird klar, dass die saubere Definition von Objektklassen von entscheidender Bedeutung ist.

4.2.2.2 Die Chance

Komplementär zum Risiko ist die Chance definiert als

Chance = Eintrittswahrscheinlichkeit × Nutzen

$$R = E_N \cdot N \tag{2}$$

Als Beispiel für eine Chance im technischen Bereich sei hier die Auslegung einer Stahlstruktur angenommen, die gegenüber einer den Vorschriften genügenden Beschichtung einen Korrosionsschutz besitzt, der erheblich längere Standzeiten erwarten lässt, wenn die Umweltparameter konstant bleiben. Die Chance besteht nun darin, dass der Mehrpreis (dieser geht in das Risiko ein) durch geringere Instandhaltungskosten (die Kostendifferenz ist der Nutzen) zumindest kompensiert wird.

Zur Optimierung technischer Systeme genügt es nicht, Risiken zu minimieren; vielmehr sind gleichzeitig die Chancen zu betrachten. Dies geschieht vorteilhaft durch die Minimierung des Quotienten

$$k = \frac{R}{C} = \frac{E_S \cdot S}{E_N \cdot N}$$

Bereits an einfachen Beispielen kann gezeigt werden, dass die Minima von *k* nicht notwendigerweise mit dem Minimum von *R* und dem Maximum von *C* zusammenfallen müssen (Bild 1).

4.3 Übergreifende Konzepte

4.3.1 Lebenszyklus eines Bauwerks

Bauwerke unterliegen wie alle natürlichen und künstlichen Systeme einem Alterungspro zess, der die Fähigkeit, den erwünschten Zweck zu erfüllen, mit der Zeit abnehmen lässt.

Zur Darstellung dieses Vorgangs lassen sich vorteilhaft verzerrte cos²-Funktionen einsetzen, die die Eigenschaft besitzen, ausschließlich Werte zwischen 0 und 1 anzunehmen. Wird eine unverzerrte Funktion angenommen, so ist der 50 %-Wert nach p/4, der Nullwert bei *p*/2 erreicht. Wird *p*/2 mit der Gesamtlebensdauer gleichgesetzt, so bedeutet dies, dass bereits nach der halben Lebensdauer nur noch 50 % der Funktionalität (im folgenden als „Wert“ bezeichnet) erhalten sind. Tatsächlich wird der Wert aber in der Anfangszeit langsamer abnehmen und erst zum Ende der Lebensdauer stark abnehmen.

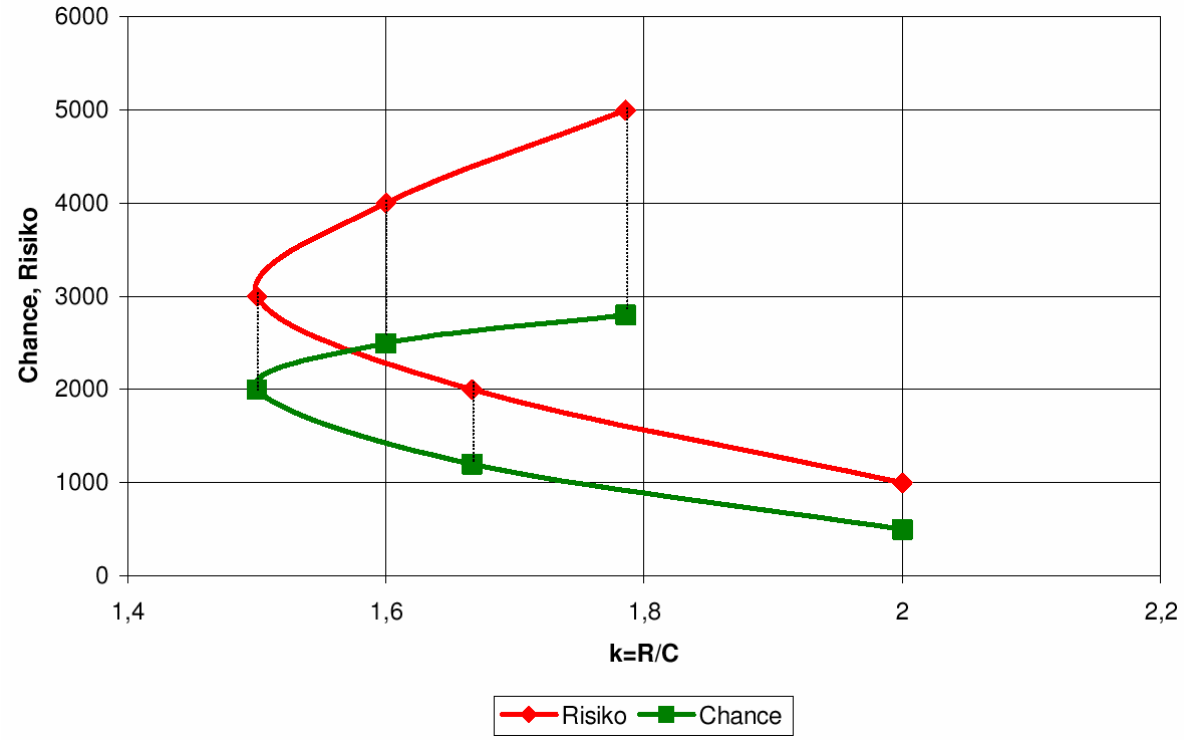

Bild 1: Minimum des Quotienten R/C (schematisch)

Dieser Effekt lässt sich durch eine Verzerrung der Zeitachse erreichen:

$$W = \cos^2 \xi$$
$$\xi = \frac{\pi}{2} \cdot \frac{t}{(1-s) \cdot t + s \cdot t_e} \qquad (3)$$

Darin ist

t_e Lebensdauer

s Streckung bei $t = 0$

Die Streckung s in obiger Formel bewirkt, dass die Funktion längs x so verzerrt wird, dass bei $t = 0$ eine Streckung um s und bei $t = t_e$ keine Streckung erfolgt.

Bild 2 zeigt einen so erhaltenen Wertverlauf über die Zeit für zwei Varianten mit der Gesamtlebensdauer von 30 bzw. 50 Jahren.

Tatsächlich wird sich der Wertverlauf für jedes Objekt individuell ergeben, eine Verallgemeinerung ist somit auf statistischen Methoden zu basieren. Infolge der verhältnismäßig langen Betrachtungszeiträume ergibt sich dabei aber das Dilemma, dass unvorhersehbare Ereignisse (z.B. geänderte Nutzung, Kriege) einen nicht vorher abschätzbaren Einfluss ausüben. Damit ist die Stationarität als Grundlage der Anwendbarkeit stochastischer Methoden nicht mehr gegeben.

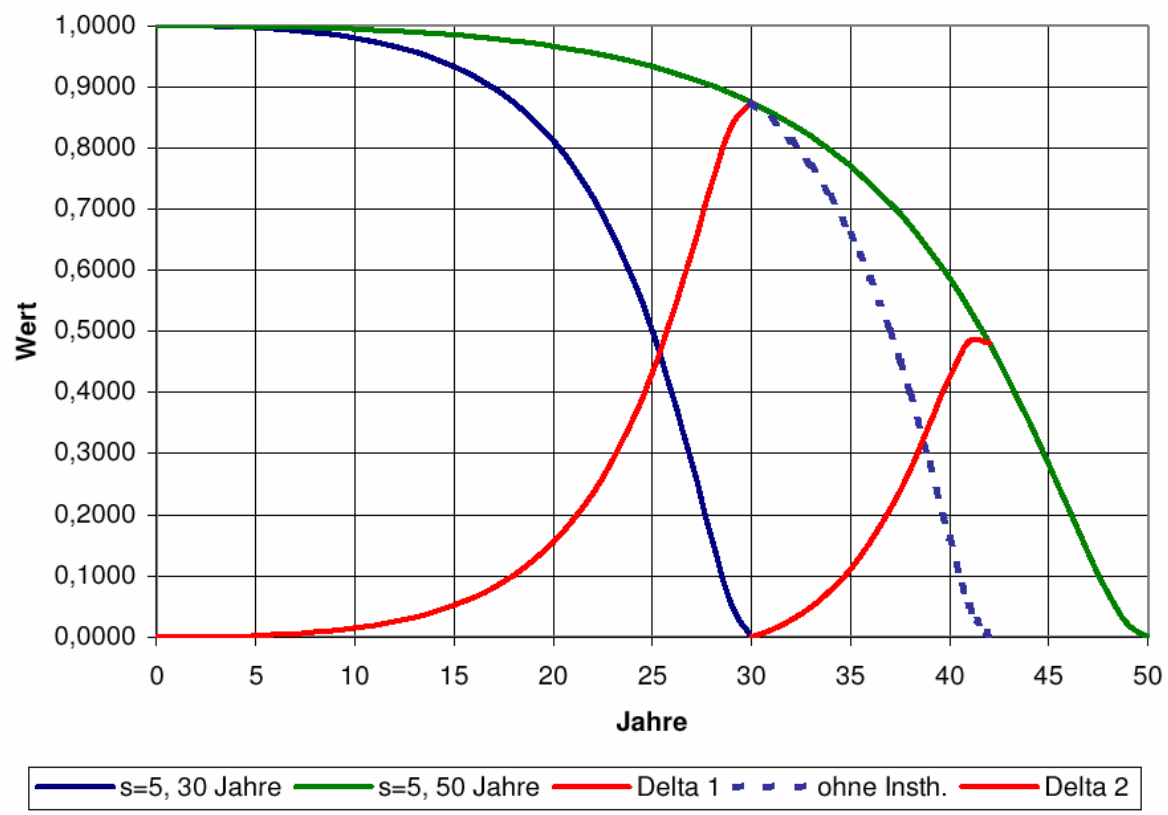

Bild 2: Lebensdauerzyklen zweier Varianten mit Darstellung der Wertdifferenz

Wird angenommen, dass es sich bei Variante den Verlauf ohne Instandhaltungsaufwand darstellt und Variante 2 ein entsprechendes Bauwerk mit Instandhaltung abbildet, so ist die Wertdifferenz bis zur Lebensdauer der Variante 1 (Annahme 30 Jahre) durch die Differenz Delta 1 und den restlichen Verlauf der Kurve für Variante 2 gegeben. Würde die Instandhaltung der Variante 2 nach 30 Jahren eingestellt, so würde der Wert sich entsprechend der gestrichelten Kurve ändern und die Restlebensdauer nur noch 12 Jahre statt 20 Jahre betragen. Wird weiter instandgehalten, ist eine Wertdifferenz entsprechend der Kurve Delta 2 zu erreichen. Diese Betrachtung kann weiter fortgesetzt werden, wobei die Wertdifferenz stets geringer wird, je näher man der Lebensdauer der Variante 2 kommt.

Die Wertdifferenz-Kurven stellen zugleich den maximalen wirtschaftlich vertretbaren Instandhaltungsaufwand dar. Um den tatsächlichen Mehrwert zu erhalten, müssen von diesen selbstverständlich die Bewertungen des Instandhaltungsaufwandes abgezogen werden.

Der Begriff des Wertes ist hier nicht ausschließlich monetär zu sehen, vielmehr kann dieser auch die Funktionalität abbilden, etwa dergestalt, dass die Tragfähigkeit einer Konstruktion bewertet wird.

Wird beispielsweise angenommen, dass die Funktionalität eines Bauwerks bis zu einer Tragfähigkeitsminderung von 10 % des zugrunde gelegten Wertes erhalten ist, so wäre diese Grenze bei Variante 1 nach 16 Jahren, bei Variante 2 nach 28 Jahren erreicht. Nach Ablauf dieser Zeit ist dann eine Sanierung erforderlich, um den ursprüngliche Tragfähigkeit wieder herzustellen. Modellhaft ist der Aufwand in Bild 3 dargestellt, wobei die kumulierten Kosten betrachtet werden (bei Variante 2 fallen im Unterschied zu Variante 1 auch Instandhaltungskosten an).

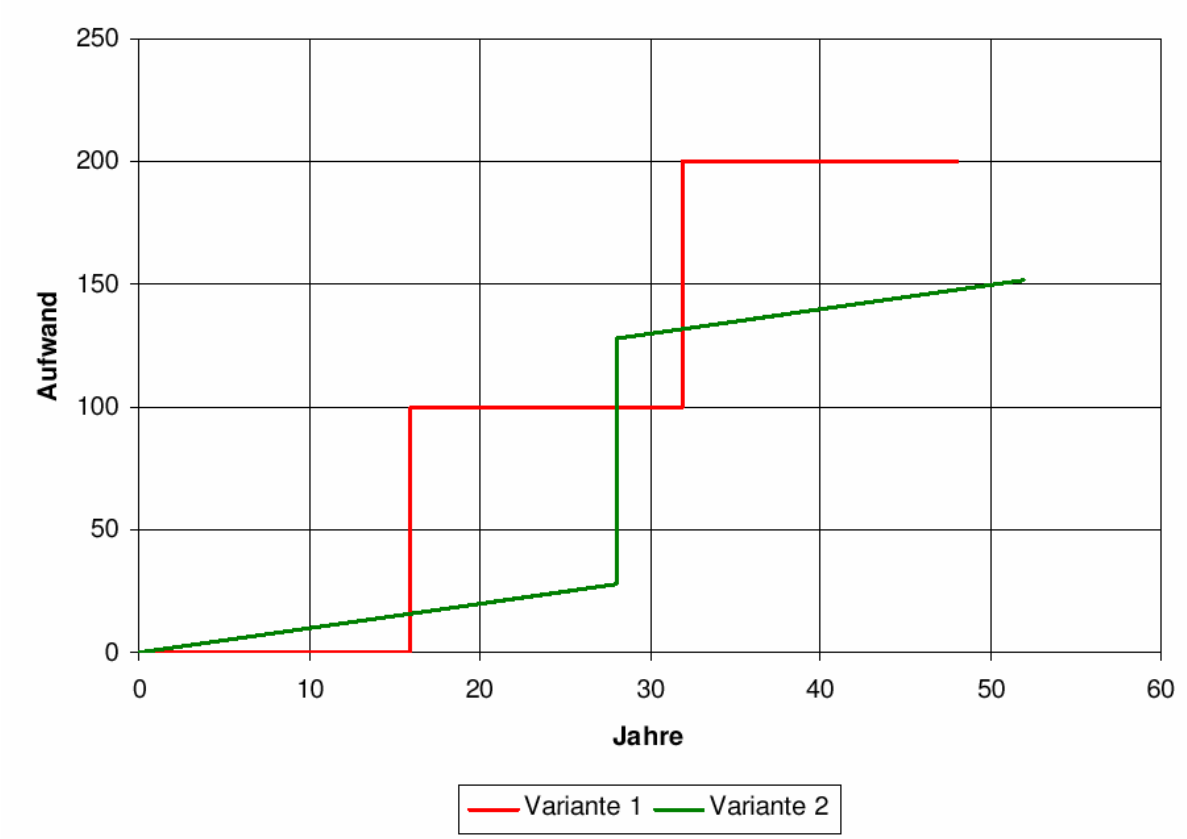

Bild 3: Kumulierter Aufwand für Instandhaltung und Sanierung (Modell)

Alle hier getroffenen Feststellungen setzen voraus, dass der Zustand des Bauwerks während des Zeitablaufs auch tatsächlich bekannt ist. Nur dann lassen sich Instandhaltungsmaßnahmen auf ihre Wirksamkeit hin überprüfen und Sanierungen zum notwendigen Zeitpunkt einleiten.

4.3.2 Risikomanagement

Als Basis der Betrachtung soll hier die Darstellung eines immobilienspezifischen Risikomanagements für Kommunen dienen, das von BRADLER ausführlich in [9] dargestellt wurde.

Dabei beschränkt sich die Ausführung auf die Nutzungs- bzw. Betriebsphase des Bauwerks beginnend mit dessen Fertigstellung.

Die Bausteine des Modells für das Risikomanagement sind in Bild 4 dargestellt.

Grundsätzlich sind die folgenden Fragen zu stellen und zu beantworten:

- Welche Risiken entstehen durch den Betrieb der baulichen Anlage?
- Welche Auswirkungen haben diese Risiken und wie hoch ist deren Eintrittswahrscheinlichkeit?
- Welche Risikofaktoren können durch geeignete Maßnahmen verändert werden?

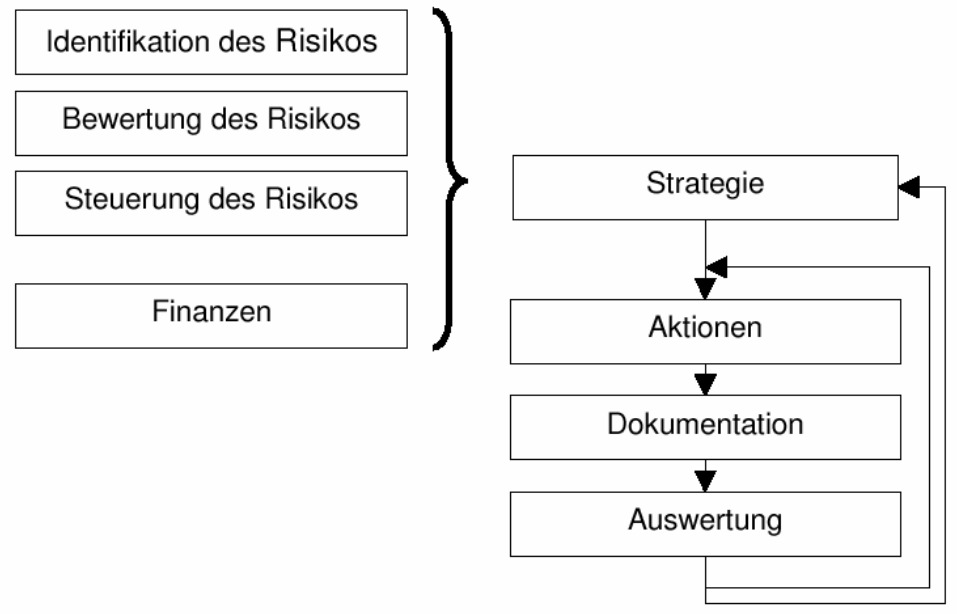

Bild 4: Modell des Risikomanagements

Unter Ansatz der zur Verfügung stehenden Finanzmittel – Einsparungspotentiale durch zu ergreifende Maßnahmen sind hier zu berücksichtigen – wird dann eine Strategie zur Steuerung des Risikos in dem Sinne entwickelt, dass das Verhältnis Risiko/Chance minimiert wird.

Aus der Strategie leiten sich Aktionen wie beispielsweise die Aufstellung von Wartungs- und Inspektionsplänen, Instandhaltungsarbeiten und bauliche Veränderungen ab. Alle Aktionen werden dokumentiert und ausgewertet, um so eine Anpassung der Aktionen, im weiteren Schritt möglicherweise der Strategie zu erreichen.

Dieser Regelkreis ist in bestimmten Zeitabständen auf die erneute Betrachtung der Risiken zu erweitern, da anfänglich lediglich mit Abschätzungen gearbeitet werden kann, die durch die gesammelten Erfahrungen zu korrigieren sind.

Als Risiken sind zu unterscheiden:

- Betriebsrisiken
- Marktrisiken
- Umfeldrisiken.

Markt- und Umfeldrisiken sollen hier nicht näher betrachtet werden, da sie nur in geringem Maße durch technische Eigenschaften des Bauwerks bestimmt werden.

Die Betriebsrisiken können weiter untergliedert werden in:

- Objektschäden
- Haftungsschäden

- Schäden infolge krimineller Handlungen
- Schäden durch Betriebsunterbrechung

Oft wird argumentiert, diese Schäden seien durch entsprechende Versicherungen gedeckt. Nicht beachtet wird dabei häufig der tatsächliche Umfang des Versicherungsschutzes, ins besondere im Hinblick auf unterlassene Handlungen zur Minderung des Risikos (unterlassene Wartung und Instandhaltung, grobe Fahrlässigkeit u.a.). Auch sind typische Betriebsrisiken wie Nutzungsausfall und Funktionsstörungen in der Regel nicht versicherbar.

Unverzichtbar sind somit im Rahmen der Gesamtstrategie die Teilstrategien

- Präventivstrategie
- Inspektionsstrategie
- Korrektivstrategie

Die Präventivstrategie umfasst alle Maßnahmen, die dem Erhalt der Funktionalität dienen. Dies sind vor allem Wartungs- und Instandhaltungsaktivitäten, die nach einem definierten Plan vorzunehmen sind.

Die Inspektionsstrategie hat alle Prüfungen der Anlage zum Inhalt, die Aufschluss über deren Fähigkeit geben, den festgelegten Zweck zu erfüllen. Dabei ist eine Vorausschau über das Verhalten in der Zeit bis zur nächsten Prüfung notwendig. Aus der zu erwartenden Veränderung der Anlage ergibt sich der Inspektionsplan sowohl in Form eines Fristenplans als auch des Prüfumfangs. Die Inspektionen sind die Grundlage zur Anpassung der Wartungs- und Instandhaltungspläne und geben vorzunehmende Reparaturen, den Austausch von Bauteilen bis hin zu größeren Sanierungen oder der Außerbetriebnahme des Bauwerks vor.

Die Korrektivstrategie ist bei Anwendung der Präventiv- und Inspektionsstrategie in der Regel überflüssig. Sie kommt nur dann zum Tragen, wenn außergewöhnliche Ereignisse wie etwa die Kollision eines LKW mit einer Gebäudewand eintreten und Sofortmaßnahmen nötig werden, die die Sicherheit und den Wert des Bauwerks wieder herstellen.

Der heute im Immobilienmanagement beschrittene Weg führt eindeutig aus Gründen der Kostenminimierung zu einer Abkehr von der Korrektivstrategie auch bei vorhersehbaren und regulären Betriebsrisiken hin zur Anwendung der Präventiv- und Inspektionsstrategie.

4.3.3 Risikoklassen

Zur Definition einer Präventiv- und Inspektionsstrategie ist es erforderlich, einen verlässlichen Beurteilungsmaßstab für das dem Bauwerk zuzuordnende Risiko zu entwickeln.

Im Zusammenhang mit der Risikoabschätzung eines Bauwerks sind folgende Gesichtspunkte zu betrachten und zu bewerten:

- Vulnerabilität

- äußere Einwirkungen
- Nutzung

Die Vulnerabilität ist der Maßstab für die Anfälligkeit eines Bauwerks, d.h. für das Maß der möglichen Änderungen der hinsichtlich der Stand- und Funktionssicherheit charakteristischer Eigenschaften. Hier gehen beispielsweise die Bauweise, die verwendeten Werkstoffe sowie die Eigenschaft der Fehlertoleranz (Redundanzen, Sicherheitsreserven) in die Bewertung ein.

Die Vulnerabilität ist stets in Zusammenhang mit den zu erwartenden und bereits erfolgten äußeren Einwirkungen auf das Bauwerk zu betrachten, da erst diese zu einer Veränderung der Eigenschaften führen. Hier sind nicht nur die Lasten (z.B. als Lastkollektive oder Maximallasten), sondern auch Einflüsse aus Feuchtigkeit, Temperatur und chemischer Substanzen (z.B. Chlor in Schwimmbädern) zu erfassen.

Die Nutzung entscheidet über die möglichen Personen- und Sachschäden sowie die Folgen eines Betriebsausfalls.

Obwohl die angesprochenen Problemkreise seit langem bekannt sind, fehlen für Bauwerke im Allgemeinen verlässliche Zahlenangaben. Lediglich für Brückenbauwerke lassen sich aus den Berichten der Brückenprüfungen nach DIN 1076 entsprechende Statistiken gewinnen, die für sonstige Ingenieurbauwerke aber keine Rückschlüsse zulassen. Für den Bereich des Stahlbaus lassen sich Erkenntnisse der Betriebsfestigkeitsrechnung heranziehen.

Die einfachste Klassierung wäre hier im Sinne einer Abgrenzung nach der Anzahl der sich in dem Gebäude aufhaltenden Personen möglich, die auch mittelbar über die Geschossfläche angegeben sein kann. Diesem Weg folgen viele Verordnungen der Bundesländer wie beispielsweise die Versammlungsstättenverordnung oder die Verkaufsstättenverordnung. Im Vergleich zu den oben aufgeführten Kriterien ist hier aber ausschließlich der Faktor der Nutzung berücksichtigt.

Seitens der LGA wurde eine Klassierung entsprechend Bild 5 vorgeschlagen [10]. Die grundsätzlichen Gesichtspunkte scheinen hier zwar implizit zumindest ansatzweise berücksichtigt zu sein, jedoch ist eine nachvollziehbare Risikoeinstufung nicht gegeben. Insbesondere ist hier der Aspekt der Vulnerabilität hinsichtlich Bauweise und verwendeter Werkstoffe nicht erfasst.

Ein umfassender Ansatz für eine Klassierung ist in RiL 804.8004 [4} gegeben, der die Einstufung eines Bauwerks nach obigen Kriterien zumindest teilweise vornimmt und danach entscheidet, ob es sich um ein Buch- oder Heftbauwerk handelt oder ob die dort vorgesehenen Prüfungen entfallen können. Es werden dabei folgende Merkmale berücksichtigt:

- Belastung des Bauwerks oder des Bauwerksteils
- statische Verhältnisse
- Konstruktive Ausbildung

- Zugänglichkeit zu den zu untersuchenden Bauwerksteilen bzw. Verbindungen
- Möglichkeit, einen Schaden zu erkennen
- Schadensfolge

Die Bewertung der Zugänglichkeit und des Schwierigkeitsgrades der Schadenserkennung hat hier nur eine mittelbaren Einfluss auf das Risiko, etwa dergestalt, dass durch das Nichterkennen von Schäden das Risiko für das Bauwerk zunimmt. Somit handelt es sich hierbei nicht um Gefährdungen des Gebäudes an sich, sondern um Erschwernisse bei der Schadensaufnahme, die aber durch erhöhten Prüfaufwand kompensiert werden können (z.B. Öffnen von Bauteilen, Vorrichtungen zur Überwachung).

Gefährdungspotential/ Schadensfolgen	Gebäudetypen	Beispielhafte, nicht abschließende Aufzählung
Kategorie 1	Versammlungsstätten mit mehr als 5000 Personen, bauliche Anlagen mit über 60 m Höhe	Stadion, Fernsehturm, Hochhaus
Kategorie 2a	Gebäude und Gebäudeteile mit Stützweiten *) > 12 m sowie großflächige Überdachungen	Schwimmbäder, Mehrzweck-, Sport-, Reit-, Tennis-, Passagier- abfertigungs-, Pausen-, Produktionshallen, Kinos, Theater
Kategorie 2b	Exponierte Bauteile von Gebäuden	große Vordächer, angehängte Balkone, vorgehängte Fassaden, Kuppeln
Kategorie 3	Sonstige Gebäude, ausgenommen Wohn- und Bürogebäude in herkömmlicher Bauweise	

Bild 5: Risikoklassierung nach einem Vorschlag der LGA [10]

4.4 Entwurf einer Inspektionsstrategie für Ingenieurbauwerke

4.4.1 Voraussetzungen und Randbedingungen

4.4.1.1 Planung des Bauwerks

Bei der Planung des Bauwerks werden auch alle die Vulnerabilität bestimmenden Größen festgelegt. Zusammen mit der vorgegebenen Nutzung und den anzusetzenden äußeren Einwirkungen ist damit das Betriebsrisiko bestimmt, aus dem sich als Konsequenz auch die erforderlichen Wartungs- und Instandhaltungsmaßnahmen ergeben, die in die Präventivstrategie eingehen. Die Dauerhaftigkeit der Teilkonstruktionen bestimmt sowohl die Gesamtlebensdauer als auch den Aufwand für Reparaturen und Sanierungen.

Aus wirtschaftlichem Gesichtspunkt sind demnach die Gesamtkosten über den Lebenszyklus des Gebäudes zu betrachten und nicht ausschließlich die Herstellkosten:

Gesamtkosten = Herstellkosten + Betriebskosten + Sanierungskosten + Beseitigungskosten

Da die Präventivstrategie durch die Inspektionsstrategie gestützt und ständig angepasst und verbessert wird, ist bereits bei Entwurf und Planung die Möglichkeit der Prüfung hinsichtlich der zeitlichen Veränderungen der maßgeblichen Parameter des Bauwerks sicherzustellen.

Dies kann durch Planung der Zugänglichkeit und/oder das Vorsehen von geeigneten Messvorrichtungen erfolgen. Nur so ist zu erreichen, dass Abweichungen frühzeitig erkannt und entsprechende korrektive Maßnahmen ergriffen werden können.

Dieser Aspekt ist im Bauwesen im Gegensatz beispielsweise zur Anlagentechnik und zum Fahrzeugbau zur Zeit noch stark unterentwickelt. So ist es auch heute noch weitgehend üblich, Spannglieder im Spannbetonbau (z.B. bei Brücken) so einzubauen, dass eine Überwachung der Spannkräfte praktisch nicht möglich ist. Deren Veränderung wird dann erst durch Folgeschäden sichtbar, was zu erheblichen Sanierungskosten führt. In Einzelfällen ist hier auch schon plötzliches Versagen mit der Folge des Systemkollapses eingetreten.

Forderung I: Wartungs- und inspektionsfreundliche Planung

4.4.1.2 Errichtung des Bauwerks

In der Realisierungsphase entsteht das Bauwerk auf der Basis der Planung durch das Zusammenwirken einer Vielzahl von Gewerken, wobei industrielle Verfahren der Massen- oder Serienfertigung in der Regel lediglich bei Komponenten Anwendung finden. Bei der überwiegenden Zahl von Bauten handelt es sich um im Prinzip handwerklich erstellte Unikate. Dies führt dazu, dass die in der industriellen Fertigung angewandten Verfahren der Qualitätssicherung nicht unmittelbar übertragbar sind. Unverzichtbar ist als Teil des Projektmanagements hier ein Qualitätsmanagement, das die Übereinstimmung der Ausführung mit der Planung sicherstellt.

Insbesondere größere Bauvorhaben sind durch Planungsänderungen während der Bauphase gekennzeichnet, die oft unter erheblichem Zeitdruck zustande kommen. Jedoch sind auch hier die oben für die Planungsphase aufgeführten Grundsätze in jedem Falle einzuhalten. Dies wird nur dann gelingen, wenn das Projektmanagement bereits in der Planungsphase zumindest informativ beteiligt wurde und die Planungsgrundsätze verstanden hat.

Forderung II: Qualitätsmanagement als Teil des Projektmanagements

4.4.1.3 Prüfung vor Inbetriebnahme

Neben den bereits durch Verordnungen vorgeschriebnen Prüfungen an Bauwerken vor der Inbetriebnahme ist eine generelle Prüfung des baulichen Substanz auf Übereinstimmung mit der Baugenehmigung und der Planung sinnvoll, um eine verlässliche Basis für spätere Inspektionen zu erhalten. Auch kann hier die Beseitigung von Abweichungen im Rahmen der Gewährleistung eingefordert werden.

Eine sogenannte Endabnahme gibt jedoch letztlich nur einen Augenblickszustand wieder. Ein Großteil der Eigenschaften des Bauwerks ist zu diesem Zeitpunkt verdeckt und nicht mehr oder nur mit unvertretbarem Aufwand prüfbar. Aus diesem Grunde kann die Prüfung vor Inbetriebnahme letztlich nur den Abschluss einer baubegleitenden Qualitätssicherung sein, die entsprechend dokumentiert sein muss.

Forderung III: Durchführung einer Prüfung vor Inbetriebnahme

4.4.1.4 Erarbeiten einer Präventivstrategie

Der Erhalt der integralen Sicherheit und des Wertes des Bauwerks erfordert die Festlegung von Plänen für die Wartung und Instandhaltung sowohl des baulichen Teils als auch der technischen Gebäudeausrüstung. Für letztere sind hier die Vorschriften der Hersteller maßgeblich, für das Bauwerk an sich sind diese anhand von Erfahrungswerten festzulegen.

Forderung IV: Erstellen von Wartungs- und Inspektionsplänen

4.4.1.5 Dokumentation

Auch heute ist die Dokumentation für die meisten Bauwerke äußerst lückenhaft. Eine Ausnahme bilden hier eigentlich nur die Brücken, für die verpflichtend Brückenbücher zu führen sind.

Sowohl im Sinne der Qualitätssicherung bei der Errichtung als auch für den Betrieb des Bauwerks und der damit verbundenen Wartungen, Instandhaltungen, Reparaturen und Prüfungen ist die Einführung eines Bauwerkbuches unabdingbar.

Der Inhalt des Bauwerkbuches soll umfassen:

- Übersichtsplan, Lageplan
- Baugenehmigung
- Geprüfte Statik
- Ausführungspläne und Spezifikationen, jeweils auch für einzelne Gewerke
- Unterlagen zur technischen Gebäudeausrüstung mit Bedienungs- und Wartungsanleitungen, ggf. Prüfbücher und zugehörige Prüfberichte
- Abnahmeprotokolle
- Verzeichnis der am Bau Beteiligten
- Auflistung der Termine des Ablaufs der Gewährleistung
- Wartungs- und Instandhaltungspläne mit Bestätigung der Durchführung
- Inspektionspläne und Protokolle der Inspektionen
- Verzeichnis der baulichen Veränderungen (ggf. mit Zeichnungen)
- Liste vorgenommener Reparaturen und Sanierungen (mit Spezifikationen, Zeichnungen und Abnahmeprotokollen)

Bei größerem Umfang kann das Bauwerksbuch aus mehreren sinnvoll zu gliedernde Teilen bestehen.

Forderung IV: Erstellen und Führen eines Bauwerkbuches

4.4.2 Festlegung der Risikoklasse

Die Risikoklasse ist maßgeblich für Umfang, Prüftiefe und Fristen der anzusetzenden Inspektionen. Unabhängig von einem erwünschten Resultat kann eine Bewertungssystematik erstellt werden, die die Charakteristika des Bauwerks, die wirkenden Lasten und die Nutzungsparameter mit Einzelbewertungen versieht nach Gewichtung zu einer Gesamteinstufung führt. Ähnliche Verfahren werden üblicherweise bei populären Tests von Waren (z.B. durch die Stiftung Warentest) angewandt.

Das Gesamtergebnis hängt hier maßgeblich von der Gewichtung der Teilergebnisse ab und wird je nach individuellem Bedürfnis und Kenntnisstand höchst unterschiedlich ausfallen. Um hier einen breiten Konsens zu erzielen, ist die Anwendung der Delphi-Methode zu empfehlen, die auf der These beruht, dass eine Vielzahl subjektiver Expertenmeinungen zu einem objektiven Gesamtergebnis führt (PATZAK [11]). HERTZ [12] hat hierauf basierend ein Verfahren zur finanziellen Risikoanalyse durch stochastische Simulation entwickelt, das durchaus auf das hier vorliegende Problem einer Risikoklassierung hin angepasst werden kann. Allerdings wird empfohlen, das Verfahren um die Bestimmung des Vertrauensbereichs (z.B. unter Anwendung der *t*-Verteilung [13]) und die Berechnung der Varianz zu erweitern, um einerseits stark abweichende Meinungen einzelner Experten identifizieren zu können und andererseits die Bandbreite der Aussagen darzustellen.

Dabei sollte vorerst die Bewertungsskala der Einzelergebnisse und deren Gewichtung durch die Experten vorgeschlagen werden. Anhand festzulegender Musterobjekte wird dann unabhängig von den Experten eine Bewertung und Gewichtung mit den Mittelwerten und den oberen und unteren Quartilen vorgenommen. Die Gesamtergebnisse werden dann den Experten zusammen mit den Angaben zu den Musterobjekten mit der Frage vorgelegt, ob sie der Rangfolge der Objekte zustimmen. Gegebenenfalls sind darauf hin Adaptionen vorzunehmen, um zu einem breit anerkannten Verfahren zu gelangen.

Ein Vorschlag des Verfassers ist in Bild 6 wiedergegeben.

4.4.3 Inspektionen

4.4.3.1 Inspektionsarten

In Anlehnung an bereits vorhandene und bewährte Inspektionsschemata wird die Stufung in

- Eigenüberwachung
- Untersuchungen
- Begutachtungen

Vorgeschlagen, die sich sowohl hinsichtlich ihrer Intensität als auch in der vorauszusetzenden Qualifikation des Durchführenden unterscheiden. Neben diesen turnusmäßig zu planenden Inspektionen werden in besonderen Fällen (z.B. Havarie, unerwartet auftretende größere Schäden) Sonderinspektionen notwendig.

Die Eigenüberwachung ist eine Kontrolle des Bauwerks durch entsprechend eingewiesenes Personal des Betreibers, die in kurzen Zeitabständen im Rahmen des Wartungs- und Instandhaltungskonzepts durchgeführt wird. Hierbei werden Erkenntnisse über Veränderungen am Bauwerk anhand einer Checkliste dokumentiert und einer sachkundigen Person zur Beurteilung und Veranlassung entsprechender Maßnahmen zur Beseitigung von Schäden oder Veranlassung einer Sonderinspektion vorgelegt.

Untersuchungen erstrecken sich auf die Kontrolle der zugänglichen Teile der Konstruktion auf Mängel und Schäden, deren Vorhandensein die Eignung hinsichtlich der Sicherheit, der Dauerhaftigkeit, der Tragfähigkeit und der Funktionssicherheit beeinträchtigen kann. Die zerstörende Öffnung von Bauteilen ist grundsätzlich nicht vorgesehen, kann aber auf Grund der Erkenntnisse als Sonderinspektion empfohlen werden. Diese Prüfungen können nur von Personen vorgenommen werden, die gemäß ihrer Berufsausbildung und der fachlichen Qualifikation in der Lage sind, die statischen Verhältnisse des Bauwerks zu beurteilen.

Begutachtungen erstrecken sich auf alle die Stand- und Funktionssicherheit des Bauwerks betreffenden Teile, soweit diese nicht bereits bei andere vorgeschriebenen Prüfungen inspiziert wurden (z.B. Brandschutz, E-Technik, Aufzüge, HLK). Auch nur mit Hilfsmitteln zugängliche Bauteile sind in den Inspektionsumfang einzubeziehen, die optische Prüfung ist ggf. durch zerstörungsfreie Prüfverfahren und Messungen zu ergänzen. Auch hier können weitergehende Sonderinspektionen (z.B. Öffnung, Ausbau von Bauteilen, Entnahme von Werkstoffproben, Laboruntersuchungen) erforderlich werden. Die Art der Inspektion setzt voraus, dass über die Anforderungen für Untersuchungen Personen mit langjähriger Erfahrung in der Prüfung von Bauwerken eingesetzt werden, die mit den üblichen Schadensbildern vertraut sind und den Einfluss von Mängeln auf die Sicherheit beurteilen können.

Alle Inspektionen sind so zu dokumentieren, dass dem Betreiber Hinweise für einzuleitende Maßnahmen und eventuelle Nutzungseinschränkungen eindeutig mitgeteilt werden.

4.4.3.2 Prüffristen

Anhand der Risikoklasse des Bauwerks sind die Fristen für die einzelnen Inspektionsarten so festzulegen, dass eine Veränderung am Bauwerk, die die Stand- und/oder Funktionssicherheit gefährdet, frühzeitig genug erkannt wird, um durch geeignete Reparatur- und Sanierungsmaßnahmen oder die Außerbetriebnahme Schaden von Personen und Gütern abzuwenden.

Als Anhaltswert sollen hier die Prüffristen für Brücken nach DIN 1076 herangezogen werden. Unter Verwendung des Bewertungsschemas in Bild 6 würden Stahlbetonbrücken in der Regel eine Gesamtbewertung von etwa 4,0 erreichen. Solche Bauwerke sind alle drei Jahre einer Untersuchung und alle sechs Jahre einer Begutachtung (bei Brücken Hauptprüfung genannt) zu unterziehen.

A Vulnerabilität		Punkte	G	W x G
A1 Statische Verhältnisse				
Träger auf 2 Stützen, Kragarme		2		
Durchlaufträger, Fachwerk,Stahlbetonrahmen		5		
Stahlrahmen, Scheiben, Theorie 2. Ordnung,		10		
	Auswahl W	5	50%	2,5
A2 Konstruktion				
Einfache Konstruktion (z.B. Decken in Wohnhäusern oder Bürogebäuden) oder Kragdach lk <= 3,0 m		2		
genietete, geschraubte **Stahlkonstruktion**, Kragdächer lk >3,0 m, einzelne Schweißnähte an gut zugänglichen Stellen		5		
Stahlbeton, Betonfertigteile, Spannbeton, Kragdächer lk >3,0 m		5		
geschraubte **Holzkonstruktion** aus Vollholz, Leimbinder, Kragdächer lk >3,0 m		5		
Stahlbau mit geschweißter Haupttragkonstruktion		7		
Brettschichtholz, genagelte Konstruktionen		9		
Hohlkästen		10		
	Auswahl W	5	50%	2,5
	Summe A			**5,0**
B Einwirkungen				
B1 Lasten				
vorwiegend ruhende Lasten mit großen Sicherheits-reserven		2		
vorwiegend ruhende Lasten ohne großen Sicherheits-reserven		4 4		
dynamische Lasten		8		
Eingebaute Kranbahnen		10		
	Auswahl W	4	70%	2,8
B2 Sonstige Einwirkungen				
keine		0		
Feuchtigkeit		6		
chemischer Angriff		10		
starke Temperatureinwirkung		4		
	Auswahl W	4	30%	1,2
	Summe B			**4,0**
C Nutzung				
C1 Personenschäden				
Kein Publikumsverkehr		1		
zeitweise Publikumsverkehr		5		
ständiger Publikumsverkehr		10		
	Auswahl W	5	70%	3,5
C2 Geschossfläche				
unter 1000 m²		2		
bis 5000 m²		5		
über 5000 m²		10		
	Auswahl W	5	30%	1,5
	Summe C			**5,0**
Gesamteinstufung				
Vulnerabilität		5,0	30%	1,5
Einwirkungen		4,0	20%	0,8
Nutzung		1,5	50%	0,75
	Gesamtwert			3,05

Bild 6: Vorschlag Bewertungsschema zur Ermittlung der Risikoklasse

Als unterer Grenzfall werde ein kleineres Bürogebäude mit geringem Publikumsverkehr in herkömmlicher Bauweise betrachtet. Die Gesamtbewertung nach dem Vorschlag in Bild 6 würde etwa den Wert 2,0 ergeben. Für solche Bauwerke dürfte eine Eigenüberwachung in der Regel hinreichend sein.

Hieraus ergibt sich auf der Grundlage der Bewertungsziffern und Gewichtungen des Vorschlags etwa die in Bild 7 zusammengefasste Festlegung von Prüffristen.

Gesamtbewertung	Eigenüberwachung	Untersuchung	Begutachtung
< 2,5	6 Monate	Keine	Keine
2,5 bis 3,5	6 Monate	5 Jahre	Keine
> 3,5	6 Monate	3 Jahre	6 Jahre

Bild 7: Vorschlag für Inspektionsfristen an Bauwerken (bautechnischer Teil)

5 Zusammenfassung

Auf der Grundlage der haftungs- und strafrechtlichen Bedingungen und bereits bestehender deutscher Normen und Regelwerke wurde eine Inspektionssystematik für Bauwerke entwickelt, die die bereits heute vorgeschriebenen Prüfungen um den Aspekt der Stand und Funktionssicherheit der baulichen Substanz erweitert. Dabei wurde auch die Tatsache berücksichtigt, dass in neuerer Zeit im Immobilienmanagement eingeführte Präventions- und Inspektionsstrategien die Gesamtkosten mindern und zu einem wirtschaftlichen Betrieb maßgeblich beitragen.

6 Literatur

[1] Bürgerliches Gesetzbuch in der Fassung der Bekanntmachung vom 2. Januar 2002. BGBL. I 42, ber. 2909.

[2] Strafgesetzbuch, Neufassung vom 13. November 1998. BGBl I 3322, zuletzt geänd. 1. September 2005, BGBl I 2674.

[3] DIN 1076: Ingenieurbauwerke im Zuge von Straßen und Wegen; Überwachung und Prüfung. November 1999.

[4] Richtlinie 804.8001: Ingenieurbauwerke planen, bauen u. Instand halten; Inspektion von Ingenieurbauwerken. DB Netz AG, 01.11.2000.
RiL 804.8001: -; Allgemeine Grundsätze.
RiL 804.8002: -; Eisenbahnüberführungen.
RiL 804.8003: -; Überbauungen von Betriebsanlagen und sonstige Überbauungen.
RiL 804.8004: -; Sonstige Ingenieurbauwerke.

[5] DIN 1045-1: Tragwerke aus Beton, Stahlbeton und Spannbeton Teil 1: Bemessung und Konstruktion. Juli 2001 mit Berichtigung Juli 2002.

[6] DIN 18 800-1: Stahlbauten; Teil 1: Bemessung und Konstruktion. November 1990.

[7] Kuhlmann, A.: Einführung in die Sicherheitswissenschaft. Wiesbaden/Köln 1981.

[8] Switaiski, B., Bücker, J.: Betriebliche Umsetzung des Risk-managements; Planungsphase und Bauüberwachung. In: Lutz, U., Klaproth, T. (Hrsg.): Risikomanagement im Immobilienbereich. Berlin/ Heidelberg 2004.

[9] Bradler, A: Immobilienspezifisches Riskmanagement in der Kommune – ein Ansatz zur Bewältigung anstehender öffentlicher Aufgaben im Spannungsfeld zwischen Versorgungsauftrag und sinkenden Kassen. In: Lutz, U., Klaproth, T. (Hrsg.): Risikomanagement im Immobilienbereich. Berlin/Heidelberg 2004.

[10] Weierganz, Th.: TÜV Erfahrungsaustausch „Sicherheit von öffentlichen Hallen". Berlin, 15.03.2006.

[11] Patzak, G.: Systemtechnik – Planung komplexer innovativer Systeme. Berlin, Heidelberg 1982.

[12] Hertz, D. B.: Risk Analysis in Capital Investment. Havard Business Review, Jan./Feb. 1964, pp. 95 – 106.

[13] Abramowitz, M., Segun, I. A.: Handbook of Mathematical Functions. New York 1968.

Uncertainties of material properties in nonlinear computer simulation

Radomír Pukl[1], Drahomír Novák[2], Miroslav Vořechovský[2] and Konrad Bergmeister[3]
[1] Červenka Consulting, Praha, Czech Republic
[2] Institute of Structural Mechanics, Brno University of Technology, Czech Republic
[3] University of Natural Resources and Applied Life Sciences, Vienna, Austria

Abstract: Nonlinear finite element method and advanced stochastic package were coupled in order to account uncertainties, randomness and spatial variability of material properties in computer simulation of structural behaviour and failure. The nonlinear FE program ATENA contains advanced constitutive models for concrete based on damage mechanics, fracture mechanics and plasticity theories with smeared crack approach. The advanced stochastic simulation software FREET is employed for the stochastic treatment. New and updated (significantly improved) methods were developed and verified in the simulation of uncertainties, e.g. small-sample simulation of Monte Carlo type Latin hypercube sampling for both random variables and random fields with focus on correlation control among variables, accurate representation of random fields based on spectral decomposition of covariance matrix and employing very small number of underlying random variables, hierarchical nonlinear material models etc. The complex simulation tool SARA which efficiently combines both above mentioned packages has been introduced at the 3rd International Probabilistic Symposium 2005 for the level of random variables. It can evaluate statistical properties of response variables (stresses, deflections, crack widths etc.) and consequently reliability analysis of the structure can be performed. Here the upgrade to the level of random fields is described. An efficient method encapsulating the existing material models has been developed and implemented in the nonlinear finite element framework to account the spatial variability of material properties generated by the random fields technology or measured in-situ. Several illustrative examples of the stochastic fracture mechanics simulation accounting the spatial variability of material properties are presented.

1 Introduction

Computer simulation based on nonlinear finite element analysis is a well established and widely used methodology for investigation of structural behaviour under severe conditions. Input parameters like material properties for such a simulation are usually considered as deterministic values. In reality, these values are uncertain and random, which can considerably affect structural behavior, response and damage processes. It has been shown (Pukl & Bergmeister 2005, Novák 2005) that this subject can be satisfactorily solved in a rational and mathematically precise way and the random characteristics of nature can be addressed by computational models based on stratified sampling of random variables. A higher level and also very natural (physical) technique of uncertainties modeling is their representation by random fields. The stochastic numerical results from both random variables and random fields analyses can be statistically evaluated and used for assessment of structural safety and reliability.

2 Nonlinear Computer Simulation of Building Structures

The nonlinear finite element program ATENA employs advanced constitutive models for concrete based on damage mechanics, nonlinear fracture mechanics (as illustrated in Fig. 1) and plasticity theories with smeared crack approach. It is a proven tool for computer simulation of reinforced structures including failure mechanism and post-peak behaviour (Červenka & Bergmeister 1999, Červenka 2000, Bergmeister 2005). The program consists of solution core and user-friendly graphical environment. The graphical user interface serves for creating of structural model and evaluation of results, even already during the analysis. The solution core includes finite element modelling, numerical equation solver, nonlinear solution methods and nonlinear material models.

For computer simulation of concrete and reinforced concrete structures including its interaction with neighbourhood the program offers variety of nonlinear material models for concrete (plain, reinforced, pre-stressed, fibre reinforced concrete), quasi-brittle materials like masonry, rock, soils and metals, namely:

- damage-based material model
- fracture-plastic cementitious material
- microplane material model
- Drucker-Prager plasticity model
- Von Mises plasticity model
- plasticity with hardening for reinforcement
- etc.

All these material models contain number of parameters, which define the numerical model and describe the nonlinear behaviour. Typical parameters for concrete are Young's modulus of elasticity, compressive and tensile strength, fracture energy, Poisson's ratio etc. In the standard (deterministic) solution these parameters are treated as deterministic values, constant within the structure or its parts. This assumption allows calculating a response to given actions in terms of mean values. Safety issues at the deterministic level should be addressed by means of global safety factors (Červenka 2006).

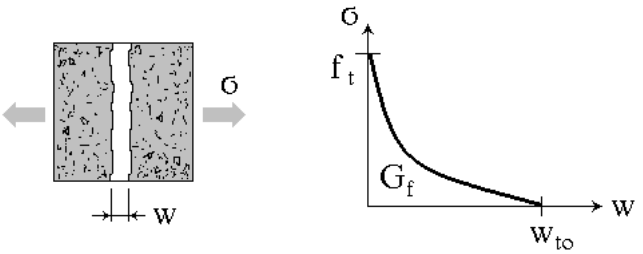

$$\frac{\sigma}{f_t} = (1+c_1\frac{w}{w_{to}})^3 \exp(-c_2\frac{w}{w_{to}}) - \frac{w}{w_{to}}(1+c_1^3)\exp(-c_2)$$

$$c_1 = 3, \quad c_2 = 6.93, \quad w_{to} = 5.14\frac{G_f}{f_t}$$

Fig. 1: Nonlinear fracture mechanics approach for concrete in tension: exponential stress – crack-opening law

3 Uncertainty and randomness of input parameters

Solution to the variety of complex engineering problems, involving randomness in the mechanical properties and in the excitations they are subjected to, can be found by means of simulation. The Monte Carlo type of simulation is usually used for this purpose. However, a requirement of large number of samples can be time consuming and thus can be a serious limiting obstacle in practical cases. An efficient solution of this problem is offered in software SARA, which couples the nonlinear finite element analysis with appropriate stochastic methods (Pukl et al. 2003, Pukl and Bergmeister 2005, Bergmeister 2006). Part of the SARA package is the software FREET for stochastic functions (Novák et al. 2003). It is used in two stages of analysis:

(i) Generation of random samples, which are passed to the deterministic solver.

(ii) Statistical assessment of random response together with information on dominating and non-dominating variables (sensitivity analysis) and estimation of reliability using reliability index and/or theoretical failure probability.

For time-intensive calculations like nonlinear fracture mechanics of concrete, the small-sample simulation techniques based on stratified sampling of Monte Carlo type represent a rational compromise between feasibility and accuracy. Therefore Latin hypercube sampling (LHS) was selected in FREET as a key fundamental technique. The method belongs

to the category of stratified simulation methods. It is a special type of the Monte Carlo simulation, which uses the stratification of the theoretical probability distribution function of input random variables. It requires a relatively small number of simulations to estimate statistics of response – repetitive calculations of the structural response (tens or hundreds).

The basic feature of LHS is that the probability distribution functions for all random variables are divided into N_{Sim} equiprobable intervals (where N_{Sim} is number of simulations); the values from the intervals are then used in the simulation process (random selection, median of interval or the probabilistic mean value of an interval). This means that the range of the probability distribution function of each random variable is divided into intervals of equal probability (McKay et al. 1979, Iman & Conover 1980). The samples are chosen directly from the distribution function based on an inverse transformation of distribution function, as illustrated in Fig. 2.

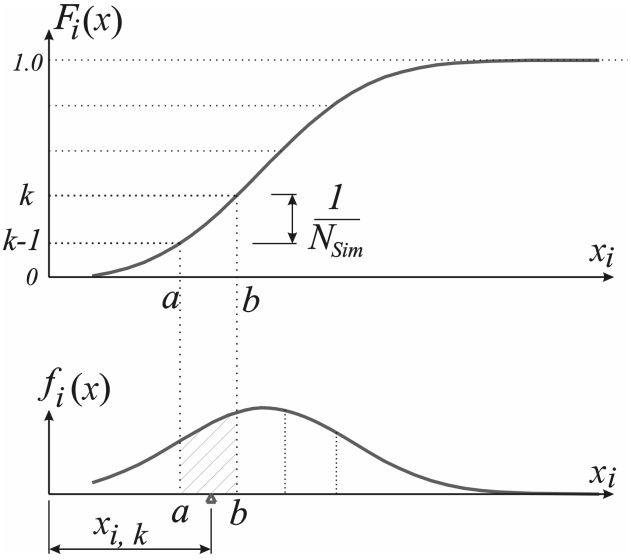

Fig. 2: Scheme of the Latin hypercube sampling

The order of representative parameters of variables are selected randomly, being based on random permutations of integers 1, 2, ..., j, N_{Sim}. Every interval of each variable must be used only once during the simulation. Being based on this precondition, a table of random permutations can be used conveniently, each row of such a table belongs to a specific simulation and the column corresponds to one of the input random variables. Once the samples of each input random variable alone are generated, the correlation structure according to the target correlation matrix must be taken into account. There are generally two problems related to the statistical correlation: First, during sampling an undesired correlation can occur between the random variables. For example, instead of the correlation coefficient zero for the uncorrelated random variables an undesired correlation can be generated. It can happen especially in the case of a very small number of simulations (tens), where the number of interval combination is rather limited. Another task is to introduce the prescribed statistical correlation between the random variables defined by the correlation matrix. The columns in LHS simulation plan should be rearranged in such a way that they may fulfil the following two requirements: to diminish the undesired random correlation and to introduce the prescribed correlation. A robust technique to impose statistical

correlation based on the stochastic method of optimization called simulated annealing has been proposed recently by Vořechovský & Novák (2003). The imposition of the prescribed correlation matrix into the sampling scheme can be understood as an optimization problem: The difference between the prescribed and the generated correlation matrices should be as small as possible. In such a way, the optimal sets of input parameters are generated and passed to the solver.

The nonlinear finite element solver, represented in SARA by program ATENA, performs analyses of the structure with generated sets of input variables in order to obtain more realistic structural response. The results are evaluated by stochastic methods according to paragraph (ii). Safety of the structure is assessed directly by built-in reliability methods. The basic level of introducing randomness into the nonlinear finite element analysis by SARA system is treatment of the input parameters as random variables. Selected parameters are randomized as described above, and their values differ from sample to sample, but inside of a single sample they are constants over the structure or structural part respectively. Thus, the spatial variability of the structural properties is neglected at the level of random variables.

4 Spatial variability of material properties

Spatial variability of structural properties, in particular of material properties, is an important phenomenon, which can have substantial influence on the structural damage and failure – e.g. crack initiation and localization in homogeneous stress state region as it occurs in four point bending tests. Therefore, it should be properly accounted in the computer simulation of structures if realistic results are desired. The ATENA program has been extended in order to be able to account for the spatial variability of material properties. General parameters for the material models are updated according to the predefined values over the structure.

The parameters of material models in the nonlinear finite element analysis are created and stored individually for each integration (material) point, since they can have individual settings and can locally change during the solution (e.g. due to damage processes or stress redistribution). Standard treatment of the local material models can be itemized as follows:

- input of general parameters
- adjustment of local parameters in integration (material) point (e.g. scaling to the finite element size)
- changes of local parameters during nonlinear solution (e.g. reduction of lateral strength and shear stiffness in cracks, increase of compressive strength due to lateral compression etc.)

If the spatial variability should be reflected, the above scheme will change as follows:

- input of general parameters
- substitution of general parameters with predefined local parameters

- adjustment of local parameters in integration points (here comes the association with a random field realization)
- changes of local parameters during solution.

Since the number of material models in ATENA is rather high, and the spatial variability should be enabled for all of them, an efficient methodology has been developed for substitution of the general parameters with the local ones by encapsulating the existing material models into an envelope. This envelope provides transfer of the local material parameters from the predefined geometrical matrix to the influenced material model. The value from the nearest geometrical point is adopted for the material point. If the parameter values are defined in the material points (Gaussian integration points), they are directly used for substitution of the general parameters.

The geometrical matrix describing the spatial distribution of the material parameters is stored in an ASCII file with coordinates and corresponding parameter values. It can be created in several ways:

- it can contain the values from (in situ) measurements
- it can be written arbitrary by user – e.g. for introducing of (a local) inhomogeneity
- it can be generated in a scientific and mathematically precise way – by random fields methodology

5 Random fields approach

The term stochastic or probabilistic finite element method (SFEM or PFEM) is used to refer to a methodology, which accounts for uncertainties in the geometry or material properties of a structure, as well as the applied loads. The representation of spatial variability of structural properties by random fields is a high level of their modelling with a scientific background. Random fields describe the spatial distribution of a structural (material) property over the region representing the structure. The spatial correlation of the generated random fields, defined by correlation length (and the autocorrelation function), is of crucial importance. Randomly selected examples of realizations of 2D random fields over a rectangular support for different correlation lengths are shown in Fig. 3 for illustration.

Because of the discrete nature of the finite element formulation, the random field must also be discretized into random variables. This process is commonly known as random field discretization. The computational effort in reliability problem generally increases with the number of random variables. Therefore it is desirable to use small number of random variables to represent a random field. To achieve this goal, the transformation of the original random variables into a set of uncorrelated random variables can be performed through a well-known eigenvalue orthogonalization procedure. It has been demonstrated that a few of these uncorrelated variables with largest eigenvalues are sufficient for the accurate representation of the random field.

The utilization of the above described LHS method for simulation of Gaussian uncorrelated variables is a new simple idea for improvement of random field simulation using orthogonal transformation of covariance matrix suggested by Novák et al. (2000). The superiority of this stratified technique remains here also for accurate representation of random field, thus leading to the decrease of number of simulations needed (Vořechovský & Novák 2005). The approach is based on utilization of stratified sampling technique LHS for simulation of dominating uncorrelated random variables. The result is that only a few random variables and quite small number of simulations is necessary for accurate representation of a random field.

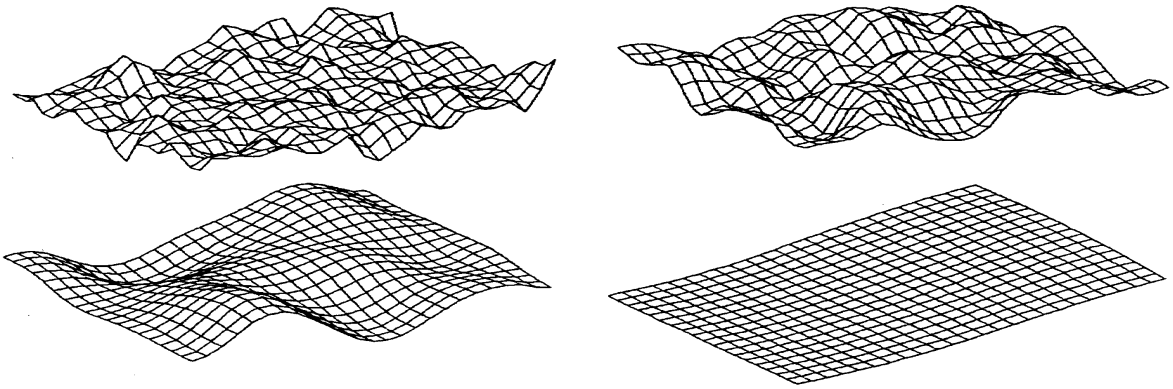

Fig. 3: Realizations of 2D random fields with increasing spatial correlation

This methodology is implemented in FREET as a level of random fields, which can represent the spatial variability of material properties for the structural analysis in ATENA. The above described technology of encapsulating existing nonlinear material models and spatial distribution matrix are utilized in SARA system at this level. It enables to model the spatial variability and material inhomogenities in the nonlinear finite element solution in a highly scientific and systematic way. The results can be therefore directly statistically evaluated and used for statistical assessment of response variables, sensitivity analysis and estimation of structural reliability and failure probability, as recommended by Červenka (2006).

6 Selected application examples

The use of the SARA system at level of random fields is illustrated on several selected examples. Another example of utilizing the SARA system is described in a separate paper submitted to this Symposium (Strauss 2006).

Random crack initiation and localization in numerical simulation of four-point bending tests is shown in Fig. 4. The first (uniformly grey) beam was analyzed with the deterministic strength value, which was constant over the whole structure. Two major symmetrical cracks and symmetrically distributed microcracks appear in this case. In the next four beams the strength is randomly distributed over the structure. The regions with lower con-

crete strength are red (dark) coloured. The localized cracks are depicted by short black lines in the damaged material points; the thicker line the larger crack width. Random appearance of cracks in the beam and various crack patterns are obvious.

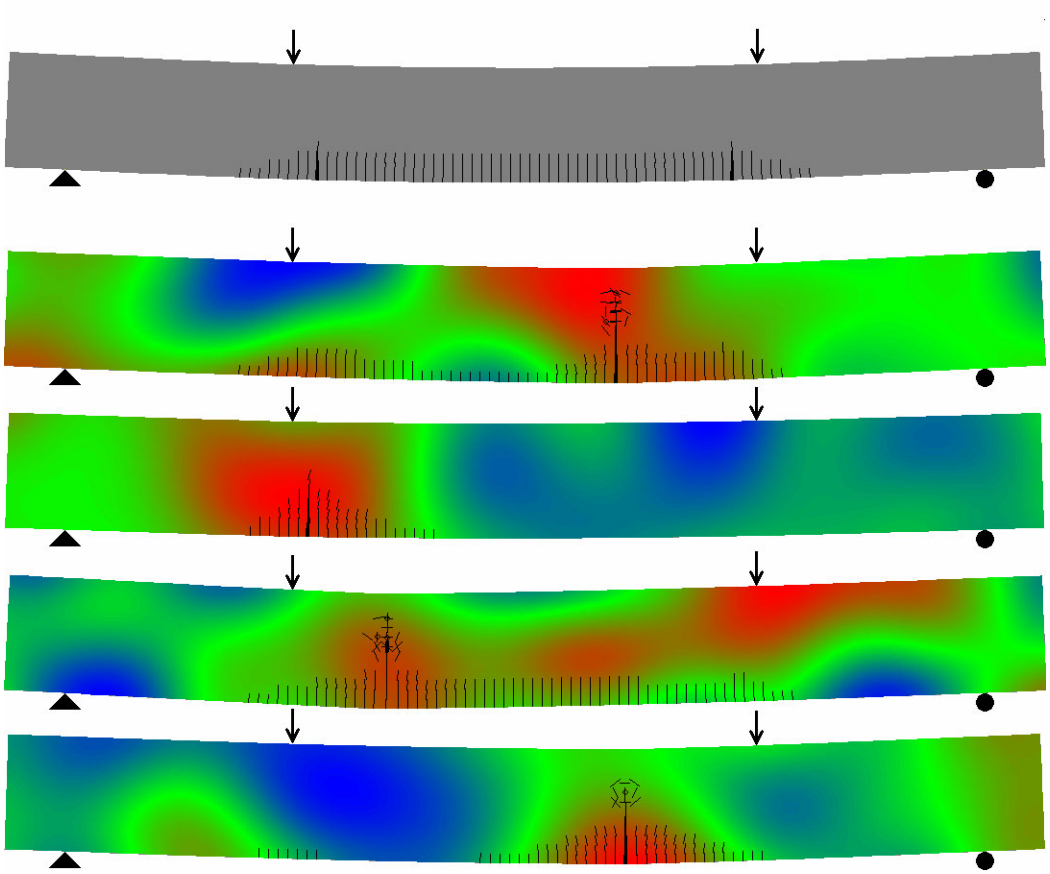

Fig. 4: Four-point bending tests - random fields of strength and crack patterns

A bundle of normalized load-deflection curves from the extensive random-fields simulation of those four-point bending beams is presented in Fig. 5. Due to spatial randomness the mean of the peak load decreases comparing to the deterministic capacity. Note that also the average plus one sample standard deviation does not reach the peak deterministic nominal stress. This is an important fact with serious consequences in rational design and assessment of structures.

A complex example based on the random field's methodology was published by Vořechovský and Matesová (2006). It presents numerical simulation of experimentally obtained size effect in dog-bone shaped concrete specimens under uniaxial tension (illustrative Fig. 6). In the cited paper it is shown how the statistical size effect can be computationally captured. Since the deterministic model automatically models the energetic size effects caused by stress redistribution, the complex statistical-energetic size effect gets truly modelled by the presented software tools.

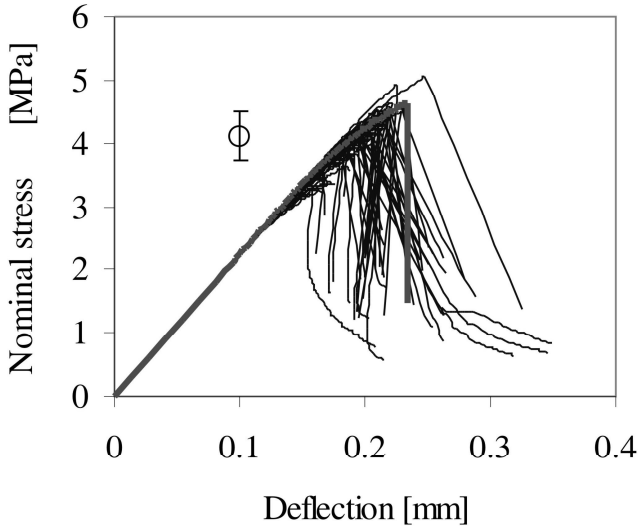

Fig. 5: Random stress–deflection curves (the thick red curve represents deterministic calculation)

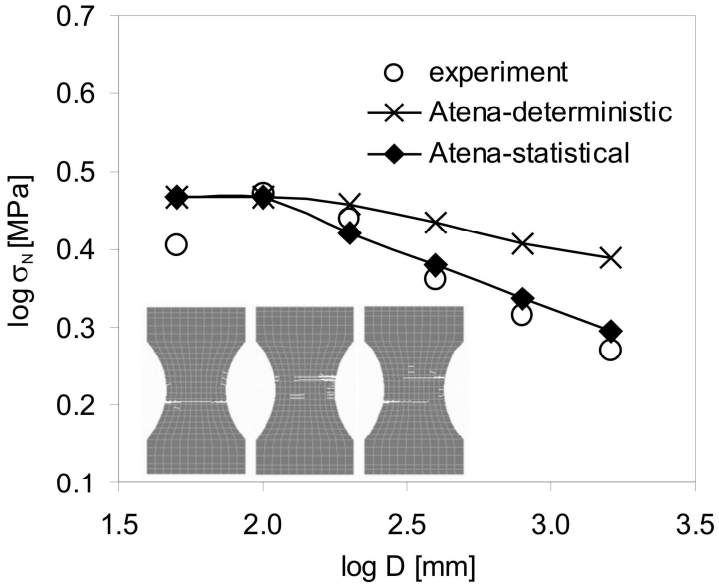

Fig. 6: Random crack initiation and size effect curves – experiment vs. simulation

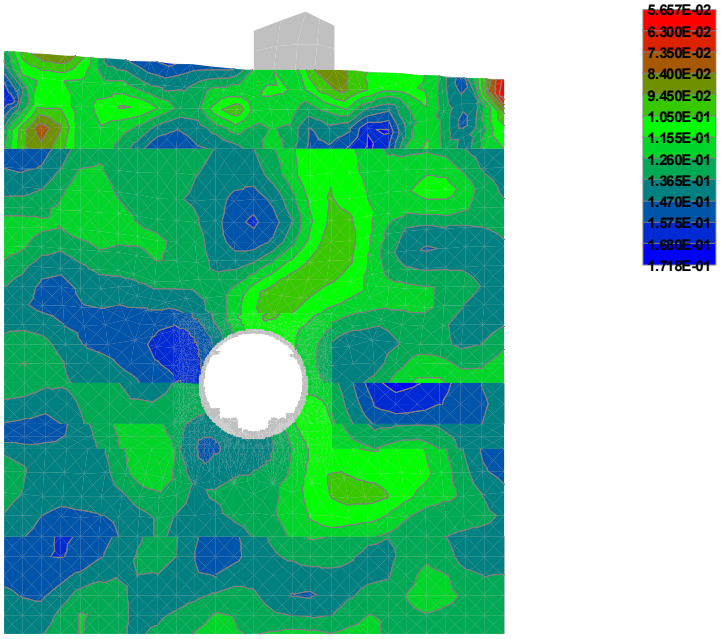

Fig. 7: Random field of soil property (Drucker-Prager parameter α) around a concrete tunnel tube

The application of random fields is also very suitable for solution of soil-structure interaction tasks. The influence of spatial variation of Young's modulus and material constants of Drucker-Prager failure criterion (based on cohesion and angle of internal friction) was studied. The stability of concrete tunnel tube in complicated geological conditions has been analyzed. The thickness of geological layers was between 10 and 25 m, the diameter of the tunnel tube was 11 m, the typical wall thickness 0.5 m. The whole analyzed part of the soil with tunnel had the dimensions of 50 × 60 m. It was solved in plane strain state and discretized in 5000 finite elements. Drucker-Prager plasticity was used for modelling of soil behaviour. The spatial variability was simulated using Gaussian random fields with correlation length of 2 m. A model sample is shown in Fig. 7.

7 Conclusion

The random nature and variability of structural features are widely recognized by both industry and researchers. The object of uncertainty can be solved in a scientific and mathematically precise way and the random characteristics of nature can be addressed by computational models. A high level technique of uncertainties modelling is its representation by auto-correlated random fields. An efficient method encapsulating the existing material models has been developed and implemented in order to account for spatial variability of material properties in the nonlinear finite element framework. The variable structural properties used for calculation can be measured in-situ or generated by random fields technology.

The presented technology enables to model material inhomogenities in the nonlinear finite element solution, which can simulate random occurrence of structural damage (crack) even

in a homogeneous stress state (four-point bending beams), capture complex statistical-energetic size effect etc. These features are in particular important in materials with high variability and uncertainty of their properties like fibre reinforced concrete, masonry or soil.

The numerical results can be directly statistically evaluated and used for structural reliability assessment.

8 Acknowledgement

The related research was partially supported by grant No. 1ET409870411 "VITESPO" of Czech national research program "Information society".

9 References

[1] Bergmeister, K. "Integrierte Bau- und Energietechnik beim Universitätsgebäude Brixen", *Beton- und Stahlbetonbau* 100, (2), p. 161, 2005.

[2] Bergmeister, K. "Stochastic structural modeling", *4th International Probabilistic Symposium*, BAM, Berlin, Germany, 2006.

[3] Červenka, V. and Bergmeister, K. "Nichtlineare Berechnung von Stahlbetonkonstruktionen", *Beton- und Stahlbetonbau* 94, Heft 10, 413-419, 1999 (in German).

[4] Červenka, V. "Simulating a Response", *Concrete Engineering International* 4 (4), 45-49, 2000.

[5] Červenka, V. "Safety Assessment in Non-linear Analysis of Concrete Structures", ***fib*** 2nd International Congress, Naples, Italy, 2006.

[6] Iman R.C. & Conover W.J. "Small Sample Sensitivity Analysis Techniques for Computer Models with an Application to Risk Assessment", *Communications in Statistics Theory and Methods* A9 (17), 1749-1842, 1980.

[7] McKay, M.D., Conover, W.J. & Beckman, R.J. "A Comparison of Three Methods for Selecting Values of Input Variables in the Analysis of Output from a Computer Code", *Technometrics* 21, 239-245, 1979.

[8] Novák, D., Lawanwisut, W. and Bucher, C. "Simulation of Random Fields Based on Orthogonal Transformation of Covariance Matrix and Latin Hypercube Sampling", *Int. Conference on Monte Carlo Simulation MC 2000*, Monaco, Monte Carlo, 129-136, 2000.

[9] Novák, D., Rusina, R. & Vořechovský, M. 2003. "Small-sample statistical analysis - software FREET", *9th International conference on applications of statistics and probability in civil engineering (ICASP9)*, Berkeley, California, USA, 2003.

[10] Novák, D. "Small sample simulation methods for statistical sensitivity and reliability analysis", *3rd Probabilistic workshop – Technical systems + Natural hazards*, BOKU, Vienna, Austria, 2005.

[11] Pukl, R., Červenka, V., Strauss, A., Bergmeister, K. & Novák, D. "An advanced engineering software for probabilistic-based assessment of concrete structures using nonlinear fracture mechanics", *9th Int. Conf. on Applications of Statistics and Probability in Civil Engineering – ICASP 9*, San Francisco, USA, Rotterdam Millpress, 1165-1171, 2003.

[12] Pukl, R. and Bergmeister, K. "Safety and Reliability Assessment of Concrete Structures and Practical Applications", *3rd Probabilistic Workshop: Technical Systems + Natural Hazards*, BOKU, Vienna, Austria, 2005.

[13] Strauss, A. "Lifetime assessment of concrete structures considering material uncertainties", *4th International Probabilistic Symposium*, BAM, Berlin, Germany, 2006.

[14] Vořechovský, M. and Novák, D. "Statistical correlation in stratified sampling", *9th Int. Conf. on Applications of Statistics and Probability in Civil Engineering – ICASP 9*, San Francisco, USA, Rotterdam Millpress, 119-124, 2003.

[15] Vořechovský, M. and Novák, D. "Simulation of random fields for stochastic finite element analysis", *9th Int. conf. on Structural Safety and Reliability – Icossar 2005*, Rome, Italy, 2005.

[16] Vořechovský, M. and Matesová, D. "Interplay of sources of size effect in concrete specimens", *Computational modeling of concrete structures* – Euro-C 2006, Mayrhofen, Austria, 2006.

Reliability of RC Members Strengthened with Externally Bonded Reinforcement

Stefan Daus, Carl-Alexander Graubner
Institute of Concrete and Masonry Structures, University of Technology Darmstadt

Summary: Bonding additional reinforcement on the surface of concrete members is a common technique for strengthening nowadays. For those strengthenings the proof of the bond strength, is an essential part of the design. To adapt a new proof concept for the bond strength to the German design codes, the partial safety factors are presently calibrated such that the required safety level is reached of all strengthened members as equally as possible. This includes the determination of the important basic variables as well as the size of the safety factors by means of a reliability analysis using Adaptive Importance Sampling. At first some characteristic of the bond between concrete and external reinforcement and of the considered proof concept are described briefly. Subsequently the reliability analysis is addressed paying special attention to the kind of safety factor, the stochastic model and the model uncertainties.

1 Introduction

Strengthening of concrete members by gluing additional reinforcement on its surface is a common technique nowadays, that has proved to be superior compared to other techniques in many cases. While in the beginning only steel plates were used as external reinforcement, fiber reinforced polymers (FRP) became more and more established over the past 15 years. FRP are used in the form of fabrics or lamellas and strips respectively. For the latter the fibers are embedded in a matrix of resin ex work, whereas fabrics are worked into the resin while gluing them onto the surface of the concrete.

Concerning the effectiveness of those strengthenings the force-fit connection of the additional reinforcement and the concrete member is essential. Thus the proof of the bond strength is an important part of the structural analysis of strengthened concrete members, which is – when FRP is used as external reinforcement – decisive in most cases.

However the most codes or technical approvals respectively concerning those strengthenings use design concepts for the bond strength, which are treating the bond of the externally glued reinforcement insufficiently. In the meantime however newer and more appropriate proof procedures are available. As one of these new concepts shall be included in the German technical approvals, a reliability-based calibration of the partial safety factors of that concept is conducted, to assure, that using the new concepts results in reaching the required safety level.

2 Structural Strengthening with Externally Bonded Reinforcement

2.1 Bond Between Concrete and Externally Glued Reinforcement

In contrast to the bond between concrete and reinforcement bars the bond between concrete and external reinforcement glued on the surface behaves very brittle and fails already at very small relative displacements and shear stresses respectively. Therefore – in contrast to reinforcement bars – only forces can be transferred at the plate end or end of laminate respectively, which are considerably smaller than the ultimate load of the element (s. e. g. NEUBAUER [8] or NIEDERMEIER [9]). For steel plates with common thickness only about 20 % to 40 % of the yield stress can be transferred and for lamellas of FRP the bond strength corresponds to only about 15 % of the ultimate load. To transfer larger forces, cracks along the adhesive surface are needed, in which the slip between concrete and external reinforcement can be reduced. The axial force in the external reinforcement is then increased gradually over the several sections between the cracks. Therefore bond failure can occur not only at the end of plate or laminate respectively but also on other locations as e. g. at concentrated loads or the point where the internal reinforcement starts yielding. Thus the bond strength has to be verified over the entire area being stressed by shear forces regarding the crack pattern along the adhesive surface, the more so as the location of failure is not known a priori.

2.2 New Design Concepts for the Bond Strength of External Reinforcement

Both NEUBAUER [8] and NIEDERMEIER [9] developed design concepts, which enable to prove the bond strength over the entire length of the external reinforcement. Within the scope of the own research only the concept of NIEDERMEIER is regarded, because it is planned to included it in the technical approvals in Germany. The concept is described below in few words. A detailed description of the concepts can be found in [8] and [9].

At first the crack pattern of the member has to be determined in the ultimate limit state. Subsequently the stresses in the external reinforcement σ_L must be calculated in every crack as well as the differences of stresses $\Delta\sigma_{L,eff}$ for each section of external reinforcement lying between two cracks. Afterwards the differences of stresses $\Delta\sigma_{L,tol}$, that can be

transferred by the bond strength between two cracks is calculated by means of the formulas given in [9]. Amongst others $\Delta\sigma_{L,tol}$ is a function of the lower one of the stresses σ_L in the bordering cracks. At last the differences of stresses $\Delta\sigma_{L,eff}$ and $\Delta\sigma_{L,tol}$ have to be compared. Because the location of the maximum utilization of the bond strength is unknown a priori, this comparison is necessary over the entire length of the external reinforcement (i. e. for every section lying between two cracks and at the end of the reinforcement), what is exemplified in Fig. 1. In Fig. 1 every triangle is standing for the difference of stresses of one section. That proof concept of the bond strength is rather extensive. As every section between two cracks has to be investigated and the number of cracks depends on the load, there have to be regarded several limit state functions, whose number is depending on the loading.

Fig. 1: Proving of the bond strength according to NIEDERMEIER [9]

In Fig. 1 the differences of stresses $\Delta\sigma_{L,eff}$ and $\Delta\sigma_{L,tol}$ are displayed as a function of σ_L. It is also possible to chart the totals stresses $\sigma_{L,eff}$ and $\sigma_{L,tol}$ over the length of the member. That type of chart is shown in Fig. 2 for the left half a one-span beam (length $l = 4.40$ m) and for two levels of loading. Fig. 2 clearly shows, that the bond strength depends on the bond action. Furthermore it can be seen, that for $q_i = 2.0 * q_0$ the failure of the bond occurs at the point $x \approx 0.85$ m, where the lines of $\sigma_{L,eff}$ and $\sigma_{L,tol}$ have an intersection. Thus the location of bond failure coincides neither with the end of the lamella nor with the maximum of the bending moment nor with concentrated loads and could not be detected a priori.

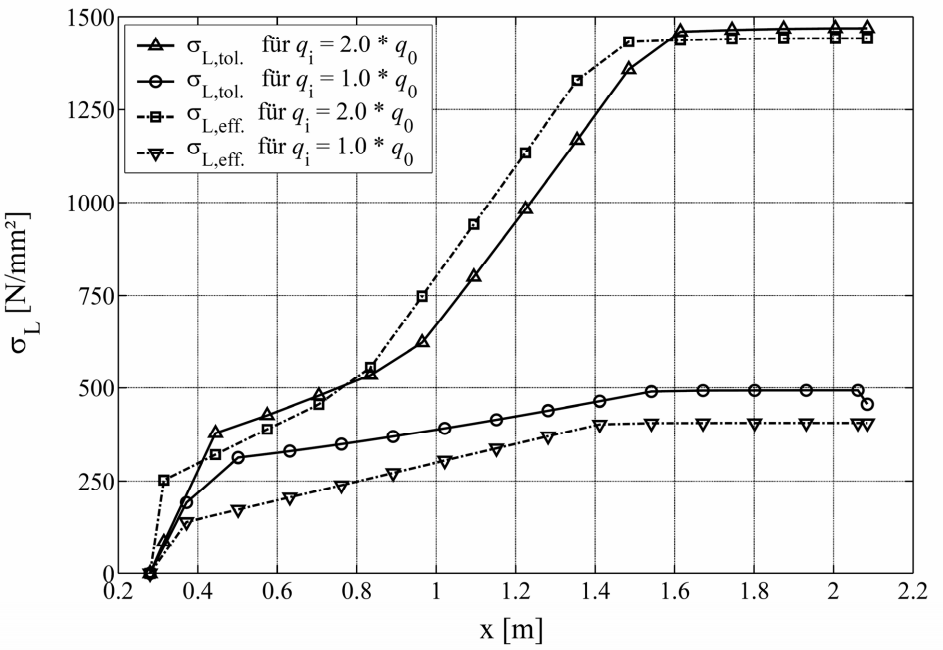

Fig. 2: Tolerable and existing stresses in the external reinforcement of the left half of an one-span beam for two levels of loading

2.2.1 Conclusions

The mentioned characteristics of the bond between concrete and external reinforcement result in some particularities which have to be considered at the calibration of the partial safety factors:

- The bond strength is a function of the loading.
- The location where bond failure occurs as well as the relevant limit state function are not known a priori.
- The number of limit state functions is variable for one regarded member depending on the load.
- Setting up the limit state function is rather difficult and may be impossible as the regarded new proof concepts consists of several extensive steps.
- In some cases a concrete member holds a sufficient residual load bearing capacity after bond failure of the external reinforcement. So bond failure not necessarily results in failure of the member.
- As the up-to-date valid technical approvals in Germany comprise insufficient proof concepts for the bond strength, they cannot be used for the calibration of the partial safety factors for the new proof concept.

3 Reliability-based Calibration of Partial Safety Factors

3.1 Scope and Object

The aim of the reliability analysis is calibrating the safety concept for the proof of the bond strength so that the proof concept can be included into the German technical approvals. Because these approvals are applied together with the German design codes for structural concrete (e. g. DIN 1045-1 [2]) and the other accessory codes, the characteristic values of loads and material properties (except for the FRP) as well as the partial safety factors are given. Thus only the partial safety factors of the bond strength must be determined. The required safety level is prescribed by DIN 1055-100 [4] to $\beta = 4.7$ for a period of 50 years and $\beta = 3.8$ for one year respectively.

3.2 Kinds of Safety Factors

According to the partial factor method the characteristic values of the material strengths are to reduce by partial safety factors to determine the resistance of a structure. Applying this on the proof of the bond strength the concrete compressive and tensile strength, the yield stress of the internal reinforcement and the ultimate stress of the external reinforcement are to reduce. As mentioned above $\Delta\sigma_{L,tol}$ is also a function of the stresses σ_L. Subsequently reducing the material strengths leads to the ratio of characteristic and design value of bond strength $\gamma_{b,eff} = R_k / R_d$ being a function of the stresses σ_L too. This is exemplified in Fig. 3 for the partial safety factor for concrete compressive strength $\gamma_c = 1.50$. It is evident, that this approach leads to a lower reduction of the bond strength for small stresses ($\sigma_L \rightarrow 0$) (i. e. close to the end of the external reinforcement) than for large stresses. Alternatively within this study it is investigated, whether it is feasible to reduce only the transferable differences of stress $\Delta\sigma_{L,tol}$.

Whereas choosing which basic variables are to reduce by partial safety factors, governs the constancy of the safety level for different types of structures, load cases etc. the size of the partial safety factors governs which safety level is reached. Concerning this it is of importance that bond failure does not necessarily lead to failure of the member. For this reason in the up-to-date valid German technical approvals (e. g. [1]) the tolerable stresses of the external reinforcement must be reduced for high grades of strengthening η_b (i. e. the ration of moment capacity after and before strengthening). Hence in the present study a variation of the safety factors depending on η_b is considered too.

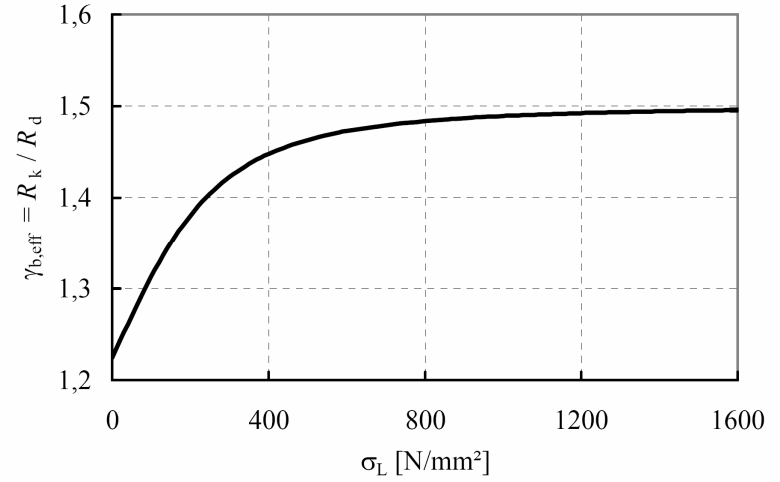

Fig. 3: Effect of stresses in the external reinforcement on the ratio $\gamma_{b,eff} = R_k / R_d$ for $\gamma_{b,eff} = 1.50$

3.3 Chosen Reliability Method

The characteristics of the regarded proof concept are of importance for the choice of the reliability method. Using the first- and second-order reliability method (FORM and SORM), which is desirable because of the little numerical effort, is abandoned here because of the problems connected with setting up the limit state function as well as the variable and unknown number of limit state functions as mentioned above.

Here the determination of the failure probabilities is carried out using optimized Monte-Carlo methods. This is comparatively easy because all possible kinds of bond failure are considered and the location of failure is detected automatically. It is easy to identify and – if desired – to sort out the cases of members having a sufficient residual load bearing capacity after bond failure.

To keep the numerical effort small, and because scarce information about the possible location of the design point or point of maximum likelihood (PML) respectively is available, Adaptive Importance Sampling (AIS) is used with normal distributions as importance sampling functions. The search of the expected value of the importance sampling function is conducted by means of a simple algorithm. After each iteration the vector, that provides the largest density and the minimal value for the limit state functions, is chosen as an improved expected value.

To reduce the number of basic variables before starting the reliability analysis a sensitivity analysis is conducted, by means of which the most important variables are identified. For this purpose the load bearing capacity is calculated using the mean values for all of the variables. In the next step each variable is increased or decreased (so that the bond strength is reduced or the stresses are enlarged) by twice the standard deviation. All variables affecting the proof of the bond strength more than the average are regarded as important. Using this method reduces the number of basic variables approximately to the half (s. e. g. KLEINSCHMITT [7]).

3.4 Stochastic Model

The stochastic model is based on the specifications of the PROBABILISTIC MODEL CODE [6], VROUWENVELDER AND SIEMES [13], RACKWITZ [10], SPAETHE [11] and STRAUSS [12]. A sample of the selected models is given in Tab. 1. The modeling of the concrete strength, live loads and the model uncertainties are briefly described below.

Tab. 1: Stochastic model and characteristic values of basic variables

Variable	Coefficient of Variation	Distribution Type	Quantiles used in design
Permanent loads	10 %	N	50 %
Variable loads:			
- Office	37 %	G	97,8 %
- Residence	28 %	G	97,5 %
- Hotel guest room	16 %	G	97,5 %
- Merchant / retail	45 %	G	98,0 %
- Industrial (light)	77 %	G	99,2 %
- Snow	25 %	G	98,0 %
Strengths:			
Concrete compression strength	≈ 8 ÷ 18 % [1)]	LN	≈ 2 ÷ 20 % [1)]
Concrete tension strength	8 % [2)]	LN	50 % [2)]
Reinforcement Steel	5 %	N	2 %
FRP-Reinforcement	5 %	LN	5 %
Model uncertainty:			
Lamellas	-	DET	-
Fabrics	12 %	LN	10 %

Distribution Types: N: Normal, LN: Lognormal, G: Gumbel, DET: deterministic

1) Derived by updating the parameters given in [6] with test data
2) Derived from test results

3.4.1 Concrete Compressive and Tensile Strength

While in the design of structures which still have to be built, the properties of the structure (e. g. the concrete compressive strength) are unknown and only target values are determined as the result of the structural analysis, in the case of structural strengthening the regarded member already exists. Thus its properties can be measured at the structure, and if this is done are having usually a smaller uncertainty. The determination of all relevant characteristics of the structure is very expensive and therefore unusual. However according

to the German technical approvals [1], the compressive strength and the tensile strength of the concrete must always be ascertained which is considered in the stochastic model.

For the concrete compressive strength both prior and additional information is used for the stochastic model. It is refrained from using only the test data because it is often gained by means of a concrete test hammer, which is leading to a little bit more uncertain results than other test methods. The prior information is taken from the PROBABILISTIC MODEL CODE [6] for a given concrete strength class, and it is updated with the test results. Because no test results are available for the reliability analysis, plausible assumptions are made. The mean of the sample of test results is chosen so that the concrete still belongs to the given concrete strength class. According to SPAETHE [11] the coefficient of variation for tests of the compression strength is in the range of $C_{vx} = 0.005 \div 0.08$ with a mean value of $C_{vx} \approx 0.04$. Because of the larger uncertainty of results from the concrete test hammer, the upper value is used here. Within the reliability analysis for each concrete strength class only one set of distribution parameters is determined, which is derived using a representative (i. e. mean) assumption for the test data.

Deriving the concrete tensile strength form the compressive strength leads to results subjected to a rather large scattering. Therefore only the measured values are used for the stochastic model. The coefficient of variation is assumed to $C_{vx} = 0.08$ again. This value is confirmed by test results, which were collected from a construction company during structural strengthenings.

3.4.2 Live Loads

As concrete members are usually strengthened while the self weight of the structure and in many cases also a part of the additional dead load are acting on it, the additional external reinforcement mainly is stressed by the live loads. Hence a closer look on those loads seems to be appropriate and it is refrained from regarding only one type of live load with one coefficient of variation and one characteristic value.

Instead of that the stochastic models from the PROBABILISTIC MODEL CODE [6] are used were different kinds of live loads depending on the type of use are distinguished. According to [6] live loads are divided into two components, which are sustained loads with a fairly large relative duration and intermittent loads, which are acting only for a short time and changing very often. Using their parameters given in [6] for the different types of loading and as a function of the size of the considered area, the sustained and the intermittent loads are simulated and combined over the hole life-time of a structure (here 50 years) by means of an algorithm from GLOWIENKA AND HAUSMANN [5]. Subsequently the maximum value in that period is determined and the whole procedure is repeated for several times (say 1000) leading to a representative sample of extreme values, which can be described quite well by a Gumbel distribution. The parameters of these distributions are printed in Tab. 1 for some types of use were only the decisive size of area is regarded. From Tab. 1 it is evident that primarily the coefficient of variation, which is lying within in a range from 16 % to 77 %, is fairly various for the different types of use. Furthermore the characteristic values given in DIN 1055-3 [3], concerning the imposed loads, are corresponding to different quantiles of the Gumbel distributions.

These results assert the necessity to distinguish between the different types of loads within in the reliability analysis and furthermore indicate to do so in the design codes by defining different partial safety factors. However all safety factors (except for the bond strength) are given by the design codes and in these codes only one factor for all types of live loads is defined. Therefore it is expected, that the reliability levels of several regarded members are scattering if they are subjected to different kinds of live loads, the more so as the external reinforcement is predominantly stressed by the live loads.

3.4.3 Model Uncertainties

The model uncertainties of the regarded design concept were determined by comparing the results of conducted experiments (i. e. the observed ultimate load) with the ultimate loads calculated using the proof concept. About 40 of the several experiments, which are documented in the literature, were selected, from which one half were strengthened with FRP strips and the other half with fabrics. Further documented experiments were not used, since either the documentation was incomplete or the test specimens did not fail by debonding of the external reinforcement. The ratios of experimental and calculated ultimate Load $\xi = F_{u,exp} / F_{u,calc}$ for the regarded Tests are shown in Fig. 4. It is evident that the values of ξ are quite different for strips and fabrics.

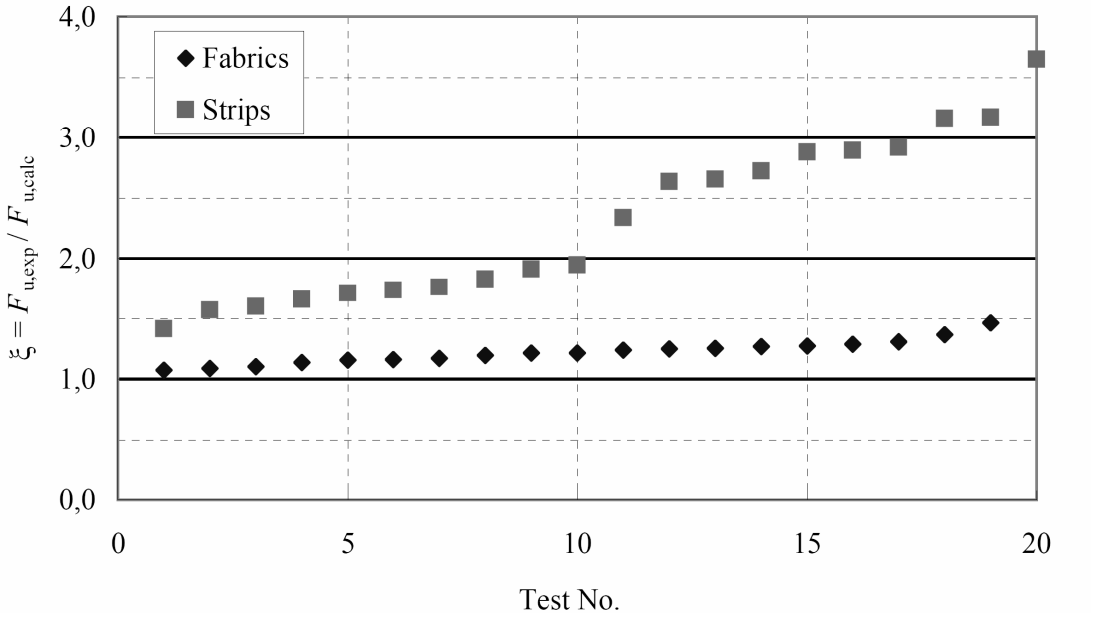

Fig. 4: Ratio of experimental and calculated ultimate Load $\xi = F_{u,exp} / F_{u,calc}$ for several Tests on strengthened beams

Regarding FRP fabrics there is found a quite good agreement of test results and results of the calculation. All obtained values of ξ are within a range of about 1.07 to 1.46 and the controlling boundaries of the confidence interval (with a confidence of 95%) are $\mu_\xi = 1.18$ and $\sigma_\xi = 0.14$ (i. e. the coefficient of variation is $C_{vx} = 0.12$). These are reasonable values compared to the model uncertainties for other model types, which can be found in the literature. For example in the PROBABILISTIC MODEL CODE [6] or in VROUWENVELDER AND

SIEMES [13], the range of the coefficient of variation for concrete resistance models is $C_{v\xi} = 0.10 \div 0.30$. According to [6] and [13] a lognormal distribution is chosen for ξ. In the reliability analysis ξ is regarded as a further basic variable, that is multiplied with the calculated values of $\sigma_{L,tol}$.

On the other hand for FRP strips or lamellas respectively the model uncertainties are considerably larger ($\mu_\xi = 2.0$, $\sigma_\xi = 0.98$ and $C_{vx} = 0.49$). As in all cases the bond strength was clearly underestimated by the regarded proof concept, it is assumed that the results of the proof concept are always conservative. Therefore in the reliability analysis the model uncertainties are neglected for lamellas, and it is presumed that the proof concept matches the bond strengths exactly. Otherwise, because it is multiplied with $\sigma_{L,tol}$, ξ would have – besides the live loads – by far the largest sensitivity and maybe dominate the results of the reliability analysis. Considering these results it has to be asked, if the regarded proof concept is still applicable for strengthenings with lamellas, even though it is mechanically reasonable, or if further research and an improvement of the concept are necessary at first, before incorporating it into the technical approvals.

3.5 Example Structures for the Reliability Analysis

The reliability analysis will be conducted for a sample of several fictitious members, covering the range of application admitted by the German technical approvals. The sample comprises slabs, rectangular beams and T-beams as one- and two-span systems. The varied parameters are beside some others the grade of strengthening, the reinforcement ratio and the type of loading (ratio of permanent loads to live load, type of live load).

Slabs are regarded mainly, because strengthening of beams requires an additional external reinforcement for shear in most cases. As this external reinforcement for shear encloses the longitudinal external reinforcement and is increasing its bond strength, and as this effect still cannot be described sufficiently, only beams with a low grade of strengthening and no external reinforcement for shear are regarded.

4 Summary and Outlook

New proof concept for the bond strength of external reinforcement glued on the surface of concrete members shall be incorporated into the German technical approvals for structural strengthenings. For this purpose suitable safety factors for the proof concept are determined by means of a reliability analysis. Because the choice for the reliability method is restricted by the characteristics of strengthened members as well as of the regarded design concept, the probabilities of failure are determined by means of Adaptive Importance Sampling. The stochastic modeling is done regarding the variable loads and the concrete strengths in particular. The latter were modeled by using additional information, which is obtained through test results. The determined model uncertainties differ for the two kinds of FRP used (fabrics and lamellas) and thus two stochastic models are chosen for them. First results of the reliability analysis will soon be available.

5 References

[1] DIBt: Allgemeine bauaufsichtliche Zulassung Nr. Z-36.12-39, Verstärkung von Stahlbeton- und Spannbetonbauteilen durch schubfest aufgeklebte Kohlefaserlamellen Sika CarboDur. Berlin: Deutsches Institut für Bautechnik, 2002.

[2] DIN 1045-1: Tragwerke aus Beton, Stahlbeton und Spannbeton, Teil 1: Bemessung und Konstruktion. Beuth-Verlag, Berlin, 2001.

[3] DIN 1055-3: Einwirkungen auf Tragwerke - Teil 3: Eigen- und Nutzlasten für Hochbauten. Beuth-Verlag, Berlin, 2006.

[4] DIN 1055-100: Einwirkungen auf Tragwerke, Teil 100: Grundlagen der Tragwerksplanung, Sicherheitskonzept und Bemessungsregeln. Beuth-Verlag, Berlin, 2001.

[5] Glowienka, S.; Hausmann, G.: Hintergründe zur Festlegung der charakteristischen Werte von Nutzlasten. Unpublished Manuscript, 2006.

[6] JCSS: *Probabilistic Model Code. Joint Committee on Structural Safety* (www.jcss.ethz.ch), 2000.

[7] Kleinschmitt, J.: Probabilistisch fundierte Bewertung nichtlinearer Berechnungskonzepte für die Traglastermittlung von Verbundstützen aus einbetonierten I-Profilen. Dissertation, University of Technology Darmstadt, 2003.

[8] Neubauer, U.: Verbundtragverhalten geklebter Lamellen aus Kohlenstofffaser-Verbundwerkstoff zur Verstärkung von Betonbauteilen. Dissertation, University of Technology Braunschweig, 2000.

[9] Niedermeier, R.: Zugkraftdeckung bei klebearmierten Biegeträgern. Dissertation, University of Technology München, 2001.

[10] Rackwitz, R.: Einwirkungen auf Bauwerke. In Mehlhorn, G. (Editor): *Der Ingenieurbau: Grundwissen, Band 8 Tragwerkszuverlässigkeit, Einwirkungen.* Ernst & Sohn Verlag, Berlin, 1997.

[11] Spaethe, G.: Die Sicherheit tragender Baukonstruktionen. Springer Verlag, Wien, 1992.

[12] Strauss, A.: *Stochastische Modellierung und Zuverlässigkeit von Betonkonstruktionen.* Dissertation, University of Natural Resources and Applied Life Sciences, Wien, 2003.

[13] Vrouwenvelder, A. C. W. M.; Siemes, A. J. M.: Probabilistic calibration procedure for the derivation of partial safety factors for the Netherlands building codes. *Heron*, Vol. 32, No. 4, S. 9-29, 1987.

Probabilistic Modelling of the Load Carrying Capacity of Modern Masonry

Simon Glowienka, Carl-Alexander Graubner
Institute of Concrete and Masonry Structures, Darmstadt University of Technology

Summary: Since probabilistic calculations to assess the reliability of structural elements and buildings are gaining a higher importance, the estimation of statistical parameters of material properties plays a major role. Whereas for steel and concrete structures the required information based on extensive data of test results is existent, there is a lack for masonry structures. This is valid especially for modern masonry. In this paper the main statistical parameters for the assessment of the reliability of big sized masonry are provided.

1 Introduction

Within the scope of the harmonisation of the European design codes the partial safety concept is recommended also for masonry structures. Thus the question of the required value of the partial safety factors has to be discussed. The comparison of the international masonry codes (see Table 1) shows, that especially the safety factors on the resistance for unreinforced masonry are contradictory. Possibly the provided safety factors were calibrated on basis of experience and traditions of the different countries. Up to now only some reliability studies on masonry have been conducted (GALAMBOS et. al [1], HOLICKY & MARKOVA [2], SCHUEREMANNS [3]). The reason for this can be found in the lack of required statistical data especially for industrially produced masonry. Due to the great amount of different unit-brick combinations with different properties of modern masonry the estimation of the statistical parameters is difficult, too.

In the following sections some required statistical parameter for the assessment of the reliability of masonry, made of big sized units (in the following called big sized masonry) will be given. The focus will be set on axial loading. The main parameter for the assessment of the reliability of masonry structures is its compressive strength. Other important material parameters as the modulus of elasticity are correlated with the compressive strength and may be defined on this basis. Hence the compressive strength needs to be analysed care-

fully. For the assessment of masonry walls subjected to out of plane shear the statistical properties of the friction coefficient and the initial shear strength have to be estimated. Beside the influence of the material parameters on the reliability of masonry structures, uncertainties due to the model used to calculate the load capacity play a major role and will be analysed, too.

Table 1: Summary of safety factors for the ultimate limit state design of unreinforced masonry in different countries

Country	Masonry	Action[1)]	
		permanent	variable
	γ_M	γ_G	γ_Q
Germany	1.50	1.35	1.50[2)]
Austria	2.20	1.35	1.50
Switzerland	2.00	1.30	1.50[2)]
U.K.	2.50÷3.50[5)]	1.20÷1.40[2)]	1.40÷1.60[2)4)]
Netherlands	1.80	1.20÷1.35[2)]	1.50[2)]
Sweden	1.50÷2.76[3)5)]	1.00÷1.15	1.30[2)]
Australia	1.67÷2.22[6)]	1.20÷1.35[2)]	1.50[2)]
USA	1.25÷2.5[6)]	1.20	1.30÷1.60[2)4)]
Canada	1.67	1.4÷1.25	1.50[2)]

1) Unfavourable effect
2) Depending on the load combination
3) Depending on the structural class an kind of building stones
4) Depending on the effect
5) Depending on the quality of building stones and the building inspection
6) Depending on the analysed design situation (e.g. shear, axial, bending)

2 Specification of Big Sized Masonry

Big sized masonry is made of big sized units in combination with thin layer mortar and is common in Germany, as it safes on construction time and so reduces the cost of the structure. In the following big sized units are defined as stones with a height of 248mm and more, while the length of the stones reaches 998mm in special cases. The most common materials for this kind of masonry are porous concrete and calcium silicate unit. In the case of calcium silicate unit more or less solid stones are used for big sized masonry.

The units provide a plane surface and geometrical deviations from the nominal size are negligible. The units are stone walled in stretcher course with the aid of small chain hoists if the weight of the units exceeds 25kg. The compressive strength and the weight of units made of porous concrete are significantly smaller in comparison to calcium silicate units. In the following the most important statistical parameters for the determination of the reliability of big sized masonry made of porous concrete and calcium silicates units will be analysed.

3 Compressive Strength

3.1 Definition of the Calculation Model

The compressive strength of masonry is affected by the compressive strength of the units and the mortar used. Direct measurements of the compressive strength of masonry are expensive and thus reduced to minimum. However, the properties of units and mortar are subjected to quality control, so that the statistical parameters of the basic materials can be obtained on basis of extensive data. These reasons make clear that a calculation model should be defined which uses all sources of information for the estimation of the compressive strength of masonry. The model according to equation (1), was proposed by MANN [4] and provides a good adjustment with experimental investigations. It is also used in Eurocode 6 for the calculation of the compressive strength of masonry:

$$f_m = a \cdot f_b^b \cdot f_{mo}^c \tag{1}$$

Where: f_m is the compressive strength of masonry
f_b is the compressive strength of the unit (brick)
f_{mo} is the compressive strength of the mortar
a, b, c are factors which characterise the kind of masonry

The factors a, b and c may be obtained using a regression analysis based on experimental investigations. It should be mentioned that for $b+c \neq 1$ equation (1) is restricted to a special dimension. For the estimation of the required statistical parameter of the compressive strength of masonry the model uncertainties due to the transformation of experimental data to a mathematical model have to be considered. Thus model uncertainties M must to be added to equation (1).

$$f_m = M \cdot a \cdot f_b^b \cdot f_{mo}^c \tag{2}$$

Where: M is a variable with a mean value of 1.0 which considers model uncertainties

In the probabilistic model a, b and c can be regarded as deterministic parameters, since the uncertainties due to the definition of these factors will be included in the model uncertainty M. Besides the model uncertainty the compressive strength of the bricks and the mortar will be treated as random variables. Prior values for the factors a, b and c can be found at SCHUBERT [5]. However it should be mentioned, that the values provided by SCHUBERT [5] are valid for a slenderness of the masonry specimens the defined as height-to-thickness ratio of 10, whereas in Eurocode 6 these factors are related to a (theoretical) slenderness of 0.

For thin layer mortar, the influence on the compressive strength of masonry is negligible and thus the factor c can be set to zero (see SCHUBERT [5]), so that equation (2) becomes:

$$f_m = M \cdot a \cdot f_b^b \quad \text{for masonry with thin mortar layers} \tag{3}$$

3.2 Parameter Estimation

The required parameters *a* and *b* in equation (3) for big sized masonry are calculated on basis of a regression analysis of experimental investigations, where the compressive strength of the units and the masonry were analysed. Note that all variables in equation (3) are treated as deterministic values within this stage of the analysis. Also the parameter *M* remains constant with value of 1.0.

Since the height of the units has a significant influence on the compressive strength a reference value for the slenderness has to be defined. The specimens used for the following calculation had a slenderness λ defined as height-to-thickness ratio of 3 up to 10. The compressive strengths provided by the tests were converted into a slenderness of zero using an approach of MANN [4] so that a standardised basis for the parameter estimation was provided. On these basis the parameter *a* and *b* are estimated to determine the mean value of f_m in such a way that the squared mean error is minimized.

Table 2 shows the results of the analysis. These parameters may be used to calculate the mean value of the compressive strength of big sized masonry. The parameter *a* also considers also the slenderness on which the compressive strength of masonry is related to.

Table 2: Parameters for the calculation of the compressive strength

Masonry	Parameter	
	a	*b*
Calcium silicate unit	0.23	1.31
Porous concrete	0.96	0.88

3.3 Determination of the Model Uncertainties

Since no calculation model exactly fits to experimental results model uncertainties have to be regarded in a probabilistic calculation. In Fig. 1 the adjustment of the model to the data using the parameters according to Table 2 is shown. The statistical properties of the model uncertainties *M* are determined by the comparison of the compressive strength provided by the model and experimental data. Due to the fact that the model uncertainties are considered multiplicative in equation (3), the following relationship was used to calculate the mean value and the coefficient of variation of the model uncertainties:

$$m = \frac{f_{m,experiment}}{f_{m,model}} \tag{4}$$

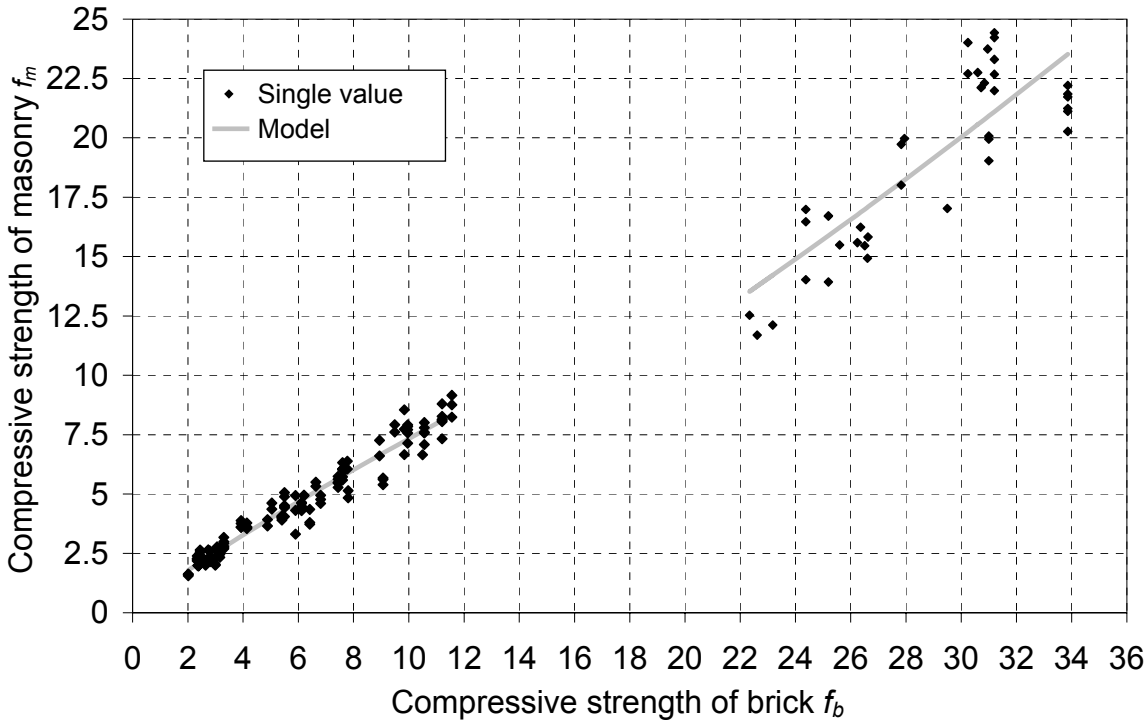

Fig. 1: Compressive strength of masonry against compressive strength of brick

Considering that these values come from a limited amount of data the confidence provided by the estimation may be obtained. Table 3 shows the results.

Table 3: Parameters for the model uncertainties of the compressive strength of masonry

Masonry	Parameter		Model uncertainty M			Model uncertainty M considering the amount of data[1)]		
	a	b	m_M	σ_M	V_M	m_M[2)]	σ_M[3)]	V_M
Calcium silicate unit	0.23	1.31	1.00	0.10	0.10	0.97	0.13	0.13
Porous concrete	0.96	0.88	1.00	0.10	0.10	0.98	0.11	0.11
1) α = 95 % (confidence) 2) Lower limit 3) Upper limit								

3.4 Resulting Statistical Properties

Due to the fact that the compressive strength of the units and the model uncertainties are random variables the compressive strength of masonry is random variable, too. Since a log-normal distribution is assumed for the units and the model uncertainty the resulting mean value and the coefficient of variation of the compressive strength of masonry may be calculated by equation (5) and (6):

$$E[f_m] = E[M] \cdot a \cdot E[f_b]^b \tag{5}$$

$$V[f_m] = \sqrt{V_M^2 + \left(1 + V_{f_b}^2\right)^{b^2} - 1} \tag{6}$$

On the basis of investigations in the context of quality control the required statistical properties of the bricks are obtained. For calcium silicate units the coefficient of variation of the compressive strength is about 8% whereas for porous concrete it is about 9%. Using all information the statistical properties of the compressive strength of masonry can be calculated. The results are summarized in Table 4. According to [1], [2], [3], [6] the compressive strength of masonry is (approximately) assumed to be lognormal.

Table 4: Statistical Parameters of the compressive strength of masonry

Masonry	Parameter		Mean value			Coefficient of Variation			Class[2)]
	a	b	f_b[1)]	M	f_m[1)]	f_b	M	f_m	
Calcium silicate unit	0.23	1.33	22.9	0.97	13.5	0.07	0.13	0.16	16
			29.5	0.97	18.8				20
			38.9	0.97	27.0				28
Porous concrete	0.96	0.88	2.9	0.98	2.4	0.09	0.12	0.14	2
			5.3	0.98	4.1				4
			7.5	0.98	5.5				6

1) [N/mm²]
2) Characteristic compressive strength of the brick (common values)

In comparison to the variations of other types of masonry, big sized masonry provides a smaller coefficient of variation, as Table 5 shows. These values are considered for various materials of the units (e.g clay, calcium silicate unit, porous concrete etc.) and thus represent a mean value for the compressive strength of the masonry.

Table 5: Parameters for the calculation of the compressive strength

Author	V	Basic variable
GALAMBOS et al. [1]	0.18	Resistance
HOLICKY & MARKOVA [2]	0.20	Compressive strength
SCHUEREMANS[1)] [3]	0.19	Compressive strength
KIRTSCHIG & KASTEN [6]	0.17	Compressive strength
TSCHÖTSCHEL [7]	0.25	Compressive strength
1) For historical masonry made of bricks (clay)		

Using the estimated parameter according to Table 4 the characteristic values for the compressive strength can be calculated. These are usually defined as 5%-quantile of the distribution of the dependent parameter. Fig. 2 shows the results in comparison to the characteristic values according to Eurocode 6. While for porous concrete a good conformance is provided, there are significant variations between the values according to Eurocode 6 and the results on the basis of experimental investigations for calcium silicate units.

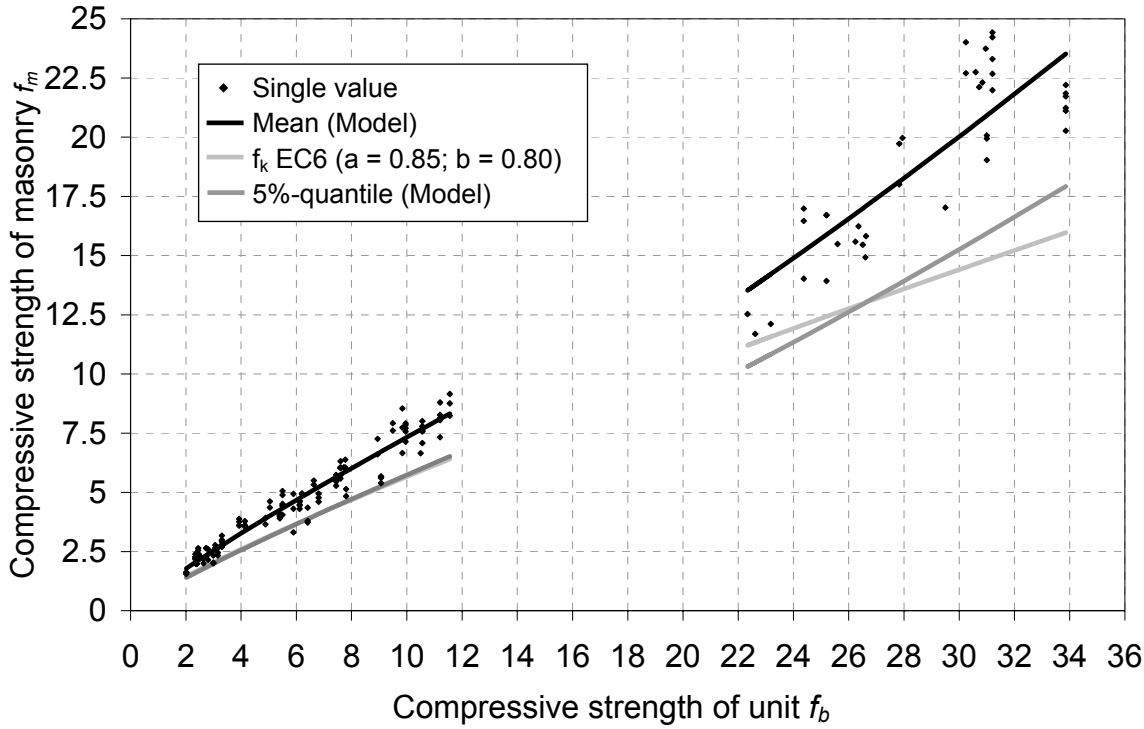

Fig. 2: Compressive strength of masonry against compressive strength of unit and characteristic values according to EC 6 and the model according to equation (3)

4 Statistical Parameters for the Shear Resistance

For the calculation of the shear resistance of masonry walls subjected to out of plane shear models based on the shear theory by Mohr-Culoumb are common, in which the shear resistance is dependent on friction and cohesion. For in plane shear the following model, which is based on Eurocode 6 is recommended:

$$V_R = t \cdot l_c \cdot \left(f_{v0} + \mu \cdot \frac{N_E}{t \cdot l_c} \right) = t \cdot l_c \cdot f_{v0} + \mu \cdot N_E \tag{7}$$

Where: t is the thickness of the wall
f_{v0} is the initial shear strength under zero compression
μ is the coefficient of friction
N_E, M_E is the axial force and bending moment on the section under consideration
l_c is the length of the compressed part of the wall $l_c = 3/2 \cdot (l - 2 \cdot M_E/N_E) \leq l$
l is the length of the wall

For a probabilistic calculation the statistical properties of the initial shear strength and the coefficient of friction have to be determined. However a lack of data values is existent in this case. Especially in the case of the friction coefficient no direct measurements for big sized masonry are available. Because of this the statistical properties of the coefficient of friction will be approximated according to SCHUEREMANS [3] in this case. Values for the

required parameters are summarized in Table 6. However these values should be considered as prior parameter in a probabilistic calculation, as the data base for the estimation is poor.

Table 6: Parameters for the calculation of the shear resistance (in plane shear)

Variable	masonry	mean	V	Source
coefficient of friction μ	Calcium silicate unit	0.8	0.19	SCHUEREMANS [3]
	Porous concrete	0.8	0.19	SCHUEREMANS [3]
initial shear strength[1] f_{v0}	Calcium silicate unit	1.27	0.37	SCHUBERT [5]
	Porous concrete	1.00	0.15	SCHUBERT [5]
1) Under zero compression				

5 Model Uncertainties for the Carrying Capacity of Unreinforced Masonry Walls

For a probabilistic assessment of structures uncertainties due to the calculation models used have to be considered. The statistical parameters of the model uncertainties are influenced by the accuracy of the chosen resistance model and by the amount of information available on the properties of the analysed masonry. The resulting model uncertainties can be estimated by comparison with the results of experimental tests. In this approach it is approximately assumed that the tests provide the exact load carrying capacity. However in many cases experimental investigations are rare, because of to the cost associated with the tests.

For the maximum load carrying capacity of slender masonry walls subjected to axial load, the model according to Eurocode 6 will be analysed in this paper, which is characterised by equation (8) and (9):

$$N_R = \Phi \cdot b \cdot t \cdot f_m \tag{8}$$

$$\Phi = \left(1 - 2\frac{e_I}{t}\right) \cdot exp\left(-\frac{u^2}{2}\right) \text{ where } u = \frac{\frac{h_{ef}}{t} \cdot \sqrt{\frac{f_m}{E_0}} - 0{,}063}{0{,}73 - 1{,}17 \cdot \frac{e_I}{t}} \tag{9}$$

Where: b is the thickness of the wall
t is the width of the wall
e_I is the eccentricity of the axial load $e_I = M_E/N_E$
h_{ef} effective height of the wall $h_{ef} = \rho \cdot h_s$
E_0 is the modulus of elasticity of masonry

To estimate the modulus of elasticity only a few tests with contradictory results are available. For calcium silicate unit no tests using big sized masonry units have been done at all. For this reason the parameter f_m/E_0 is chosen in such a way that the mean value of the

model uncertainty becomes 1.0 to provide an unbiased model. For porous concrete and calcium silicate unit an amount of 18 tests of masonry walls under representative boundary conditions were available to calculate the model uncertainties due to the model according to equation (8) and (9). As the results in Table 7 show the model uncertainties of calcium silicate units have a higher coefficient of variation compared to porous concrete.

Unfortunately no experimental investigations on walls subjected to in plane shear are available. Hence the statistical properties of the coefficient of friction will approximately be chosen as for concrete structures basing on the recommendations of the JCSS Probabilistic Model Code [8]. Table 7 summarizes the statistical parameters of the model uncertainty for the calculation of big sized masonry.

Table 7: Parameters for model uncertainties due to the calculation model

Model	Masonry	Model uncertainties	
		mean	V
Load carrying capacity of masonry subjected to axial load	Calcium silicate unit[1)]	1.0	0.17
	Porous concrete[2)]	1.0	0.15
Shear resistance[3)]	Calcium silicate unit	1.0	0.10
	Porous concrete	1.0	0.10

1) $f_m/E_0 = 1/900$
2) $f_m/E_0 = 1/525$
3) Based on the JCSS Probabistic Modelcode [8] for concrete structures

6 Conclusion

This paper provides statistical parameters for a probabilistic assessment of masonry structures made of big sized units, focusing on axial loading. Beside the required material parameters, model uncertainties have to be regarded in a probabilistic calculation and are quantified in this paper, too. The estimated values are based on experimental tests of masonry walls and where test results are missing on basis of expert opinions and literature research. The determined parameters can be used as prior parameters when additional tests become available. In comparison to other kinds of masonry, the statistical parameters of big sized masonry provide a smaller scatter.

7 References

[1] Galambos, T. V.; Ellingwood, B.; MacGregor J. G.; Cornell, C. A.: Probability Based Load Criteria: Assessment of Current Design Practice, *Journal of the Structural Division,* Vol. 108 No. St5 (1982), S.959-977

[2] Holicky, M.; Markova, J.: Calibration of Reliability Elements for a column, *JCSS workshop on reliability based code calibration*, Zürich 2002

[3] Schueremans, L.: *Probabilistic evaluation of structural Reliability unreinforced masonry*, Katholieke Universiteit Leuven, Belgium 2002 - PhD-Thesis

[4] Mann, W.: Druckfestigkeit von Mauerwerk – Eine statistische Auswertung von Versuchsergebnissen in geschlossener Darstellung mithilfe von Potenzfunktionen – *In Mauerwerk-Kalender* (1983), Verlag Ernst & Sohn, Berlin

[5] Schubert P.: Eigenschaftswerte von Mauerwerk, Mauersteinen und Mauermörtel – *In Mauerwerkkalender* (2005), Verlag Ernst & Sohn, Berlin

[6] Kirtschig K.; Kasten D.: Zur Festlegung von Mauerwerksklassen bei Ingenieurmauerwerk – *In Mauerwerk-Kalender* (1980), Verlag Ernst & Sohn, Berlin

[7] Tschötschel, M.: *Zuverlässigkeitstheoretisches Konzept für Mauerwerkskonstruktionen*, TH Leipzig 1989 – Dissertation

[8] JCSS: *The probabilistic model code*, (2003) available on the internet on www.jcss.ethz.ch

Reliability Analysis of the Fire Protection Lining in the High Speed Train Tunnel 'Groene Hart'

Alfons Krom & Sten de Wit
Structures and Safety
TNO Built Environment and Geosciences

Abstract: Sprayed fire protection linings in bored, high speed train tunnels are a new field of application. Questions were raised on the failure probability of the lining during the service life of the Groene Hart tunnel. The fire protection lining is reinforced with a wire mesh fixed to the tunnel lining. A systematic failure analysis has been carried out to identify possibly causes and growth mechanisms of delaminations of the protection lining. The research shows how the reliability of a new system can be analysed. The analysis uses standard reliability methods, and a combination of analytical and numerical modelling, small and full-size experiments and expert judgments. The conclusion is that sprayed fire protection linings can be applied in the high speed train tunnel Groene Hart for short service periods. For long service periods an additional inspection regime has to be established.

1 Introduction

Fire protection linings are applied in tunnels to protect the concrete against fire. The aim of the fire protection lining is to reduce the risks during a fire: to protect the tunnel against collapse so that people in the tunnel can leave the tunnel, and to have time to rescue casualties. Naturally the fire protection lining should not increase the risk during normal use of the tunnel.

The Groene Hart Tunnel in The Netherlands is a 7 km long high speed railway tunnel with an inner diameter of about 13 m, see Fig. 1. A partition wall separates the two tracks. High speed trains will pass the tunnel at speeds of more than 300 km/h. Inside the tunnel 200,000 m^2 fire resistant plaster with a wire mesh reinforcement was applied within a very short period of time. More information is given by Van de Linde et al. [1].

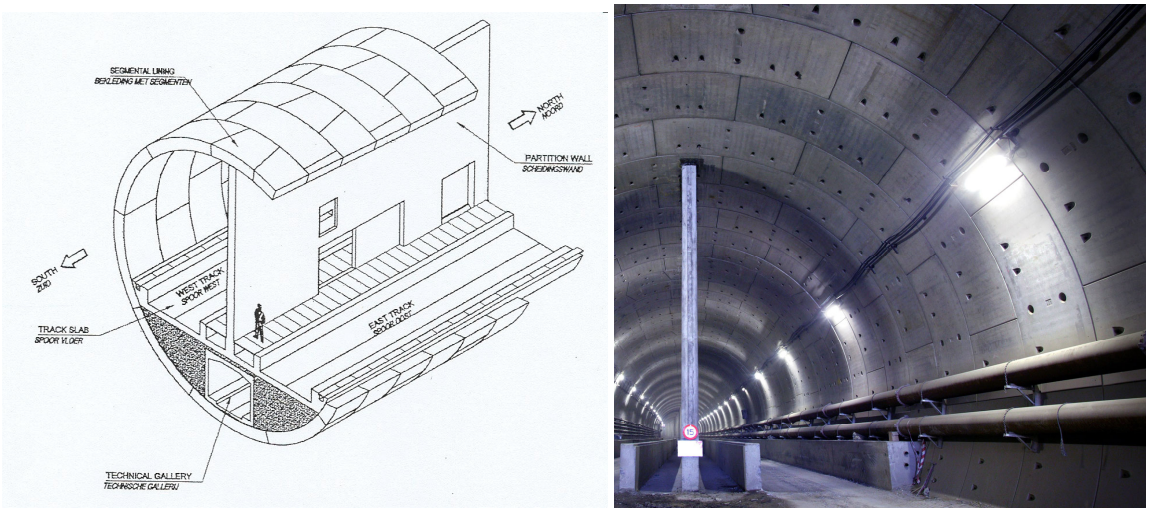

Fig. 1: Illustration of the high speed train tunnel (left) and a photo of the tunnel lining without the fire protection lining (right). Note that the partition wall is not protected by the fire protection lining.

The fire protection lining should not significantly contribute to the probability of failure accepted for a structure complying with the Dutch Building Decree during a reference period of 100 years. The requirements for safety class nr. 3 (primary structure) are applicable, i.e. the reliability index $\beta_t = 3.6$, corresponding to a probability of failure of approximately 10^{-4} in the reference period of 100 year.

It is assumed that the fire protection lining fails when a part of the lining is released from the tunnel lining. This part must be large enough to cause any potential serious damage, e.g. penetration of the front window of a train.

This paper gives an overview of the reliability analysis of the fire protection lining. It includes a description of the fire protection lining, the failure analysis, the modelling of the structural behaviour of the lining and the reliability calculations.

2 System description

The fire resistant layer consists of a reinforced plaster (Fendolite MII). The average thickness is 42 mm. This thickness is large enough to withstand the HSL fire test (1000 °C for 1 hour). The reinforcement is a wire mesh of stainless steel quality AISI 316, consisting of wires of diameter of 1.5 mm and a mesh of 50 mm in both directions. The wire mesh is anchored to the concrete lining using stainless steel anchors. The anchors are fixed to the wire mesh with specially bend washers, see Fig. 2. The fixation with the anchors also acts as a backup system of the fire protection lining to the concrete lining, which starts to function in the event that the normal bond between the two lining has failed.

Spacings in the segments (see Fig. 1) of the tunnel lining, used during the construction, are covered with a bonded plate. There are around 150.000 spacing in the tunnel.

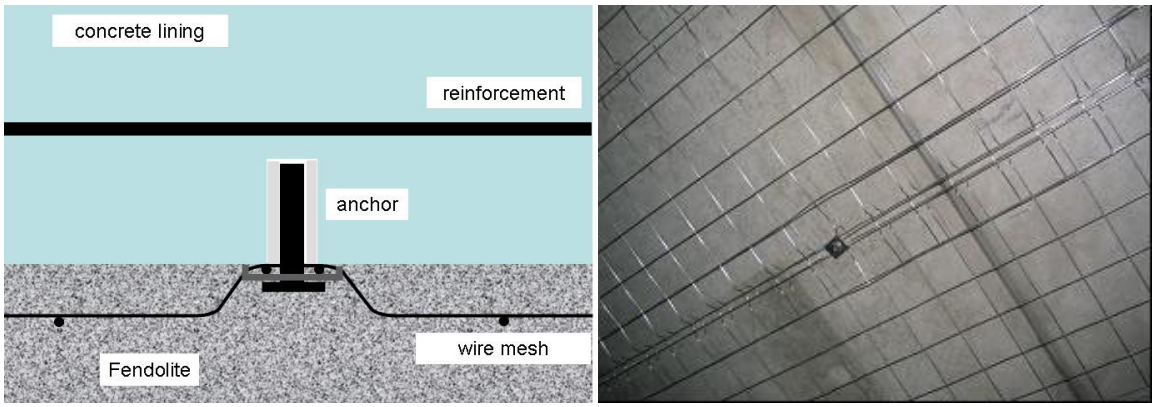

Fig. 2: Detail of the fire protection lining (left) and anchored wire mesh fixed to concrete lining before spraying (right)

3 Failure analysis

Failure is defined as the situation in which the fire protection lining is not connected to the concrete lining neither by bond nor by the backup system (wire mesh). In this situation the risk is considered as realistic that in the end parts of the lining fall down.

Note that failure is not defined as the situation in which parts of fire protection lining fall down but as the situation in which parts of the lining are not connected to the tunnel. In this way some additional safety may be built in the analysis. The reason for this approach is that statements can be made on the cracking of the protection lining and the failure of the wire mesh on the basis of modelling. Statements on the release of parts from a cracked delaminated fire protection is very difficult.

When parts of the fire protection lining are released from the lining, the bond between the linings was not good. A part of the lining which is still intact but has no bond with the lining is called a *delamination*, see Fig. 3. Delaminations may be present from the beginning due to application errors. Delaminations may also grow in time due to degrading actions. There are several causes for the initial lack of bond. For example the surface of the tunnel lining was not clean before the plaster was applied. Because of the large area involved, delaminations cannot be ruled out.

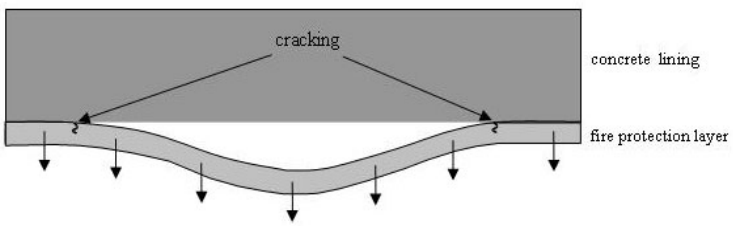

Fig. 3: Illustration of a delamination of the fire protection lining and the position of the cracking. Note that the anchored wire mesh is not shown.

High speed trains can develop large pressures cycles. As a consequence, delaminations are subjected to fatigue. Firstly the lining at the delamination can break due to this fatigue loading and parts of the protection lining can fall down. Secondly the delamination can grow and once its size is too large to withstand the pressure variation, the lining also breaks and parts of the lining fall down. In both cases we are dealing with a highly unwanted situation.

The sequences of events, which may lead to failure of the fire protection lining are presented in an event tree, shown in Fig. 4. The tree starts with the situation that a delamination is present. The first branch deals with the detection of the delamination. If the delamination is detected it is assumed that some repair or monitor procedure is taken to prevent failure. The second branch deals with the cracking of a part of the delamination. An illustration of the cracking of the delamination is shown in Fig. 3.

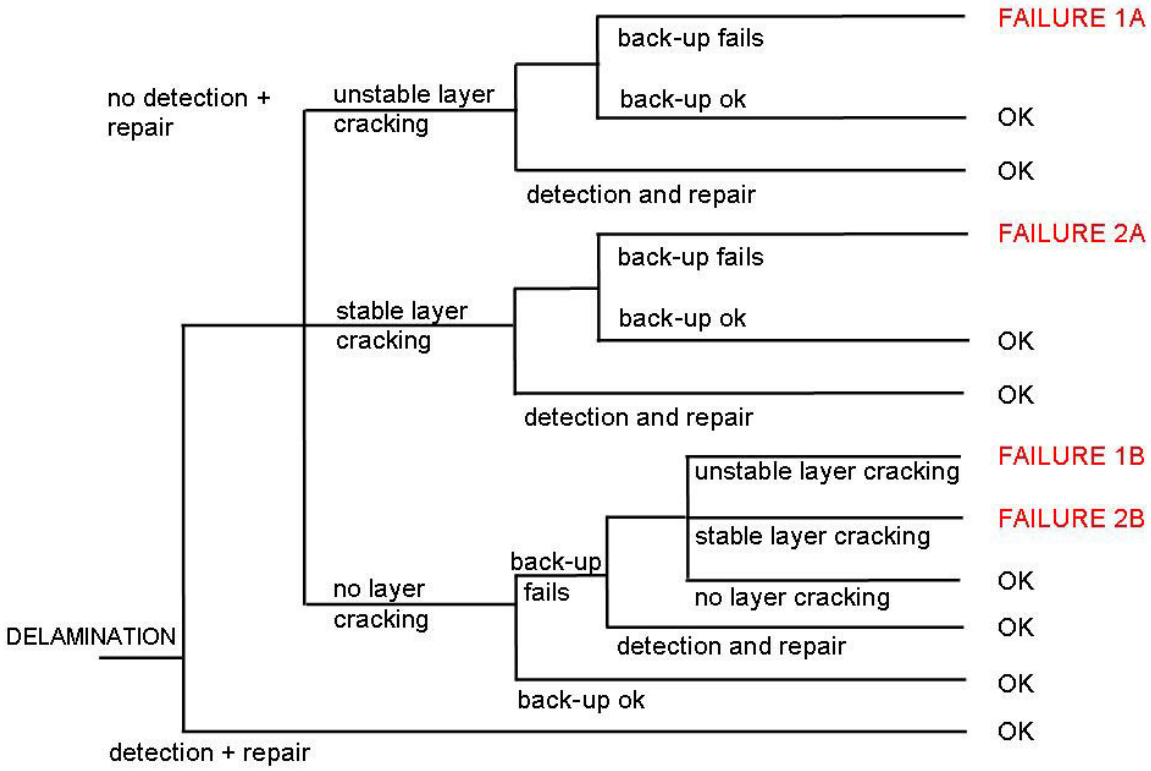

Fig. 4: Sequence of events leading to failure and non failure situations of delaminations (layer).

Failure of a delamination may occur in three different scenarios. The first scenario is that cracking occurs in a unstable way: the delamination cracks due to one single train passage. If the backup system also fails, this will lead to failure (1A). There is no failure when the backup is ok or the cracked delamination is detected and repaired. The second scenario is that cracking occurs in a stable way due to repeated train passages (fatigue). Again, if the backup system also fails, this will lead to failure (2A). There is no failure when the backup is ok or the cracked delamination is detected and repaired. The third scenario is that no cracking of the delamination occurs. If the backup system is ok, then no failure occurs. If the backup is not ok then unstable or stable cracking occurs, leading to failure 1B and 2B,

respectively. No failure occurs when the failure of the backup is detected and repaired and when no delamination cracking occurs.

The backup system may fail several in several ways. For example the anchor may be pulled out of the tunnel lining. On the basis of experiments, the relevant failure mechanism is fatigue of the wires around the anchors.

The difference between failure modes A and B is the sequence of events. In case of failure modes A, first the delamination fails, followed by failure of the backup system. In case of modes B it is the other way round. Here failure mode B is assumed to be dominant. This assumption is supported by experiments, see the next section. Presumably this is a conservative approach because if the delamination cracks first, the load on the delamination decreases due to the direct pressure adjustment behind the delamination.

4 Analytical and Numerical Modelling

4.1 Mechanical load on the delamination

Due to the high speed of the trains, high pressure differences will occur in the tunnel. During the passage of a train at a certain position in the tunnel, the pressure on the lining first increases and then decreases. From small-scale experiments it is concluded that a pressure drop of about 3 kPa over 0.01 s exists within the pressure fluctuation. It is assumed that in case of a delamination the pressure drop is so fast that the pressure in the delamination cannot adjust to the pressure in the tunnel. Therefore a pressure difference exists at the delamination. As a consequence the volume of the delamination will increase, the pressure in the delamination will decrease, and the delamination will be stressed: it will bulged out. The pressure difference over the delamination can be estimated by taking the universal gas law and assuming the delamination as circular plate clamped at the edge, see Fig. 5.

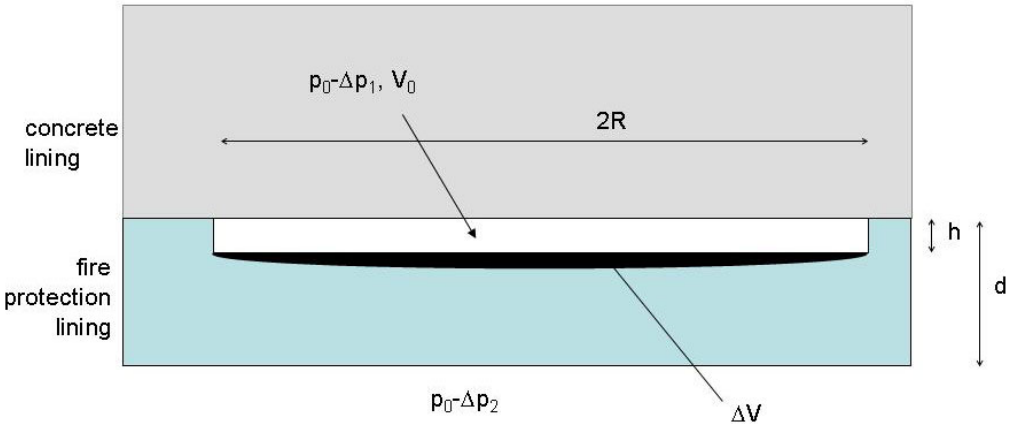

Fig. 5 Illustration of a circular delamination with radius R, initial volume V_0 and height h. The volume increase ΔV, due to Δp_2 the pressure drop in the tunnel, is indicated by the shaded area. p_0 = initial pressure in the tunnel and in the delamination, Δp_1 = pressure decrease at the delamination.

It can be derived that the pressure difference over the delamination Δp_f is:

$$\Delta p_f = \Delta p_2 - \Delta p_1 = \frac{1}{2}\left(- p_0 + \Delta p_2 - \frac{V_0}{k} + \sqrt{(p_0 - \Delta p_2 + \frac{V_0}{k})^2 + 4\frac{V_0}{k}\Delta p_2} \right) \quad (1)$$

with k the compliance of the delamination (1/k = the stiffness)
the other symbols are given in Fig. 5.

In case of a circular delamination with radius R, initial volume V_0 and height h, V_0/k is given by:

$$\frac{V_0}{k} = \frac{16E}{(1-\nu^2)}\frac{d^3 h}{R^4} \quad (2)$$

with E the elastic modulus of the lining
ν Poisson's ratio of the lining
d the thickness of the lining
ρ the density of the lining

As the height of the delamination will be very small, the ratio V_0/k will also be small. Consequently also the pressure difference will be small. However, the volume of the delamination depends on the weight of delamination and the number of spacings behind by the delamination. These spacings were used for the handling of the tunnel segments during the construction of the tunnel. The volume of the spacings within a segment is spread over the surface resulting in a spacing thickness $d_{spacing}$. When the volume behind the delamination is determined by the weight and the number of spacings behind the delamination, the ratio V_0/k is given by:

$$\frac{V_0}{k} = \frac{16Ed^3}{(1-\nu^2)}\left(\frac{\rho g(1-\nu^2)}{16Ed^2} + \frac{d_{spacing}}{R^4} \right) \quad (3)$$

with g the acceleration of gravity.

Note that no difference is made in the position along the tunnel lining. The above relation is valid for delaminations at the ceiling of the tunnel. For delaminations on the side Eq. 3 is conservative. The pressure difference on the delamination as function of the radius of the delamination is given in Fig 6. At small radii of the delamination the pressure difference is equal to the pressure drop. There is no pressure adjustment because small delaminations are relatively stiff. So the pressure behind the delamination will not decrease. As the radius increases the pressure difference over the delamination decreases. The stiffness decreases and the volume behind the delamination increases. As a consequence the pressure behind delamination decreases.

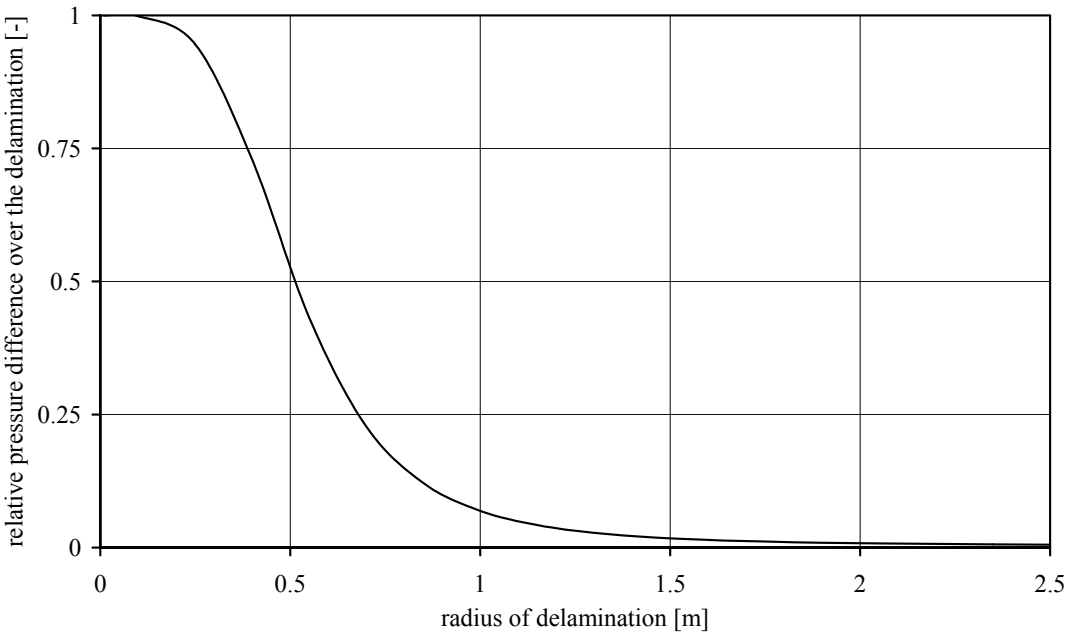

Fig. 6 The relative pressure difference over the delamination ($=\Delta p_f/\Delta p_2$) as a function of the radius of the delamination.

4.2 Stress at the delamination

The pressure difference over the delamination and its self weight causes stresses in the layer. The stresses in the layer can be estimated by considering the delamination as circular plate clamped at the edge. The maximum stress in the layer occurs at the edge of the delamination, see Fig. 3. Using the thin plate theory, this stress is given by [2]:

$$\sigma_{layer} = \frac{3R^2}{4d^2}\left(\Delta p_f + \rho g d\right) \tag{4}$$

with Δp_f the pressure difference on the delamination caused by the fast pressure drop, see Eq. 1.
$\rho g d$ the weight of the delamination

In Fig. 7 the stress in the fire protection lining is shown at a delaminated layer in which the spacings are averaged over the delamination. As a reference the stress in the layer is shown without the pressure adjustment due to the deformation of the layer.

The radius of the delamination has two effects: the pressure Δp_f decreases and the stress increases with increasing radius. The result is that there is a (local) minimum in the stress in the layer as a function of the radius. At small radii the pressure difference is equal to the pressure drop but the stress in the layer remains low. When the radius increases, the pressure difference becomes small compared with the self weight contribution. As a result, the stress in the layer becomes large with increasing radius.

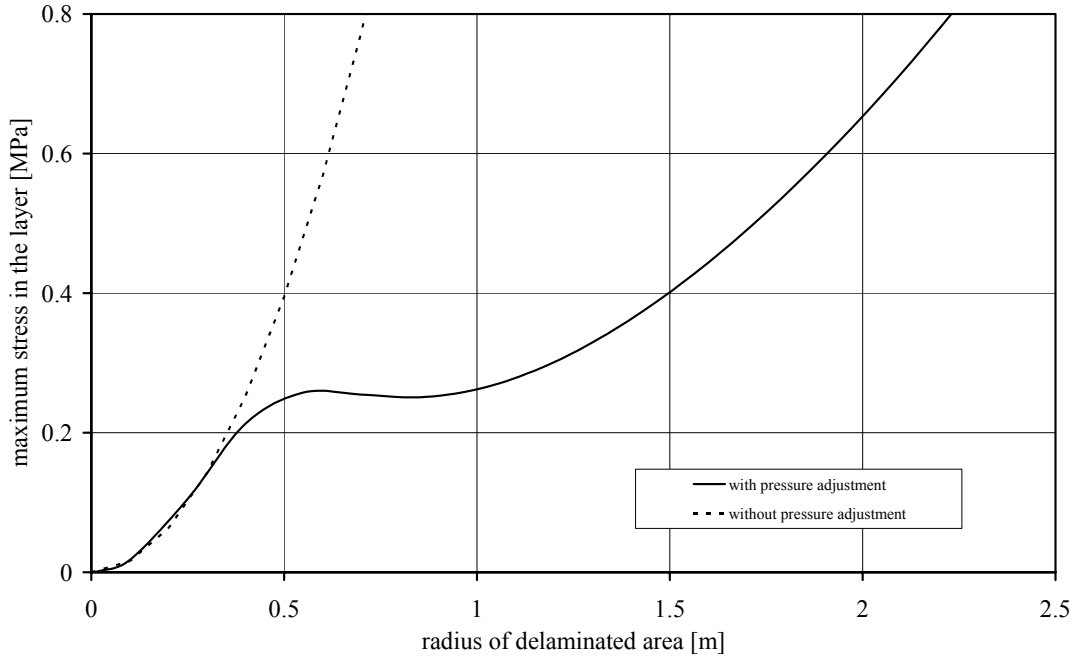

Fig. 7 Maximum stress in the layer as a function of the radius of the delaminated due to a pressure drop of 4 kPa according to Eq. 4. The dashed line indicates the stress when the effect of the volume increase is not taken into account (Eq. 4 with $\Delta p_f = \Delta p_2 = 4$ kPa). The layer thickness is 43 mm.

4.3 Modelling of the backup system

When there is a delamination the backup system (anchored wire mesh) is activated. The response of the backup system to pressure loads was determined by both small and large scale experiments. The backup fixation system was tested in the TNO laboratory using large test panels (4 m^2) with 18 anchor connections and small test panels (0.25 m^2) with 1 anchor connection. Both static and fatigue tests were carried out, the latter in connection with the large number of load cycles to the system caused by fast pressure variations due to passing high speed trains (300 km/h) during the service life of the tunnel.

Fig. 8 shows the wire mesh being pulled out of the layer during the static test on a single anchor and a typical load displacement diagram for this test. The decreases in load during the test occur when the wire mesh is gradually pulled out of the plaster. The static strength was in all cases approximately 3 kN. The static requirement was 12 kN/m^2 or, with 8 anchors per m^2, 1.5 kN per anchor. With a value of 3 kN the static requirement is fulfilled.

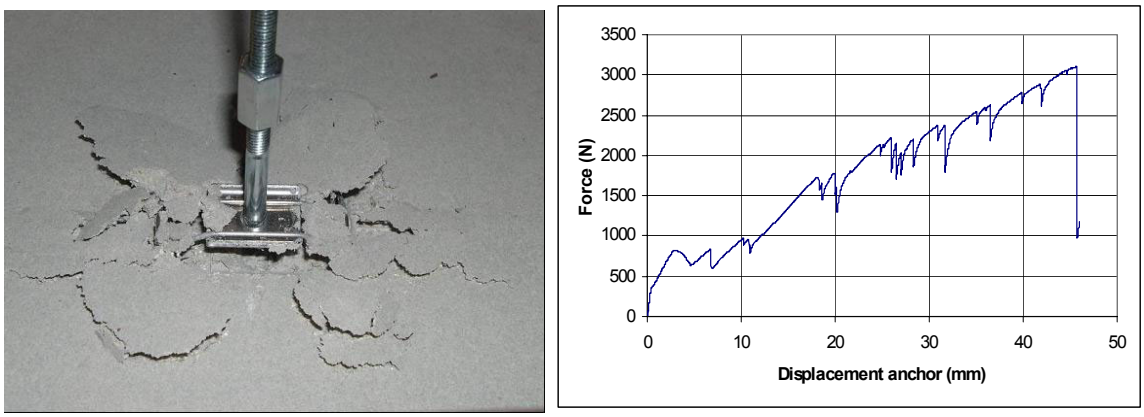

Fig. 8: Static test of the anchor and the layer (l) and the load displacement diagram (r).

Finite element analyses were carried out to assess the effect of the back-up system. In the finite element model the anchors were modelled as non-linear springs, see Fig. 9. The wire mesh was not modelled as its effect on the stiffness of the layer was insignificant. The spring characteristics were derived from the experiments (see e.g. Fig. 2). By calculating the volume (change) as a function of the applied pressure, the compliance k was calculated. This compliance was compared with the compliance of the delamination without the anchors. This resulted in a correction on the compliance in Eq. 3. The correction depends on the radius of the delamination. In order to keep the reliability analysis simple, the correction was taken conservatively at pressure drop of 6 kPa.

The same finite element approach was used to calculate the effect of the backup on the stresses in the layer. By comparing the stresses with and without backup, a correction factor was derived.

Another correction was applied because the stiffness was derived using the thin plate theory which is correct when the layer thickness is small compared to the size of the delamination. Using the same finite element model as used for the anchor effects, a correction was derived for the analytical model. The analytical model is used in order to keep the reliability calculations simple.

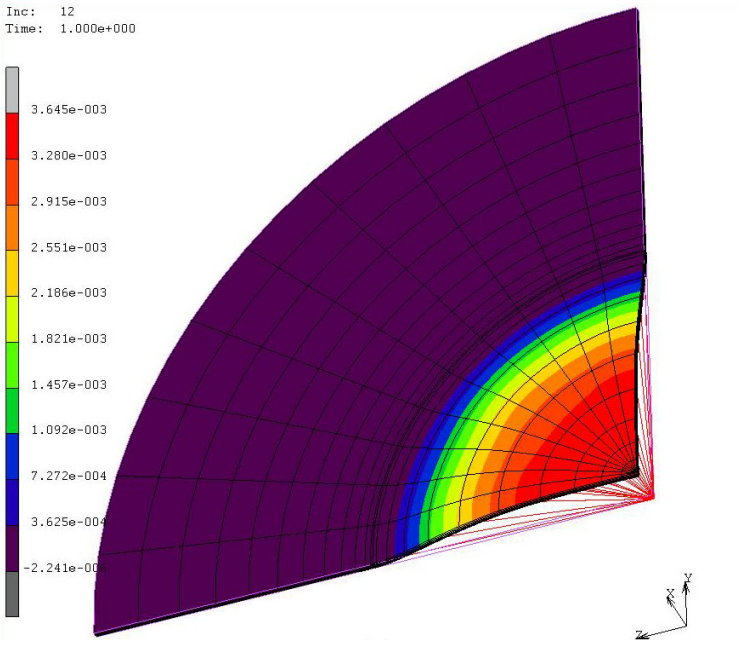

Fig. 9 An example of a finite element mesh of delamination with anchors (R = 2 m). The figure shows the displacements in x-direction in an exaggerated deformed mesh The anchors are visualised by (red) lines running from the position of the anchor to the origin. Because of symmetry only one quarter needs to be modelled.

5 Reliability analysis

In this section limit state functions are defined for the events presented in Fig. 4. The functions are used to calculate the reliability index. For most of the variables given in the limit state functions statistical distributions were set up. The reliability index was determined using the FORM method. Checks were made using SORM and crude Monte Carlo. ProBox [3], a probabilistic toolbox developed within TNO, was used to calculate the reliability as function of the radius of a the delamination.

5.1 Failure of the backup system due to repeated train passages

On the basis of the full scale experiments, failure due to a single train passage was not considered as a relevant failure mechanism. Only failure due to fatigue is considered. Failure of the backup is defined as failure of the anchor in the centre of the delamination. The experiments support the assumption that once an anchor (wires around the anchor) has failed, anchors in the vicinity fail shortly afterwards. The load acting upon the backup depends on the pressure difference over the delamination, the size of the delamination, the number of anchors behind the delamination, and the anchor stiffness. Using the fore mentioned finite element modelling, the ratio $C_{K/p}$ between the force on the (centre) anchor and the pressure difference over the layer could be determined. The limit state is given by:

$$Z = K - \gamma C_{K/p} \Delta p_f \tag{5}$$

with K is the fatigue resistance of the backup determined by full scale tests. The fatigue resistance depends on the reference period considered

$C_{K/p} = 0.14(1 - e^{-(1.27R)^2})$

γ a variable to taken into account the variation in $C_{K/p}$

Δp_f is the pressure over the delamination (Eq. 1)

The reliability index as function of the radius of the delamination is given in Fig. 10. The result can be explained by considering the pressure difference in Fig. 7 and the function $C_{K/p}$.

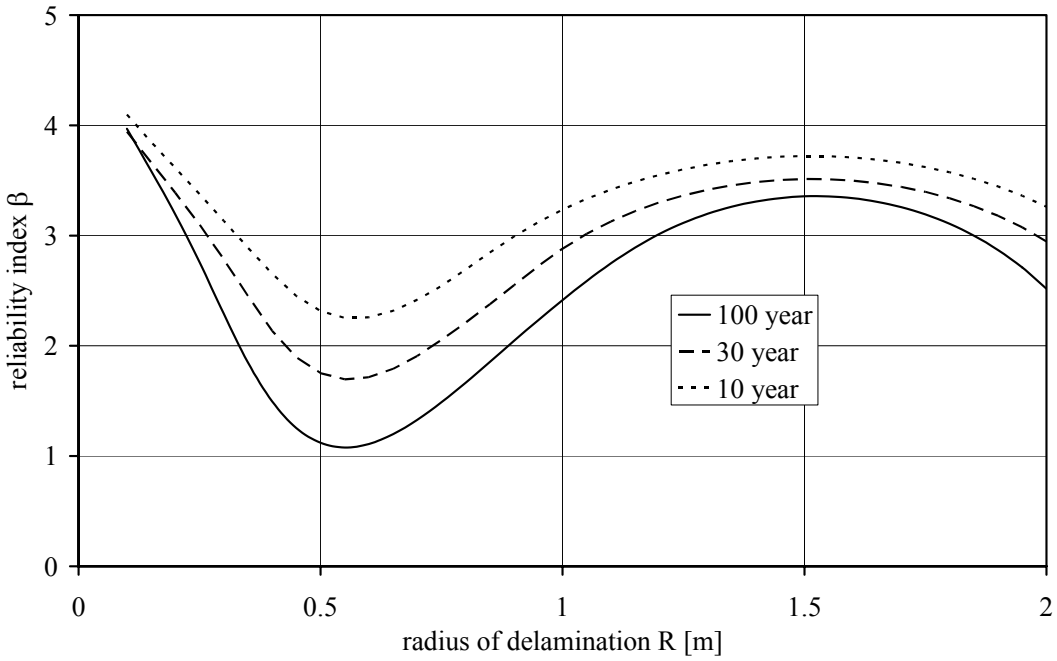

Fig. 10 Reliability of the backup as function of the radius of the delamination for three reference periods. Failure due to repeated train passages.

5.2 Failure of a delamination due to a single train passage

This failure mechanism of the fire protection lining is defined as the stress state by a single train passage which exceeds the critical stress. Then the layer will crack by a single pressure load. The largest stress will occur at the edge of the delamination. The delamination will bend outwards. Therefore the critical stress is taken equal to the flexural strength of the layer. The limit state is given by:

$$Z = f_c - \frac{3}{4}\frac{R^2}{d^2}\left(\Delta p_f + \rho dg\right) \tag{6}$$

with f_c the flexural strength of the layer

Δp_f the pressure difference over the layer

The reliability index as a function of the radius of the delamination is given in Fig 11. The result can be explained by considering Fig. 7. The backup system has a reducing effect on the stress. But its effect is only apparent at radii larger than 0.5 m.

Discarding inspection and maintenance, the following relation is used for probability of failure mode 1 given a certain delamination:

$$\begin{aligned} P(\text{mode 1}) &= P(\text{instable cracking of delamination AND backup fails}) \\ &= P(\text{instable cracking of delamination} \mid \text{backup fails}) \times P(\text{backup fails}) \\ &< P(\text{instable cracking of delamination, no backup}) \times P(\text{backup fails}) \end{aligned} \quad (7)$$

The first term can be determined from the *solid* line in Fig. 11. This corresponds to the situation that no backup is present. This is a conservative approach because the backup is not present from the beginning which is not the case in reality. The second term can be determined from Fig. 10. The result of Eq. 7 is given in Fig. 12.

For radii up to 2 m the reliability index is above the target (=3.6) independent of the reference period. For larger radii (> 2.5 m) the reliability becomes below the target value. So these delamination have to be found by an inspection program.

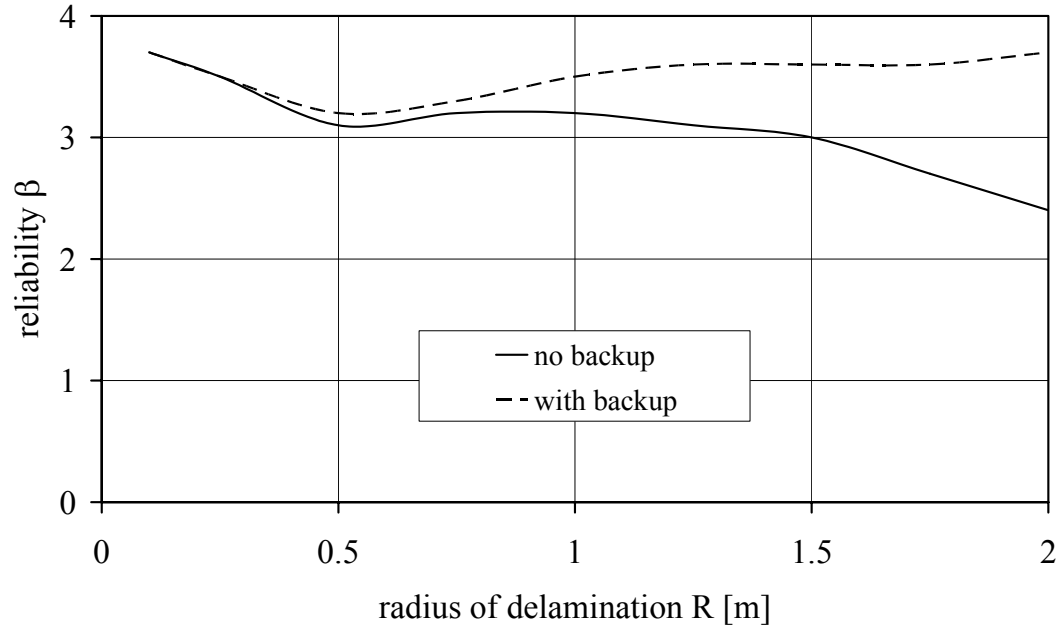

Fig. 11 The reliability index as a function of the radius of delamination, single train passage (unstable cracking). The dashed line is shown for illustration only and not used to calculate the reliability.

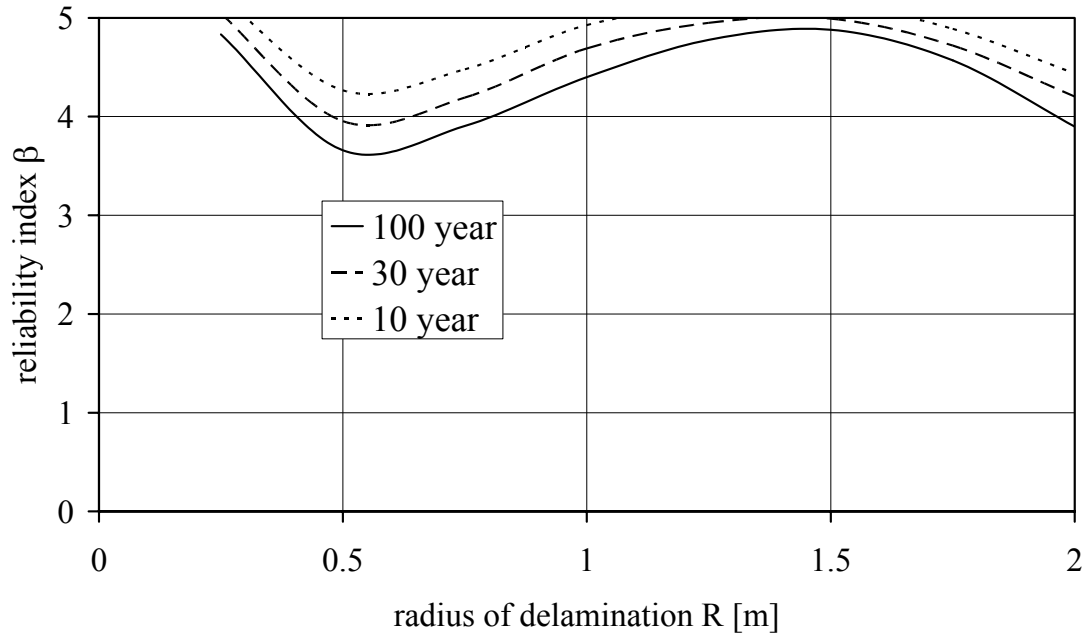

Fig. 12 Reliability index of failure as a result of instable cracking of the delamination and fatigue of the backup for three reference periods.

5.3 Failure of a delamination due to due to repeated train passages

This failure mechanism of the fire protection lining is defined as the stress state exceeding the fatigue strength due to repeated train passages. Then the layer will crack by repeated pressure loads in a stable way. The limit state is the same as for failure mode 1 except there are two modifications: a correction for fatigue on the flexural strength and without the constant load, i.e. the weight of the layer. The limit state is given by:

$$Z = C_{fatigue} f_c - \frac{3}{4}\frac{R^2}{d^2}\Delta p_f \tag{8}$$

with $C_{fatigue}$ a correction factor due fatigue on the flexural strength. This factor depends on the time period considered
Δp_f the pressure difference over the layer (Eq. 1).

The reliability index as a function of the radius of the delamination is given in Fig. 13. Comparing with the situation of a single train passage, the reliability is lower up to 1.5 m. This is caused by correction for fatigue. At radii larger than 1.5 m, the index remains constant because the load, the pressure difference, becomes constant. Note that for the single train passage the load increases as the radius increases due to the weight of layer. The backup system has a reducing effect on the stress. But its effect is only apparent at radii larger than 0.5 m.

The same approach as with failure mechanism 1 is used to calculate the probability of failure mode 2. Discarding inspection and maintenance, the following relation is used for probability of mode 2 given a certain delamination:

P(mode 2) = P(stable cracking of delamination AND backup fails)

= P(stable cracking of delamination | backup fails) x P(backup fails)

< P(stable cracking of delamination, no backup) x P(backup fails) (9)

The first term can be determined from the *solid* line in Fig. 13. This corresponds to the situation that no backup is present. The second term can be determined from Fig. 10. The result of Eq. 9 is given in Fig. 14.

Between R = 0.3 m and 0.85 m the target reliability is not met for a reference period of 100 year. The reliability index is clearly below the value of 3.6. For a reference period of 10 year the target reliability is obtained, and considering the various conservative assumptions this may also be assumed for a period of 30 year.

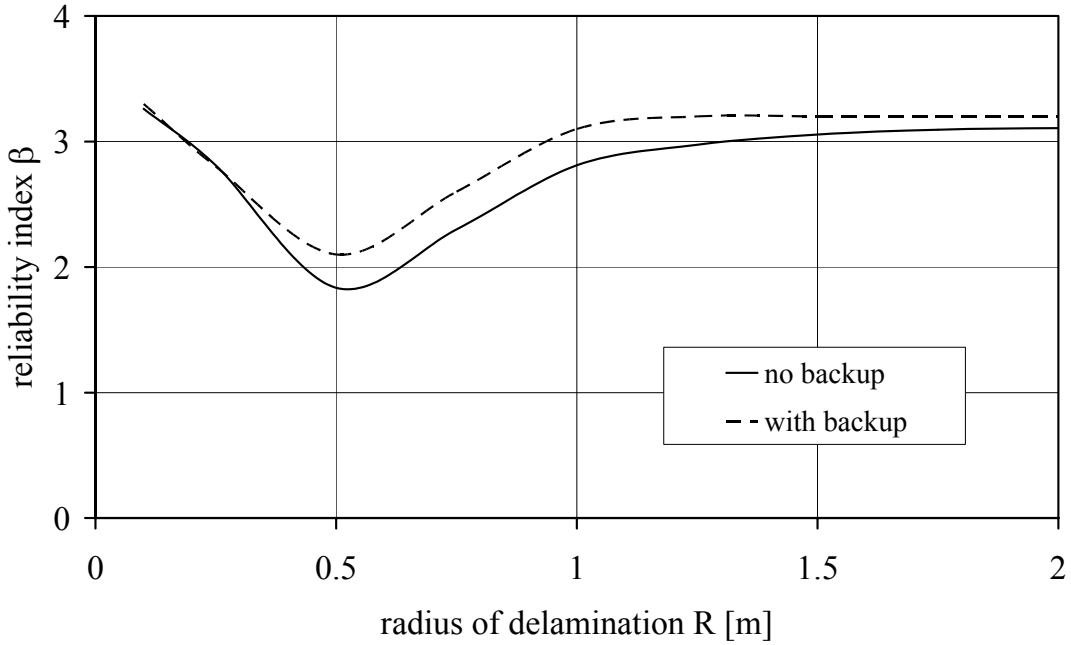

Fig. 13 The reliability as a function of the radius of delamination, repeated train passages (stable cracking). The dashed line is shown for illustration only and not used to calculate the reliability.

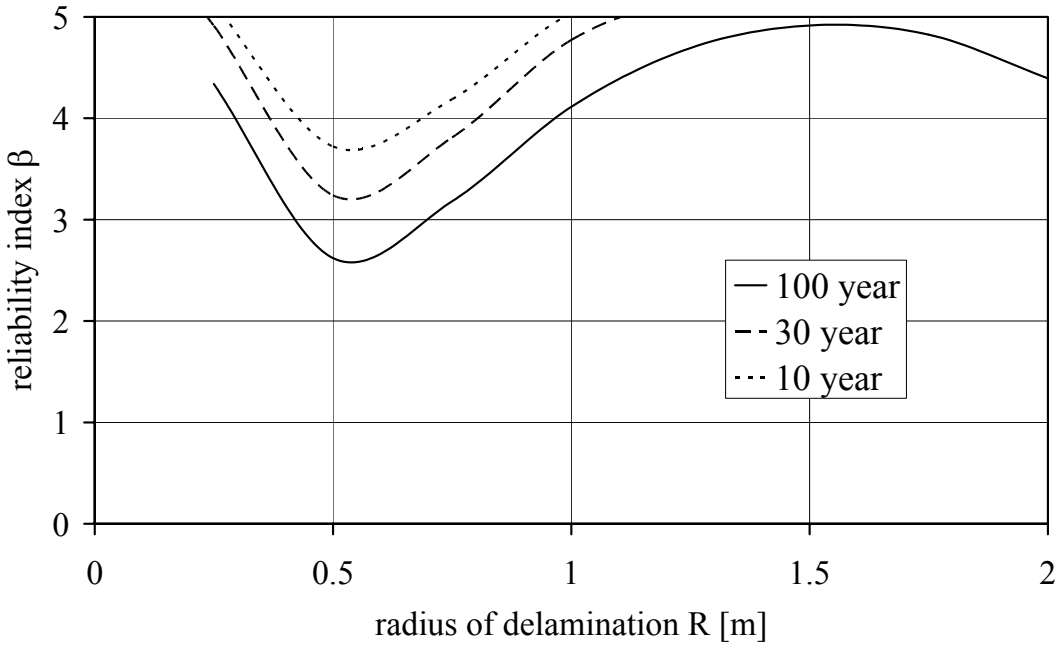

Fig. 14 Reliability of the lining as a result of stable cracking of the delamination and fatigue of the backup for three reference periods.

6 Conclusions

The reliability of the sprayed fire protection lining in the high speed tunnel Groene Hart has been analysed. The analysis shows how the reliability of a new system can be assessed on the basis of probabilistics, standard reliability methods, a combination of analytical and numerical modelling, small and full-size experiments and expert judgments. The conclusion is that the sprayed fire protection linings can be applied in the high speed train tunnel for short service periods (10-30 year). For longer service periods an additional inspection regime has to be established.

7 References

[1] Van de Linde, F.W.J., Gijsbers, F.B.J., Klok, G.J.: Fire Protection for High Speed Line Tunnels; Risk Analysis and Exceptional Robotic Application Results. ITA WTC 2006.

[2] Timoshenko, S.P., Woinowsky-Krieger, S.: Theory of plates and shells, second edition, 1970

[3] ProBox, a generic probabilistic toolbox, TNO, Delft, The Netherlands

Life cycle assessment of structures based on reliability analysis

Ralf Schnetgöke, Christoph Klinzmann, Dietmar Hosser
Institute for Building Materials, Concrete Construction and Fire Protection
Technical University of Braunschweig

Abstract: A modern lifetime oriented design of structures includes inspection and monitoring strategies. Structural health monitoring guarantees that the load bearing capacity, the serviceability and the durability of the structure remain ensured and that the costs of rehabilitation are limited. In the collaborative research centre 477 (CRC 477) at Braunschweig University of Technology methods for the optimisation of structural health monitoring are developed. In project field A1 the possibilities of reliability-based structural health monitoring are investigated. The methodology bases on a combination of recognized procedures of system and reliability theory. In reliability analysis using the First/Second-Order-Reliability-Method (FORM/SORM) the critical weak points and failure paths of the structure are identified. The optimisation is achieved when the structural health monitoring measures are concentrated on these weak-points and failure paths. This is utilized in the knowledge-based computer program PROBILAS (PRObabilistic Building Inspection and Life ASsessment). The program was designed to assist engineers to plan structural health monitoring measures for civil engineering structures. In this paper the assessment process is explained using a bridge as an example.

1 Introduction

1.1 Motivation

The lifetime oriented design of structures includes maintenance strategies. Structural health monitoring is essential to evaluate these strategies in such a way that the bearing capacity, serviceability and the durability remain ensured and the costs of rehabilitation are limited. The aim of structural health monitoring is the continuous monitoring and assessment of the

actual state of the structure. The outcome of this is the base for the optimisation of further measures.

In the Collaborative Research Centre 477 (CRC 477) "Life cycle assessment of structures via innovative monitoring" funded by the German Research Council (DFG) at the Braunschweig University of Technology, methods for the optimisation of SHM are investigated (see http://www.sfb477.tu-braunschweig.de). In project field A1 of the CRC 477 a framework for reliability-based system assessment based on data from SHM is developed. Its main objective is the optimisation of SHM measures with the help of probabilistic methods. The methodology is able to identify relevant parameters, to weigh the critical areas and to determine the actual safety level of a structure.

1.2 Life cycle assessment

Nowadays, the design and management of structures is becoming more and more performance orientated. Modern building management systems (BMS) are starting to combine system assessment with regular inspections and monitoring. The proportion of probabilistic models within BMS is increasing steadily (e.g. FABER [1]). In the USA, probabilistic models for life cycle considerations are primarily developed and tested for bridge networks (e.g. FRANGOPOL et al. [2]), but it is only a question of time until these technologies are applied to complex buildings as well.

In contrast to Germany, bridges in the USA are often constructed in well-proven and uniform configurations. Therefore, the variation of structural elements, types of deterioration and development of deteriorations is significantly smaller than in Germany. Additionally, the large amount of similar bridge structures provides a sufficient statistic basis to determine the leading influences on typical deteriorations (e.g. deterioration due to chloride ingress). In this case it is possible to draw conclusions from the totality of all bridges onto single bridges in a network (Top-down principle). In Germany, this is not possible due to a large variety of types of constructed bridges. Here, conclusions can only be drawn from a single structure to the totality of structures (Bottom-up principle). According to the conditions in Germany, the developed frame-work concentrates on the individual assessment of structures based on results from SHM.

2 Reliability-based life cycle assessment

2.1 Framework

The framework for reliability-based life cycle assessment bases on methods of system and reliability theory. The main idea is that, after a thorough anamnesis of a structure, typical weak points and failure paths are identified. The gained knowledge about the structural system is used to formulate a probabilistic model for the whole system. This model consists of limit-state equations for components of the system, information about the random variables and other uncertain parameters and a logical model, which describes the in-

teractions between the components. This model is evaluated in a reliability analysis with FORM/SORM.

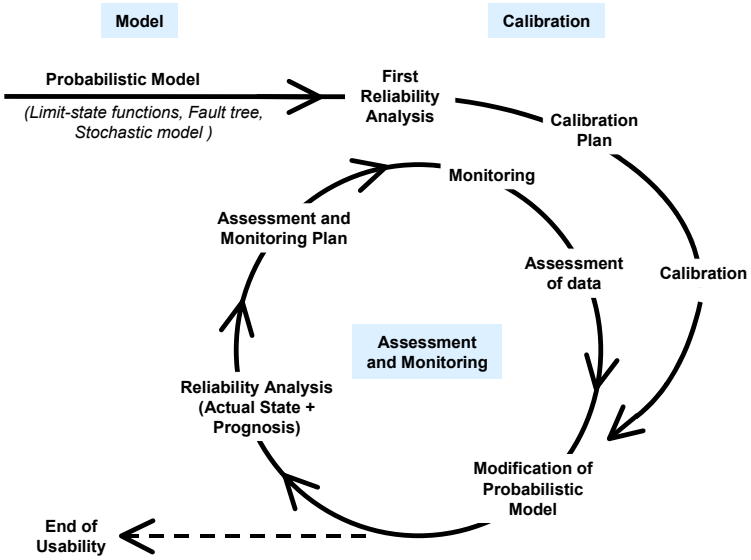

Fig. 1. Structural evaluation process of the framework

With the help of the results of this analysis, further decisions concerning an inspection and monitoring plan can be made, e.g. it is possible to identify the most significant parameters of a model. Additionally the weak points of the structure can be weighted. The knowledge gained can be used to derive a cost optimised monitoring plan for a continuous monitoring process.

2.2 System reliability analysis

The analysis of the structure starts with the identification of the different sources of risk for the structure. This information has to be translated into components and subsystems. The relations between the components are described using logical trees, which combine causes, intermediate events and their consequences. Two types of logical trees are used for further analysis.

The event tree shows all consequences of an occurring event and is used to identify all relevant failure paths of the structure. *The fault tree* regards all possible causal sequences of component and sub-system failures that lead to a system failure. The root element of the fault tree is called “Top Event” and represents e.g. an overall system failure. The logical dependence between the subsequent failures of components is described with the help of logical conjunctions.

There are two basic types of conjunctions between the elements of the fault tree: the serial system (disjunction), which fails if one of its elements fails and the parallel system (conjunction), which fails if all of its elements fail. Real systems, in most cases, can be represented by a combination of these two types.

For all components in a fault tree an ultimate limit state has to be defined. A limit state is described by quantities that represent the resistance of a structure (e.g. material strength) and by quantities, which represent the actions imposed on the structure (e.g. live load). Then the limit state equation can be described in the form:

$$G = R - S \tag{1}$$

The component fails, when the resistance quantity (R) is smaller than the action quantity (S). Both quantities are functions of parameters, which are stochastic and/or uncertain and are generally described by probability distributions. The parameters of the distributions can either be estimated from measurements or be found in the literature, e.g. (JCSS [3]). If the random variations of an input parameter are small, the parameter can be assumed as deterministic.

For the reliability analysis the first or second order reliability method (FORM/SORM) (DITLEVSEN et al. [4]) is utilised. In these calculations a probability of failure (p_f), a safety index b ($p_f=\Phi(-\beta)$) and sensitivity values (α-values) for each parameter can be determined. The weak points ("hot spots") of the structure can be identified with the help of the system reliability analysis. Based on the calculated values, the failure path with the highest probability of occurrence can be found. Especially the parameters of the limit-state equations within this failure path should be investigated further.

The first reliability analysis of the actual state of the system is carried out with values for the parameters of the structure according to the prescriptions in the structural design. In reality, these values may not be identical to the real values of the parameters in the structure. An example is the compression strength of concrete, which is usually higher than the value assumed in the design calculation. Therefore, the probabilistic model of the structure has to be calibrated prior to the further probabilistic assessment of the structure. The calibration can be limited to the important and time-independent parameters identified in the reliability analysis. Usually, random samples from the regular quality control can be used for this purpose. With statistic tests the random samples are tested for conformity with the values assumed in the design process. Afterwards, prior information about the parameter and the random sample are used to compute new stochastic information about the parameter using Bayesian procedures.

Beside the reliability of the actual state of the structure, a prognosis calculation will be carried out. The difference is that in his case, the reliability index is calculated in a time-step procedure. For each time-step, the time-dependent alteration functions are evaluated for the mean and/or the standard deviation of each considered parameter, before the reliability analysis is started. This results in a time-dependant curve of the safety index.

2.3 Monitoring and inspection

Based on the calculation results, a monitoring plan can be determined. It contains information about the parameters which should be monitored, as well as monitoring, inspection and probabilistic assessment intervals. The monitoring plan mainly depends on the capabilities of sensors.

The monitoring interval is unique for each sensor and is dependent on the phenomenon to be monitored and its significance. For very slow processes, e.g. chloride ingress, a suitable monitoring interval can be once or twice a year. When the deformation of a deteriorated bridge is monitored, this is surely insufficient. In these cases the interval must be extended to several times a day.

The monitoring interval is usually not identical to assessment and inspection intervals. The assessment interval describes the time between two probabilistic assessments of the structure based on the monitored data. The inspection interval describes the time between regular inspections of the structure to identify new deteriorations or errors of the structure. Due to slow degradation processes, it is not necessary to conduct a probabilistic assessment or an inspection of the structure every time when new data is available. The ideal time intervals for assessment and inspection can be defined adaptively in conjunction with the results from the prognosis calculations. In addition, new data is investigated for negative trends in the behavior of the structure. If negative behavior of the structure is detected, an extraordinary inspection should be carried out. If the outcome of this inspection indicates that the probabilistic model has to be modified, a complete probabilistic re-assessment of the structure has to take place, too. If the prognosis calculations indicate no significant change in the reliability, an assessment and inspection interval of 2 to 3 years is sufficient. This interval would be smaller, if the actual safety level of the structure is near to the prescribed target reliability.

3 Life cycle assessment of a bridge

3.1 Bridge structure

The function of a building regarding the bearing capacity and serviceability has to be guaranteed over the intended lifetime without substantial loss of the usage characteristics. The detection of safety-relevant deviations from planned properties of the structure requires an optimised structural health monitoring process.

For illustration purposes a bridge example is used. The main focus in this article lies on the ultimate limit states for the flexure and fatigue failure of the bridge structure. The structure is a multi-span plate-girder bridge over two fields with two girders and a span width of 32 m for each field (Fig 1, 2). The bridge is pre-stressed with post-tensioning tendons. The tendons have a cross-sectional area of 180 cm² per girder with normative yield strength of 1570 MN/m² and a normative ultimate strength of 1770 MN/m². A concrete strength class C 35 according to EN 1992 [5] was chosen in the design.

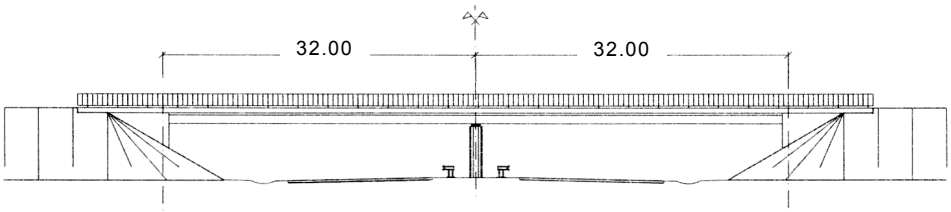

Fig. 2. Bridge structure, elevation

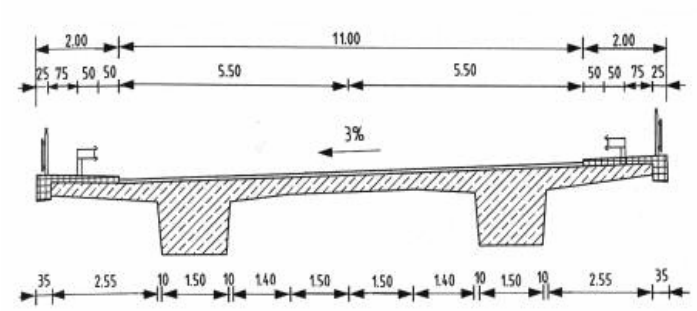

Fig. 3. Bridge structure, cross section

3.2 Probabilistic model

The risk-orientated assessment starts with a survey of possible weak points. First information about weak points of structures can be acquired by damage analyses. These analyses are the basis for the determination of failure scenarios. Further information about possible weak points and failure scenarios can be derived from the structural design process. In this example, the weak point analysis is based on the structural design.

The structural design for the bridge structure shows a high action effect in the cross section at midspan and at the support. At these so called "failure points" the structure can fail due to the exceeding of the flexure capacity or the fatigue capacity respectively. Further investigations will be concentrated on these failure modes. The different failure modes are summarised in the fault tree as serial system (Fig. 4). A system effect like load redistribution is neglected. The failure of more then one component for the collapse of the system is considered as system effect. Prior analyses of this type of a bridge showed a so-called "zip-effect" (SCHNETGÖKE et al. [6]).That means that after the failure of the first component the redistributed load effect on the second component jumps up extensively. Therefore the reliability of the second component decreases significantly, which results in a small influence on the system reliability.

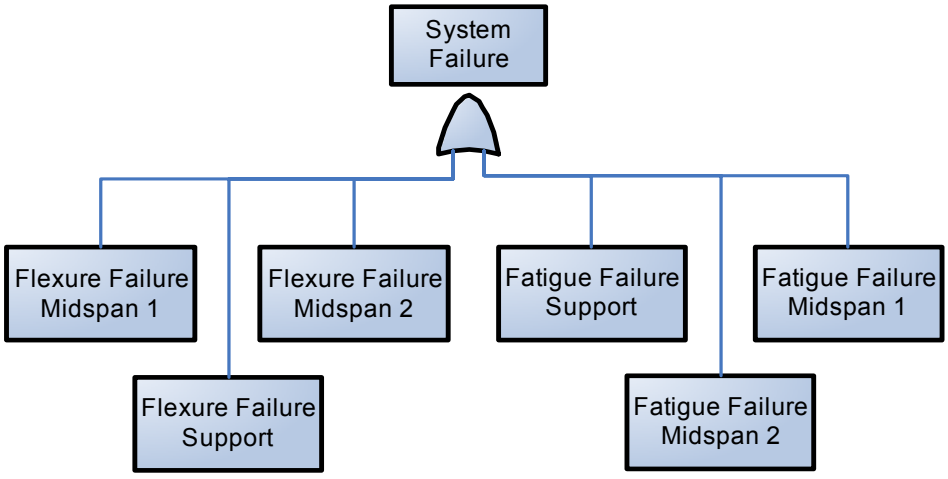

Fig. 4. Fault tree

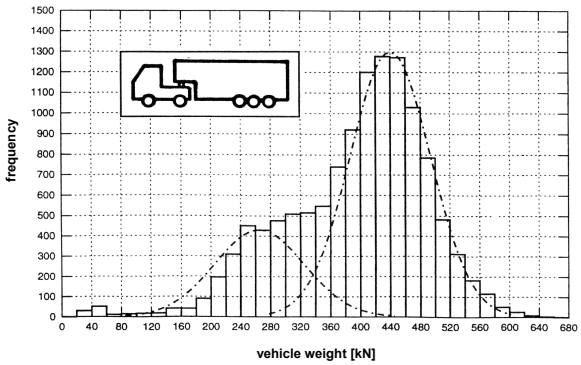

Fig. 5. distribution of the weight for a semitrailer truck

For all components in the fault tree the limit state functions have to be defined. The first component illustrated in this chapter is the flexure failure. The flexure capacity for the bridge section can be calculated using the equilibrium of internal forces. The associated equation for the flexure capacity can be described as follows:

$$M_R = A_s \cdot f_y \cdot d - \frac{1}{2} \cdot A_s \cdot f_y \cdot \frac{A_s \cdot f_y}{b \cdot f_c)} \tag{2}$$

The resisting moment according to equation (2) will be compared with the acting moment due to dead load and live load. The dead load results from the concrete weight of the construction and the additional load (e.g. surfacing, parapet). The load effect of the live load due to the traffic is carried out with a Monte Carlo simulation. A vehicle classification as well as the stochastic model of the vehicle weight, axle weight, axle spacing, vehicle length, vehicle spacing etc. is required for the simulation. In this investigation the necessary input is based on the data in MERZENICH et al. [7]. A typical twin peaked bimodal distribution of the weight for a semi-trailer truck is shown in Fig. 5. This form of distribution is typical for trucks. The first mode contains the partially loaded trucks, whereas the second involves the fully loaded trucks. The moment-time curve is derived from the traffic flow simulation and the influence line for the bending moment.

In the next step the distribution for the bending moment will be described with an extreme-value distribution type I (Gumbel) (Fig. 6).

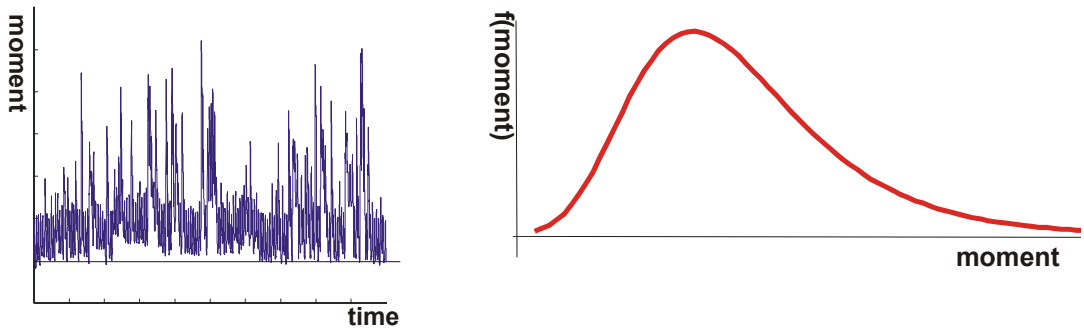

Fig. 6. Time series and distribution of the bending moment

Beside the flexure capacity also the limit state for fatigue failure of the tendons has to be analysed. The describing model for fatigue failure is based on the PALMGREN-MINER hypothesis. This hypothesis describes the damage of the material due to alternating loads of the construction. The damage accumulates until a critical value is reached. In the theory a fracture occurs with the exceeding of this value. The damage progress of the tendon is described by the dimensionless damage factor D:

$$D = \sum_i \frac{n(\Delta\sigma_i)}{N(\Delta\sigma_i)} \tag{3}$$

In the equation $n(\Delta\sigma_i)$ stands for the number of load cycles with the stress difference $\Delta\sigma_i$. $N(\Delta\sigma_i)$ is the maximum number of alternations for the stress difference $\Delta\sigma_i$. This maximum number can be read off directly from the *S-N* curve. Per definition the fatigue failure occurs when the dimensionless damage factor D reaches a value of 1. Based on the Palmgreen-Miner hypothesis, the limit state equation for the fatigue failure can be defined to be:

$$Z = D_R - D_S \tag{4}$$

In the context of the first building assessment the number of $0.5 \cdot 10^6$ trucks is assumed to be the annual volume of traffic. Further the distribution of the stress differences $\Delta\sigma_i$ is needed. The stress-time curve results with the relationship between the bending moment and the stress in the tendon. In the next step the relevant information for the fatigue failure like stress differences $\Delta\sigma_i$ and associated frequency will be calculated from this curve. Therefore the so-called counting methods, e.g. the rainflow hysteresis counting method (CLORMANN et al. [8]), are used. The maximum number of alternations can be read of the S-N curve with the stress differences determined in this way.

The probabilistic approach to fatigue failure is based on the stochastic model for the *S-N* curve. An appropriate relationship between the number of stress cycles and the stress differences can be found in MAES et al. [9]:

$$\log N(\Delta\sigma) = g(\Delta\sigma) + \theta_N \tag{5}$$

where $g(\Delta\sigma)$ is a deterministic function of the stress range and θ_N a zero mean normal random variable. The traditional function $g(\Delta\sigma)$ is the linear respectively bilinear relationship between log N and log $\Delta\sigma$. The resulting relationship is:

$$g(\Delta\sigma) = \log N(\Delta\sigma) = c_m - m \cdot \log(\Delta\sigma) \tag{6}$$

where m is an exponent, which ranges typically from 3 to 5 and c_m is a constant. Often the *S-N* curve is made bilinear to account for the absence of fatigue failure when the stress range $\Delta\sigma$ becomes very small.

The PALMGREN-MINER hypothesis is an empirical description of the complex mechanical fatigue behaviour procedures and comparatively simple to handle. Therefore the dimensionless damage factor D will be considered as random variable to keep the shortcoming of the mechanical model (SPAETHE [10]) in mind.

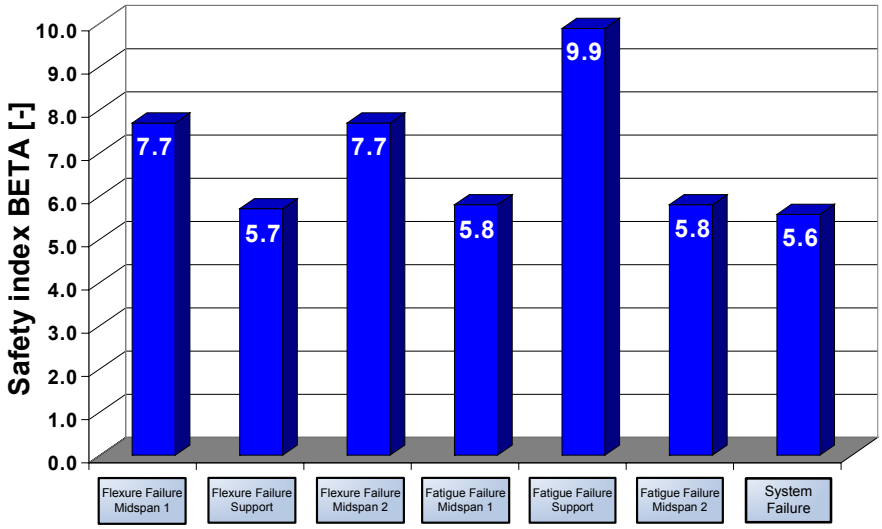

Fig. 7. Result of the reliability analysis (actual state)

3.3 Reliability analysis and life cycle assessment

The result of the reliability analysis for the actual state is shown in Fig. 7. The figure shows the reliability index β for every component and for the system. The components which are significant for the system reliability become obvious based on these results. The strength of the concrete and the pre-stressing steel and the live load show a prevalent influence on the reliability due to the high sensitivity factors α for these parameters.

A further reliability analysis is the prognosis calculation to estimate the development of the reliability of the structure in the future. Therefore a possible degradation and/or a change in the load configuration of the structure are assumed. The rising amount of traffic of highway bridges and the related higher loading of bridges can be taken as an example. Following the bottom-up principle, the degradation of the structure is modelled using time-

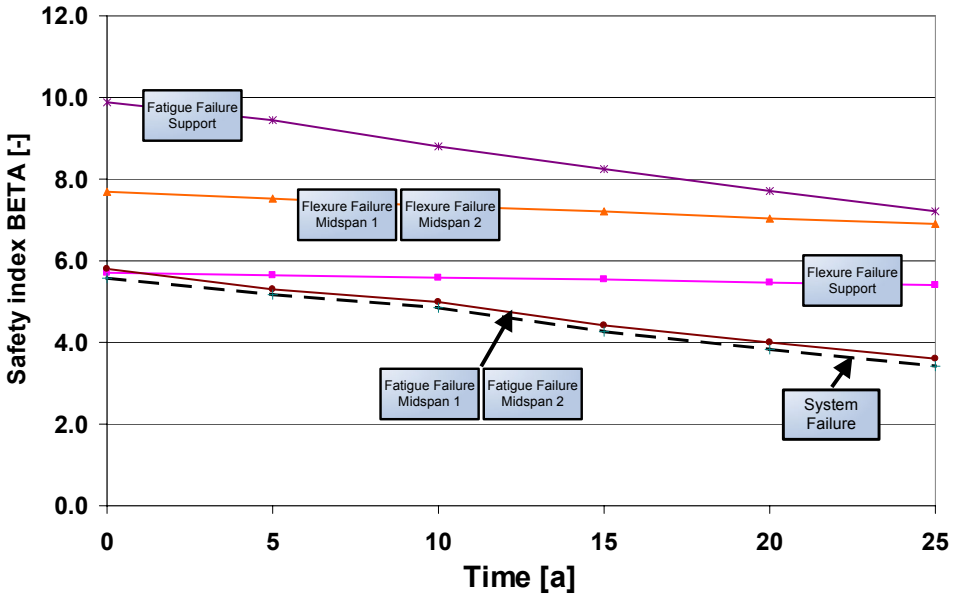

Fig. 8. Result of the reliability analysis (prognosis)

dependant alteration functions for the parameter affected. Due to the small change of the material strength during the time and the high sensitivity value α for the live load in the prognosis calculation an increase of the live load by 2 % of the initial value a year will be assumed. This results in a time-dependent reliability index β shown in fig. 8.

The monitoring plan can now be determined with this curve. On the one hand there is the regular inspection every 3 respectively every 6 years, on the other hand a measurement of the traffic load will be suggested after ten years at the latest. The next step will be the reassessment of the structure based on measured data and the update of the monitoring plan. Within the first 10 years there is a sufficient safety margin between the prognosis and the target reliability according to structural codes (e. g. $\beta_{1\text{year}} = 4.7$ according to EN 1990 [11]).

If the inspections show new weak points, a modification of the probabilistic model follows. A new reliability analysis including a new prognosis calculation leads to a modification of monitoring plan if necessary.

The durability of the concrete can be important for the structural behaviour besides to an increase of the live load. The analysis of past damages shows the environmental influence on the structure, e.g. steel corrosion due to chloride attack. In the future, the probabilistic model of a bridge structure will have to consider this deterioration if necessary. Based on the monitoring of concrete durability, first pieces of information about deviations from the designed properties can be received. An approach to include a corrosive degradation of the reinforcement in the reliability analysis is shown in SCHNETGÖKE et al. [12]. The methods developed in the Collaborative Research Centre 477 which enable the monitoring of the concrete durability are described in e.g. (SCHMIDT-DÖHL et al. [13]).

4 Conclusion

This article shows the application of the methods of system and reliability theory to the life cycle assessment of civil engineering structures. On this basis the inspection, monitoring and safety assessment of structures can be optimised. The whole procedure is summarised in the explained framework.

The procedure is illustrated with a bridge structure. After the set up of the probabilistic model for the structure in form of a fault tree, the modelling of the limit states for the components is shown. With the result of the reliability analysis for the actual state and the prognosis consequences for the further structural health monitoring process became apparent.

Further research will focus on the modelling of different types of structures and extended usage of the results from monitoring in the assessment process of structures. The integration of the methodology of the framework into the computer code PROBILAS (PRObabilistic Building Inspection and Life ASsessment) is one additional research topic of project field A1 of CRC 477.

Acknowledgments

The research presented in this paper is supported by the German Research Council (DFG) within the Collaborative Research Centre 477 (CRC 477). The authors would like to express their appreciation for the financial support.

References

[1] Faber, M. H. (ed.): Risk Based Inspection and Maintenance Planning, Institute of Structural Engineering, *Report Nr. 266*, Swiss Federal Institute of Technology, Zurich 2001.

[2] Frangopol, D. M. & Liu, M.: Optimal Bridge Maintenance Planning Based on Probabilistic Performance Prediction, in *Engineering Structures Vol. 26, No. 7* (2004), pp 991-1002.

[3] Joint Committee on Structural Safety (JCSS): *Probabilistic Model Code*, 12th draft. http://www.jcss.ethz.ch, 17.05.2002.

[4] EN 1992-1-1: Eurocode 2: Design of concrete structures – Part 1-1: General rules and rules for buildings, 2004.

[5] Ditlevsen, O. & Madsen, H.O.: *Structural Reliability Methods*, Lyngby, Department of Mechanical Engineering, Technical University of Denmark, 2003.

[6] Schnetgöke, R.; Klinzmann, C.; Hosser, D.: Reliability-based life cycle assessment for civil engineering structures, *The 3rd International Conference on Bridge Maintenance, Safety and Management*, Porto, Portugal, 2006.

[7] Merzenich, G.; Sedlacek, G.: *Hintergrundbericht zu Eurocode 1 – Teil 3.2: „Verkehrslasten auf Straßenbrücken“*, Forschung Straßenbau und Straßenverkehrstechnik, Heft 711. 1995.

[8] Clormann, U.H., Seeger, T.: RAINFLOW-HCM, Ein Zählverfahren für Betriebsfestigkeitsnachweise aus werkstoffmechanischer Grundlage, in *Stahlbau 55*, 1986. Berlin, Verlag Ernst & Sohn.

[9] Maes, M.A., Wei, X., Dilger, W.H.: Fatigue reliability of deteriorating prestressed concrete bridges due to stress corrosion cracking in *Canadian Journal of Civil Engineering, 28,* 2001.

[10] Spaethe, G.: *Die Sicherheit tragender Baukonstruktionen*, Wien, Springer-Verlag, 1992.

[11] EN 1990: Eurocode: Basis of structural design. 2002.

[12] Schnetgöke, R. & Hosser, D.: Application of reliability-based system assessment using a bridge example. *Proceedings of 22nd CIB-W78 Conference Information Technology in Construction*, Dresden. 2005.

[13] Schmidt-Döhl, F., Bruder, S. & Budelmann, H.: Monitoring and Prognosis of Concrete Durability under Chemical Attack, *Proceedings of the Second European Workshop on Structural Health Monitoring*, Munich. 2004.

Life cycle assessment of structures based on reliability analysis

Ralf Schnetgöke, Christoph Klinzmann, Dietmar Hosser
Institute for Building Materials, Concrete Construction and Fire Protection
Technical University of Braunschweig

Abstract: A modern lifetime oriented design of structures includes inspection and monitoring strategies. Structural health monitoring guarantees that the load bearing capacity, the serviceability and the durability of the structure remain ensured and that the costs of rehabilitation are limited. In the collaborative research centre 477 (CRC 477) at Braunschweig University of Technology methods for the optimisation of structural health monitoring are developed. In project field A1 the possibilities of reliability-based structural health monitoring are investigated. The methodology bases on a combination of recognized procedures of system and reliability theory. In reliability analysis using the First/Second-Order-Reliability-Method (FORM/SORM) the critical weak points and failure paths of the structure are identified. The optimisation is achieved when the structural health monitoring measures are concentrated on these weak-points and failure paths. This is utilized in the knowledge-based computer program PROBILAS (PRObabilistic Building Inspection and Life ASsessment). The program was designed to assist engineers to plan structural health monitoring measures for civil engineering structures. In this paper the assessment process is explained using a bridge as an example.

1 Introduction

1.1 Motivation

The lifetime oriented design of structures includes maintenance strategies. Structural health monitoring is essential to evaluate these strategies in such a way that the bearing capacity, serviceability and the durability remain ensured and the costs of rehabilitation are limited. The aim of structural health monitoring is the continuous monitoring and assessment of the

actual state of the structure. The outcome of this is the base for the optimisation of further measures.

In the Collaborative Research Centre 477 (CRC 477) "Life cycle assessment of structures via innovative monitoring" funded by the German Research Council (DFG) at the Braunschweig University of Technology, methods for the optimisation of SHM are investigated (see http://www.sfb477.tu-braunschweig.de). In project field A1 of the CRC 477 a framework for reliability-based system assessment based on data from SHM is developed. Its main objective is the optimisation of SHM measures with the help of probabilistic methods. The methodology is able to identify relevant parameters, to weigh the critical areas and to determine the actual safety level of a structure.

1.2 Life cycle assessment

Nowadays, the design and management of structures is becoming more and more performance orientated. Modern building management systems (BMS) are starting to combine system assessment with regular inspections and monitoring. The proportion of probabilistic models within BMS is increasing steadily (e.g. FABER [1]). In the USA, probabilistic models for life cycle considerations are primarily developed and tested for bridge networks (e.g. FRANGOPOL et al. [2]), but it is only a question of time until these technologies are applied to complex buildings as well.

In contrast to Germany, bridges in the USA are often constructed in well-proven and uniform configurations. Therefore, the variation of structural elements, types of deterioration and development of deteriorations is significantly smaller than in Germany. Additionally, the large amount of similar bridge structures provides a sufficient statistic basis to determine the leading influences on typical deteriorations (e.g. deterioration due to chloride ingress). In this case it is possible to draw conclusions from the totality of all bridges onto single bridges in a network (Top-down principle). In Germany, this is not possible due to a large variety of types of constructed bridges. Here, conclusions can only be drawn from a single structure to the totality of structures (Bottom-up principle). According to the conditions in Germany, the developed frame-work concentrates on the individual assessment of structures based on results from SHM.

2 Reliability-based life cycle assessment

2.1 Framework

The framework for reliability-based life cycle assessment bases on methods of system and reliability theory. The main idea is that, after a thorough anamnesis of a structure, typical weak points and failure paths are identified. The gained knowledge about the structural system is used to formulate a probabilistic model for the whole system. This model consists of limit-state equations for components of the system, information about the random variables and other uncertain parameters and a logical model, which describes the in-

teractions between the components. This model is evaluated in a reliability analysis with FORM/SORM.

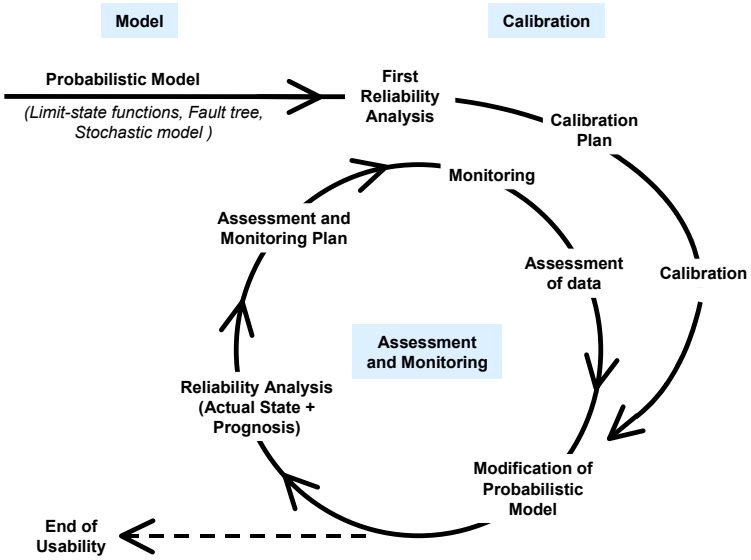

Fig. 1. Structural evaluation process of the framework

With the help of the results of this analysis, further decisions concerning an inspection and monitoring plan can be made, e.g. it is possible to identify the most significant parameters of a model. Additionally the weak points of the structure can be weighted. The knowledge gained can be used to derive a cost optimised monitoring plan for a continuous monitoring process.

2.2 System reliability analysis

The analysis of the structure starts with the identification of the different sources of risk for the structure. This information has to be translated into components and subsystems. The relations between the components are described using logical trees, which combine causes, intermediate events and their consequences. Two types of logical trees are used for further analysis.

The event tree shows all consequences of an occurring event and is used to identify all relevant failure paths of the structure. *The fault tree* regards all possible causal sequences of component and sub-system failures that lead to a system failure. The root element of the fault tree is called “Top Event” and represents e.g. an overall system failure. The logical dependence between the subsequent failures of components is described with the help of logical conjunctions.

There are two basic types of conjunctions between the elements of the fault tree: the serial system (disjunction), which fails if one of its elements fails and the parallel system (conjunction), which fails if all of its elements fail. Real systems, in most cases, can be represented by a combination of these two types.

For all components in a fault tree an ultimate limit state has to be defined. A limit state is described by quantities that represent the resistance of a structure (e.g. material strength) and by quantities, which represent the actions imposed on the structure (e.g. live load). Then the limit state equation can be described in the form:

$$G = R - S \tag{1}$$

The component fails, when the resistance quantity (R) is smaller than the action quantity (S). Both quantities are functions of parameters, which are stochastic and/or uncertain and are generally described by probability distributions. The parameters of the distributions can either be estimated from measurements or be found in the literature, e.g. (JCSS [3]). If the random variations of an input parameter are small, the parameter can be assumed as deterministic.

For the reliability analysis the first or second order reliability method (FORM/SORM) (DITLEVSEN et al. [4]) is utilised. In these calculations a probability of failure (p_f), a safety index b ($p_f=\Phi(-\beta)$) and sensitivity values (α-values) for each parameter can be determined. The weak points ("hot spots") of the structure can be identified with the help of the system reliability analysis. Based on the calculated values, the failure path with the highest probability of occurrence can be found. Especially the parameters of the limit-state equations within this failure path should be investigated further.

The first reliability analysis of the actual state of the system is carried out with values for the parameters of the structure according to the prescriptions in the structural design. In reality, these values may not be identical to the real values of the parameters in the structure. An example is the compression strength of concrete, which is usually higher than the value assumed in the design calculation. Therefore, the probabilistic model of the structure has to be calibrated prior to the further probabilistic assessment of the structure. The calibration can be limited to the important and time-independent parameters identified in the reliability analysis. Usually, random samples from the regular quality control can be used for this purpose. With statistic tests the random samples are tested for conformity with the values assumed in the design process. Afterwards, prior information about the parameter and the random sample are used to compute new stochastic information about the parameter using Bayesian procedures.

Beside the reliability of the actual state of the structure, a prognosis calculation will be carried out. The difference is that in his case, the reliability index is calculated in a time-step procedure. For each time-step, the time-dependent alteration functions are evaluated for the mean and/or the standard deviation of each considered parameter, before the reliability analysis is started. This results in a time-dependant curve of the safety index.

2.3 Monitoring and inspection

Based on the calculation results, a monitoring plan can be determined. It contains information about the parameters which should be monitored, as well as monitoring, inspection and probabilistic assessment intervals. The monitoring plan mainly depends on the capabilities of sensors.

The monitoring interval is unique for each sensor and is dependent on the phenomenon to be monitored and its significance. For very slow processes, e.g. chloride ingress, a suitable monitoring interval can be once or twice a year. When the deformation of a deteriorated bridge is monitored, this is surely insufficient. In these cases the interval must be extended to several times a day.

The monitoring interval is usually not identical to assessment and inspection intervals. The assessment interval describes the time between two probabilistic assessments of the structure based on the monitored data. The inspection interval describes the time between regular inspections of the structure to identify new deteriorations or errors of the structure. Due to slow degradation processes, it is not necessary to conduct a probabilistic assessment or an inspection of the structure every time when new data is available. The ideal time intervals for assessment and inspection can be defined adaptively in conjunction with the results from the prognosis calculations. In addition, new data is investigated for negative trends in the behavior of the structure. If negative behavior of the structure is detected, an extraordinary inspection should be carried out. If the outcome of this inspection indicates that the probabilistic model has to be modified, a complete probabilistic re-assessment of the structure has to take place, too. If the prognosis calculations indicate no significant change in the reliability, an assessment and inspection interval of 2 to 3 years is sufficient. This interval would be smaller, if the actual safety level of the structure is near to the prescribed target reliability.

3 Life cycle assessment of a bridge

3.1 Bridge structure

The function of a building regarding the bearing capacity and serviceability has to be guaranteed over the intended lifetime without substantial loss of the usage characteristics. The detection of safety-relevant deviations from planned properties of the structure requires an optimised structural health monitoring process.

For illustration purposes a bridge example is used. The main focus in this article lies on the ultimate limit states for the flexure and fatigue failure of the bridge structure. The structure is a multi-span plate-girder bridge over two fields with two girders and a span width of 32 m for each field (Fig 1, 2). The bridge is pre-stressed with post-tensioning tendons. The tendons have a cross-sectional area of 180 cm² per girder with normative yield strength of 1570 MN/m² and a normative ultimate strength of 1770 MN/m². A concrete strength class C 35 according to EN 1992 [5] was chosen in the design.

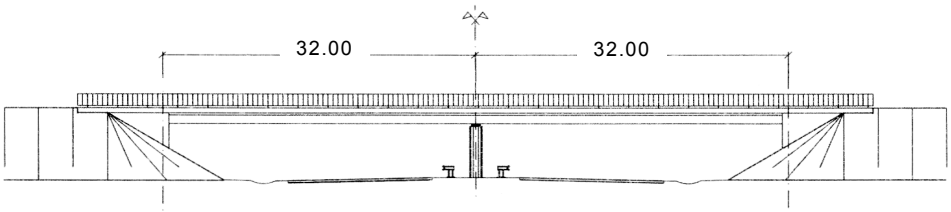

Fig. 2. Bridge structure, elevation

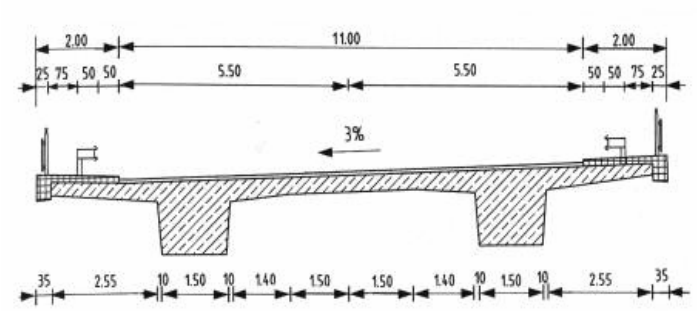

Fig. 3. Bridge structure, cross section

3.2 Probabilistic model

The risk-orientated assessment starts with a survey of possible weak points. First information about weak points of structures can be acquired by damage analyses. These analyses are the basis for the determination of failure scenarios. Further information about possible weak points and failure scenarios can be derived from the structural design process. In this example, the weak point analysis is based on the structural design.

The structural design for the bridge structure shows a high action effect in the cross section at midspan and at the support. At these so called "failure points" the structure can fail due to the exceeding of the flexure capacity or the fatigue capacity respectively. Further investigations will be concentrated on these failure modes. The different failure modes are summarised in the fault tree as serial system (Fig. 4). A system effect like load redistribution is neglected. The failure of more then one component for the collapse of the system is considered as system effect. Prior analyses of this type of a bridge showed a so-called "zip-effect" (SCHNETGÖKE et al. [6]).That means that after the failure of the first component the redistributed load effect on the second component jumps up extensively. Therefore the reliability of the second component decreases significantly, which results in a small influence on the system reliability.

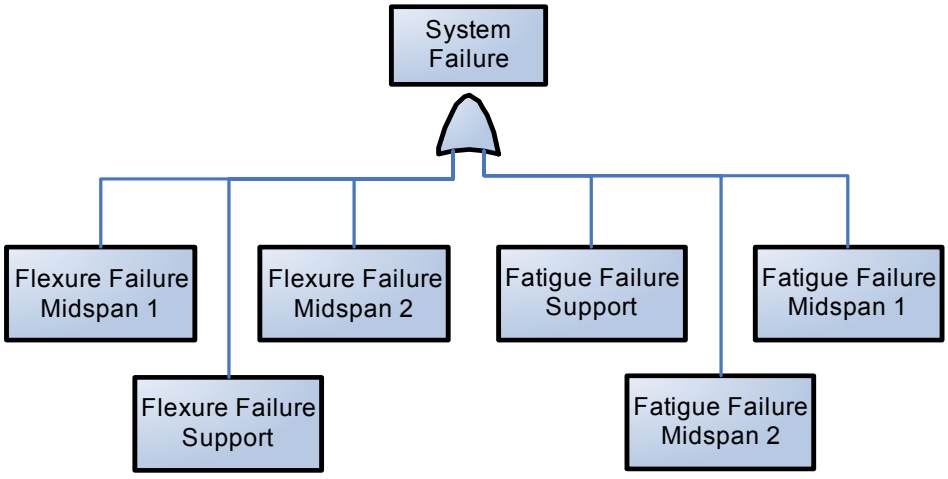

Fig. 4. Fault tree

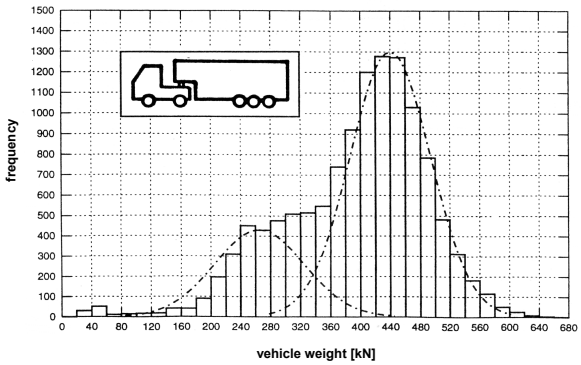

Fig. 5. distribution of the weight for a semitrailer truck

For all components in the fault tree the limit state functions have to be defined. The first component illustrated in this chapter is the flexure failure. The flexure capacity for the bridge section can be calculated using the equilibrium of internal forces. The associated equation for the flexure capacity can be described as follows:

$$M_R = A_s \cdot f_y \cdot d - \frac{1}{2} \cdot A_s \cdot f_y \cdot \frac{A_s \cdot f_y}{b \cdot f_c)} \tag{2}$$

The resisting moment according to equation (2) will be compared with the acting moment due to dead load and live load. The dead load results from the concrete weight of the construction and the additional load (e.g. surfacing, parapet). The load effect of the live load due to the traffic is carried out with a Monte Carlo simulation. A vehicle classification as well as the stochastic model of the vehicle weight, axle weight, axle spacing, vehicle length, vehicle spacing etc. is required for the simulation. In this investigation the necessary input is based on the data in MERZENICH et al. [7]. A typical twin peaked bimodal distribution of the weight for a semi-trailer truck is shown in Fig. 5. This form of distribution is typical for trucks. The first mode contains the partially loaded trucks, whereas the second involves the fully loaded trucks. The moment-time curve is derived from the traffic flow simulation and the influence line for the bending moment.

In the next step the distribution for the bending moment will be described with an extreme-value distribution type I (Gumbel) (Fig. 6).

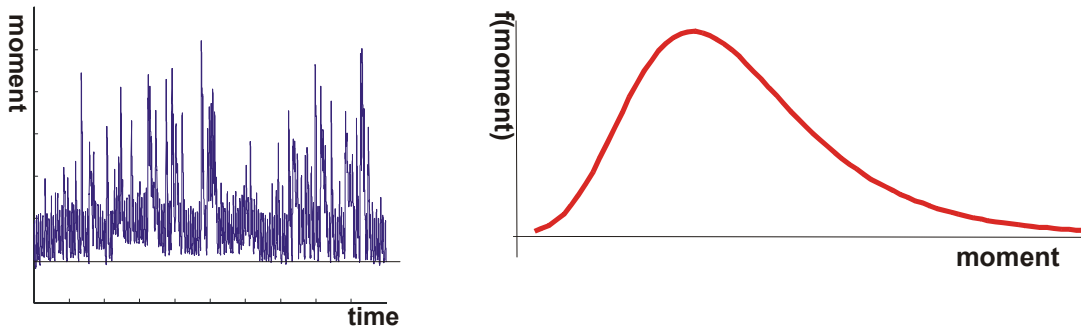

Fig. 6. Time series and distribution of the bending moment

Beside the flexure capacity also the limit state for fatigue failure of the tendons has to be analysed. The describing model for fatigue failure is based on the PALMGREN-MINER hypothesis. This hypothesis describes the damage of the material due to alternating loads of the construction. The damage accumulates until a critical value is reached. In the theory a fracture occurs with the exceeding of this value. The damage progress of the tendon is described by the dimensionless damage factor D:

$$D = \sum_i \frac{n(\Delta\sigma_i)}{N(\Delta\sigma_i)} \tag{3}$$

In the equation $n(\Delta\sigma_i)$ stands for the number of load cycles with the stress difference $\Delta\sigma_i$. $N(\Delta\sigma_i)$ is the maximum number of alternations for the stress difference $\Delta\sigma_i$. This maximum number can be read off directly from the *S-N* curve. Per definition the fatigue failure occurs when the dimensionless damage factor D reaches a value of 1. Based on the Palmgreen-Miner hypothesis, the limit state equation for the fatigue failure can be defined to be:

$$Z = D_R - D_S \tag{4}$$

In the context of the first building assessment the number of $0.5 \cdot 10^6$ trucks is assumed to be the annual volume of traffic. Further the distribution of the stress differences $\Delta\sigma_i$ is needed. The stress-time curve results with the relationship between the bending moment and the stress in the tendon. In the next step the relevant information for the fatigue failure like stress differences $\Delta\sigma_i$ and associated frequency will be calculated from this curve. Therefore the so-called counting methods, e.g. the rainflow hysteresis counting method (CLORMANN et al. [8]), are used. The maximum number of alternations can be read of the S-N curve with the stress differences determined in this way.

The probabilistic approach to fatigue failure is based on the stochastic model for the *S-N* curve. An appropriate relationship between the number of stress cycles and the stress differences can be found in MAES et al. [9]:

$$\log N(\Delta\sigma) = g(\Delta\sigma) + \theta_N \tag{5}$$

where $g(\Delta\sigma)$ is a deterministic function of the stress range and θ_N a zero mean normal random variable. The traditional function $g(\Delta\sigma)$ is the linear respectively bilinear relationship between log N and log $\Delta\sigma$. The resulting relationship is:

$$g(\Delta\sigma) = \log N(\Delta\sigma) = c_m - m \cdot \log(\Delta\sigma) \tag{6}$$

where m is an exponent, which ranges typically from 3 to 5 and c_m is a constant. Often the *S-N* curve is made bilinear to account for the absence of fatigue failure when the stress range $\Delta\sigma$ becomes very small.

The PALMGREN-MINER hypothesis is an empirical description of the complex mechanical fatigue behaviour procedures and comparatively simple to handle. Therefore the dimensionless damage factor D will be considered as random variable to keep the shortcoming of the mechanical model (SPAETHE [10]) in mind.

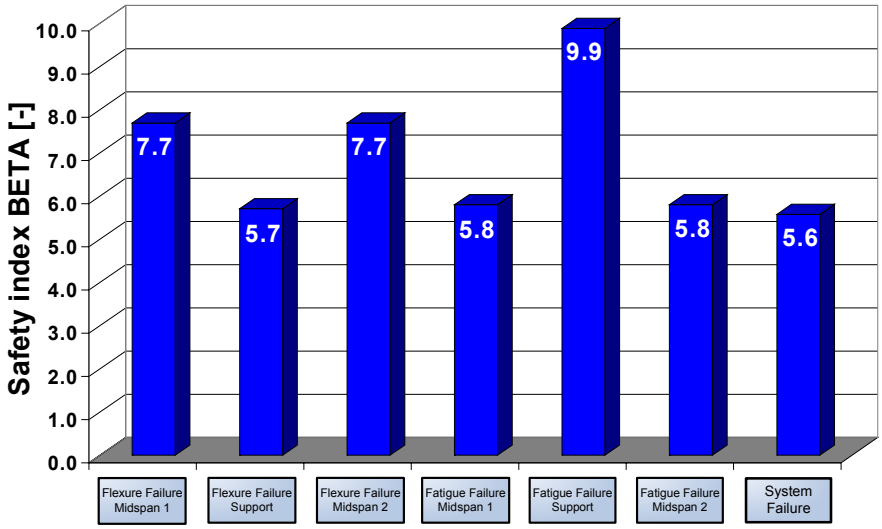

Fig. 7. Result of the reliability analysis (actual state)

3.3 Reliability analysis and life cycle assessment

The result of the reliability analysis for the actual state is shown in Fig. 7. The figure shows the reliability index β for every component and for the system. The components which are significant for the system reliability become obvious based on these results. The strength of the concrete and the pre-stressing steel and the live load show a prevalent influence on the reliability due to the high sensitivity factors α for these parameters.

A further reliability analysis is the prognosis calculation to estimate the development of the reliability of the structure in the future. Therefore a possible degradation and/or a change in the load configuration of the structure are assumed. The rising amount of traffic of highway bridges and the related higher loading of bridges can be taken as an example. Following the bottom-up principle, the degradation of the structure is modelled using time-

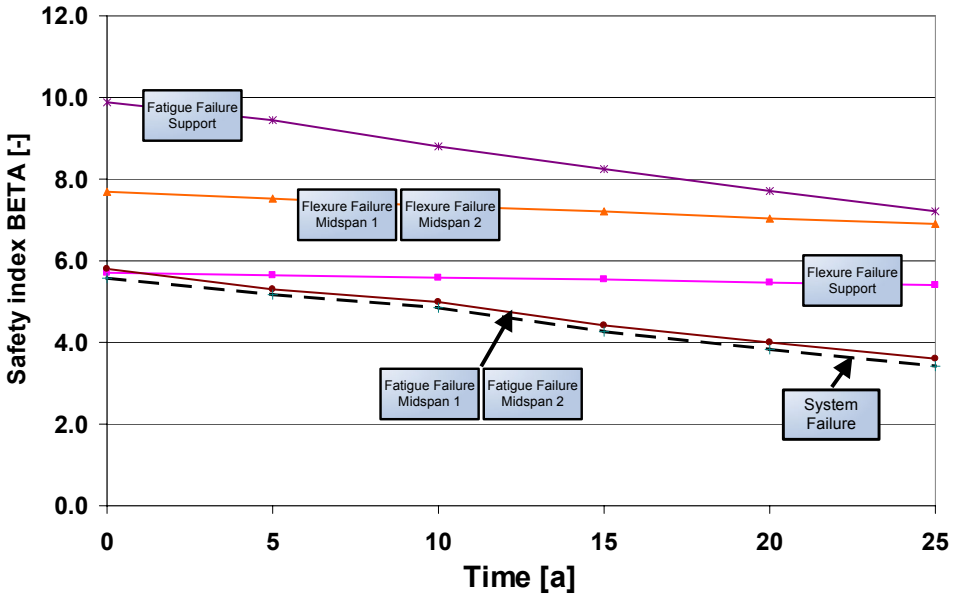

Fig. 8. Result of the reliability analysis (prognosis)

dependant alteration functions for the parameter affected. Due to the small change of the material strength during the time and the high sensitivity value α for the live load in the prognosis calculation an increase of the live load by 2 % of the initial value a year will be assumed. This results in a time-dependent reliability index β shown in fig. 8.

The monitoring plan can now be determined with this curve. On the one hand there is the regular inspection every 3 respectively every 6 years, on the other hand a measurement of the traffic load will be suggested after ten years at the latest. The next step will be the reassessment of the structure based on measured data and the update of the monitoring plan. Within the first 10 years there is a sufficient safety margin between the prognosis and the target reliability according to structural codes (e. g. $\beta_{1\text{year}} = 4.7$ according to EN 1990 [11]).

If the inspections show new weak points, a modification of the probabilistic model follows. A new reliability analysis including a new prognosis calculation leads to a modification of monitoring plan if necessary.

The durability of the concrete can be important for the structural behaviour besides to an increase of the live load. The analysis of past damages shows the environmental influence on the structure, e.g. steel corrosion due to chloride attack. In the future, the probabilistic model of a bridge structure will have to consider this deterioration if necessary. Based on the monitoring of concrete durability, first pieces of information about deviations from the designed properties can be received. An approach to include a corrosive degradation of the reinforcement in the reliability analysis is shown in SCHNETGÖKE et al. [12]. The methods developed in the Collaborative Research Centre 477 which enable the monitoring of the concrete durability are described in e.g. (SCHMIDT-DÖHL et al. [13]).

4 Conclusion

This article shows the application of the methods of system and reliability theory to the life cycle assessment of civil engineering structures. On this basis the inspection, monitoring and safety assessment of structures can be optimised. The whole procedure is summarised in the explained framework.

The procedure is illustrated with a bridge structure. After the set up of the probabilistic model for the structure in form of a fault tree, the modelling of the limit states for the components is shown. With the result of the reliability analysis for the actual state and the prognosis consequences for the further structural health monitoring process became apparent.

Further research will focus on the modelling of different types of structures and extended usage of the results from monitoring in the assessment process of structures. The integration of the methodology of the framework into the computer code PROBILAS (PRObabilistic Building Inspection and Life ASsessment) is one additional research topic of project field A1 of CRC 477.

Acknowledgments

The research presented in this paper is supported by the German Research Council (DFG) within the Collaborative Research Centre 477 (CRC 477). The authors would like to express their appreciation for the financial support.

References

[1] Faber, M. H. (ed.): Risk Based Inspection and Maintenance Planning, Institute of Structural Engineering, *Report Nr. 266*, Swiss Federal Institute of Technology, Zurich 2001.

[2] Frangopol, D. M. & Liu, M.: Optimal Bridge Maintenance Planning Based on Probabilistic Performance Prediction, in *Engineering Structures Vol. 26, No. 7* (2004), pp 991-1002.

[3] Joint Committee on Structural Safety (JCSS): *Probabilistic Model Code*, 12th draft. http://www.jcss.ethz.ch, 17.05.2002.

[4] EN 1992-1-1: Eurocode 2: Design of concrete structures – Part 1-1: General rules and rules for buildings, 2004.

[5] Ditlevsen, O. & Madsen, H.O.: *Structural Reliability Methods*, Lyngby, Department of Mechanical Engineering, Technical University of Denmark, 2003.

[6] Schnetgöke, R.; Klinzmann, C.; Hosser, D.: Reliability-based life cycle assessment for civil engineering structures, *The 3rd International Conference on Bridge Maintenance, Safety and Management*, Porto, Portugal, 2006.

[7] Merzenich, G.; Sedlacek, G.: *Hintergrundbericht zu Eurocode 1 – Teil 3.2: „Verkehrslasten auf Straßenbrücken“*, Forschung Straßenbau und Straßenverkehrstechnik, Heft 711. 1995.

[8] Clormann, U.H., Seeger, T.: RAINFLOW-HCM, Ein Zählverfahren für Betriebsfestigkeitsnachweise aus werkstoffmechanischer Grundlage, in *Stahlbau 55*, 1986. Berlin, Verlag Ernst & Sohn.

[9] Maes, M.A., Wei, X., Dilger, W.H.: Fatigue reliability of deteriorating prestressed concrete bridges due to stress corrosion cracking in *Canadian Journal of Civil Engineering, 28,* 2001.

[10] Spaethe, G.: *Die Sicherheit tragender Baukonstruktionen*, Wien, Springer-Verlag, 1992.

[11] EN 1990: Eurocode: Basis of structural design. 2002.

[12] Schnetgöke, R. & Hosser, D.: Application of reliability-based system assessment using a bridge example. *Proceedings of 22nd CIB-W78 Conference Information Technology in Construction*, Dresden. 2005.

[13] Schmidt-Döhl, F., Bruder, S. & Budelmann, H.: Monitoring and Prognosis of Concrete Durability under Chemical Attack, *Proceedings of the Second European Workshop on Structural Health Monitoring*, Munich. 2004.

Probabilities and uncertainties in natural hazard risk assessment

Sven Fuchs
Institute of Mountain Risk Engineering,
University of Natural Resources and Applied Life Sciences, Vienna, Austria

Abstract: In recent years, risk management procedures expanded into the assessment of natural hazards in the European Alps. The risk assessment methodology requires information on both, the natural process and the affected damage potential. While determining hazard potential and the related probability of occurrence of defined design events is quite sophisticated, little attention has been given to the possible range of input parameters needed for modeling. Furthermore, the affected damage potential has only been evaluated roughly so far, in particular concerning temporal dynamics and vulnerability. Consequently, uncertainties emerging from risk modeling techniques have only been addressed recently. In this study, those uncertainties are discussed with respect to the input parameters needed for the risk assessment procedure. Long-term as well as short-term shifts in the values at risk are presented for different study areas and on different scales. A conceptual framework for the consideration of those changes in risk analyses for natural hazards is developed.

1 Introduction

The term natural hazard implies the occurrence of a natural condition or phenomenon which threats disastrous to anthropogenic spheres of interest in a defined space and time[1]. Natural hazards pose a threat to settlements and infrastructure in European mountain areas,

[1] Notwithstanding from this definition, some authors characterise the 'natural process' as 'hazard', and the 'natural hazard' as 'disaster', and argue that hazards are natural, but in general, disasters are not, and that disasters should not be seen as inevitable outcome of a hazard's impact (for a relatively early attempt, see O'KEEFE et al., 1976). They stress on the conditions of people which make it possible for a hazard to become a disaster (e.g., CANNON, 1993). This includes the extent and types of people's vulnerability, in combination with the technical issue of how society deals (or does not deal) with the hazard in terms of mitigation and preparedness.

particularly due to the relative scarceness of areas suitable for land development; e.g., in Austria, only about 20 % of the whole area is suitable for development activities (BEV, 2006). Thus, since the outgoing 19th century, technical mitigation measures have been implemented to avoid damage to assets and people. Since the late 1970s, those measures have progressively more been supplemented by non-technical mitigation, such as land-use restrictions and preparedness activities in periods of increased jeopardy (e.g., evacuation).

In recent years, the method of risk management, originally derived from technical sciences, has become a common tool to deal with natural hazards in Alpine countries (e.g., KIENHOLZ, 1977; KIENHOLZ et al., 1991; HOLLENSTEIN, 1997; HEINIMANN, 1998; BORTER, 1999; FUCHS et al., 2001). Within the risk management framework (e.g., KIENHOLZ et al., 2004), risk is defined as a function of probability of occurrence of a natural process and the corresponding extent of damage (VARNES 1984), see Equation (1).

$$R_{i,j} = f(p_{Si}, A_{Oj}, v_{Oj,Si}, p_{Oj,Si}) \quad (1)$$

where $R_{i,j}$ risk, dependent on scenario i and object j
p_{Si} probability of scenario i
A_{Oj} value of object j
$v_{Oj,Si}$ vulnerability of object j, dependent on scenario i
$p_{Oj,Si}$ probability of exposure of object j to scenario i

The traditionally technical approach of risk assessment, resulting from the application of Equation (1), is subject to inherent uncertainties resulting from the fact that the natural system can only partly be described by stochastic or deterministic models. Those uncertainties have effects on the result of risk assessment, in particular regarding the extent of the area affected by the hazard process, and consequently on the predicted damage height. This paper provides an overview of such uncertainties with respect to snow avalanche risk based on case studies carried out in Davos, Switzerland (FUCHS et al., 2004). Snow avalanches have caused high damage in mountain areas within the last century (e.g., EDI, 1951; SLF, 2000; JÓHANNESSON and ARNALDS, 2001; JAMIESON and STETHEM, 2002; FUCHS and BRÜNDL, 2005), and had been subject to comprehensive research even earlier during the period of the penultimate turn of the century (e.g., COAZ, 1888; HEIM, 1885; PENCK, 1912).

2 Probability of occurrence of snow avalanches

Within the risk management procedure, reliable and precise modelling is a key tool considering the area potentially affected by avalanches. A variety of models have been derived to calculate snow avalanche motion and/or run-out distance in the past. Early attempts in physical modelling of avalanche phenomenon (PERLA et al., 1980; VOELLMY, 1955) based on "sliding block" descriptions had been further developed towards "continuum" models (e.g., BARTELT et al., 1999; NETTUNO, 1996) in recent years. Apart from such deterministic approaches for avalanche motion, empirical procedures for run-out calculation have been developed as well (LIED and BAKKEHØI, 1980; MCCLUNG and LIED, 1987; LIED et al., 1995). Although the use of empirical models is more immediate and involves a relatively

low degree of subjectivity in the choice of input parameters, the information they can provide is more limited than that obtained from dynamic approaches (BARBOLINI et al., 2002). With reference to avalanche risk assessment, empirical models can give no information concerning impact pressures and thus potential damage. Furthermore, the return period of an avalanche event is not considered because the models had been developed for one specific frequency class (typically "extreme" events). Conversely, dynamical models allow for a wide range of information on the avalanche event (velocity, impact pressure, shape of the deposit). Moreover, the deterministic nature of such an approach guarantees the reproduction of a specific avalanche event, once certain initial and boundary conditions and model parameters have been fixed (BARBOLINI et al., 2002). This opens the possibility of simulating events with different return periods, and therefore to deal with avalanche risk assessment, correlating the frequency of the avalanche with its potential degree of damage. However, the substantial degree of uncertainty in the definition of either initial conditions (release area and release depth) and model parameters (friction coefficients) represent one of the main weakness still connected with the use of dynamical models in practical applications. Thus, because land-use planning decisions rely on the calculated avalanche run-out distances, these modelling uncertainties could have large effects on the risk assessment procedure.

Within the present study, a case study related to the long-term development of risk has been carried out in Davos, Switzerland (FUCHS et al., 2005). Methodologically, the areas affected by avalanches were deduced using the incident cadastre of former events, the legally valid hazard maps, and the avalanche models AVAL1-D. AVAL-1D is a one-dimensional avalanche dynamics program that predicts run-out distances, flow velocities and impact pressure of both flowing and powder snow avalanches. Calibrated depth-average continuum models are used to track the motion of the avalanches from initiation to run-out. AVAL-1D consists of two computational modules for dense flow avalanches and powder snow avalanches. These modules solve the governing equations of mass, energy and momentum balance using a finite difference scheme (CHRISTEN et al., 2002). The dense flow simulation model employs a "Voellmy-fluid" flow law. This law assumes that the shear strains in the flow body are small and that the flow resistance, given by a dry-Coulomb type friction (μ) and a velocity squared friction (ξ), is concentrated at the base of the avalanche. The magnitude of these two friction parameters is based on extensive model calibration (BARTELT et al., 1999) as well as observed field events. The powder snow simulation follows Norem's description of powder flow avalanche formation and structure (NOREM, 1995). The model consists of a suspension layer and a saltation layer, mass and momentum exchange between those two layers being determined by particle settling, turbulent diffusion against the concentration gradient, and aerodynamic shear forces (CHRISTEN et al., 2002). The net erosion or deposition rate is a function of the kinetic energy of the impacting forces. More details about the model and its validation are described in ISSLER (1998) and FÖRSTER (2000).

During the sets of calculation, the run out zones of 30-year and 300-year avalanche scenarios were determined for the community of Davos. In doing so, the release conditions uncertainties resulting from the combination of input parameters were considered following a procedure outlined in BARBOLINI et al. (2002). Thus, based upon a 95 % confidence interval, the run out length of the 30-year events varied ± 20 m and the run out length of the

300-year events varied ± 30 m, which resulted in significant effects on the affected values at risk.

3 Values at risk

For those avalanche scenarios, the values at risk were obtained analysing the zoning plan with respect to location and perimeter of every building. Additional information, such as building type, year of construction and replacement value[2], as well as the number of residents was provided by the official authorities and the mandatory building insurer, and was joint using a GIS. The number of endangered tourists was derived using the number of beds within endangered hotels and guest houses and the respective degree of utilisation.

A general shift in damage potential resulted from the development of the study area from a traditionally agricultural society towards a tourism centre within the 20th century. This development could be evaluated since the year 1950, using decadal study periods, and provided a general idea about the development of assets in endangered areas. This approach mainly focused on the development of values in areas endangered by avalanches, such as the number and value of buildings, or the number of persons inhabiting those buildings.

A second development of damage potential, particularly focusing on mobile values and intangible assets, is based on a seasonal and diurnal assessment of variations in damage potential. This approach had also been applied related to the number of tourists staying temporally at a specific endangered location.

3.1 Long-term development of values at risk

Regarding the long-term development in numbers and values of endangered buildings, a significant increase could be proven for the period between 1950 and 2000 (FUCHS et al., 2004, 2005). The total number of buildings has almost tripled, from 161 in 1950 to 462 in 2000 (Fig. 1). This increase was due to the shift from 51 to 256 in the category of residential buildings, while in the other categories the number of buildings was approximately unchanging. A significant increase in number dated back in the 1960s and 1970s before the legally binding hazard map came into force. The total value of buildings increased by a factor of almost four. In 1950, the total sum of buildings was € 240 million and in 2000, the total sum was € 930 million. In 1950, the proportion of residential buildings was less than 15 %, compared to the total amount of endangered buildings. Until 2000, this ratio changed to almost 50 %. Regarding the category of hotels and guest houses as well as the

[2] Regarding the discussion of market values versus reconstruction costs, see FUCHS and MCALPIN (2005) and FUCHS et al. (2006a): The first choice for revealing the societal preferences toward buildings would be the market price. However, since it is the philosophy of mandatory building insurers like in Switzerland to underwrite the risk due to the replacement value to be able to compensate for an eventual total loss and to enable a replacement of the damaged building at any time, it does make sense to use the replacement value within this study, neglecting any risk-dependent change in the demand within the real estate market. Furthermore, this value serves as a basis for the expressed preferences of the societal accepted value of protection against natural hazards.

category of special risks, nearly no increase in value could be observed. However, those categories showed a higher average value per building than residential buildings. The number of endangered permanent residential population increased slightly. In 1950, a population of 1,098 persons was exposed to avalanche hazards, until 2000 this value increased to 1,137 persons. This is a relatively moderate increase of 3.6 %, compared to the increase in tangible assets. If the classification into different building functions is carried out, this increase turned out to be larger. In residential buildings, 673 persons were concerned in 1950 and 1,116 in 2000, which is an increase of two thirds.

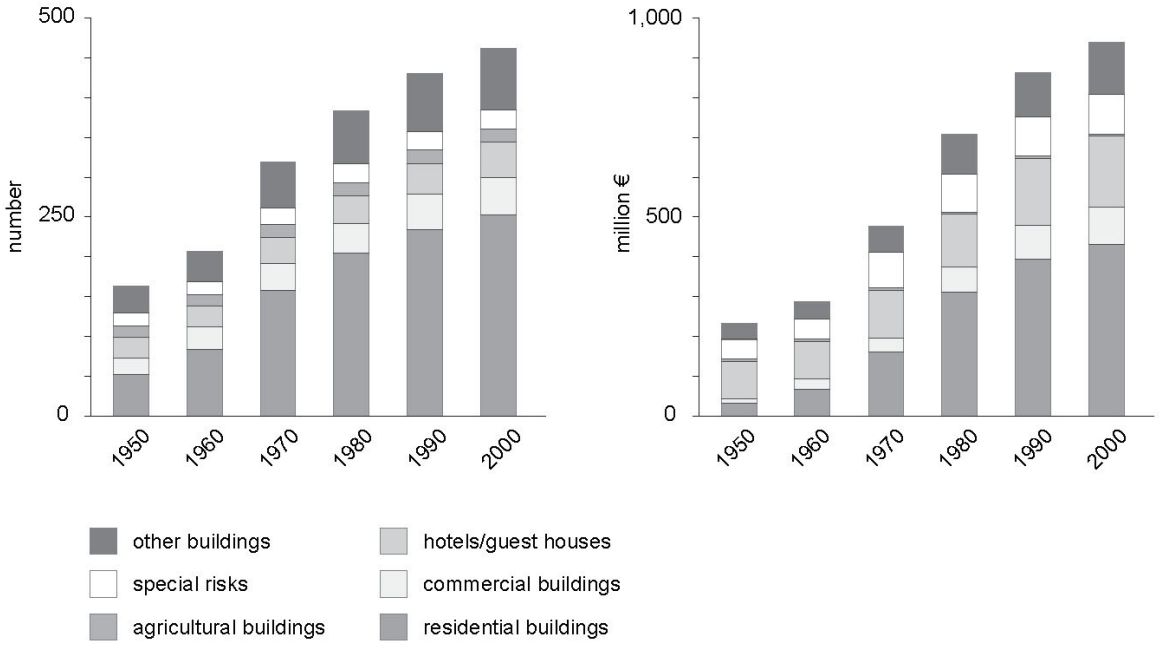

Fig. 1: Development of values at risk in Davos, Switzerland related to the respective avalanche-prone areas, subdivided in decades and building categories. In the left bar plot, information on the number of affected buildings is given, while on the right bar plot the respective reconstruction value is presented.

3.2 Short-term development of values at risk

Parallel to the long-term increases described in the previous section, remarkable short-term variations of persons at risk are detectable in mountain areas. Those variations could be determined on seasonal, weekly and hourly resolution, and are exemplarily presented using results from a case study carried out in Galtür, Austria (KEILER et al., 2005). This work complemented the studies in Davos with respect to rapid changes in avalanche risk, and had shown considerable similarities between mountain communities featuring different historical roots.

Between 1950 and 2000, the total number of endangered persons fluctuated by a factor of almost six, however, strong variations could be observed during the winter season as well as in daytime (Fig. 2). The seasonal fluctuation was characterised by a strongly increasing number of tourists at Christmas time and the Easter travel season. The end of the winter

season was highlighted by a sharp decrease in the number of persons to nearly the amount of the permanent population. Considering the diurnal fluctuation, the weekly structure could be easily followed. From the beginning of the winter season on, these patterns were overlapped by general movements of the tourists during daytime. The number of persons varied by a factor of 1.4 between minimum and maximum in the off-season, and by a factor of 3.4 in the period of the main season. These changes could occur extremely rapid within one or two hours.

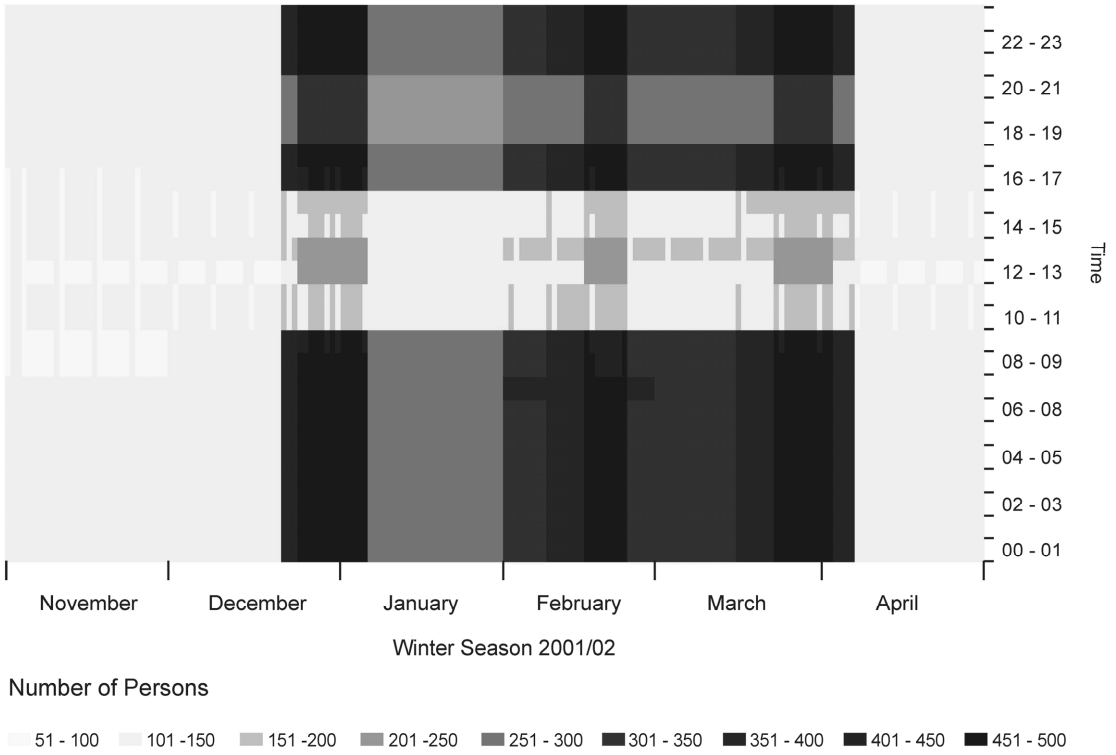

Fig. 2: Monthly, weekly, and diurnal fluctuations of the number of exposed persons in the study area of Galtür, Austria (KEILER et al., 2005, with permission).

3.3 Multi-temporal development of values at risk

As presented in the previous sections, the development of values at risk due to socioeconomic transformation in the European Alps varies remarkably on different temporal levels. Long-term changes and short-term fluctuations have to be considered when evaluating risk resulting from natural hazards.

Long-term changes in values at risk could be considered as basic disposition. To reduce the risk resulting from this basic disposition, permanent constructive mitigation measures could be constructed and land-use regulations implemented. As a consequence, the basic risk could be reduced due to a spatial reduction of the process area. As pointed out in (FUCHS et al., 2004) for the study area of Davos, the risk due to snow avalanches decreased fundamentally since the 1950s, even if the values at risk increased in the municipality. This development could be mainly attributed to the construction of permanent mitigation measures, and is strongly related to immobile values. Similar results were obtained for the study

area Galtür (KEILER et al., 2006). However, extraordinary losses could be estimated if rare events with severe effects occur, since the delimitation of the respective process areas is based on defined design events. This problem emerged during the avalanche winter 1999 in Switzerland (SLF, 2000) and Austria.

Short-term fluctuations in damage potential supplement this continuing development of damage potential within a specific range. Thus, they have to be considered as variable disposition. To mitigate those fluctuations, temporal measures could be applied, such as evacuations or temporary road closures.

Long-term as well as short-term variations in damage potential should be implemented into risk management approaches. In Fig. 3, the significance for a consideration of variable as well as basic damage potential is presented. As shown in example a) the event will not hit any values at risk, and thus, the level of risk reduction is sufficient. In example b), due to high amounts of variable values at risk, damage will occur. As a result, temporal mitigation strategies could reduce the variable damage potential until a critical level. In example c), basic and variable values at risk are affected by a process. Thus, temporal measures are no more sufficient enough for an effective risk reduction. These examples clearly indicate the strong need for an incorporation of dynamic assessments of damage potential in community risk management strategies.

Furthermore, since the socioeconomic development differs within Alpine regions, studies on the long-term behaviour of values at risk contribute to the ongoing discussion of passive and active developing regions and suburbanisation (FUCHS and BRÜNDL, 2005). However, if a potentially dangerous natural event will occur, it depends on the actual amount of values at risk (basic and variable disposition) within the process area whether or not damage will be triggered.

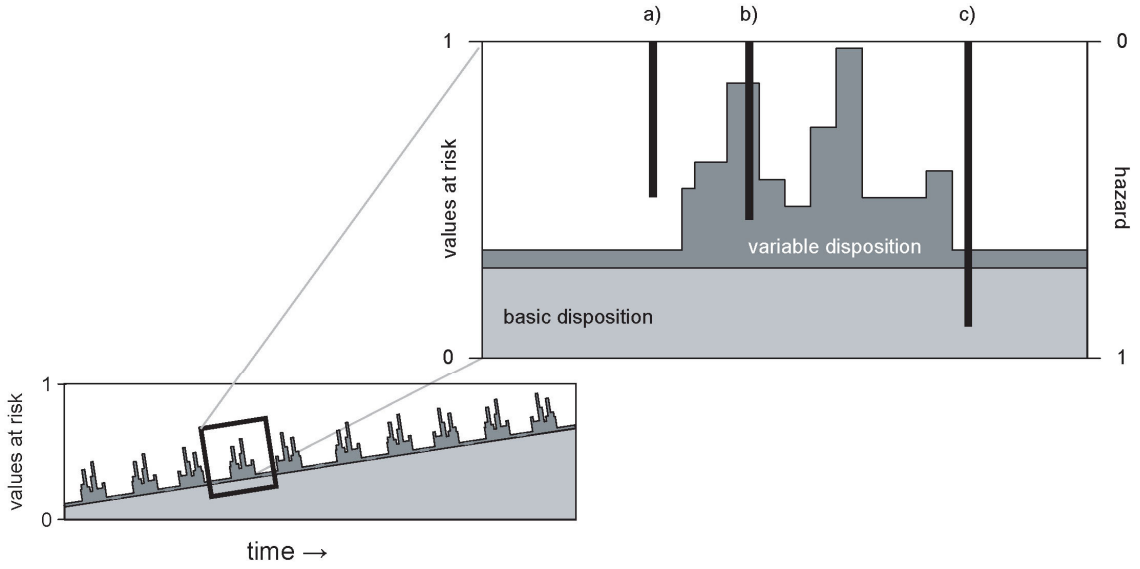

Fig. 3: Schematic description of the concept of basic (long-term) and variable (short-term) damage potential and the relation to triggering events.

4 Vulnerability

The term vulnerability is used in hazard and risk management in a large number of ways. Without controversy, vulnerability is related to the consequences of a natural hazard. Those consequences are generally measured in terms of damage or losses, either on a metric scale (e.g., as monetary unit), or on a non-numerical scale based on social values or perceptions and evaluations. This is not necessarily a matter of ambiguity or semantic drift, but disciplinary focus. Essentially, these different uses have invisible, implied adjectives preceding them, hence structural engineering vulnerability, lifeline infrastructural vulnerability, communications system vulnerability, macro-economic vulnerability, regional economic vulnerability, commercial vulnerability (including insurance exposure), and social vulnerability (WISNER et al., 2004). Consequently, two diverse perspectives on the concept of vulnerability exist; (1) the perspective from social science and (2) the perspective from natural science.

From social sciences' perspective, there are no unique definitions of vulnerability (CUTTER, 1996). Approaches not only differ between several degrees of voluntariness when dealing with natural hazards, but also consider individual as well as social influences, filtered by certain conditions that determine an individual's perception of risk. Depending on various guiding elements such as probability of occurrence, extent of damage, perception, uncertainty, ubiquity, persistence, reversibility, time delay, and mobilisation potential (GERMAN ADVISORY COUNCIL ON GLOBAL CHANGE, 1998), vulnerability is subject to considerable changes.

From a natural science perspective, vulnerability is usually considered as a function of a given intensity of a process, and is defined as the expected degree of loss for an element at risk as a consequence of a certain event (VARNES, 1984; FELL, 1994). The vulnerability value ranges generally between 0 (no damage) to 1 (complete destruction). Its assessment involves in many cases the evaluation of several different parameters and factors such as building materials and techniques, state of conservation, presence of protection structures, presence of warning systems and so on (FELL, 1994; FELL and HARTFORD, 1997). On the process side, parameters such as the process intensity have to be analysed, usually by mapping the geomorphologic disposition and previous events, and/or modelling (defined design) events. However, with respect to avalanches, it has recently been claimed that standardised approaches to evaluate the impacts to buildings are still missing (HOLLENSTEIN et al., 2002).

BARBOLINI et al. (2004) proposed an empirical vulnerability relation for alpine buildings based on the studies of JÓNASSON et al. (1999) and KEYLOCK and BARBOLINI (2001). Knowing the degree of damage and the deduced specific loss of the buildings, the vulnerability function was analysed for five impact pressure ranges (BARBOLINI et al., 2004). However, heterogeneous construction methods of buildings in alpine countries as well as socio-economic changes have not been sufficiently addressed in the study of BARBOLINI et al. (2004), an issue that is very important in the vulnerability analysis, particularly for a temporal approach of avalanche risk assessment.

To partially close this gap, KEILER et al. (2006) applied an empirical approach outlined in WILHELM (1997) to determine vulnerability functions for different construction types of buildings (building categories) related to avalanche pressure (Fig. 4). The susceptibility of loss to the building categories is partly based on the analyses of destroyed buildings during the avalanche winter 1954 in Vorarlberg, Austria, by VOELLMY (1955). WILHELM (1997), and accordingly BORTER (1999) differentiate between four vulnerability thresholds (see Fig. 4):

- The general damage level (p_u) corresponds to an avalanche pressure of 2–3 kPa and causes mentionable damage (estimated at 3 %), such as destroyed windows and doors.

- The specific damage level (p_{ui}) is the consequence of an avalanche impact pressure that inflicts damage on the building structure. Thus, each building category has a different specific damage level due to its different construction type.

- The destruction level (p_{oi}) describes the avalanche pressure that can produce maximum loss within each building category.

- The detach limit (p_{ai}) of each building category describes a damage threshold below the destruction level, but demolition and reconstruction of the buildings is necessary. Therefore, maximum loss is postulated for a degree of susceptibility to loss of 50 % and more because additional costs arise for the demolition and reconstruction that can add up to the maximum loss.

However, since the construction type of buildings has typically to be identified by field studies, this procedure is very time-consuming and thus costly. Furthermore, the effects of avalanches in the run-out area is not yet completely known[3], consequently, modelled impact pressures can only be a rough estimate of the real system behaviour. There were examples where an avalanche destroyed a building situated perpendicular to the avalanche axis (e.g., in the hamlet of Valzur, Paznaun, Austria, in February 1999), but there were cases where such a building was able to stop such an avalanche completely (e.g., in the village of Airolo, Ticino, Switzerland, February 1951). To conclude, the vulnerability component of risk analysis is still poorly specified, mainly due to a lack of intensive experimental or observational data.

[3] Future research concerning the behaviour of avalanches in the run-out areas is needed, in particular related to the structure of buildings. Buildings can have similar effects on avalanches as avalanche retarding mounds. Thus, due to a shift in the building pattern within the accumulation area, buildings oriented towards the valley bottom tend to result in smaller risk than buildings that are located closer towards the transit area. Independent from the related political implications and the associated impacts on land-use planning, further studies on this effect should be carried out due to the probable reduction of the run-out areas and, as a consequence, the resulting risk.

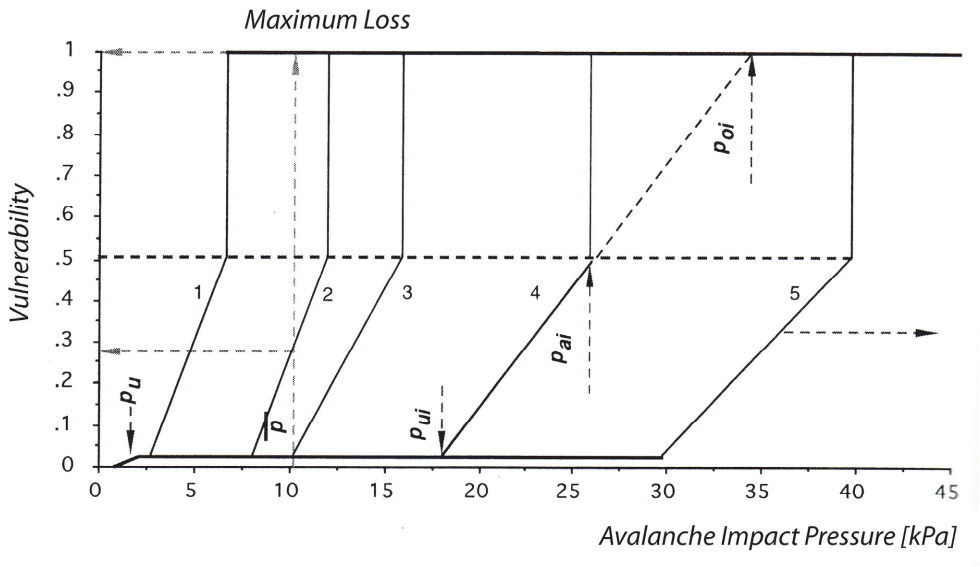

Fig. 4: Degree of possible loss as a function of avalanche impact pressure and vulnerability of buildings, the latter varies due to the material used for construction (building categories). Building categories: 1 = lightweight construction, 2 = mixed construction, 3 = massive construction, 4 = concrete (reinforced) construction, 5 = reinforced construction. Limiting values: p_u = damage level, p_{ui} = specific damage level, p_{ai} = detach limit, p_{oi} = destruction level, p = avalanche pressure [kPa] (modified according to WILHELM, 1997:72).

5 Discussion and Conclusions

Natural hazard risk management is subject to a range of uncertainties which have to be taken into account. Regarding the probability of occurrence p_{Si}, uncertainties resulting from avalanche modelling have to be considered. In addition to some basic limitations that occur when using models, the major uncertainties result from the use of the input parameters. As outlined in BARBOLINI et al. (2002), data related to the fracture depth and the potential extent of the release area is concerned, in addition to the length and angle of the accumulation area in consequence of topographic conditions. As a result, the range resulting from these uncertainties within the avalanche run-out areas was calculated regarding the variations outlined in section 2. This procedure caused a wide range of results which traced back to the high concentration of assets in the study area (see Fig. 5); and represented the typical problems when dealing with design events in the area of risk analyses resulting from alpine natural hazards.

In the year 1950, 83 buildings with a total replacement value of approximately € 107.6 million had been located inside the run-out areas affected by the 30-year avalanche scenarios. In the year 2000, 33 buildings with a replacement value of € 19.3 million were situated inside the areas affected by a 30-year avalanche, which is nearly 40 % in number and 18 % in value of the 1950s calculation. The endangered residential population amounted to 591 persons living in the areas of a 30-year avalanche run-out zone in 1950. In 2000, in consequence of the construction of permanent mitigation measures, 87 residents remained exposed, which is an 85 % reduction. However, the range of these results was considerable:

Inside the areas of a 30-year avalanche event, the number of buildings scattered almost 25 % in number and value for the scenario 1950 and 50 % for the scenario 2000. Concerning residential population, the values ranged from ± 20 % for the scenario 1950 to a remarkable factor of around 450 % for the scenario 2000. Compared to the results of the 300-year avalanche scenarios, those values were relatively small.

Even if the number of buildings affected by the 300-year scenarios has decreased from 161 to 125, the upper limit decreased only from 178 to 174. Thus it could be deduced that when interpreting the scenarios adversarial (accumulation length of the avalanche +30 m), no fundamental shift in the risk occurred in spite of the construction of mitigation measures. Concerning the values of endangered buildings it becomes apparent that the upper limit of the $scenario_{2000}$ (€ 162.2 million) is near to the lower limit of the $scenario_{1950}$ (€ 172.3 million), which is far below the development of the precise scenario. Using the results of the exact scenario, nearly a bisection of the endangered building values is detectable, from € 239.4 million to € 121.7 million. The average number of persons (residential population), which was 2.4 per dwelling, might be an upper limit in the category of vacation homes in the area under investigation. However, more exact data related to vacation homes are missing in the official statistics. Comparing $scenario_{1950}$ to $scenario_{2000}$, the number of endangered persons increased from 1,098 to 1,137 persons. Considering the minimum values (accumulation length of the 300-year scenario – 30 m), this value decreased from 832 to 636 persons. Considering the maximum values (accumulation length of the 300-year scenario + 30 m), nearly a doubling is detectable from 1,156 to 1,971 persons. Particularly in the category of endangered persons it becomes evident that the range of the scenarios is higher than the difference between the scenario under consideration of mitigation measures and the scenario without mitigation measures.

As shown in the previous section, short-term fluctuations in damage potential might lead to a temporal increase in risk, resulting from a modified recreational behaviour within the society. Until now, there is a particular lack in information related to short-term fluctuations of values at risk. In contrast to the immobile damage potential (buildings and infrastructure, etc.), persons and mobile values can either leave or be removed out of hazard-prone areas in case of dangerous situations. For developing efficient and effective evacuation and emergency plans, information on numbers of persons and mobile values as well as their location and movements in the area is needed. In consequence, permanent mitigation structures could be complemented by temporal measures to achieve an efficient and effective risk reduction.

If uncertainties in the vulnerability of objects would have been included within this study, the ranges would have been considerably higher. However, until now, there is no reliable methodology to account for such values within the risk management procedure. Thus, expressions regarding the range of uncertainty in natural hazard risk management will rather increase than decrease in the future. Possible improvements could be achieved applying the promising approach by GRÊT-REGAMEY and STRAUB[4], however, large uncertainties will

[4] GRÊT-REGAMEY and STRAUB, Integrating Bayesian networks into a GIS for avalanche risk assessment, this issue; and GRÊT-REGAMEY and STRAUB, Spatially explicit avalanche risk assessment linking Bayesian networks to a GIS, *Natural Hazards and Earth System Sciences*, forthcoming.

remain in a sustainable dealing with natural hazards in mountain areas. Until now, the spatial planning authorities need to have a precise boundary to draw the outline of endangered areas not or only to a certain extent appropriate for land development. Consequently, a dichotomy arises between the (scientifically) accurate and precise delimitation of areas endangered by natural hazards including confidence intervals, and the practical requirements emerging from the implementation of legal requirements (FUCHS et al., 2006b).

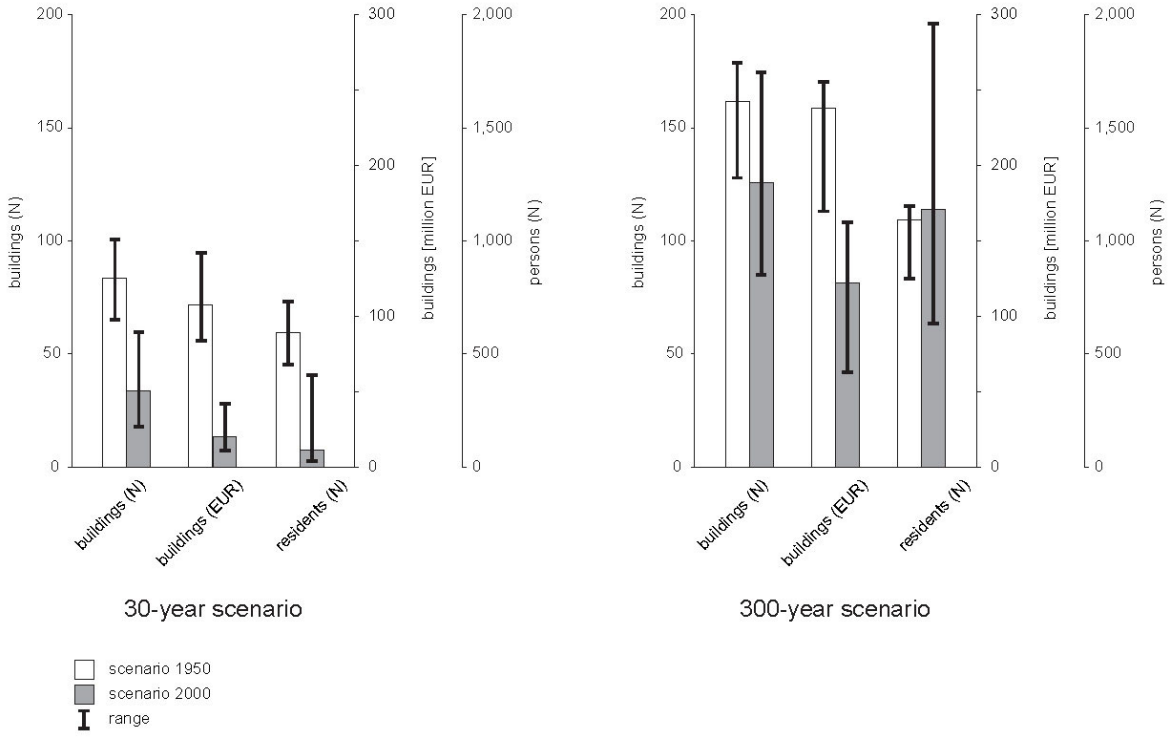

Fig. 5: Scenario$_{1950}$ and scenario$_{2000}$ related to a 30-year and a 300-year avalanche event and presentation of the associated uncertainties following the suggestions outlined in BARBOLINI et al. (2002). Modified from FUCHS et al. (2005, with permission).

Information on the temporal variability of values at risk both from a long-term as well as from a short-term point of view provide in combination with process knowledge provides the basis for dynamic risk visualisation. Such information may help to recognise high-risk situations more easily and enables a situation-oriented and risk-based decision-making (e.g., ZISCHG et al., 2004; SCHWAB et al., 2005; ZISCHG et al., 2005). Apart from the damage potential, risk analyses are based on the concept of recurrence intervals of hazard processes. If due to 'global change'-processes those defined design events have to be exceeded, the remarkable increase of values at risk would result in a significant shift in monetary losses (and presumably fatalities). First results on risk associated with torrent hazards suggest an increase in the probabilities of the design events in the Alpine region, however, these results still need some additional analyses to be verified, and are subject to ongoing research.

To conclude, risk analyses concerning natural hazards should be carried out with respect to a dynamic change of input parameters, particularly with respect to exposed values at risk. This is essential for efficient disaster risk reduction and contributes to the concept of resil-

ience as part of proactive adaptation. Regarding snow avalanches in the European Alps, the most important input parameter is the temporal variability of damage potential, since the natural avalanche activity did not vary substantially during the past decades (LATERNSER and SCHNEEBELI, 2002). Thus, future research is needed to quantify the impact of modifications in damage potential on (1) the result of risk analyses, (2) the assessment of risk in the cycle of integrated risk management, (3) the adjustment of coping strategies, and (4) the perception of risk by all parties involved, including policy makers.

The latter is the most crucial issue in Europe, since until now, dealing with natural hazards is based on mono-disciplinary approaches. In Austria, the forest law of 1975 restricts all hazards planning to forestry engineers (REPUBLIK ÖSTERREICH, 1976, 2004), in France, experts responsible for these issues are predominantly geologists (STÖTTER et al., 1999), while in Italy, the requirement for those specialists is a PhD in agriculture or a master's degree in forestry or geology (AUTONOME PROVINZ TRENTINO-SÜDTIROL, 1998). However, since risk resulting from natural hazards is a subject matter affecting life and economy within the whole society, multiple stakeholders' interests have to be considered when mitigation measures and coping strategies are developed and decisions are made. Thus, there is a particular need to involve (1) economists with respect to an efficient and effective use of public expenditures, (2) social scientists with respect to both, society's risk perception and an enhanced risk communication, (3) geographers and land-use planners as well as (4) all other disciplines representing any other party involved.

6 References

[1] Autonome Provinz Trentino-Südtirol, *Beiblatt Nummer 5 zum Amtsblatt der Autonomen Region Trentino-Südtirol vom 28. April 1998 18–I/II*, Trient, 1998.

[2] Barbolini, M., Natale, F., and Savi, L., Effects of release conditions uncertainty on avalanche hazard mapping, *Natural Hazards* 25, 2002, 225–244.

[3] Barbolini, M., Cappabianca, F., and Sailer, R., Empirical estimate of vulnerability relations for use in snow avalanche risk assessment, Brebbia, C. (ed.), *Risk Analysis IV*, Southampton, WIT, 2004, 533–542.

[4] Bartelt, P., Salm, B., and Gruber, U., Calculating dense-snow avalanche run-out using a Voellmy-fluid model with active/passive longitudinal straining, *Journal of Glaciology* 45, 1999, 242–254.

[5] BEV: *Regionalinformation der Grundstücksdatenbank des Bundesamtes für Eich- und Vermessungswesen*. 2004, www.bev.gv.at (access August 08, 2006).

[6] Borter, P., *Risikoanalyse bei gravitativen Naturgefahren*, Bern, Bundesamt für Umwelt, Wald und Landschaft, 1999.

[7] Christen, M., Bartelt, P., and Gruber, U., AVAL-1D: An avalanche dynamics program for the practice, Anonymous (ed.), *INTERPRAEVENT 2002 in the Pacific Rim*, October 14–18, 2002, Matsumoto, 2002, 715–725.

[8] Coaz, J., *Die Lauinen der Schweizeralpen*, Bern, Schmid, Franke & Co, 1888.

[9] Cutter, S., Vulnerability to environmental hazards, *Progress in Human Geography* 20, 1996, 529–539.

[10] EDI (ed.), Der Lawinenwinter 1950/51, *Veröffentlichungen über Verbauungen* 6, Bern, Eidgenössische Inspektion für Forstwesen, Jagd und Fischerei, 1951.

[11] Fell, R., Landslide risk assessment and acceptable risk, *Canadian Geotechnical Journal* 31, 1994, 261–272.

[12] Fell, R. and Hartford, D., Landslide Risk Management, Cruden, D. and Fell, R. (eds.), *Proceedings of the International Workshop on Landslide Risk Assessment* – Honolulu, Hawaii, USA, February 19–21, 1997, Rotterdam, Balkema, 1997, 51–109.

[13] Förster, M., *Ausführliche Dokumentation ausgewählter Staublawinenereignisse und Bestimmung ihrer Eingangsparameter für die Verifikation von Staublawinenmodellen*, Interner Bericht 730, SLF, Davos, 2000.

[14] Fuchs, S., Keiler, M., and Zischg, A., *Risikoanalyse Oberes Suldental (Vinschgau), Konzepte und Methoden für die Erstellung eines Gefahrenhinweis-Informationssystems*, Innsbrucker Geographische Studien 31, Innsbruck, Institut für Geographie, 2001.

[15] Fuchs, S., Bründl, M., and Stötter, J., Development of avalanche risk between 1950 and 2000 in the municipality of Davos, Switzerland, *Natural Hazards and Earth System Sciences* 4, 2004, 263–275.

[16] Fuchs, S. and Bründl, M., Damage potential and losses resulting from snow avalanches in settlements of the canton of Grisons, Switzerland, *Natural Hazards* 34, 2005, 53–69.

[17] Fuchs, S., Keiler, M., Zischg, A., and Bründl, M., The long-term development of avalanche risk in settlements considering the temporal variability of damage potential, *Natural Hazards and Earth System Sciences* 5, 2005, 893–901.

[18] Fuchs, S. and McAlpin, M.C., The net benefit of public expenditures on avalanche defence structures in the municipality of Davos, Switzerland, *Natural Hazards and Earth System Sciences* 5, 2005, 319–330.

[19] Fuchs, S., Thöni, M., McAlpin, M.C., Gruber, U., and Bründl, M., Avalanche hazard mitigation strategies assessed by cost effectiveness analyses and cost benefit analyses – evidence from Davos, Switzerland, *Natural Hazards*, 2006a, online first: http://dx.doi.org/10.1007/s11069-006-9031-z (access August 09, 2006).

[20] Fuchs, S., Khakzadeh, L., and Weber, K. (eds.), *Recht im Naturgefahrenmanagement*, Innsbruck, Studienverlag, 2006b.

[21] German Advisory Council on Global Change (ed.), *Strategies for managing global environmental risks*, Berlin, Springer, 1998.

[22] Heim, A., *Handbuch der Gletscherkunde*, Stuttgart, Engelhorn, 1885.

[23] Heinimann, H., Der Umgang mit Naturrisiken aus ingenieurwissenschaftlicher Sicht, *Schweizerische Zeitschrift für Forstwesen* 9, 1998, 691–705.

[24] Hollenstein, K., *Analyse, Bewertung und Management von Naturrisiken*, Zürich, vdf, 1997.

[25] Hollenstein, K., Bieri, O., and Stückelberger, J., *Modellierung der Vulnerability von Schadenobjekten gegenüber Naturgefahrenprozessen*, ETH Zürich, Forstliches Ingenieurwesen, 2002, http://e-collection.ethbib.ethz.ch/show?type=bericht&nr=173 (access August 09, 2006).

[26] Issler, D., Modelling of Snow Entrainment and Deposition in Powder-Snow Avalanches, *Annals of Glaciology* 26, 1998, 253–258.

[27] Jamieson, B. and Stethem, C., Snow Avalanche Hazards and Management in Canada: Challenges and Progress, *Natural Hazards* 26, 2002, 35–53.

[28] Jóhannesson, T. and Arnalds, Þ., Accidents and economic damage due to snow avalanches and landslides in Iceland, *Jökull* 50, 2001, 81–94.

[29] Jónasson, K., Sigurðsson, S., and Arnalds, Þ., *Estimation of avalanche risk*, Reykjavík, Rit Veðurstofu Íslands VÍ-R99001-ÚR01, 1999.

[30] Keiler, M., Zischg, A., Fuchs, S., Hama, A.M., and Stötter, J., Avalanche related damage potential – changes of persons and mobile values since the mid-twentieth century, case study Galtür, *Natural Hazards and Earth System Sciences* 5, 2005, 49–58.

[31] Keiler, M., Sailer, R., Jörg, P., Weber, C., Fuchs, S., Zischg, A., and Sauermoser, S., Avalanche risk assessment – a multi-temporal approach, results from Galtür, Austria, *Natural Hazards and Earth System Sciences* 6, 2006, 637–651.

[32] Keylock, C. and Barbolini, M., Snow avalanche impact pressure–vulnerability relations for use in risk assessment, *Canadian Geotechnical Journal* 38, 2001, 227–238.

[33] Kienholz, H., *Kombinierte geomorphologische Gefahrenkarte 1:10.000 von Grindelwald*, Geographica Bernensia G4, Bern, Geographisches Institut, 1977.

[34] Kienholz, H., Erismann, T., Fiebiger, G., and Mani, P., Naturgefahren: Prozesse, Kartographische Darstellung und Massnahmen, Barsch, D. and Karrasch, H. (eds.), *Kurzfassungen der Vorträge zum 48. Deutschen Geographentag*, Basel, Geographisches Institut, 1991, 293–312.

[35] Kienholz, H., Krummenacher, B., Kipfer, A., and Perret, S., Aspects of integral risk management in practice – considerations with respect to mountain hazards in Switzerland, *Österreichische Wasser- und Abfallwirtschaft* 56, 2004, 43–50.

[36] Laternser, M. and Schneebeli, M., Temporal trend and spatial distribution of avalanche activity during the last 50 years in Switzerland, *Natural Hazards* 27, 2002, 201–230.

[37] Lied, K. and Bakkehøi, S., Empirical calculations of snow avalanche run-out distance based on topographic parameters, *Journal of Glaciology* 26, 1980, 165–177.

[38] Lied, K., Weiler, C., Bakkehøi, S., and Hopf, J., Calculation methods for avalanche run-out distance for the Austrian Alps, Sivardière, F. (ed.), *The contribution of scientific research to safety with snow, ice and avalanche*, Grenoble, Association nationale pour l'étude de la neige et des avalanches, 1995, 63–68.

[39] McClung, D. and Lied, K., Statistical and geometrical definition of snow avalanche run-out, *Cold Regions Science and Technology* 13, 1987, 107–119.

[40] Nettuno, L., *La modellazione delle valanghe di neve densa: aspetti modellistici e sperimentali*, Dipartimento di Ingegneria Idraulica, University of Pavia, PhD thesis, 1996.

[41] Norem, H., *Shear stresses and boundary layers in snow avalanches*, Oslo, Norwegian Geotechnical Institute, Technical Report 581240-3, 1995.

[42] O'Keefe, P., Westgate, K., and Wisner, B., Taking the naturalness out of natural disasters, *Nature* 260, 1976, 566–567.

[43] Penck, W., *Naturgewalten im Hochgebirge*, Stuttgart, Strecker & Schröder, 1912.

[44] Perla, R., Cheng, T., and McClung, D., A two-parameter model of snow-avalanche motion, *Journal of Glaciology* 26, 1980, 197–207.

[45] Republik Österreich, *Forstgesetz 1975*, Bundesgesetzblatt Nr. 440/1975, in der Fassung BGBl. I Nr. 83/2004, http://recht.lebensministerium.at/file-manager/download/6119/, 2004 (access August 08, 2006), and additional executive order, *Verordnung über Gefahrenzonenpläne*, BGBl. Nr. 436/1976, http://recht.lebensministerium.at/filemanager/download/6128/, 1976 (access August 08, 2006).

[46] Schwab, J., Gori, P., and Jeer, S. (eds.), *Landslide hazards and planning*, Planning Advisory Service Report 533/534, Washington, American Planning Association, 2005.

[47] SLF (ed.), *Der Lawinenwinter 1999*, Davos, Eidgenössisches Institut für Schnee- und Lawinenforschung, 2000.

[48] Stötter, J., Belitz, K., Frisch, U., Geist, T., Maier, M., and Maukisch, M., *Konzeptvorschlag zum Umgang mit Naturgefahren in der Gefahrenzonenplanung*, Innsbrucker Geographische Gesellschaft (ed.), Jahresbericht 1997/98, Innsbruck, Institut für Geographie, 1999, 30–59.

[49] Varnes, D., *Landslide hazard zonation: A review of principles and practice*. Paris, UNESCO, 1984.

[50] Voellmy, A., Über die Zerstörungskraft von Lawinen, *Schweizerische Bauzeitung* 73, 1955, 159–165, 212–217, 246–249, 280–285.

[51] Wilhelm, C., *Wirtschaftlichkeit im Lawinenschutz*, Davos, Eidgenössisches Institut für Schnee- und Lawinenforschung, 1997.

[52] Wisner, B., Blaikie, P., Cannon, T., and Davis, I., *At risk*, London, Routledge, 2004.

[53] Zischg, A., Fuchs, S., and Stötter, J., Uncertainties and fuzziness in analysing risk related to natural hazards – a case study in the Ortles Alps, South Tyrol, Italy, Brebbia, C. (ed.), *Risk Analysis IV*, Southampton, WIT, 2004, 523–532

[54] Zischg, A., Fuchs, S., Keiler, M., and Stötter, J., Temporal variability of damage potential on roads as a conceptual contribution towards a short-term avalanche risk simulation, *Natural Hazards and Earth System Sciences* 5, 2005, 235–242.

Integrating Bayes'ian Networks into a GIS for avalanche risk assessment

Adrienne Grêt-Regamey [1, 2] , Daniel Straub [3]
[1] WSL Swiss Federal Institute for Snow and Avalanche Research,
Division Alpine Environment, Davos, Switzerland
[2] Eidgenössiche Technische Hochschule Zürich, ETH Hönggerberg, Zürich
[3] Department of Civil and Environmental Eng., University of California, Berkeley, USA

Abstract: Considering the significant monetary losses associated with avalanche disasters, it is crucial that decisions made in regard to hazard mitigation are based on a consistent assessment of the risks. This in turn necessitates a proper assessment of the uncertainties involved in the modeling of the avalanche frequencies and intensities, the possible avalanche extent, as well as the estimations of the damage potential. In this study, we link a BAYES'ian network to a Geographic Information System for avalanche risk assessment. We identify the major sources of uncertainty and show the potential of BAYES'ian inference techniques to improve the avalanche model using observed data. The probabilistic model, which consistently incorporates available information, can serve as a basis for spatial risk assessment. It is implemented here in a test area in the Swiss Alps.

1 Introduction

Economical damages from natural hazards are on the rise (MunicheRe, 2006). In mountainous areas such as the Swiss Alps, costs associated with damages due to snow avalanches and floods have grown exponentially in the last decade. In order to deal with these expenditures, decision makers are recognizing the need for a risk-based strategy, which explicitly addresses the involved uncertainties together with the consequences of such events (PLANAT, 2004). This type of strategy requires, on one hand, a probabilistic avalanche hazard model, which includes all available information on the physical processes and the observations of past events, on the other hand, a risk assessment procedure, which combines the available observational information and expert opinions.

Probabilistic approaches to avalanche hazard are not new (HARBITZ et al., 2001; BARBOLINI et al., 2002, 2003; ANCEY, 2004, 2005). These studies use observations to ei-

ther estimate release probability and/or the parameters of the dynamic avalanche models. ANCEY (2005) applies BAYES'ian inference, but only to investigate the dependency of the friction parameters in the dynamic avalanche model on the avalanche volume. To our knowledge, BAYES'ian inference has never been used to update both uncertainties in the release and the flow process based on avalanche observations.

In order to facilitate the explicit modeling of uncertainties in risk assessment procedures, several authors (e.g. FRIIS-HANSER, 2000; FABER et al., 2002) suggest the use of BAYES'ian Networks (BN). There are only few reported applications of BN in the field of natural hazards (e.g. AMENDOLA et al., 2000; ANTONUCCI et al., 2003; HINCKS et al., 2004; BAYRAKTARLI et al., 2005; STRAUB, 2005). All these studies, however, do not estimate risk in a spatially explicit manner, which is essential for land-use planning. Geographic Information Systems (GIS) have the capacity to incorporate the complexities of spatial dimension within such analyses. A large number of GIS applications for natural hazards have been developed (e.g., WADGE et al., 1993; CARRARA and GUZZETTI 1995, CHEN et al., 2003; BELL and GLADE, 2004). However, until now, in spite of the recognized uncertainties in spatial models and data, we are only aware of one previous attempt at considering the output of GIS in probabilistic terms (STASSOPOULOU et al.,1998).

It is thus the aim of this study to (1) develop a probabilistic avalanche hazard model (2) to integrate this probabilistic hazard model into a BN linked to a GIS (3) to show, how BAYES'ian inference modify the risk assessment results. We illustrate the approach by assessing the risk of avalanches in a run-out zone located in the municipality of Davos (Switzerland). This paper links the findings of two previous studies (STRAUB and GRÊT-REGAMEY, 2006; GRÊT-REGAMEY and STRAUB, 2006).

2 Method

2.1 BAYES'ian probabilistic avalanche hazard model

We apply a state-of-the-art two-dimensional dynamic simulation model, the AVAL-2D, used in Switzerland for avalanche prediction and hazard zoning (GRUBER, 1999; MAGGIONI and GRUBER, 2003). The avalanche process can be divided into the release process and the dynamic avalanche flow. Both parts are associated with uncertainties, which must explicitly be addressed.

In the AVAL-2D, the avalanche release process is represented by the annual maximum detached snow volume, described by the area A_r and the snow depth H of the detached snow mass. We focus on five release scenarios (r_{10}, r_{30}, r_{100}, and r_{300}) with different return periods (R); typical values of the return periods are 10 years, 30 years, 100 years, and 300 years. Representative values for the size of the release areas and the snow depths under these release scenarios are based on calibration of the model at different sites (U. GRUBER, pers. communication 11/2005, SLF). We introduce a sixth scenario, r_1, with an annual exceedance frequency equal to 1, which is assumed to correspond to no avalanche, as avalanches that occur every year will not lead to damages in the built environment. In order to

include both the uncertainty related to the type of release scenario and its probability of occurrence, we determine different alternative exceedance probability curves for each return period (Θ_R). The probability of r_1 is represented by a separate random variable Φ, as the probability of occurrence of the nil-scenario is dependent on the definition of a relevant avalanche. The annual probability of any release scenario r, conditional on φ and θ_R, is written as $p_{R|\theta_R,\varphi}(r)$ and following the total probability theorem, the unconditional annual probability is:

$$p_R(r) = \sum_{\Phi}\sum_{\Theta_R} p_{R|\theta_R,\varphi}(r)\, p_{\Theta_R,\Phi}(\theta_R,\varphi)$$

where $p_{\Theta_R,\Phi}(\theta_R,\varphi)$ is the joint probability of $\Theta_R = \theta_R$ and $\Phi = \varphi$.

The AVAL-2D calculates flow resistance at the base of the avalanche using two parameters: the dry-Coulomb type friction (μ) and a velocity squared friction (ξ). In this study, the parameter μ is modeled probabilistically, while the parameter ξ is modeled as a deterministic parameter, with different values for slope angles, topographical classifications, and surfaces. As the parameter μ depends on different topographical classifications, we identify nine different parameter scenarios for $\theta_{\mu 1 \ldots}$ $\theta_{\mu 9}$, corresponding to a set of values for μ.

In summary, the input parameters to the AVAL-2D are a set of four random variables $\boldsymbol{\Theta} = \{\Theta_R, \Phi, R, \Theta_\mu\}$. The dynamic avalanche model itself can be interpreted as a deterministic function f_{Aval}, which, for given values of $\boldsymbol{\Theta}$, gives the annual maximum pressure P for any spatial coordinate **u** on a 5m x 5m raster as:

$$P(\mathbf{u},\boldsymbol{\theta}) = f_{AVAL}(\mathbf{u},\boldsymbol{\theta}) + \varepsilon(\mathbf{u})$$

Because the model is only a simplified representation of reality and because some of the deterministic input parameters of the model are actually uncertain, we consider the additive error term ε in the formulation for *P*.

2.2 Spatially explicit risk assessment using BAYES'ian Networks

We organize the risk assessment procedure including the probabilistic avalanche model in the form of a BN as suggested by STRAUB (2005). BN are directed acyclic graph, where the nodes correspond to the random variables and the arcs represent the dependency structure of the problem, see PEARL (1988) and JENSEN (2001) for a comprehensive summary. Figure 1 shows the a-priori probabilistic avalanche risk assessment model represented by a BN. A detailed description of the data and sources of the variables used in the BN are provided in GRÊT-REGAMEY and STRAUB (2006).

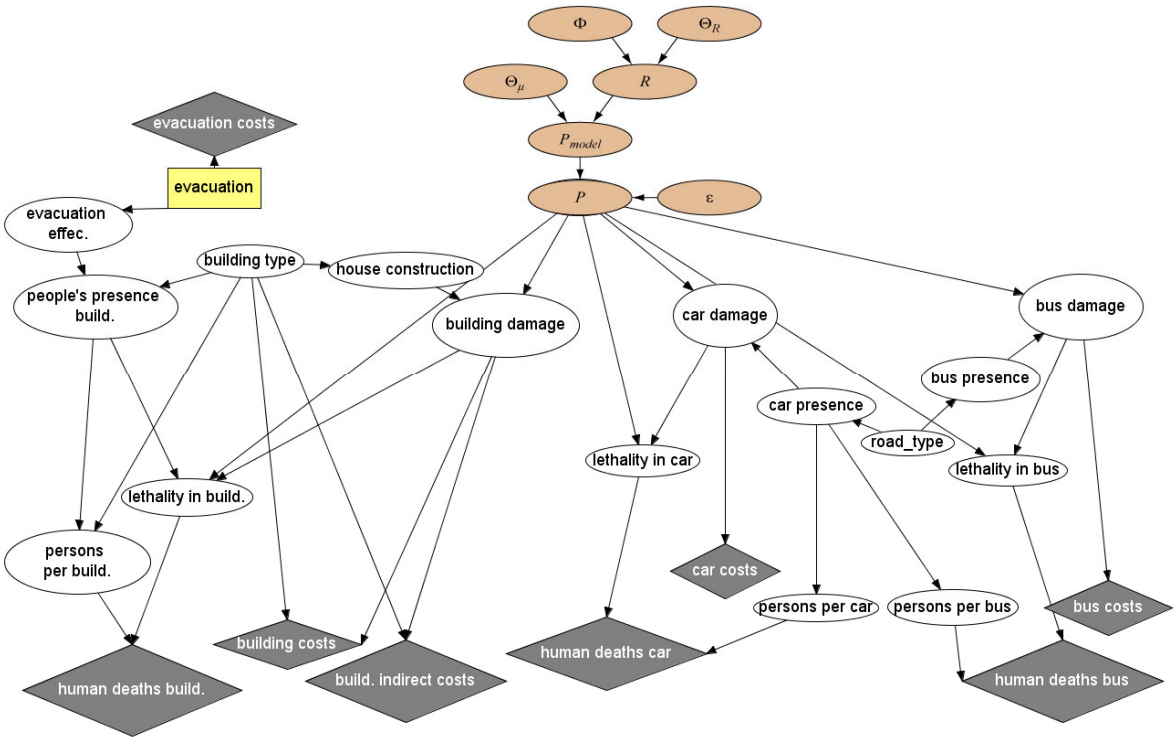

Fig. 1: BAYES'ian network of avalanche risk assessment with the a-priori probabilistic avalanche model.

In order to estimate the risk on a cell basis, we integrate the BN created in the Hugin environment into ArcGIS 9.3 (ESRI, 2000). The input nodes of the BN are initialized with values provided by spatially explicit datasets such as location and type of buildings. A digital elevation model provides information used in the AVAL-2D to calculate values used as evidence for the conditional probability tables of the "friction parameter" and the "pressure" nodes. The main output of the BN is thus the annual risk for each cell expressed in monetary terms, which includes not only costs of damaged building, but also costs associated with damaged contents, infrastructure, and societal losses.

2.3 Updating the avalanche model with BAYES'ian inference

BAYES' theorem allows for updating a prior probabilistic model with observations of the process under consideration. Finding the conditional distribution of a subset of the variables, conditional on know values for some other subset (the evidence) is the goal of inference. Here, we update the prior probabilistic model of the set of variables Θ, represented through the joint probability mass function of Θ, with observations related to the extent of past avalanches (**q**). The observations of avalanches are considered one-dimensionally along the avalanche path and were obtained from the winter reports 1950 to 2003 (unpublished data, SLF Davos, Switzerland). A threshold is introduced on the observations of the run-out distance. Observations, which are considered to correspond to a return period lower than 10 years are introduced in the analysis only through the information that the run-out distance was lower than the threshold. This threshold was chosen in the example as 1300m, which is lower than the lowest calculated run-out distance for the r_{10} scenario.

STRAUB and GRÊT-REGAMEY (2006) perform a sensitivity study to check the appropriateness of this choice.

The choice of the prior probability mass functions for the set of variables $\Theta_{\mu,}$ Θ_R, and Φ, and the impact of this choice on the updating procedure is discussed in details in STRAUB and GRÊT-REGAMEY (2006).

In the posterior model, the updated variables Θ_R, Φ and R may be collapsed into the single variable R. The posterior model is then fully described by the two parameters Θ_μ and R.As derived in details in STRAUB and GRÊT-REGAMEY (2006). The posterior joint probability mass function is calculated as

$$\mathrm{p}_{R,\Theta_\mu|\mathbf{q}}\left(r,\theta_\mu\right)=\sum_{\Theta_R}\sum_{\Phi}\mathrm{p}_{R|\theta_R,\varphi}\left(r\right)\mathrm{p}_{\Theta_\mu,\Theta_R,\Phi|\mathbf{q}}\left(\theta_\mu,\theta_R,\varphi\right)$$

When neglecting the error term (which is a reasonable assumption for engineering applications) and based on the posterior model of the parameters, we can apply the following BN in the risk assessment procedure, simplified to three nodes (Fig. 2). For more details on the probabilistic avalanche model, the reader is referred to STRAUB and GRÊT-REGAMEY (2006).

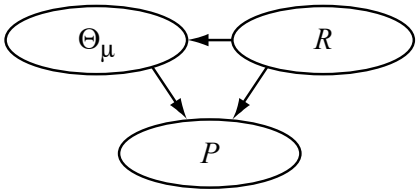

Fig. 2: BAYES'ian network representing the posterior avalanche model.

3 Results

The probabilistic risk assessment model is applied to a run-out zone, the "Frauentobel", located in the municipality of Davos, Switzerland.

In a first step, we update the prior probabilistic model of the set of variables Θ. Fig. 3 shows the posterior marginal probability mass function of the parameter scenario Θ_μ. To illustrate the fact that Θ_μ is dependent on the release scenario R, we also show the posterior probability mass function conditional on r_{10} and r_{100}. Higher values of the friction parameter are more likely for smaller release scenarios, respectively lower snow volumes, which is in accordance with general experience (ANCEY, 2005).

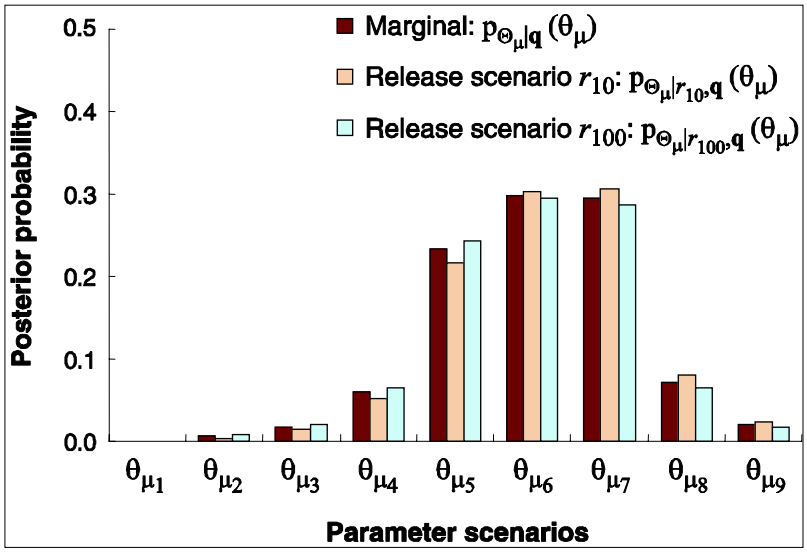

Fig. 3: Posterior probability mass function of Θ_μ .

In a second step, we introduce the new values for the friction parameters in the posterior avalanche model. Figure 4 shows the annual probability that an avalanche occurs, as evaluated with the prior model (a) and the posterior model (b). The updated model predicts a larger amount of shorter avalanches, whereas the presented probabilistic model predicts fewer but larger avalanche.

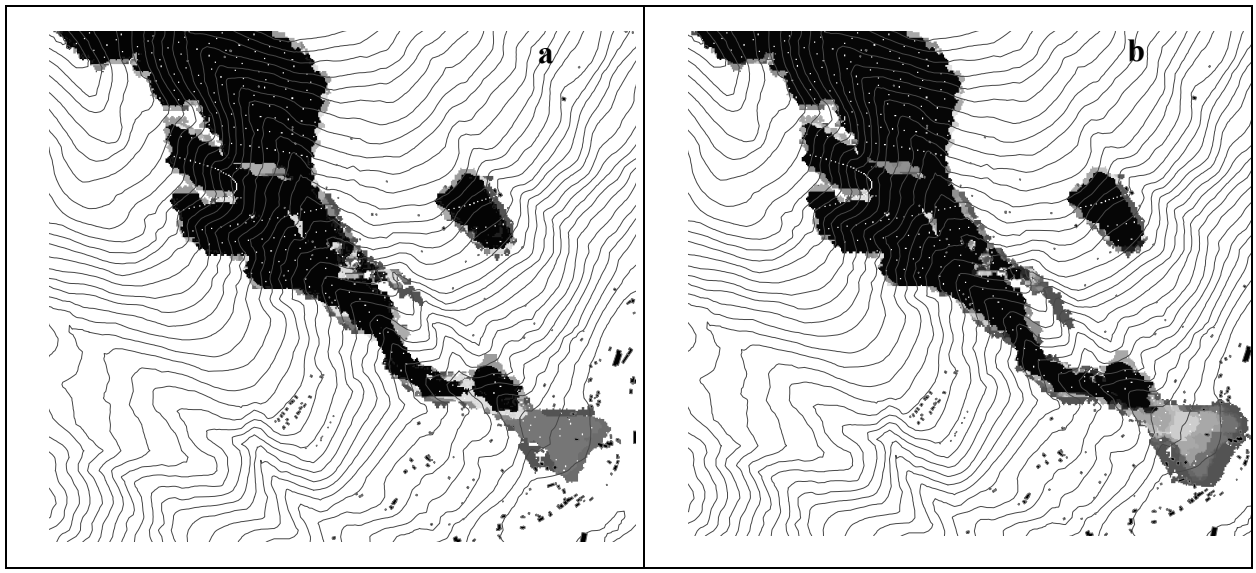

Fig. 4: Annual probability that an avalanche occurs, as evaluated with the prior model (a) and the posterior model (b) model. The annual probabilities range from 2.5*10-9 (brown) to 0.15 (blue).

In a third step, we calculate annual risks using the original avalanche model and the improved probabilistic model. Annual risks calculated using the updated avalanche model in the "Frauentobel" (4970 CHF/year) exceed the annual risk calculated using the original model (3850 CHF/year) by 22 % considering the five avalanche release scenarios. Total annual risks are lowest under a 30-year release scenario. This suggests that frequent but smaller avalanches do not reach highly populated areas.

Finally, we conduct a sensitivity analysis to identify the variables having the greatest influence on the risk. We use the SHANNON's mutual information indicator. Details about its calculation are provided in GRÊT-REGAMEY and STRAUB (2006). The variables "house construction", followed by "people's presence in buildings", and "pressure" are identified as having the largest impact on the uncertainty in the total risk. BAYES'ian credible intervals allow representing these uncertainties in a spatially explicit manner (Figure 5).

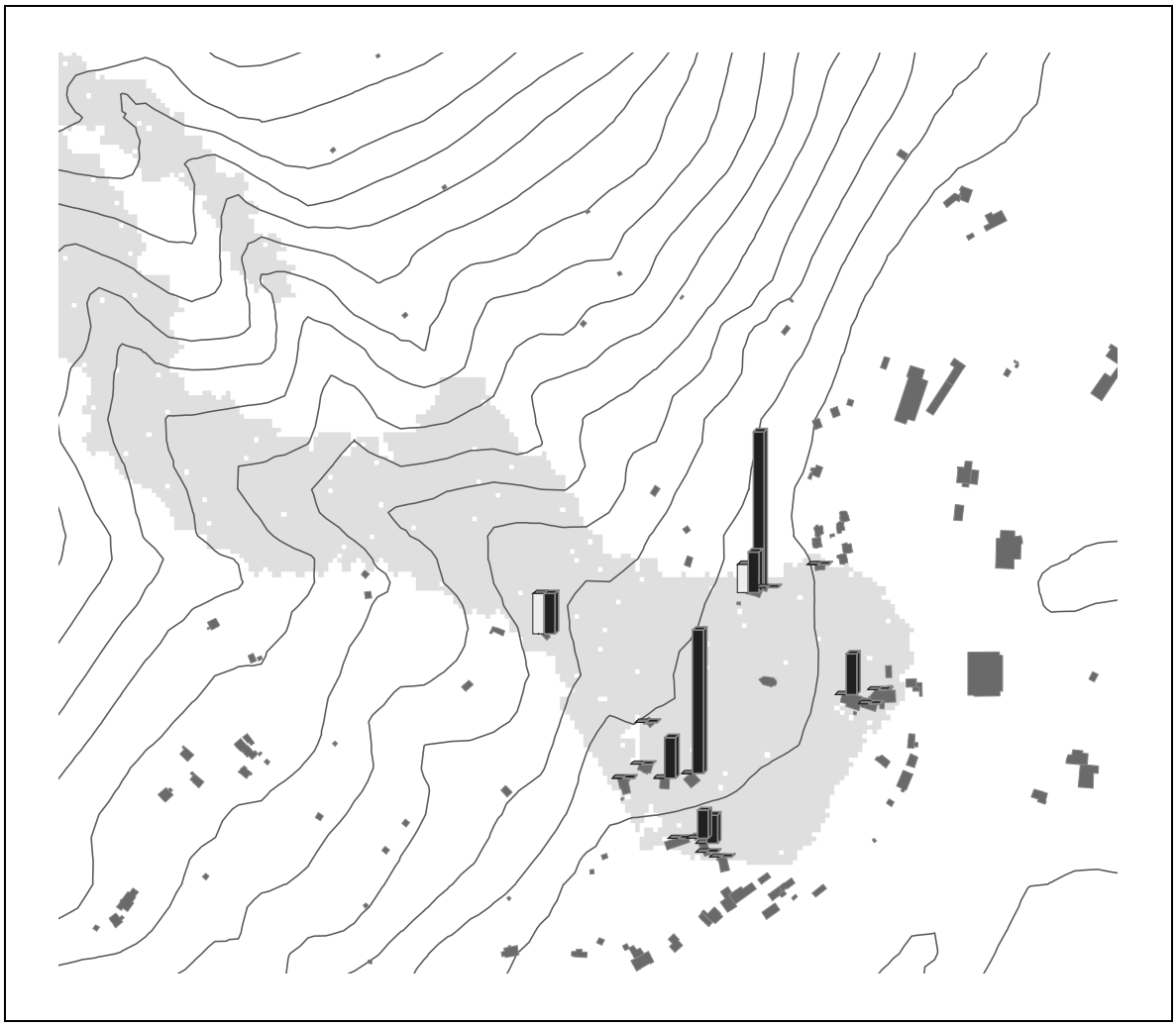

Fig. 5: BAYES'ian credible intervals map. The white bars represent the expected cost value at each location [log CHF]; the black bars are the upper bound values of the credible interval. The grey area represents the avalanche extent under a 300-year scenario.

The maximum credible interval calculated from the uncertainty distributions in the BN is large (2680 CHF/year) compared to the maximal expected annual cost of 800 CHF. Risk values located at the border of the avalanche run-out zones have large confidence intervals, pointing to the large uncertainties in the estimation of the risks at these locations, and showing that a more reliable calculation of the avalanche pressures are crucial for reducing the uncertainty in the risk assessment.

4 Discussion

In this study, we show the potential of embedding a BN into a GIS for natural hazard risk assessment. The approach unifies human expertise and quantitative knowledge in a coherent framework, which overcomes a major limitation of previous approaches. By updating the avalanche model with observations, we show that the risk estimates can increase by approximately 20% in the considered run-out zone. Furthermore, the integration of the probabilistic approach into a GIS allows quantifying and visualizing uncertainties in a spatially explicit manner, which is a basis to provide credible information to planners.

A distinct feature of the presented probabilistic avalanche model is that it allows calibrating the model parameters to observations, not deterministically as done in previous studies, but using BAYES'ian inference, which ensures the consistent use of all available information, and facilitates learning the processes in a regional context. In the future, for example, the approach could be used to investigate the dependency of the friction parameters on the snow release volume.

The proposed framework offers many other possibilities for further development. In its present version, the model is run for each cell individually, and thus the spatial and temporal dependency structure of the risk is not evaluated. These dependencies can be included in the framework by combining individual BN in the model into one single model. This will allow using the information obtained from similar sites for the determination of the prior probability distributions of the parameters, which can be of particular relevance at sites where little information on past events is available.

Furthermore, many important characteristics of an integral risk management strategy, as presented e.g. in FABER and STEWART (2003), are not covered in this paper. Such aspects include the identification of mitigation actions or the determination of risk acceptance criteria. Yet it is believed that the presented framework for risk assessment supports a structured approach to all tasks involved in the management of natural hazards, and could be extended to provide a tool for optimal risk-based decision making.

Acknowledgments

We would like to thank URS GRUBER from the SLF for providing the AVAL-2D with the data and continuous support, PETER BEBI from the SLF and MICHAEL FABER from ETH for their support in this study. This work was partly funded by the Marie Heim-Vögtlin Fellowship 3234-69265 of the Swiss National Science Foundation (SNF). The second author is supported by the SNF through grant PA002-111428.

5 References

[1] Amendola, A., Ermoliev, Y., Ermolieva, T., Gitits, V., Koff , G., Linnerooth-Bayer, J.: A systems approach to modeling catastrophic risk and insurability, Natural Hazards Journal, 21 (2000), pp. 381–393

[2] Ancey, C., Gervasoni, C., Meunier, M.: Computing extreme avalanches. *Cold Regions Science and Technology* 39 (2004), pp. 161-180

[3] Ancey, C.: Monte Carlo calibration of avalanches described as Coulomb fluid flows. *Philosophical Transactions of the Royal Society,* 363 (2005), pp. 1529-1550

[4] Antonucci, A., Salvetti, A., Zaffalon, M.: Hazard assessment of debris flows by credal net-works. *Technical report IDSIA-02-04*, IDSIA, Available online: www.idsia.ch/idsiareport/IDSIA-02-04.pdf, 2004.

[5] Barbolini, M., Cappabianca, F., Savi, F.: A new method for the estimation of avalanche distance exceeded probabilities. *Surveys in Geophysics* 24 (2003), pp. 587-601

[6] Barbolini, M., Natale, L., Savi, F.: Effects of release conditions uncertainty on avalanche hazard mapping. *Natural Hazards* 25 (2002), pp. 225-244

[7] Bayraktarli, Y.Y., Ulfkjaer, J., Yazgan, U., and Faber, M.H.: On the application of Bayesian probabilistic networks for earthquake risk management. Paper presented at the *9th International Conference on Structural Safety and Reliability (ICOSSAR 05)*, Rome, Italy, June 19 – 23, 2005.

[8] Bell, R., Glade, T.: Quantitative risk analysis for landslides – Examples from Bíldudalur, NW-Iceland, *Natural Hazards and Earth System Sciences* 4 (2004), pp. 117—131

[9] Carrara, A., Guzzetti, F. (eds.): Geographical information systems in assessing natural hazards. Kluwer Academic Publishers, Dordrecht, 1995

[10] Chen, K., Blong, R. Jacobson, C.: Towards an integrated approach to natural hazards risk assessment using GIS: With reference to bushfires, *Environmental Management* 31(2003), pp. 546–560

[11] ESRI (Environmental System Research Institute): ArcGIS 8.3. ESRI INC, Redlands, CA. http://www.esri.com, 2000

[12] Faber, M.H., Kroon, I.B., Kragh, E., Bayly, D., Decosemaeker, P.: Risk assessment of decommissioning options using Bayesian networks. *Journal of Offshore Mechanics and Arctic Engineering*, *Trans. ASME* 124 (2002), pp. 231-238

[13] Faber, M.H., Stewart, M.G.. Risk assessment for civil engineering facilities: critical overview and discussion. *Reliability Engineering and System Safety* 80 (2003), pp. 173-184

[14] Friis-Hansen, A.: *Bayesian networks as a decision support tool in marine applications*, Technical University of Denmark, 2000 - PhD thesis

[15] Grêt-Regamey, A., Straub D.: Accommodating uncertainties in avalanche risk assessment by linking Bayesian networks to a GIS. *Natural Hazards and Earth System Science,* 2006 (submitted)

[16] Harbitz, C., Harbitz, A., Nadim, F.: On probability analysis in snow avalanche hazard zoning. *Annals of Glaciology* 32 (2001), pp. 290-298

[17] Hincks, T., Aspinall A., and Woo, G.: An evidence science approach to volcano hazard forecasting. Paper presented at the *International Association of Volcanology and Chemistry of the Earths Interior (AVCEI)*, 2004.

[18] Jensen F.V.: *Bayesian networks and decision graphs*. Springer, New York, 2001

[19] Maggioni, M., Gruber, U.:. The influence of topographic parameters on avalanche release dimension and frequency. *Cold Regions Science and Technology*, 37 (2003), pp. 407-419.

[20] MunichRe: Topics Geo – Annual review: *Natural catastrophes 2005*. Order No. 302-04772. http://www.munichre.com. August 2006

[21] Pearl. J.: *Probabilistic reasoning in intelligent systems*. Morgan Kaufmann Publishers, San Mateo, California, 1988

[22] Planat: *Sicherheit vor Naturgefahren - Vision und Strategie*. Report 7/2004, National Platform for Natural Hazards (PLANAT), Switzerland. Available online: www.planat.ch, 2004

[23] Straub D.: Natural hazards risk assessment using Bayesian networks. Paper presented at the *9th International Conference on Structural Safety and Reliability (ICOSSAR 05)*, Rome, Italy, June 19 – 23, 2005.

[24] Straub, D., Grêt-Regamey, A.: A Bayesian probabilistic framework for avalanche modelling based on observations, in revision by *Cold Regions Science and Technology*, 2006

[25] Wadge, G., Wislocki, A., Pearson, E.J., Whittow, J.B.: Mapping natural hazards with spatial modelling systems. In Mather, P.M. (ed.): *Geographic information handling: research and applications*. John Wiley & Sons, Chichester, UK, 1993, 239–250

Utilisation of Probabilistic Investigations to Support Safety Assessment and Risk Management

Cornelia Spitzer
TÜV SÜD Energietechnik Baden-Württemberg, Mannheim

Abstract: Probabilistic Safety Assessments (PSAs) performed within the Periodic Safety Reviews are utilised thereafter in the regulatory procedures related to specific issues to be dealt with and to be decided upon as well as regular plant changes applied for by the utilities. In this paper the status of PSAs available, the objectives of performing additional probabilistic analyses as well as probabilistic investigations actually conducted in different cases of application are described. Significant results and insights obtained which are able to support the safety assessment and the decision making process in the regulatory procedures are addressed. Further, basic facts of a concept developed to perform an integrated safety assessment within the usual Regulatory Plant Change Procedure (RPCP) will be outlined.

1 Background

The licensing and supervision procedures referring to Nuclear Power Plants (NPPs) in Germany are essentially based on deterministic principles and criteria laid down in the corresponding regulatory framework. Probabilistic analyses and investigations have firstly been conducted in the context of the so-called Periodic Safety Reviews (PSR; lately, only called Safety Review (SR)) regularly to be carried out.

After the conclusion of the 1st round of the PSRs, Probabilistic Safety Assessments (PSAs) for all NPPs in Baden-Württemberg have been available which have also been reviewed. It was felt meaningful to utilise these PSAs afterwards also to assess specific issues to be dealt with in the usual regulatory procedures as well as to up-date and expand the existing PSAs with respect to recommendations given with the conclusion of the 1st PSR.

Thus, in various cases probabilistic investigations have been conducted in the past years in order to be able to address the safety relevance of issues to be decided upon.

Further, the utilities applied for regular plant changes by supplementing the usually requested deterministic reasoning with a probabilistic analysis, i. e. investigating the impact of the change to the safety level of the plant explicitly.

2 Status of PSAs available

The analysed plant reference states of the PSAs conducted in the framework of the 1st round of the PSRs range from 1994 to 1997, partly including plant modifications already planned at the time, but realised afterwards. The scope of a PSA in the framework of this 1st PSR corresponded to the GERMAN PSR GUIDELINE [1], i. e. a level 1 PSA without the analysis of low power and shutdown plant states (LPSS), Accident Management (AM) measures, internal fires or external events. Meanwhile, these topics have been addressed by the utility – also due to recommendations given by the reviewing body (TÜV) with the final statement of the 1st PSR – but not completely been reviewed.

It has to be stressed that the PSR GUIDELINE [1] has recently been considerably up-dated and supplemented [2]. Thereby, also other recommendations given by the reviewer with the objective of a continuation and up-dating of the existing PSAs will be tackled – like an extension of the existing Human Reliability Assessments (HRAs) and the additional probabilistic analysis of LPSS.

In the meantime, the 2nd round of the Safety Review (SR) has been started according to the fixed schedule since the amendment of the Atomic Law. Recently, we started with the reviewing process of the PSA of one of the NPPs concerned, which represents a considerable expansion regarding the scope in comparison to the PSAs submitted and finally reviewed during the 1st PSR.

That means, the eventually reviewed PSAs available up-to now for the NPPs do reflect a conservative result with respect to the quantification of the safety level (plant hazard states, because AM measures are not credited); on the other hand, the scope of the PSAs conducted is not comprehensive with respect to risk contributions. Moreover, the current plant states do no longer correspond to these existing reviewed PSAs, for not every plant changes realised after the performance of the PSAs are reflected in the plant modelling.

3 Objectives

Main objective of additional probabilistic analyses is to obtain different, safety relevant insights that can support the safety assessment and decision making process in the regulatory procedures. In particular, the regulatory body is interested in acquiring as much relevant insights as possible for the safety assessment to be conducted and the decisions to be taken. Moreover, it is possible to quantify safety benefits, to assess the balance of the

safety concept and to be able to concentrate on safety relevant issues, i. e. to prioritise actions to be taken. All in all, such an approach provides an additional instrument to support the necessary safety assessment and the decision making process for the regulatory body (UM) as well as for the utility.

The utilities have the same objective in performing additional probabilistic analyses, i. e. gathering as much safety relevant insights and results as possible. In addition, their goal can be related more to the concentration on really safety relevant issues, i. e. to prioritise their activities and efforts against the background of cost – benefit considerations.

However, the regulatory procedures are deterministic for the time being, and a structured and systematic implementation of supplementing probabilistic investigations – in particular concerning regular plant changes – is primarily voluntary, and thus subject to arguments and convincing.

Therefore, TÜV had already in the end of the 90th developed a concept, see SPITZER et al. [3], on how to conduct an integrated safety assessment by utilising PSAs with respect to regular plant changes to provide a discussion basis within the regulatory procedures and to develop a common understanding at the parties involved.

Some time later, TÜV developed an expanded concept, see SPITZER et al. [4], on request of UM related to the documentation to be provided by the utility in case of the performance of additional probabilistic analyses within the usual Regulatory Plant Change Procedure (RPCP) as well as the formal processing of a future supplemented probabilistic assessment, in particular addressing the issue of when such additional assessments should be performed.

Hereafter, recent activities being carried out are described in some detail, i. e. examples related to the present practice of supplementing probabilistic investigations to support safety assessment and risk management in the decision making processes will be given. Further, basic facts of the concept developed, i. e. the formal processing of a future supplemented probabilistic assessment within the usual RPCP and the topics in terms of content will be described to some extent, for details see SPITZER et al [4].

4 Probabilistic Investigations

The areas where supplementing probabilistic investigations outside the by now mandatory SR have in practice been conducted can roughly be identified firstly as principal issues the regulators wanted to be investigated in order to benefit from the different approach with respect to possibly different safety relevant insights for the NPPs under consideration.

Further, additional probabilistic analyses have been carried out regarding necessary assessments which had a very specific reason.

Last but not least, usual plant modifications resp. changes planned have been supplemented by the utilities with probabilistic analyses with the objective to investigate the impact of the modification to the safety level of the plant.

4.1 Principal Issues

Recommendations given with the conclusion of the 1st PSR e. g. referred to the probabilistic analysis of LPSS, internal fire events as well as AM measures.

These topics, that had not been subject of the investigations within the 1st PSR, were felt to be very important to assess the respective contributions to the plant risk, and to possibly identify safety relevant plant improvements and optimisations.

A major initiative in this context for example referred to the performance and subsequent review of probabilistic analyses for the LPSS for the NPPs in Baden-Württemberg. Main emphasis of the review work performance for these LPSS analyses referred to the

- documentation and plant reference state
- evaluation of the plant operating states (POS) according to the operational experience, outage scheduling, available system technique and containment state
- determination of potential initiating events to be considered and the identification of relevant events to be analysed explicitly
- evaluation of all parameters needed
- Human Reliability Assessments (HRA) and Human Factors (HF) analyses
- definition and categorisation of final states of event tree analyses.

For the performance of LPSS probabilistic analyses (by the way also for the analysis of AM measures), the HRA resp. the HF analysis can no longer be considered only to a limited extend, they have a major relevance, see SPITZER [5]. The reason for it is that in contrast to the Full Power Operating State (FPOS) the control of malfunctions has basically to be carried out manually. Besides, in most plants the operating procedures – event and symptom oriented as well as AM measures – have been developed, designed and implemented for the FPOS (including an extensive training), and therefore do not inevitably match with the requirements and demand of the LPSS; the latter also applies to the so far used HRA approach which had initially been developed for FPOS circumstances – evidently for historical reasons.

Another issue that requires much more attention in the LPSS refers to the analysis of the consequences of human erroneous behaviour related to pre-accident human actions which have to be addressed adequately for these LPSS probabilistic analyses, see SPITZER [5].

The most important HF relevant issues that have been identified during the review of the LPSS analyses and consequently need to be addressed refer to a larger scope for making a

decision, relatively large time windows, the communication between members of several teams in different places in the plant and knowledge based behaviour; further, there are higher demands for administrative and organisational coordination and communication, physical restrictions due to the environment (like radiation, high temperature, steam) as well as a potential for the so-called Errors of Commission (EoC).

The most important insights from the review of the LPSS probabilistic analyses subsequently concerned the necessity to

- ensure an available system technique in the different POS
- develop strategies for the control of incidents, malfunctions and accidents during the LPSS in corresponding operating procedures
- preferably utilise an advanced HRA resp. HF methodology, see SPITZER [5], instead of the mostly used conventional approach THERP [6].

Based on these results and insights, a comprehensive project has been initiated regarding the further development of operating procedures for the LPSS for all NPPs in Baden-Württemberg. Thus, consistent symptom oriented procedures related to LPSS have been developed and submitted for review. These procedures are based on action guiding schemes for all POS, including the adaptation of safety goals to follow-up and control under the circumstances of LPSS.

The regulatory body has been very satisfied about the identification of the safety relevant plant improvements and optimisations obtained related to the LPSS; this can also be stated for other principal issues being subject of probabilistic analyses and subsequent review, e. g. internal fire events and AM measures.

4.2 Assessments with Specific Reason

In case of some unexpected occurrences in the plant operation or requests resulting from certain technical constraints, probabilistic analyses and investigations had eventually to be performed in the regulatory procedures in order to be able to really assess the safety relevance of the issue to be decided upon.

Different cases of application have successfully been conducted in the regulatory procedures depending on the occurrences and on request; in this paper, selected representative case studies will be outlined – also with respect to plant modifications planned and addressed in the next chapter.

A corresponding example referred to the realisation of a certain plant change, namely the reconstruction of two redundant electrical trains planned and scheduled for two consecutive outages of the corresponding NPP.

The reconstruction work in one of the electrical trains has been carried out in the first outage after the approval of the regulatory body. The implementation of the changes in the second electrical train has been scheduled for the subsequent outage.

Thereafter, the following circumstances turned out: due to the limited space in the affected electronic equipment rooms, the usual inspections and maintenance tasks would have to be carried out temporally after the implementation of the plant changes related to the electrical train affected, i. e. the reconstruction work. This consecutive work performance would have resulted in a significantly longer outage period.

The utility therefore requested to disconnect the affected electrical train two months before the 2nd outage to carry out the reconstruction work. They substantiated this request by probabilistic investigations and corresponding assessments.

TÜV then conducted quite expanded analyses in order to assess the safety relevance of this request. In the course of this, the time dependent unavailability related to system functions, event sequences and initiating events has been analysed with regard to the impact of disconnecting the affected electrical train during the FPOS two months before the scheduled outage.

Thereby, the evidence could be demonstrated that the reconstruction already carried out during the precedent outage resulted in such a safety relevant improvement, that the disconnecting of the other electrical train two months before the subsequent outage implied only a very minor relative risk increase in comparison to not disconnecting.

On basis of the integral view provided by the probabilistic investigations and assessments taking into account the risk development in the course of time, the utilities´ request could be supported and approved by the regulatory body.

In another case, during the periodic testing a slightly increased leakage had been identified at the mechanical shaft seal of a component cooling pump which is part of safety system of the respective NPP.

The utility requested to replace the component cooling pump instantaneously during FPOS by disconnecting the corresponding train – though the reliable operation on demand of the component cooling pump was still assumed, also in consideration of the finding during the test procedure. The reviewer affirmed the functional capability of the component cooling pump given the very minor leakage identified during the testing. Nevertheless, it could not be excluded that the deterioration mechanism at the mechanical shaft seal would progress. This would then result in an increased failure probability of the component cooling pump up to the total loss on demand.

In order to support the decision to be taken by the regulatory body, the following two strategies related to the time period up to the next periodic testing have probabilistically been investigated and assessed:

- instantaneous replacement of the component cooling pump with a defined disconnecting of the corresponding train
- no replacement of the component cooling pump resulting in a likely increase of the failure rates up to the total loss on request.

TÜV performed detailed sensitivity and uncertainty analyses for the two strategies to be decided upon by also considering possible variations in the disconnecting time period and the potential increase in the failure probability of the component cooling pump.

As result of the probabilistic analyses, the two strategies showed practically no difference with respect to the impact on the safety level of the plant - assuming a limited disconnecting time period which could be expected and a certain increase in the failure rates which has been estimated.

The utilities´ request to replace the component cooling pump instantaneously during FPOS could be approved by the regulatory body – but on basis of substantial results and safety relevant insights provided.

4.3 Plant Modifications Planned

For the regular plant modifications planned and applied for by the utilities within the RPCP, the a. m. expanded concept of an integrated safety assessment has been developed. This concept aims at a systematic and structured procedure on when and how such plant modifications should be supplemented by probabilistic analyses.

As this concept is not yet formally implemented in the RPCP, plant modifications have been applied for in a case-by-case approach. Due to the lack of binding guidelines agreed up-to-now in Baden-Württemberg for the performance of supplemented probabilistic assessments within the RPCP, in most cases TÜV had to conduct a quite expanded analysis on the basis of the reviewers´ PSA in order to assess the impact of the change on the safety level of the plant thus being able to assess the safety relevance of the modification. The review and subsequent assessment essentially followed the concept developed and explained in this paper afterwards on how to conduct such an integrated safety assessment.

In quite a number of cases replacements and/or changes in the maintenance respectively surveillance test intervals in various electrical systems have been applied for and supplemented by the utilities with probabilistic assessments with the objective to investigate the impact of the modification to the safety level of the plant. A representative example will be outlined hereafter.

One of the applied plant changes in the framework of the RPCP referred to the prolongation of the surveillance test interval (doubling) of digital protective relay. The impact of this plant change has been assessed by the utility in a quite global manner therefore TÜV had to conduct more detailed probabilistic investigations.

First of all, the possible impact of the proposed change, i. e. the prolongation of the surveillance test interval of the digital protective relay concerned had to be evaluated. The potential impact could only be assed indirectly with respect to the respective assigned technical component to be protected by the protective relay. One of the consequences evaluated in case of a possible degradation in the function of the digital protective relay could for example result in an erroneous turning-off of the assigned technical component.

After the identification of all assigned technical components affected by the prolongation of the surveillance test interval of the digital protective relay concerned, sensitivity analyses have been performed addressing the potential indirect impact on the technical components´ failure behaviour. The probabilistic analyses have been carried out successively for the initiating events, event sequences as well as system functions affected.

The probabilistic analyses related to the potential erroneous turning-off of the assigned technical components revealed a non-negligible safety relevance of the modification for a certain system function. This system function however has been dominated by the operational failure behaviour of a pump basically resulting from a rather short observation period. Consequently, the potential indirect impact of the prolongation of the surveillance test interval of the digital protective relay modelled in this case represented a gross overestimation.

Nevertheless, it has been recommended to follow-up and to evaluate the failure modes of the technical components affected in particular with respect to possible contributions of the digital protective relay in order to address this insight obtained.

On basis of the overall probabilistic investigations and assessments, the applied prolongation of the surveillance test interval of digital protective relay could be approved, but the a. m. recommendations as well as some further aspects addressed by the reviewer have to be observed.

Though the approach for these case by case reviews and integrated safety assessments has not fully been satisfying (the plant reference state has not been up-dated in the framework of the RPCP), additional insights could always be achieved – in contrast to a purely deterministic approach – in order to support the necessary decision making process.

5 Integrated Safety Assessment

In order to perform an integrated safety assessment – that means the performance of deterministic and supplemented probabilistic assessments within the usual RPCP – in a more structured way, a consistent concept has been proposed addressing the prerequisites, the formal processing, the documentation to be provided and the topics in terms of content. Hereafter, basic facts of this concept developed will be outlined, for details see SPITZER et al [4].

5.1 Prerequisites

Prerequisite for the performance of an integrated safety assessment including additional probabilistic analyses is a plant specific PSA which has been reviewed in detail.

Further, the existing PSAs should be up-dated and reviewed referring to the plant reference state, including the realisations of the recommendations given with the final statement in the previous PSR.

Moreover, very detailed and specified procedures should be agreed on in order to carry out this up-dating consistently and efficiently. Besides, changes reflected in the PSA model should remain there, also in such cases which initially have no risk impact.

5.2 Formal Processing

The formal processing of a future supplemented probabilistic assessment within the RPCP has been proposed as a step by step procedure: only plant changes applied for, where a risk impact is generally expected and consequences on the existing PSAs are identified, should be subject of an immediate supplemented probabilistic assessment; the remaining plant changes are probabilistically assessed later in a summarised form (see figure 1).

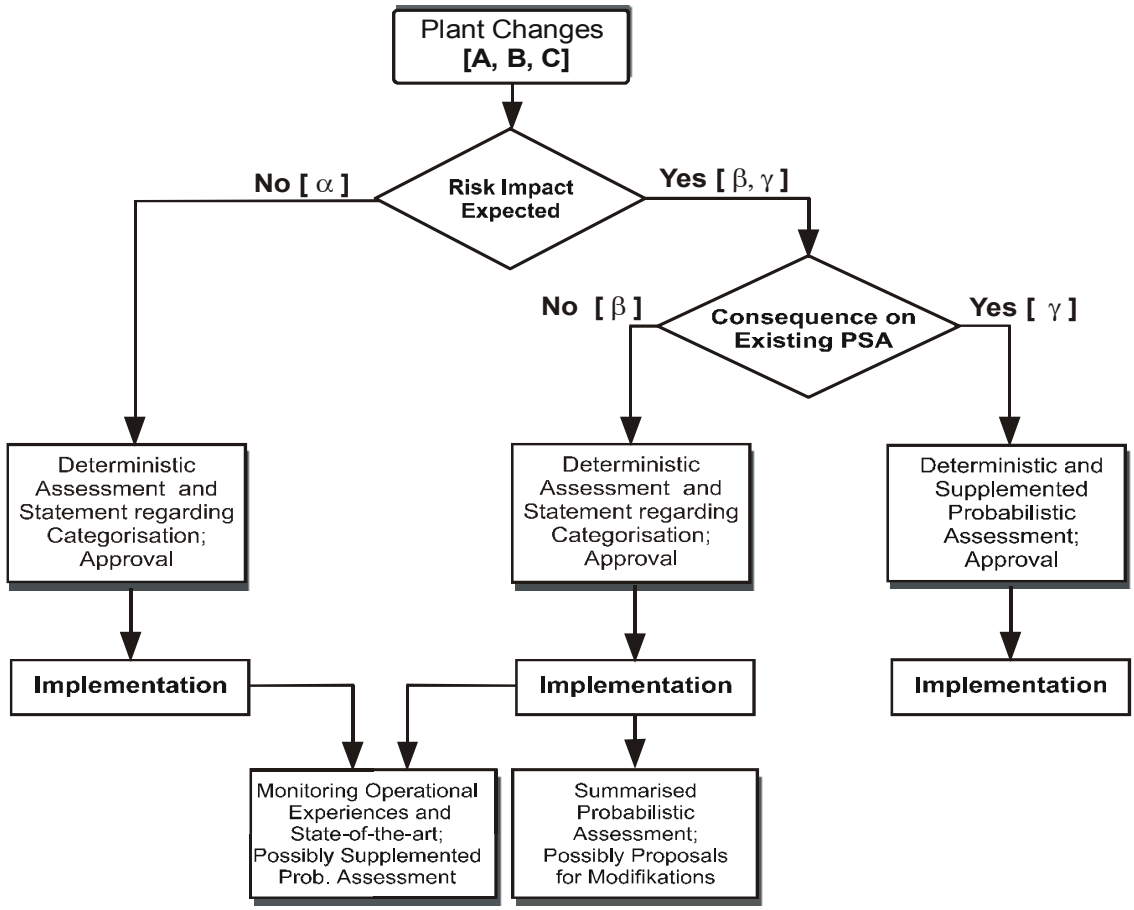

Fig. 1: Formal processing of a supplemented probabilistic assessment within the Regulatory Plant Change Procedure (RPCP)

5.3 Documentation

The documentation to be provided and submitted for γ plant changes, i. e. in case of the performance of additional probabilistic analyses, should be comprised of the following parts:

A definition of the plant change with a detailed description of the current and planned status including the prevailing impacts

B performance of deterministic evaluations as well as probabilistic assessments

C development of monitoring strategies for the plant change

D application of the plant change according to the formal RPCP.

The utilities´ documentation should aim at the evidence that the following principles are met:

I The proposed plant change is consistent with the current regulations and safety concept (defence-in-depth philosophy).

II Including the plant change, there are still sufficient safety margins.

III Including the plant change, the safety level of the plant is maintained.

IV The impact of the plant change is monitored by corresponding strategies.

The submittal of such a γ plant change applied for would then be subject of a concrete review in the framework of the formal RPCP with the objective of an integrated safety assessment before the regulators´ approval and the utilities´ implementation.

5.4 Assessment in Terms of Content

For the demonstration of the adherence of a proposed plant change to the principles listed above, the following issues should be addressed in the submittal and have to be reviewed specifically:

All safety impacts of a proposed plant change are evaluated and assessed in an integrated manner. An e. g. minor risk increase due to a slight increase in some evaluated frequencies of plant hazard states can be compensated by the qualitative description of the safety relevant benefit of the change.

The scope and quality of the evaluations and analyses conducted are suitable to justify the plant change and to support a risk-informed assessment and decision making; they are based on the current plant state and reflect the existing operating experience.

Appropriate consideration is given to the associated uncertainties in the analyses and the interpretation of the insights obtained. Significant uncertainties should be monitored and a feedback as well as possibly needed corrective actions should be anticipated.

Basis of the probabilistic assessment are the currently available and reviewed frequencies of plant hazard states; thereby, a categorisation of the hazard states should be carried out, particularly with respect to the potential of a large early release.

A proposed plant change has eventually to be analysed and assessed in accordance with the usual deterministic principles and criteria; additionally, probabilistic analyses and assessments have to be performed.

The probabilistic assessment is carried out on basis of the analyses performed and the robustness of the insights and results obtained, particularly considering the uncertainties in data, models and assumptions. In this context, a possible further impact of the plant change on not explicitly reflected subject areas has to be addressed and assessed appropriately.

The deterministic evaluations and probabilistic assessments have to be brought together aiming at demonstrating the evidence that the plant change is consistent with the current regulations and safety concept, that there are still sufficient safety margins and the safety level of the plant is maintained, and that the impact of the plant change is monitored by corresponding strategies.

6 Conclusions

After the conclusion of the 1st PSR, PSAs for all NPPs in Baden-Württemberg have been available which have also been reviewed. It was felt meaningful to utilise these PSAs afterwards also to assess specific issues to be dealt with in the usual regulatory procedures as well as to up-date and expand the existing PSAs with respect to recommendations given.

Thus, in various cases probabilistic investigations have been conducted in the past years in order to be able to address the safety relevance of issues. Further, the utilities applied for regular plant changes by supplementing the usually requested deterministic reasoning with a probabilistic analysis, i. e. investigating the impact of the change on the safety level of the plant explicitly.

Additional probabilistic investigations are performed in order to support decisions to be taken in the regulatory procedures. As the legal basis is still mainly deterministic, such a performance – in particular concerning regular plant changes – is voluntary.

Nevertheless, regulators, utilities and reviewers appreciate the explicit usefulness and benefit, i.e. the safety relevant insights exceeding a purely deterministic consideration.

The areas where supplementing probabilistic investigations have been conducted refer to principal issues the regulators wanted to be investigated, issues regarding necessary assessments which had a specific reason as well as plant changes planned within the RPCP aiming at an integrated safety assessment.

A major initiative in this context for example referred to the performance and review of probabilistic analyses for the LPSS for the NPPs in Baden-Württemberg resulting in significant results and insights consequently leading to major safety relevant plant improvements and optimisations.

Further cases of application – also related to assessments which had a specific reason as well as regular plant changes – always resulted in supplementing significant results and insights being able to support the necessary safety assessment and the decision making process in the regulatory procedures. In order to perform an integrated safety assessment within the usual RPCP in a less case-by-case approach, i. e. in a more structured way, a consistent concept has been proposed addressing the prerequisites, the formal processing, the documentation to be provided and the topics in terms of content.

The performance of additional probabilistic analyses in regulatory procedures related to specific issues to be dealt with and to be decided upon as well as regular plant changes in a step by step way of proceeding within the RPCP is regarded to be feasible, appropriate and beneficial for all parties involved.

7 References

[1] *Bundesanzeiger*. Public Announcement of the Guidelines for the Performance of Periodic Safety Reviews (PSRs) for Nuclear Power Plants in the Federal Republic of Germany. Number 232 a, 18.08.1997

[2] *Bundesanzeiger*. Public Announcement of the Guideline for the Performance of the Safety Review (SR) according to §19a of the Atomic Law – Guideline Probabilistic Safety Assessment – for Nuclear Power Plants in the Federal Republic of Germany (30.08.2005). Number 207a, 03.11.2005

[3] Spitzer C., Heermann M. (1998). Concept of an Extended Application of PSAs in Regulatory Procedures. *Proceedings of the 4th International Conference on Probabilistic Safety Assessment and Management* (PSAM 4). A. Mosleh, R. A. Bari (Eds.), New York City, USA, 13-18 September 1998, pp 307-312. Springer-Verlag, London, UK

[4] Spitzer C., Wildermann T. (2004). Extended Application of PSAs in Regulatory Procedures: Practice and Concept of an Integrated Safety Assessment. *Proceedings of the International Conference on Probabilistic Safety Assessment and Management*: PSAM 7 – ESREL ´04. C. Spitzer, U. Schmocker, V.N. Dang (Eds.), June 14-18, 2004, Berlin, Germany, pp 1401- 1407. Springer-Verlag, London (UK)

[5] Spitzer C., (2004). Human Factors Analysis: Central Needs for Practical Applications. *Proceedings of the International Conference on Probabilistic Safety Assessment and Management*: PSAM 7 – ESREL ´04. C. Spitzer, U. Schmocker, V.N. Dang (Eds.), June 14-18, 2004, Berlin, Germany, pp 1727-1733. Springer-Verlag London (UK).

[6] Swain A. D., Guttmann H. E. (1983). Handbook of Human Reliability Analysis with Emphasis on Nuclear Power Plant Applications. *NUREG/CR-1278*, Sand 80-0200 RX, AN. Final Report, 1983

Probability-of-Detection-Evaluation of NDT Techniques for Cu-Canisters for Risk Assessment of Nuclear Waste Encapsulation

Christina Müller[(1)], Mstislav Elaguine[(1)], Carsten Bellon[(1)], Uwe Ewert[(1)], Uwe Zscherpel[(1)], Martina Scharmach[(1)], Bernhard Redmer[(1)], Hakan Ryden[(2)], Ulf Ronneteg[(2)]
[(1)] BAM - Federal Institute for Materials Research and Testing,
Unter den Eichen 87; 12205 Berlin; Germany,
[(2)] SKB – Svensk Kärnbränslehantering AB; Oskarshamn; Sweden

Abstract. In order to handle long living radioactive waste Sweden is planning to build a deep repository that requires no monitoring by future generations. The spent nuclear fuel will be encapsulated in copper canisters consisting of a graphite cast iron insert shielded by an outer 30-50 mm thick copper cylinder for corrosion and radiation protection. The cast iron insert provides the necessary strength and shielding of radiation. The critical part of the encapsulation of spent fuel is the sealing of the canister which is done by welding the copper lid to the cylindrical part of the canister. Two welding techniques have been developed in parallel at the canister lab in Oskarshamn, Electron Beam Welding (EBW) and Friction Stir Welding (FSW). Mid 2005 SKB decided that FSW is the preferred sealing technique.A subpart of the final risk assessment for the deep repository is to determine the risk of premature canister leak caused by discontinuities in the insert, in the sealing weld or elsewhere in the copper shielding. Therefore the quality of the production processes and the reliability of the NDT system must be satisfactorily determined and combined to derive assumptions regarding the frequency of undetected production discontinuities in relation to the acceptance criteria for the ensemble of canisters. The reliability of the NDT systems can be derived from POD curves which are investigated for X-ray and ultrasonic techniques applied by SKB. The POD evaluation was carried out by BAM in a joint project for SKB and is evaluated within the common "$\hat{a}$ versus a" approach according to the MIL1823 and some extensions due to the more complex flaw situations in the canisters compared to the original aerospace applications.

1 The Swedish Deposit Project

Svensk Kärnbränslehantering AB (SKB, Swedish Nuclear Fuel and Waste Management Co) is responsible for the final disposal of spent nuclear fuel in Sweden.

In order to handle the long living radioactive waste (spent nuclear fuel) SKB is planning to build a deep repository that requires no monitoring by future generations. The spent nuclear fuel will be encapsulated in copper canisters consisting of a graphite cast iron insert. The KBS-3 system is based on a multi barrier system where the canister is the primary barrier. The cast iron insert gives the canister the necessary strength and the outer shell that gives corrosion protection is made of oxygen free copper.

Fig. 1: Svensk Kärnbränslehantering AB (SKB, Swedish Nuclear Fuel and Waste Management Co) is responsible for the final disposal of spent nuclear fuel in Sweden.

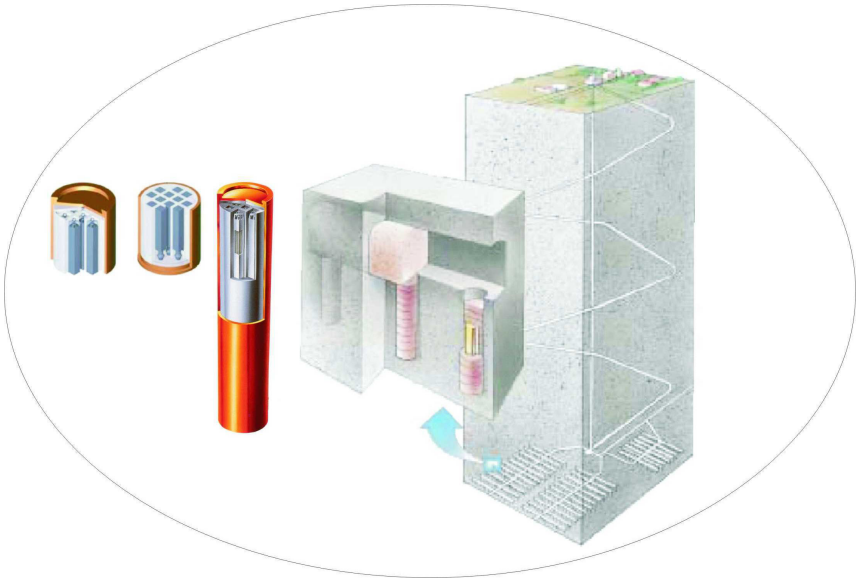

Fig. 2: The canisters will then be deposited in the bedrock, embedded in bentonite clay, at a depth of 500 meters.

SKB's efforts are based on a stepwise program for the implementation of deep geological disposal of spent fuel including concurrent activities in the areas of deep repository- and encapsulation technology. Major milestones in the program are application for construction and building of an encapsulation plant in 2006 and a deep repository in 2008. According to the program initial operation for the system will start in 2017. The most critical part of the encapsulation process is the sealing of the canister, which is done by welding the copper lid to the cylindrical part of the copper shell. The canisters will then be deposited in the bedrock, embedded in bentonite clay, at a depth of 500 meters.

Fig. 3: Outfit of the Copper Canister

The safety and reliability of the whole systems i.e. the well sealed deposit of the radioactive material under all possible influencing scenarios will be guaranteed by modern means of risk assessment and management.

2 Welding and risk assessment

The welding techniques studied are electron beam welding (EBW) and friction stir welding (FSW). Both techniques are developed in parallel at the SKB Canister Laboratory (see Fig. 1) in Oskarshamn (Sweden) [1]. According to the different metallurgical welding processes they reveal a quite different variety of discontinuity's to be detected by NDT techniques and different material micro-structure.

A subpart of the final risk assessment of the deep repository construction is to determine the risk of premature canister leak caused by discontinuities in the sealing weld. The discontinuities occurring during the production welding process create a diminishing of the wall thickness. The possible additional reduction of the wall thickness by ground water corrosion makes a minimum rest wall thickness of 15 mm copper necessary. A consequence for the applied NDT methods is to detect all critical discontinuities which would reduce the wall thickness to an amount near or below the 15 mm with a validated high reliability the value of which needs to be known for the further risk assessment.

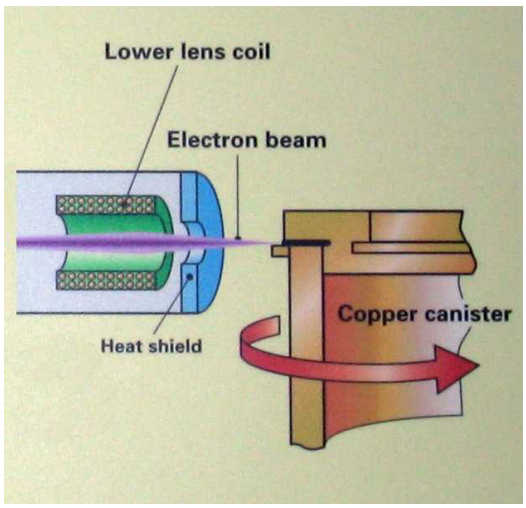

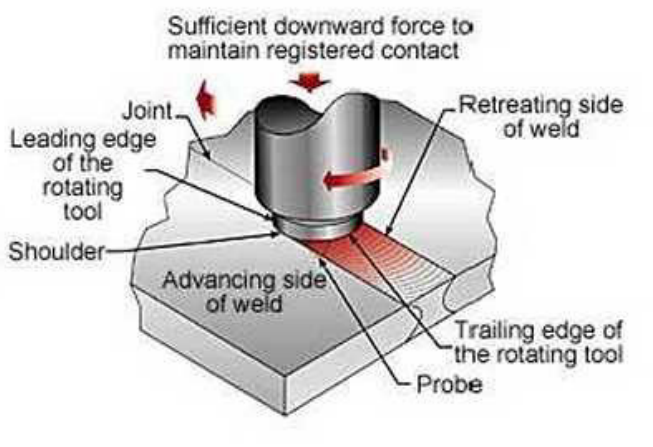

a: Principle of the electron beam welding b: Principle of the friction stir welding

Fig. 4: Principe of the Electron beam welding and Stir friction welding

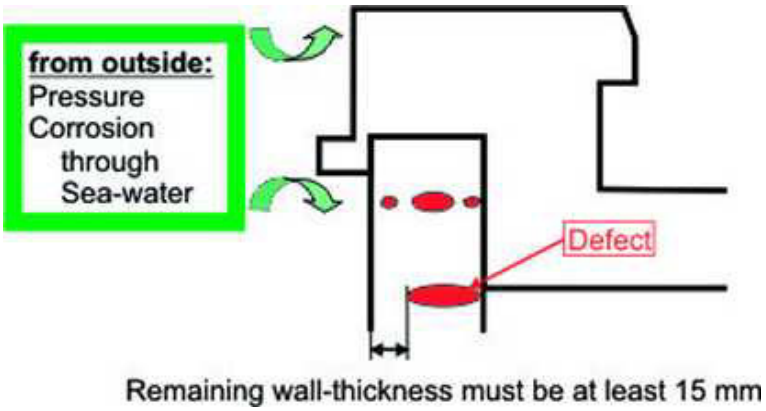

Fig. 5: The weld with possible discontinuity configurations

The NDT techniques applied and adapted by SKB are high energy (9 MeV) X-ray-technique and mechanized ultrasonic phased array technique (2…5 MHz) according to the material structure [1]. Since the materials structures and connected possible discontinuity scenarios created by the welding techniques are different the development of NDT techniques and reliability measurement has also been tailored to the particular welding methods – e.g. higher frequencies for UT were possible for FSW. Mid 2005 SKB decided that FSW is the preferred sealing technique.

The BAM was providing its expertise in optimizing non-destructive testing to a certain extent and the corresponding reliability assessment to the project during 2004-2005. The applied non-destructive testing methods are in a first step checked and optimized concerning the physical parameters and set up according to the latest European and American standards. For the detailed optimization of the radiographic technique the BAM "X-ray" simulation tool [2] is applied to various parameter options thus saving lots of expensive experiments. BAM UT-simulation was used to understand the UT-signal response from special discontinuities types better as input for the POD. [3]

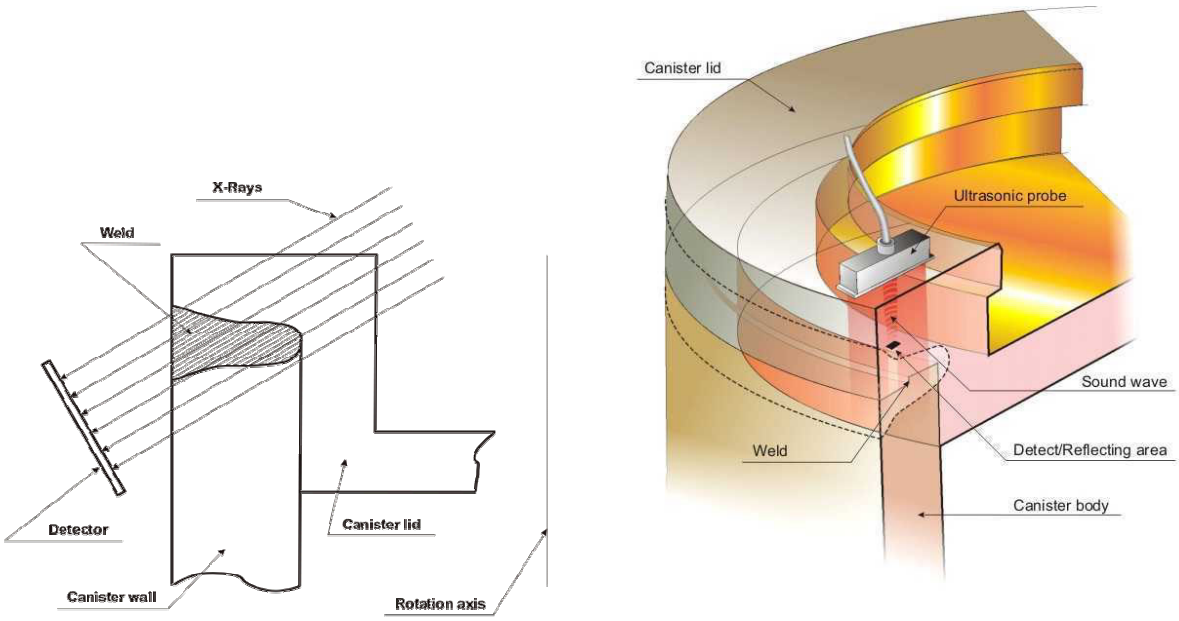

a: Radiographic testing

b: Mechanized ultrasonic testing with phased array technique

Fig. 6: Non-destructive testing methods used in the project.

3 Reliability Assessment using POD

Steered by the plan of experiments for the welding procedure optimization and verification, the POD (Probability of Detection) for the discontinuities is determined using a systematic statistical methodology. The POD method, where the detection probability is determined as a function of discontinuity size, was originally developed for the US military aerospace sector [4] for 1-dimensional signals. For the more complex 3-dimensional discontinuity situation in the canister welds and 2-dimensional data fields the method needs to be developed further. From the POD curve and its lower confidence bound the discontinuity size is derived that will be detected with sufficient reliability and compared to the demand for integrity. This procedure includes a series of experiments with the SKB X-ray and ultrasonic methods foreseen for the production.

These results have to be compared to true discontinuity configurations in the welds. To determine these “true discontinuity configurations” the welds have to be tested destructively or tested with a more comprehensive non-destructive reference method. To save the parts and the effort for the destruction, the BAM selected a high energy computed tomography (HECT, or CT) method as reference completed by focussed ultrasonic transmission measurement. Finally all reference measurements were verified or corrected by destructive tests. Fig. 7 shows all the results for a wormhole in weld No. FSW 5 at 136° position. In figure part a) a JLH is seen in addition (green colour).

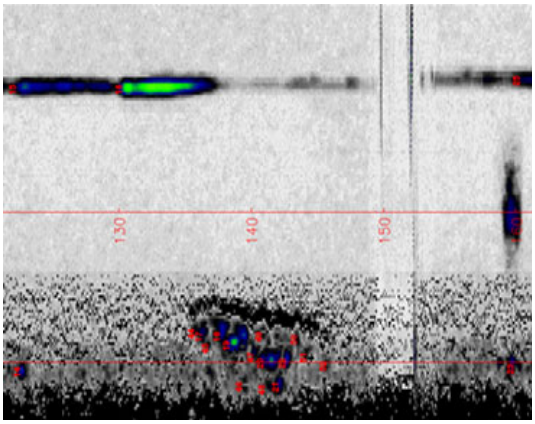

(a) SKB UT-scan (JLH+wormhole)

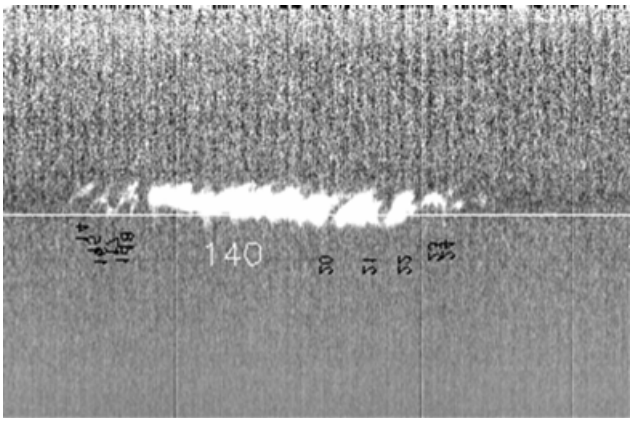

(b) SKB-RT scan (wormhole)

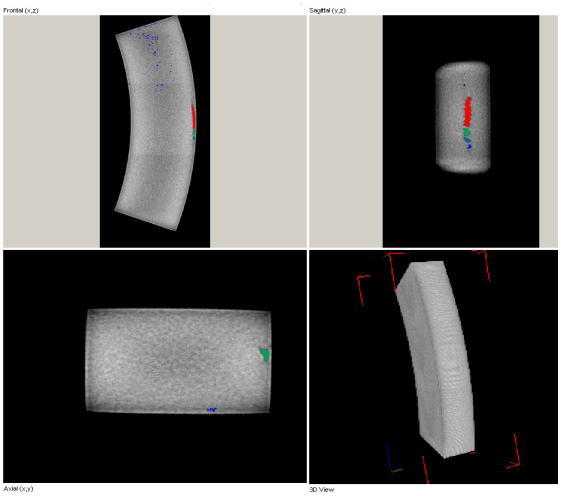

(c) CT of wormholes

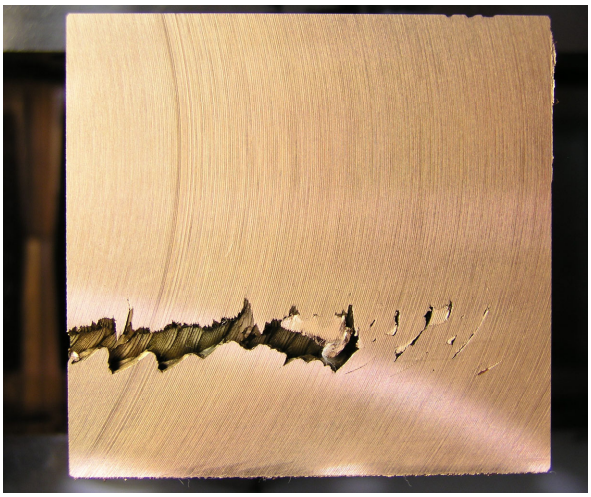

(d) Wormhole cross section FSW5-136

Fig. 7: Example: Weld FSW5 Section 136°

The basic principle of the signal response analysis or "$\hat{a}$ versus a" evaluation is shown in Fig. 8. A discontinuity of size a (crack depth in Fig. 8) is causing a signal of height $\hat{a}$. The statistical distribution of the signals in dependence of the discontinuity size yields a certain POD curve which is described in more exact terms in the following section.

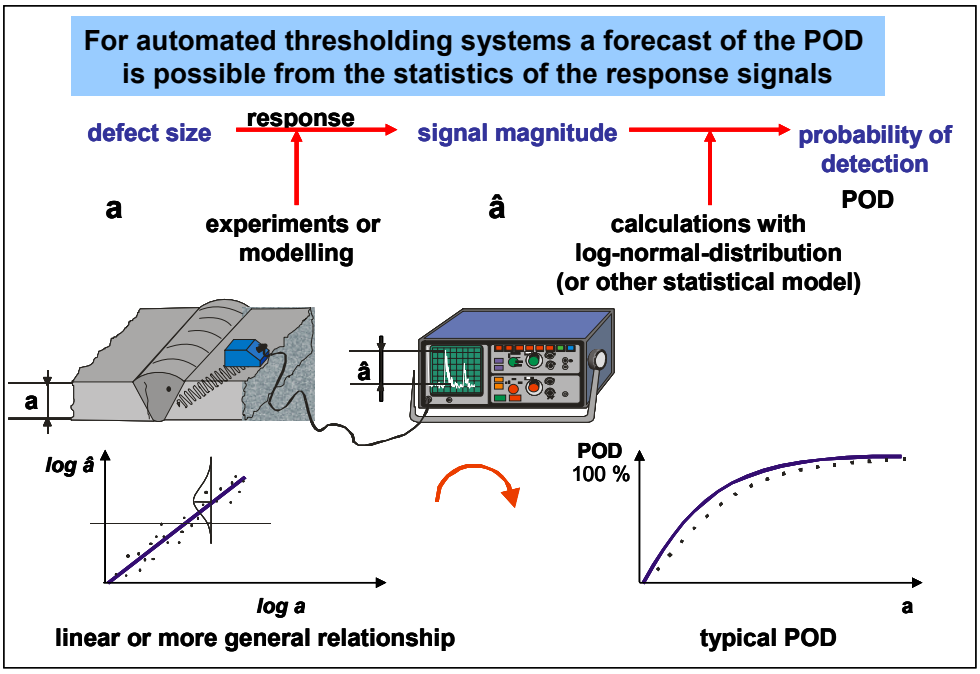

Fig. 8: Quantify the risk: „â versus a“

3.1 â versus a analysis

3.1.1 General description [2]

Consider a quantitative NDT system. As a result of the investigation of a discontinuity having size a, it generates a signal $\hat{a}$. If the signal exceeds a certain decision threshold $\hat{a}_{dec}$, the system registers a flaw detection. As the NDT system is influenced by uncontrolled factors, discontinuities of the same size can cause signals of different strength. For this reason the strength of the signal $\hat{a}$ to the discontinuity of size a is considered as a random value and associated with a probability density $g_a(\hat{a})$. The relation between a and $\hat{a}$ can be expressed as follows:

$$\hat{a} = \mu(a) + \delta \tag{1}$$

Here $\mu(a)$ equals the mean value of $g_a(\hat{a})$ and δ is the random error whose distribution determines the probability density $g_a(\hat{a})$.

In practice, it is often assumed that δ is distributed normally with zero mean and constant (independent of a) variance. $g_a(\hat{a})$ is then the normal density function with mean $\mu(a)$ and variance equal to that of δ.

The probability of detection (POD) as function of the size of the discontinuity is:

$$\mathrm{POD}(\hat{a}) = P[\hat{a}(a) > a_{dec}] = \int_{\hat{a}_{dec}}^{+\infty} g_a(\hat{a})\, d\hat{a} \tag{2}$$

Fig. 9 illustrates this formula. The probability of detection is represented as hatched part of the area under the bell curve.

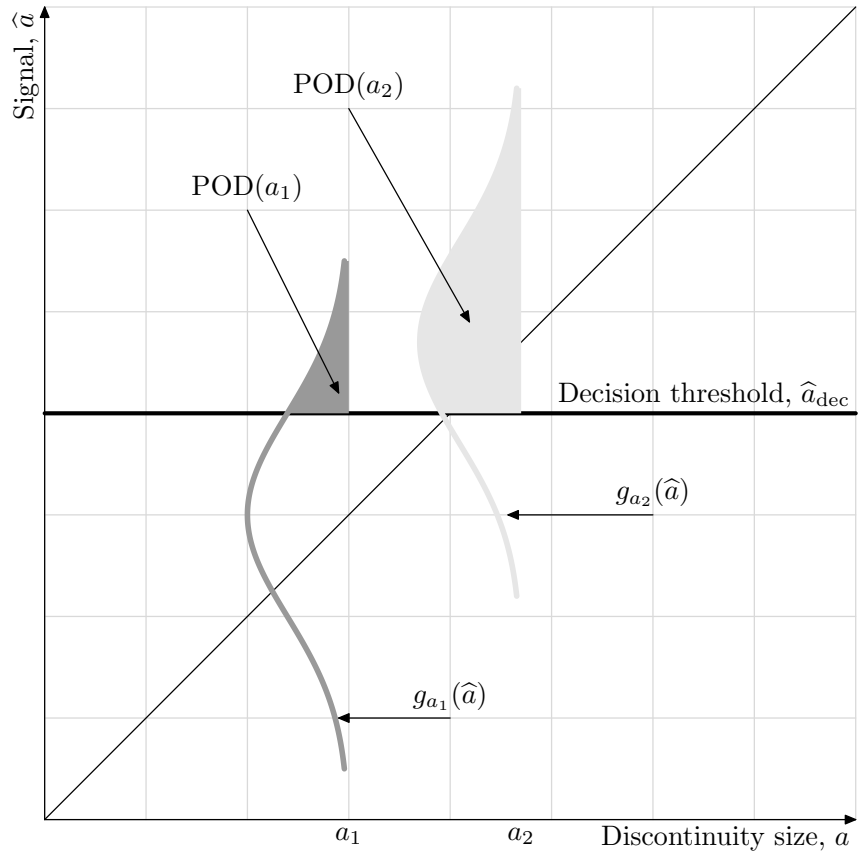

Fig. 9: Probability of detection

3.1.2 Calculation of the POD

Source data are a and $\hat{a}$ – arrays of length n that contain sizes of the discontinuities and response magnitudes, respectively, and the decision threshold $\hat{a}_{\mathrm{dec}}$. Note that the theory for dealing with censored data has been developed (see [5]) but is not used here, because the data sets available to us do no contain censored data. The censored data are the signals that cannot be registered by the system because they are either under the recording threshold or above the saturation threshold.

3.1.3 Calculation of the POD function parameters

The following formula is commonly used to model the relation between a and $\hat{a}$:

$$\ln \hat{a} = \beta_0 + \beta_1 \cdot \ln a + \delta \qquad (3)$$

Here δ is normally distributed with zero mean and constant variance σ_δ^2.

Under the assumptions of the model, the POD function has the following form:

$$\mathrm{POD}(a) = P[\hat{a} > a_{\mathrm{dec}}] = P[\ln(\hat{a}) > \ln(\hat{a}_{\mathrm{dec}})] = \Phi\left(\frac{\ln a - \mu}{\sigma}\right) \tag{4}$$

where Φ is the standard normal distribution function, and

$$\mu = \frac{\ln \hat{a}_{\mathrm{dec}} - \beta_0}{\beta_1} \tag{5}$$

$$\sigma = \frac{\sigma_\delta}{\beta_1} \tag{6}$$

The parameters β_0, β_1 and σ_δ describe the linear dependency of $\hat{a}$ on a and have the following meaning:

β_0	Intercept
β_1	Slope
σ_δ	Standard deviation of the residuals

Their values are estimated from the arrays a and $\hat{a}$ using the method of maximum likelihood.

3.1.4 The 95% lower confidence POD

The 95% lower confidence bound is given by the following formula:

$$\mathrm{POD}_{95}(a) = \Phi\left(\hat{z} - h\right) \tag{7}$$

where $\hat{z} = \frac{\ln a - \mu}{\sigma}$ and the variable h reflects the sample size and the scatter of the source data. The calculation of h is thoroughly described in [5].

This general formalism has now to be applied to the discontinuity detection problem within the scope of welding optimization and risk assessment.

3.2 POD - The Original Task (full programs)

The original task (together with the welding optimization) is to make sure that only one of 1000 canisters might contain a critical discontinuity situation where in total more or equal 35 mm of the Cu-wall is missing.

From the naturally real existing POD as a function of all possible influencing parameters we have to extract the POD as function of the flaw radial dimension by a dedicated „Plan of Experiments“ and reasonable mean value operations (see Formula 1). The full program

is only feasible with a number of additional experiments. But in order to learn where we are with our current NDT technique and where to optimize, we need a POD assessment of the state of the art using an "Adapted POD Assessment".

$$\mathrm{POD} = f(a_1,\ldots,a_n) \rightarrow \mathrm{POD} = g(a_{\mathrm{radial}}) \qquad (8)$$

Formula 1: Extraction of the POD as a function of the radial size.

3.3 „Adapted POD Assessment"

Volumetric flaws and area-like (non-volumetric) flaws will be treated separately – for EB as well as for FSW

- Volumetric flaws RT
- area like flaws UT

The physically reasonable „$\hat{a}$ versus a" PODs are applied to the parameter configurations shown on 13.

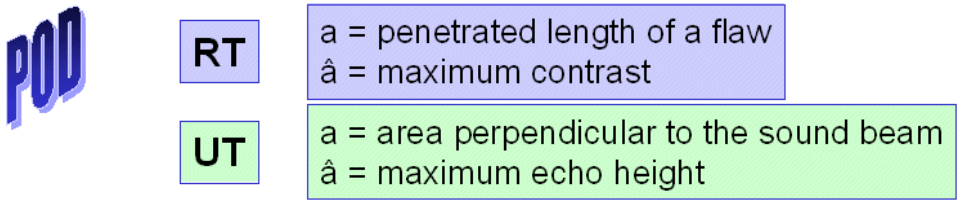

Fig. 10: Input parameters to the POD

We determine the $a_{90/95}$ magnitudes i.e. the size a of the flaw for which the lower 95% confidence bound crosses the 90% POD level i.e. it is guaranteed that flaws with a size of $a_{90/95}$ will be detected with 90% probability where only 5% might fall outside this confidence limit in case the experiment is repeated. We work with the assumption – given by the manufacturing experts – that only one of 100 canisters might have a critical flaw. Then the above argumentation yields: Only each of 1000 canisters might have a leakage.

3.4 Integrity Requirement

The flaw radial size has to be limited so that a remaining wall thickness of 15 mm is guaranteed against ground water corrosion. The maximum allowed flaw size in the radial direction is 35 mm. Together with the above POD an additional flaw geometry statistics has to provide for the four groups

- FSW volumetric area-like
- EB volumetric area-like

separately, no flaws of $a_r \geq 35$ mm will be present. No flaw of radial size $a_r \geq 35$ mm can be among the flaw assembly below $a_{90/95}$, that means no $a \leq a_{90/95}$ should have at the same time an $a_r \geq 35$ mm. This would yield a reasonable justification of the system to meet the above integrity requirement, as long as the existing flaw configurations are representative for the welds. Look for the "correlation" in the scatter diagrams:

- penetrated flaw length by X-ray ←→ radial dimension
- area perpendicular to UT beam ←→ radial dimension

3.5 Results

In the following diagrams we illustrate the results for several examples of flaws for EBW and FSW detected by X–rays (RT) and ultrasound (UT).

3.5.1 Results for Electron Beam Welding (EBW)

Fig. 11 shows the basic "$\hat{a}$ versus a" logarithmic diagram for the radiographic maximum contrast as a function the discontinuity size penetrated by the X-rays. The dependence is quite linear but shows a considerable scatter. The original values are shown in the diagram on the upper side. The lower diagram shows the values without outliers. This version is more reasonable because the discontinuities behind the outliers were created with perturbations to the welding process far outside the normal parameter window.

The corresponding probability of detection and its lower confidence bound (Fig. 12) yield an $a_{90/95}$ value of about 2 mm for the penetrated size (2.3 with outliers and 1.9 without). Now we have to make sure the corresponding radial dimension will not exceed the critical size for all penetrated sizes below $a_{90/95}$.

Fig. 13 shows the discontinuity size statistics, where the penetrated sizes are plotted against the radial dimensions for all observed volumetric discontinuities for the EBW. The critical region is the red hatched area, where discontinuities with critical radial dimensions above the critical size would occur belonging to sizes a below $a_{90/95}$. As seen in Fig. 13, the real discontinuity configurations are far away from this. The radial discontinuity dimension a_r belonging to $a_{90/95}$ is about 3.6 mm. For an exact determination of the corresponding radial dimension a complete geometrical model for the discontinuities shape would be necessary. The data points were too few for this. That is why we turned to an empirical assessment: The value a_r is taken as the maximum radial size between the discontinuities with the area/penetrated length less than $a_{90/95}$ plus 1 mm. The 1 mm is for the uncertainty in the radial dimension from destructive testing/reference methods.

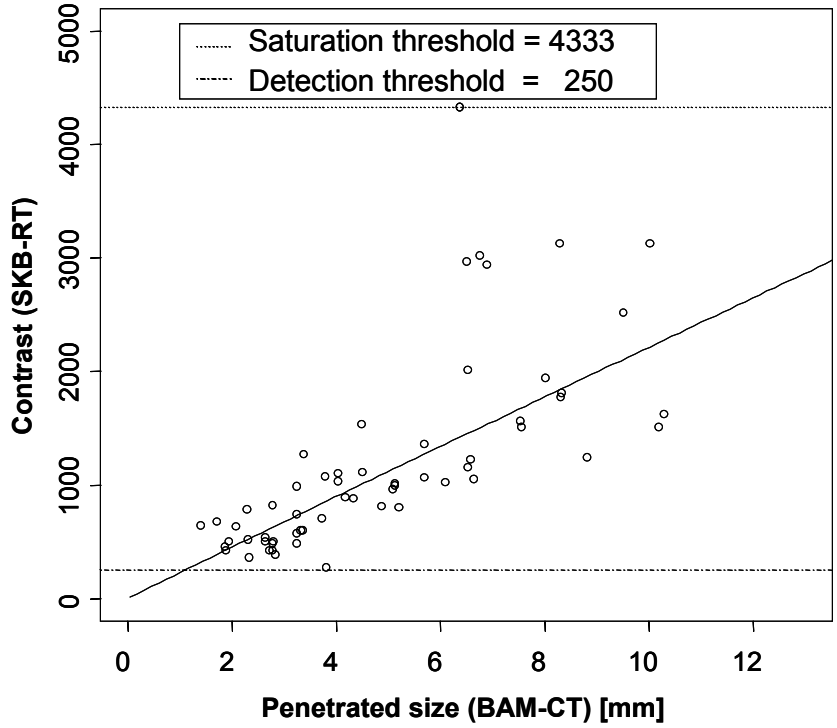

with-outliers

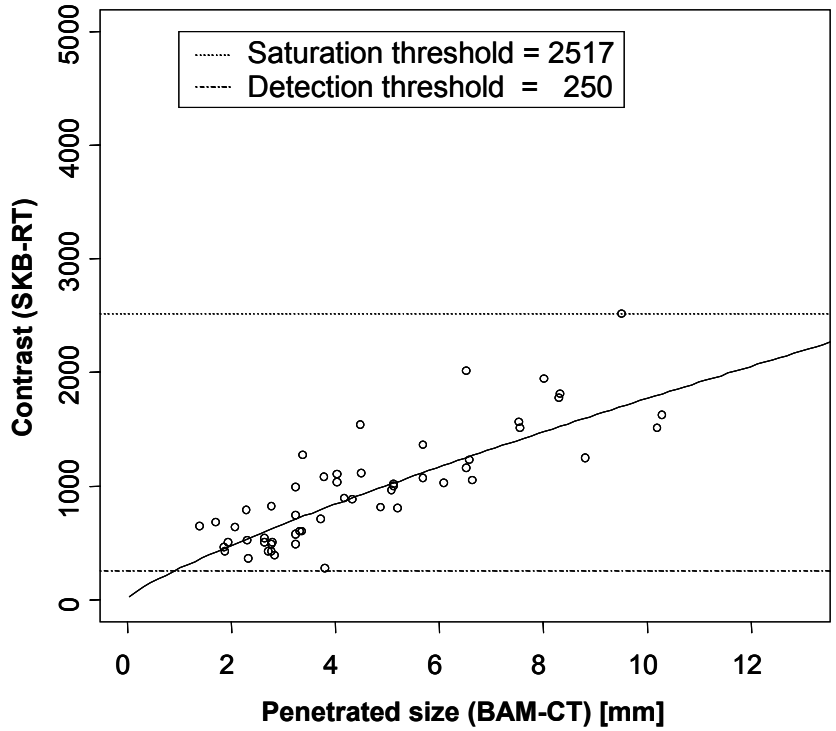

no-outliers

Fig. 11: L025 RT scatter diagram

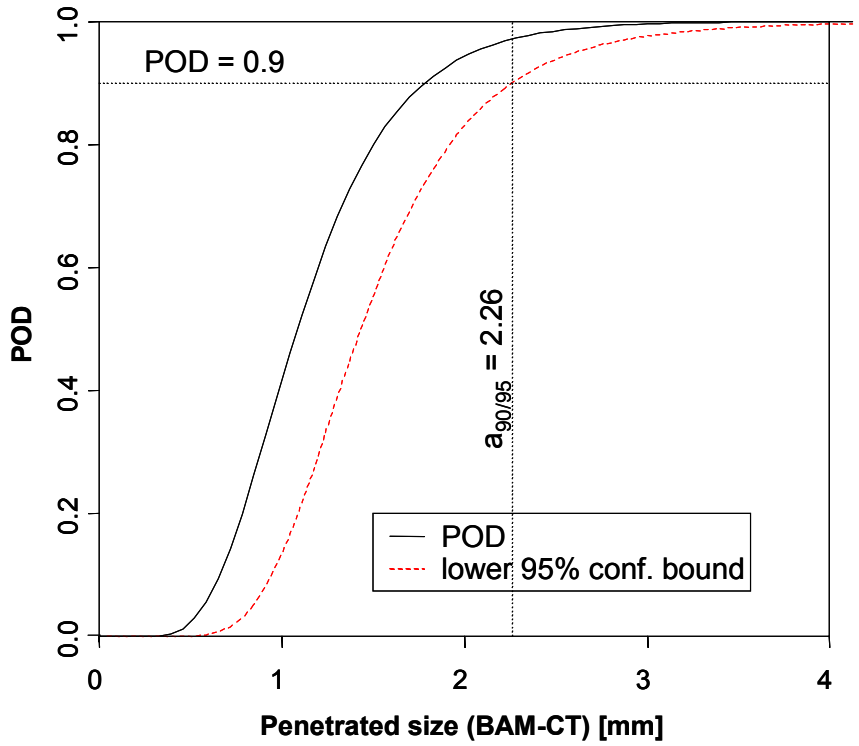

with-outliers

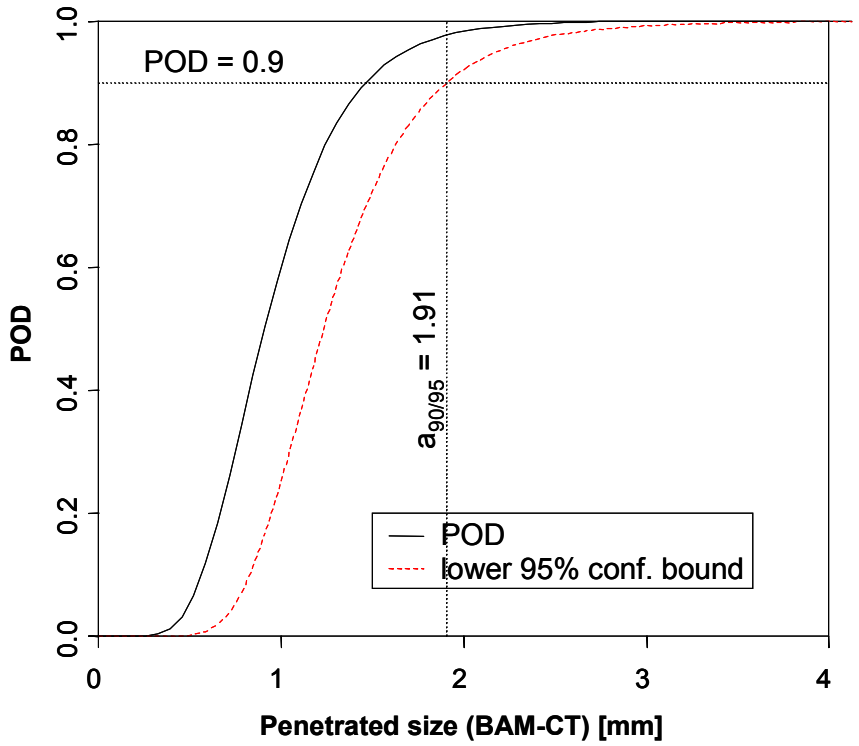

no-outliers

Fig. 12: L025 RT POD

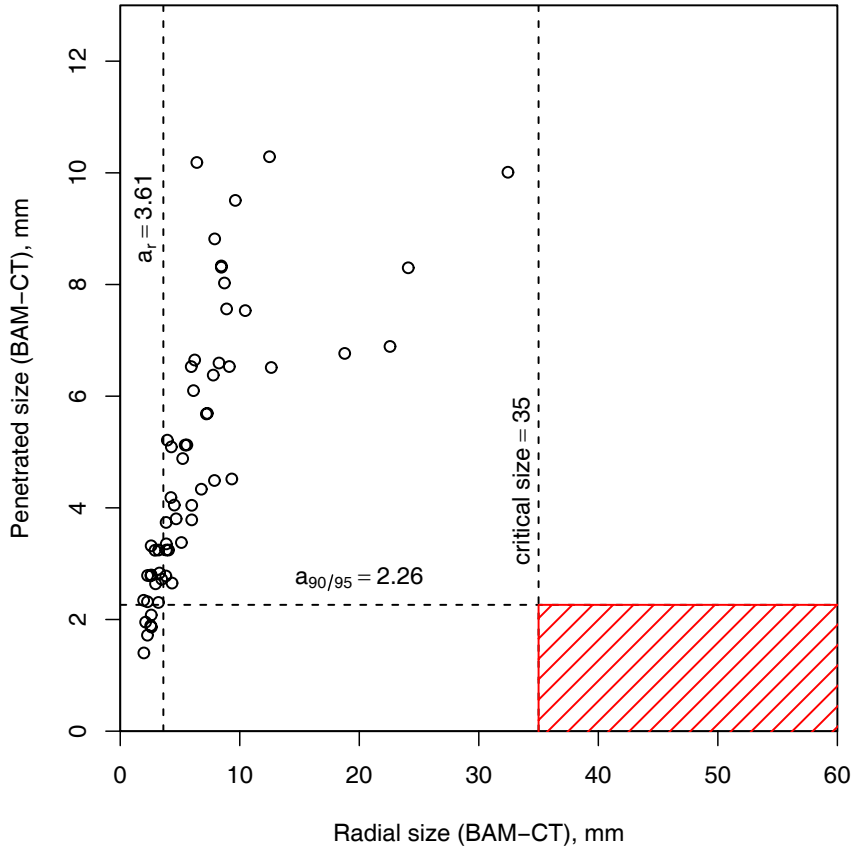

with-outliers

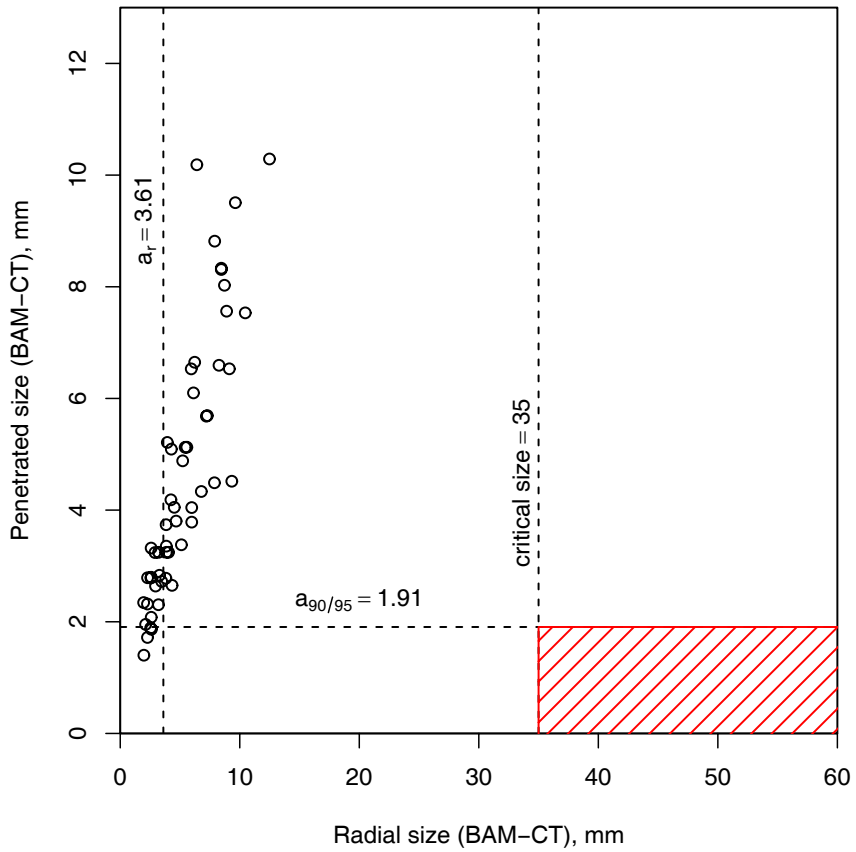

no-outliers

Fig. 13: L025 RT critical region

The Fig. 14 to Fig. 16 show the same types of diagrams (as presented in Fig. 11 to Fig. 13 for RT) for the UT- investigation of area like discontinuities for EBW. The $\hat{a}$ is the ultrasonic echo height and a is the reflecting area of the discontinuity. The scatter of signals is wider and the $a_{90/95}$ is larger. When the area is plotted in a logarithmic scale the "*$\hat{a}$ versus a*" looks quite linear even when the bigger flaws of the right hand side are taken into account which are not so typical for the EBW process. As seen in Fig. 16, again all observed discontinuities are far away from the critical region.

These results should be taken as a rough confirmation that the SKB NDT system is able to detect the volumetric discontinuities with X-ray technique and the area like discontinuities with UT phased array technique with high probability already far below all critical values. Since for EBW no destructive tests have been carried out the $a_{90/95}$ might change a couple of millimetres due to the uncertainty of the true values determined via reference methods.

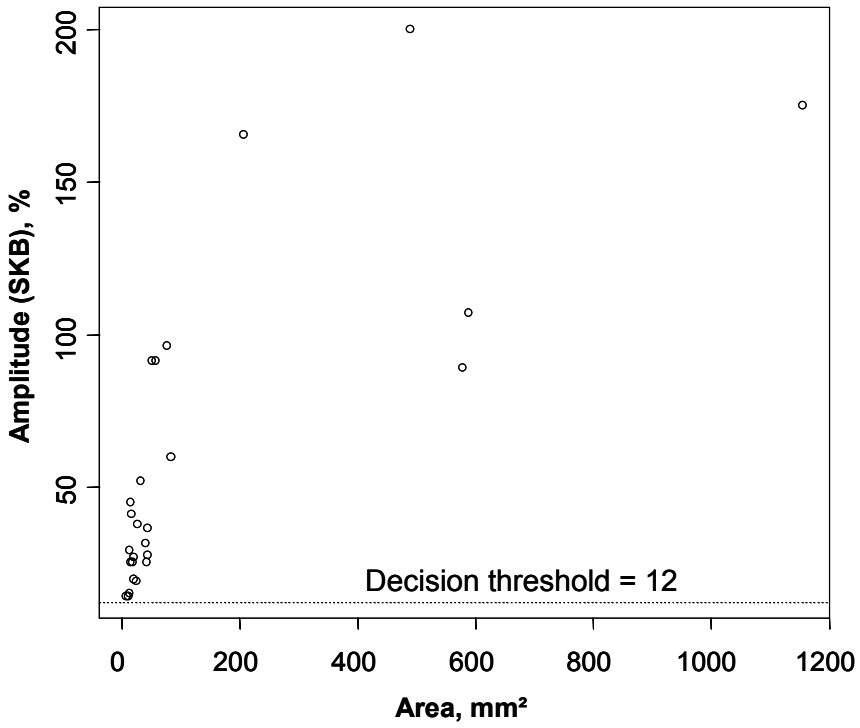

Fig. 14: L025 UT scatter diagram

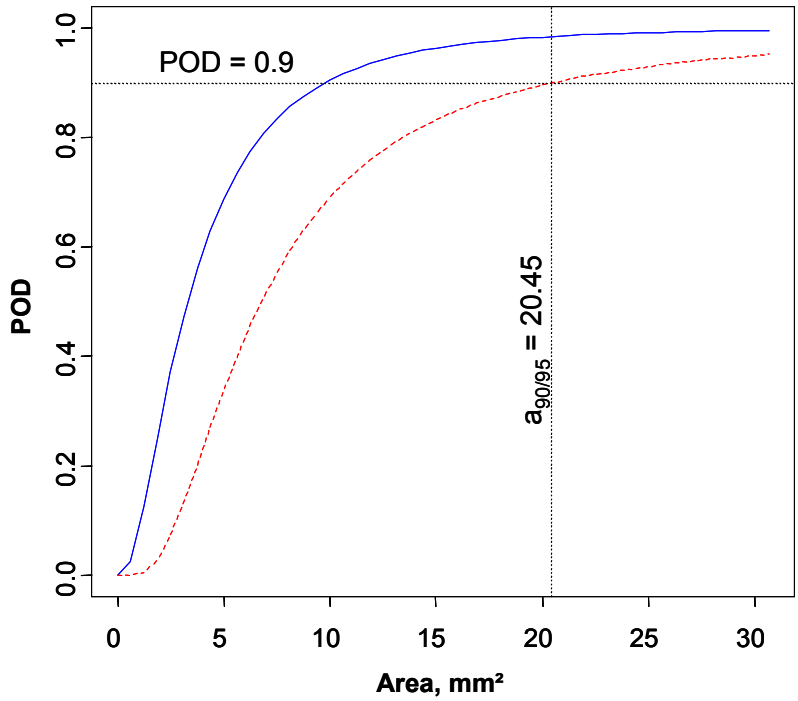

Fig. 15: L025 UT POD

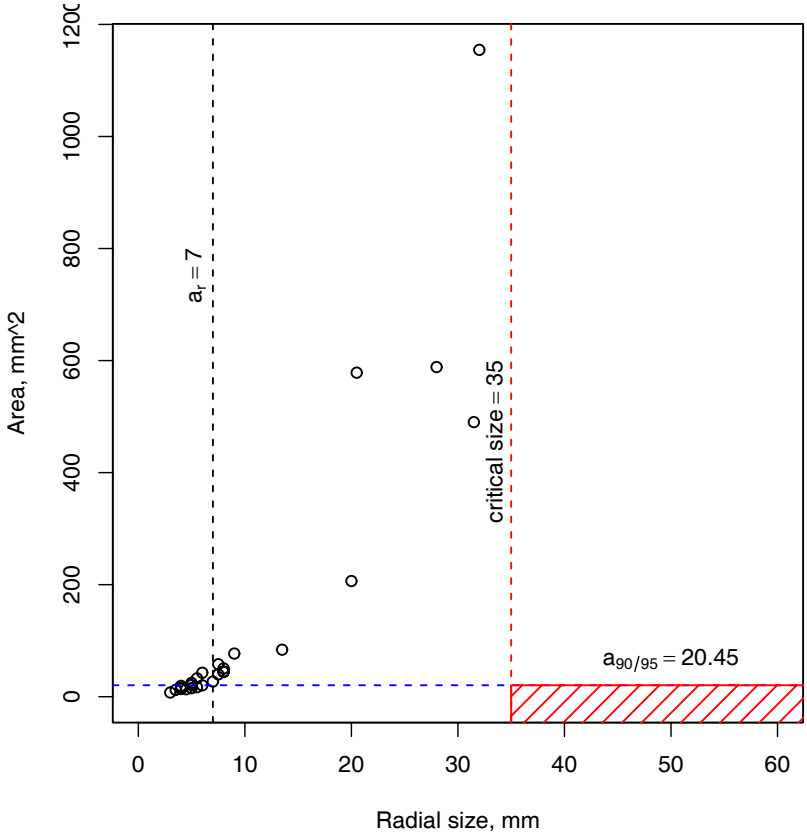

Fig. 16: L025 UT critical region

3.5.2 Results for Friction Stir Welding (FSW)

Below the "Adapted POD Results" for the wormholes for RT- and UT-inspection are presented with the following pattern: First we present the "$\hat{a}$ versus a" scatter diagrams where the $\hat{a}$'s in terms of maximum radiographic contrast and the maximum echo height, respectively are plotted in dependence of the "a" in terms of penetrated length and area perpendicular to the sound beam. For these signal sizes the actual thresholds are applied yielding the mean POD curves and the 95% confidence bound and the $a_{90/95}$ as key parameter. As discussed above the additional scatter diagram showing the statistics of the "a" dimension in dependence of the radial dimension reveals for all cases that the "critical" region with critical radial dimensions belonging to "a"-values below $a_{90/95}$ are far away from the actually occurring configurations.

RT wormhole

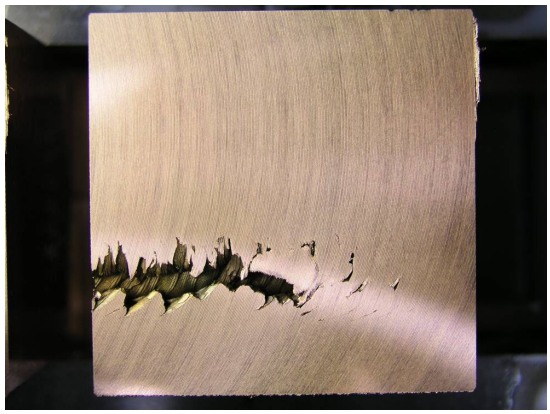

Fig. 17: Volumetric Discontinuity

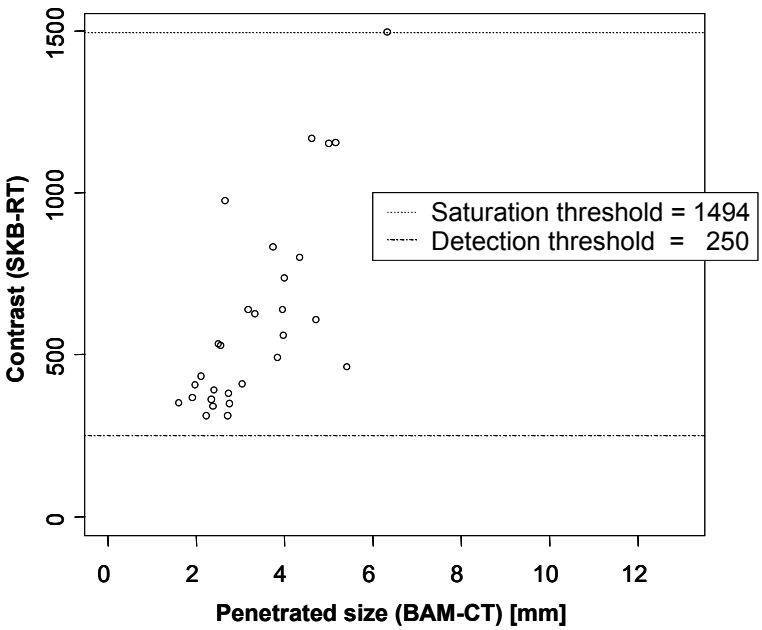

Fig. 18: FSW5 RT scatter diagram

Fig. 18 shows the "â versus a" scatter diagram in terms of maximum radiographic contrast versus the by the X-rays penetrated length. A linear behaviour can be seen but with considerable scatter which might be due to the zig-zag shape (see Fig. 17) causing uncertainties in the determination of the penetrated length.

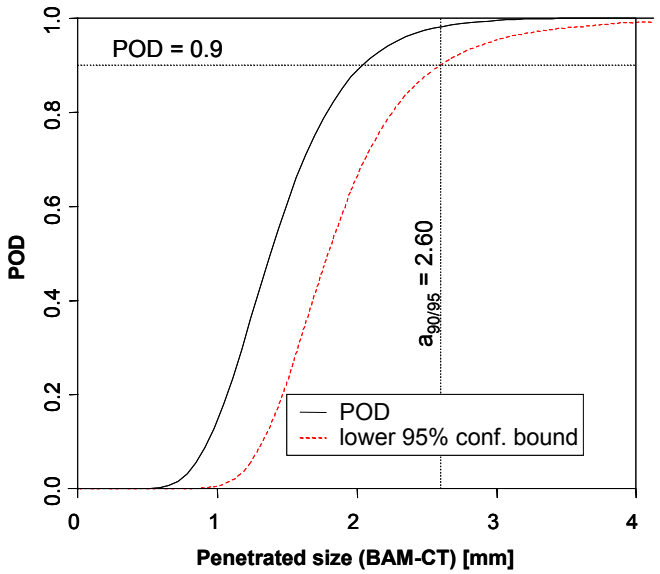

Fig. 19: FSW5 RT POD

The resulting POD curve and the 95% confidence bound in Fig. 19 indicate an $a_{90/95}$ of 2.6 mm for the penetrated length. The corresponding radial dimension of the discontinuities "to detect for sure" is 4 mm as indicated in Fig. 20.

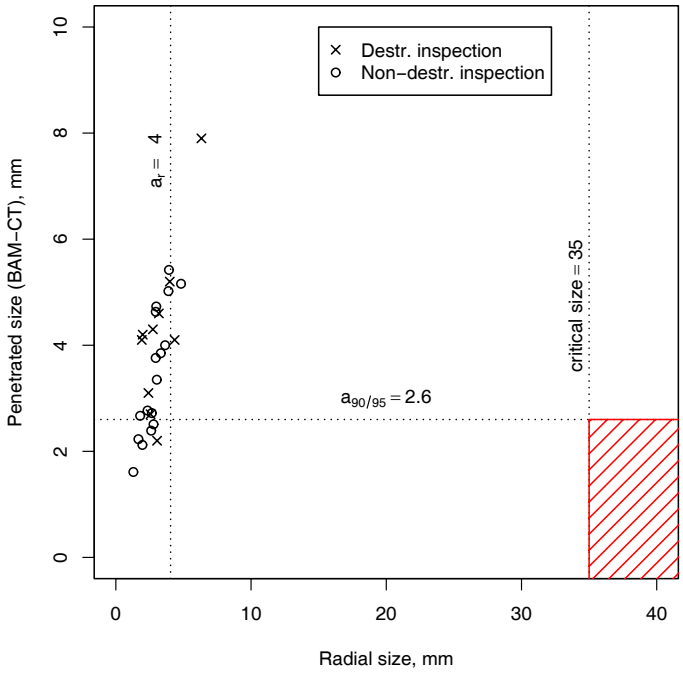

Fig. 20: Critical region based on radiographic inspection of volumetric discontinuities with the threshold 250 levels.

UT Wormhole

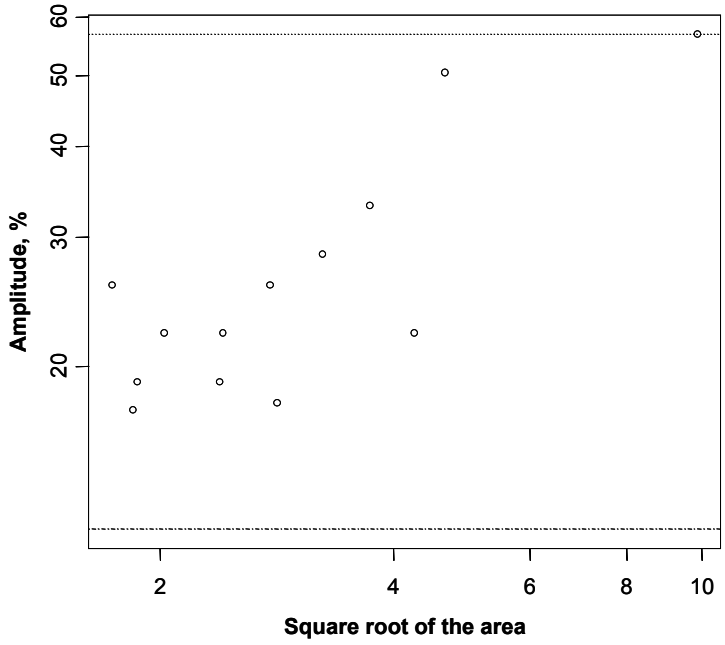

Fig. 21: FSW5 UT scatter diagram

The same set of wormhole discontinuities as investigated above were inspected by ultrasound with "a" as area perpendicular to the sound beam and $\hat{a}$ as maximum echo amplitude. The reference value for the area was taken from results from destructive tests (cubes). The scatter diagram in Fig. 21 indicates the already known fact that these discontinuities are not ideal reflectors of ultrasound and that the echo amplitude is affected by a number of other factors than the discontinuity size as listed in [6] for UT. The corresponding POD curve in Fig. 22 and the "critical region"- Fig. 23 reveals for $a_{90/95}$ 12.5 mm² and a corresponding detectable radial dimension of 6.3 mm. The crosses in Fig. 23 represent results from destructive testing.

Both methods are capable to detect the wormholes far below the required critical size but show even a potential to detect smaller discontinuities in studying the detection processes in more detail.

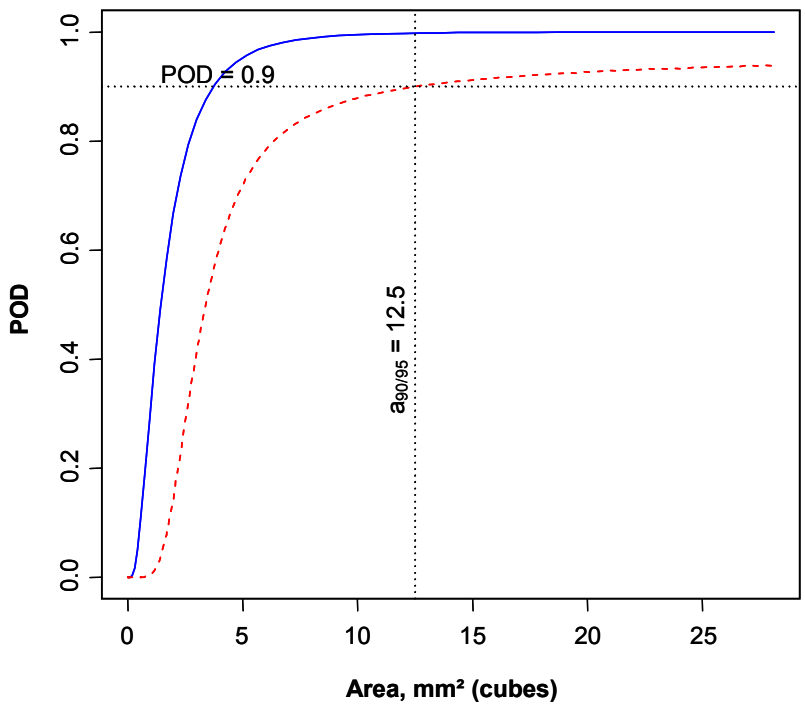

Fig. 22: POD curve based on ultrasonic inspection of volumetric discontinuities (threshold 15%).

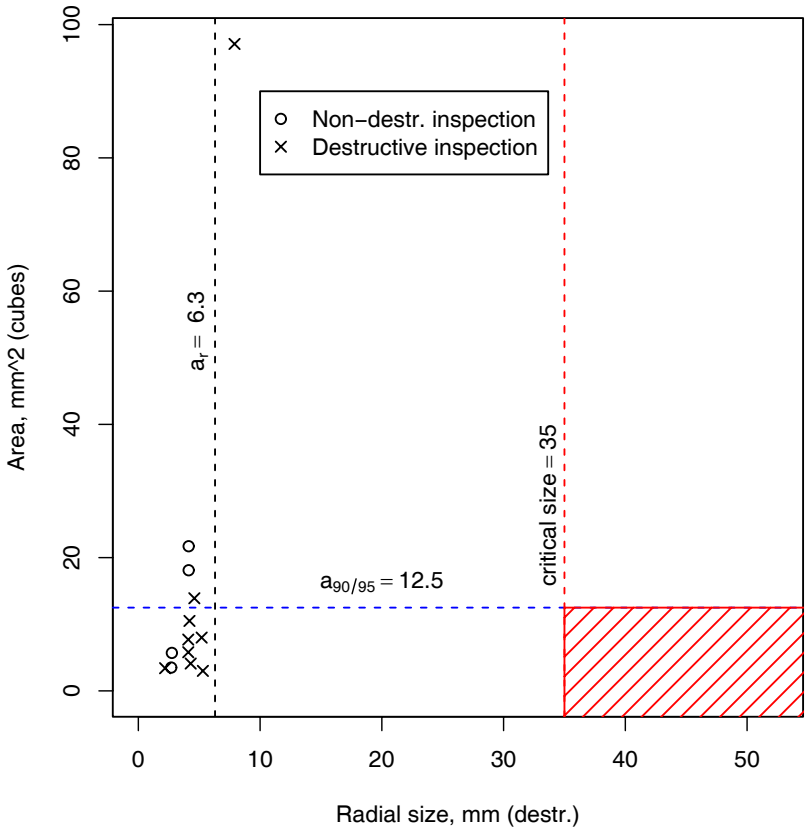

Fig. 23: Critical region based on ultrasonic inspection of volumetric discontinuities (threshold 15%).

JLH

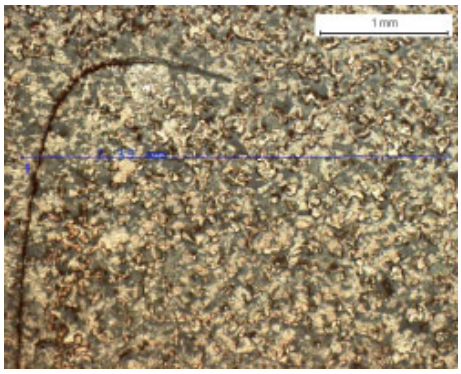

Fig. 24: Cross section of a JLH (Joint Line Hooking)

Fig. 24 shows a typical cross section of a JLH (Joint Line Hooking) discontinuity. It is clear that this shape not easily matching the empirical POD approach. *The investigation was refined* step by step: The first approach in investigating the JLH discontinuities was to apply the POD method in an empirical way. For this approach, the maximum echo amplitude was used as $\hat{a}$ as before. First, a totally empirical "$\hat{a}$ versus a" scatter (Fig. 25) diagram and POD (Fig. 26) were created. These included all the values of the SKB experiments which yields the $a_{90/95}$ equal to the detectable radial dimension of 4.0. In the next step, outliers (too small and too big values compared to a "normal" amplitude versus size behaviour), were excluded. This resulted in detectable radial dimension is 3.2 mm due to the decreased scatter.

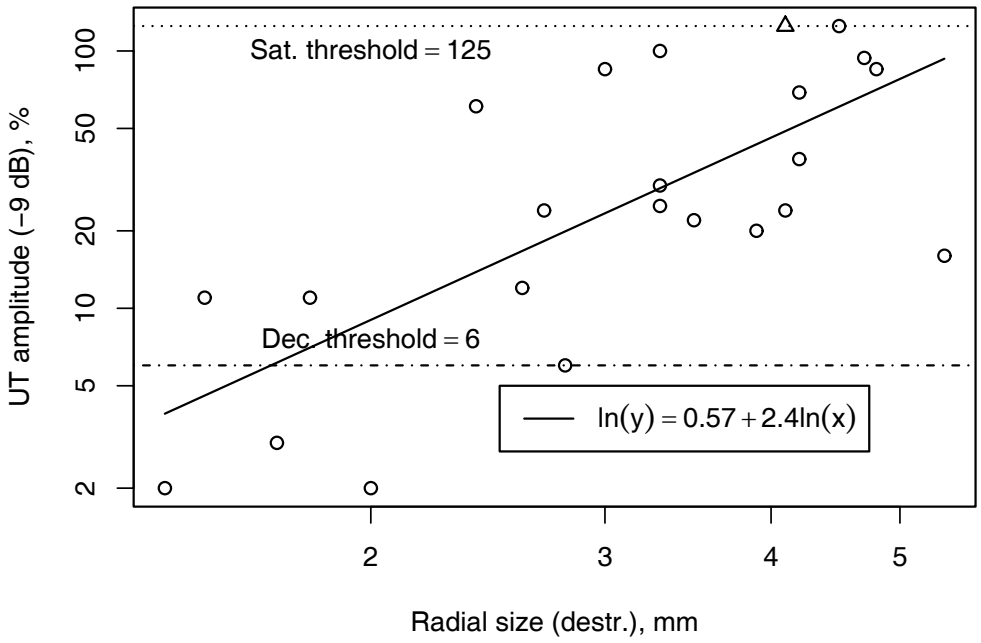

Fig. 25: Scatter diagram of the amplitude vs. radial size for the JLH-type discontinuities (log. axes).

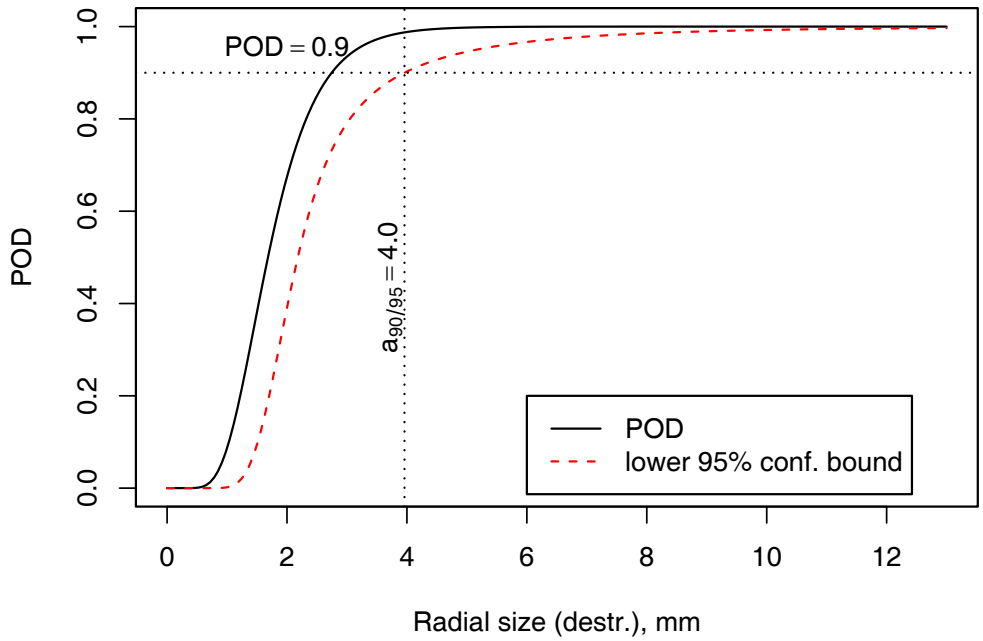

Figure 26: POD curve for the JLH–type discontinuities (with outliers).

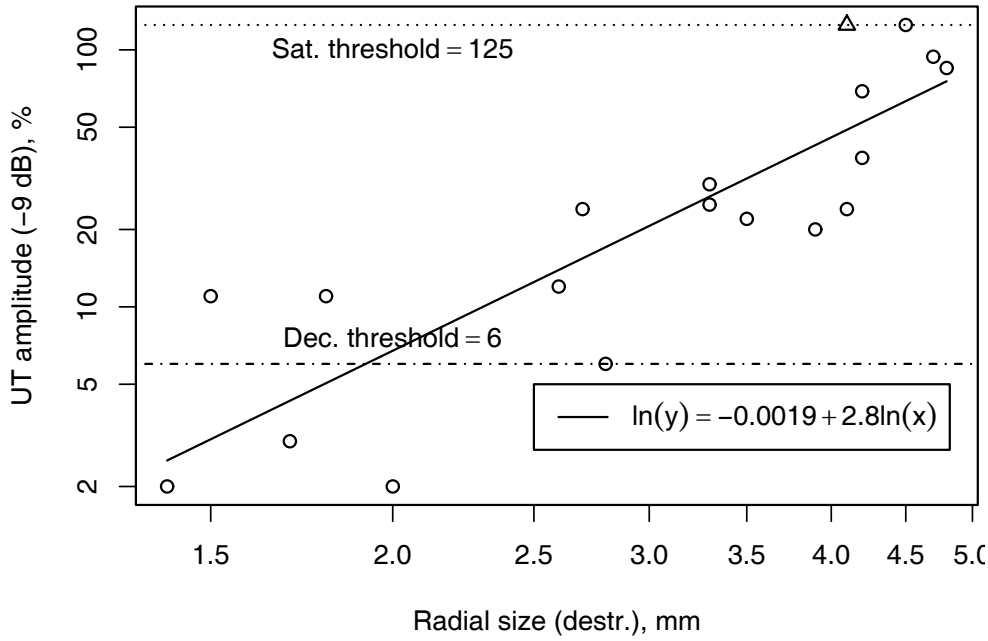

Figure 27: Scatter diagram of the amplitude vs. radial size for the JLH–type discontinuities (log. axes, without outliers).

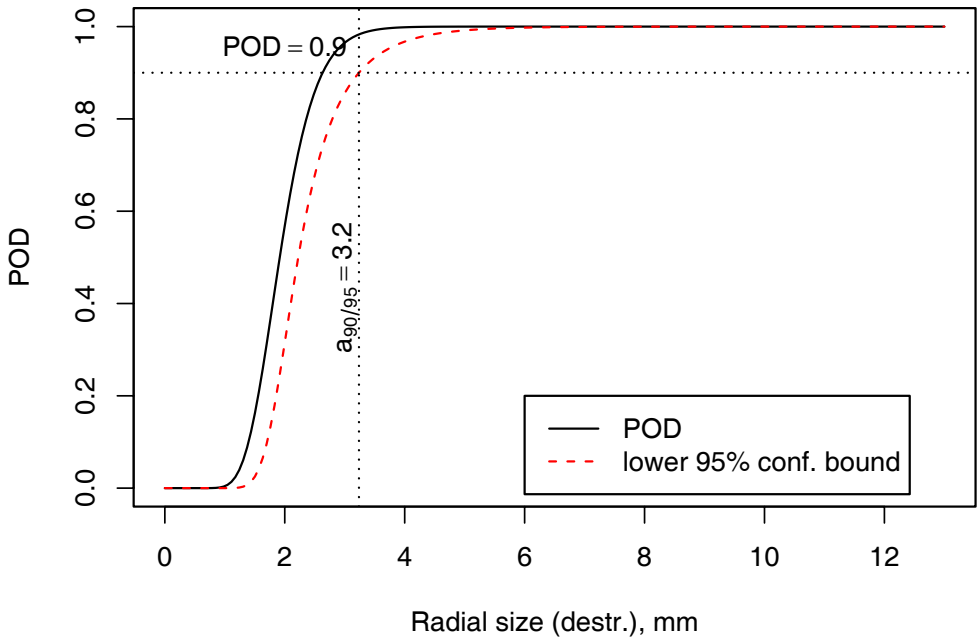

Fig. 28: POD curve for the JLH–type discontinuities (outliers excluded).

We looked deeper into the JLH geometry and echo heights and recognized that the "hook" part is in almost all cases indicated by the 0° or -10° sound beam and the straight part, the inclined plane or rectangle by the 10° and 20° sound beam. Consequently we should consider the forming of the POD separately for hook and rectangle with the corresponding angle of the sound beam. Because the number of data points becomes too small after separation we did not carry out this procedure yet. It might be considered as a future investigation to look deeper to the forming of the POD for the two parts of the JLH and the different angles separately in combining experimental and modelling insight after all the influencing factors has been listed carefully. It will depend on the importance of the JLH in the future welding process.

3.6 Consideration of the total reliability

The POD's considered so far reveal the basic or intrinsic capability of the NDT methods and do not yet take into account the final industrial application factors and the human factor. The situation for general NDT systems – as outlined in the formula (2) - is described in detail in [7] and [8] and will be applied to the canister welds on a later stage of the project. It is planned to set up the NDT–system as automatic as possible to minimize the human factors or to apply double evaluation.

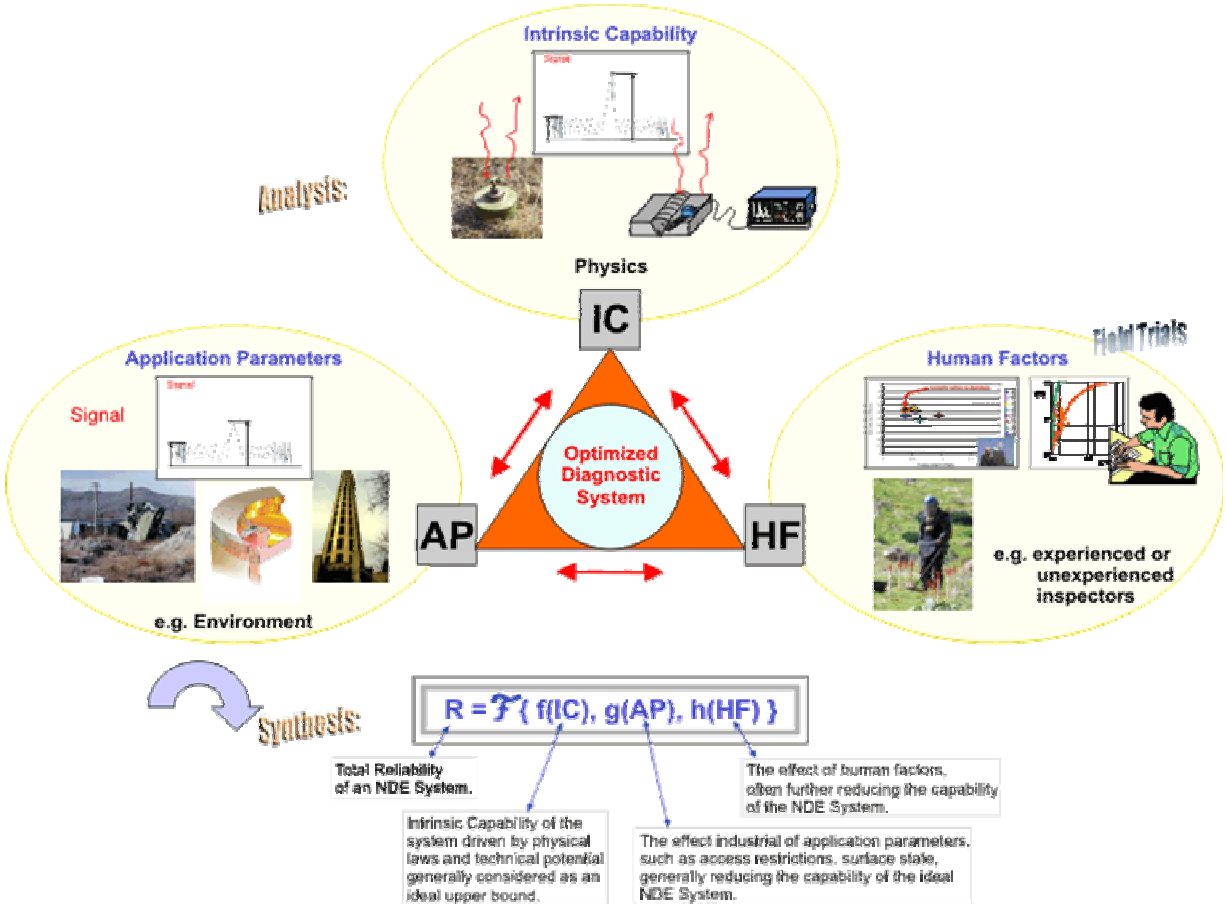

Fig. 29: Modular approach: the reliability formula

4 Conclusions

A Probability of Detection evaluation for the SKB-NDT processes has been successfully established to make sure the applied NDT techniques are able to reveal the occurring discontinuities, which might be overseen by NDT as an input for the final risk assessment. A generalization of the existing prescription for the signal response POD from the MIL 1823 standard was necessary because the EBW and FSW welds of 50 mm thick Cu-canister-welds are more complex than thin aerospace structures.

The physical reasonable $a_{90/95}$ values as discontinuity sizes, which are detected for sure need to be set in correspondence to the corresponding radial dimensions of discontinuities to provide the expected wall thickness reduction, which is of importance for the integrity requirement. For EBW these values are below 4 mm for volumetric flaws detected by radiography and are not larger than 7 mm for area like flaws detected by UT. Subject of consideration for FSW was the detectability of volumetric like wormholes and area like "Joint line hooking" with the SKB radiographic and ultrasonic methods. At the current state of the art all observed $a_{90/95}$ values are for the wormholes for radiographs not larger than 3 mm and for UT not larger than 13 mm^2. The corresponding radial dimension are at maximum 4 mm for RT and 6 mm for UT in case the flaw configurations investigated here

represent the full possible scale which might occur in the welds under production conditions.

The empirical detectable radial dimension with UT for the “joint line hooking” is 4 mm.

As result of this SKB-BAM project optimized testing techniques will be provided which are validated for the production process and which will guarantee the required rest wall thickness with sufficient reliability. The NDT reliability investigation is continued now for the iron cast insert and the copper shield. The joint SKB-BAM project is a contribution for the long term European public safety.

5 Acknowledgment

The authors like to thank Dr. Gerd-Rüdiger Jaenisch for fruitful scientific discussions and Dr. Jürgen Goebbels for providing the reference - CT-measurements on “High energy - CT”. We are also indebted to the colleagues from the ultrasonic group at BAM (Dr. Gerhard Brekow, Dr. Dirk Tscharntke) for ultrasonic reference measurements and Mrs. Sylke Bär for helpful assistance in flaw extraction from data sets.

6 References

[1] N. N. RD & D-programme 2001. Technical Report TR-01-30, Svensk Kärnbränslehantering AB, September 2001.

[2] Tillack, G.-R.; Nockemann, C.; Bellon, C.: X-ray modelling for industrial applications. *NDT & E International*, 33:481–488, 2000.

[3] Tscharnktke, D.; Boehm, R.; Müller, C.; Ronneteg, U.; Ryden, H.: Ultrasonic investigation on copper canister welds in preparation for the storage of spent nuclear fuel in a deep repository, to be published in proceedings of the 6th ECNDT

[4] US Department of defense. *Nondestructive evaluation system. Reliability assessment*, 1999. Handbook.

[5] Berens, A.P.: NDE reliability data analysis. In *Metals Handbook*, volume 17. ASM International, 9 edition, 1989.

[6] ASNT Nondestructive Testing Handbook, Second Edition, Volume 7: Ultrasonic Testing pp. 445 (Factors Determining Amplitude of Discontinuity Echo Signal)

[7] Müller, C.; Fritz, T.; Tillack, G.-R.; Bellon, C.; and Scharmach, M.: Theory and applications of the modular approach to NDT reliability. *Materials Evaluation*, 59(7), pp. 871–874, 2001

[8] Christina Müller, Mstislav Elagin, Martina Scharmach, Bernhard Redmer, Uwe Ewert, Lloyd Schaefer, and Peter-Theodor Wilrich. Reliability investigation of NDE systems by modular analysis of recorded data. In *Proceedings of the 8th European Conference on Non-Destructive Testing*, 2002.

Statistical design of experiments applied to tests of metal detectors used for mine detection

Mate Gaal, Christina Müller
Bundesanstalt für Materialforschung und –prüfung (BAM), Berlin

Summary: This paper discusses the statistical design of experiments for testing and evaluation of metal detectors used in humanitarian landmine clearance. Design of experiment is the process of planning the experiment so that appropriate data will be collected, enabling objective conclusions. In 2003 and 2005 field tests were performed on the latest models of four metal detector manufacturers. The results of these tests are discussed in this paper. The tests were executed according to the standard for testing and evaluation of metal detectors CWA 14747:2003 with the purpose of optimisation and more detailed specification of the testing procedures.

Many factors influence the reliability of a detection system, which consists of the physical and technical properties of the detector, the conditions of application and the human operator. In demining, the most important influences are the detector, the mine type, the mine depth, the soil magnetic properties and the operator. Statistical design of experiments enables an unbiased estimate of the difference between detectors, at the same time minimising the experimental error, thus reducing the necessary number of repetitions. Only a scientifically planned experiment can separate the influences of all influencing factors, with the aim to select the most appropriate device for certain conditions of application.

A full factorial design was applied to the maximum detection height measurements and a fractional factorial design to the blind tests, also called reliability tests. The performance indicators of the blind tests are the probability of detection (POD) and the false alarm rate (FAR). The statistical design of experiments is applicable also in tests of the equipment used in non-destructive testing.

1 Test and evaluation of metal detectors

Most efforts of the research and development community working on problems related to humanitarian demining were directed at improving landmine detection. Many scientists hoped to find a "silver bullet" solution among technologies not used before in the field. However, all developments in that direction have failed to meet field needs. The metal detector is still the main detection tool in humanitarian demining, and it will probably continue to be for many more years [1]. At the same time, we are witnessing substantial progress in testing and evaluation of demining equipment. A standard for testing and evaluation of metal detectors has been proposed in 2003. The CEN Workshop Agreement CWA 14747:2003 specifies standardised procedures for measuring the influences of many factors to the performance of metal detectors [2]. The purpose of testing is to find the most suitable detector for a given set of conditions.

Many tests described in the CWA 14747:2003 are based on maximum detection height measurements. The maximum detection height is the distance between the search head of the metal detector and the top of the target at which the detector starts to give clear signals in an experiment in which the position of the target is known to the operator. This quantity provides the information about the depths at which the mines in a minefield can still be detected.

The blind in-field tests called detection reliability tests are the tests receiving the highest attention by detector end users, since they are performed in conditions as close as possible to the real minefield conditions. The operators are not familiar with the positions of the targets. They mark the assumed positions of the targets and the positions of their indications are compared with the actual target positions. If an indication falls inside a prescribed circle called halo, the indication is counted as a true positive. If it falls outside, it is counted as a false positive indication. The halo radius, according to CWA 14747:2003, is "the half of the maximum horizontal extent of the metal components in the target plus 100 mm".

The two values to be estimated by the results of a detection reliability test are the probability of detection (POD) and the false alarm rate (FAR). The estimated probability of detection for a particular choice of targets, operators or detectors is the number of detected targets (true positives) divided by the total number of targets. The estimated false alarm rate is the number of false alarms (false positives) on a certain area divided by the size of that area. If we assume a binomial distribution for the number of detections, we can find 95% confidence limits for the probability of detection. Similarly, if we assume Poisson distribution for the false alarms, we can construct 95% confidence limits for the false alarm rate [3]. A ROC diagram is a diagram with the POD on the ordinate and the FAR on the abscissa, and it is a modification of a ROC diagram used in non-destructive testing, where the probability of detection is plotted against the probability of false alarms [5], [6], [7].

The other kind of diagram is the POD curve, presenting the dependence of the POD on a parameter, in our case the depth of the target. The POD curves and the corresponding regression model are described in detail in the final report of the metal detector trial performed in Benkovac, Croatia, 2005 [8].

The detection reliability tests owe their name to the concept of reliability, which is defined (CWA 14747:2003) as "the degree to which the metal detector is capable of achieving its purpose, which is to have maximum capability for giving true alarm indications without producing false alarm indications". Detection reliability tests are the only tests that include the evaluation of the ability of metal detectors to deal with false alarms. In the context of testing, the detection of metal clutter is not considered as false alarm, since metal detectors are designed to detect metal. The main source of false alarms is the soils with frequency dependent magnetic susceptibility, causing alarms without presence of a metal fragment. Most metal detectors today have some ground compensating abilities, which means that they can decrease their sensitivity to soils with much smaller decrease of sensitivity to metal.

There are many factors influencing the performance of metal detectors. They are all described in a concept called "reliability formula", first applied in non-destructive testing [5], [6]. The total reliability (R) of a detection system is described by three factors: intrinsic capability (IC) describing the physics and the basic technical capabilities of the device, and representing an upper limit of R; factors of application (AP) such as specific environmental conditions in the field generally diminishing R and finally the human factor (HF), which also lowers R. The mutual interaction of these factors is usually very complex.

An important advantage of the detection reliability tests is that they include most of the factors influencing the performance of metal detectors. In the maximum detection height measurements the influence of the operator (or the "human factor" from the reliability model) is much smaller, but it is not entirely excluded. The operator sets up the metal detector, performs the ground compensation, operates the device and decides whether the audio signal is a detection or noise.

2 Design of experiment, basic principles

The statistical design of experiments [3], [4] (sometimes called experimental design) is the process of planning the experiment considering all influencing factors so that appropriate data will be collected, enabling objective conclusions. A scientific approach to planning an experiment results in unambiguous results, which are as little affected by experimental error as possible. The use of experimental design in industry can result in products with better performance, reliability, lower production costs or shorter development time.

In a designed experiment we make a difference between the predictor variables and the response variables describing a process. The predictor variables included in the experiment by controlling their values are called factors and the specific values that these factors can take in an experiment are called factor levels, or simply levels.

The basic principles of experimental design are replication, randomisation and blocking. Replication is the repetition of the experiment. It allows the experimenter to estimate the experimental error. Randomisation is crucial for each design of experiment. Both the allocation of the experimental material and the order of execution of measurements are determined randomly. As a result, errors are usually values of independently distributed random

variables. Another important consequence of randomisation can be "averaging out" the effects of extraneous factors that might be present. A block is a portion of the experimental material that is more homogeneous than the entire set of material. Comparisons can be made within each block. This way the variability between blocks does not affect the experimental error.

3 Metal detector trial, Benkovac, Croatia, May 2005

3.1 Overview

BAM (German Federal Institute for Materials Research) has organised and performed a series of four metal detector trials [7][8]. The last of these trials was performed in Benkovac, Croatia in May 2005. That trial was conducted at the test site of the Croatian Mine Action Centre – Centre for Testing, Development and Training (HCR-CTRO) in Benkovac, Croatia. It was conducted according to the procedures prescribed in CWA 14747:2003, CEN Workshop Agreement on testing and evaluation of metal detectors for humanitarian demining [2], with the aim to verify the proposed testing procedures. Maximum detection height measurements and detection reliability tests were performed.

The metal detector models tested in the trials were products of the following companies, listed alphabetically: CEIA, Ebinger, Foerster and Vallon. It has been agreed with the manufacturers to keep the detector models anonymous, so that the models are labelled U, X, Y and Z. The detectors operated on different principles: some were time domain, some frequency domain ones; some used a single coil, some a "double-D" coil; some were static mode detectors, and some dynamic mode ones. All detectors had the possibility of ground compensation.

Two soil types were present in the trials in May 2005. There were four lanes with dimensions 1 m × 29 m, lanes 1 and 2 containing a highly magnetic soil from the surroundings of the town Obrovac, and lanes 3 and 4 containing a magnetically rather neutral soil from the area around the town Sisak.

Two mine types modified to be safe were used as targets: PMA-2 and PMA-1A. The PMA-2 is a minimum metal mine, the hardest to detect in south-eastern Europe. A surrogate of PMA-2 labelled PMA-S was used too, but only for the maximum detection height measurements. Each lane contained five mines PMA-2 buried just below the surface, five buried to 5 cm depth and five to 10 cm depth, measured to the top of the mine. The PMA-1A mines were buried similarly, but to depths 5, 10 and 15 cm.

The operators were experienced deminers of CROMAC (Croatian Mine Action Centre). They went through a one-day training for each detector model. Each of them performed one or two runs (i.e. one or two passes through a lane) per day.

3.2 Maximum detection height measurements, design of experiment

In earlier investigations it has been conjectured that repeated maximum detection height measurements give very similar results. The experiment described in this article had been designed to check this conjecture of the stability of metal detectors.

The maximum detection height measurements were performed with a full factorial design, meaning that all combinations of factor levels were present in the experiment. The investigated factors were: detector model, operator, target-soil combination. Two series of maximum detection height measurements were performed: one during the detection reliability test and the other afterwards. They both contain the same measurements; they were just performed in a different order.

The goals of this test were:

1. To assess the variability of the maximum detection height measurements.
2. To compare the detecting capabilities of four metal detectors in two soil types separately.
3. To compare the surrogate of the PMA-2 with the real mine, using the in-air measurements.
4. If the surrogate faithfully represents the real mine, to use it for comparing the two soils used in the experiment.

The first series of measurements was performed according to the design of the reliability test (see section 3.3). This series is described in more detail in the trial final report [8]. The measurements of the second series were performed according to the design presented in Table 1. PMA-S is a surrogate of the PMA-2. This is a full factorial design, meaning that all combinations of factor levels are present. The in-air measurements on the PMA-2 and the PMA-S were performed one after the other, in a random order. The execution order of starts was arranged to avoid bias, i.e. a systematic influence of unknown factors related to time (for example, gradual increase of the deminers' concentration or fatigue). If there was such an influence, it was "distributed" to all detector models equally. The operators set up the detector before each start and performed the ground compensation before the in-soil measurement. The targets were buried to depths up to 15 cm in steps of 1 cm and their positions were visibly marked.

3.3 Detection reliability tests, design of experiment

The four factors investigated in this test are detector model, operator, lane (related to the soil type), and start. A factorial design including all factor level combinations would be the optimum choice to achieve an unbiased estimate of the detectors in each soil type separately. However, such a test would require a lot of time. This is why a fractional factorial design had been proposed: each detector is tested with each level of each factor, but not with all the possible combinations of factor levels. This design is based on a Graeco-Latin

square and it is shown in Table 2. In the first week two operators (A, B) tested two detectors (alpha, beta) and the other two operators the other two detectors. In the second week they switched (A and B tested gamma and delta). Such a design, compared with an ordinary Graeco-Latin square, allowed the operators to concentrate on two in stead of four detector models in a week.

Tab. 1. Design of the maximum detection height measurements. The variable "start" indicates the order of execution. Numbers 1, 2, 3 indicate the random order of execution of the measurements within a start. The in-air measurements were executed before the in-soil measurements, but within the same start.

			in-air			in soil of lanes 1, 2	in soil of lanes 3, 4
start	operator	detector	PMA-1A	PMA-2	PMA-S	PMA-2	PMA-S
1	C	beta	*1*	*2*	*3*	*1*	*2*
2	D	alpha	*1*	*3*	*2*	*2*	*1*
3	A	delta	*1*	*2*	*3*	*2*	*1*
4	B	gamma	*3*	*2*	*1*	*1*	*2*
5	A	alpha	*1*	*3*	*2*	*1*	*2*
6	B	beta	*1*	*3*	*2*	*1*	*2*
7	C	gamma	*1*	*2*	*3*	*1*	*2*
8	D	delta	*1*	*3*	*2*	*1*	*2*
9	A	gamma	*3*	*2*	*1*	*2*	*1*
10	B	delta	*3*	*1*	*2*	*1*	*2*
11	C	alpha	*3*	*2*	*1*	*2*	*1*
12	D	beta	*1*	*3*	*2*	*2*	*1*
13	C	delta	*3*	*2*	*1*	*2*	*1*
14	D	gamma	*1*	*2*	*3*	*1*	*2*
15	A	beta	*1*	*2*	*3*	*1*	*2*
16	B	alpha	*3*	*2*	*1*	*1*	*2*

Tab. 2. Design of the detection reliability test. The design is based on a Graeco-Latin square, letters A, B, C, D representing the operators, and alpha, beta, gamma, delta the detectors.

Week 1
18-20 May

Lane \ Start	1	2	3	4
1	A alpha	C delta	B beta	D gamma
2	C gamma	A beta	D delta	B alpha
3	B beta	D gamma	A alpha	C delta
4	D delta	B alpha	C gamma	A beta

Week 2
25-27 May

Lane \ Start	1	2	3	4
1	C alpha	A delta	D beta	B gamma
2	A gamma	C beta	B delta	D alpha
3	D beta	B gamma	C alpha	A delta
4	B delta	D alpha	A gamma	C beta

4 Results of the Benkovac trial, May 2005, compared with the results of earlier trials

4.1 Results of the maximum detection height measurements

This section discusses some results of both series of maximum detection height measurements.

One of our goals was to compare the metal detectors in a specific soil. Assuming that the maximum detection heights for a specific detector-target-soil combination are independently normally distributed, we can perform some statistical tests to examine the differences between the detectors. Before doing that, it is usually helpful to present the results in a simple diagram. Fig. 1 contains the results of both measurement series. The indicated error bars are the sample standard deviations. The results of a t-test with a significance level $\alpha = 0.05$ for the soil from lanes 1 and 2 show a significant difference between all detectors except between detectors U and X and between Y and Z. In the soil from lanes 3 and 4 the only significant differences are between X and Y and between X and Z.

Let us compare the PMA-2 with its surrogate, PMA-S. The in-air measurements were analysed as paired measurements. This means that the difference between the measurements on these two targets within the same start (see Table 1) is analysed as a normally distributed variable. The result indicates that the maximum detection height of the real mine is (9.4±6.6) mm larger than that of the surrogate, where (9.4 ± 6.6) mm marks the 95% confidence limits. This result indicates that in some cases the PMA-S can be used as a surrogate of the PMA-2, since it is just a bit more difficult to detect. However, the difference is not small enough to allow the comparison of the results in two soils as if the two targets were identical.

Many metal detector trials performed before 2005 included some maximum detection height measurements, but almost all of them were performed without repetitions. However, already a quick view on the diagram in Fig. 1 reveals that the variance of the maximum detection height measurements cannot be neglected, thus pointing to the conclusion that repetitions are necessary. Further investigations have shown that the variability of the measurements is caused by the differences between the operators (deminers), by the setup of the devices, and by the remaining sources of the variability, which are the instability of the hardware between two setups, the changing subjectivity of the operators, and the uncertainty of the measurements of the distance between the search head and the target.

4.2 Results of the detection reliability tests

This section presents some of the results of the detection reliability tests performed in Benkovac in Croatia, in May 2005.

The following three diagrams are ROC diagrams are based on the complete data set, i.e. all levels of all factors: both mine types, both soil types, all four detectors and all four opera-

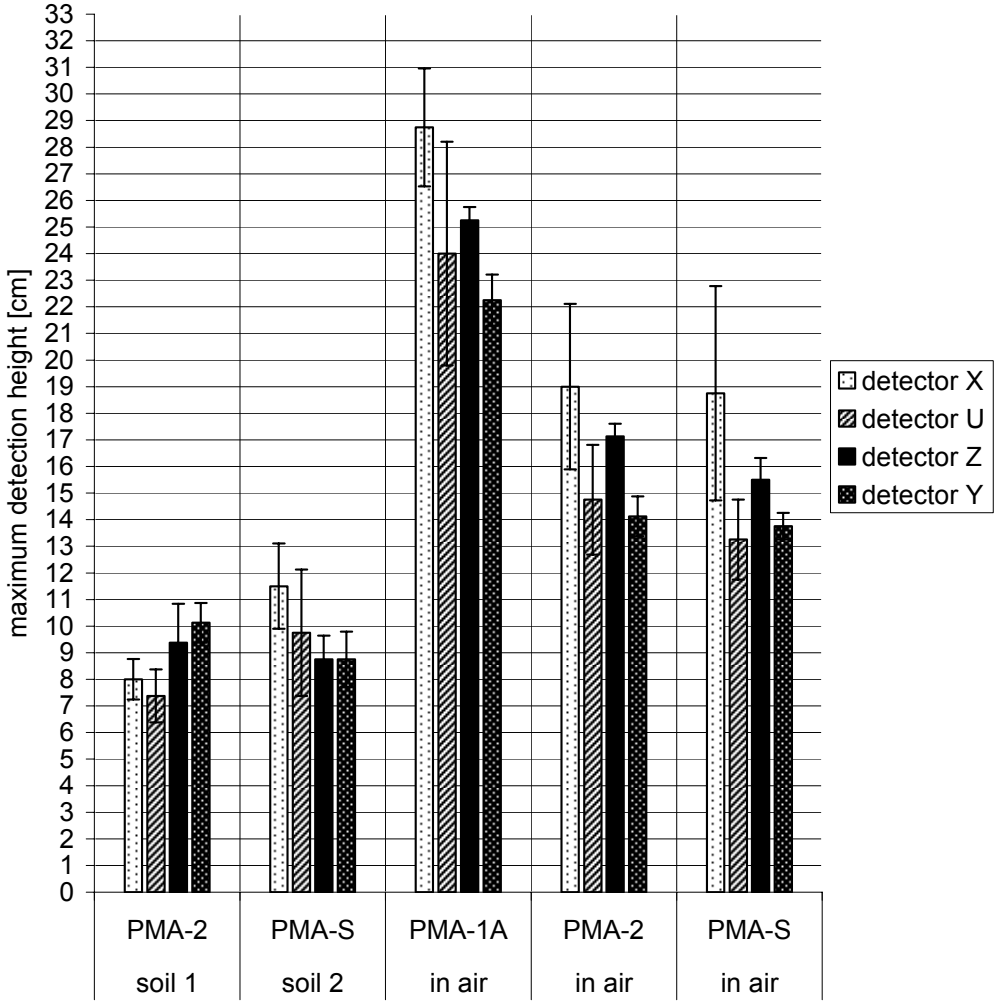

Fig. 1. Results of the maximum detection height measurements. The error bars indicate the estimated standard deviations.

tors. The first diagram, Fig. 2, shows the differences between the four detector models tested in the trials. The diagram on Fig. 3 clearly shows that all operators performed similarly: no significant differences were detected between the deminers' results. This is a consequence of the choice of skilled deminers, an adequate training, and the applied working procedures, which were close to the actual working conditions. The same was observed throughout the whole analysis, for any choice of targets or soils. The importance of operators involved in the trials has proven in all trials of demining equipment, but also in tests of NDT (non-destructive testing) detection systems [5], [6]. It has been shown that the human factor (skill of the operators and the testing procedure) can significantly influence the test results. A comparison with earlier tests in Benkovac and Oberjettenberg [7], [8] reveals a notable improvement of the test results, mostly due to human factor improvements. This can be seen in Fig. 4 and Fig. 6. Fig. 4 is a ROC diagram comparing the results of the BENKOVAC 2003 and 2005 trials. Only the factor levels common to both trials are included in the analysis.

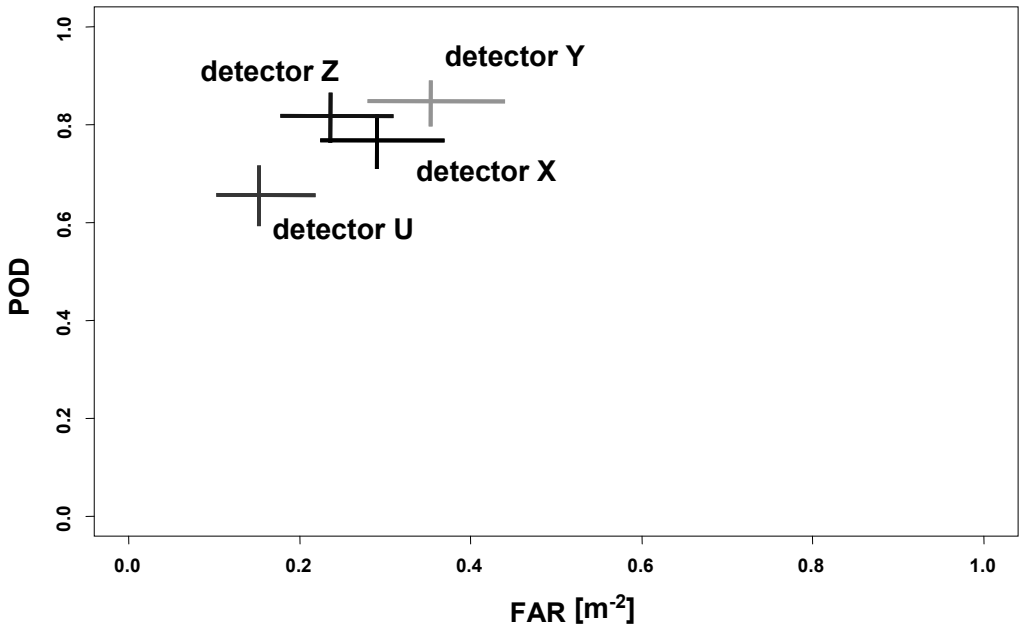

Fig. 2. Overall results, comparison of detector models. The size of the crosses indicates 95% confidence intervals.

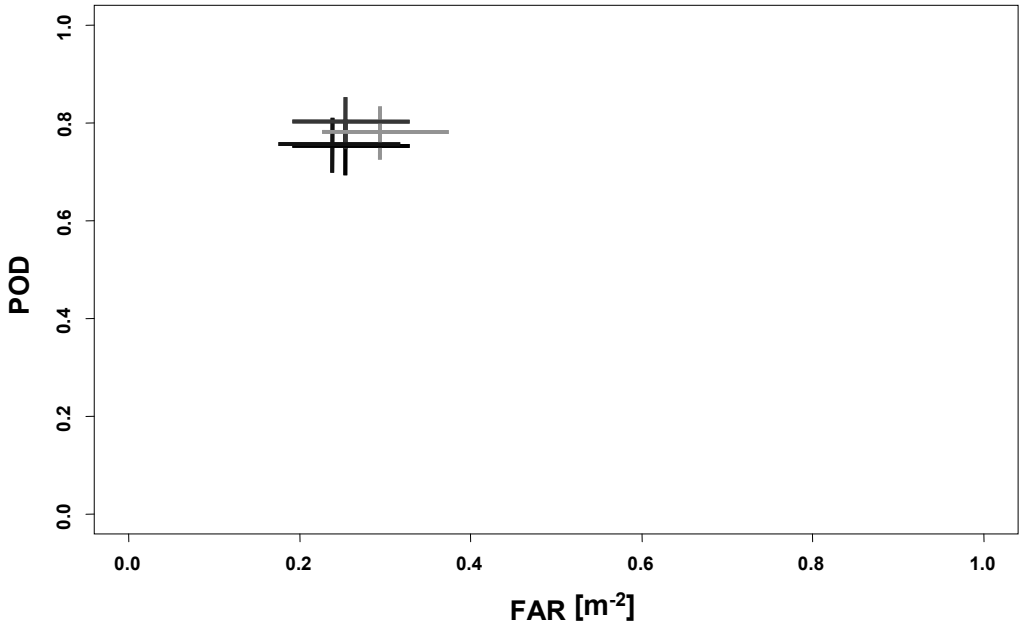

Fig. 3. Overall results, comparison of operators A, B, C and D. The size of the crosses indicates 95% confidence intervals.

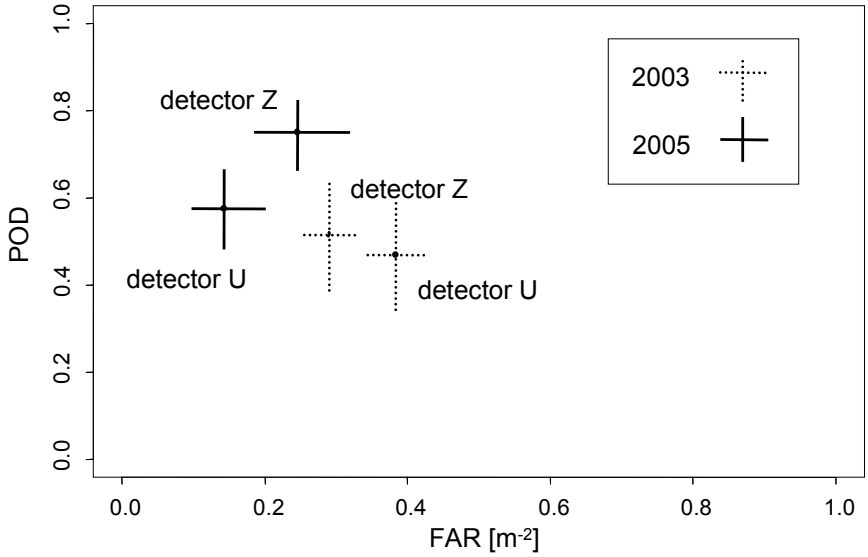

Fig. 4. Comparison of Benkovac 2003 and 2005 trials, ROC diagram. Only the factor levels common for the two trials are selected: PMA-2 at depths 0, 5 and 10 cm in Obrovac soil and Sisak soil, detectors Z and U. The size of the crosses indicates 95% confidence limits.

The next diagram (Fig. 5) presents the estimated POD curve (POD versus depth) with the corresponding confidence bounds for the selected case of PMA-2 in the soil from Obrovac area. The mine PMA-2 has the smallest metal content in the region of South-Eastern Europe. The soil from Obrovac is very difficult for metal detectors due to its magnetic properties, causing many false alarms, so that ground compensation is necessary. We can see from the diagram that detector Y, which has the highest total POD, can reliably detect the PMA-2 in the soil from Obrovac only if it is buried shallowly. Fortunately, the vast majority of mines is buried very near the surface.

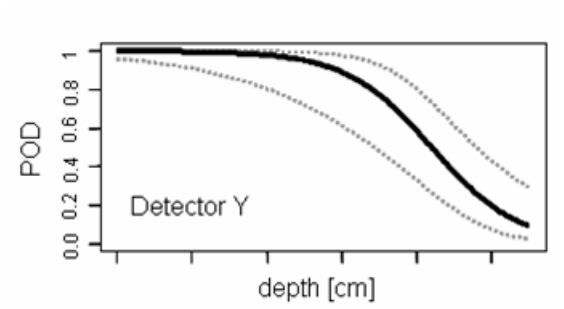

Fig. 5. POD curve, the results of detector Y in lanes 1 and 2 on the target PMA-2. The dotted curves indicate 95% confidence bounds.

Let us compare this result with the maximum detection height measurements with the same choice of detector, soil and target. The largest value being detected is (9.6 ± 0.6) cm. The best estimate of the maximum detection height is that value increased by 0.5 cm, because the targets were buried to depths in steps of 1 cm. Thus we have the estimated maximum detection height: (10.1 ± 0.6) cm. We see from Fig. 5 that many mines at that depth and even at smaller depths than (10.1 – 0.6) cm = 9.5 cm were not detected in the reliability

test. The main reason is that the operators did not know the positions of the targets during the reliability test. However, the human factor is not the only cause of this effect. There are some other sources of variation involved with blind trials. The depths of the targets can not be controlled so well as during the maximum detection height measurements. Each target is placed on another location, and the local properties of soil can vary. All these influences introduce higher unavoidable errors, both for the POD and for the target depths. This is why the POD curves obtained from a reliability trial will not fall with depth that abruptly as expected from the maximum detection height measurements. The analysis of the other detectors leads to the same conclusions.

Fig. 6 is a comparison of the POD curves of the Benkovac 2003 and 2005 results. Again we see, as in Fig. 4, a notable improvement of the test results. An important consequence of the improvements of the human factor treatment is the increase of the POD for smaller depths. This is mostly a consequence of better pinpointing, i.e. localisation of the target.

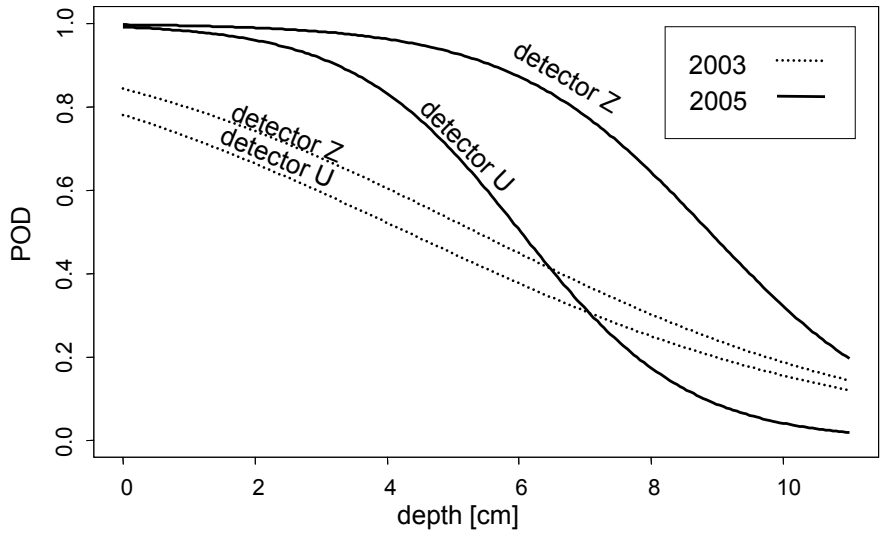

Fig. 6. Comparison of Benkovac 2003 and 2005 trials, ROC diagram. Only the factor levels common for the two trials are selected: PMA-2 at depths 0, 5 and 10 cm in Obrovac soil and Sisak soil, detectors Z and U.

5 Conclusions

Statistical design of experiment enables unbiased conclusions and minimises the experimental error, thus enabling shorter trials with lower expenses. Conclusions are unbiased when it is possible to separate the influences of different factors, for example, the influence of the detector model from the influence of the operator. Design of experiments is the only way to deal with complex experimental problems like metal detector tests.

Maximum detection height measurements are easier to perform than the more time consuming detection reliability tests. However, detection reliability tests include a large part of the human factor influences, and so come closer to actual conditions in demining. Besides, the false alarm rate can be estimated only in reliability tests. The maximum detection

height measurements should be performed with several operators and with repetitions, since they have a variance that has to be taken into account.

A comparison of the Benkovac 2005 and 2003 trials shows a notable improvement of the test results. That improvement is a consequence of a reduced time pressure on the operators, improved training and the application of some elements of the local demining practise.

ROC diagrams, POD curves and results of maximum detection height measurements are planned to be included in annual catalogues of demining detection equipment.

6 References

[1] Bruschini, C.: *A Multidisciplinary Analysis of Frequency Domain Metal Detectors for Humanitarian Demining*. PhD thesis, Vrije Universiteit Brussel, September 2002. Available at http://www.eudem.vub.ac.be/.

[2] CWA 14747:2003, *CEN Workshop Agreement, Humanitarian Mine Action – Test and Evaluation – Metal Detectors*, June 2003. Available at http://www.itep.ws/.

[3] Box, G. E. P.; Hunter, W. G.; and Hunter, J. S.: *Statistics for Experimenters*. John Wiley & Sons, 1978.

[4] Montgomery, D. C.: *Design and Analysis of Experiments*. John Wiley & Sons, third edition, 1991.

[5] Müller, C.; Fritz, T.; Tillack, G. R.; Bellon, C.; and Scharmach, M.: Theory and Application of the Modular Approach to NDT Reliability. *Materials Evaluation*, 59(7):871–874, 2001.

[6] Müller, C.; Scharmach, M.; Konchina, V.; Markucic, D.; and Piscenec, Z.: General Principles of Reliability Assessment of Nondestructive Diagnostic Systems and its Applicability to the Demining Problem. In *8th European Conference on Non-Destructive Testing (ECNDT 2002)*, Barcelona, Spain, 17-21 Jun 2002.

[7] Müller, C.; Gaal, M.; Scharmach, M.; Ewert, U.; Lewis, A.; Bloodworth, T.; Wilrich, P.-T.; and Guelle, D.: *Reliability Model for Test and Evaluation of Metal Detectors*. Final report of the ITEP Project 2.1.1.2, Federal Institute for Materials Research and Testing (BAM), Berlin, Germany, September 2004. Available at http://www.itep.ws/.

[8] Müller, C. et al: *Reliability Model for Test and Evaluation of Metal Detectors – Part 2*. Final report of the ITEP Project 2.1.1.8, Federal Institute for Materials Research and Testing (BAM), Berlin, Germany, September 2004. The report will soon be published; it will be available at http://www.itep.ws/.

Measurement uncertainty and risk analysis – examples from civil engineering products

Wilfried Hinrichs
Materialprüfanstalt für das Bauwesen Braunschweig (Germany)

Abstract: Measurement uncertainty may have a significant impact on decisions on a product's compliance with a specification. At the moment, in practice, this problem is usually treated on a qualitative or half-quantitative basis. This contribution presents quantitative models on how to link statements on measurement uncertainty and risk analysis and how this information can be used in compliance assessment. The application of the models is demonstrated in three examples. An important result of the investigation is that the probability of wrong decisions is considerably high both in classification and in statements on compliance of civil engineering products.

1 Introduction

1.1 General

In principle, new constructions meet requirements both of the owners and/or the users when four preconditions are met:

- The static system is correct.
- All reasonable loads have been taken into account.
- The construction materials have been carefully chosen.
- The realisation of the building was quality-driven.

As usability and safety are key issues in construction the probability of severe deviations from these requirements is usually very small, i.e. in a range of $p = 10^{-4} \ldots 10^{-5}$. With additional effort it is quite easy to reach even $p = 10^{-10}$. In practice, substantial mistakes in planning mainly arise from the dimensioning for bearing loads and from calculation with wrong units. This is not the subject of this contribution but it focuses on specifications for construction products and their compliance with the appropriate limit values on the background of the third and the fourth bullet above. The emphasis lies on market aspects, i.e. the question whether the materials and the constructions are in accordance with a contract.

A statement of non-compliance does not necessarily mean that the technical usability is questionable but it may have substantial financial consequences for the supplier.

1.2 Measurement uncertainty

Every measurement results is associated with an uncertainty which may be relevant in two quite different areas:

- One source of an uncertainty problem is an incomplete validation[1] of a test procedure. As a validation of test procedures is a prerogative in standardization which includes the measurement uncertainty undefined risks should not emerge from normative documents. However, this is not always the case as reported below.
- The other area is the process of compliance assessment itself which is the fulfilment of specified requirements. When assessing the compliance of a given product on the basis of a test result a decision may have to include the uncertainty associated with the test result. This is rarely done in practice.

1.3 Risk analysis

Due to measurement uncertainty there is always a certain probability that a decision about the acceptance or rejection of a product is wrong. It is possible to quantitatively address the probability using risk analysis procedures if quantitative data for the measurement uncertainty are available. A feasible approach is outlined in an international discussion paper which links risk analysis with measurement uncertainty and conformance testing [1].

The instruments for estimating probabilities for wrong decisions in compliance assessment are same whether the choice of the underlying tolerances was safety-driven and functionality-driven but the consequences are quite different. On the one hand a wrong decision may decrease the safety level unacceptably [2] or it may increase it to an inadequate extent. On the other hand construction products with wrong dimensions may cause direct reactions such as a rejection from the construction site.

1.4 Risk assessment

Quantitative details on the risk of making wrong decisions in compliance assessment which encompass measurement uncertainty are mostly lacking. In the areas investigated neither the test nor the product standards provide any help. This situation is by no means exceptional. In principle, assessment bodies are aware of the problem but it is often hardly possible to address it. Both clients and other parties involved do not want to be confronted with (avoidable) problems and a certification body would usually not have all necessary information to professionally include the results of a risk analysis in its decision.

Therefore in practice, measurement uncertainty is no issue in decisions on compliance. This situation is far from being satisfactory. Strictly speaking, in compliance assessment a

[1] Validation is the confirmation that the particular requirements for a specific use are fulfilled.

test result as such is not important: Relevant is the statement whether or not the product meets specified requirements. But as all decisions are wrong to a certain degree users of certificates should get information on the reliability of a decision. That could be done by a quantitative statement on the probability to what extent a decision may be right or wrong.

2 Models

This contribution reports about the evaluation of different models for risk analysis in compliance assessment which are presented as examples from different fields of civil engineering. Theoretically speaking, the background is how the result of the validation of a test procedure may influence the result of a compliance assessment. The basic question is therefore simply: **To what extend does the measurement uncertainty of an applied test procedure influence the probability of making a wrong decision?**

2.1 Model for measurement uncertainty

There are two basic sources of uncertainty in materials testing: the intrinsic properties of the substance as regards its internal homogeneity, texture etc and extrinsic phenomena like sampling and test procedures, environmental conditions etc. In the last years the international laboratory community has put much effort into the investigation of the extrinsic source, i.e. in measurement uncertainty. That has been triggered especially by the harmonization of requirements in quality management such as ISO/IEC 17025 [3]. The process is far from being at an end as the implementation of concepts and procedures are difficult and are also prone to incomparability. But in this course both the knowledge about specific aspects of uncertainty is broadening and the amount of reliable data on measurement uncertainty is increasing.

In many branches of civil engineering data on measurement uncertainty are rare as explicit information. But there are various sources of implicit data that may be used so that it is in many cases generally possible to arrive at quantitative data. The basic ideas of the international discussion in measurement uncertainty are accessible through different sources of uncertainty data [4] which are usually described by their evaluation procedure:

- The modelling (or mathematical) approach
- The single laboratory validation approach
- The interlaboratory validation approach
- The proficiency testing approach

The wide spectrum of such concepts to get quantitative uncertainty data opens the gate to an analysis of the risks that reflect on the measuring and/or testing procedure. However, the reliability of such data is often not sufficiently known. It is therefore of major importance to check what information these data really contain. That means for practical applications that an answer to the question is needed on how realistic the uncertainty data for the purpose of their use are.

2.2 Model for risk analysis

For risk analysis purposes a distinction between usability and the compliance of a product is irrelevant. This aspect must be addressed in the risk assessment, i.e. in the evaluation of the results. A decision on the usability of a product is a deeply technical question whereas statements on compliance are aiming at whether or not a product is fit for putting it on the market. Its technical aspect is more hidden: The putting-on-the-market is a commercial activity but it usually also means that the product is fit for putting it in service which is again a technical issue.

One focus of the international discussion in treating measurement uncertainty is its influence on statements in compliance assessment. JCGM/WG1/SC3 have produced a draft document [1] which links measurement uncertainty and conformance testing. The scope of this draft Technical Report specifies that it '*provides guidelines for setting gauging (or test) limits in support of accept/reject decisions in ... general conformance tests where uncertain numerical test results are compared with specified requirements.*' The paper provides detailed information on the theoretical background, on conditions, on procedures etc. A main figure is P_C which is the probability of conformance. Provided a Gaussian distribution of the test results the formula runs as follows:

$$P_C = \Phi\left(\frac{T_U - x_m}{u_m}\right) - \Phi\left(\frac{T_L - x_m}{u_m}\right) \tag{1}$$

with P_C probability of conformance

T_L lower tolerance limit

T_U upper tolerance limit

x_m test result

u_m measurement uncertainty associated to the test result x_m

From a mathematical point of view it is not necessary to differentiate between types of the origin of uncertainty data. But as the results of such calculations are not comparable it is useful to specify different probabilities and to concentrate on the basic question of this contribution. Firstly, the probability of making a wrong decision is expressed as the probability of non-compliance P_{NC}. Secondly, it is necessary to distinguish some types of probabilities of non-compliance, mainly because in practice there are two main testing situations:

- In factory production control test results are produced under very similar circumstances, i.e. personnel, instruments, environmental conditions etc. This is a first party (producer) business. In interlaboratory validation testing s_r is used as the standard deviation for the repetition of measurement as defined in ISO 5725-2 [5]. When comparing test results with specifications the term 'conformance testing' is used. The probability of non-compliance in this case is $P_{\mathrm{NC,conformance}}$.
- The spread of test results is usually wider when tests are performed by different persons using similar instruments but, of course, applying specified procedures. This is specific for a third party (impartial laboratory) business. A useful term for standard de-

viations under such reproducibility conditions is s_R as defined in ISO 5725-2. This is a 'conformity testing' with $P_{\mathrm{NC,conformity}}$ as the probability of non-compliance in these situations.

- Figures both for the repetition and reproduction are well understood in the laboratory community as they are linked with interlaboratory validation schemes. The situation is different with other kinds of uncertainty data because they usually need further explanation. The probability of non-compliance is specified as $P_{\mathrm{NC,model}}$.

The transformed formula runs as follows:

$$P_{NC,x} = 1 - \left[\Phi\left(\frac{T_L - x_m}{u_x} \right) + \Phi\left(\frac{T_U - x_m}{u_x} \right) \right] \qquad (2)$$

with $P_{NC,x}$ specific probability of non-compliance
T_L lower tolerance limit
T_U upper tolerance limit
x_m test result
u_x measurement uncertainty associated to the test result x_m

2.3 Assessment of non-compliance

When assessing compliance the model input data both of the risk analysis and of the measurement uncertainty must be quantitatively known. A statement on non-compliance encompasses the measurement uncertainty approaches used.

The problem with test results close to specification limits is an old one. The treatment of such situation in practice is a formal rather than a mathematical or a technical one. As the procedures are internationally quite different, an international discussion in measurement on this subject has just started. An example is given in a draft for public comment [6].

3 Examples

Aggregates for concrete and fire protective products are tested before putting them in service. The evenness is usually tested immediately after completion of a floor.

3.1 Risk analysis

Formula (2) allows to directly calculate the probability of non-compliance P_{NC}. As most laboratory people are more familiar with P_C, the probability of compliance is presented in the diagrams.

3.1.1 Aggregates for concrete

EN 12620 [7] specifies aggregates for concrete. It refers to numerous properties. Nearly all test procedures specified in the product standard contain information on precision data in

informative annexes. Two examples are treated here: the Flakiness index *FI* and the content of acid-soluble sulphates *MS* of an aggregate product (table 1).

Requirement	Test procedure	Standard deviations
Flakiness index (FI)	EN 933-3	$s_r = 0{,}001 \cdot \sqrt{\frac{FI \cdot (100 - FI) \cdot D^3}{M}}$ $s_R = 0{,}082 \cdot FI + 0{,}343$
Magnesium sulphate index (MS)	EN 1367-2	$s_r = 0{,}054 \cdot \sqrt{MS \cdot (100 - MS)}$ $s_R = 0{,}188 \cdot \sqrt{MS \cdot (100 - MS)}$

Table 1: Uncertainty data of test results of aggregates

The Flakiness index *FI* represents a geometrical property of an aggregate. It is important both for the workability of the material and the necessary amount of cement in concrete. The content of magnesium sulphates *MS* indicates how much of $MgSO_4$ would be introduced in the concrete with the aggregate. The substance is harmful for the durability of concrete.

EN 12620 specifies 5 product categories for *FI* (FI_{15}, FI_{20}, FI_{35}, FI_{50} and $FI_{>50}$) and 4 for *MS* (MS_{18}, MS_{25}, MS_{35}, $MS_{>35}$). The appropriate category is chosen on the basis of test results. For CE-marking it has to be formally stated in a declaration of conformity by the supplier. This document is therefore an important basis for contracts. The buyer of aggregates will compare the data with his requirements usually specified in an advertised bidding.

Graphs for the sums of the relative distributions of the probability of compliance P_C are given in Fig. 1 and Fig. 2. The small line is for results arrived at under repetition conditions (conformance testing), the bold line is based on data from reproduction (conformity testing). More details are given in [8].

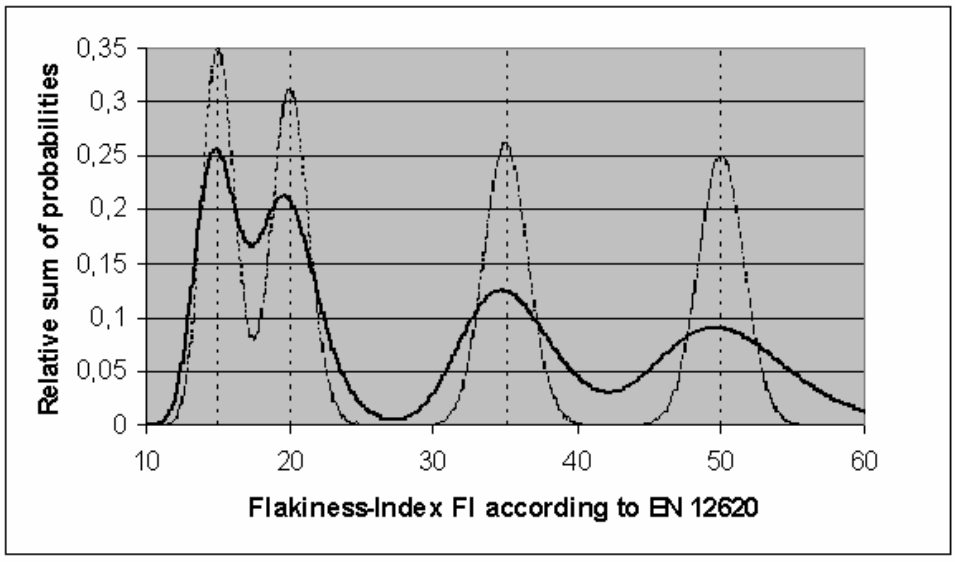

Fig. 1: Classification for the Flakiness-Index of aggregates

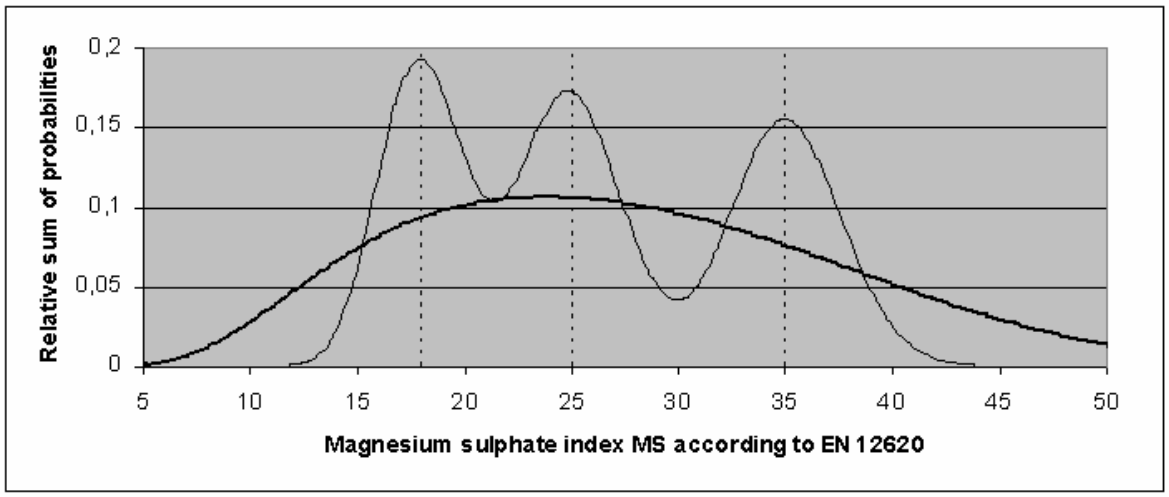

Fig. 2: Classification for the magnesium sulphate index MS of aggregates

3.1.2 Fire protective products

A basic requirement of fire protective products is the reaction to fire. That means that the material must not only withstand fire attacks but it shall also not contribute to the development of a fire. Technical approval papers call for a non-combustibility test according to ISO 1182 [9]. This standard contains quantitative data on the precision of test methods. They include the increase of temperature (ΔT) and the flaming time (t_f) which were produced in interlaboratory comparisons and in proficiency testing (table 2):

Parameter	Standard deviations
Increase of temperature ΔT	$s_r = 1{,}26 + 0{,}10 \cdot \Delta T$
	$s_R = 0{,}96 + 0{,}26 \cdot \Delta T$
Flaming time tf	$s_r = 0{,}14 \cdot t_f$
	$s_R = 0{,}32 \cdot t_f$

Table 2: Uncertainty data of test results of fire protective products

Fig. 3 and Fig. 4 show the sums of the probability of compliance P_C for ΔT and t_f. Again the small line is for conformance testing, the bold line for conformity testing.

3.1.3 Industrial floors

Evenness or flatness of industrial floors is a basic requirement which necessary ‘degree’ strongly depends upon the intended use. It is usually acceptable that unfinished upper surfaces of floors and concrete bases are more uneven than finished floors or those with more stringent requirements. For example, evenness is an important requirement in warehouses with high fixed path forklift trucks or in similar storages such as archives. Due to dynamic components caused by the movements and impacts of static lean even relatively small geometrical deviations in the floor can reduce the usability of the trucks as regards safety of operation and collision with other trucks.

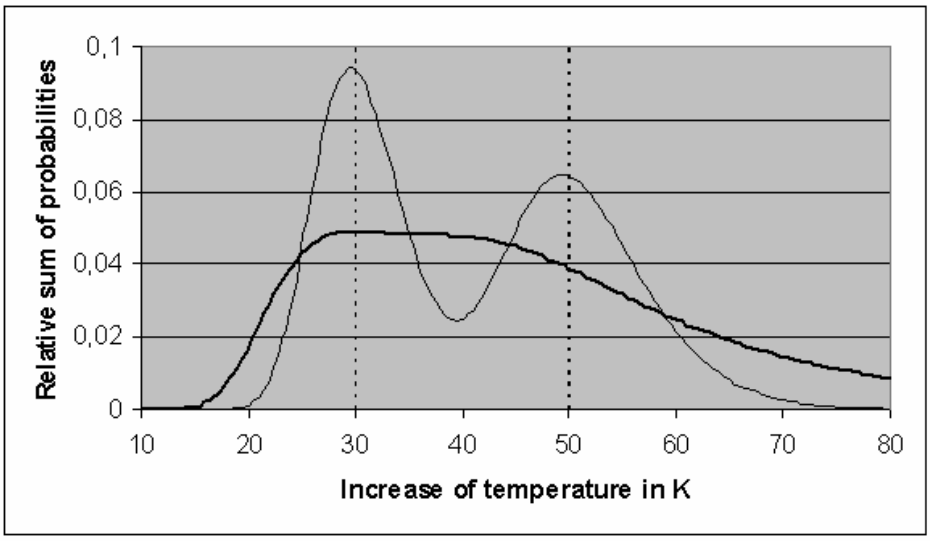

Fig. 3: Classification for the increase of temperature ΔT of fire protective products

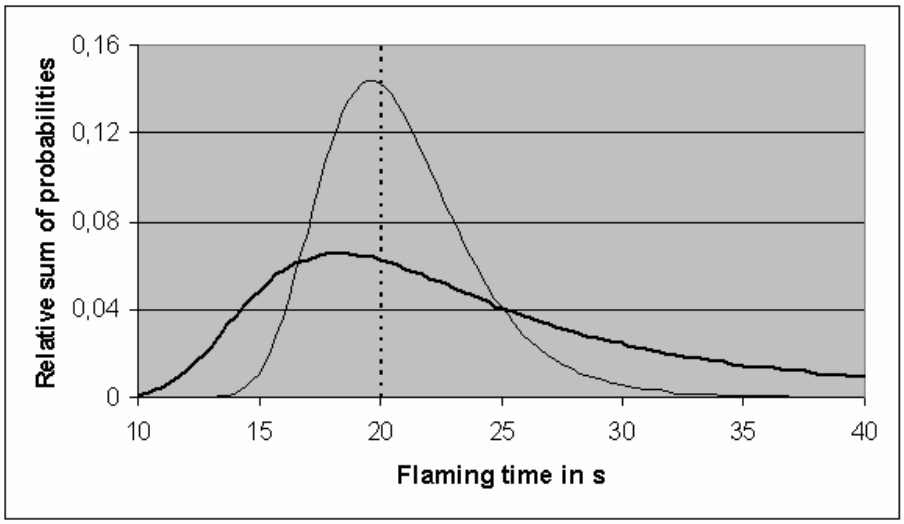

Fig. 4: Classification for the flaming time t_f of fire protective products

DIN 18202 [10] specifies tolerances for evenness in building constructions but it does not prescribe a test method or describe how a survey to check compliance with these limits should be conducted. Two usual methods in evenness testing of industrial floors are:

- Test procedure A: V head and straightedge / aiming stake
- Test procedure B: Grid levelling / area levelling

To quantify the risk associated with results from these methods the measurement uncertainties have been investigated using the modelling, the interlaboratory and the single laboratory validation approaches. Significant systematic components in the uncertainties were found for the test procedure A. The reason is that the V head forms bridges on the surface of the concrete. The resulting measured distance is therefore usually smaller than in reality but it cannot be larger. Further details will be presented in [11].

Independent of the test method applied a significant source of uncertainty is the floor itself. DIN 18202 does not specify how many tests should be conducted. Due to economic reasons their number is always strongly limited, with the effect that the standard deviation of the test result is far from being statistically reliable. In general the numbers of test results should vary strongly. This all leads to considerable uncertainties mainly because the presumption of homogenous surfaces is not realistic in practice. Thus the measurement uncertainty depends on various factors. The main influences are the number of measured distances per square unit, the test method applied and the measuring conditions as the calibration status of the instrumentation and the skill of the personnel. The specific uncertainties have been calculated for favourable and for unfavourable measurement conditions. 'Favourable' does not mean best measurement capability but good practice. Unfavourable conditions are those where the situation is worse than a fair practice would suggest. The results are listed in the table 3. They are valid for a straightedge of 4 m length.

Test procedure	Measurement uncertainty U in mm	Measurement situation
A: V head and straightedge	3,5	Favourable
	7,0	Unfavourable
B: Grid levelling / area levelling	2,0	Favourable
	4,0	Unfavourable

Table 3: Uncertainty data of test results in floor testing

Fig. 5 shows the results of a risk analysis. Given is the probability of a non-conformance P_{NC} of a finished floor (upper limit T_U = 10 mm) under favourable conditions. The numbers locate the limits with P_{NC} = 0,05 or P_{NC} = 0,01 respectively.

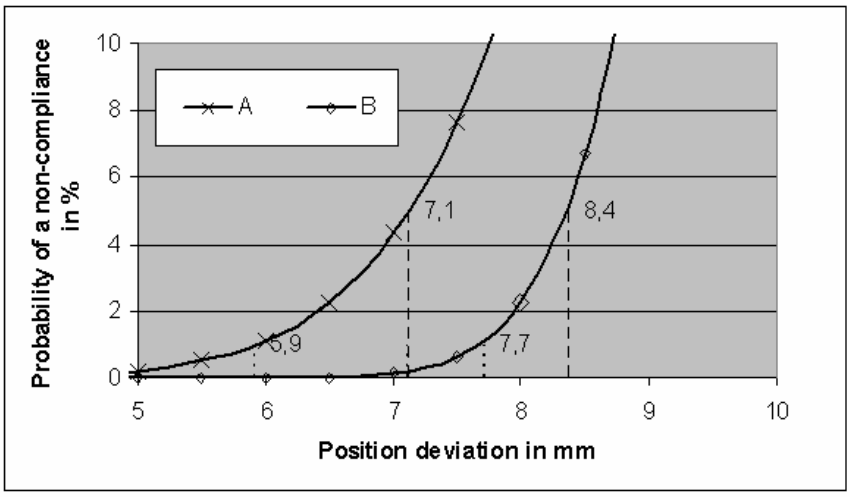

Fig. 5: Critical values for the compliance assessment in floor testing

3.2 Risk assessment

3.2.1 General example

A compliance assessment body (CAB) is asked to certify that a certain product meets a requirement with an upper tolerance limit $T_U = 21$ units and to make a statement on the risk of the certification statement for market use. The appropriate product standard refers to the two slightly different test methods A and B. The client presents two test results: the one for procedure A is 18,9 units, the other for procedure B 18,2 units. Here are three scenarios to what result a risk assessment body could reasonably come:

- Scenario 1: Both test results are below the upper tolerance limit. The requirement is met. The tolerance values encompass all possible measurement uncertainties because that is not explicitly excluded. Additionally both test methods were applied and show a positive result. The reliability of the certification is therefore very high. [The implicit probability PNC for the user is close to 0 %.]

- Scenario 2: The CAB asks both laboratories for the appropriate measurement uncertainty. The one that has chosen test method A reports that the standard deviation is 0,9 units ($\sigma = 1$, normal distribution). It has been taken from the laboratory's internal documentation based on repeatability studies. The other laboratory informs that for test method B the standard deviation is 1,1 units. This figure is mentioned in a laboratory's internal validation document. The CAB calculates a probability of non-compliance of 1 % for method A. The CAB assumes that $\sigma = 1$ and normal distribution are correct: PNC ≈ 0,6 %.

- Scenario 3: The CAB has an own risk management procedure for certification purposes which also addresses the measurement uncertainty. This document states that the calculation of compliance should generally be done using appropriate uncertainty data. It says that reproducibility data shall be used for certification purposes. The CAB asks the laboratories specifically for these data and gets the information that an annex to the test standard specifies reproducibility limits s_R which are 2,6 units for test procedure A and 2,9 units for B. That leads to PNC ≈ 7,4 % for method A and PNC ≈ 4,0 % for method B.

The CABs in the scenarios arrive at quite different results. The task called for some considerations about the risk of the decision. In the first scenario it has been formally handled with reference to the specification limit and to general contractional conditions. In the second scenario the CAB looked at the measurement uncertainty but used data for in-house testing. In the third scenario the CAB was well aware of the client's task.

3.2.2 Results of the investigation

In order to make the results better comparable the figure R_{rel} is used. It normalizes the width of a safe-guard band for compliance assessment and is defined as:

$$R_{rel} = \frac{T_U - x}{T_U} \tag{3}$$

with R_{rel} relative width of a safe-guard band
T_{U} upper tolerance limit
x measurement value at a defined PNC

Table 4 shows that in the areas investigated the probabilities for wrong decisions are sometimes highly significant. Based on a risk management as outlined in the third scenario a CAB would have to ask the client for acceptable P_{NC} for wrong decisions.

Parameter	TU	Rrel in %	
		PNC = 5 %	PNC = 1 %
Aggregates for concrete			
Flakiness index FI	30	14	18
Magnesium sulphate index MS	25	43	55
Fire protective products			
Increase of temperature ΔT	30	34	42
Flaming time tf	20	24	41
Flatness of industrial floors			
V head and straightedge	10	29	41
Grid levelling / area levelling	10	16	23

Table 4: Results for P_{NC} = 0,05 or 0,01 respectively

4 Conclusions

The probability of wrong decisions in compliance assessment depends upon its specific aim (statements on compliance with general specifications or on conformance, conformity c_i), on the associated measurement uncertainty u_m if the decision is based on laboratory results, on systematic components u_{sys}, on measurement conditions m_c etc. Hence P_{NC} is influenced by various factors:

$$P_{NC} = f\left(c_i, u_m, u_{sys}, m_c, \ldots\right) \tag{4}$$

with c_i specific aim of assessment
u_m measurement uncertainty
u_{sys} systematic component to the measurement uncertainty
m_c measurement conditions

Some or all of these influences may be significant. The investigation showed that it is quite improbable that the measurement uncertainty in general may have a significant and direct impact on aspects such as usability or safety. But it may affect, for example, the safety level.

In conformance assessments the measurement uncertainty is usually of minor importance as a repetition of measurement is usually less uncertain and systematic components are often unimportant. The probability of wrong decisions may especially be important with

conformity testing because here u_{sys} and m_c have to be taken quantitatively into account. This has been illustrated in detail in the course of the presentation of the three examples.

The problem with measurement uncertainty in the certification of construction product properties is an old one – and it is well known. The onus to handle the measurement uncertainty lies with the specialised laboratories but it remains in the responsibility of certification assessment bodies to cope with the problem. However, in practice, this fact is often ignored or at least underestimated. The usual concept to compare test results, i.e. more or less random numbers, with specification data is not appropriate from a risk management point of view. In an advanced certification process it is possible to assign an appropriate probability of the 'validity' of the statement.

Safety relevant products call for additional measures. If laboratories are involved in such reliability studies they should use strategies on how to contribute to the input of relevant data. This problem is, for example, outlined in the contribution made by SCHNETGÖKE et al [12]. Measurement uncertainty data may have two general influences on the reliability assessment of a construction. Firstly, they may affect the precision of the model through its calibration. An example is the significant influence of the dispersion of the yield point of steel on the reliability of a construction. Secondly, they may contribute to the 'weak points' when used in the assessment of the measurement values. This should especially be the case for systematic errors, at least if used as absolute figures. Data should also be available, for example, in the course of the selection of appropriate sensors.

In some cases further influences on compliance statements which are only touched in this contribution are the sampling, the identification and number of measurement spots, systematic components etc. From this point of view the task of compliance assessment bodies can be strongly supported by laboratories that are well aware of measurement uncertainty and its possible influences on the use of measurement results. In difficult situation that could include services such as testing under more precise conditions, the quantification of systematic components etc.

5 Literature

[1] JCGM/WG1/SC3: Measurement Uncertainty and Conformance Testing: Risk Analysis; Draft 2; October 2003

[2] Hinrichs, W.; Linking conformity assessment and measurement uncertainty – an example; tm – Technisches Messen 73 (2006) 10 (in print)

[3] ISO/IEC 17025:2005: *General requirements for the competence of testing and calibration laboratories*

[4] Eurolab TR No. X/2007: Measurement uncertainty revisited: How to compare and combine uncertainty estimates; draft 1, May 2006

[5] ISO 5725-2:2002: Accuracy (trueness and precision) of measurement methods and results – Part 2: Basic method for the determination of repeatability and reproducibility of a standard measurement method

[6] EURACHEM/CITAC Guidance note: *Use of uncertainty information in compliance assessment*; draft for public comment: April 2006

[7] EN 12620:2002: Aggregates for concrete

[8] Hinrichs, W.: *Conformity assessment of aggregates (in German)*; MIRO Zeitschrift für mineralische Rohstoffe 42 (2006) 4, Seite 13-18

[9] ISO 1182:2002: Reaction to fire tests for building products - Non-combustibility test

[10] DIN 18202:2005: Tolerances in building construction – Buildings

[11] Hinrichs, W.: *Flatness – a risk analysis of test methods*; 6th International Colloquium Industrial Floors '07; Esslingen, January 2007 (in preparation)

[12] Schnetgöke, R.; Klinzmann, C.; Hosser, D.; Reliability-based system assessment of civil engineering structures based on structural health monitoring (in German); Beton- und Stahlbetonbau 101 (2006) 8, Seite 585-595

Method for Risk Assessment in Water Supply Systems

Barbara Tchórzewska-Cieślak, Andrzej Włoch
Faculty of Civil and Environmental Engineering, Faculty of Mathematics,
Rzeszow University of Technology

1 Introduction

The aim of the analysis of risk connected with water supply system (WSS) operating is to create a basis of substantial critical information necessary in decision making process, process optimisation, system operating and control and while the protective actions preventing occurrence of unfavourable consequences of events are undertaken.

Lately BAYES' formula has become the basis to develop the theory and algorithms of the probabilistic deduction. BAYES' analysis is used to describe the reason of the situation in which the occurrence of the given event depends on the occurrence of the other event as well as the situation in which necessary knowledge is uncertain or incomplete.

Let Ω means a space of all the events. Events X and Y will be called independent if the occurrence of one of them has no impact on the occurrence of the other one. $P(X)$ means the likelihood that event X occurs. The likelihood that event X occurs assuming that event Y took place is marked as $P(X|Y)$ and is called the conditional likelihood. The notation $X+Y$ means the sum and $X \cdot Y$ the product of events X and Y.

$$P(X \cdot Y) = P(X/Y) \cdot P(Y) = P(Y/X) \cdot P(X) \tag{1}$$

$$P(X + Y) = P(X) + P(Y) - P(X \cdot Y) \tag{2}$$

If events X and Y are independent, then:

$$P(X \cdot Y) = P(X) \cdot P(Y)$$

There is the given event Y and there are such mutually exclusive events $X_1, X_2, ..., X_n$ that $\sum_{i=1}^{n} X_i = \Omega$ and Y can take place only together with one of the events X_i, $i=1,\ldots n$. Then the total (complete) likelihood is defined by the formula [4]:

$$P(Y) = \sum_{i=1}^{n} P(Y / X_i) \cdot P(X_i) \tag{3}$$

2 Uncertainty in WSS operation

Uncertainty concerning WSS operational reliability analysis can relate to:

- fragmentary information (eg. concerning the actual network technical condition),
- inaccurate, imprecise information (eg. concerning failure localisation, ground conditions),
- difficulties in right consequences prediction,
- uncertainty connected with expert's knowledge.

The most basic and the most effective form of knowledge about the so called uncertain environment is the conditional independence, which is described by BAYES' formula. BAYES' theory introduces the so called BAYES'ian likelihood, which means that the likelihood of event changes together with a new premise. It can be useful when we evaluate the likelihood that the given undesirable event occurs on the base of the causal likelihood of that event.

BAYES' theorem is the following: (T. BAYES 1763) [5].

If $X_1, X_2, \ldots X_n$ are such events that $X_i \cap X_j = \varnothing$ for $i \neq j$, $i, j = 1,\ldots n$, $\bigcup_{i=1}^{n} X_i = \Omega$, $P(B_i)>0$ for $i=1,2,\ldots n$ and $P(Y) > 0$, then :

$$P(X / Y) = \frac{P(Y / X) \cdot P(X)}{P(Y)} \tag{4}$$

2.1 An example of BAYES'ian deduction

Water leakage can be located by means of a digital correlator. It was assumed that the likelihood of the event with the positive result of examination (the device indicates water leakage) and when the leakage exists in reality is 0.97 and the likelihood of the event with the negative result of examination (the device did not indicate water leakage) and the presumed leakage does not exist in reality is 0.98. Moreover, it was found that within a year the failures occur in 10 % of water-pipe network kilometre segments.

The following notations have been made:

$P(+)$ - the likelihood of the event that the device will indicate leakage (the positive result of examination),
$P(\neg)$ - the likelihood of the event that the device will not indicate leakage (the negative result of examination),
$P(+\text{failure})$ - the likelihood that the failure in water- pipe network occurs,
$P(\neg\text{failure})$ - the likelihood that the failure in water- pipe network will not occur,
$P(+/+\text{failure})$ – the conditional likelihood of the event; the positive result of examination and in reality the failure in water-pipe network took place,
$P(+/\neg\text{failure})$ - the conditional likelihood of the event; the positive result of examination but in reality the

failure in water-pipe network did not take place,
P(¬/+failure - the conditional likelihood of the event; the negative result of examination but in reality the failure in water-pipe network took place,
P(¬/¬failure) - the conditional likelihood of the event; the negative result of examination and in reality the failure in water-pipe network did not take place.

The particular likelihood values are the following:

P(+failure) = 0,1 P(¬failure) = 0,9
P(+/+failure) = 0,97 P(¬/ + failure) = 0,03
P(+/¬failure) = 0,02 P(¬/¬failure) = 0,98

Next the partial likelihood has been calculated according to the formula for the complete likelihood (3):

P(+/+failure) · P(+failure) = 0,97 ·0,1 = 0,097
P(+/¬failure) ·P(¬failure) = 0,02 · 0,9 = 0,018

The complete likelihood of the event that the device will indicate leakage is:

P= 0,097 + 0,018 = 0,115

Finally the conditional likelihood has been calculated according to the formula (4):

P(+failure /+) - the conditional likelihood of the event that the failure in water-pipe network took place and the result of examination is positive,

P(¬failure/+) - the conditional likelihood of the event that the failure in water-pipe network did not take place in spite of the positive result of reading.

$$P(+\ failure/+) = \frac{P(+/+\ failure)\cdot P(+\ failure)}{P} = \frac{0{,}97\cdot 0{,}1}{0{,}115} = 0{,}8435$$

$$P(\neg failure/+) = \frac{P(+/\neg failure)\cdot P(\neg failure)}{P} = \frac{0{,}02\cdot 0{,}9}{0{,}115} = 0{,}1565\ .$$

Calculated likelihood a posteriori shows that the positive device reading concerning the possibility of the failure in water-pipe network (water leakage reading) comes true in reality with the likelihood ~ 0,84 and does not come true with the likelihood ~0,16.

3 BAYES'ian network basis

Let us consider a configuration of random events mutually connected by cause and effect relation. The occurrence of event X (cause) has some influence on the occurrence of event Y (effect). However, this influence is not "certain" and can be defined only by means of the likelihood. Such configuration of events and their mutual relations can be modelled by means of the directed graph D. Every event is interpreted as the graph node which is identified with the point on the plane. Relations between events are represented by edges. If the

occurrence of event X has an influence on the occurrence of event Y (Y depends on X) then in the graph model there is an edge (X, Y) going from X into Y direction is marked by an arrow). The node X will be called the parent of node Y. $\pi(X)$ means the set of all nodes X parents [1, 2].

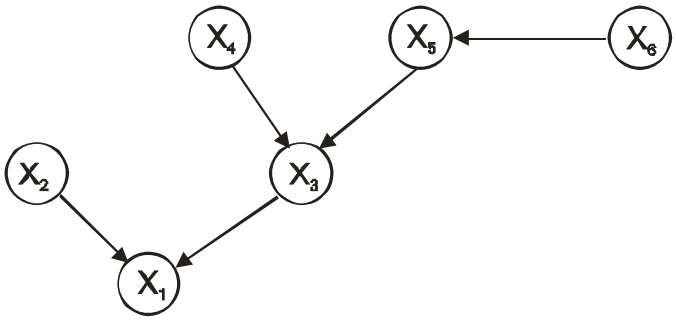

Fig. 1: The example of BAYES'ian network

For the graph D in fig.1 we have $\pi(X_1) = \{X_2, X_3\}$, $\pi(X_5) = \{X_6\}$. Events X_5, X_6 are the dependent events, and X_3 depends on X_4, X_5, that means on their parents. Additionally we assume the independence of every node of the nodes which are not its parents. In our example X_1 is independent of X_4, X_5, X_6.

To simplify the notation every event X_i will be identified with the corresponding random variable with the same name. In our considerations all the random variables corresponding to events are bivalent.

The dependence between nodes (events) is expressed by means of the conditional likelihood. For the node X whose parents are in the set $\pi(X)$ these dependences are represented by the conditional likelihood tables CLT. In CLT for the variable X must be defined the likelihood values $P(X|\pi(X))$ for all possible combinations of variable values from the set $\pi(X)$. The table for node without parents contains the likelihood that random variable X will take its particular values.

Formally the definition of BAYES'ian network (BN) can be written as follows:

BAYES'ian network B(D,CLT) is a pair (D, CLT), where D is an acyclic directed graph on whose nodes the function CLT has been defined, which assigns the conditional likelihood tables CLT to each node X. The table CLT for node X contains $P(X|\pi(X))$ [1, 2].

If the net has n nodes: $X_1,...,X_n$ then the joint probability distribution of all random variables can be shown as the formula

$$P(X_1,...X_n) = \prod_{n=1}^{n} P(X_i / \pi(X_i)) : \qquad (5)$$

For the network in fig. 1 this formula can be unfolded as:

$$P(X_1, X_2, X_3, X_4, X_5) = P(X_1/ X_2, X_3) \cdot P(X_2) \cdot P(X_3/ X_4, X_5) \cdot P(X_4) \cdot P(X_5/ X_6) \cdot P(X_6)$$

To determine the joint probability distribution without using BN it is necessary to know all values $P(X_1,...,X_n)$ for all possible combinations of variable values $X_1,...,X_n$ which means $2n$ values to be memorised. Using BAYES network it is enough to know the conditional likelihood for each node at the given values of its direct ancestors (parents) that means:

$$LN = \sum_{i=1}^{n} 2^{|\pi(X_i)|} \tag{6}$$

where $|\pi(X_i)|$ means a number of elements in set $\pi(X_i)$.

For the example presented in fig.2 the likelihood number is:

LN = $2^2+2^0+2^2+2^0+2^1+2^0$=13. To calculate the joint probability distribution by the conventional method it would be necessary to determine 2^6= 64 likelihood values.

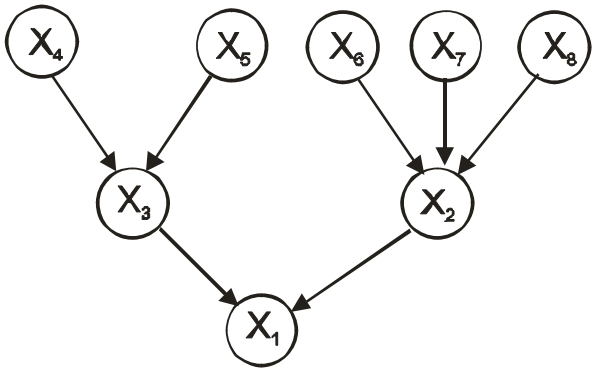

Fig. 2: Bayesian network diagram for the event - the contaminated water occurs in water-pipe network

4 Possibility of BAYES'ian network application in WSS risk analysis

Let us assume the following notation of the particular events:

X_1 – secondary water contamination in water-pipe network,
X_2 – failure in water-pipe network,
X_3 – contaminated water in the water treatment plant outlet,
X_4 – incidental contamination in water intake,
X_5 – water treatment process failed,
X_6 – wear-out failure occurred (water-pipe network is over 50 years old).
X_7 – stress failure occurred (sudden changes of ground temperature),
X_8 - water-pipe network failure caused by external factors (eg. mechanical damage).

The configuration of cause and effect relation for the events defined above is shown as BAYES'ian network in fig.2.

We assume the independence of events X_i of all $X_j \notin \pi(X_i)$ (not parents).

The number of necessary likelihood is LN = 2^3 + 2·22 +5·20 = 21 according to the formula (6). For the particular network nodes the appropriate tables of the conditional likelihood have been made assuming the following notions: $+X$ – means that the event takes place, $\neg X$ – means that the event does not take place, X – means that the event takes place or does not take place.

The particular likelihood values are:

Node,, X_1"

X_3	X_2	$P(X_1/ X_3, X_2)$
+	+	0,05
+	¬	0,50 **
¬	+	0,50 *
¬	¬	0,90

Node,,X_2"

X_6	X_7	X_8	$P(X_2/ X_6, X_7, X_8)$
+	+	+	0,15
+	+	¬	0, 40
+	¬	+	0,50
¬	+	+	0,60
+	¬	¬	0,70 *
¬	+	¬	0,65
¬	¬	+	0,55
¬	¬	¬	0,95 **

Node,, X_3"

X_4	X_5	$P(X_3/ X_4, X_5)$
+	+	0,05 **
+	¬	0,50
¬	+	0,50
¬	¬	0,95 *

Node,, X_4", ,, X_5"

X_4	$P(X_4)$	X_5	$P(X_5)$
+	0,25 **	+	0,35**
¬	0,75 *	¬	0,65 *

Node,, X_6", ,, X_7", ,, X_8"

X_6	$P(X_6)$	X_7	$P(X_7)$	X_8	$P(X_8)$
+	0,3 *	+	0,2	+	0,4
¬	0,7 **	¬	0,8 *·**	¬	0,6 *·**

*) - values in CLT for the example ①
**) - values in CLT for the example ②

The joint probability distribution for the example presented in fig.2 is:

$$P(X_1, X_2, X_3, X_4, X_5, X_6, X_7, X_8) = P(X_1/ X_2, X_3) \cdot P(X_2/X_6,X_7,X_8) \cdot P(X_3/ X_4, X_5) \cdot P(X_4) \cdot P(X_5) \cdot P(X_6) \cdot P(X_7) \cdot P(X_8) \quad (7)$$

4.1 Example ①

One must determine the likelihood of water contamination in water-pipe network (event $+X_1$) if:

- failure in water-pipe network occurred (event $+X_2$),
- wear-out failure occurred (event $+X_6$),
- stress failure did not occur (event $\neg X_7$),
- failure contributed by external factors did not occur (failure$\neg X_8$),
- contaminated water in the water treatment plant outlet did not occur (failure$\neg X_3$),
- contamination in water intake did not occur (failure$\neg X_4$),
- water treatment process did not fail (failure $\neg X_5$).

Assuming that the events are not dependent on their primogenitors and only on their parents we obtain the joint probability distribution:

$$P(+X_1, +X_2, +X_6, \neg X_7, \neg X_8, \neg X_3, \neg X_4, \neg X_5) = 0{,}5 \cdot 0{,}7 \cdot 0{,}3 \cdot 0{,}8 \cdot 0{,}6 \cdot 0{,}95 \cdot 0{,}75 \cdot 0{,}65 = 0{,}023$$

4.2 Example ②

One must determine the likelihood of water contamination in water-pipe network (event $+X_1$) if:

- failure in water-pipe network did not occur (event $\neg X_2$),
- wear-out failure did not occur (event $\neg X_6$),
- stress failure did not occur (event $\neg X_7$),
- failure contributed by external factors did not occur (failure$\neg X_8$),
- contaminated water in the water treatment plant outlet occurred (failure $+X_3$),
- contamination in water intake occurred (failure $+X_4$),
- water treatment process failed (failure $+X_5$).

Assuming that the events are not dependent on their primogenitors and only on their parents we obtain the joint probability distribution:

$$P(+X_1, \neg X_2, \neg X_6, \neg X_7, \neg X_8, +X_3, +X_4, +X_5) = 0{,}5 \cdot 0{,}95 \cdot 0{,}7 \cdot 0{,}8 \cdot 0{,}6 \cdot 0{,}05 \cdot 0{,}25 \cdot 0{,}35 = 0{,}0007$$

4.3 Example ③

There is the failure in water-pipe network contributed *y* the external factors (event $+X_8$). What is the likelihood of the secondary water contamination in water- pipe network (event $+X_1$) if we do not have any information about the other events. Deduction that we use is called the cause-and-effect deduction. We determine the likelihood of the consequence when we know the cause. $P(+X_1|+X_8)$ must be calculated.

$$P(+X_1|+X_8)=\frac{P(+X_1,+X_8)}{P(+X_8)}=\frac{\sum_{X_2,X_3,X_4,X_5,X_6,X_7} P(+X_1,X_2,X_3,X_4,X_5,X_6,X_7,+X_8)}{\sum_{X_1,X_2,X_3,X_4,X_5,X_6,X_7} P(+X_1,X_2,X_3,X_4,X_5,X_6,X_7,+X_8)}$$

Taking into account the formula (7) we obtain:

$$P(+X_1|+X_8)=\frac{P(+X_1,+X_8)}{P(+X_8)}=$$

$$\frac{\sum_{X_2,X_3,X_4,X_5,X_6,X_7} P(+X_1/X_2,X_3)\,P(X_2/X_6,X_7,+X_8)P(X_3/X_4,X_5)P(X_3/X_4,X_5)\,P(X_4)\,P(X_5)P(X_6)\,P(X_7)\,P(+X_8)}{\sum_{X_1,X_2,X_3,X_4,X_5,X_6,X_7} P(+X_1/X_2,X_3)\,P(X_2/X_6,X_7,+X_8)P(X_3/X_4,X_5)P(X_3/X_4,X_5)\,P(X_4)\,P(X_5)P(X_6)\,P(X_7)\,P(+X_8)}$$

= 0,48

4.4 Example ④

There is the secondary failure in water- pipe network (event $+X_1$). Calculate the likelihood that the cause of it was the damage in water-pipe network contributed by the external factors (event $+X_8$). $P(+X_8|+X_1)$must be calculated. Deduction that we use now is called the diagnostic deduction. Using the same deduction as in the example 3 we obtain:

$P(+X_8|+X_1)=$

$$\frac{\sum_{X_2,X_3,X_4,X_5,X_6,X_7} P(+X_1/X_2,X_3)\,P(X_2/X_6,X_7,+X_8)P(X_3/X_4,X_5)P(X_3/X_4,X_5)\,P(X_4)\,P(X_5)P(X_6)\,P(X_7)\,P(+X_8)}{\sum_{X_1,X_2,X_3,X_4,X_5,X_6,X_7} P(+X_1/X_2,X_3)\,P(X_2/X_6,X_7,+X_8)P(X_3/X_4,X_5)P(X_3/X_4,X_5)\,P(X_4)\,P(X_5)P(X_6)\,P(X_7)\,P(+X_8)}$$

=0,4

5 Conclusion

- WSS is a complex technological system and its reliable operation conditions water consumer's safety.
- To determine the likelihood of different undesirable events scenarios in WSS and to cause and effect analysis of these events we can use Bayesian networks.
- The advantages of using Bayesian network are, among others, the following: a lower number of necessary likelihood values, instead of $2n$ we need only (for the example presented in fig.3: 21 instead of 256), we can choose any direction of deduction, network is easy to be modified and expanded.

- The right Bayesian network construction requires the base of historical date in order to assess the conditional likelihood and the knowledge of the experts in the given field [3].
- Bayesian networks can be a very good tool to analyse risk connected with water supply system operating, they can be used to calculate different scenarios of causes and consequences of undesirable events which, however, often requires to build the expanded networks and to use computer software for calculations (eg.3 and 4).
- The methods and procedures concerning the cause and effect analysis of the undesirable events in WSS that have been known and used up to the present can be completed by Bayesian networks.

6 References

[1] Better SAG, Dethlefsen C. Learning Bayesian Networks with R. http:// www.ci.tuwien.ac.at/Conferences/ DSC-2003/.

[2] Chavira M. Darwiche A. Jaeger M. Compiling Relational Bayesian Network for Exact Inference. Computer Science Department . UCLA. CA. 900095.

[3] Oniśko A. i inni. Uczenie parametrów sieci bayesowskich z danych z wykorzystaniem bramek NOSY –OR. Badania operacyjne i systemowe wobec wyzwań XXI wieku. Problemy współczesnej nauki. P-IV.S19-26. Akademicka Oficyna wydawnicza ELIT. Warszawa 2002.

[4] Ross K., Wright Ch., Matematyka dyskretna, PWN, 1996.

[5] Sysło M., Deo N., Kowalik J., Algorytmy optymalizacji dyskretnej, PWN, 1999.

Restricted water area optimization with risk consideration

Lucjan Gucma
Maritime University of Szczecin, Poland

Abstract: The paper presents method of waterway width optimization with risk as the optimization criterion and limitation. The data possessed from real time ship simulations conducted in first stage of researches are processed and accident intensity in several ship passages are calculated. In further step the cost optimization model based on risk of accident is used to find optimal solution of waterway modernization.

1 Navigational risk

Navigational risk R is expressed as potential losses during the waterway operation. The navigational accidents on restricted water areas usually do not involve human fatalities nor injuries so economical expression of consequences is used. The main factors of risk are probability of accident P_a and accident consequences C:

$$R = P_a \cdot C \tag{1}$$

The most important aspects in navigational risk assessment are concerned with:

- accident probability is changing during the ship passage;
- necessity to consider many manoeuvring ships;
- different conditions during ship passages;
- long time of waterway operation.

Some of above aspects have been considered in presented optimization model.

1.1 Probability of accident and cumulative accident intensity

Real time simulations are conducted with use of computer model of ship and environment in simulated meteorological conditions (Fig. 1). These researches are rather expensive and time consuming so they should to be reduced to the minimum that guarantee statistical significance to achieved results. Human navigators are used as ships operators. The naviga-

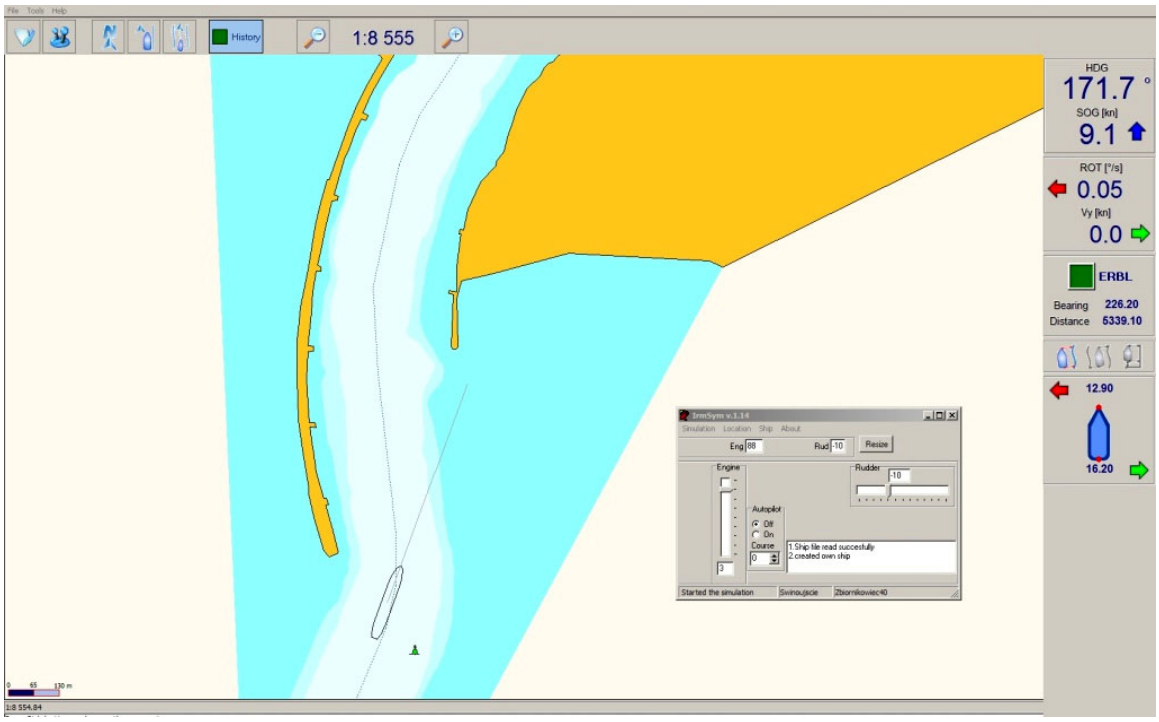

Fig. 1: Typical real time PC-based ship maneuvering simulator

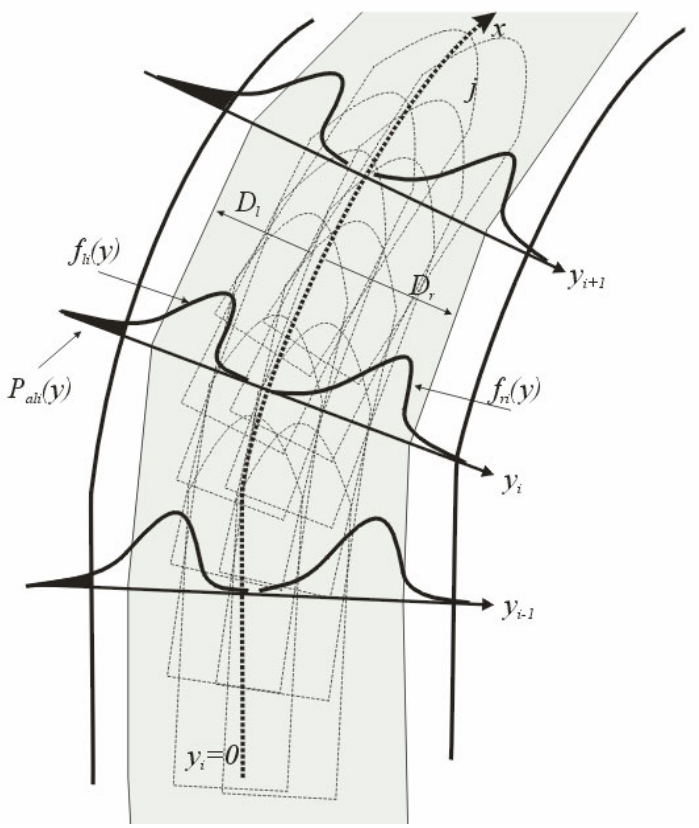

Fig. 2: Graphical explanation of safety water area definition and probability of collision with the embankments assessment.

tor influence is therefore propagated through presented model and described by means of estimated statistical distributions.

Let us consider that the ships of breadth B move along the waterway trying to keep as close as possible to the centre of the waterway described by the curve line y=0. The distances of the most extreme points of the waterway are considered as random variables and denoted as $f_r(y)$ and $f_l(y)$ (Fig.1). To allow further calculations the waterway is divided into discrete sections with length Δx.

Based on empirical distributions of ship positions achieved in simulations (Fig. 2) the simplified formula for probability of accident due to safe waterway exit can be evaluated in every i^{tch} waterway section as follows:

$$P_{ari} = \int_{d_{ri}}^{+\infty} f_{ri}(y)\, dy \tag{2}$$

where: $f_{ri}(y)$ = density function of ship extreme positions; d_{ri} = distance from the waterway centre to its border.

The above formula does not consider the phenomenon that on narrow waterways it is not possible to exit the waterway on the left side of the waterway while considering the probability on the right side of the waterway. Thus the truncated distribution at the point of $d_{tli}=(d_{li}-B)$ should be considered as more appropriate. This distribution is created with use distribution $f_r(y)$ in point d_{li} by normalizing for $y < d_{li}$:

$$f_{tri}(y) = \begin{cases} k \cdot f_{ri}(y) & for \quad y > d_{tli} \\ 0 & for \quad y \le d_{tli} \end{cases} \tag{3}$$

where: k – normalizing constant $k = 1/F_R(d_{tli})$.

Then probability of accident on right side of i^{tch} section of the waterway can be expressed as:

$$P_{ari} = \int_{d_{ri}}^{+\infty} f_{tri}(y)\, dy \tag{4}$$

The probability of accident changes during the passage of ships due to conditions and proximity to the waterway borders is the function of x:

$$P_{ari} = f(x) \tag{5}$$

The function $f(x)$ is usually determined as empirical by means of simulation and presented method.

The probability on the right and left side are should be treated as independent so to the final calculations the maximum value should be considered if or when consequence assessment is available the one with maximum risk:

$$p_{\mathrm{ai}} = \max(P_{\mathrm{ali}}; P_{\mathrm{ari}}) \tag{6}$$

The time of ship passage through the section is random and depends of ships speed distribution *v(x)* and can be express as:

$$t_{\mathrm{i}} = \Delta x_{\mathrm{i}} / v_{\mathrm{i}} \tag{7}$$

With assumption that accidents occurrence could be described be the Poisson process [2], the accident intensity of single ship in given section λ_{i} could be calculated as:

$$p_{\mathrm{ai}} = p_{\mathrm{ai}}(n \geq 1) = 1 - e^{-\lambda_{\mathrm{i}} \cdot t_{\mathrm{i}}} \tag{8}$$

thus intensity of accident in given section estimated as:

$$\lambda_i = -\ln(1 - p_{\mathrm{ai}}) / t_{\mathrm{i}} \tag{9}$$

It was assumed that ship speed is constant and accident intensity were constant in single section The intensity calculated in [accident/km] units can be evaluated as:

$$\lambda_{\mathrm{i}} = -\ln(1 - p_{\mathrm{ai}}) \bar{t}_{\mathrm{i}} / \Delta x_{\mathrm{i}} \tag{10}$$

where: $\bar{t}_{\mathrm{i}}$ – mean time of given section passing.

The whole passage of the ship can be treated as nonhomogeneous Poisson processes (NHPP) with probability function:

$$p_{\mathrm{n}}(N) = \frac{\lambda(x) \cdot t^n \cdot e^{-\lambda(x) \cdot t}}{n!} \tag{11}$$

where: $\lambda(x)$ – intensity function,

and the probability of *n*-event occurrence in i^{tch} section can be defined as:

$$p_{\mathrm{n}}(N = n) = \frac{\int_{\Delta x_{\mathrm{i}}} \lambda(x) \cdot t^n \cdot e^{-\int \lambda(x) t}}{n!} \tag{12}$$

cumulative intensity function can be expressed as:

$$\Lambda(x) = \int_0^{x_{\mathrm{i}}} \lambda(x)\, dx \tag{13}$$

and estimated by:

$$\hat{\Lambda}(x_{\mathrm{i}}) = \sum_{i=1}^{m} \lambda(x_{\mathrm{i}}) / (x_{\mathrm{i}} - x_{\mathrm{i}-1}) \tag{14}$$

1.2 Accident consequences – cost of typical navigational accident

Usually during the investigation of ship grounding accident on restricted waters it is not necessary to take into consideration the possibility of human fatalities nor injures. The cost of accident *Ca* could be divided into following costs:

$$Ca = Cr + Cra + Cos + Cpc \tag{15}$$

where:

Cr – cost of ships repair,
Cra – cost of rescue action,
Cos – cost of potential oil spill,
Cpc – cost of port closure.

2 Optimization model

The optimization model with risk consideration is relatively simple and can be expressed as follows:

$$CT = \sum CM + \sum Ca \rightarrow \min \quad \text{with} \quad R \le R_t \tag{16}$$

where:

CT – total cost,
CM – modernization costs,
Ca – accident costs,
R – risk,
R_t – tolerable risk.

The cost of modernization can be evaluated by the cost of dredging material that should removed from the waterway and protection works that should be done on the waterway embankments. The cost is nearly linear and depends mostly of desired width (Fig. 7, 8, 9).

3 The case study – cost optimization of the waterway

As an example the 5 km long part of Szczecin – Świnoujście waterway have been chosen. The total length of the waterway is more than 40 km. Analyzed 5 km long part of the fairway consist of two bands and one straight line (Fig. 3).

The analysis has been conducted due to modernization projects of bringing into service on this waterway much bigger ships (Length = 250 m, Breadth = 38.5 m, Draught = 10.5m) than ones presently used (Length = 210m, Breadth = 31 m, Draught = 9.15 m).

The real time simulation models of ships have been applied for researches. Due to fact that at the moment there is no reliable mathematical model of human navigator available the real navigators have been used for these researches (captains, pilots).

After executing series of simulation trials with number guaranteed the former set up level of confidence the shape of distribution of maximum ship's point's distances from the centre of the fairway have been determined (Fig. 1, 2). There have been also estimated parameters of these distributions. As it was proven in former researches [2], [3] normal distribution usually well estimates process of ship passage through the waterway, even on the curved parts of it. Two such distributions were analyzed (starboard and port side of the waterway) for each section of the waterway. The length of the section was set to avoid loosing important information about ship movement.

Estimated mean (m) and variance (σ) of normal distribution was used for the navigation reliability (P_n) calculation (Fig. 3). The following formula was used:

$$P_a(d) = P(X \geq d_{max}) \tag{17}$$

where:

d_{max} – distance from the centre of the fairway to the fairway bank,

X – normal distribution with parameters X: N(m, σ).

The above probability of collision with bank was calculated twice one for starboard and one for port side of the fairway.

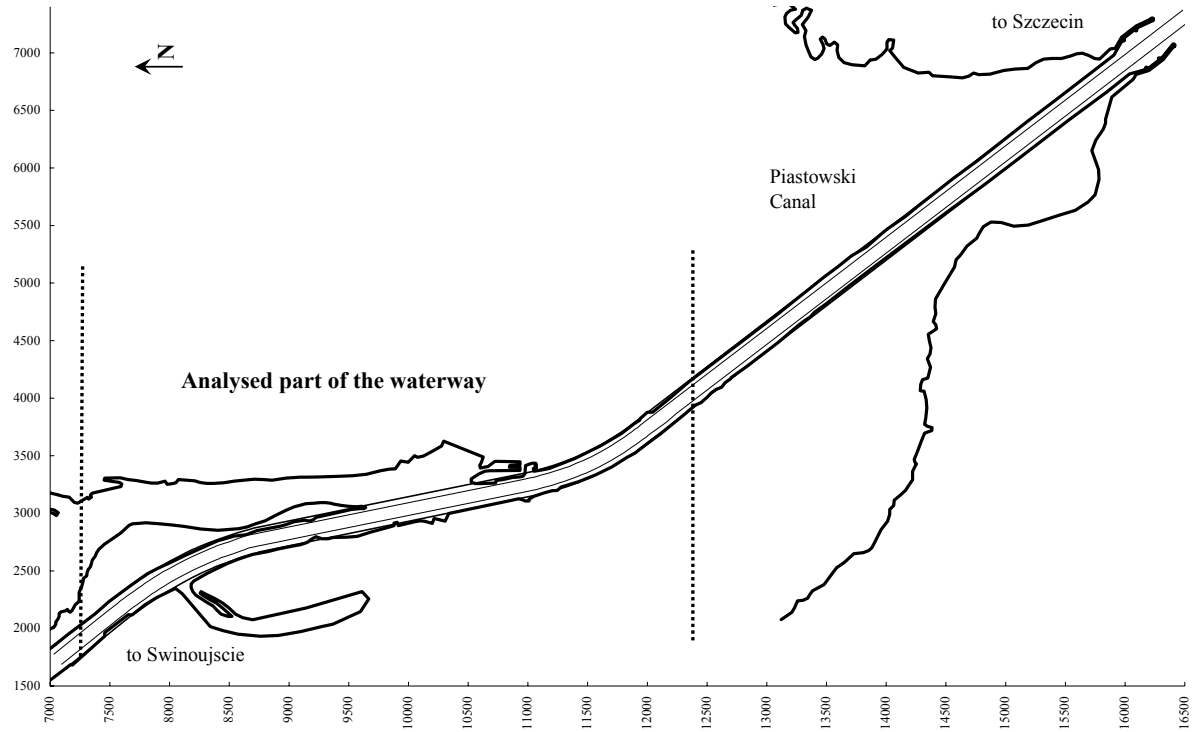

Fig. 3: The layout of investigated waterway

The probability of accident P_a in single passage of ship is presented on Fig. 4. As it could be expected the probability of accident is highly dependent of waterway part and increases on curved sections.

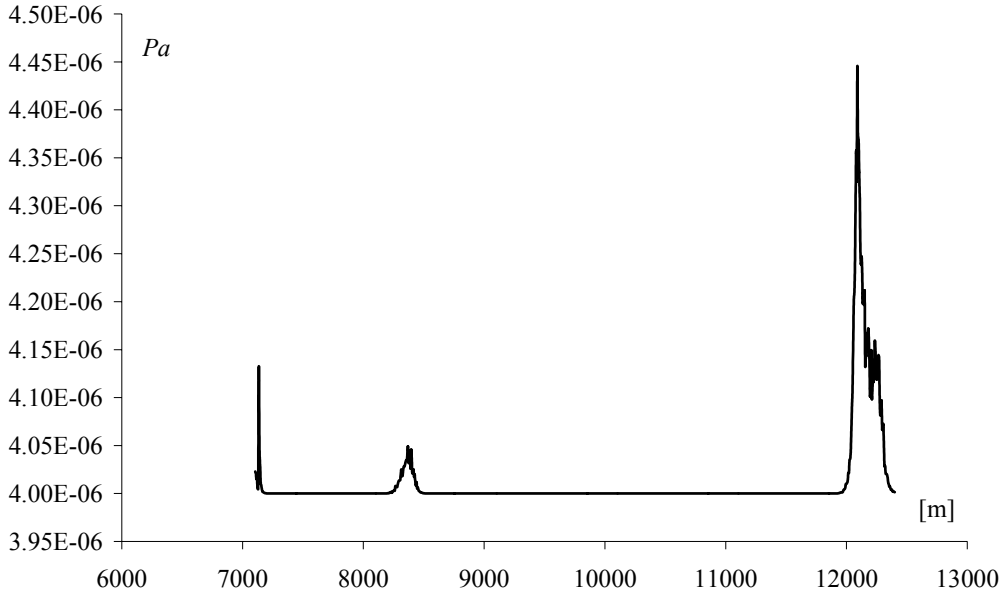

Fig. 4: Probability of accident in ships single passage

The presented model of accident intensity cumulating is used for determination of accident intensity in single passage (Fig. 5). In the next step several passages were taken into consideration.

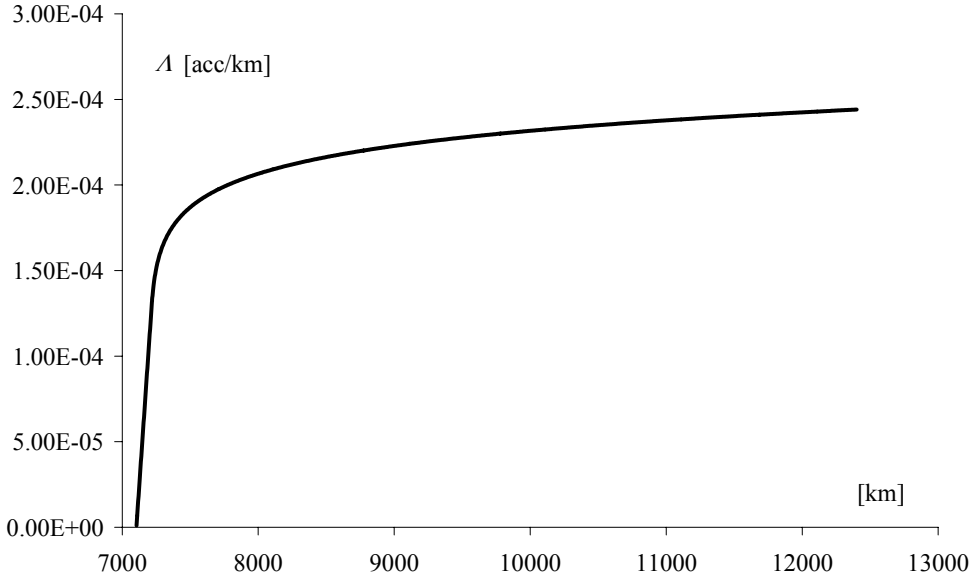

Fig. 5: Cumulative number of accident in single passage of ship through the waterway

The waterway modernization is based on increasing of its width. The widening of waterway increases the safety and decrease the number of expected accidents. This could be

observed on the Fig. 6 where one year is considered. In presented researches average traffic intensity is assumed as 200 movements of given ships per year.

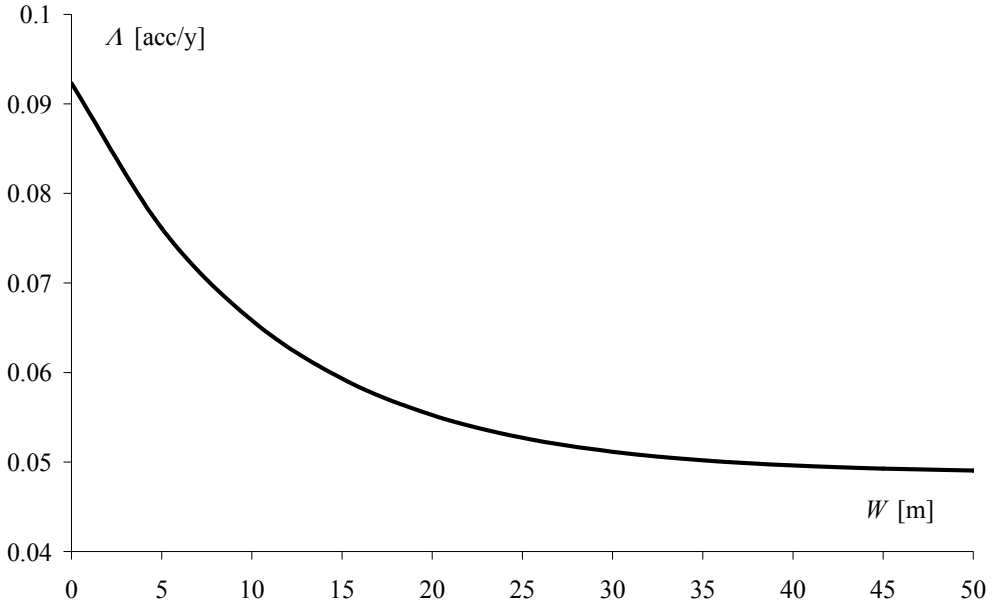

Fig. 6: Decreasing of yearly accident intensity in 200 maneuvers of given ships with waterway widening up to 50 meters

The total cost of accidents *CAn* throughout the waterway lifetime *n*=20 years could be defined as a product of accident cumulative intensity and mean cost of single accident:

$$CAn = \Lambda_n \cdot Ca \tag{18}$$

where:

- CAn – cost of accidents throughout the lifetime of the waterway,
- Λ_n – cumulative intensity of accidents,
- n – expected lifetime of the waterway (n = 20 years),
- Ca – mean cost of single accident.

The mean cost of accident is very important in these researches and was calculated for typical ship. The mean estimated cost of serious ship accident is assumed as C_1 = 600.000 €. The oil spill cost was not considered. Following assumption has been taken in calculations:

- number of tugs taking part in rescue action: 3 tugs,
- mean time of rescue action.: 1 day,
- trip to nearest shipyard: 0,5 day,
- discharging of ship: 4 days,
- repair on dry dock: 2 days,
- total of oil spilled:0 tons.

The results of optimization are presented on Fig. 7. One could observe that there is no necessary of waterway widening with assumed mean cost of accidents. The most important problem in these researches is relatively high uncertainty to the cost of accident. It depends

of many factors like kind of ship, bottom characteristic ships kinetic energy and finally cargo on board.

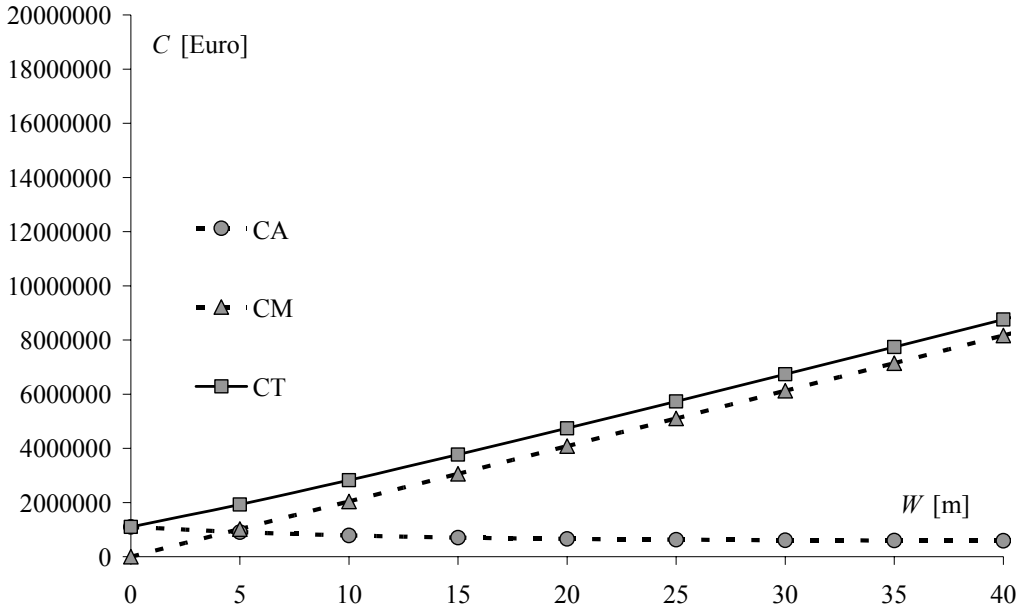

Fig. 7: Cost-Benefit Analysis for mean accident cost

On the Fig. 8 and 9 the cost of single accident has been increased by the factor of 10 and 20 up to 6 million € and 12 million € respectively. In these cases the optimal increase of waterway width should be around 10 and 15 meters respectively.

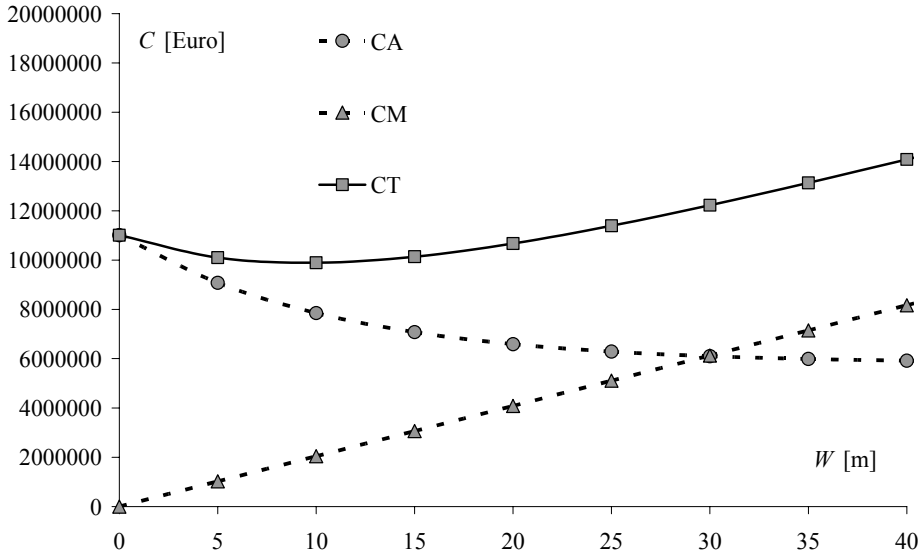

Fig. 8: Cost-Benefit Analysis for the accident cost increased by the factor of 10

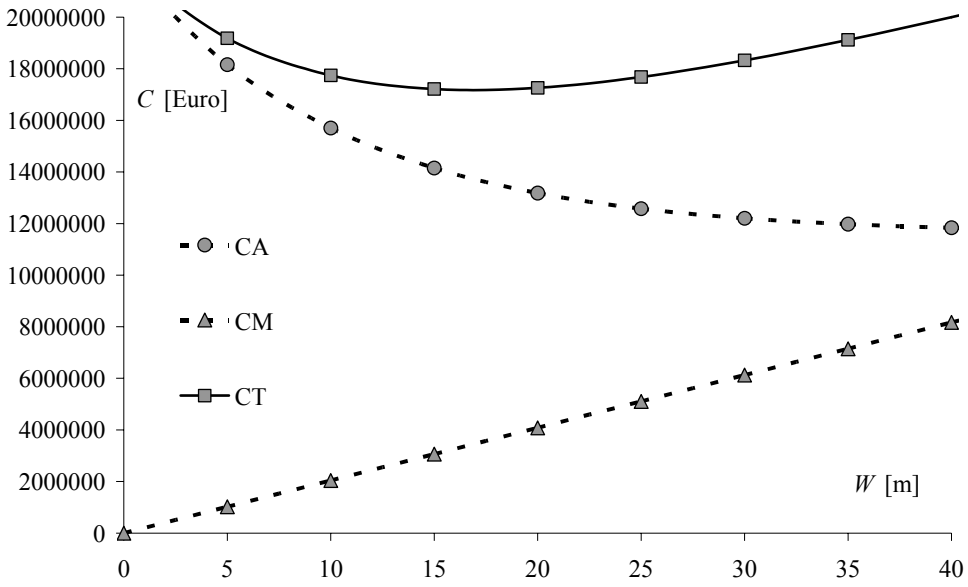

Fig. 9: Cost-Benefit Analysis for the accident cost increased by the factor of 20

4 Conclusions

The paper presents the optimal waterway modernization method with consideration of navigational risk. The presented case study and sensitivity analysis revealed that cost determination is most important in optimization process. It should be stressed that from the other side that the cost of navigational accident is highly undetermined and serious methods of uncertainty evaluations should be applied.

The Cost-Benefit Analysis is powerful technique and with combination of acceptable risk could be used in helping of decision making process during optimization of waterway width.

References

[1] Gucma, L.: *Navigation risk assessment for vessels maneuvering in various conditions*. Risk Analysis III, WIT Press Computational Mechanics Publications, Southampton-Boston 2002

[2] Gucma, L.: *Risk Models of Ship Collision with Fixed Objects* (in Polish), Maritime University of Szczecin Press, Szczecin, 2005

[3] Gucma, L.: *The method of average navigation risk assessment with consideration of inequality of ship's accident probability along the waterway*. Risk Analysis II Bologna, Wit Press Southampton Boston, 2000; pp. 125-134.

[4] Sand, S.E., Nielsen, D.S., Jakobsen, V.B.: *Risk Analysis of Simulated Ship Approaches to Ports*. Proc. of the Permanent International Association of Navigation Congresses. Seville 1994

[5] Savenije, R.Ph.: *Probabilistic Admittance Policy*, PIANC Bulletin No 91. Bruxelles 1996

Estimating Convolution Density Function by Monte-Carlo-Simulation-Method

Lech Kasyk
Institute of Mathematics in Maritime University, Szczecin

Abstract: The paper presents a few problems from the area of Marine Traffic Engineering and a few theoretical problems with the sum of continuous random variables. In order to describe the probability distribution of density function of the summed random variables, function convolution was applied. The formulae of particular convolutions were derived, and the distributions were estimated by means of Monte Carlo simulation method.

1 Introduction

Marine Traffic Engineering is preoccupied with numerous problems of probabilistic nature [3, 4, 5, 6, 7]. In the problems solved, known probability distributions are frequently used, as well as various methods to make the matched theoretical distribution differ as little as possible from real data. The application of density function convolutions of random variables also serves this purpose; it describes the probability distribution of sums of random variables [9]. The density function of the convolution is defined as the boundary density of two-dimensional random variable. For this purpose variable $Z=(U, V)$ is created, where $U=X+Y$ and $V = Y$. Random variable $U=X+Y$ has a boundary distribution of two-dimensional variable Z. Assuming variables X and Y to be independent, random variable Z is described by density function [9]:

$$g(u,v) = f_1(u-v) \cdot f_2(v) \tag{1}$$

where

f_1 probability density function of variable X

f_2 probability density function of variable Y

The density of single variable U is obtained as boundary distribution, integrating density $g(u,v)$ in relation to variable v, in limits proper for particular distributions.

2 Convolution of exponential with normal distribution

The process of reporting by fairway vessels, when they report individually and independently of each other, is a Poisson process [2, 7]. If T_1 denotes the time of waiting for the successive vessel at point P_1, and T_2 denotes the time of passing section P_1P_2, then the time $T = T_1 + T_2$ denotes the time of waiting for the successive vessel to report at point P_2. Time T_1 is a random variable with exponential distribution [6, 7, 8]; therefore, the probability distribution density of variable T is the boundary density of function:

$$g(u,v) = \begin{cases} \lambda e^{-\lambda(u-v)} \cdot \dfrac{1}{\sigma\sqrt{2\pi}} e^{-\frac{(v-m)^2}{2\sigma^2}} & \text{for } u \geq v \wedge v \in R \\ 0 & \text{for other } u, v \end{cases} \tag{2}$$

where

λ exponential distribution parameter of random variable T_1

m expected value of random variable T_2

σ^2 variance of random variable T_2

The density of random variable T is equal to:

$$\begin{aligned} g(u) &= \int_{-\infty}^{u} \lambda e^{-\lambda(u-v)} \cdot \frac{1}{\sigma\sqrt{2\pi}} e^{-\frac{(v-m)^2}{2\sigma^2}} dv = \\ &= \frac{1}{2}\sqrt{e^{\lambda\left(2m-2u+\lambda\sigma^2\right)}} \cdot \lambda\left(1 - \mathrm{Erf}\left[\frac{m-u+\lambda\sigma^2}{\sigma\sqrt{2}}\right]\right) \end{aligned} \tag{3}$$

where Erf (x) denotes the function of error used in Mathematica program in probabilistic problems; [1]:

$$\mathrm{Erf}(x) = \frac{2}{\sqrt{\pi}} \int_0^x e^{-t^2} dt$$

.

A graph of function $g(u)$ is presented in Fig. 1. The shape of the graph depends on particular parameters of the summed variables. The figure below was prepared for $\lambda = 2$, $m = 15$, $\sigma = 5$.

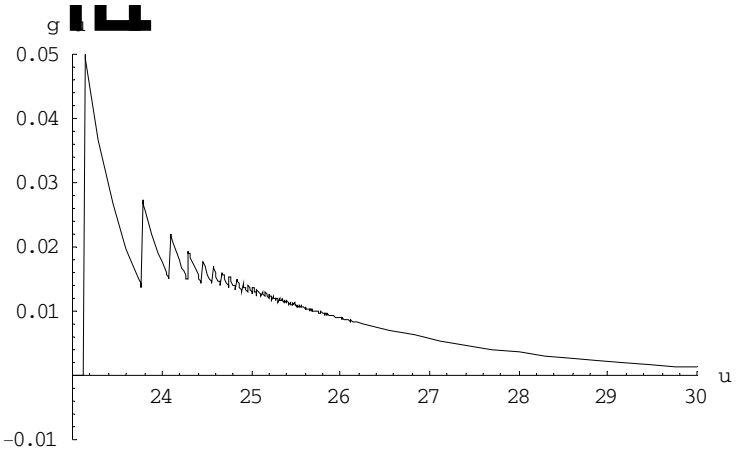

Fig.1. Graph of density function of the sum of random variables with exponential and normal distributions

By use of the Monte Carlo method 1000 values of random variable T_1 with uniform distribution were determined by way of simulation and 1000 values of variable T_2 with normal distribution. Next they were summed and a distribution of variable $T = T_1 + T_2$ was obtained. A histogram of this variable is presented in Fig. 2.

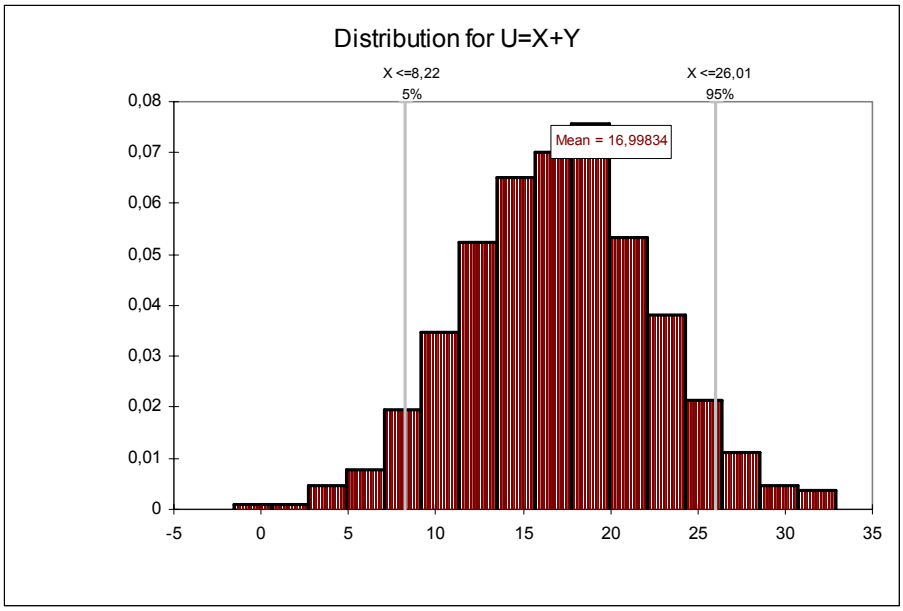

Fig.2. A histogram of sum distribution of simulated random variables with exponential and normal distributions

Among distributions matched, variable T is best described by Inverse Gauss distribution with parameters 731 and 13263517. The conformity of these distributions is high, as the χ^2 coefficient is equal to 23.24 at critical value 41.33 (on confidence level 0.95).

3 Convolution of two normal distributions

If B_1 denotes an error of a vessel's position determination in a given direction, resulting from measurement accuracy, and B_2 an error resulting from the method assumed, then the random variable $B = B_1 + B_2$ can be assumed as the total error of the vessel's position determination in a given direction.

In the case of both B_1 and B_2 errors being random variables with normal distributions, the two-dimensional density function has the following shape:

$$g(u,v) = \frac{1}{2\pi\sigma_1\sigma_2} \cdot e^{-\frac{(u-v-m_1)^2}{2\sigma_1^2} - \frac{(v-m_2)^2}{2\sigma_2^2}} \tag{4}$$

where m_1 expected value of random variable B_1
σ_1^2 variance of random variable B_1
m_2 expected value of random variable B_2
σ_2^2 variance of random variable B_2

After integrating this function in relation to v, within the range of $(-\infty,\infty)$, the density of random variable B is equal to

$$g(u) = \frac{1}{\sqrt{2\pi\left(\sigma_1^2+\sigma_2^2\right)}} \cdot e^{-\frac{(u-m_1-m_2)^2}{2\left(\sigma_1^2+\sigma_2^2\right)}} \tag{5}$$

This is the density of normal distribution with mean $m_1 + m_2$ and with variance $\sigma_1^2 + \sigma_2^2$.

Using the Monte Carlo method 1000 values of random variable B_1 with normal distribution N(70;2) were determined by way of simulation as well as 1000 values of random valuable B_2 with normal distribution N(14;5). Next, they were summed and the distribution of variable $B = B_1 + B_2$ was obtained. This distribution was compared with normal distribution described by density function (5). The conformity of these distributions is high, as the chi^2 coefficient is equal to 15.17 at critical value 41.33, on confidence level of 0.95.

4 Convolution of normal distribution with uniform distribution

In the case of B_1 being a random variable with normal distribution, and B_2 a random variable with uniform distribution, the two-dimensional density function has the following shape:

$$g(u,v)=\frac{1}{b-a}\cdot\frac{1}{\sqrt{2\pi}\sigma}\cdot e^{-\frac{(v-m)^2}{2\sigma^2}} \tag{6}$$

where b, a limits of uniform distribution
m, σ parameters of normal distribution.

After integrating this function in relation to *v*, within the limits of $(u-b,u-a)$, the density of random variable *B* is equal to:

$$g(u)=\frac{1}{2(b-a)}\cdot\left(\mathrm{Erf}\left[\frac{b+m-u}{\sigma\sqrt{2}}\right]-\mathrm{Erf}\left[\frac{a+m-u}{\sigma\sqrt{2}}\right]\right) \tag{7}$$

Fig. 3 presents the graph of *g(u)* function for the following parameters: $a = 4$, $b = 10$, $m = 5$, $\sigma = 0.5$.

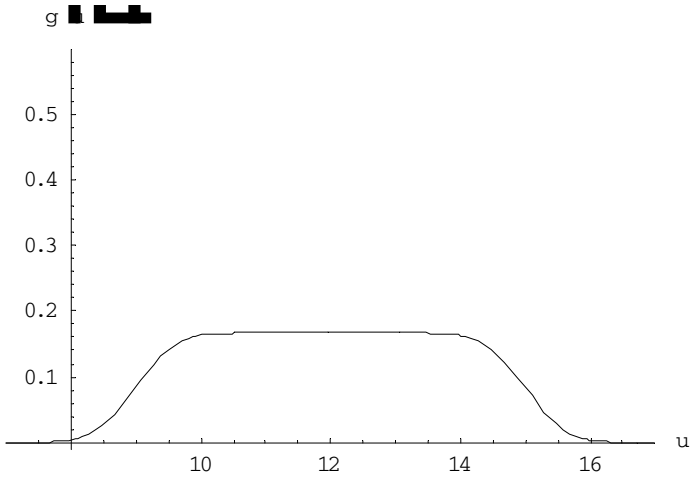

Fig.3. Graph of density function of random variables sum with uniform and normal distribution

Using the Monte Carlo method, 1000 values of variable B_1 with uniform distribution U(4;10) were determined by way of simulation, as well as 1000 values of variable B_2 with normal distribution N(5;0.5). Next they were summed, and the distribution of variable $B = B_1 + B_2$ was obtained. A histogram of this variable is presented in Fig. 4.

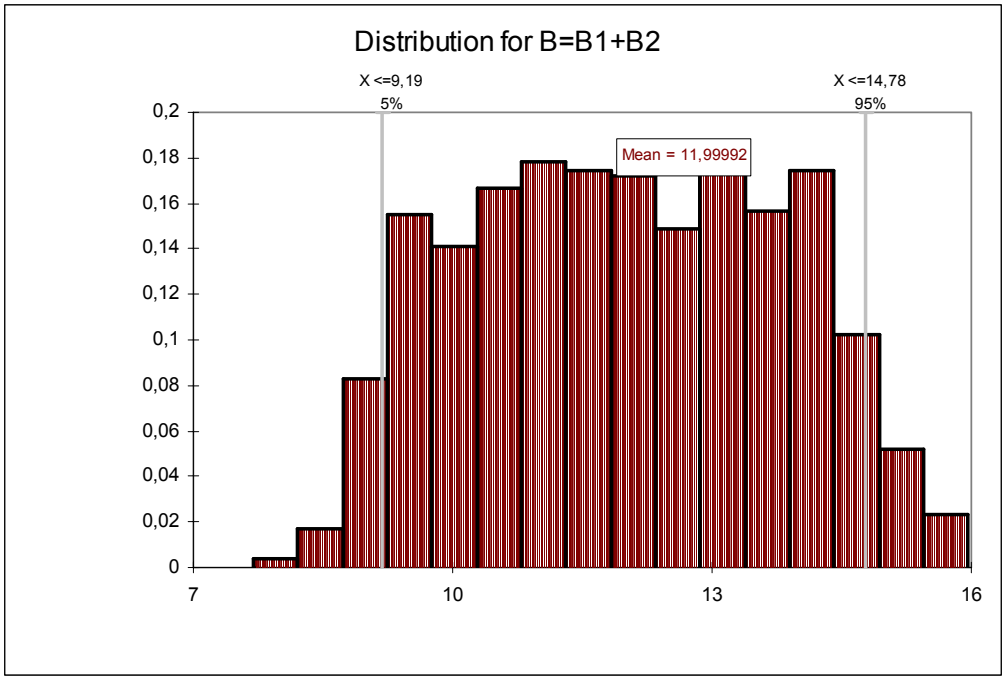

Fig.4. A histogram of sum distribution of simulated random variables with uniform and normal distributions

Among distributions matched, variable *B* is best described by Beta distribution with parameters (2.48; 2.32; 7.63; 16.12). The conformity of these distributions is very low, as the chi^2 coefficient is equal to 60.53 at critical value 41.33 (on confidence level 0.95).

5 Convolution of three normal distributions

The ferry's movement on a ferry crossing can be divided into 3 phases. The first is "gathering speed", i.e. the time from leaving the initial berth to reaching full crossing speed. The second phase is the ferry's movement at full speed. The third phase is "braking", i.e. the time from starting to brake to the mooring at final harbour. The times of covering particular stages of the crossing are random variables with normal distributions [3, 8]. Hence, the total time of covering the crossing is equal to $T = T_1 + T_2 + T_3$.

Formula (5) presents the density function of the convolution of two normal distributions. By repeating the operation of this distribution's convolution with normal distribution, the density function of the convolution of three normal distributions was obtained:

$$g(u) = \frac{1}{\sqrt{2\pi\left(\sigma_1^2 + \sigma_2^2 + \sigma_3^2\right)}} \cdot e^{-\frac{(u-m_1-m_2-m_3)^2}{2\left(\sigma_1^2+\sigma_2^2+\sigma_3^2\right)}} \tag{8}$$

where m_i, σ_i parameters of normal distribution of variable T_i

Function *g(u)* is equal to the density of normal distribution with mean $m_1 + m_2 + m_3$ and variance $\sigma_1^2 + \sigma_2^2 + \sigma_3^2$.

Using the Monte Carlo method 1000 values of variable T_1 with normal distribution were determined, 1000 values of variable T_2 with normal distribution and 1000 values of variable T_3 with normal distribution. Next they were summed and the distribution of variable $T = T_1 + T_2 + T_3$ was obtained. This distribution was compared with normal distribution described by density function (8). The conformity of these distributions is not high, as the chi^2 coefficient is equal to 38.78 at critical value 41.33 (on confidence level of 0.95). Variable *T* is better described by Inverse Gauss distribution (chi^2 equal to 29.44 at critical value 41.33, on confidence level of 0.95).

6 Convolution of two uniform distributions

A vessel proceeding along a narrow fairway usually attempts to sail along the axis of the fairway; yet a lot of phenomena make it practically impossible. The distance of the vessel's gravity centre from the fairway axis is a random variable which can be described by uniform distribution [4]. If D_1 denotes the distance of the vessel's gravity centre from the fairway axis caused by factor C_1, and D_2 denotes the distance of the vessel's gravity centre from the fairway axis caused by factor C_2, then the summary deviation $D = D_1 + D_2$ will have a distribution equal to the convolution of uniform distributions. The two-dimensional density function, from which the convolution was calculated, has the following form:

$$g(u,v) = \begin{cases} \dfrac{1}{b-a} \cdot \dfrac{1}{d-c} & \text{for } v+a \le u \le v+b \wedge c \le v \le d \\ 0 & \text{for other } u,v \end{cases} \tag{9}$$

where

b, a limits of uniform distribution of variable D_1
d,c limits of uniform distribution of variable D_2

If $c+b < d+a$, then after integrating this function in relation to *v*, in the range $(c, u-a)$, $(u-b, u-a)$ and $(u-b, d)$, the density of random variable *D* will amount to:

$$g(u) = \begin{cases} \dfrac{u-a-c}{(b-a)\cdot(d-c)} & \text{for } c+a \le u < c+b \\ \dfrac{1}{d-c} & \text{for } c+b \le u < d+a \\ \dfrac{-u+d+b}{(b-a)\cdot(d-c)} & \text{for } d+a \le u < d+b \end{cases} \tag{10}$$

If $c+b>d+a$, then after integrating this function in relation to v, in the range $(c,u-a)$, (c,d) and $(u-b,d)$, the density of random variable *D* will amount to:

$$g(u)=\begin{cases}\dfrac{u-a-c}{(b-a)\cdot(d-c)} & \text{for } c+a\le u<d+a\\ \dfrac{1}{d-c} & \text{for } d+a\le u<c+b\\ \dfrac{-u+d+b}{(b-a)\cdot(d-c)} & \text{for } c+b\le u<d+b\end{cases} \tag{11}$$

If $c+b=d+a$, then after integrating this function in relation to v, in the range $(c,u-a)$ and $(u-b,d)$, the density of random variable *D* will amount to:

$$g(u)=\begin{cases}\dfrac{u-a-c}{(b-a)\cdot(d-c)} & \text{for } c+a\le u<c+b\\ \dfrac{-u+d+b}{(b-a)\cdot(d-c)} & \text{for } c+b\le u<d+b\end{cases} \tag{12}$$

The above function $g(u)$ is the density of triangular distribution.

Using the Monte Carlo method 1000 values of random variable D_1 with uniform distribution U(3;6) were determined by way of simulation as well as 1000 values of random valuable D_2 with uniform distribution U(4;10). Next, they were summed and the distribution of variable $D = D_1 + D_2$ was obtained. This distribution was compared with triangular distribution. The conformity of these distributions is not high, as the chi^2 coefficient is equal to 35.71 at critical value 41.33, on confidence level of 0.95.). Variable *D* is better described by Beta distribution (chi^2 equal to 27.93 at critical value 41.33, on confidence level of 0.95).

7 Convolution of two exponential distributions

The two-dimensional density function, for sum of two exponential random variable, has the following form:

$$g(u,v)=\begin{cases}\lambda_1\lambda_2\cdot e^{-\lambda_1(u-v)}\cdot e^{-\lambda_2 v} & \text{for } u\ge v\wedge v\ge 0\\ 0 & \text{for rest } u,v\end{cases} \tag{13}$$

where

λ_1 exponential distribution parameter of random variable *X*

λ_2 exponential distribution parameter of random variable *Y*.

After integrating this function in relation to *v*, within the limits of $(0,u)$, the density of random variable $U=X+Y$ is equal to:

$$g(u)=\frac{\lambda_1\lambda_2}{\lambda_1-\lambda_2}\cdot\left(e^{-\lambda_2 u}-e^{\lambda_1 u}\right) \tag{14}$$

Fig. 7 presents the graph of *g(u)* function for the following parameters: $\lambda_1=3$ and $\lambda_1=7$.

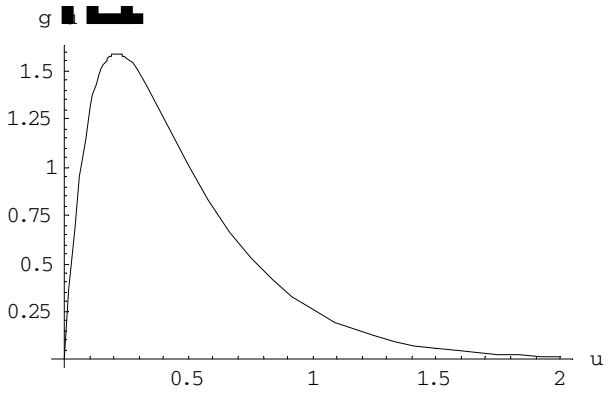

Fig.7. Graph of density function of random variables sum with exponential distribution

Using the Monte Carlo method, 1000 values of variable *X* with exponential distribution E($\lambda_1=3$) were determined by way of simulation, as well as 1000 values of variable *Y* with exponential distribution E($\lambda_1=7$). Next they were summed, and the distribution of variable *U=X+Y* was obtained. A histogram of this variable is presented in Fig. 8.

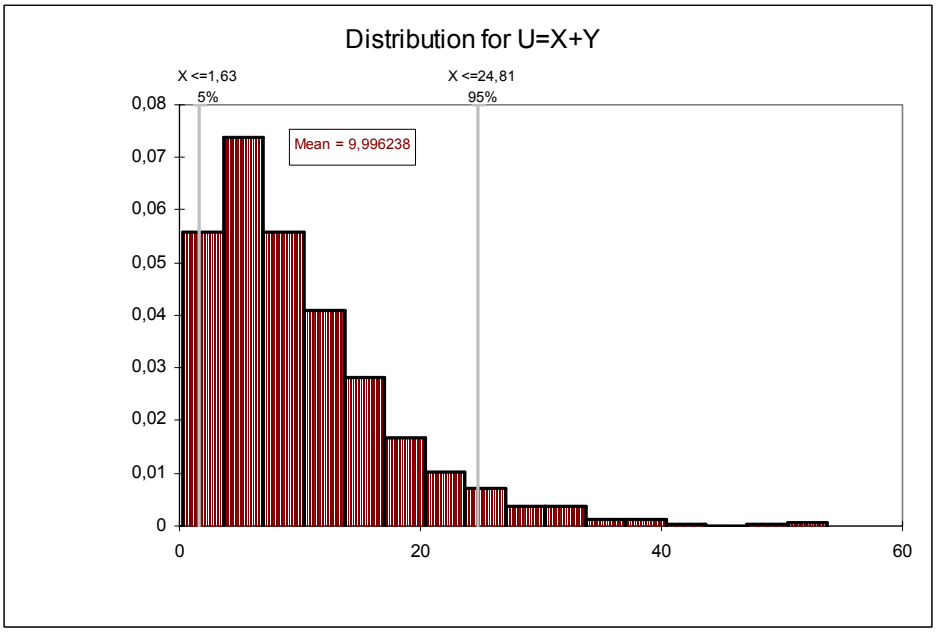

Fig.8. A histogram of sum distribution of simulated random variables with exponential distributions

Among distributions matched, variable *U* is best described by Gamma distribution with parameters (1.71; 5.7). The conformity of these distributions is high, as the chi^2 coefficient is equal to 17.9 at critical value 41.33 (on confidence level 0.95).

8 Resumé

The convolution of particular density functions of random variables makes it possible to distribute a given phenomenon over a number of smaller elements, which can be examined more easily and profoundly. Knowing the distributions of particular component elements of the variable, the distribution of this variable can be determined. What is also interesting is the fact that knowing the distribution of the variable and knowing that this distribution is a convolution of other distributions, it is possible to search for component elements of this variable with known distributions. This process is possible due to matching the distribution to the sum of simulated random variables.

References

[1] Drwal G., Grzymkowski R., Kapusta A., Słota D., *Mathematica 4*, Wydawnictwo Pracowni Komputerowej Jacka Skalmierskiego, Gliwice 2000.

[2] Gajek L., Kałuszka M., *Wnioskowanie statystyczne*, WNT Warszawa 1996.

[3] Galor W., *Wybrane modele oceny ryzyka zderzenia statku z budowlami hydrotechnicznymi*, Zeszyty Naukowe nr 70, WSM Szczecin 2003.

[4] Gucma L., *Modele probabilistyczne do oceny bezpieczeństwa statków na akwenach ograniczonych oparte na splotach rozkładów jednostajnego i normalnego*, Zeszyty Naukowe nr 11(83), AM Szczecin 2006.

[5] Gucma S., *Podstawy teorii linii pozycyjnych i dokładności w nawigacji morskiej*, WSM Szczecin, Szczecin 1995

[6] Kasyk L., *Empirical distribution of the number of ship reports on the fairway Szczecin – Świnoujście*, XIV-th International Scientific and Technical Conference The Part of Navigation in Support of Human Activity on the Sea, Gdynia 2004.

[7] Kasyk L., *Rozkład prawdopodobieństwa czasu oczekiwania na zgłoszenie statku na torze wodnym Szczecin – Świnoujście*, Zeszyty Naukowe nr 74, AM Szczecin 2004.

[8] Montgomery D. C., Runger G. C., *Applied statistics and probability for engineers*, John Wiley & Sons, Inc., New York 1994.

[9] Nowak R., *Statystyka dla fizyków*, Wydawnictwo Naukowe PWN, Warszawa 2002.

Risk assessment for LNG carrier maneuvers in a restricted sea area

Maciej Gucma
Institute of Marine Traffic Engineering, Maritime University Szczecin

Abstract: Increase of LNG (Liquefied Natural Gas) terminals development, especially in sea areas where other ports are located, leads to growth of marine traffic. This affects safety factors in such area. Article presents method for assessing navigational risk of maneuvering LNG carrier in area where dense traffic and movement restrictions occurs. Methods used in marine traffic engineering discipline are presented. Some conceptions of specific LNG terminals, with its particulars related to maneuvering safety factors are showed as well.

1 Introduction

Over the last few years, there has been a substantial increase in the worldwide production and transportation of Liquefied Natural Gas (LNG). This situation leads to growth of traffic in areas where LNG terminal are located. While many studies have been conducted to assess the consequences and risks of potential LNG land based accident, the increasing importance of marine LNG imports suggests that, consistent methods and approaches shall be identified and implemented to help improve safety.

One of possible regulations for safety assessment of waterways for LNG has been developed by United States Coast Guard. The Waterway Suitability Assessment (WSA) outlined in the Navigation Vessel and Inspection Circular (NVIC) No. 05-05: "Guidance on Assessing the Suitability of a Waterway for Liquefied Natural Gas Marine Traffic" is a qualitative assessment of a waterway. The WSA is considered crucial to the objective evaluation of proposals to build and operate shoreside LNG terminals. The Coast Guard Captain of the Port (COTP) reviews and validates the applicant's assessment, ensuring it adequately addresses the inherent safety, security, and environmental risks associated with the terminal and LNG marine traffic.

From the European Union point of view there are no common politics related to LNG maritime safety measures. Each country has own procedures for implementation and op-

eration of shore based LNG terminals. In such case it is a desirable to create own risk criterions for maneuvering of LNG tanker carrier in confined waters. Although such criterions should be based on well described and accepted models. This work is introduction study in maritime safety field for development of LNG system in Polish coast.

2 LNG Terminal Waterway Suitability Assessments

The WSA described in NVIC 05-05 is a relatively new process for the LNG industry and the Coast Guard in the United States of America. The new process calls for the applicant to complete a comprehensive WSA that considers all aspects of safety, security, and the marine environment. Major factors and risks assessed include [5]:

- density and character of marine traffic, including detailed analysis of recreational, commercial, military and other movements,
- identification of critical sea infrastructure – for traffic of LNG carrier,
- key assets along the transit route,
- consequences resulting from possible LNG spills,
- demographical situation in proximity of terminal,
- detailed characterization of LNG facility with, so called 'Zones of Concern' giving applied to the length of the transit to determine the main areas of concern along the waterway.
- maneuvers required to berth to terminal, and their impact for traffic in vicinity,
- availability of resources for maintaining security and safety,

In addition, the process outlined in WSA requires the Coast Guard to conduct a review and validation of the applicant's to ensure it presents a realistic and credible analysis of the public safety and security implications for introducing LNG marine traffic into the port and evaluates the measures intended to responsibly manage identified risks [5].

Risk Assessments in Means of WSA determines both safety and security aspects. After the port environment and transit route have been characterized, the WSA should analyze the risks that arise from the introduction to LNG operations into the port. The goal of this section of the WSA is to discern and understand the individual risks, in terms of probabilities, threats, vulnerabilities and consequences, so that appropriate risk management strategies can be developed in the next section. The WSA should go into as much detail as possible [5]. Key assumptions should be identified and a sensitivity analysis performed.

User of terminal may use any assessment methodology deemed appropriate. However, it is recommended that the applicant use a methodology that meets generally accepted risk-based decision-making industry standards and that the assessment is as objective and

transparent as possible. The Risk Assessment portion of the WSA looks at the conditions that could result in a release of LNG. The events that could trigger a release may be accidental (collisions, groundings, spills, etc.) or intentional (terrorist act, sabotage, etc) [5]. The accidental releases should be considered in a safety assessment that looks at the probability and consequences of various incidents. For the unique case of intentional releases a security assessment is performed.

3 MTE tools for assessment of risk factors

The Marine Traffic Engineering as a regular science was initiated due to the increasing number of vessel accidents, due to the higher intensity of vessels traffic. Such circumstances are of special interest in confined water regions. Along with the increased number, size and speed of ships, there was no corresponding change in the size of waterways, canals and maneuvering areas.

A vessel can maneuver safely only in an area where she fulfils at every point the condition of required depth. Such an area is called **accessible navigational** area, which can be presented in the form of area **D** of sets of point fulfilling the condition of required depth at moment t [3].

The vessel performing a given maneuver in an accessible navigational area occupies a certain area determined by her successive locations in the area. The parameters of this area are random and depend on various factors. This area, calculated on a definite reliability level is called **safe maneuvering** area. A safe maneuvering area so defined can be presented in the form of area $\mathbf{d}_{ijk}$ (set of points) and the **basic navigational safety condition** can be written down as follows [3]:

$$\left.\begin{array}{c} \mathbf{d}_{ijk} \subset \mathbf{D}(t) \\ p(x,y) \in \mathbf{D}(t) \quad h(x,y,t) \geq T(x,y,t) + \Delta(x,y,t) \end{array}\right\} \tag{1}$$

where:

- $\mathbf{D}(t)$ – accessible navigational area (meeting the condition of accessible depth at moment t,
- $\mathbf{d}_{ijk}$ – accessible maneuvering area (traffic lane) of the i-th vessel, performing the j-th maneuver in k-th navigational conditions,
- $h(x, y, t)$ – the depth of the area at point with coordinates (x, y) at moment t,
- $T(x, y, t)$ – the draft of the vessel at area point with coordinates (x, y) at moment t,
- $\Delta(x, y, t)$ – underkeel clearance at area point with coordinates (x, y) at moment t.

Sets of points of the accessible navigational area $\mathbf{D}(t)$, as also the safe maneuvering area $\mathbf{d}_{ijk}$ can be identified with areas of definite linear parameters (Fig. 1). P represents actual

position of vessel in moment t, and P_2 represents position in moment t_2, and for its moment probability of grounding and touching the bottom is visualized.

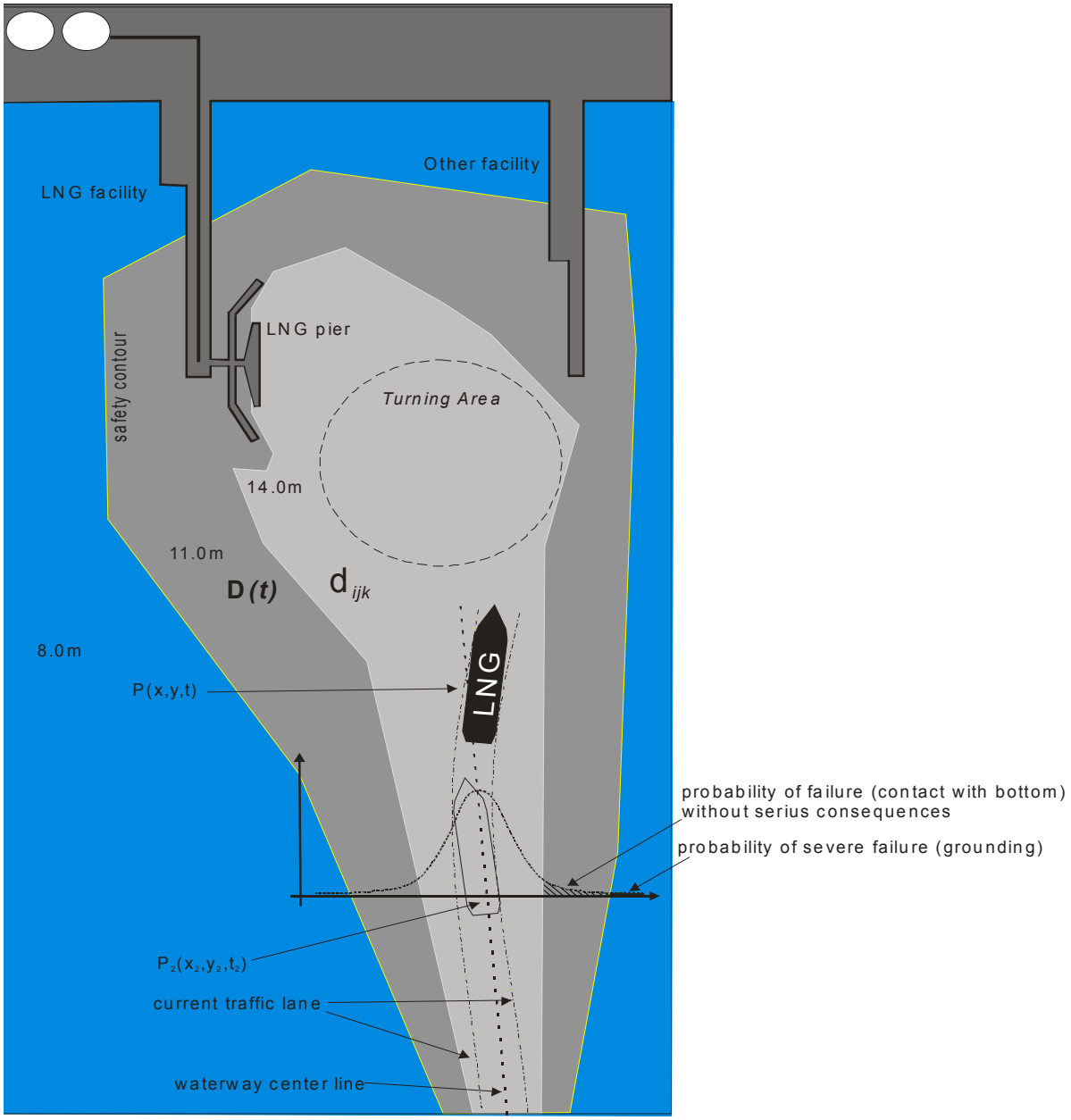

Fig. 1: Sets of accessible navigational area $\mathbf{D}(t)$ and safe manoeuvring area $\mathbf{d}_{jk}$ for LNG tanker in virtual port

Navigational safety in restricted areas is a concept which covers all problems bound with conducting the vessel from point A to point B, fulfilling the basic navigational safety condition on the confined water.

Such defined safety can be presented in the form of the function [2]:

$$P_i = f(A_i, S_i, N_i, H_i, M_i, I_i, R_i) \tag{2}$$

where:

A_i – area parameters,

S_i – vessel parameters,

N_i – position fixing systems parameters,

H_i – parameters of hydrometeorological conditions,

M_i – parameters of manoeuvre performed taking into consideration the human factor,

I_i – traffic intensity parameters,

R_i – traffic control system parameters.

4 Simulation researches

Computer based simulations are used for assessment of traffic lane and after analysis an actual level of risk at given area and given conditions. Navigational risk is defined as the product of probability of failure occurrence and the consequences it can cause. Additionally, the definition of risk was supplemented by relative frequency of performing the maneuver under research. Assuming that failure and its results are independent occurrences, navigational risk can be presented in the form of product [3]:

$$R_{ijkxy} = I_{ijkxy} \cdot P^{a}_{ijkxy} \cdot S_{ijkxy} \tag{3}$$

where:

I_{ijkxy} – average annual intensity (frequency) of performing the *j*-th maneuver by the *i*-th vessel in *k*-th navigational conditions in area (xy),

P^{a}_{ijkxy} – probability of particular failure occurrence when performing the *j*-th maneuver by the *i*-th vessel in *k*-th navigational conditions in area (xy),

S_{ijkxy} – results caused by this failure when performing the *j*-th maneuver by the *i*-th vessel in *k*-th navigational conditions in area (xy).

At the same time it should be noted that the product $I_{ijkxy} \cdot P^{a}_{ijkxy}$ is the probable number of a definite failure occurrence in a year that is [3]:

$$a_{ijkxy} = I_{ijkxy} \cdot P^{a}_{ijkxy} \tag{4}$$

The estimation of navigational risk consists of:

- calculation of the probability of failure occurrence of a certain type when performing the *j*-th kind of maneuver in a set area restricted by the *i*-th kind of vessel in *k*-th navigational conditions,
- estimating failure consequences of a certain type due to performing the *j*-th kind of manoeuvre in a set area restricted by the *i*-th kind of vessel in *k*-th navigational conditions.

Based on the definition of navigational risk the condition of safe definition of safe navigation has been determined [2]:

$$R_{ijkxy} \leq R_{xy}^{acc} \tag{5}$$

and after transformation:

$$I_{ijkxy} \cdot P_{ijkxy}^{a} \cdot S_{ijkxy} \leq R_{xy}^{acc} \tag{6}$$

Simulations are performed by expert users – captains on LNG tankers. Simulations environment is visualized at navigational chart (Fig. 2) or at 3D models. After completion of significant number of runs (usually 20 runs gives statistically significant results) over given area in given conditions and in given time, the analysis began. The mean traffic lane is evaluated and then risk criterions are checked again for fulfillment of acceptability.

Simulations results from performed in Marine Traffic Engineering Institute, Maritime University of Szczecin for entering large crude carrier to port Swinoujscie in Poland, are presented at Fig. 3.

Along with simulation runs, expert opinions elicitation, will give an answer for probabilities of failures of such events that could not be assed directly as for example:

- Fatal:
  - Grounding;
  - Collision;
  - Stranding;
  - Loss of stability;
  - Extreme weather during cargo operations;
  - Failure of cargo system in port;
- Non fatal:
  - Electrical system breakdown;
  - Mechanical system breakdown;
  - Steering system breakdown;
  - Other.

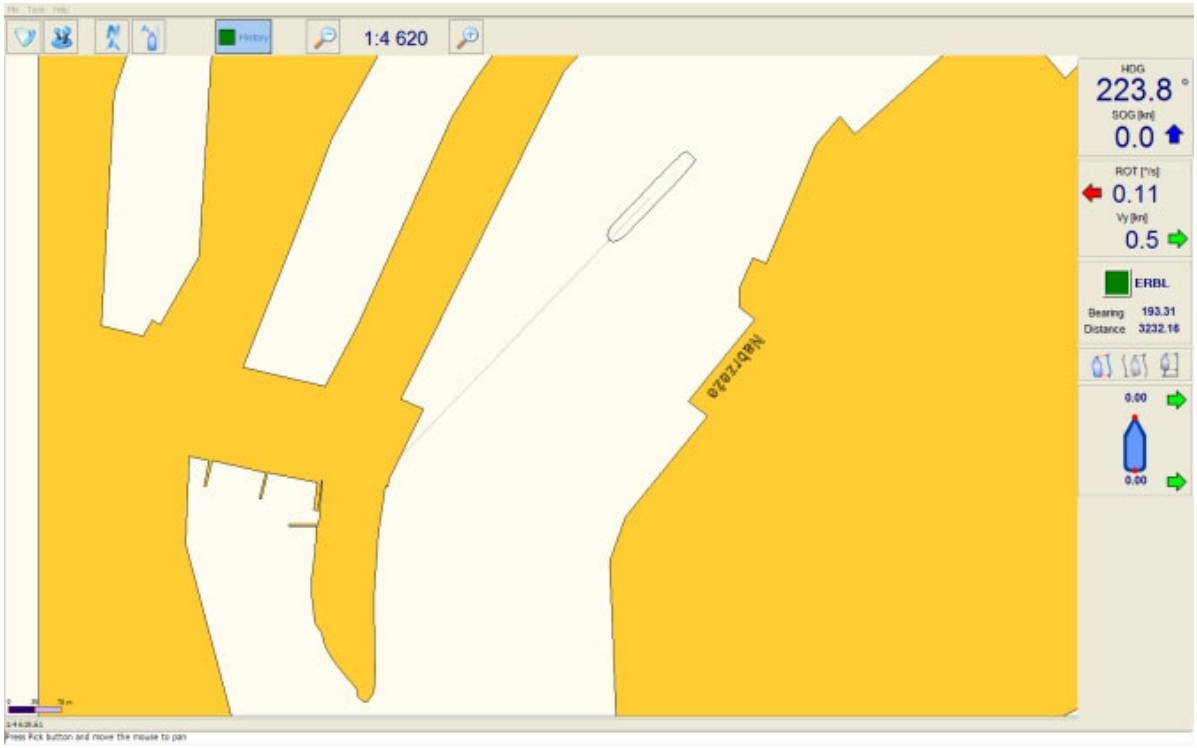

Fig. 2: Visualization during simulation runs

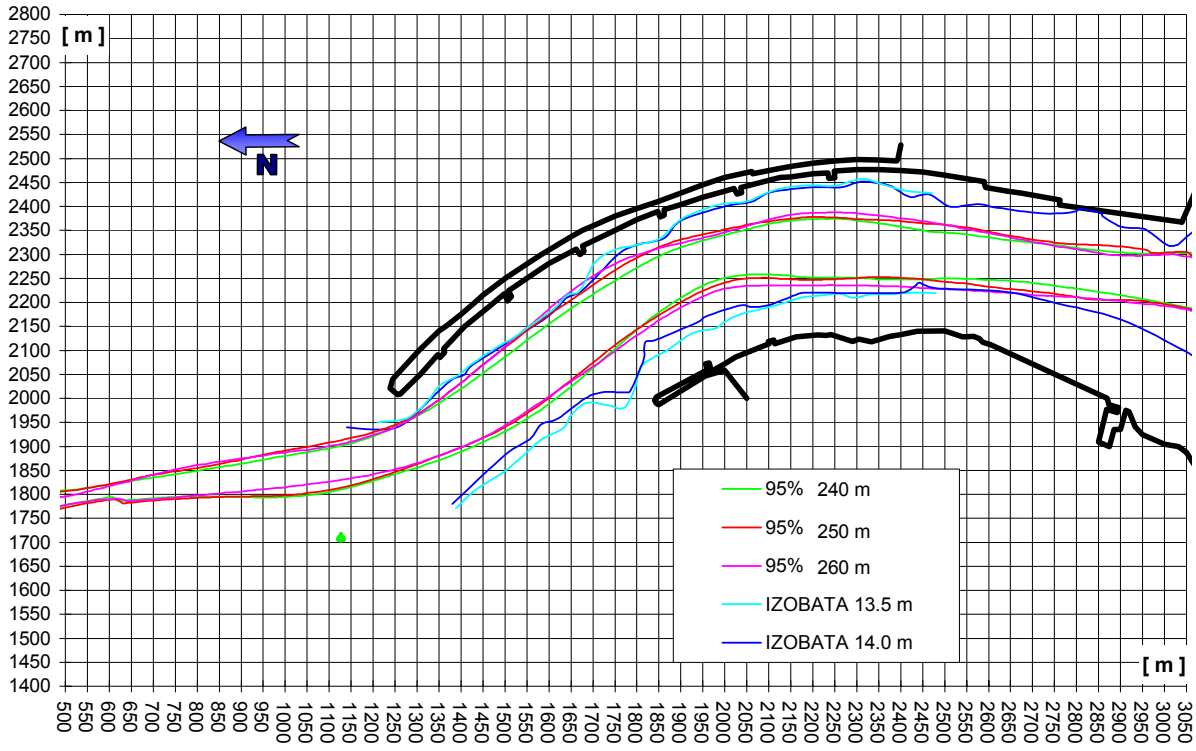

Fig.3. Traffic lanes during entrance of crude carrier to the inner port of Swinoujscie with lengths of: 240 m, 250 m and 260 m. [6]

This method gives values accident occurrence values for QRA reports that are desired for WSA in USA and for local regulations in UE. For example powered collision of merchant vessels with LNG tanker using coastal traffic lanes was estimated at value of $6.1 \cdot 10^{-6}$ for given port – studies for Cabrillio LNG port [4]. Other risks were calculated for among 70 different situations both fatal and non fatal [4].

5 Conclusions

Detailed study over localization of LNG terminal should be based on analysis of area and facilities in surroundings. Criterions used for risk assessment shall comply with the accepted methods used in MTE science.

Qualitative risk assessment method proposed by companies like DNV (Det Norske Veritas), do not give an answers for measurable risk in field of vessel movement, other than expert based factors. Such methodology is not effective for LNG carrier traffic safety assessment, due to the fact that potential accident might lead to many casualties. Proposed method has following features:

- Gives detailed risk factors for specific maneuvers,
- Describes conditions of performed maneuvers,
- Is directly implemental for new structures (not existing terminals).

6 Bibliography

[1] Eriksen, R., Brandstorp, J.E., Cramer, E., *Evaluating the Viability of Offshore LNG Production and Storage*, DNV Consulting, Gastech, Qatar 2002.

[2] Gucma, S., *Marine Traffic Engineering*, Shipbuilding Foundation, Gdansk 2003

[3] Gucma, S., Model *of navigational safety at confined areas*, Safety and Reliability Conference KONBIN 2006 Proceedings, Krakow 2006.

[4] Independent Risk Assessment, *Cabrillo Port LNG Deepwater Port,* Risknology, Inc. January 2006

[5] *USCG, Guidance On Assessing The Suitability Of A Waterway For Liquefied Natural Gas (LNG) Marine Traffic* U.S. Department Of Homeland Security, United States Coast Guard, NVIC 05-05, 2005;

[6] *Simulation-based determination of maximum parameters of vessels that can safely enter the port of Swinoujscie conditions (possibilities of handling ships up to 280 m,)* WSM Szczecin, 2003 (research report in Polish, leader of project: prof. S. Gucma).

Graue Zahlen – Ein mathematisches Modell zur Beschreibung von Unbestimmtheit

Dirk Proske[1], Alfred Strauss[2], Konrad Bergmeister[2], Pieter van Gelder[3]
[1] Institut für Alpine Naturgefahren, Universität für Bodenkultur Wien
[2] Institut für Konstruktiven Ingenieurbau, Universität für Bodenkultur Wien
[3] Structural Hydraulic Engineering and Probabilistic Design, Technische Universität Delft

Zusammenfassung: Unbestimmtheit ist eine inhärente Eigenschaft der Welt. Unbestimmtheit kann durch geeignete mathematische Modelle beschrieben werden. Derartige Modelle sind z.B. die Wahrscheinlichkeitsrechnung, Fuzzy-Modelle, Neuronale Netze, Expertensysteme oder eben die Theorie der Grauen Systeme. Im Folgenden wird kurz auf die letztgenannte Theorie eingegangen. Anschließend werden zwei Beispiele vorgestellt, bei denen die Grauen Zahlen zur Erfassung von Unbestimmtheit verwendet wurden.

1 Einleitung

Die vollständige Vorhersage zukünftiger Ereignisse ist nach dem derzeitigen Verständnis der Welt unmöglich. Unbestimmtheit ist ein wesentlicher Bestandteil der bekannten Welt. Aber die aktive Rolle des Menschen und die damit verbundenen notwendigen Vorhersagen zukünftiger Ereignisse zwingen den Menschen, die Unbestimmtheit zu berücksichtigen. Im letzten Jahrhundert haben sich theoretisch-mathematische und empirisch-mathematische Modelle zur Extrapolation zukünftiger Ereignisse in nahezu allen Fachgebieten durchgesetzt und die reinen empirischen Regeln verdrängt. Im Gegensatz zu den reinen empirischen Regeln, die implizit Unbestimmtheit beinhalten, bedürfen die mathematischen Modelle einer besonderen Berücksichtigung der Unbestimmtheit. Dazu stehen verschiedene Verfahren bereit, wobei hierbei zu allererst die Statistik und Wahrscheinlichkeitsrechnung zu nennen wären. Weitere Verfahren sind die in den 60er Jahren des 20. Jahrhunderts von ZADEH entwickelten Fuzzy-Modelle [20], aber auch Entropie basierte Werte (z.B. SHANNON's Entropie als Maß fehlender Informationen), Degrees of belief (Subjektive Wahrscheinlichkeit), Expertensysteme (Delphi-Befragungen), Künstliche Intelligenz, Neuronale Netzwerke, Datamining, Rought Sets, Chaostheorie oder genetische Verfahren.

WEN & CHANG [10] verweisen in diesem Zusammenhang darauf, dass mehr als 300 mathematische Verfahren zur Entwicklung von Vorhersagemodellen existieren.

In den 80er Jahren wurde in China die Theorie der Grauen Zahlen durch DENG eingeführt [15]. Seither wurde dieses mathematische Verfahren zur Beschreibung der Unbestimmtheit auf vielen Gebieten in China verwendet. So wurden Graue Zahlen für die Abschätzung des Aufkommens an Schmutzwasser [4], für Temperaturvorhersagemodelle [5], Transportprobleme [6], Energieverbrauchsvorhersagen [7], für die Planung von Unterhaltungsmaßnahmen [2] oder für Flut- und Murenprognosen [12] verwendet. Auch eine Überführung von Fuzzymodellen in Graue Modelle wurde bereits vorgestellt [8].

Auf Grund der Tatsache, dass die Veröffentlichungen überwiegend in chinesischer Sprache gehalten waren, fand dieses Verfahren nur sehr wenig Beachtung im europäischen Raum. Deshalb soll hier im Folgenden eine kurze Einführung in das Thema der Grauen Zahlen erfolgen.

Der Name Graue Zahlen beschreibt den Informationsgehalt, welche eine Zahl besitzt. Im Vergleich dazu ist eine Schwarze Zahl eine Zahl, über die keine Informationen vorliegen und eine Weiße Zahl ist eine vollständig bekannte Zahl. Eine Zusammenstellung der Eigenschaften der Schwarzen, Grauen und Weißen Zahlen findet sich in Tab. 1.

Tab. 1: Eigenschaften von Zahlen

Eigenschaft	Schwarz	Grau	Weiß
Information	Unbekannt	Unvollständig	Vollständig
Darstellung	Dunkel	Grau	Leuchtend
Resultat	Keine Lösung	Mehrere Lösungen	Eine Lösung
Prozess	Neu	Erfahrungen liegen vor	Alt
Eigenschaften	Chaotisch	Komplex	Ordnung
Vorstellung	Negativ	Übergang	Positiv

1.1 Begriffe

Eine Graue Zahl wird mathematisch als $\otimes$ dargestellt. Innerhalb der Definition Grauer Zahlen sind verschiedene Klassen bekannt (GUO & LOVE [1]):

Graue Zahl mit Untergrenze	$\otimes \in [\underline{a}, \infty]$
Graue Zahl mit Obergrenze	$\otimes \in [\infty, \overline{a}]$
Graue Zahl mit Intervall	$\otimes \in [\underline{a}, \overline{a}]$
Kontinuierliche Graue Zahl	$\otimes \in [\underline{a} \le n \le \overline{a}]$
Diskrete Graue Zahl	$\otimes \in [\underline{a} \le n_1 \le n_2 \le n_3 ... \le n_i \le \overline{a}]$
Schwarze Zahl	$\otimes \in [\infty, \infty]$ oder $\otimes \in [\otimes_1, \otimes_2]$
Weiße Zahl	$\otimes \in [\underline{a}, \overline{a}]$ mit $\underline{a} = \overline{a}$
Aufhellungsprozess	Prozess zur Ermittlung einer repräsentativen Grauen Zahl. Bei Grauen Zahlen, die um einen Wert schwan-

ken, wählt man hier in der Regel den Mittelwert
$\tilde{\otimes} = \alpha \cdot a + (1-\alpha) \cdot b = 0,5 \cdot a + 0.5 \cdot b$

Eine Graue Zahl muss jedoch nicht als reiner Zahlenintervall definiert werden, sondern kann auch als Funktion abgebildet werden. Beispiele dafür werden in Tab. 2 gezeigt.

Tab. 2: Verschiedene Formen von Grauen Zahlen nach DENG [15]

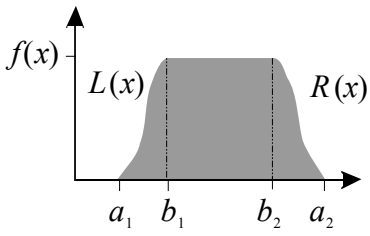

Graue Zahl

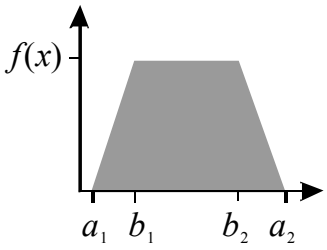

Graue Zahl mit linearen Funktionen

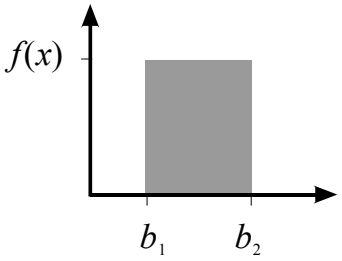

Zahlenintervall

Der Kenntnisstand einer Zahl kann über den Grauwert oder die Graustufe der Zahl beurteilt werden. Vergleichbar dazu wäre die Standardabweichung oder Varianz einer Zahl in der Statistik. Im Gegensatz dazu ist die Graustufe aber einheitenlos. Es gibt verschiedene Formen von Graustufen, wie z.B.

die relative Graustufe einer Zahl: $g^0 = \left(\frac{2 \cdot |b_2 - b_1|}{b_2 + b_1} + \max\left\{ \frac{|b_1 - a_1|}{b_1}, \frac{|b_2 - a_2|}{b_2} \right\} \right)$,

die absolute Graustufe einer Zahl: $g^0 = |b_2 - b_1| + 0,5 \cdot \left(|b_1 - a_1| + |b_2 - a_2| \right)$,

die Graustufe einer Intervall-Zahl: $g^0 = \frac{2 \cdot |b_2 - b_1|}{b_2 + b_1}$.

Berechnet man für eine Intervallzahl 8 bis 16 die Graustufe, so erhalt man:

$$g^0 = \frac{2 \cdot |16 - 8|}{16 + 8} = 0,667 .$$

In Abb. 1 wird die Entwicklung der Graustufe einer Intervallzahl in Abhängigkeit der Veränderung der oberen Schranke gezeigt.

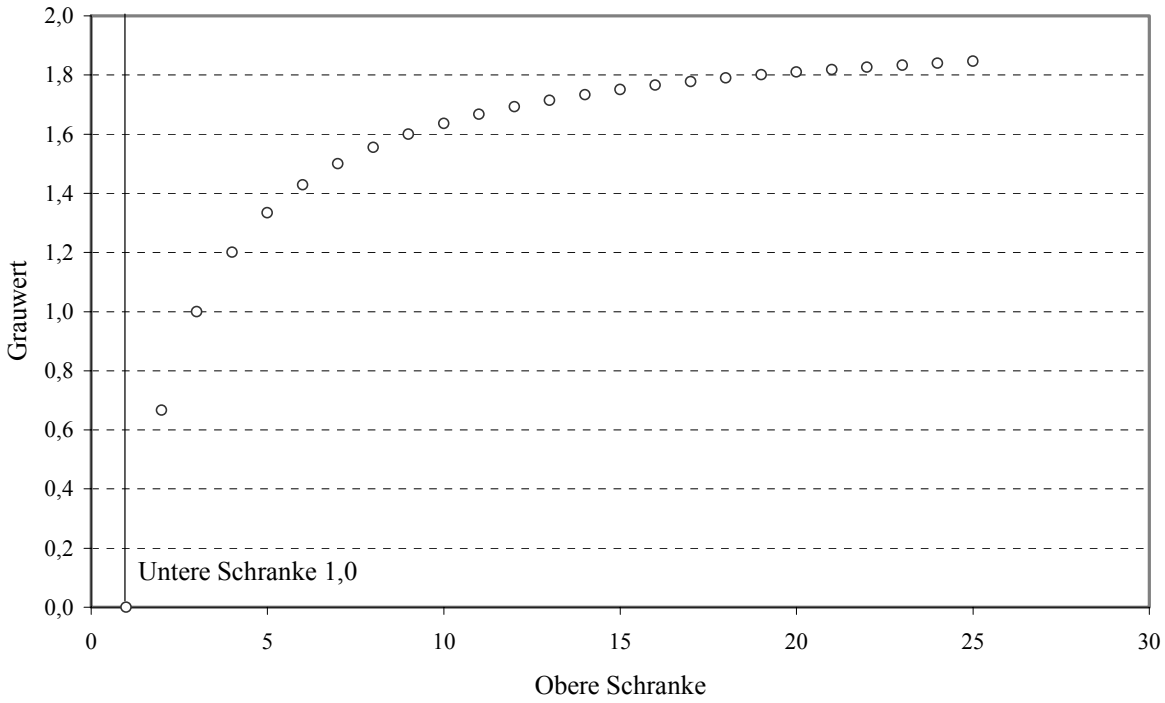

Abb. 1: Verlauf der Graustufe für eine Intervallzahl, bei der die untere Schranke mit 1,0 konstant gehalten wird und die obere Schranke kontinuierlich erhöht wird.

1.2 Prognose

Die grundlegende Annahme für die Modellbildung ist das Vorhandensein stetiger und differenzierbarer Funktionen zur Beschreibung von Abhängigkeiten. Diese Annahme kann auf Grund der begrenzt vorliegenden Daten in der Regel nicht geprüft werden. Die in vielen Gebieten auftretenden Probleme bei der Prognose, so z.B. in den Sozialwissenschaften, können möglicherweise auf die Korruption dieser Annahme zurückgeführt werden.

Die Idee bei der Anwendung Grauer Zahlen liegt nun darin, die Differential- und Integralrechnung auf diskrete Zahlenreihen anstelle von Funktionen zu erweitern. Die im Folgenden dargestellte Herleitung der Prognoseverfahren ist DENG [15] und GUO & LOVE [1] entnommen. Es soll eine Zahlenreihe, z.B. Messwerte in der Form

$$X^{(0)} = \begin{pmatrix} x^{(0)}(1) \\ x^{(0)}(2) \\ x^{(0)}(3) \\ \dots \\ x^{(0)}(k) \end{pmatrix}$$

vorliegen.

Zunächst wird das Integral dieser Zahlenreihe behandelt:

$$F(x) = \int_a^b f(x)dx = \lim_{\Delta x \to 0} \sum_{k=0}^{n-1} f(x_k)\Delta_k$$

Eine integrierte Funktion besitzt weniger Extremstellen, sie verläuft in der Regel gleichmäßiger als die ursprüngliche Funktion. Betrachtet man solche Extremwerte als Ausreißer, so werden diese Ausreißer durch den Integrationsprozess eliminiert. Die gegebene Zahlenreihe $X^{(0)}$ wird nun integriert, in dem gilt:

$$x^{(1)} = \sum_{i=0}^{k} x^{(0)}(i)$$

Die Integration soll als Operator *D* bezeichnet werden $D: X^{(0)} \to X^{(1)}$. Weitere Operationen sind möglich:

$$x^{(r)} = \sum_{i=0}^{k} x^{(r-1)}(i)$$

.

Im nächsten Schritt wird die Ermittlung des Differenzials betrachtet. Dazu wird die Reihe

$$X^{(r)} = \begin{pmatrix} x^{(r)}(1) \\ x^{(r)}(2) \\ x^{(r)}(3) \\ \dots \\ x^{(r)}(k) \end{pmatrix}$$

herangezogen. Das Differential ergibt sich dann zu:

$$\frac{d}{dt} X^{(r)}(k) = \lim_{\Delta t \to 0} \frac{x^{(r)}(k) - x^{(r)}(k-1)}{\Delta t}$$

Berücksichtigt man die Ermittlung von $X^{(r)}$, so erkennt man, dass gilt:

$$\frac{d}{dt} X^{(r)}(k) = \frac{\sum_{i=1}^{k} x^{(r-1)}(i) - \sum_{i=1}^{k-1} x^{(r-1)}(i)}{1} = x^{(r-1)}(k)$$

Damit können Summen bzw. Differenzen der Messreihen als Integrale und Differentiale betrachtet werden und sind ineinander überführbar. Die Überführung der Reihen kann nun auf Differentialgleichungen angewendet werden.

Zunächst soll die Differentialgleichung 1. Ordnung:

$$\frac{dx}{dt} + a \cdot x = b$$

betrachtet werden. Diese Gleichung ist die Grundlage für das so genannte Graue Model GM(1,1). Dazu wird zunächst $x = x^{(1)}$ gewählt und man erhält:

$$\frac{dx^{(1)}}{dt} + a \cdot x^{(1)} = b$$

Da $\frac{dx^{(1)}}{dt} = x^{(0)}$ gilt, kann man schreiben:

$$x^{(0)} + a \cdot x^{(1)} = b$$

Allerdings stimmen jetzt die Zeitpunkte nicht mehr. Deutlich wird dies allein durch die Tatsache, dass $x^{(0)}$ einen Zahlenwert mehr hat als $x^{(1)}$. Diese Zeitverschiebung wird korrigiert, in dem man anstelle von $x^{(1)}$ mit dem Mittelwert zweier benachbarter $x^{(1)}$ rechnet. Das entspricht auch einem Aufhellungsprozess, also der Berücksichtigung zusätzlicher Informationen: $z^{(1)}(k) = 0.5 \cdot x^{(1)}(k) + 0.5 \cdot x^{(1)}(k-1)$. Der Wert 0.5 ist variable. Im Rahmen der vorliegenden Untersuchungen wurde ein Verfahren umgesetzt, welches den Wert im Sinne des kleinsten Fehlerquadratsumme optimiert, wobei gilt

$$z^{(1)}(k) = f \cdot x^{(1)}(k) + (1/f) \cdot x^{(1)}(k-1)$$

Die Differentialgleichung wird nun zu:

$$x^{(0)} + a \cdot z^{(1)} = b$$

Mit den Originaldaten und den Umrechnungen der Reihen können nun die noch unbekannten Parameter *a* und *b* der Differentialgleichung bestimmt werden. Dazu wird das folgende Gleichungssystem aufgestellt.

$$x^{(0)}(2) = -a \cdot z^{(1)}(2) + b$$
$$x^{(0)}(3) = -a \cdot z^{(1)}(3) + b$$
$$x^{(0)}(4) = -a \cdot z^{(1)}(4) + b$$
...

Schreibt man dieses Gleichungssystem in Matrixform, so erhält man die Matrix

$$B = \begin{bmatrix} -z^{(1)}(2) & 1 \\ -z^{(1)}(3) & 1 \\ -z^{(1)}(4) & 1 \end{bmatrix}, \text{ und den Vektor } Y = \begin{bmatrix} x^{(0)}(2) \\ x^{(0)}(3) \\ x^{(0)}(4) \end{bmatrix}.$$

Die Bestimmungsgleichung für die noch unbekannten Parameter ist

$$A = \begin{bmatrix} a \\ b \end{bmatrix} = (B^T \cdot B)^{-1} \cdot B^T \cdot Y .$$

Die gegebene inhomogene Differentialgleichung 1. Ordnung

$$\frac{dx}{dt} + a \cdot x = b$$

gehorcht der Form

$$\frac{dx}{dt} = r \cdot x + k$$

Diese Differentialgleichung kann wie folgt gelöst werden:

$$\frac{dx/dt}{x + k/r} = r$$

Beide Seiten werden integriert und man erhält: $\ln(x + k/r) = r \cdot t + C$

Weiter kann man beide Seiten exponieren:

$$x + k/r = \pm \exp(r \cdot t) \cdot \exp(C) .$$

Isoliert man im nächsten Schritt x, so ergibt sich:

$$x = \exp(r \cdot t) \cdot \exp(C) - \frac{k}{r}$$

Jetzt verwendet man wieder die ursprünglichen Bezeichnungen und Vorzeichen:

$$x = C \cdot \exp(-a \cdot t) + \frac{b}{a}$$

Die Variable C beschreibt die Startbedingungen:

$$C = \left(x^{(0)}(1) - \frac{b}{a} \right) .$$

Basierend auf den vorliegenden Datenreihen, kann man gemäß der Formel Daten extrapolieren:

$$\hat{x}^{(1)}(k+1) = \left(x^{(0)}(1) - \frac{b}{a} \right) \cdot e^{-a \cdot k} + \frac{b}{a}$$

$$\hat{x}^{(0)}(k+1) = \hat{x}^{(1)}(k+1) - \hat{x}^{(1)}(k) .$$

Neben dem Grauen Model GM (1,1)-Modell gibt es weitere Modelle, die auf anderen Ansätzen beruhen, wie z.B. DGDMMI(1,1,1) [21], GDM(2,2,1) [26], GFM(1,1) [26], GM(2,2) [23], GM(0,N) [12], UIRGM(1,1) [25] oder DGDM(1,1,1) [22].

■ Beispiel

Im Folgenden soll die Anwendung an einem sehr einfachen Beispiel gezeigt werden. Dazu wird ein exponentieller Wachstumsprozess für eine zu extrapolierende Größe angenommen. Die Eingangsgrößen für die Funktion sind in Tabelle 3 angegeben. Der Wert für 2010 wurde mittels Regression Grauer Zahlen geschätzt.

Tab. 3: Eigenschaften von Zahlen

Jahr	Messwert
1995	1,412
2000	1,050
2005	0,720
2010 extrapoliert	0,4933

Die Berechnung wurde mit dem Programm MATLAB durchgeführt. Die Variablen gemäß der bisher verwendeten Nomenklatur sind links Die Einzelwerte der Berechnung ergeben sich zu:

```
X0 =    1.4120    1.0500    0.7200                 x^(0)
Y0 =      1995      2000      2005                 Zeitachse
X1 =    1.4120    2.4620    3.1820                 x^(1)
Z1 =         0    1.9370    2.8220                 z^(1)
B  =   -1.9370    1.0000                           Matrix B
       -2.8220    1.0000
Y =     1.0500                                     Matrix Y
        0.7200
BT =   -1.9370   -2.8220                           Matrix B^T
        1.0000    1.0000
A =     0.3729                                     Matrix A
        1.7723
alpha = 0.3729                                     α
beta =  1.7723                                     β
X0SG =   1.4120    1.0500    0.7200    0.4937      x̂^(0)
```

1.3 Grauer Relationskoeffizient

Vergleichbar zum PEARSON'schen Korrelationskoeffizienten in der Statistik existiert innerhalb der Theorie der Grauen Zahlen auch ein Grauer Relationskoeffizient, der den Grad der Abhängigkeit zwischen Zahlenreihen beschreiben soll. Dazu müssen zwei Zahlenreihen in der Form

$$X_0 = \begin{pmatrix} x_0(1) \\ x_0(2) \\ x_0(3) \\ \\ x_0(k) \end{pmatrix} \quad X_1 = \begin{pmatrix} x_1(1) \\ x_1(2) \\ x_1(3) \\ \\ x_1(k) \end{pmatrix};$$

vorliegen. Es können auch mehrere Zahlenreihenpaare vorliegen. Im ersten Schritt werden die Beträge der Differenzen der Zahlenreihen ermittelt:

$$X_1 = \begin{pmatrix} |x_1(1) - x_0(1)| \\ |x_1(2) - x_0(2)| \\ |x_1(3) - x_0(3)| \\ \dots \\ |x_1(4) - x_0(4)| \end{pmatrix}, \quad X_i = \begin{pmatrix} |x_i(1) - x_{i-1}(1)| \\ |x_i(2) - x_{i-1}(2)| \\ |x_i(3) - x_{i-1}(3)| \\ \dots \\ |x_i(4) - x_{i-1}(4)| \end{pmatrix}$$

Der Relationskoeffizient ist definiert als:

$$\xi_{(i)}(k) = \frac{\min_i \min_k X + \alpha \max_i \max_k X}{X + \max_i \max_k X} \text{ mit } 0 \le \alpha \le 1$$

Der Wert α ist abhängig von den Umgebungsbedingungen:

$\alpha = 1$	Umgebungsbedingungen identisch
$\alpha = 0$	Umgebungsbedingungen unabhängig

Der berechnete Relationskoeffizient kann wie folgt interpretiert werden:

$0,9 < \xi \le 1$	Vollständige Abhängigkeit
$0,8 < \xi \le 0,9$	Gute Übereinstimmung
$0,6 < \xi \le 0,8$	Mittlere Übereinstimmung
$0,0 < \xi \le 0,6$	Keine Übereinstimmung

Bei Relationskoeffizient zwischen 0,0 und 0,6 besteht also ein signifikanter Unterschied zwischen den Zahlenpaaren.

2 Beispiele

2.1 Abschätzung von Hochwasserständen

In den Niederlanden befindet sich 40 % der Landesfläche unterhalb des Meeresspiegels. Diese Zahl zeigt die Bedeutung des Hochwasserschutzen in diesem Land. Um Schutzbauwerke gegen Hochwasser zu errichten ist die Prognose von Hochwasserständen erforderlich.

Für die Abschätzung von sturminduzierten Hochwasser in den Niederlanden gibt es eine Vielzahl von Verfahren und Veröffentlichungen. Die Verfahren lassen sich in der Regel in zwei Gruppen einteilen: rein stochastische Verfahren oder Mischverfahren, die sowohl

deterministische Zusammenhänge als auch stochastische Eingangsparameter berücksichtigen können. Beide Verfahrensarten müssen sich einer gewaltige Aufgabe stellen: nämlich der beachtlichen Extrapolation von Daten für die Bemessung von Dämmen. In der Regel wird ein Hochwasserpegeln mit einer Rückkehrperiode von 10.000 Jahren herangezogen. Die längsten Messungen von Hochwasserpegeln liegen bei ca. 130 Jahren. Im vorliegenden Fall wurden die Regional Frequency Analysis für Messungen an der niederländischen Nordseeküste verwendet, um die Datenmenge durch die Vermengung der Messungen an verschiedenen Küstenorten zu erhöhen.

Anschließend wurde für die Häufigkeit der Hochwasserpegel eine Wahrscheinlichkeitsverteilung gewählt. Basierend auf zahlreichen Vorarbeiten, die u.a. eine GUMBEL, Exponential-, Weibull- oder Logistische Verteilung nennen, wurden eine Exponential- und eine Logistische Verteilung gewählt. Für diese Verteilungen wurden die Verteilungsparameter basierend auf den Daten nicht mittels Maximum-Likelihood, wie üblich, sondern mittels Regressionsverfahren für Graue Zahlen berechnet (GM 1). Es zeigte sich, dass die errechneten Werte zum Teil deutlich über den bisher ermittelten Werten lagen (Abb. 2). Weitere Angaben zu der Berechnung finden sich bei PROSKE & VAN GELDER [21].

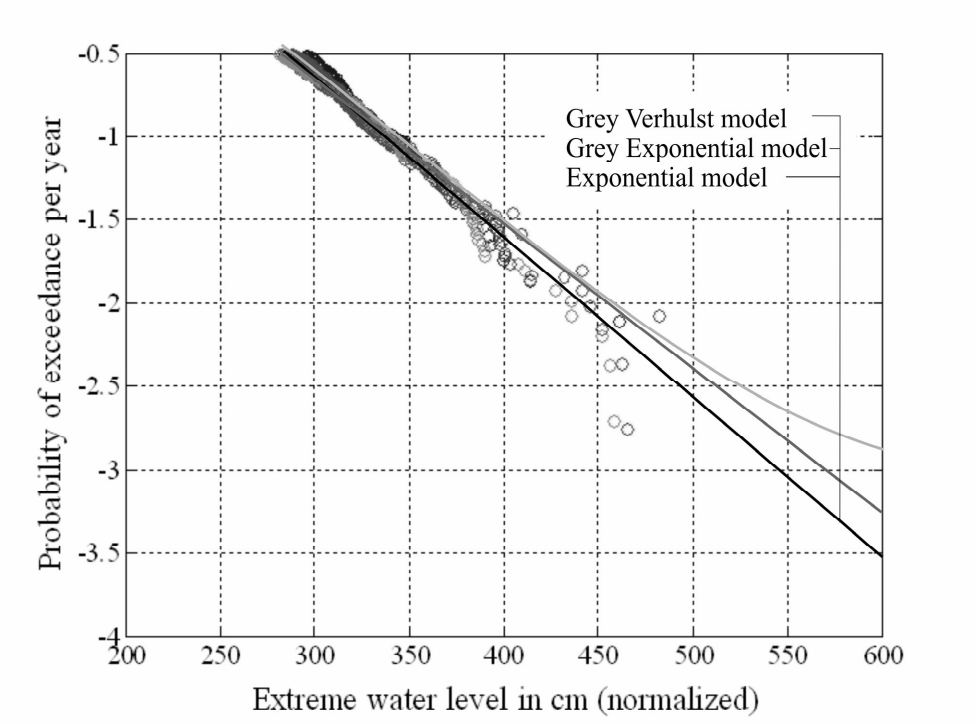

Abb. 2: Prognose von Hochwasserpegeln mittel Grauem Exponential Modell (GM 1), Grauem Verhulst Modell und der klassischen Exponentialverteilung

2.2 Identifikation von Schädigungen in Baukonstruktionen

Die Anwendung des Grauen Relationskoeffizienten soll am Beispiel der Identifikation von Schäden an einem Kragarm gezeigt werden. Grundlage für die hier vorgestellte Untersuchung waren Vorarbeiten von CHEN, ZHU & CHEN [3]. Untersuchungsgegenstand ist ein Kragarm, der verschiedenen Belastungen unterworfen wird. Die dabei auftretenden Ver-

formungen sollen an zwölf verschiedenen Stellen des Kragarmes erfasst werden. Zunächst werden die Messungen am unbeschädigten Originalsystem und anschließend am beschädigten System durchgeführt. Ziel der Untersuchung ist die Identifizierung von lokalen Schäden am Kragarm. Unter Schäden werden Bereiche mit einer überdurchschnittlichen Abnahme der Steifigkeit unter Belastung verstanden. Es wird davon ausgegangen, dass die Umweltbedingungen identisch sind. Die Untersuchung hier vorgestellte Untersuchung ist allein numerischer Art.

Zunächst werden die Verformungen im unbeschädigten und im beschädigten Zustand ermittelt. Anschließend werden die Krümmungen vereinfacht mittels Differenzverfahren berechnet. Weiterhin wird die Differenz der Krümmungen ermittelt, wobei die Minimal- und Maximalwerte berechnet werden. Damit kann der Graue Relationskoeffizient bestimmt werden. In Abhängigkeit von der Vorschädigung zeigt der Relationskoeffizient Veränderungen der Steifigkeiten der einzelnen Elemente des Kragarms an. Die drei Laststellungen, denen der Kragarm unterworfen wird, sind eine Einzellast am Kragarmende, drei Einzellasten verteilt über den Kragarm und sieben Lasten regelmäßig verteilt über den Kragarm. Abb. 3 zeigt nun die mittels Grauem Relationskoeffizienten identifizierten Schädigungen bei den jeweiligen Laststellungen (Linien) und die tatsächlich vorgegebene Schädigung (Graue Balken)

Das Problem bei dieser Untersuchung liegt nun darin, dass die Schädigungen oft durch andere Einflüsse überdeckt werden. Im vorliegenden Fall wurde deshalb ein sehr starkes weißes Rauschen über die Messwerte (Variationskoeffizient 30 %) gelegt. Dadurch wird die Identifikation der geschädigten Elemente deutlich schwieriger. Abb. 4 zeigt die Ergebnisse. Während bei den Messungen ohne weißes Rauschen die geschädigten Bereiche (Messpunkte) eindeutige identifiziert werden können, gelingt dies bei starkem weißem Rauschen deutlich schwieriger. Abb. 5 verdeutlicht den Umfang der Störungen in den Daten durch das weiße Rauschen. Trotzdem scheint der Graue Relationskoeffizient die geschädigten Bereiche identifizieren zu können.

Bei zwei Lastfällen wird die Schädigung an der Stelle 3 identifiziert. Lastfall 1 und Lastfall 2 weisen auf eine Schädigung am Messpunkt 5, die nicht existiert. Die leichte Schädigung in der Nähe der Messstelle 7 scheint bei allen drei Laststellungen erkannt zu werden. Allerdings wird die Schädigung an der Messstelle 8 vermutet. Auch die Schäden an der Messstelle 9 werden weiter nach hinten geschoben.

3 Ergebnisse

Das Verfahren der Grauen Zahlen ist eine weitere mathematische Möglichkeit der Behandlung von Unbestimmtheit. Die Anwendung wurde an zwei einfachen Beispielen gezeigt. Die Frage, in welchen Bereichen die Vorteile des Verfahrens der Grauen Zahlen im Vergleich zu andere mathematische Verfahren zur Erfassung von Unbestimmtheit liegen, erfordert aus Sicht der Autoren weitere Forschungsarbeit.

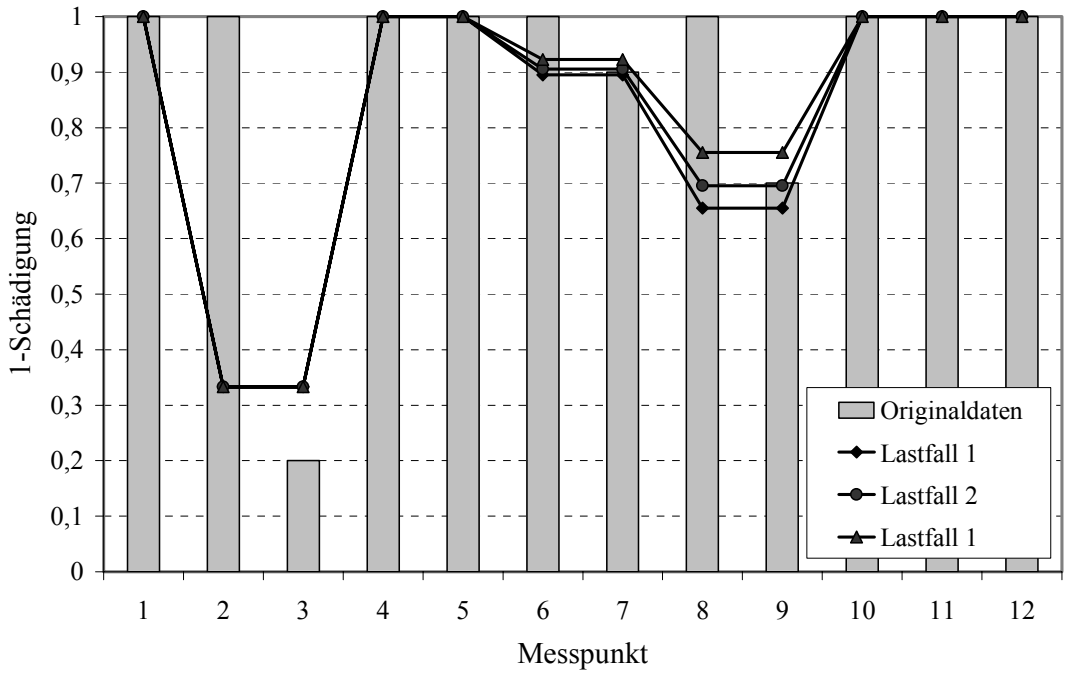

Abb. 3: Identifikation von Schädigungen durch den Grauen Relationskoeffizienten bei Messungen ohne weißes Rauschen.

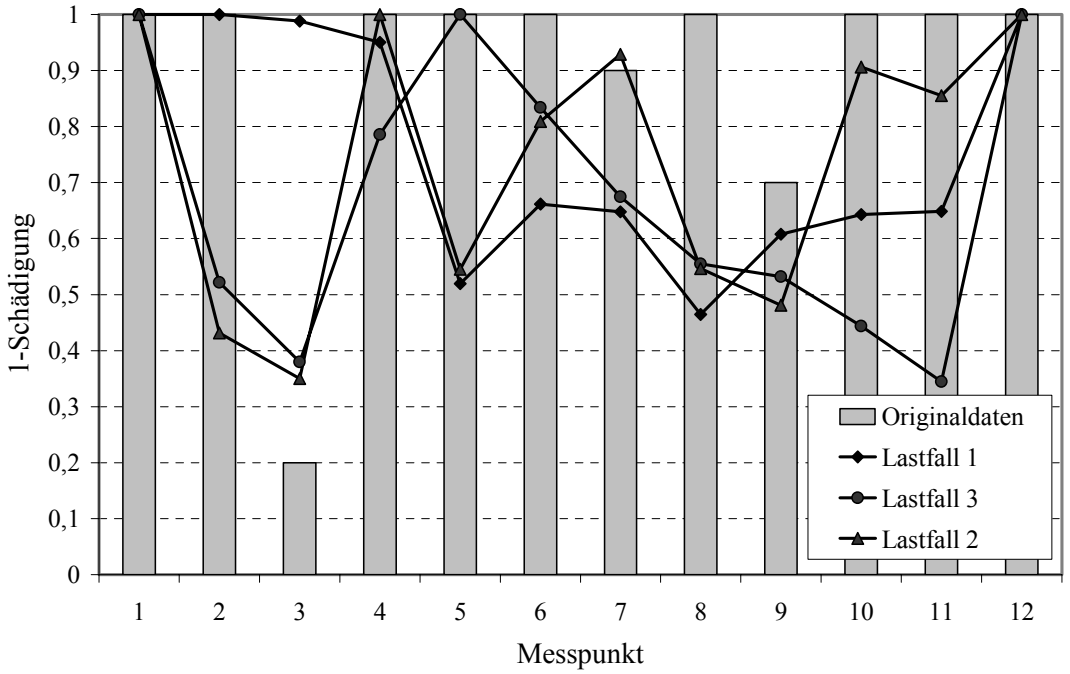

Abb. 4: Identifikation von Schädigungen durch den Grauen Relationskoeffizienten bei Messungen mit weißem Rauschen

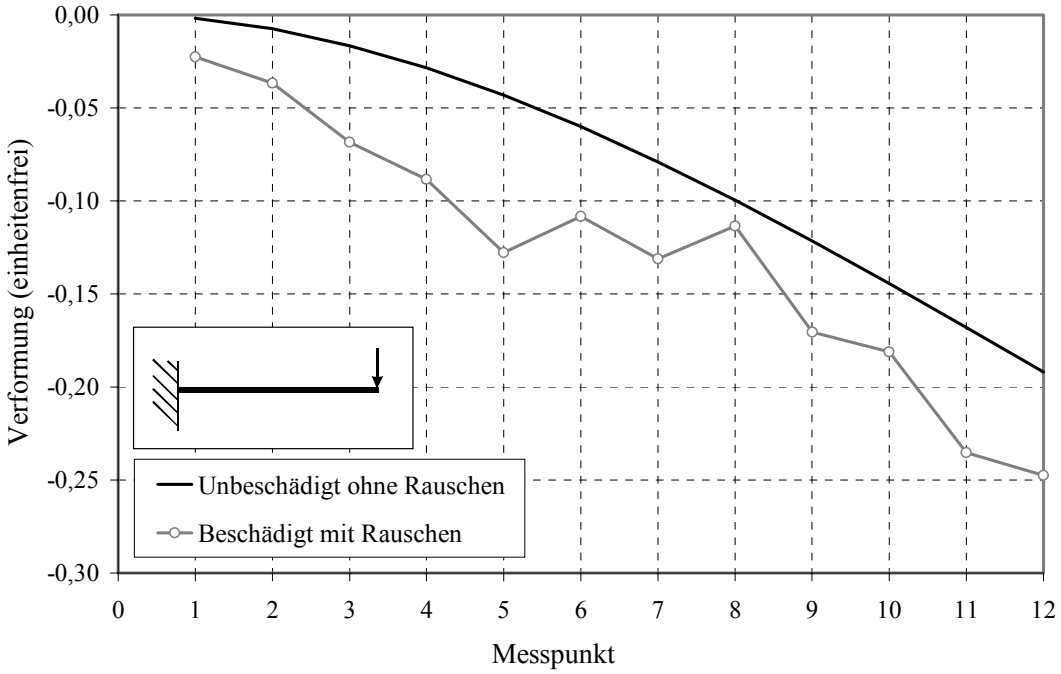

Abb. 5: Verformungsbild des Kragarmes mit und ohne weißes Rauschen

4 Literatur

[1] Guo, R.; Love, C.E.: Keynote lecture: Grey repairable system analysis. K. Kolowrocki (Edr.) *Advances in Safety and Reliability - ESREL 2005*, Taylor and Francis Group. London 2005, page 753-765

[2] Guo, R.; Dunne, T.: Stochastic system age processes. K. Kolowrocki (Edr.) *Advances in Safety and Reliability - ESREL 2005*, Taylor and Francis Group. London 2005, page 745-752

[3] Chen, X.; Zhu, H.; Chen, C.: Structural damage identification using test static data based on grey system theory. *Journal of Zhejiang University Science*, 2005 6A (8), page 790-796

[4] Jun, X.; Baoqing, H.: A grey system model for predicting trend change of urban waste water load. *Journal of Environmental Hydrology*, Paper 2, Volume 5, 1997

[5] Dounis, A.I.; Tiropanis, P.; Tseles, D.; Nikolaou, G.: Grey model for time series ambient temperature prediction, magazine unknown

[6] Bai, G.; Mao, J.; Lu, G.: Grey transportation problem. *Kybernetes*, Vol. 33 No. 2, 2004, Page 219-224

[7] You-xin, L.: Long-ting, Z.; An-hui, C.; Zhi-ming, H.: Grey GM(1, 1) model with function-transfer method and application to energy consuming prediction. *Kybernetes*, Vol. 33 No. 2, 2004, Page 322-330

[8] Tsaur, R.-C.: Fuzzy grey GM(1,1) model under fuzzy systems. *International Journal of Computer Mathematics*, Volume 82, Number 2, February 2005, page 141-149

[9] Yan, T.; Zhou, C.; Yan, L.: Prognoses of environmental geoscientific problems by grey systems. Magazine unknown

[10] Wen, K.-L.; Chang, T.-C.: The research and Development of Completed GM(1,1) Model Toolbox using Matlab. *International Journal of Computational Cognition*, Volume 3, No. 3, September 2005, Seite 41-47

[11] Lin, Y.; Chen, M.-Y.; Liu, S.: Theory of grey systems: capturing uncertainties of grey information. *Kybernetes*, Vol. 33 No. 2, 2004, Page 196-218

[12] Tien, T.-L.: The indirect measurement of tensile strength of material by the grey prediction model GMC(1,n). *Measurement Science and Technology* 16 (2005) Page 1322-1328

[13] Wong, K.-W.: Grey Tuple Dependency and Grey Relation Algebra. *Association of Computing Machinery*, 1995, Page 203-207

[14] Brown, C.B.: Self-organised critically and Jaynes Entrophy. *Applications of Statistics and Probability in Civil Engineering.* Der Kiureghian, Madanat & Pestana (Eds.), Millpress Rotterdam 2003, Seite 149-153

[15] Deng, J.: *Essential Topics on Grey Systems. Theory and Applications*, China Ocean Press, Bejing 1988

[16] Tien, T.-L.: A research on the deterministic grey dynamic model with multiple inputs DGDMMI(1,1,1). *Applied Mathematics and Computation*, 139 (2003), Seite 401-416

[17] Tien, T.-L.; Chen, C.-K.: The indirect measurement of fatigue limits of structural steel by the deterministic grey dynamic model DGDM(1,1,1). *Applied Mathematics Modelling*, Vol. 21, Oktober 1997, Seite 611-619

[18] Zhang, H.; Li, Z.; Chen, Z.: Application of grey modelling method to fitting and forecasting wear trend of marine diesel engines. *Tribology International* 36 (2003), Seite 753-756

[19] Chen, H.W.; Chang, N.B.: Prediction analysis of solid waste generation based on grey fuzzy dynamic modelling. *Ressource, Conservation and Recycling* 29 (2000), Seite 1-18

[20] Zadeh, L.A.: Fuzzy-Sets. *Information and Controll* 8 (1965), Page 338-353

[21] Proske, D.; van Gelder, P.: Analysis about extreme water levels along the Dutch north-sea using Grey Models: preliminary analysis. *ESREL 2006 Conference*, September 2006, Portugal

List of Referents & Authors

Bellon, Carsten
Bundesanstalt für Materialforschung und -prüfung
Unter den Eichen 87, 12205 Berlin
Germany

Bergmeister, Konrad, Prof. DDr.
Universität für Bodenkultur, Wien
Institut für Konstruktiven Ingenieurbau
Peter Jordan Strasse 82, 1190 Wien
Austria

Bierbrauer, Kerstin, Dipl.-Ing.
Universität der Bundeswehr München, Institut für
Konstruktiven Ingenieurbau - Massivbau
Werner-Heisenberg-Weg 39, 85577 Neubiberg
Germany

Caspeele, Robby, Dr.
Ghent University
Department of Structural Engineering
Magnel Laboratory for Concrete Research
Technologiepark Zwijnaarde 904, B-9052 Gent
Belgien

Courage, Wim , Dr.ir.
Structures and Safety
Business Unit of TNO Built Environment
and Geosciences
P.O. Box 49, 2600 AA Delft
The Netherlands

Daus, Stefan, Dipl.-Ing.
Technische Universität Darmstadt
Institut für Massivbau
Petersenstraße 12, 64287 Darmstadt
Germany

de Wit, Sten, Dr.-ing.
Structures and Safety
Business Unit of TNO Built Environment
and Geosciences
P.O. Box 49, 2600 AA Delft
The Netherlands

Elaguine, Mstislav, Dipl.-Math.
Bundesanstalt für Materialforschung und -prüfung
Unter den Eichen 87, 12205 Berlin
Germany

Ewert, Uwe, Prof. Dr. rer. nat., Dir.
Bundesanstalt für Materialforschung und -prüfung
Unter den Eichen 87, 12205 Berlin
Germany

Frangopol, Dan, Prof.
College of Engineering and Applied Science
University of Colorado at Boulder
422 UCB, Boulder, CO 80309-0422
U.S.A.

Fuchs, Sven, Dr. Geo.
Universität für Bodenkultur, Wien
Institut für Alpine Naturgefahren
Peter Jordan Strasse 82, 1190 Wien
Austria

Gaal, Mate, Dipl.-Phys.
Bundesanstalt für Materialforschung
und –prüfung, Berlin
Unter den Eichen 87, 12205 Berlin
Germany

Gelder, Pieter van, Prof. dr.-ir.
TU Delft
Hydraulik and Offshore Engineering Section
Postbus 5, 2600 AA Delft
The Netherlands

Glowienka, Simon, Dipl.-Ing.
Technische Universität Darmstadt
Institut für Massivbau
Petersenstraße 12, 64287 Darmstadt
Germany

Graubner, Carl-Alexander, Prof. Dr.-Ing.
Technische Universität Darmstadt
Institut für Massivbau
Petersenstraße 12, 64287 Darmstadt
Germany

Grêt-Regamey, Adrienne, M.A., M.S.
LEP, Landscape and Environmental Planning,
IRL, HIL H 31.2, ETH Hönggerberg
CH - 8093 Zürich
Switzerland

Gucma, Lucjan , Prof.
Institute of Marine Traffic Engineering
Maritime University of Szczecin
Wały Chrobrego 1-2, 70 – 500 Szczecin
Poland

Gucma, Maciej, MSc.
Institute of Marine Traffic Engineering
Maritime University of Szczecin
Wały Chrobrego 1-2, 70 – 500 Szczecin
Poland

Hausmann, Guido, Dipl.-Ing.
Technische Universität Darmstadt
Institut für Massivbau
Petersenstraße 12, 64287 Darmstadt
Germany

Hinrichs, Wilfried, Dr.-Ing.
MPA Braunschweig
Beethovenstraße 52, 38106 Braunschweig
Germany

Hoffmann, Simon, Dipl.-Ing.
Universität für Bodenkultur, Wien
Institut für Konstruktiven Ingenieurbau
Peter Jordan Strasse 82, 1190 Wien
Austria

Hosser, Dietmar, Prof. Dr.-Ing.
Institute for Building Materials,
Concrete Construction and Fire Protection
Technical University of Braunschweig
Beethovenstr. 52, 38106 Braunschweig
Germany

Klinzmann, Christoph, Dipl.-Ing.
Institute for Building Materials,
Concrete Construction and Fire Protection
Technical University of Braunschweig
Beethovenstr. 52, 38106 Braunschweig
Germany

Krom, Alfons H. M., Dr. ir.
Structures and Safety
Business Unit of TNO Built Environment
and Geosciences
P.O. Box 49, 2600 AA Delft
The Netherlands

Lech, Kasyk
Institute of Mathematics
Maritime University of Szczecin
Wały Chrobrego 1-2, 70 – 500 Szczecin
Poland

Maultzsch, Matthias, Dr.-Ing.
Bundesanstalt für Materialforschung
und –prüfung, Berlin
Unter den Eichen 87, 12205 Berlin
Germany

Mehdianpour, Milad, Dr.-Ing.
Bundesanstalt für Materialforschung und -prüfung
Unter den Eichen 87, 12205 Berlin
Germany

Müller, Christina, Dr. rer. nat., ORRin
Bundesanstalt für Materialforschung und -prüfung
Unter den Eichen 87, 12205 Berlin
Germany

Novák, Drahomír, Prof. Ing. DrSc
Institute of Structural Mechanics
Faculty of Civil Engineering
Brno University of Technology
Veveří 95, 662 37 Brno
Czech Republic

Pietrzykowski, Zbigniew, Prof
Maritime University of Szczecin
Waly Chrobrego 1-2, 70-500 Szczecin
Poland

Proske, Dirk, Dr.-Ing. MSc.
Universität für Bodenkultur, Wien
Institut für Alpine Naturgefahren
Peter Jordan Strasse 82, 1190 Wien
Austria

Pukl, Radomir, Ing. CSc.
Cervenka Consulting Prag
Predvoje 22, 160 00 Praha 6
Czech Republic

Redmer, Bernhard, Dipl.-Ing., RR
Bundesanstalt für Materialforschung und -prüfung
Unter den Eichen 87, 12205 Berlin
Germany

Ronneteg, Ulf
Bodycote Materials Testing AB
Box 1340, SE-581 13 Linköping
Sweden

Rydén, Håkan
Canister Laboratori
Box 925, SE-572 29 Oscarsamn
Sweden

Schnetgöke, Ralf, Dipl.-Ing.
Institute for Building Materials,
Concrete Construction and Fire Protection
Technical University of Braunschweig
Beethovenstr. 52, 38106 Braunschweig
Germany

Schweckendiek, Timo, Dipl.-Ing.
Structures and Safety
Business Unit of TNO Built Environment
and Geosciences
P.O. Box 49, 2600 AA Delft
The Netherlands

Scharmach, Martina, Dipl.-Ing.
Bundesanstalt für Materialforschung und -prüfung
Unter den Eichen 87, 12205 Berlin
Germany

Spitzer, Cornelia, Dipl-Math.
TÜV Süddeutschland
Dudenstraße 28, 68167 Mannheim,
Germany

Straub, Daniel, Dr.-Ing.
Department of Civil and Environmental Engineering,
University of California
Berkeley, CA 94720-1710
U.S.A.

Strauss, Alfred, Dr.-Ing.
Universität für Bodenkultur, Wien
Institut für Konstruktiven Ingenieurbau
Peter Jordan Strasse 82, 1190 Wien
Austria

Switaiski, Burkhard, Dr.-Ing.
TÜV Rheinland Industrie Service GmbH
Geschäftsfeld Bautechnik
Am Grauen Stein
51105 Köln
Germany

Taerwe, Luc, Prof.dr.ir.
Ghent University
Department of Structural Engineering
Magnel Laboratory for Concrete Research
Technologiepark Zwijnaarde 904, B-9052 Gent
Belgien

Tchórzewska-Cieślak, Barbara, Dr.
Faculty of Civil and Environmental Engineering
Rzeszow University of Technology
Wincentego Pola 2, 35-959 Rzeszów
Poland

Vořechovský, Miroslav, Ing. PhD
Institute of Structural Mechanics
Faculty of Civil Engineering
Brno University of Technology
Veveří 95, 662 37 Brno
Czech Republic

Włoch, Andrzej, Dr.
Faculty of Mathematics
Rzeszow University of Technology
Wincentego Pola 2, 35-959 Rzeszów
Poland

Zscherpel, Uwe, Dr. rer. nat., ORR
Bundesanstalt für Materialforschung und -prüfung
Unter den Eichen 87, 12205 Berlin
Germany

List of Probabilistic Symposiums in this Series

1st Dresden Probabilistic Symposium –
Safety and Risk in Civil Engineering (in German)
14th November 2003, Dresden
Dresden University of Technology
2nd Edition, 2006
ISBN-10: 3-00-019234-4 & ISBN-13: 978-3-00-019234-0
Price: 30 €
Order: Dirk Proske, Goetheallee 35, 01309 Dresden, Germany
E-mail: dirk.proske@boku.ac.at

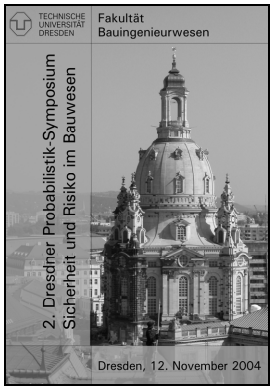

2nd Dresden Probabilistic Symposium –
Safety and Risk in Civil Engineering (in German)
12th November 2004, Dresden
Dresden University of Technology
2nd Edition, 2006
ISBN-10: 3-00-019235-2 & ISBN-13: 978-3-00-019235-7
Price: 30 €
Order: Dirk Proske, Goetheallee 35, 01309 Dresden, Germany
E-mail: dirk.proske@boku.ac.at

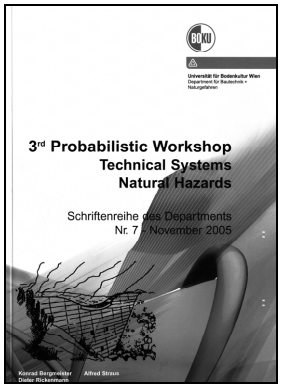

3rd Probabilistic Workshop –
Technical Systems & Natural Hazards,
12th-13th October 2005, Vienna
University of Natural Resources and Applied Life Sciences,
Vienna, Austria
Order: Department of Civil Engineering and Natural Hazards,
Peter Jordan Strasse 82, 1190 Vienna, Austria

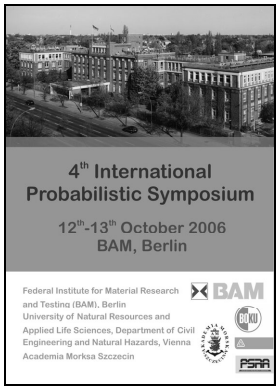

4th International Probabilistic Symposium
12th-13th October 2006, Berlin
BAM - Federal Institute for Materials Research and Testing
ISBN-10: 3-00-019232-8 & ISBN-13: 978-3-00-019232-6
Order: Dirk Proske, Goetheallee 35, 01309 Dresden, Germany
E-mail: dirk.proske@boku.ac.at
or: Milad Mehdianpour, BAM-Fachgruppe VII.2 Ingenieurbau
Bundesanstalt für Materialforschung und –prüfung,
Unter den Eichen 87, 12205 Berlin

ISBN-10: 3-00-019232-8
ISBN-13: 978-3-00-019232-6